



SHAHID BEHESHTI UNIVERSITY

Development of Exotic Harmonium Model  
to Investigate Electron-Positively Charged  
Particle Correlation in Two-Component  
Quantum Systems

By:

Nahid Sadat Riyahi

A Thesis Submitted for the Degree of Doctor of Philosophy in Physical Chemistry

Faculty of Chemistry and Petroleum Sciences

January 2024

This thesis was originally written in Persian at Shahid Beheshti University as per university regulations. It has been translated into English to facilitate broader accessibility and academic exchange while maintaining the integrity of the original content.

## Abstract

The problem of calculating the electron- positively charged particle correlation energy poses a challenge in the field of quantum chemistry beyond the adiabatic approximation. In this study, a toy model called Exotic Harmonium is developed to enhance our understanding of this type of correlation. Since the analytical methods to solve eigenvalue equation for exotic harmonium lead to the excited rather than the ground state of the system, we employ the variation method in this study to obtain an approximate ground state wave function. By considering the asymptotic behavior of the wave function, we derive a compact but highly accurate variational wave function. Using this wave function, we are able to determine various properties of the system, including energy and its components, as well as single-particle densities. Additionally, we extend key concepts and quantities specifically tailored to study electron correlation in the harmonium model to the Exotic harmonium model. For instance, the "correlation hill" concept effectively highlights the distinct nature of electron-positively charged particle correlation compared to electron-electron correlation. Furthermore, we utilize Exotic Harmonium to assess the accuracy of five electron-positively charged particle correlation functionals developed within the context of the two-component density functional theory. Through a regression process, we obtained a compact yet precise analytical form for wave function which explicitly depends on the two crucial variables: oscillator field frequency and positively charged particle's mass. This analytical form provides valuable insights into the behavior of the system. Also, the Exotic Harmonium model enables the investigation of electron-positively charged particle correlation in a vast range of particle masses

To my parents, two angels in human guise

And to my sixteen-year-old self, who, upon discovering this path,  
imbued me with an unwavering passion for this remarkable journey,  
and whose whispers reminded me that even on this Pale Blue Dot<sup>1</sup>,  
"Knowledge Is Power<sup>2</sup>."

---

<sup>1</sup> Carl Sagan

<sup>2</sup> Sir Francis Bacon



With heartfelt gratitude, I acknowledge the esteemed guidance  
and support of  
my supervisor, Dr. Shant Shahbazian,  
and my advisor, Dr. Mohammad Goli.

# Contents

1	Introduction.....	1
1.1	Quantum Chemistry .....	1
1.1.1	The Success of Quantum Chemistry .....	2
1.2	Computational Chemistry.....	4
1.3	Electronic Structure Theory .....	5
1.3.1	The Nature of Approximations.....	7
1.3.2	Equations.....	10
1.4	Why Go Beyond the Born-Oppenheimer Approximation? .....	12
1.5	Exotic Atoms and Molecules .....	14
1.6	Multi-Component Non-BO Ab Initio Methods .....	20
1.6.1	Overview .....	22
1.6.2	Multi-Component Hartree-Fock Equations.....	28
1.7	Multi-Component Non-BO Density Functional Theory.....	32
1.7.1	Equations.....	34
1.8	Challenges and Motivation .....	40
2	Development of the Exotic Harmonium Model .....	44
2.1	Harmonium Model.....	44
2.2	Analytical Solution of the EHM .....	47
2.2.1	Separability of the Hamiltonian.....	51
2.2.2	Analytical Solution .....	52
2.3	EHM.....	61
2.3.1	Finding the Relative Motion Wave Function Using the Variational Method.....	62
2.3.2	Examining the Asymptotic Behavior of the Trial Wave Function.....	63
2.3.3	Other Possibilities for Variational Trial Functions .....	64
2.3.4	Variational Theorem.....	65
2.3.5	Calculating the Gradient and Hessian of the Energy .....	67

2.4	Coordinate System Transformations.....	73
2.4.1	Single-Particle Wave Function .....	73
2.4.2	Intermediate Wave Function .....	75
2.5	Energy Components.....	78
2.5.1	Single-Particle Coordinate System.....	78
2.5.2	Energy Components in Pseudo particle Coordinates.....	82
2.6	Single-Particle Densities .....	85
3	Electron-Positively Charged Particle Correlation .....	91
3.1	Fundamental Definition of Correlation in Physics.....	91
3.2	E-PCP Correlation .....	93
3.2.1	Nature.....	93
3.2.2	History .....	93
3.3	Mathematical Framework.....	95
3.3.1	Pair Correlation Factor .....	95
3.3.2	Correlation Hill .....	96
3.3.3	Correlation Hill Sum Rule .....	99
3.3.4	Correlation Energy.....	100
3.3.5	Two-Particle Distribution Functions .....	104
3.3.6	Mean Inter-Particle Distance and Its Variance .....	109
3.3.7	The Kato Condition.....	110
4	Numerical Data for Model Solution.....	113
4.1	Computational Details.....	113
4.2	Optimized Variational Parameters .....	117
4.3	Energy and Its Components .....	124
4.4	Exponents and Coefficients of MC-HF Calculations.....	148
4.5	Asymptotic Behavior of the Variational Wave Function and System Nature .....	158
5	Electron-Positively Charged Particle Correlation in the Exotic Harmonium Model .....	170

5.1	Correlation in Wavefunction-Based Approaches.....	170
5.1.1	Correlation Energy.....	170
5.1.2	Single-Particle Densities .....	182
5.1.3	Correlation Hill .....	198
5.1.4	Two-Particle Distribution Functions .....	220
5.1.5	Mean Inter-particle Distance and its Variance .....	226
5.2	E-PCP Correlation in Density Functional Theory .....	232
5.2.1	Simplification of Densities .....	233
5.2.2	Calculating Correlation Potentials via Inversion of Kohn-Sham Equations .....	241
5.2.3	Evaluating the Efficiency of Existing Electron-PCP Functionals .....	252
5.2.4	Calculating the Correlation Potentials of the Functionals .....	255
5.3	Data Fitting.....	261
5.3.1	Fitting Variational Parameters.....	261
5.4	Comparison of Non-Adiabatic and Correlation Energy Contributions.....	266
5.4.1	Analysis of the EHM in the Adiabatic Framework .....	266
5.4.2	Calculation of Electronic Energy .....	267
5.4.3	Comparison of Non-Adiabatic and Correlation Energy Contributions .....	272
6	Conclusion .....	280
7	Appendix A .....	285
8	Appendix B .....	314
9	Appendix C .....	329
10	References.....	355

# 1 Introduction

## 1.1 Quantum Chemistry

Theoretical chemistry provides a systematic picture of the laws governing chemical phenomena and uses physics and mathematics to describe the structure and interaction of atoms and molecules. By the end of the 19th century, chemistry was still largely considered a descriptive science, based on concepts such as atomic and molecular weights, combinatorial ratios, thermodynamic quantities, and fundamental ideas of molecular stereochemistry. Although much more logical compared to its ancient roots in alchemy, it was still largely a collection of empirical facts about the behavior of matter. Immanuel Kant, in his famous book "Critique of Pure Reason," asserts: " In any special doctrine of nature there can be only as much proper science as there is mathematics therein." This assertion can be considered a

rational and philosophical reason for emphasizing the use of mathematical methods in chemistry.

The developments in physics at the beginning of the 20th century made it possible to explain all of chemistry fundamentally within the framework of quantum mechanics. As Paul Dirac succinctly stated: "The underlying physical laws necessary for the mathematical theory of a large part of physics and the whole of chemistry are thus completely known, and the difficulty is only that the exact application of these laws leads to equations much too complicated to be soluble." Quantum mechanics, by its nature, is mathematical physics. However, the gap that Dirac pointed out, namely the existence of chemically complex problems from a mathematical perspective, justifies the survival of parts of chemistry as an experimental science. Semi-empirical concepts of chemical bonding and reactivity fall into this category.

The primary goal of theoretical chemistry is to provide a coherent picture of the structure and properties of atomic and molecular systems. Techniques adapted from mathematics and theoretical physics are employed in an effort to explain and correlate the structures and dynamics of chemical systems. Given the extreme complexity of chemical systems, theoretical chemistry, unlike theoretical physics, generally uses more approximate mathematical techniques, which are often supplemented by experimental or semi-empirical methods [1].

### 1.1.1 The Success of Quantum Chemistry

Modern science has struggled to explain the most significant phenomena in the universe, such as the accelerated expansion of galaxies (apparently due to "dark energy") and the fundamental nature of the universe's matter (a significant portion of which is "dark

matter"). Quantum chemistry is in a much better position and may even be exceptional in the entire field of science. Chemical phenomena can be explained using contemporary theories down to the level of individual molecules (the subject of quantum chemistry). Comparing theory and experiment has shown that solving the Schrödinger equation provides a quantitatively accurate picture in most cases, and only molecules with very heavy atoms, due to the importance of relativistic effects, need to be treated using the Dirac equation. When exceptionally high precision is rarely required, we may ultimately consider quantum electrodynamics (QED) corrections, a method whose necessity is currently very unlikely for routine applications but feasible for small multi-particle systems. This success of computational quantum chemistry is based on the following conditions:

- Atoms and molecules are made up of only two types of particles: nuclei and electrons.
- The components of atoms and molecules are usually considered as point charges. Although nuclei have a nonzero size (electrons are considered point-like particles), this size is so small compared to atomic and molecular dimensions that its effect on computational results is much less than chemical accuracy<sup>3</sup>.
- QED corrections are much smaller than energy changes in chemical phenomena (e.g., 1:10,000,000) and can therefore be ignored in most applications.
- Nuclei are a thousand times heavier than electrons and, therefore, except in some special cases, move a thousand times slower than electrons. This makes it possible to solve the Schrödinger equation for electrons under the assumption that

---

<sup>3</sup> Chemical accuracy is considered to be equivalent to 1 kcal/mol or 4 kJ/mol.

the nuclei are stationary, i.e., their positions in space are fixed (clamped nuclei).

It is generally believed that an exact analytical solution to the Schrödinger equation for any atom (except for hydrogen-like atoms) or molecule is not possible. Instead, reasonable approximate solutions can be obtained, which almost always involve calculating a large number of electron integrals and performing some algebraic manipulations on matrices constructed from these integrals. The reason for this is the computational efficiency of what is known as the algebraic approximation (algebraization) of the Schrödinger equation.

## 1.2 Computational Chemistry

Fortunately, a large part of quantum chemistry relies on conditions such as negligible relativistic and electrodynamic corrections and the significant mass ratio of the nucleus to the electron. Rapid advancements in computer technology have revolutionized theoretical chemistry, leading to the birth of computational quantum chemistry. Computational quantum chemistry provides researchers with new, ready-to-use tools that offer powerful insights into the internal molecular structure and dynamics. Commercial computational chemistry programs allow us to perform calculations for molecules and examine each molecule independently of its chemical relationship with other molecules.

In chemistry, as in any other science, it is essential not to study only specific cases one by one but to extract important general laws whenever possible. However, since these general laws are initially derived for specific cases with certain approximations, they are not necessarily applicable to all similar cases and are sometimes only partially valid. Nonetheless, such laws enable chemists to predict,



explain, and ultimately be efficient. If we relied exclusively on the exact solutions of the Schrödinger equation, chemistry would not exist at all, and people would lose the ability to rationalize this branch of science, especially for designing the synthesis of new molecules. Chemists rely on the spatial structure of molecules (nuclear configurations), concepts of valence electrons, chemical bonds, single-electron pairs, and so on. These concepts sometimes do not have a unique and precise quantum definition but remain important and highly effective for describing molecular models [2].

### 1.3 Electronic Structure Theory

Solving quantum mechanics problems always begins with writing the Schrödinger equation for the system under study. Quantum chemistry, which aims to study the quantum nature of chemical systems and processes, is no exception. Therefore, quantum chemistry starts with solving the Schrödinger equation for the simplest natural chemical system, the hydrogen atom (just as the historical development of quantum mechanics began with it). It then progresses from multi-electron atoms to more complex chemical systems, namely molecules, and their corresponding Schrödinger equations. The time-independent form of this equation is as follows:

$$\hat{H}\Psi(r^e, r^n) = E\Psi(r^e, r^n) \tag{1.1}$$

where,  $r^e$  and  $r^n$  are the sum of electronic and nuclear coordinates, respectively, and the molecular non-relativistic Hamiltonian  $\hat{H}$  for a molecule with  $N$  electrons and  $N'$  nuclei in atomic units is as follows<sup>4</sup>:

---

<sup>4</sup> Throughout this thesis, the quantities related to nuclei or positively charged particles are denoted by prime, n or p depending on the conditions.

$$\begin{aligned}
\hat{H} = & - \sum_i^N \frac{1}{2} \nabla_i^2 - \sum_{i'}^{N'} \frac{1}{2m_{i'}} \nabla_{i'}^2 \\
& + \sum_i^N \sum_{j>i}^N \frac{1}{r_{ij}} - \sum_i^N \sum_{i'}^{N'} \frac{Z_{i'}}{r_{ii'}} + \sum_{i'}^{N'} \sum_{j'>i'}^{N'} \frac{Z_{i'}Z_{j'}}{r_{i'j'}}
\end{aligned} \tag{1.2}$$

The first and second terms represent the kinetic energy of the electrons and nuclei, while the subsequent terms refer to the Coulomb potential energies (electron-electron repulsion, electron-nucleus attraction, and nucleus-nucleus repulsion, respectively). Here,  $m_{i'}$  and  $Z_{i'}$  denote the masses of the nuclei and the atomic number, respectively. Additionally,  $r_{ij} = |\vec{r}_i - \vec{r}_j|$  represents the distance between two electrons,  $r_{i'j'}$  represents the distance between two nuclei, and  $r_{ii'}$  represents the distance between an electron and a nucleus.

If we want to describe the distribution of electrons in detail, there is no alternative to quantum mechanics. Electrons cannot even be qualitatively described by classical mechanics. Therefore, we will focus on solving the time-independent Schrödinger equation (1-1).

Methods in which solutions are generated without reference to experimental data, in contrast to semi-empirical models, are called "ab initio" methods. The first step in solving the Schrödinger equation in quantum chemistry is the Born-Oppenheimer approximation, which neglects the coupling between nuclear and electronic motions. This approximation allows us to solve the electronic part of the Schrödinger equation by considering the positions of the nuclei as parameters and using the resulting potential energy surface as the basis for solving the nuclear Schrödinger equation. A significant portion of computational efforts in quantum chemistry is dedicated to solving the electronic

Schrödinger equation for a given nuclear arrangement, which collectively forms the "electronic structure theory."

### 1.3.1 The Nature of Approximations

Unfortunately, the undeniable fact is that equation (1-1) cannot be solved analytically even for the simplest molecule,  $H_2^+$  (which consists of three particles). As a result, we must resort to approximation from the very beginning to simplify as much as possible [3]. The most famous approximation in this context is the Born-Oppenheimer approximation, or BO for short, named after a perturbative study published in 1927 by Max Born and Robert Oppenheimer [4]. However, the BO approximation itself belongs to a broader school of thought called the adiabatic approximation, which has its roots in classical physics. The adiabatic approximation in quantum mechanics was first introduced by Max Born and Vladimir Fock in 1928 under the title of the adiabatic theorem [5]. Therefore, the BO approximation can be considered a special case of the adiabatic approximation.

The word "adiabatic" is derived from the Greek word  $\alpha\delta\iota\alpha\beta\alpha\tau\omicron\varsigma$ , which literally means a situation where "nothing passes through something else." In fact, the response of a system to a time-dependent perturbation depends on the time scale of the perturbation. Gradual changes in external conditions characterize an adiabatic process, whereas rapid movements that result in chaotic responses indicate a non-adiabatic process. In other words, the essence of the adiabatic approach arises from the coexistence of two time scales in some phenomena: fast and slow scales [6].

In thermodynamics, an adiabatic process is one in which energy exchange occurs without the exchange of heat between a system and its surroundings, meaning that heat does not pass through the system's

boundary. Similarly, in quantum mechanics, an adiabatic process refers to a process in which no sudden transition from one state to another occurs relative to the continuous change of some parameters. Therefore, the adiabatic theorem in quantum mechanics is stated as follows: "If a given perturbation acts on a physical system slowly enough and if there is a gap between the eigenvalue of the state it is in and the rest of the Hamiltonian's eigenvalue spectrum, that system remains in its instantaneous eigenstate" [5].

The main strategy for analyzing an adiabatic process is to initially solve the system's behavior with fixed external parameters and then allow those parameters to change at the end of the calculations [7]. In quantum chemistry, this strategy is precisely used as a starting point, where the change in nuclear positions is considered a change in parameter.

In fact, to overcome the difficulty of solving equation (1-1) for molecules, we adopt this strategy and take advantage of the significant difference in mass between electrons and nuclei. Due to this difference, electrons can almost instantaneously respond to the displacement of nuclei, whereas nuclei cannot do so practically, resulting in the coexistence of two different time scales. Therefore, we can adopt the conventional strategy in such a situation: instead of trying to solve the Schrödinger equation simultaneously for all particles, we first consider the nuclei as fixed and solve the Schrödinger equation for the electrons in the static electric potential created by a specific arrangement of nuclei. Then, we change the arrangement of the nuclei and repeat the calculations.

In general, the eigenvalues of the electronic Hamiltonian are obtained for a specific arrangement of nuclei, and then the arrangement that yields the lowest energy is identified. In quantum

chemistry and condensed matter and molecular physics, this different behavior regarding nuclear and electronic motions is famously known as the Born-Oppenheimer approximation [6]. However, if we want to speak in more precise and technical terms, we should call it the adiabatic approximation.

The set of solutions obtained from the electronic Schrödinger equation, i.e., the relationship between molecular electronic energies and molecular geometry, allows us to reach one of the most effective concepts in theoretical chemistry: the Potential Energy Surface (PES). This concept is highly practical, functioning like a white cane for a blind chemist. A minimum on the PES curve indicates the equilibrium configuration of a molecule [8]. Additionally, the PES enables the identification of reaction pathways.

In the BO approximation, when we solve the electronic Schrödinger equation for fixed nuclear configurations and vary the nuclear coordinates, we assume that the electronic state of the system remains the same. In other words, we assume that we remain on the same PES. However, this is only true when the PES for different electronic states is well-separated; thus, in nuclear configurations where the PES of different electronic states come close or even intersect, the BO approximation is insufficient [6]. The BO approximation is generally reliable for ground states but less so for excited states [8]. Nevertheless, most chemical systems can be described using the BO approximation because it provides accurate answers. For this reason, nearly all quantum chemistry textbooks begin by introducing the BO approximation.

### 1.3.2 Equations

The electronic Hamiltonian operator can be expressed as the sum of the electronic kinetic energy and the potential energies involving the nuclei and electrons:

$$\hat{H}_e = \hat{T}_e + \hat{V}_{ee} + \hat{V}_{ne} \quad 1.3$$

Suppose a complete set of solutions of the electron Schrödinger equation is available as follows:

$$\hat{H}_e \psi_i(r^e; r^n) = E_i(r^n) \psi_i(r^e; r^n) \quad 1.4$$

where  $r^e$  and  $r^n$  refer to the total electronic and nuclear variables, respectively, with the eigenfunctions and energies parametrically dependent on  $r^n$ . By solving the electronic Schrödinger equation for all conceivable configurations of the nuclei, the potential energy surface is obtained. Without introducing any approximations, the exact total wave function can be written as an expansion of a complete set of electronic functions, with the condition that the coefficients of this expansion are functions of the nuclear coordinates:

$$\Psi(r^e, r^n) = \sum_{i=1}^{\infty} \psi_i(r^e; r^n) \psi_{ni}(r^n) \quad 1.5$$

In the adiabatic approximation, the form of the total wave function is limited to a single electronic surface, and it is assumed that the expansion (5-1) can be reduced to a single term [2], that is:

$$\Psi(r^e, r^n) \approx \psi_l(r^e; r^n) \psi_{nl}(r^n) \quad 1.6$$

This assumption is the essence of the adiabatic approximation. Except for spatially degenerate wave functions, the first-order diagonal

non-adiabatic coupling elements are zero. Finally, we arrive at the nuclear Schrödinger equation in the following form:

$$\left(\hat{T}_n + E_j(r^n) + U(r^n)\right)\psi_{nj}(r^n) = E_{tot}\psi_{nj}(r^n) \quad 1.7$$

The term  $U(r^n)$  is known as the diagonal correction and is approximately smaller than  $E_j(r^n)$  by a factor roughly equal to the ratio of the mass of the electron to the nucleus. This term usually depends on  $r^n$  and varies slowly, so the shape of the potential energy surface is well determined by  $E_j(r^n)$ . In the adiabatic approximation, the diagonal correction is ignored, and the resulting equation takes the form of the ordinary nuclear Schrödinger equation, where the electronic energy acts as the local potential energy surface:

$$\left(\hat{T}_n + E_j(r^n)\right)\psi_{nj}(r^n) = E_{tot}\psi_{nj}(r^n) \quad 1.8$$

The diagonal Born-Oppenheimer correction (DBOC) can be easily evaluated, as it only involves the second derivative of the electronic wave function with respect to the nuclear coordinates, and thus has a close relation to the nuclear gradient and the second derivative of the energy [9]. Solving equation (1-8) for the nuclear wave function leads to energy levels for molecular vibrations and rotations, which in turn form the basis for many forms of spectroscopy, such as infrared, Raman, microwave, and others [9].

Sometimes, the BO approximation is mistaken for the clamped nucleus approximation, where the nuclear kinetic energy is entirely ignored in the molecular Hamiltonian. Similarly, the BO approximation is occasionally equated with the classical nucleus approximation, where nuclei are considered classical point particles.

However, molecular energies, even in the Born-Oppenheimer approximation, include contributions from the nuclear kinetic energy operator [10]. Thus, the clamped nucleus approximation can be regarded as the initial stage in the BO approximation. Born and Huang, or BH for short, developed a variational alternative to the BO approximation [11] and presented it in the sense we know today (equation 1-5).

## 1.4 Why Go Beyond the Born-Oppenheimer Approximation?

There are significant molecular phenomena that cannot be sufficiently analyzed using conventional methods based on the Born-Oppenheimer approximation. Generally, two major reasons compel us to go beyond the BO approximation and extend our framework to a non-adiabatic approach:

1. Achieving Spectroscopic Accuracy<sup>5</sup>: One of the most critical challenges in quantum chemistry is achieving spectroscopic accuracy. All the systems we study possess some degree of non-adiabaticity [12], which prevents us from achieving such accuracy. To describe these small effects, we need a suitable new formalism. The most common approach is to introduce some non-adiabatic corrections to the results obtained from separate electronic-nuclear Hamiltonian calculations.

---

<sup>5</sup> Indeed, spectroscopic accuracy varies across different types of spectroscopies. For example, in vibrational spectroscopy, spectroscopic accuracy is approximately equivalent to  $1\text{ cm}^{-1}$ .



## 2. Inherently Non-Adiabatic Systems and Phenomena:

There are systems and phenomena that are inherently non-adiabatic, where the BO approximation is ineffective from the outset. Specifically, we cannot describe systems that include strongly coupled particles (e.g., slight differences in particle masses) or coupled states (e.g., closely spaced electronic levels) within the adiabatic framework [13].

It is important to note that when methods beyond the Born-Oppenheimer approximation are employed, concepts such as molecular geometries become ambiguous, and energy levels no longer have unique definitions. In a quantum description, nuclei are delocalized, and "bond lengths" do not have unique definitions. The largest Born-Oppenheimer diagonal correction (DBOC) is expected for molecules containing hydrogen atoms since hydrogen has the lightest nucleus. The absolute magnitude of the DBOC for a water molecule is approximately 7 kcal/mol. These effects are expected to be much smaller for systems with heavier nuclei [9]. Proton-coupled electron transfer (PCET) reactions [14], [15] are examples of phenomena where there is strong coupling between electron and proton dynamics. Therefore, while we know the BO approximation is generally suitable for protons under normal conditions, it is no longer effective in situations such as PCET reactions. Another example includes atoms and molecules containing exotic particles such as positrons and muons, which have garnered increasing interest in recent decades. Given that these particles are lighter than atomic nuclei, using the BO approximation to separate the wave functions of these system components can introduce significant errors in calculations [16].

In addition to the above, there are other ancillary reasons for extending fully non-adiabatic computations: these calculations in

fundamental physics represent a technological advancement for calculating the stationary states of atoms and molecules with very high accuracy. Although a non-adiabatic quantum theory is a natural starting point for quantum chemistry, it has historically been applied only to specific systems due to a lack of computational resources. However, with advancements in computational chemistry and increasing computational capabilities, there will be less emphasis on low-cost methods, and non-BO methods may be chosen for problems where high accuracy is desired [17]. Moreover, interest in non-adiabatic effects has been growing, inspired by the maturation of fields such as ultrafast spectroscopy and molecular dynamics. Experimental studies in these areas are more likely to encounter BO failure and observe non-adiabatic effects [17].

## 1.5 Exotic Atoms and Molecules

An exotic atom refers to a system where the nucleus of a hydrogen atom is replaced with another positively charged fundamental particle (such as a positive muon to form a muonium atom or a positron to form a positronium atom), or an electron in a regular atom is replaced with another negatively charged fundamental particle (such as a muon, pion, or antiproton), or even both simultaneously (such as in antihydrogen) [18].

Table 1-1 : Properties of particles. The mass  $m$  refers to the rest mass of the particle.

Particle	Symbol	Spin	Half-life (s)	Mass relative to e ( $m/m_e$ )	Energy (MeV)	Type
Electron	$e^-$	1/2	$\infty$	1	0.511	Lepton
Positive Muon	$\mu^+$	1/2	$2.197 \times 10^{-6}$	207	105.7	Lepton
Positive Pion	$\pi^+$	0	$2.603 \times 10^{-8}$	273	139.6	Meson
Positive Kaon	$K^+$	0	$1.237 \times 10^{-8}$	966	493.6	Meson
Proton	$p^+$	1/2	$\infty$	1836	938.3	Baryon
Sigma	$\Sigma^+$	1/2	$1.48 \times 10^{-10}$	2343	1197.4	Baryon

When a negatively charged particle with a sufficient lifetime slows down and comes to rest in a material, it replaces an atomic electron and becomes bound in an atomic orbit. Exotic atoms formed in this way are named after the particles they contain, with the most common examples presented in Table 1-1. Depending on the particle type, we refer to muonic atoms, pionic atoms, kaonic atoms, antiprotonic atoms, or sometimes mesonic or hadronic atoms. Additionally, atoms formed by a positive particle and an electron (such as positronium or muonium) also belong to the family of exotic atoms. Due to their extensive applications in positron annihilation and muon spin research in solid-state physics and chemistry, they have been studied much more than exotic atoms with negatively charged particles.

In positronium, the positron and electron, each with the same mass, orbit around a common center of mass. This system is exactly similar to the hydrogen atom, except that the proton is approximately 1836 times heavier than the electron, giving the appearance that the latter orbits the former. By modifying the Bohr model of the hydrogen atom

for positronium, we can show that the radius of the electron's ground state orbit in positronium is twice that of the corresponding orbit in the hydrogen atom. In muonium, a positive muon becomes the effective nucleus, and since the muon has a mass of about one-ninth that of the proton, the muonium atom has a larger radius than hydrogen.

Muons are unstable fundamental particles found in cosmic rays and can also be produced by particle accelerators. They have various applications in fundamental science and engineering. Scientific research using muons focuses on both the fundamental properties of this particle and the microscopic interactions (at the atomic level) between muons and surrounding particles such as nuclei, electrons, atoms, and molecules. Examples of research that can be conducted using muons include muon-catalyzed fusion, the use of muon spin probes to study the microscopic magnetic properties of materials, electron tagging to help understand the microscopic level of electron transfer in proteins, and non-destructive elemental analysis. Cosmic ray muons can even be used to study the internal structure of volcanoes [19].

Muonium is the bound atomic state of a positive muon and an electron, with a mass of  $1/9$  that of a regular hydrogen atom. This exotic atom is of significant interest in both physics and chemistry. In particle physics, it is used for testing fundamental symmetries of matter. In solid-state physics, it serves as a probe for measuring local magnetic fields. In chemistry, it is employed as a traceable lightweight hydrogen atom. From a field theory perspective, muonium is a bound state of two point-like leptons, making it an ideal system for studying quantum effects.

$\mu SR$  stands for Muon Spin Rotation, Relaxation, or Resonance. As mentioned above, positive muons are used to measure local magnetic fields. When polarized muons come to rest in a sample material with

a magnetic field, they align along the field lines, and positrons from their decay are preferentially emitted along the muon's spin direction. This method uses the detection of emitted positrons to obtain information about the local magnetic fields in the system under study [20]. Muonium, also known as a lightweight radioisotope of hydrogen, can be considered the second radioisotope of hydrogen after tritium. It forms chemical bonds with unsaturated organic molecules and creates free radicals. The muon in these radicals acts as a radioactive probe of kinetic and structural properties [21]. Figure 1-1 shows how some of these radicals are formed [22].

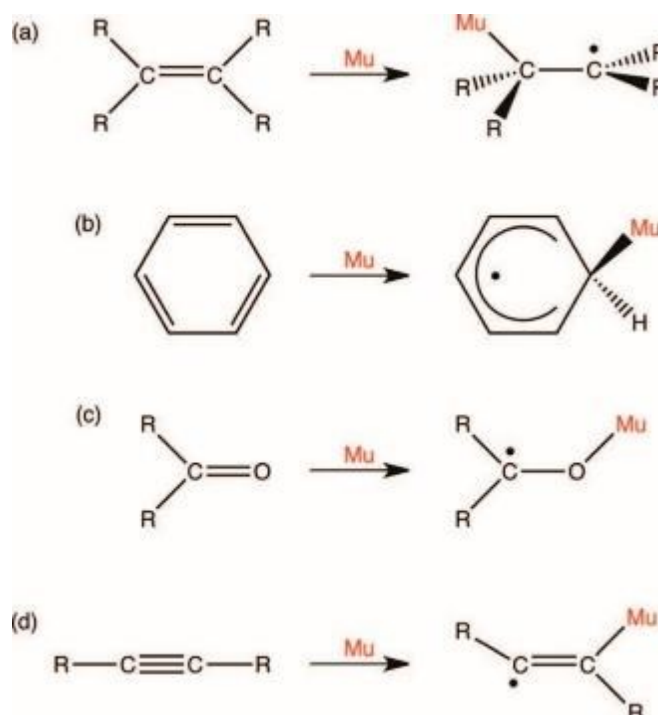


Figure 1-1: Formation of muoniated radicals; (a) alkyl radical; (b) cyclohexadienyl radical; (c) muonoxo-alkyl radical; (d) vinyl radical.

The equivalents of these radicals are also produced as a result of the reaction of hydrogen atoms with unsaturated organic molecules.

However, due to the mass difference between these two atoms, some properties of muonic bonds (such as vibrational frequency) differ from their hydrogen counterparts. This mass difference also causes the reaction rates of muonic and hydrogen radicals to differ, despite having the same mechanism.

Muoniated radicals, which can be detected by  $\mu$ SR spectroscopy, provide a unique opportunity to obtain information about solids such as zeolites, solutions, or even unusual solvents like supercritical water [22]. Additionally, positive muons embedded in semiconductors with diamond and zinc sulfide structures often form paramagnetic muonium states, the characteristics of which can also be studied using the  $\mu$ SR technique [23].

Positron attachment to molecules also has significant applications in material science and chemistry. When a positron comes into contact with a molecule, it annihilates with a molecular electron through a process called positron annihilation, resulting in gamma radiation. However, before this annihilation occurs, the positron can temporarily form a positronium atom, providing valuable information about the electronic structure of molecules [24]. Various experimental methods based on positron annihilation have become important tools for investigating the structure and properties of condensed matter, such as studying defects in solids [25]. Positron annihilation spectroscopy is especially suitable for studying vacancy defects in semiconductors. Combining advanced experimental and theoretical methods allows for precise identification of defects and the surrounding chemical environment. Charge states and defect levels in the energy gap can also be examined [26].

Positron Emission Tomography (PET) is a powerful metabolic imaging technique that provides high-quality images. Clinical PET

imaging is currently used in oncology, cardiology, cardiac surgery, and neurology [27].

Studies of positronium in a vacuum and its decay in the environment provide useful information about the structure of matter and the biological processes of living organisms on a nanoscale. Positronium in biological materials is sensitive to intermolecular and intramolecular structures and the metabolism of living organisms, from single cells to humans. This leads to new ideas for positronium imaging in medicine, utilizing the fact that 40% of positron annihilation through the production of positronium atoms during PET occurs inside the patient's body. A new generation of highly sensitive multi-photon PET systems opens fresh windows for clinical applications of positronium as a biomarker of tissue pathology. Figure 1-2 shows a schematic diagram of such a new PET spectroscopy [28].

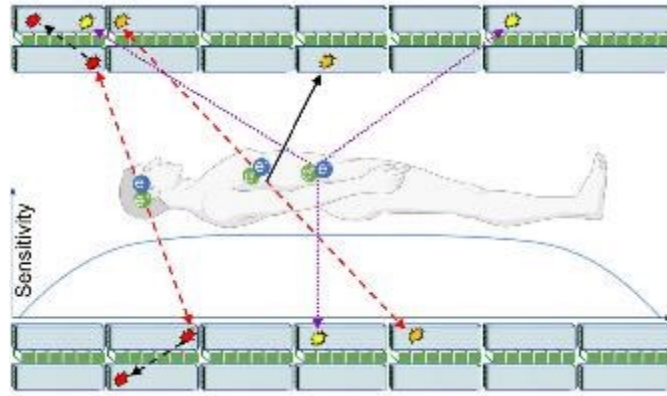


Figure 1-2: Schematic of a whole-body PET scanner for positronium imaging and quantum entanglement. This figure illustrates an axial cross-section of a tomograph design consisting of two detector layers. The red dashed arrows indicate sample responses originating from the positron annihilation process.

The spectrum of the hydrogen atom has been studied more precisely and comprehensively than any other atom. Similarly, the spectroscopy

of exotic "atoms" reveals their characteristics and provides opportunities for testing physical theories. For instance, unlike the proton, which is made up of quarks, both the positron and muon are particles with no internal structure. This means that the energy state separations in these exotic atoms are determined solely by electromagnetic interactions. This makes such exotic atoms an ideal arena for testing Quantum Electrodynamics (QED), as demonstrated by recent research conducted by RIKEN Institute scientists using muonic neon [29]. All these exotic atoms, like the hydrogen atom, serve as laboratories for testing the efficiency of physical theories [30]. Research on exotic atoms is ongoing at all major and medium-energy accelerators where low-energy charged particles are produced [31]–[35].

## 1.6 Multi-Component Non-BO Ab Initio Methods

The mean-field description of electrons moving in the external electric field of clamped nuclei forms the basis of most models currently used in quantum chemistry. However, due to the presence of significant non-adiabatic systems and phenomena mentioned in sections 1-4 and 1-5, it becomes necessary to develop a more general non-BO theory that describes both electrons and nuclei in a mean-field approximation. Such a self-consistent field formulation provides a natural starting point for molecular structure theory (as opposed to electronic structure theory) and yields an initial electron-nuclear wave function reference for all hierarchies of models that include inter-particle correlation, such as Many-Body Perturbation Theory (MBPT), Configuration Interaction (CI), Coupled-Cluster (CC), and Multi-Component Self-Consistent Field (MC-SCF) [36].



A theory that describes all electrons and nuclei in a molecule simultaneously abandons the concept of the potential energy surface. This radical step enables geometry optimization in a non-iterative calculation and the calculation of dynamic processes (e.g., tunnelling of light atoms). However, hidden difficulties exist in this seemingly straightforward approach, including the invariance of the molecular Hamiltonian with respect to rotational and translational motions [37], as well as the lack of explicit dependence of wave functions (except explicitly correlated functions) on inter-particle distances [36].

In this section, we review methods that, from the start of calculations, consider at least one other component of the system in addition to electrons, simultaneously and quantum-mechanically. These methods, which can be termed Multi-Component (MC) non-BO methods, exhibit significant diversity compared to conventional methods in electronic structure theory. In these MC methods, single-particle wave functions for electrons and other quantum species are separately constructed using Gaussian-type basis sets. A notable feature of MC schemes is that nuclear quantum effects on electronic structure and molecular properties are directly obtained from single-point calculations rather than additional corrections based on previous adiabatic calculations [16].

In contrast to the uniformity of computational methods in the adiabatic approach (aiming to derive discrete eigenvalues of the electronic Hamiltonian spectrum), non-adiabatic *ab initio* computational strategies vary significantly [37]. Given the diversity of these methods, the following section will provide a brief overview of the most important ones that have yielded better results or have been further developed.

### 1.6.1 Overview

The first MC method was proposed by Thomas in papers from 1969 and 1970 [38], [39]. He proposed a non-adiabatic molecular orbital theory to simultaneously obtain electronic and protonic wave functions, where electrons and protons are treated quantum-mechanically while heavier nuclei are treated classically. In Thomas' method, all basis functions are placed at the origin on the clamped nucleus, creating a spherical symmetry that avoids the problem of rotational invariance. However, the main limitation of this method is the increasing computational complexity as the number of particles grows.

After Thomas, Adamowicz and colleagues [40] in 1991 proposed a non-BO computational method using explicitly correlated Gaussian (ECG) basis functions, which included the internal coordinates between nuclei and electrons. The ECG method is the most accurate and successful research program in non-BO calculations, based on initially separating the center of mass from the system and then employing the variational principle using trial wave functions that explicitly include rotational invariance [17], [41]–[43]. In this method, the  $n+1$ -particle problem is reduced to an  $n$ -pseudo particle problem, and by placing the reference particle (particle 1 with mass  $M_1$  and usually the heaviest particle) at the center of the coordinate system, the Hamiltonian for internal motion is obtained as follows [43]:

$$\hat{H}_{ECG} = -\frac{1}{2} \left( \sum_i^n \frac{1}{m_i} \nabla_i^2 - \sum_{i \neq j}^n \frac{1}{M_1} \nabla_i' \nabla_j \right) + \sum_{i=1}^n \frac{Z_0 Z_i}{r_i} + \sum_{j>i}^n \frac{Z_i Z_j}{r_{ij}} \quad 1.9$$

In this equation,  $Z_0$  represents the charge of the reference particle, and  $m_i$  is the reduced mass of the  $n$ -pseudo particle system given by

$m_i = \frac{(M_1 M_{i+1})}{(M_1 + M_{i+1})}$  with charges  $Z_i$ . The challenge with the ECG approach is that the complexity of the integrals required to solve the problem increases rapidly with the number of particles, necessitating different coding for various  $n$ -values [44]. Additionally, since the ECG method treats system particles as pseudo-particles, previous computational strategies derived from electronic structure theory are not necessarily applicable. Therefore, other research groups have developed more practical, albeit less accurate, non-adiabatic methods to avoid these computational limitations. The goal of these methods is to develop non-adiabatic approaches that are analogous to familiar methods like Hartree-Fock, post-Hartree-Fock, and Density Functional Theory [37].

In 1998, the multi-component non-BO Hartree-Fock theory was introduced by Tachikawa, Nakai, and colleagues [45], [46]. Subsequently, in 2002, Nakai refined the initial method and introduced the Nuclear Orbital plus Molecular Orbital (NOMO) approach [47]. Nakai and his team described the Nuclear Orbital (NO) as a single-nucleus wave function, similar to the Molecular Orbital (MO) for single-electron wave functions. The total wave function is constructed by multiplying determinants made from NOs and MOs, and the coupled Hartree-Fock equations for NOs and MOs are derived within the single-particle approximation framework. The Configuration Interaction (CI) method applied to the NOMO theory yields not only electronically excited states but also vibrationally excited states of nuclei, while many-body effects in the NOMO theory are examined using Many-Body Perturbation Theory (MBPT) and Coupled-Cluster (CC) theory [48]. These studies revealed that electron-nucleus correlation energy has a larger absolute value compared to nucleus-nucleus correlation energy in the NOMO theory [49].

In the NOMO method, Gaussian-Type Functions (GTFs), which are commonly used as nuclear basis functions as well as electronic basis functions, can accurately describe a vibrational state. However, rotational and translational states are not reproduced well enough using GTFs. Therefore, accounting for rotational and translational motions is necessary to achieve high accuracy in the NOMO method [44]. Accordingly, Nakai proposed a scheme based on Sutcliffe's idea [50] to completely separate the translational motion component from the total Hamiltonian and obtain a Translation-Free Hamiltonian ( $\hat{H}_{TF}$ ) [49]. This Hamiltonian is simply obtained by subtracting the center-of-mass kinetic energy operator (the translational Hamiltonian) from the total Hamiltonian (2-1). For this, we need the center-of-mass kinetic energy operator of nuclei, derived from a coordinate transformation [49]:

$$\hat{T}_{COM} = -\frac{1}{2M} \sum_{\mu} \nabla(x_{\mu})^2 - \frac{1}{M} \sum_{v>\mu} \nabla(x_{\mu}) \cdot \nabla(x_v) \quad 1.10$$

where  $M$  represents the total mass of the nuclei, and the first and second terms are the single-particle and two-particle operators, respectively. By subtracting this operator from the total Hamiltonian (1-2), which is contaminated by translational motion ( $\hat{H}_{TRC}$ ), we obtain the translation-free Hamiltonian ( $\hat{H}_{TF}$ ).

$$\hat{H}_{TF} = \hat{H}_{TRC} - \hat{T}_{COM} = \hat{T}^e + \hat{T}^p + \hat{V}^{ee} + \hat{V}^{ep} + \hat{V}^{pp} - \hat{T}_{COM} \quad 1.11$$

On the other hand, we can subtract  $\hat{T}_{COM}$  separately from each of the above operators and redefine them as follows:

$$\hat{H}_{TF} = \hat{T}_{TF}^e + \hat{T}_{TF}^p + \hat{V}_{TF}^{ee} + \hat{V}_{TF}^{ep} + \hat{V}_{TF}^{pp} \quad 1.12$$

where their explicit form is as follows:

$$\hat{T}_{TF}^e = - \sum_i^N \frac{1}{2} \left( 1 - \frac{1}{M} \right) \nabla_i^2 = \sum_i^N \hat{t}_{TF}^e \quad 1.13$$

$$\hat{T}_{TF}^p = - \sum_i^{N'} \frac{1}{2} \left( \frac{1}{m_p} - \frac{1}{M} \right) \nabla_{i'}^2 = \sum_i^{N'} \hat{t}_{TF}^p \quad 1.14$$

$$\hat{V}_{TF}^{ee} = \sum_i^N \sum_{j>i}^N \left( \frac{1}{r_{ij}} + \frac{1}{M} \nabla_i \cdot \nabla_j \right) \quad 1.15$$

$$\hat{V}_{TF}^{ep} = \sum_i^N \sum_{i'}^{N'} \left( -\frac{Z_{i'}}{r_{ii'}} + \frac{1}{M} \nabla_i \cdot \nabla_{i'} \right) \quad 1.16$$

$$\hat{V}_{TF}^{pp} = \sum_{i'}^{N'} \sum_{j'>i'}^{N'} \left( \frac{Z_{i'} Z_{j'}}{r_{i'j'}} + \frac{1}{M} \nabla_{i'} \cdot \nabla_{i'} \right) \quad 1.17$$

where  $m_p$  denotes the mass of nuclei (or positive particles). Equations (1-13) and (1-14) represent the kinetic energy of electrons and nuclei, respectively. Equations (1-15) and (1-17) indicate the Coulomb repulsion potential between electrons and between nuclei, respectively. Finally, Equation (1-16) shows the Coulomb attraction between electrons and nuclei. Using  $\hat{H}_{TF}$ , the accuracy of an orbital approach such as the NOMO method is significantly improved at the HF, CI, MBPT, and CC levels [51].

Nakai and his colleagues, in the next step and to remove the contribution of rotational motions, subtracted the rotational energy operator from  $\hat{H}_{TF}$  and introduced a new Hamiltonian called the Translation- and Rotation-free Hamiltonian ( $\hat{H}_{TRF}$ ) [49]. Based on these modifications, the initial total Hamiltonian, contaminated by translational motion, is referred to as  $\hat{H}_{TRC}$ , and the corresponding

formulation is called TRC-NOMO. Similarly, the formulations related to  $\hat{H}_{TF}$  and  $\hat{H}_{TRF}$  are referred to as TF-NOMO and TRF-NOMO, respectively. It is noteworthy that in all versions of NOMO-HF, the total wave function is defined as the product of the Slater determinants of the electronic and nuclear wave functions.

Since the NOMO method uses Gaussian-Type Functions (GTFs) as both electronic and nuclear basis sets, efficient algorithms can be applied to evaluate the two-particle integrals. However, this method has limited accuracy, especially when used to evaluate nucleus-dependent properties such as zero-point energies. The electron-nucleus correlation in the NOMO method is not efficiently recoverable by Configuration Interaction (CI), Many-Body Perturbation Theory (MBPT), or Coupled-Cluster (CC) methods [52].

Finally, in 2002, Hammes-Schiffer and her colleagues proposed a hybrid method to simplify multi-component ab initio methods. They suggested that some nuclei in a molecule could be treated as clamped, and only the lightest nuclei (e.g., protons, deuterium) should be treated quantum-mechanically. Therefore, this method deals with three types of entities: electrons, quantum nuclei, and clamped nuclei. This approach is called the Nuclear-Electronic Orbital (NEO) method, and its Hamiltonian in atomic units is given as follows [53]:

$$\begin{aligned}
\hat{H}_{NEO} &= \hat{T}_{NEO}^e + \hat{V}_{ext}^e + \hat{T}_{NEO}^p + \hat{V}_{ext}^p + \hat{V}_{NEO}^{ee} + \hat{V}_{NEO}^{ep} + \hat{V}_{NEO}^{pp} \\
&= -\sum_i^N h(i) - \sum_{i'}^{N'} h'(i') \\
&\quad + \sum_i^N \sum_{j>i}^N \frac{1}{r_{ij}} - \sum_i^N \sum_{i'}^{N'} \frac{Z_i}{r_{ii'}} + \sum_{i'}^{N'} \sum_{j>i'}^{N'} \frac{Z_{i'} Z_{j'}}{r_{i'j'}}
\end{aligned} \tag{1.18}$$

where the first and second terms, considering the external potential that is typically interaction with clamped nuclei ( $N_c$ ), are defined as follows:

$$h(i) = -\frac{1}{2}\nabla_i^2 - \sum_A^{N_c} \frac{Z_A}{r_{iA}} \quad 1.19$$

$$h'(i') = -\frac{1}{2M_{i'}}\nabla_{i'}^2 + \sum_A^{N_c} \frac{Z_A Z_{i'}}{r_{i'A}} \quad 1.20$$

In this method, due to the presence of clamped nuclei, the issue of the total Hamiltonian's invariance with respect to translational and rotational motions is resolved. Therefore, this method is suitable for systems where only certain nuclei exhibit non-adiabatic behavior and need to be considered coupled with electrons from the outset. The mathematical details of this method will be discussed in Section 1-6-2, as this approach is directly used in this study.

Since the NEO method does not face issues related to translational and rotational invariance, the primary focus has been on improving the wave function. Initially, the Hartree-Fock wave function was extended to a multi-configurational version [54], and the following improvements were made: adding explicit electron-nucleus correlations using geminal functions to the total wave function, developing the Nuclear-Electronic Orbital Explicitly Correlated Hartree-Fock (NEO-XCHF) method [55] and extending it to multi-electron systems [56], introducing a new wave function called NEO-XCHF2 [57], developing the Nuclear-Electronic Orbital Reduced Explicitly Correlated Hartree-Fock (NEO-RXCHF) method [58], and extending it to open-shell electronic systems [59]. Reviews of the NEO method are available in [60] and [61].

Therefore, the ECG, NOMO, and NEO methods form the main approaches to multi-component non-BO ab initio methods, and other proposed methods have not been developed as extensively as these. Specifically, the NEO and NOMO methods have been developed for recovering interspecies correlations within the MC framework, starting from their own Hartree-Fock methods and extending to post-Hartree-Fock methods like Configuration Interaction, Møller–Plesset (MP) Many-Body Perturbation Theory, and Coupled-Cluster theory [61]. Additionally, Multi-Component Kohn–Sham Density Functional Theory (to be discussed in Section 1-7) has been developed as an alternative to wave function-based methods for recovering inter-particle correlations.

### 1.6.2 Multi-Component Hartree-Fock Equations

In this section, the principal equations of multi-component Hartree-Fock (MC-HF) methods are presented, with detailed derivations reported in the appendix A. In this study, the introduction of the Exotic Harmonium Model (hereafter EHM) allows for the exact variational solution of the Schrödinger equation. However, since the Hartree-Fock method is a mean-field theory, comparing it with exact solutions will reveal the correlation effects.

Since we aim to simultaneously and equally treat both electrons and nuclei as quantum particles, we need to propose a wave function that satisfies these symmetry properties of particle statistics. The most straightforward proposal for a composite two-component total wave function, using electronic and nuclear Slater determinants (assuming the nuclei are fermions), is as follows:

$$\Psi_{tot}(x^e, x^p) = \Phi_0^e(x^e) \Phi_0^p(x^p) \quad 1.21$$



where

$$\Phi_0^e(x_1^e, x_2^e, \dots, x_N^e) = (N!)^{-1/2} \begin{vmatrix} \chi_1^e(x_1^e) & \cdots & \chi_k^e(x_1^e) \\ \vdots & \ddots & \vdots \\ \chi_1^e(x_N^e) & \cdots & \chi_k^e(x_N^e) \end{vmatrix} \quad 1.22$$

$$\Phi_0^p(x_1^p, x_2^p, \dots, x_{N'}^p) = (N'!)^{-1/2} \begin{vmatrix} \chi_1^p(x_1^p) & \cdots & \chi_k^p(x_1^p) \\ \vdots & \ddots & \vdots \\ \chi_1^p(x_{N'}^p) & \cdots & \chi_k^p(x_{N'}^p) \end{vmatrix} \quad 1.23$$

The notation conventions in the above equations are as follows:

$\Phi_0^e$ : total electron wave function or electron Slater determinant

$\Phi_0^p$ : total nuclear wave function or nuclear Slater determinant

$x^e$ : set of spatial and electron spin coordinates

$x^p$ : the set of spatial and nuclear spin coordinates

$k$ : number of electron spin-orbitals

$k'$ : number of nuclear spin-orbitals

$N$ : number of electrons

$N'$ : number of nuclei (or, in general, PCPs)

Therefore:

$$\chi^e(x^e) = \begin{cases} \psi^e(r^e)\alpha(\omega) \\ \text{or} \\ \psi^e(r^e)\beta(\omega) \end{cases} \quad 1.24$$

$$\chi^p(x^p) = \begin{cases} \psi^p(r^p)\alpha(\omega) \\ \text{or} \\ \psi^p(r^p)\beta(\omega) \end{cases} \quad 1.25$$

Similar to electronic structure theory, the total energy and spatial orbitals are obtained by simultaneously optimizing the system's energy with respect to both electronic and nuclear orbitals. To achieve this

goal, we need to evaluate the expectation value of the energy, which has the general form:

$$E_0 = \langle \Psi_0 | \hat{H}_{NEO} | \Psi_0 \rangle \quad 1.26$$

By minimizing the energy expression (1-26) and after applying certain mathematical considerations, we arrive at the final form of the coupled electron-nuclear Hartree-Fock equations for the closed-shell case:

$$f^e(1) \psi_i^e(1) = \varepsilon_i \psi_i^e(1) \quad 1.27$$

$$f^p(1) \psi_i^p(1) = \varepsilon_i \psi_i^p(1) \quad 1.28$$

where  $f^e$  and  $f^p$  are the electronic and nuclear Fock operators, respectively, and are equal to the expressions within the brackets in the following equations:

$$\begin{aligned} & \left[ h^e(1) + \sum_j^{\frac{N}{2}} \left( 2J_{NEOj}^e(1) - K_{NEOj}^e(1) \right) + \sum_{i'}^{N'} J_{NEOi'}^e \right] \psi_i^e(1) \\ & = \sum_j^{\frac{N}{2}} \varepsilon_{ij} \psi_j^e(1) \end{aligned} \quad 1.29$$

$$\begin{aligned} & \left[ h^p(1) + \sum_{j'}^{N'} \left( J_{NEOj'}^p(1) - K_{TFj'}^p(1) \right) + 2 \sum_i^{\frac{N}{2}} J_{NEOi}^p \right] \psi_i^p(1) \\ & = \sum_{j'}^{N'} \varepsilon_{i'j'} \psi_{j'}^p(1) \end{aligned} \quad 1.30$$

where the Coulomb operators are as follows:

$$J_{NEOj}^e(1)\psi_i^e(1) = \left[ \int dr_2^e \psi_j^{e*}(2) \hat{V}_{NEO}^{ee} \psi_j^e(2) \right] \psi_i^e(1) \quad 1.31$$

$$J_{NEOj'}^p(1)\psi_i^p(1) = \left[ \int dr_2^p \psi_j^{p*}(2) \hat{V}_{NEO}^{pp} \psi_j^p(2) \right] \psi_i^p(1) \quad 1.32$$

$$J_{NEOi}^e(1)\psi_i^e(1) = \left[ \int dr_2^p \psi_i^{p*}(2) \hat{V}_{NEO}^{pe} \psi_i^p(2) \right] \psi_i^e(1) \quad 1.33$$

$$J_{NEOi}^p(1)\psi_i^p(1) = \left[ \int dr_2^e \psi_i^{e*}(2) \hat{V}_{NEO}^{ep} \psi_i^e(2) \right] \psi_i^p(1) \quad 1.34$$

and the exchange operators are also defined as follows:

$$K_{NEOj}^e(1)\psi_i^e(1) = \left[ \int dr_2^e \psi_j^{e*}(2) \hat{V}_{NEO}^{ee} \psi_i^e(2) \right] \psi_j^e(1) \quad 1.35$$

$$K_{NEOj'}^p(1)\psi_i^p(1) = \left[ \int dr_2^p \psi_j^{p*}(2) \hat{V}_{NEO}^{pp} \psi_i^p(2) \right] \psi_j^p(1) \quad 1.36$$

The nuclear and electronic orbitals are expanded using Gaussian-type basis functions ( $\phi_v^e$ ). This approach transforms the Hartree-Fock integro-differential equations into matrix equations, which are easier to solve:

$$\psi_i^e(1) = \sum_v^B c_{vi}^e \phi_v^e(1) \quad 1.37$$

$$\psi_i^p(1) = \sum_{v'}^{B'} c_{v'i}^p \phi_{v'}^p(1) \quad 1.38$$

where  $B$  and  $B'$  represent the number of nuclear and electronic basis functions, respectively. By substituting the above expansions into the Hartree-Fock equations (1-27) and (1-28), we arrive at the algebraic coupled Roothaan-Hall-Hartree-Fock equations:

$$\sum_v^B F_{\mu\nu}^e c_{vi}^e = \varepsilon_i \sum_v^B c_{vi}^e S_{\mu\nu}^e \quad 1.39$$

$$\sum_{v'}^{B'} F_{\mu'v'}^p c_{v'i'}^p = \varepsilon_{i'} \sum_{v'}^{B'} c_{v'i'}^p S_{\mu'v'}^p \quad 1.40$$

In equation (1-39), which is written for electrons,  $c$  and  $\varepsilon$  are  $B \times B$  square matrices (similarly for nuclear equation 1-40) and overlap matrices are defined as follows:

$$S_{\mu\nu}^e = \int dr_1^e \phi_\mu^{e*}(1) \phi_\nu^e(1) \quad 1.41$$

$$S_{\mu'v'}^p = \int dr_1^p \phi_\mu^{p*}(1) \phi_{v'}^p(1) \quad 1.42$$

And the Fock matrices are defined as follows:

$$F_{\mu\nu}^e = \int dr_1^e \phi_\mu^{e*}(1) f^e(1) \phi_\nu^e(1) \quad 1.43$$

$$F_{\mu'v'}^p = \int dr_1^p \phi_\mu^{p*}(1) f^p(1) \phi_{v'}^p(1) \quad 1.44$$

The Fock matrix can be defined using the expansion of the basis function. For this purpose, new quantities known as density matrices need to be defined.

## 1.7 Multi-Component Non-BO Density Functional Theory

The non-BO versions of Density Functional Theory were first introduced by Parr [62] and colleagues in 1982, and later by Shigeta [63] and colleagues in 1998. Subsequently, in 2001, Gross and his collaborator published the Multi-Component Density Functional

Theory (MC-DFT) [64]. The first development of NEO-DFT dates back to 2007 when Hammes-Schiffer's group incorporated electron-electron correlation into the NEO framework, hence naming it NEO-DFT(ee) [65]. In 2009, Hammes-Schiffer's group took the initial step towards obtaining an electron-proton correlation functional by introducing exact universal functional features in a multi-component density functional theory [66], and their development continued over the following years.

In 2011, the second electron-proton correlation functional, known as EPC2, was introduced within the NEO-DFT framework [67]. In 2012, the previous functional was improved using the adiabatic connection formula in multi-component DFT and was presented as EPC2-KE [68]. A significant step was taken in 2017 with the introduction of an efficient functional called epc17 [69]. In the same year, a parameter-improved version of epc17 was introduced, named epc17-2, and the original functional was renamed epc17-1 [70]. A year later, in 2018, two more functionals, epc18-1 and epc18-2, were introduced, which performed similarly to the 2017 versions [71]. In 2019, another improved functional named epc19 was introduced, which depended on both density and density gradients [72].

A significant challenge in implementing multi-component Kohn-Sham DFT is designing accurate and practical functionals for electron-proton correlation. When electron-proton correlation is ignored, proton densities become highly localized, leading to non-physical results for dependent properties. Early attempts by Hammes-Schiffer's group to estimate electron-proton correlation functionals by analyzing the relationship between electron-proton pair density and the total wave function or specific orbitals improved proton densities, but were computationally expensive or not easily applicable to multi-particle

systems. Additionally, these efforts treated functionals as post-self-consistent field energy corrections, which did not affect highly localized proton densities and, thus, were not useful for describing proton-density-based properties [69]. In 2022, the first functional for examining electron-positron correlation was proposed as part of developing electron and positive particle correlation functionals [73].

An important advantage of the NEO-DFT method is its low computational cost, making it practical for a wide range of molecular systems. However, a drawback of the NEO-DFT method is the lack of a clear path toward systematic functional improvement [74]. Unlike the NEO-DFT approach, wave function-based methods within the NEO framework are inherently improvable and free of parameters. Some of these methods include NEO-MP2 [75], [76], NEO-CI [53], and NEO-CC [74].

### 1.7.1 Equations

In this section, the final equations of the multi-component density functional theory (MC-DFT) are presented. Since this dissertation employs the inversion of two-component Kohn-Sham equations (rather than solving them self-consistently), only the main equations are provided without detailing their derivations.

MC-DFT starts with the Hohenberg-Kohn theorems, similar to its single-component counterpart. However, the form of these theorems is not obvious for different conditions and systems and must be redefined. Nevertheless, the essence of the two theorems remains the same across various DFT versions: the first theorem pertains to the existence theorem, and the second theorem proposes the variational principle in terms of single-particle densities. In a multi-component system, quantities for each component are defined separately. For example, in

a two-component system consisting of electrons and positively charged particles (hereafter PCP), we deal with two single-particle densities  $\rho_e(\mathbf{r}_e)$  and  $\rho_p(\mathbf{r}_p)$  and their respective external potentials  $v_e^{ext}(\mathbf{r}_e)$  and  $v_p^{ext}(\mathbf{r}_p)$ .

The first Hohenberg-Kohn theorem for multi-component systems states that the ground state of a multi-component system with a given inter-particle interaction is a unique functional of all single-particle densities and the mass ratio of the particles. By integrating the single-particle densities, we can determine the number of particles for each component. Using the mass ratios, we can construct their kinetic energy operators, and due to the one-to-one correspondence, we can derive the external potential for each component from its single-particle density.

In a two-component system consisting of an arbitrary number of electrons and one type of PCP, the single-particle densities are defined as follows:

$$\begin{aligned} & \rho_e(r_e) \\ &= N \sum_{spin} \int \dots \int \Psi^*(\mathbf{r}_e^1, \mathbf{r}_e^2, \dots, \mathbf{r}_e^N, \mathbf{r}_p^1, \mathbf{r}_p^2, \dots, \mathbf{r}_p^{N'}) \Psi(\mathbf{r}_e^1, \mathbf{r}_e^2, \dots, \mathbf{r}_e^N, \mathbf{r}_p^1, \mathbf{r}_p^2, \dots, \mathbf{r}_p^{N'}) d\mathbf{r}_e^2 d\mathbf{r}_e^3 \dots d\mathbf{r}_e^N d\mathbf{r}_p^1 d\mathbf{r}_p^2 \dots d\mathbf{r}_p^{N'} \end{aligned} \quad \begin{matrix} 1 \\ .45 \end{matrix}$$

$$\begin{aligned} & \rho_p(r_p) \\ &= N' \sum_{spin} \int \dots \int \Psi^*(\mathbf{r}_e^1, \mathbf{r}_e^2, \dots, \mathbf{r}_e^N, \mathbf{r}_p^1, \mathbf{r}_p^2, \dots, \mathbf{r}_p^{N'}) \Psi(\mathbf{r}_e^1, \mathbf{r}_e^2, \dots, \mathbf{r}_e^N, \mathbf{r}_p^1, \mathbf{r}_p^2, \dots, \mathbf{r}_p^{N'}) d\mathbf{r}_e^1 d\mathbf{r}_e^2 \dots d\mathbf{r}_e^N d\mathbf{r}_p^2 d\mathbf{r}_p^3 \dots d\mathbf{r}_p^{N'} \end{aligned} \quad \begin{matrix} 1 \\ .46 \end{matrix}$$

The method for calculating these single-particle densities based on the system model's wave function is discussed in detail in Section 2-6.

The second Hohenberg-Kohn theorem for multi-component systems describes a constrained search process with respect to the components'

densities, leading to the determination of the wave functions, densities, and ground state energy of the system [77]:

$$E_0 = \mathbf{Min}_{\rho_e, \rho_p} E[\rho_e, \rho_p] = \mathbf{Min}_{\Psi \rightarrow \rho_e, \rho_p} \langle \Psi | \hat{H} | \Psi \rangle \quad 1.47$$

The energy functional can be written as follows:

$$\begin{aligned} E[\rho_e, \rho_p] = & \int \rho_e(\mathbf{r}_e) v_e^{ext}(\mathbf{r}_e) d\mathbf{r}_e \\ & + \int \rho_p(\mathbf{r}_p) v_p^{ext}(\mathbf{r}_p) d\mathbf{r}_p + F_{HK}[\rho_e, \rho_p] \end{aligned} \quad 1.48$$

where  $v^{ext}$  represents the external potentials, which often but not always refer to the field caused by clamped nuclei, and  $F_{HK}[\rho_e, \rho_p]$ , which is equivalent to the universal functional in single-component DFT (but here, due to its implicit dependence on the masses of the components, it is not universal), is defined as follows:

$$\begin{aligned} F_{HK}[\rho_e, \rho_p] = & (T_e[\rho_e, \rho_p] + T_p[\rho_e, \rho_p]) \\ & + (V_{ep}[\rho_e, \rho_p] + V_{ee}[\rho_e, \rho_p] + V_{pp}[\rho_e, \rho_p]) \end{aligned} \quad 1.49$$

where  $T_e$  and  $T_p$  represent the expectation values of the kinetic energies of electrons and PCPs, respectively, using the wave function (1-1). Additionally,  $V_{ep}$ ,  $V_{ee}$ , and  $V_{pp}$  correspond to the total interaction energies of electron-positive particle, electron-electron, and positive particle-positive particle interactions, respectively, which will be discussed in detail in Chapter 3.

The Hohenberg-Kohn theorems and the formalism of Density Functional Theory primarily apply to the ground state; however, researchers have recently extended it to ensemble states (EDFT) to explore excited states [78].



After defining the multi-component Hohenberg-Kohn theorems, the next step is to define multi-component Kohn-Sham systems, which, like their single-component counterparts, are the practical equations of computational DFT. Multi-component Kohn-Sham systems are reference, non-interacting systems whose single-particle densities for each component match those of the corresponding component in the actual interacting system. The DFT equations are then solved based on the orbitals assigned to the particles in these reference systems (Kohn-Sham orbitals).

The total wave function of the non-interacting system is also defined as the product of the Kohn-Sham determinants of electrons and PCPs:

$$\Psi^{ks}(\mathbf{r}_e, \mathbf{r}_p) = \Phi_e^{ks}(\mathbf{r}_e) \Phi_p^{ks}(\mathbf{r}_p) \quad 1.50$$

where  $\Phi_e^{ks}$  and  $\Phi_p^{ks}$  are obtained using the Kohn-Sham orbitals, similar to equations (1-22) and (1-23). For a two-component two-particle system, the above equation reduces to:

$$\Psi^{ks}(\mathbf{r}_e, \mathbf{r}_p) = \phi_e^{ks}(\mathbf{r}_e) \phi_p^{ks}(\mathbf{r}_p) \quad 1.51$$

The right-hand side of the above equation represents the electronic and positive particle Kohn-Sham orbitals, respectively, and their orthonormality condition is expressed as follows:

$$\int \phi_i^{ks*}(1) \phi_j^{ks}(1) dr_1 = [\phi_i^{ks} | \phi_j^{ks}] = \delta_{ij} \quad 1.52$$

$$\int \phi_{i'}^{ks*}(1) \phi_{j'}^{ks}(1) dr_1' = [\phi_{i'}^{ks} | \phi_{j'}^{ks}] = \delta_{i'j'} \quad 1.53$$

The electron and positive particle densities, expressed in terms of Kohn-Sham orbitals for a two-component system, are defined as follows using equations (1-45) and (1-46):

$$\rho_e(\mathbf{r}_e) = \sum_i n_i |\phi_i^{ks}(\mathbf{r}_e)|^2 \quad 1.54$$

$$\rho_p(\mathbf{r}_p) = \sum_{i'} n_{i'} |\phi_{i'}^{ks}(\mathbf{r}_p)|^2 \quad 1.55$$

where  $n_i$  and  $n_{i'}$  are the orbital occupation numbers. The kinetic energies of the Kohn-Sham system are obtained from the following equations:

$$T_e^s[\rho_e] = \left\langle \psi^{ks*}(\mathbf{r}_e, \mathbf{r}_p) \left| \sum_i^N \left( -\frac{1}{2m_e} \nabla_{i,e}^2 \right) \right| \psi^{ks}(\mathbf{r}_e, \mathbf{r}_p) \right\rangle \quad 1.56$$

$$T_p^s[\rho_p] = \left\langle \psi^{ks*}(\mathbf{r}_e, \mathbf{r}_p) \left| \sum_{i'}^{N'} \left( -\frac{1}{2m_p} \nabla_{i',p}^2 \right) \right| \psi^{ks}(\mathbf{r}_e, \mathbf{r}_p) \right\rangle \quad 1.57$$

To derive the two-component Kohn-Sham equations, we must first (similar to the single-component DFT process) write the ground state energy functional expression of a two-component system in terms of the components' densities.  $F[\rho_e, \rho_p]$  in the Kohn-Sham method (Equation 1-48) can be defined as follows:

$$\begin{aligned} F[\rho_e, \rho_p] = & (T_e^s[\rho_e] + T_p^s[\rho_p]) \\ & + (J_{ee}[\rho_e] + J_{pp}[\rho_p] + J_{ep}[\rho_e, \rho_p]) \\ & + (E_{exc}[\rho_e] + E_{pxc}[\rho_p] + E_{epc}[\rho_e, \rho_p]) \end{aligned} \quad 1.58$$

The third parenthesis in the above expression includes the exchange-correlation energy of electrons ( $E_{exc}$ ), the exchange-correlation energy of PCPs ( $E_{pxc}$ ), and the electron-PCP correlation energy ( $E_{epc}$ ). The definitions of these three energies are as follows:

$$E_{epc}[\rho_e, \rho_p] = V_{ep}[\rho_e, \rho_p] - J_{ep}[\rho_e, \rho_p] \quad 1.59$$

$$E_{exc}[\rho_e] = (T_e[\rho_e, \rho_p] - T_e^s[\rho_e]) + (V_{ee}[\rho_e, \rho_p] - J_{ee}[\rho_e]) \quad 1.60$$

$$E_{pxc}[\rho_p] = (T_p[\rho_e, \rho_p] - T_p^s[\rho_p]) + (V_{pp}[\rho_e, \rho_p] - J_{pp}[\rho_p]) \quad 1.61$$

And their classical parts are defined as follows:

$$J_{ep}[\rho_e, \rho_p] = - \iint \frac{\rho_e(r_1^e) \rho_p(r_1^p)}{|\mathbf{r}_1^e - \mathbf{r}_1^p|} d\mathbf{r}_1^e d\mathbf{r}_1^p \quad 1.62$$

$$J_{ee}[\rho_e] = \frac{1}{2} \iint \frac{\rho_e(r_1^e) \rho_e(r_2^e)}{|\mathbf{r}_1^e - \mathbf{r}_2^e|} d\mathbf{r}_1^e d\mathbf{r}_2^e \quad 1.63$$

$$J_{pp}[\rho_p] = \frac{1}{2} \iint \frac{\rho_p(r_1^p) \rho_p(r_2^p)}{|\mathbf{r}_1^p - \mathbf{r}_2^p|} d\mathbf{r}_1^p d\mathbf{r}_2^p \quad 1.64$$

Ultimately, by minimizing the energy functional expression with respect to the Kohn-Sham orbitals, the coupled electron and PCP Kohn-Sham equations are obtained as follows:

$$\left( -\frac{1}{2m_e} \nabla_e^2 + V_{\text{eff}}^e(\mathbf{r}_e) \right) \phi_i^{ks} = \varepsilon_i^e \phi_i^{ks} \quad 1.65$$

$$\left( -\frac{1}{2m_p} \nabla_p^2 + V_{\text{eff}}^p(\mathbf{r}_p) \right) \phi_i^{ks} = \varepsilon_i^p \phi_i^{ks} \quad 1.66$$

where  $V_{\text{eff}}^e$  and  $V_{\text{eff}}^p$  are called the effective Kohn-Sham potentials, and are respectively equal to the sum of the external potential, Coulomb potential, single-particle exchange-correlation, and two-particle correlation potentials as follows:

$$V_{\text{eff}}^e(\mathbf{r}_e) = v_e^{\text{ext}}(\mathbf{r}_e) + v_e^{\text{ee}}(\mathbf{r}_e) + v_e^{\text{ep}}(\mathbf{r}_e) + v_e^{\text{xc}}(\mathbf{r}_e) + v_e^{\text{epc}}(\mathbf{r}_e) \quad 1.67$$

$$\begin{aligned}
v_{\text{eff}}^p(\mathbf{r}_p) = & v_p^{\text{ext}}(\mathbf{r}_p) + v_p^{Jpp}(\mathbf{r}_p) + v_p^{Jep}(\mathbf{r}_p) + v_p^{xc}(\mathbf{r}_p) \\
& + v_p^{\text{epc}}(\mathbf{r}_p)
\end{aligned}
\tag{1.68}$$

The explicit form of these potentials will be presented when calculating the correlation potential (Section 5-2-2) for the model under consideration. In general, the above equations are provided for a generic two-component system (with an arbitrary number of particles), and the equations for the EHM will be presented in the relevant sections (Sections 3-3-4 and 5-2-2).

## 1.8 Challenges and Motivation

To investigate the specific systems discussed in Section 1-4, we need computational methods beyond the Born-Oppenheimer approximation. However, the orbital-based examples of these methods introduced in Section 1-6 have fundamental issues. Research indicates that solving these problems requires a deeper understanding of a new type of correlation, namely electron-PCP (hereafter e-PCP) correlation.

Multi-component methods based on electronic and nuclear orbitals typically produce highly localized nuclear wave functions, leading to overestimated vibrational frequencies. The magnitude of errors in the stretching frequencies for hydrogen vibrations often ranges from 2000 to 3000  $\text{cm}^{-1}$ , which is of the same order as the frequencies themselves. Bending frequencies involving hydrogen are often qualitatively incorrect. The excessive localization of the nuclear wave function affects not only the frequencies but also the geometries, isotopic effects, and tunneling splittings [55].

The lack of electron-PCP correlation in the product wave function leads to the unphysical localization of the nuclear wave function.

Electron-electron correlation can be included using traditional electronic structure theory methods. However, incorporating electron-PCP correlation into the wave function is more challenging due to the attractive Coulomb interaction between them. Unfortunately, for most applications, the NEO-MP2 and NEO-MCSCF methods do not provide sufficient electron-PCP correlation to overcome the localization problem. Additionally, recovering this correlation by increasing the order of perturbation theory or the orbital active space converges very slowly [56].

Providing a deeper understanding of not only electron-nucleus correlation (which is often equivalent to electron-proton correlation) but also the more general case of electron-PCP correlation with arbitrary mass is the motivation behind the present study. Based on this, the main objective of this dissertation can be summarized in one phrase: dissecting electron-PCP correlation by introducing a simple model that allows for exact solutions.

To simulate the environment of exotic molecules, we've aimed to build a theoretical laboratory using a simple model. This laboratory features an exotic hydrogen-like atom trapped in the potential well of a harmonic oscillator, with different force constants for the electron and the PCP with arbitrary mass. We were inspired by a similar model used years ago for the analytical examination of electron-electron correlation, namely the harmonium or Hooke's atom, which consists of two electrons trapped in the potential of a harmonic oscillator. Accordingly, we named our model "Exotic Harmonium," referring to a harmonium with exotic particles.

The EHM, as it only involves electron-PCP correlation, is essentially the simplest system in which this type of correlation can be studied. By adjusting the oscillator field frequencies to match real

chemical environments, we can effectively simulate the effects of molecular environments within this model. Additionally, manipulating the field frequencies and the masses of the PCPs allows us to examine a wide range of systems and correlation effects within them. For instance, selecting very high frequencies can simulate environments with extremely high pressure, such as metallic hydrogen, and gradually changing the mass of the PCP can provide interesting information, such as the approximate boundary of the system's adiabatic transition.

In the case of the harmonium model, a quasi-analytical solution for the ground state wave function can be obtained [79]. However, our calculations show that using the same strategy for Exotic Harmonium only yields the wave functions of excited states. For this reason, this study employs the variational method for closed-form solutions. The initial idea involves proposing a simple yet efficient variational wave function, fitting the variational parameters, and extracting an accurate and compact analytical wave function. The parameters of this model include the mass of the PCP and the harmonic oscillator field frequency, covering a wide range of exotic particles (Section 1-5) and both weak and strong field frequencies.

Such a wave function can be used for the analytical calculation of any property concerning this system within different frameworks. In this dissertation, after developing and examining various aspects of the EHM, we also explore its more important applications, such as extracting accurate electron-PCP correlation potentials within the two-component density functional theory (TC-DFT) framework, testing the existing correlation functionals in the related literature within the TC-DFT framework, and computing the exact non-adiabatic energy of systems. It is hoped that this model and its derived results will contribute to the development of a novel first-principles

method for accurately estimating electron-PCP correlation energy in the future. The simplicity of this model allows for the exact solution of the resulting mathematical expressions, embodying physics at its finest.

## 2 Development of the Exotic Harmonium Model

Since the EHM was inspired by the harmonium model, the harmonium model will first be explained. In subsequent sections, the developed model and the results obtained from it will be described.

### 2.1 Harmonium Model

The harmonium model, as we know it today, which involves two electrons repelling each other through Coulombic forces and trapped in the field or well of a harmonic oscillator, was first introduced by Kestner and Sinanoglu in 1962 [80]. At the time of its introduction, there was no exact solution for two-electron systems exhibiting electron correlation, and the best solution available was the explicitly correlated variational wavefunction proposed by



Hylleraas in 1928 [81], [82]. As a result, the harmonium model, for which an exact numerical solution could be obtained, garnered significant attention. The paper begins with an introduction that highlights the significance of the proposed model.

The Hamiltonian of the simplest harmonium model is defined as follows:

$$\begin{aligned}\hat{H}(\mathbf{r}_1, \mathbf{r}_2) &= -\frac{1}{2}(\nabla_1^2 + \nabla_2^2) + \frac{1}{|\mathbf{r}_1 - \mathbf{r}_2|} + \frac{1}{2}k(\mathbf{r}_1^2 + \mathbf{r}_2^2) \\ &= -\frac{1}{2}(\nabla_1^2 + \nabla_2^2) + \frac{1}{|\mathbf{r}_1 - \mathbf{r}_2|} + \frac{1}{2}\omega^2(\mathbf{r}_1^2 + \mathbf{r}_2^2)\end{aligned}\tag{2.1}$$

where  $k$  is the force constant of the oscillator and is related to the oscillator frequency  $\omega$  by the following relation:

$$k = m\omega^2\tag{2.2}$$

where  $m$  is the mass of the particle. Additionally,  $\mathbf{r}_1$  and  $\mathbf{r}_2$  are defined relative to the center of the oscillator well. In general, the Hamiltonian of a bound two-electron system is given by:

$$H(\mathbf{r}_1, \mathbf{r}_2) = -\frac{1}{2}(\nabla_1^2 + \nabla_2^2) + V + W_1 + W_2\tag{2.3}$$

where  $V$  is the Coulombic repulsion potential between the two electrons ( $\frac{1}{|\mathbf{r}_1 - \mathbf{r}_2|}$ ).  $W_1$  and  $W_2$  are the external potentials for the first and second electrons, respectively, with  $\mathbf{r}_1$  and  $\mathbf{r}_2$  defined relative to the centers of these external potentials. The most natural form of these external potentials, as they occur in atoms and molecules, is their sum as electron-nucleus Coulombic interactions, that is:

$$W_1 + W_2 = -\sum_{i=1}^2 \sum_{A=1}^{N_c} \frac{Z_A}{|\mathbf{r}_i - \mathbf{r}_A|}\tag{2.4}$$

where  $Z_A$  is the atomic number of nucleus A. However, as mentioned above, such a system (the simplest case of which is equivalent to a helium atom) cannot be solved analytically. Another possibility is to replace the electron-nucleus interaction with a different potential. One option is to substitute this potential with that of an isotropic harmonic oscillator:

$$W_1 + W_2 = \frac{1}{2}k(\mathbf{r}_1^2 + \mathbf{r}_2^2) = \frac{1}{2}\omega^2(\mathbf{r}_1^2 + \mathbf{r}_2^2) \quad 2.5$$

Harmonium is the simplest model that not only has an exact numerical solution but also retains electron correlation. In the three decades following the proposal of the harmonium model, it was not only examined from various aspects but eventually also had a quasi-analytical solution found for it. In this regard, in 1986, Laufer and Krieger used the harmonium model to test functionals designed within the framework of density functional theory [83]. Subsequently, in 1990, Samanta and Ghosh obtained an analytical solution for the modified harmonium model by adding a linear interaction term to the Hamiltonian (2-1) [84], [85]. However, in 1993, Taut succeeded in finding an analytical solution for the harmonium model for certain frequencies of the oscillator field [79], thereby categorizing this model under quasi-exactly solvable models in quantum mechanics [86]. After separating the center of mass (with mathematical details provided in the following section), Taut started from a general power series and obtained the ground state wave function of the internal motion (without the normalization constant) for specific oscillator frequencies ( $\omega = \frac{1}{2(l+1)}$ ) as follows:

$$u(r) = r^{l+1}e^{-r^2/8(l+1)} \left[ 1 + \frac{r}{2(l+1)} \right] \quad 2.6$$

and obtained its energy as follows:

$$\varepsilon = \frac{(2l + 5)\omega}{2} \tag{2.7}$$

where  $l$  is the orbital quantum number ( $l = 0, 1, 2, \dots$ ).

After presenting this quasi-analytical solution, numerous studies have been conducted by many researchers, including Karwowski and others, on the Harmonium model and its solutions [87]–[92]. The model has also been extended to 3- to 6-particle systems [93]. Additionally, this model resembles an important class of quantum systems known as confined atoms [94], [95], and thus, it can also be used as a simple model for quantum dots, which are one of the practical quantum technologies [96].

## 2.2 Analytical Solution of the EHM

We initially attempted to obtain an analytical solution for the EHM using the methods of Karwowski [87] and Taut [79] for two particles with arbitrary masses and an attractive Coulombic potential (as opposed to the repulsive Coulombic potential of electrons in the Harmonium). Trapping such a system in the potential of a harmonic oscillator leads to the quantization of the center-of-mass motion and eliminates the issues related to subtracting the center Hamiltonian, as mentioned in the NOMO method discussed in Chapter 1. In other words, the harmonic oscillator trap prevents the emergence of a continuous energy spectrum.

However, assuming variable masses and changing the type of interaction has implications that result in significant differences from the harmonium model, which will be discussed later. As mentioned in Section 1-8, using conventional approaches for the analytical solution of harmonium for this new model, which is a two-component system trapped in a dual harmonic oscillator well, does not yield an analytical solution for the ground state.

Instead, it results in the excited states of the system (the computational details of this analytical solution are provided in Section 2-2-2).

The Hamiltonian of two interacting particles trapped in the potential of a harmonic oscillator, in its most general form, is given as follows:

$$H(\mathbf{r}_1, \mathbf{r}_2) = \frac{1}{2m_1} \nabla^2 + \frac{1}{2m_2} \nabla^2 + \frac{1}{2} k_1 r_1^2 + \frac{1}{2} k_2 r_2^2 + V \quad 2.8$$

where  $m_1$  and  $m_2$  represent the masses of the first and second particles, respectively. The potential  $V$  specifies the type of interaction between the two particles, as it can take various forms. The most well-known type is the Coulombic potential, which is represented as follows:

$$V = \frac{\zeta}{|\mathbf{r}_1 - \mathbf{r}_2|} \quad \zeta = \pm 1 \quad 2.9$$

where the sign of  $\zeta$  indicates whether the interaction between the two particles is repulsive or attractive, respectively. The Hamiltonian (2-8) for electrons reduces to the Hamiltonian (2-1), which is the main Hamiltonian of the harmonium.

By introducing the center of mass and relative coordinates as follows:

$$\mathbf{R} = \frac{(m_1 \mathbf{r}_1 + m_2 \mathbf{r}_2)}{(m_1 + m_2)} \quad 2.10$$

$$\mathbf{r} = |\mathbf{r}_1 - \mathbf{r}_2| \quad 2.11$$

The initial coordinates are expressed in terms of these two new coordinates as follows:

$$\mathbf{r}_1 = \mathbf{R} - \frac{m_2}{(m_1 + m_2)} \mathbf{r} \quad 2.12$$

$$\mathbf{r}_2 = \mathbf{R} + \frac{m_1}{(m_1 + m_2)} \mathbf{r} \quad 2.13$$

With this change of variables, the Hamiltonian is separated into two distinct parts, expressed as the sum of the center of mass (COM) and the relative motion components:

$$H(\mathbf{r}_1, \mathbf{r}_2) = H_R(\mathbf{R}) + H_r(\mathbf{r}) \quad 2.14$$

$$H_R(\mathbf{R}) = -\frac{1}{2M} \nabla_R^2 + \frac{M}{2} \omega^2 \mathbf{R}^2 \quad 2.15$$

$$H_r(\mathbf{r}) = -\frac{1}{2\mu} \nabla_r^2 + \frac{\mu}{2} \omega^2 \mathbf{r}^2 + V \quad 2.16$$

where  $M = m_1 + m_2$  and  $\mu = m_1 m_2 / M$ . This also leads to the complete decoupling of the Hamiltonian or energy spectrum into the center-of-mass and relative motion parts. We can analyze these two parts separately:

$$H_R(\mathbf{R}) \eta_{klm}(\mathbf{R}) = E_{kl} \eta_{klm}(\mathbf{R}) \quad 2.17$$

$$H_r(\mathbf{r}) \chi_{k'l'm'}(\mathbf{r}) = E_{k'l'} \chi_{k'l'm'}(\mathbf{r}) \quad 2.18$$

In equation (2-17), the function  $\eta_{klm}(\mathbf{R})$  consists of radial and angular parts as follows:

$$\eta_{klm}(\mathbf{R}) = N_{kl} \tau_{kl}(\mathbf{R}) Y_{lm}(\theta, \phi) \quad 2.19$$

where  $N$  is the normalization constant,  $(l, m)$  are the angular momentum quantum numbers, and  $Y_{lm}(\theta, \phi)$  are the spherical harmonics. Therefore, the energy of this component is equal to that of a three-dimensional spherical harmonic oscillator:

$$E_{kl} = \omega(2k + l + \frac{3}{2}) \quad 2.20$$

For  $\chi_{k'l'm'}(\mathbf{r})$  in equation (2-17), we have:

$$\chi_{k'l'm'}(\mathbf{r}) = N_{k'l'} \sigma_{k'l'}(\mathbf{r}) Y_{l'm'}(\theta, \phi) \quad 2.21$$

Using spherical coordinates to separate  $\mathbf{r}$  from the angular variables, we can write:

$$\Phi(\mathbf{r})_{nlm} = \frac{1}{r} \phi(\mathbf{r})_{nl} Y_{lm}(\mathbf{r}) \quad 2.22$$

Once again, the  $Y_{lm}$  are the spherical harmonics, and the  $\phi(\mathbf{r})_{nl}$  are determined by the following radial Schrödinger equation:

$$\left[ -\frac{1}{2\mu} \frac{d^2}{dr^2} + \frac{l(l+1)}{2\mu r^2} + \frac{\mu\omega^2}{2} r^2 + \frac{\zeta}{r} - E \right] \phi(\mathbf{r})_{nl} = 0 \quad 2.23$$

The exact wave function of the entire system is written as the product of the wave functions of the two parts, center of mass and relative motion:

$$\Xi(\mathbf{R}, \mathbf{r}) = \eta_{klm}(\mathbf{R}) \chi_{k'l'm'}(\mathbf{r}) \quad 2.24$$

And the total energy is equal to the sum of the energies of these two parts:

$$E_{klk'l'} = E_{kl} + E_{k'l'} \quad 2.25$$

Equation (2-24) shows that, after defining coordinates (2-10) and (2-11), the wave function of the system will be the product of two functions, one of which depends only on the relative coordinates and the other only on the center of mass coordinates. In such a coordinate system, we will be dealing with pseudo particles (pseudo particle  $\mu$  and pseudo particle  $M$ ).

### 2.2.1 Separability of the Hamiltonian

In general, separating the Hamiltonian of a trapped or confined two-particle system, like equation (2-3), into center-of-mass and relative motion components, as in equation (2-14), is only possible for specific potentials, such as the harmonic oscillator described by equation (2-8), and with the separability condition being satisfied. To obtain this condition, we substitute equations (2-12) and (2-13) into equation (2-8), resulting in:

$$W(\mathbf{r}_1, \mathbf{r}_2) = \frac{R^2}{2}(k_1 + k_2) + \frac{r^2}{2} \left( \frac{k_1 m_2 + k_2 m_1}{M} \right) - k_1 \left( \frac{m_2}{M} R r \right) + k_2 \left( \frac{m_1}{M} R r \right) \quad 2.26$$

For  $W$  to be separable, the sum of the third and fourth terms (the mixed terms) must be zero. As a result, the separability condition is obtained as follows:

$$\frac{k_1}{k_2} = \frac{m_1}{m_2} \quad 2.27$$

For the harmonium model, this ratio is equal to one, that is:

$$\frac{k_1}{k_2} = \frac{m_1}{m_2} = 1 \quad 2.28$$

However, in a model where the masses of the two particles are different, according to equation (2-2) and to satisfy condition (2-27), it is necessary for the following equations to hold:

$$\frac{k_1}{k_2} = \frac{m_1}{m_2} \quad \& \quad \frac{\omega_1^2}{\omega_2^2} = 1 \Rightarrow \omega_1^2 = \omega_2^2 = \omega \quad 2.29$$

$$\frac{1}{2} k_1 \mathbf{r}_1^2 + \frac{1}{2} k_2 \mathbf{r}_2^2 = \frac{1}{2} \omega^2 (m_1 \mathbf{r}_1^2 + m_2 \mathbf{r}_2^2) \quad 2.30$$

On the other hand, if we initially consider the force constant in equation (2-8) to be the same for both particles, according to equation (2-27), we conclude that the masses of the two particles must also be equal. Therefore, both methods lead us to the same result (2-29).

The above explanations clearly show that changing the masses of the particles in the harmonium model results in the creation of two harmonic oscillator traps with different force constants (proportional to the mass of each particle). In this case, although the field frequencies of the two oscillators are the same, the particles experience different harmonic potentials from the traps.

### 2.2.2 Analytical Solution

The above model, due to the variability in particle masses, can be applied to a diverse range of systems. Several specific systems are listed in the table below:

Table 2-1: Examples of Various Systems with Harmonic Oscillator Potentials

System Type	$\mu$	$\varsigma$
Harmonium	1/2	1
Positronium	1/2	-1
Hydrogen-like atom (with infinite nuclear mass)	1	-Z
Hydrogen-like atom (with finite nuclear mass)	$\frac{m_n}{1 + m_n}$	-Z

In this model, there are two parameters that allow us to change the system's state: the strength of the external field by  $\omega$  and the interaction



strength between the two particles by  $\varsigma$ . In other words, this model has two limits: strong correlation and weak correlation. When  $\omega \rightarrow \infty$ , we have a system with strong oscillator confinement where the Coulomb interaction is weak in comparison, and the particle correlation is also weak in this limit. Conversely, when  $\omega \rightarrow 0$ , we are in the strong correlation limit.

To begin the analytical approach (based on Karwowski's approach [87]), we first substitute the following equation into equation (2-23), leading us to the next equation:

$$x = \sqrt{2\mu\omega} r \quad 2.31$$

$$\left[ -\frac{d^2}{dx^2} + \frac{l(l+1)}{x^2} + \frac{x^2}{4} + \frac{s}{x} - \frac{E}{\omega} \right] \phi(x) = 0 \quad 2.32$$

where

$$s = \varsigma \sqrt{\frac{2\mu}{\omega}} \quad 2.33$$

We then obtain the asymptotic solutions (2-32) in the two limits  $r \rightarrow 0$  and  $r \rightarrow \infty$ . Thus, for the limit  $r \rightarrow 0$  (or equivalently  $x \rightarrow 0$ ), we have:

$$\begin{aligned} \lim_{x \rightarrow 0} \left( \left[ -\frac{d^2}{dx^2} + \frac{l(l+1)}{x^2} + \frac{x^2}{4} + \frac{s}{x} - \frac{E}{\omega} \right] \phi(x) = 0 \right) \\ = \left( \left[ -\frac{d^2}{dx^2} + \frac{l(l+1)}{x^2} - \frac{E}{\omega} \right] \phi(x) = 0 \right) \\ = \left( -\phi''(x) + \frac{l(l+1)}{x^2} \phi(x) = \frac{E}{\omega} \phi(x) \right) \end{aligned} \quad 2.34$$

which has the following solution:

$$\phi(x) \sim x^{l+1} \quad 2.35$$

On the other hand, for the limit  $r \rightarrow \infty$  (or equivalently  $x \rightarrow \infty$ ), we have:

$$\begin{aligned}
\lim_{x \rightarrow \infty} \left( \left[ -\frac{d^2}{dx^2} + \frac{l(l+1)}{x^2} + \frac{x^2}{4} + \frac{s}{x} - \frac{E}{\omega} \right] \phi(x) = 0 \right) \\
= \left( \left[ -\frac{d^2}{dx^2} + \frac{x^2}{4} - \frac{E}{\omega} \right] \phi(x) = 0 \right) \\
= \left( -\phi''(x) + \frac{x^2}{4} \phi(x) = \frac{E}{\omega} \phi(x) \right)
\end{aligned} \tag{2.36}$$

which results in the one-dimensional harmonic oscillator equation, and we know its solution is given by:

$$\phi(x) \sim e^{-x^2/4} \tag{2.37}$$

As a result, the general solution can be written as the product of these two limits, with the addition of an arbitrary polynomial such as  $P(x)$ , as follows:

$$\phi(x) = x^{l+1} e^{-x^2/4} P(x) \tag{2.38}$$

The first and second derivatives of this wave function are obtained as follows:

$$\begin{aligned}
\phi'(r)_{nl} &= (l+1)x^l e^{-x^2/4} P(x) - \frac{1}{2} x^{l+2} e^{-\frac{x^2}{4}} P(x) \\
&\quad + x^{l+1} e^{-\frac{x^2}{4}} P'(x)
\end{aligned} \tag{2.39}$$

$$\tag{2.40}$$

$$\begin{aligned}
\Phi''(r)_{nl} = & l(l+1)x^{l-1}e^{-x^2/4}P(x) - \frac{1}{2}(l+1)x^{l+1}e^{-x^2/4}P(x) \\
& + (l+1)x^le^{-x^2/4}P'(x) \\
& - \frac{1}{2}(l+2)x^{l+1}e^{-x^2/4}P(x) + \frac{1}{4}x^{l+3}e^{-x^2/4}P(x) \\
& - \frac{1}{2}x^{l+2}e^{-x^2/4}P'(x) + (l+1)x^le^{-x^2/4}P'(x) \\
& - \frac{1}{2}x^{l+2}e^{-x^2/4}P'(x) + x^{l+1}e^{-x^2/4}P''(x)
\end{aligned}$$

By substituting the two above equations into (2-32), we obtain:

$$\begin{aligned}
& -l(l+1)x^{l-1}e^{-x^2/4}P(x) + \frac{1}{2}(l+1)x^{l+1}e^{-x^2/4}P(x) \\
& - (l+1)x^le^{-x^2/4}P'(x) \\
& + \frac{1}{2}(l+2)x^{l+1}e^{-x^2/4}P(x) - \frac{1}{4}x^{l+3}e^{-x^2/4}P(x) \\
& + \frac{1}{2}x^{l+2}e^{-x^2/4}P'(x) - (l+1)x^le^{-x^2/4}P'(x) \tag{2.41} \\
& + \frac{1}{2}x^{l+2}e^{-x^2/4}P'(x) - x^{l+1}e^{-x^2/4}P''(x) \\
& + l(l+1)x^{l-1}e^{-x^2/4}P(x) + s x^le^{-x^2/4}P(x) \\
& + \frac{1}{4}x^{l+3}e^{-x^2/4}P(x) - \frac{E}{\omega}x^{l+1}e^{-x^2/4}P(x) = 0
\end{aligned}$$

After combining the terms of equal degree  $P(x)$  and then eliminating  $e^{-x^2/4}$  terms, we obtain:

$$\begin{aligned}
& -x^{l+1} P''(x) + \left[ \frac{1}{2} x^{l+2} - (l+1)x^l - (l+1)x^l \right. \\
& \quad \left. + \frac{1}{2} x^{l+2} \right] P'(x) \\
& + \left[ l(l+1)x^{l-1} + s x^l + \frac{1}{4} x^{l+3} - \frac{E}{\omega} x^{l+1} \right. \\
& \quad - l(l+1)x^{l-1} + \frac{1}{2} (l+1)x^{l+1} + \frac{1}{2} (l+2)x^{l+1} \\
& \quad \left. - \frac{1}{4} x^{l+3} \right] P(x) = 0
\end{aligned} \tag{2.42}$$

By multiplying the above expression by  $-x^{-(l+1)}$ , we arrive at the following expression:

$$P''(x) + \left[ \frac{2(l+1)}{x} - x \right] P'(x) + \left[ \frac{E}{\omega} - \frac{s}{x} - l - \frac{3}{2} \right] P(x) = 0 \tag{2.43}$$

$$\left[ \frac{d^2}{dx^2} + \left( \frac{2(l+1)}{x} - x \right) \frac{d}{dx} + \left( \varepsilon - \frac{s}{x} \right) \right] P(x) = 0 \tag{2.44}$$

where

$$\varepsilon = \frac{E}{\omega} - l - \frac{3}{2} \tag{2.45}$$

In equation (2-44), we can identify three terms with different degrees of homogeneity:

$$\Omega_{-2} = \frac{d^2}{dx^2} + \frac{2(l+1)}{x} \frac{d}{dx}, \quad \Omega_{-1} = -\frac{s}{x}, \quad \Omega_0 = -x \frac{d}{dx} + \varepsilon \tag{2.46}$$

$P(x)$  can be defined as a polynomial:

$$P(x) = \sum_{m=0}^{\infty} a_m x^m \tag{2.47}$$

Since we are interested in solutions with the expansion (2-47) and truncated at  $m = p$ , we can write the following conditions for  $a_m$ :

$$a_m \begin{cases} \neq 0 & 0 \leq m \leq p \\ = 0 & m > p \text{ or } m < 0 \end{cases} \quad 2.48$$

Using equations (2-46) and (2-47), we have:

$$P'(x) = \sum_{m=0}^{\infty} m a_m x^{m-1} \quad 2.49$$

$$P''(x) = \sum_{m=0}^{\infty} m(m-1) a_m x^{m-2} \quad 2.50$$

To transform equation (2-44) into a single sum with the same power of  $x$ , we use the following expressions:

$$\begin{aligned} \Omega_{-2} x^n &= n(n+2l+1) x^{n-2} \text{ , } \Omega_{-1} x^{n-1} \\ &= -s x^{n-2} \text{ , } \Omega_0 x^{n-2} = (\mathcal{E} - n + 2) \end{aligned} \quad 2.51$$

$$[\Omega_{-2} + \Omega_{-1} + \Omega_0]P(x) = 0 \quad 2.52$$

After substituting and combining the terms, we arrive at a single sum as follows:

$$\sum_{m=0}^{\infty} [m(m+2l+1)a_m - s a_{m-1} + (\mathcal{E} - m + 2)a_{m-2}] x^{m-2} = 0 \quad 2.53$$

The coefficients of each power of  $x$  must be equal to zero, therefore we have:

$$\begin{aligned} m = 0 & \quad 0 \\ m = 1 & \quad (2l+2)a_1 - s a_0 = 0 \\ m = 2 & \quad 2(2l+3)a_2 - s a_1 + \mathcal{E} a_0 = 0 \end{aligned} \quad 2.54$$

$$m = 3 \quad 3(2l + 4)a_3 - sa_2 + (\mathcal{E} - 1)a_1 = 0$$

...

$$m = p \quad p(2l + p + 1)a_p - sa_{p-1} + (\mathcal{E} - p + 2)a_{p-2} = 0$$

$$m = p + 1 \quad -sa_p + (\mathcal{E} - p + 1)a_{p-1} = 0$$

$$m = p + 2 \quad (\mathcal{E} - p)a_p = 0$$

Since  $a_p \neq 0$ , the last term of the above equations shows that  $\mathcal{E} = p$ , which, as a result, gives us the following according to equation (2-45):

$$E = \omega \left( p + l + \frac{3}{2} \right) \quad 2.55$$

Therefore, the determinant of the coefficients is given by:

$$\begin{vmatrix} -s & (2l + 2) & 0 & 0 & \dots & 0 \\ p & -s & 2(2l + 3) & 0 & \dots & 0 \\ 0 & (p - 1) & -s & 3(2l + 4) & \dots & 0 \\ \vdots & \vdots & \vdots & \vdots & \ddots & p(2l + p + 1) \\ 0 & 0 & 0 & 0 & 2 & -s \end{vmatrix} \quad 2.56$$

A non-trivial solution to equation (2-53) exists if the above determinant equals zero. We can check this condition for different values of  $p$  and determine the dependence of energy on mass. For  $p = 1$ , we have:

$$\mathcal{E} = 1, \quad a_1 = \frac{s a_0}{2l + 2}, \quad a_2 = a_3 = \dots = 0 \quad 2.57$$

$$E = \omega \left( l + \frac{5}{2} \right) \quad 2.58$$

$$\begin{vmatrix} -s & (2l + 2) \\ 1 & -s \end{vmatrix} = 0 \quad 2.59$$

$$s^2 = 2l + 2$$

Using equations (2-33) and (2-59), we obtain:

$$\omega = \frac{\mu\zeta^2}{l+1} \Rightarrow E = \mu\zeta^2 \frac{2l+5}{2l+2} \quad 2.60$$

$$P(x) = a_0 + a_1x \quad 2.61$$

In conclusion, considering equations (2-31), (2-33), and (2-57), we arrive at the following result:

$$P(x) = a_0 + \frac{a_0\sqrt{2\mu\omega}r}{2(l+1)}\zeta\sqrt{\frac{2\mu}{\omega}} = a_0\left(1 + \frac{\zeta\mu}{l+1}r\right) \quad 2.62$$

For  $p = 2$ , we have:

$$\mathcal{E} = 2 \text{ , } a_3 = a_4 = \dots = 0 \quad 2.63$$

$$\begin{vmatrix} -s & (2l+2) & 0 \\ 2 & -s & 2(2l+3) \\ 0 & (\mathcal{E}-1) & -s \end{vmatrix} = 0 \quad 2.64$$

$$s^2 = 8l+10 \Rightarrow \omega = \frac{\mu\zeta^2}{4l+5} \Rightarrow E = \mu\zeta^2 \frac{2l+7}{8l+10} \quad 2.65$$

Again, according to equation (2-47), we have:

$$P(x) = a_0 + a_1x + a_2x^2 \quad 2.66$$

And for  $P = 2$ :

$$a_1 = \frac{s a_0}{2(l+1)} \text{ , } a_2 = \frac{a_1}{s} = \frac{a_0}{2(l+1)} \quad 2.67$$

Thus, considering equations (2-31) and (2-33), we have:

$$\begin{aligned}
P(r) &= a_0 \left( 1 + \frac{sx}{2(l+1)} + \frac{x^2}{2(l+1)} \right) \\
&= a_0 \left( 1 + \frac{\mu\varsigma}{l+1}r + \frac{\mu^2\varsigma^2}{(l+1)(4l+5)}r^2 \right)
\end{aligned}
\tag{2.68}$$

The two obtained solutions, namely equations (2-62) and (2-68), are not the ground state for the attractive system ( $\varsigma = -1$ ), and there are two reasons to prove this, one of which is mathematical and the other, which is more important, is of a physical nature.

The mathematical reason is that when  $\varsigma$  is negative, the right side of these equations has positive roots, and as a result,  $P(r)$  will have nodes. Since the creation of nodes depends on having positive roots, equations (2-62) and (2-68) with negative  $\varsigma$  will have nodes and therefore cannot describe the ground state.

The physical reason is that the Karwowski approach creates a fundamental symmetry in the problem. Equations (2-60) and (2-65), as well as equation (30) in Karwowski's original paper for Harmonium [87], show that the energy is proportional to  $\varsigma^2$ . This result means that regardless of the type of interaction (repulsive or attractive), the energy value is the same, whereas we expect the ground state energies of systems with these two types of interactions to differ. Using a perturbative approach, it is easy to prove the validity of such a claim: If we consider a harmonic oscillator as the unperturbed state of the system and the Coulomb interaction as the perturbation, we can easily prove that the first-order energy of the perturbed system with attractive interaction is lower than that of the same system with repulsive interaction (in both attractive and repulsive cases, the first-order perturbation value is the same, but its sign is positive and negative, respectively, and as a result, the same value is added to and subtracted from



the unperturbed system's energy, respectively). Given that we know the energy of the exotic harmonium for any given level is lower than that of the harmonium, we conclude that using the Karwowski approach, we obtain two isoenergetic states, namely the ground state of the harmonium and the first excited state of the exotic harmonium (equation 2-63).

## 2.3 EHM

As shown in the previous section, the analytical approach used for harmonium, with changing particle mass, no longer results in the ground state wave function; therefore, we need to explore other methods. Ultimately, the variational method was used to obtain the ground state energy of the system.

In this section, the developed model in this thesis, i.e., a two-component system trapped in a double-well of harmonic oscillators, is examined using the variational method. It is worth mentioning that, unlike equations (2-8) and (2-9) which include both types of interactions, this model only considers attractive interactions, which aligns with the primary goal of this thesis, namely developing a model for investigating non-BO molecular systems. Since all numerical computations in this thesis consider one electron and one PCP (with an arbitrary mass), subscripts (superscripts)  $e$  for the negatively charged particle and  $p$  for the PCP are used in the notation of equations and relations.

The total Hamiltonian (in atomic units) for an attractive two-component system trapped in a double-well of harmonic oscillators is as follows:

$$H(\mathbf{r}_e, \mathbf{r}_p) = -\frac{1}{2m_e} \nabla_e^2 - \frac{1}{2m_p} \nabla_p^2 - \frac{1}{|\mathbf{r}_e - \mathbf{r}_p|} + \frac{1}{2} \omega^2 (m_e \mathbf{r}_e^2 + m_p \mathbf{r}_p^2) \quad 2.69$$

where  $\omega$  represents the common frequency of the oscillators, and the vectors  $\mathbf{r}_e$  and  $\mathbf{r}_p$  are defined with respect to the centers of the potential wells. The initial coordinates are expressed based on these two new coordinates as follows:

$$\begin{aligned}\mathbf{r}_e &= \mathbf{R} - \frac{m_p}{(m_e + m_p)} \mathbf{r} \\ \mathbf{r}_p &= \mathbf{R} + \frac{m_e}{(m_e + m_p)} \mathbf{r}\end{aligned}\tag{2.70}$$

Just like equation (2-14), using this new coordinate system, the Hamiltonian (2-69) can be written as the sum of two separate parts: the center of mass and relative motion. The difference is that here, the total mass is  $M = m_e + m_p$  and the reduced mass is  $\mu = m_e m_p / M$ .

### 2.3.1 Finding the Relative Motion Wave Function Using the Variational Method

Given that the wave function for the center of mass motion is known, we need to obtain the wave function for the relative motion in order to find the total wave function. The trial variational function was chosen to be as simple as possible while still accurately capturing the behavior of the system's exact ground state wave function. For this purpose, the following trial function was considered:

$$\chi'_{trial} \sim e^{-\mu(\alpha' r + \beta' r^2)}\tag{2.71}$$

where the first exponential term (Slater term) represents the hydrogen-like atom function and the second exponential term (Gaussian term) represents the harmonic oscillator function, with  $\alpha'$  and  $\beta'$  as the variational parameters. Although the presence of  $\mu$  linearly in the exponential terms is

necessary, due to the zeroing of the variational parameters at certain field frequencies and the resulting numerical problems,  $\mu$  is absorbed into the variational parameters  $\alpha'$  and  $\beta'$ , and the following wave function is used as the trial variational wave function in the subsequent calculations:

$$\chi_{trial} \sim e^{-\alpha r - \beta r^2} \quad 2.72$$

### 2.3.2 Examining the Asymptotic Behavior of the Trial Wave Function

Before applying the variational theorem to wave function (2-72), we need to ensure the correctness of its asymptotic behavior in both the strong and weak field limits of the harmonic oscillator. By substituting the Coulomb potential instead of  $V$  in Hamiltonian (2-16), it is evident that in the strong field limit ( $\omega \rightarrow \infty$ ), the harmonic oscillator potential energy term dominates the Coulomb interaction term, and it can be approximated by the Hamiltonian of a harmonic oscillator. In this case, the wave function should also reduce to the ground state eigenfunction of a three-dimensional harmonic oscillator (HO):

$$\phi_{HO}(r) = \left(\frac{\mu\omega}{\pi}\right)^{3/4} \exp\left(-\frac{1}{2}\mu\omega r^2\right) \quad 2.73$$

Conversely, in the weak field limit ( $\omega \rightarrow 0$ ), the Coulomb interaction term dominates, and Hamiltonian (2-16) can be approximated by the Hamiltonian of a hydrogen-like atom (HL) as follows:

$$\phi_{HL}(r) = \left(\frac{\mu^3}{\pi}\right)^{1/2} \exp(-\mu r) \quad 2.74$$

Therefore, at different field frequencies, we can observe the asymptotic behavior of the variational wave function and its similarity to the two aforementioned systems.

### 2.3.3 Other Possibilities for Variational Trial Functions

To increase accuracy, another term can be added to the exponent of wave function (2-72), which becomes zero under the limiting conditions discussed (thus ensuring the correct asymptotic behavior of the wave function) but remains non-zero at intermediate frequencies, thereby enhancing the accuracy of the wave function. As we will see, the accuracy of wave function (2-72) is very high even without introducing such a term, so adding an extra term to the wave function will not only provide minimal improvement in accuracy but will also increase computational burden and complexity of the equations. For example, when parameterizing the function with four parameters ( $-\alpha r - \beta r^2 - \gamma r^3 - \delta r^4$ ), the fourth parameter tends to zero during the optimization process, and the third parameter does not provide a significant improvement in energy.

Another proposal for the variational trial wave function could be as follows:

$$\chi''_{trial} \sim e^{-\mu \alpha'' r \beta''} \quad 2.75$$

The asymptotic behavior of this trial wave function also converges to the correct limits. In the strong oscillator field limit ( $\omega \rightarrow \infty$ ), the parameter  $\beta''$  approaches 2 and the parameter  $\alpha''$  approaches  $\frac{\omega}{2}$ , resulting in the shape of the wave function being exactly like the ground state wave function of a harmonic oscillator ( $e^{-\frac{\omega}{2}\mu r^2}$ ). In the weak oscillator field limit ( $\omega \rightarrow 0$ ), both

the parameter  $\beta''$  and the parameter  $\alpha''$  approach 1, resulting in the shape of the wave function being exactly like the ground state wave function of a hydrogen-like atom ( $e^{-\mu r}$ ). The results obtained from the optimization process of the wave function parameters (2-75) confirm this asymptotic behavior. Nevertheless, when the energy obtained from this wave function was compared with the energy obtained from wave function (2-72), it was found that the latter gives better results than the former.

### 2.3.4 Variational Theorem

According to the variational theorem, we have:

$$\frac{\int \chi^* \hat{H} \chi d\tau}{\int \chi^* \chi d\tau} = E \geq E_0 \quad 2.76$$

where  $E_0$  is the ground state energy of the system. The variational energy  $E_0$  of the two-component system is given by:

$$E = \frac{\int \chi^* \hat{T} \chi d\tau + \int \chi^* \hat{V} \chi d\tau}{\int \chi^* \chi d\tau} \quad 2.77$$

For the trial wave function (2-72), we have:

$$\begin{aligned}
\int \chi^* \hat{T} \chi d\tau &= \int_0^{2\pi} \int_0^\pi \int_0^\infty \chi^* \hat{T} \chi r^2 \sin \theta dr d\theta d\phi \\
&= 4\pi \int_0^\infty \chi^* \hat{T} \chi r^2 dr \\
&= -\frac{2\pi}{\mu} \left( \alpha^2 \int_0^\infty r^2 e^{-2\alpha r - 2\beta r^2} dr \right. \\
&\quad - 2\beta \int_0^\infty r^2 e^{-2\alpha r - 2\beta r^2} dr \\
&\quad + 4\alpha\beta \int_0^\infty r^3 e^{-2\alpha r - 2\beta r^2} dr \\
&\quad + 4\beta^2 \int_0^\infty r^4 e^{-2\alpha r - 2\beta r^2} dr \\
&\quad - 2\alpha \int_0^\infty r e^{-2\alpha r - 2\beta r^2} dr \\
&\quad \left. - 4\beta \int_0^\infty r^2 e^{-2\alpha r - 2\beta r^2} dr \right)
\end{aligned} \tag{2.78}$$

$$\begin{aligned}
\int \chi^* \hat{V} \chi d\tau &= 4\pi \left( - \int_0^\infty r e^{-2\alpha r - 2\beta r^2} dr \right. \\
&\quad \left. + \frac{1}{2} \mu \omega^2 \int_0^\infty r^4 e^{-2\alpha r - 2\beta r^2} dr \right)
\end{aligned} \tag{2.79}$$

$$\int \chi^* \chi d\tau = 4\pi \int_0^\infty r^2 e^{-2\alpha r - 2\beta r^2} dr \tag{2.80}$$

The values of the parameters  $\alpha$  and  $\beta$  are obtained using an optimization algorithm, in which the energy is optimized using the gradient and Hessian. For this purpose, the next section is dedicated to calculating the gradient and Hessian of the energy.

### 2.3.5 Calculating the Gradient and Hessian of the Energy

The gradient of the energy with respect to the variational parameters is defined as follows:

$$E_\alpha = \frac{\partial E}{\partial \alpha} \quad E_\beta = \frac{\partial E}{\partial \beta} \quad 2.81$$

Considering equation (2-76) for the variational energy, we have:

$$\begin{aligned} E_\alpha &= \frac{(\int \chi^* \hat{T} \chi d\tau)_\alpha + (\int \chi^* \hat{V} \chi d\tau)_\alpha - E(\int \chi^* \chi d\tau)_\alpha}{\int \chi^* \chi d\tau} \\ E_\beta &= \frac{(\int \chi^* \hat{T} \chi d\tau)_\beta + (\int \chi^* \hat{V} \chi d\tau)_\beta - E(\int \chi^* \chi d\tau)_\beta}{\int \chi^* \chi d\tau} \end{aligned} \quad 2.82$$

where the inner terms are obtained as follows:

$$\begin{aligned} (\int \chi^* \hat{T} \chi d\tau)_\alpha &= \frac{\partial}{\partial \alpha} \int \chi^* \hat{T} \chi d\tau \\ &= -\frac{2\pi}{\mu} \left[ -2 \int_0^\infty r e^{-2\alpha r - 2\beta r^2} dr \right. \\ &\quad + 6\alpha \int_0^\infty r^2 e^{-2\alpha r - 2\beta r^2} dr \\ &\quad - 2\alpha^2 \int_0^\infty r^3 e^{-2\alpha r - 2\beta r^2} dr \\ &\quad + 16\beta \int_0^\infty r^3 e^{-2\alpha r - 2\beta r^2} dr \\ &\quad - 8\alpha\beta \int_0^\infty r^4 e^{-2\alpha r - 2\beta r^2} dr \\ &\quad \left. - 8\beta^2 \int_0^\infty r^5 e^{-2\alpha r - 2\beta r^2} dr \right] \end{aligned} \quad 2.83$$

$$\begin{aligned}
(\int \chi^* \hat{V} \chi d\tau)_\alpha &= \frac{\partial}{\partial \alpha} \int \chi^* \hat{V} \chi d\tau \\
&= 8\pi \left( \int_0^\infty r^2 e^{-2\alpha r - 2\beta r^2} dr \right. \\
&\quad \left. - \mu\omega^2 \int_0^\infty r^5 e^{-2\alpha r - 2\beta r^2} dr \right)
\end{aligned} \tag{2.84}$$

$$(\int \chi^* \chi d\tau)_\alpha = \frac{\partial}{\partial \alpha} \int \chi^* \chi d\tau = -8\pi \int_0^\infty r^3 e^{-2\alpha r - 2\beta r^2} dr \tag{2.85}$$

$$\begin{aligned}
(\int \chi^* \hat{T} \chi d\tau)_\beta &= \frac{\partial}{\partial \beta} \int \chi^* \hat{T} \chi d\tau \\
&= -\frac{2\pi}{\mu} \left[ -6 \int_0^\infty r^2 e^{-2\alpha r - 2\beta r^2} dr \right. \\
&\quad + 8\alpha \int_0^\infty r^3 e^{-2\alpha r - 2\beta r^2} dr \\
&\quad - 2\alpha^2 \int_0^\infty r^4 e^{-2\alpha r - 2\beta r^2} dr \\
&\quad + 20\beta \int_0^\infty r^4 e^{-2\alpha r - 2\beta r^2} dr \\
&\quad - 8\alpha\beta \int_0^\infty r^5 e^{-2\alpha r - 2\beta r^2} dr \\
&\quad \left. - 8\beta^2 \int_0^\infty r^6 e^{-2\alpha r - 2\beta r^2} dr \right]
\end{aligned} \tag{2.86}$$

$$\begin{aligned}
(\int \chi^* \hat{V} \chi d\tau)_\beta &= \frac{\partial}{\partial \beta} \int \chi^* \hat{V} \chi d\tau \\
&= 8\pi \left( \int_0^\infty r^3 e^{-2\alpha r - 2\beta r^2} dr \right. \\
&\quad \left. - \mu\omega^2 \int_0^\infty r^6 e^{-2\alpha r - 2\beta r^2} dr \right)
\end{aligned} \tag{2.87}$$

$$(\int \chi^* \chi d\tau)_\beta = \frac{\partial}{\partial \beta} \int \chi^* \chi d\tau = -8\pi \int_0^\infty r^4 e^{-2\alpha r - 2\beta r^2} dr \tag{2.88}$$

The Hessian matrix of the energy is also defined as follows:



$$\begin{bmatrix} E_{\alpha^2} & E_{\alpha\beta} \\ E_{\beta\alpha} & E_{\beta^2} \end{bmatrix} \quad 2.89$$

where the elements of this matrix, according to the variational energy relation, are as follows:

$$\begin{aligned} E_{\alpha^2} &= \frac{\partial^2 E}{\partial \alpha^2}, & E_{\beta^2} &= \frac{\partial^2 E}{\partial \beta^2}, & E_{\alpha\beta} &= \frac{\partial^2 E}{\partial \alpha \partial \beta}, & E_{\beta\alpha} \\ &= \frac{\partial^2 E}{\partial \beta \partial \alpha} \end{aligned} \quad 2.90$$

$$\begin{aligned} E_{\alpha^2} &= \frac{(\int \chi^* \hat{T} \chi d\tau)_{\alpha^2} + (\int \chi^* \hat{V} \chi d\tau)_{\alpha^2} - E_{\alpha}(\int \chi^* \chi d\tau)_{\alpha} - E_{\alpha}(\int \chi^* \chi d\tau)_{\alpha}}{\int \chi^* \chi d\tau} \\ E_{\beta^2} &= \frac{(\int \chi^* \hat{T} \chi d\tau)_{\beta^2} + (\int \chi^* \hat{V} \chi d\tau)_{\beta^2} - E_{\beta}(\int \chi^* \chi d\tau)_{\beta} - E_{\beta}(\int \chi^* \chi d\tau)_{\beta}}{\int \chi^* \chi d\tau} \quad 2. \\ E_{\alpha\beta} &= \frac{(\int \chi^* \hat{T} \chi d\tau)_{\alpha\beta} + (\int \chi^* \hat{V} \chi d\tau)_{\alpha\beta} - E_{\alpha}(\int \chi^* \chi d\tau)_{\beta} - E_{\beta}(\int \chi^* \chi d\tau)_{\alpha}}{\int \chi^* \chi d\tau} \quad 91 \\ E_{\beta\alpha} &= \frac{(\int \chi^* \hat{T} \chi d\tau)_{\beta\alpha} + (\int \chi^* \hat{V} \chi d\tau)_{\beta\alpha} - E_{\beta}(\int \chi^* \chi d\tau)_{\alpha} - E_{\alpha}(\int \chi^* \chi d\tau)_{\beta}}{\int \chi^* \chi d\tau} \end{aligned}$$

The inner terms of equation (2-91) are obtained as follows:

$$\begin{aligned}
(\int \chi^* \hat{T} \chi d\tau)_{\alpha^2} &= \frac{\partial}{\partial \alpha} (\int \chi^* \hat{T} \chi d\tau)_{\alpha} \\
&= -\frac{2\pi}{\mu} \left[ 10 \int_0^{\infty} r^2 e^{-2\alpha r - 2\beta r^2} dr \right. \\
&\quad - 16\alpha \int_0^{\infty} r^3 e^{-2\alpha r - 2\beta r^2} dr \\
&\quad + 4\alpha^2 \int_0^{\infty} r^4 e^{-2\alpha r - 2\beta r^2} dr \\
&\quad - 40\beta \int_0^{\infty} r^4 e^{-2\alpha r - 2\beta r^2} dr \\
&\quad + 16\alpha\beta \int_0^{\infty} r^5 e^{-2\alpha r - 2\beta r^2} dr \\
&\quad \left. + 16\beta^2 \int_0^{\infty} r^6 e^{-2\alpha r - 2\beta r^2} dr \right]
\end{aligned} \tag{2.92}$$

$$\begin{aligned}
(\int \chi^* \hat{V} \chi d\tau)_{\alpha^2} &= \frac{\partial}{\partial \alpha} (\int \chi^* \hat{V} \chi d\tau)_{\alpha} \\
&= -16\pi \left( \int_0^{\infty} r^3 e^{-2\alpha r - 2\beta r^2} dr \right. \\
&\quad \left. + 2\mu\omega^2 \int_0^{\infty} r^6 e^{-2\alpha r - 2\beta r^2} dr \right)
\end{aligned} \tag{2.93}$$

$$(\int \chi^* \chi d\tau)_{\alpha^2} = \frac{\partial}{\partial \alpha} (\int \chi^* \chi d\tau)_{\alpha} = 16\pi \int_0^{\infty} r^4 e^{-2\alpha r - 2\beta r^2} dr \tag{2.94}$$

$$\begin{aligned}
(\int \chi^* \hat{T} \chi d\tau)_{\beta^2} &= \frac{\partial}{\partial \beta} (\int \chi^* \hat{T} \chi d\tau)_{\beta} \\
&= -\frac{2\pi}{\mu} \left[ 32 \int_0^{\infty} r^4 e^{-2\alpha r - 2\beta r^2} dr \right. \\
&\quad - 24\alpha \int_0^{\infty} r^5 e^{-2\alpha r - 2\beta r^2} dr \\
&\quad + 4\alpha^2 \int_0^{\infty} r^6 e^{-2\alpha r - 2\beta r^2} dr \\
&\quad - 56\beta \int_0^{\infty} r^6 e^{-2\alpha r - 2\beta r^2} dr \\
&\quad + 16\alpha\beta \int_0^{\infty} r^7 e^{-2\alpha r - 2\beta r^2} dr \\
&\quad \left. + 16\beta^2 \int_0^{\infty} r^8 e^{-2\alpha r - 2\beta r^2} dr \right]
\end{aligned} \tag{2.95}$$

$$\begin{aligned}
(\int \chi^* \hat{V} \chi d\tau)_{\beta^2} &= \frac{\partial}{\partial \beta} (\int \chi^* \hat{V} \chi d\tau)_{\beta} \\
&= -16\pi \left( \int_0^{\infty} r^5 e^{-2\alpha r - 2\beta r^2} dr \right. \\
&\quad \left. + 2\mu\omega^2 \int_0^{\infty} r^8 e^{-2\alpha r - 2\beta r^2} dr \right)
\end{aligned} \tag{2.96}$$

$$(\int \chi^* \chi d\tau)_{\beta^2} = \frac{\partial}{\partial \beta} (\int \chi^* \chi d\tau)_{\beta} = 16\pi \int_0^{\infty} r^6 e^{-2\alpha r - 2\beta r^2} dr \tag{2.97}$$

$$\begin{aligned}
(\int \chi^* \hat{T} \chi d\tau)_{\alpha\beta} &= (\int \chi^* \hat{T} \chi d\tau)_{\beta\alpha} = \frac{\partial}{\partial\beta} (\int \chi^* \hat{T} \chi d\tau)_{\alpha} \\
&= \frac{\partial}{\partial\alpha} (\int \chi^* \hat{T} \chi d\tau)_{\beta} \\
&= -\frac{2\pi}{\mu} \left[ 20 \int_0^{\infty} r^3 e^{-2\alpha r - 2\beta r^2} dr \right. \\
&\quad - 20\alpha \int_0^{\infty} r^4 e^{-2\alpha r - 2\beta r^2} dr \\
&\quad + 4\alpha^2 \int_0^{\infty} r^5 e^{-2\alpha r - 2\beta r^2} dr \\
&\quad - 48\beta \int_0^{\infty} r^5 e^{-2\alpha r - 2\beta r^2} dr \\
&\quad + 16\alpha\beta \int_0^{\infty} r^6 e^{-2\alpha r - 2\beta r^2} dr \\
&\quad \left. + 16\beta^2 \int_0^{\infty} r^7 e^{-2\alpha r - 2\beta r^2} dr \right]
\end{aligned} \tag{2.98}$$

$$\begin{aligned}
(\int \chi^* \hat{V} \chi d\tau)_{\alpha\beta} &= (\int \chi^* \hat{V} \chi d\tau)_{\beta\alpha} = \frac{\partial}{\partial\beta} (\int \chi^* \hat{V} \chi d\tau)_{\alpha} \\
&= \frac{\partial}{\partial\alpha} (\int \chi^* \hat{V} \chi d\tau)_{\beta} \\
&= -16\pi \left( \int_0^{\infty} r^4 e^{-2\alpha r - 2\beta r^2} dr \right. \\
&\quad \left. - 2\mu\omega^2 \int_0^{\infty} r^7 e^{-2\alpha r - 2\beta r^2} dr \right)
\end{aligned} \tag{2.99}$$

$$\begin{aligned}
(\int \chi^* \chi d\tau)_{\alpha\beta} &= (\int \chi^* \chi d\tau)_{\beta\alpha} = \frac{\partial}{\partial\beta} (\int \chi^* \chi d\tau)_{\alpha} \\
&= \frac{\partial}{\partial\alpha} (\int \chi^* \chi d\tau)_{\beta} = 16\pi \int_0^{\infty} r^5 e^{-2\alpha r - 2\beta r^2} dr
\end{aligned} \tag{2.100}$$

## 2.4 Coordinate System Transformations

### 2.4.1 Single-Particle Wave Function

The definition of the internal and center of mass coordinates according to equations (2-10) and (2-11), followed by the division of the Hamiltonian and the wave function into relative coordinate and center of mass parts, significantly simplifies the problem and enables us to construct an accurate variational wave function for the relative coordinate section. By substituting the variational wave function (2-72) for the relative motion part and the wave function (2-19) for the center of mass part in equation (2-24), the approximate total ground state wave function is given as follows:

$$\Psi(\mathbf{R}, \mathbf{r}) = N \exp(-\alpha r - \beta r^2 - \gamma R^2) \quad 2.101$$

where  $\gamma = \frac{1}{2}M\omega$  and  $N$  is the normalization factor of the wave function. In such a system, the volume elements for integration over the entire space will be in the form of spherical polar coordinates:

$$d\mathbf{R} d\mathbf{r} = R^2 \sin\theta_R dR d\theta_R d\phi_R r^2 \sin\theta_r dr d\theta_r d\phi_r \quad 2.102$$

which, due to the lack of explicit angular dependence in wave function (2-101), can be simplified as follows:

$$d\mathbf{R} d\mathbf{r} = 16 \pi^2 R^2 dR r^2 dr \quad 2.103$$

However, it is evident that for calculating single-particle quantities, we need a wave function explicitly dependent on single-particle coordinates. Therefore, we can rewrite wave function (2-101) in terms of single-particle coordinates using equations (2-10) and (2-11). By applying this substitution, we have:

$$\begin{aligned}
& -\gamma \left( \frac{m_e r_e + m_p r_p}{M} \right)^2 \\
& = -\frac{\gamma m_e^2 r_e^2}{M^2} - \frac{\gamma m_p^2 r_p^2}{M^2} - \frac{2\gamma m_e m_p r_e r_p \cos \theta_{ep}}{M^2}
\end{aligned} \tag{2.104}$$

$$-\beta |\mathbf{r}_e - \mathbf{r}_p|^2 = -\beta r_e^2 - \beta r_p^2 + 2\beta r_e r_p \cos \theta_{ep} \tag{2.105}$$

For simplicity and by defining three arbitrary constants as follows:

$$c_e = \frac{m_e^2 \gamma}{M^2} + \beta \tag{2.106}$$

$$c_p = \frac{m_p^2 \gamma}{M^2} + \beta \tag{2.107}$$

$$c_{ep} = 2 \left( \beta - \frac{m_e m_p \gamma}{M^2} \right) \tag{2.108}$$

The final form of the wave function will be as follows:

$$\begin{aligned}
\Psi(\mathbf{r}_e, \mathbf{r}_p) = N \exp \Big[ & -c_e r_e^2 - c_p r_p^2 + c_{ep} r_e r_p \cos \theta_{ep} \\
& - \alpha (r_e^2 + r_p^2 - 2r_e r_p \cos \theta_{ep})^{1/2} \Big]
\end{aligned} \tag{2.109}$$

The volume elements for the above wave function are also in the form of the usual polar coordinates, as follows:

$$d\mathbf{r}_e d\mathbf{r}_p = r_e^2 \sin \theta_e dr_e d\theta_e d\phi_e r_p^2 \sin \theta_p dr_p d\theta_p d\phi_p \tag{2.110}$$

where, due to the explicit presence of the angular part  $\theta$  in wave function (2-109), simplification can only be applied to the angular part  $\phi$  as follows:

$$d\mathbf{r}_e d\mathbf{r}_p = 4\pi^2 r_e^2 \sin \theta_e dr_e d\theta_e r_p^2 \sin \theta_p dr_p d\theta_p \tag{2.111}$$

### 2.4.2 Intermediate Wave Function

The two wave functions (2-101) and (2-109) have variables corresponding to the center of mass and single-particle coordinates, respectively, along with their associated differentials. However, it is possible to obtain an intermediate wave function and the associated differentials that simultaneously include both single-particle and interparticle coordinates. For this purpose, we replace  $R$  in the wave function (2-101) with the corresponding values. From equation (2-11), we have:

$$r^2 = |\mathbf{r}_e - \mathbf{r}_p|^2 = r_e^2 + r_p^2 - 2r_e r_p \cos \theta_{ep} \quad 2.112$$

As a result:

$$2r_e r_p \cos \theta_{ep} = -r^2 + r_e^2 + r_p^2 \quad 2.113$$

Therefore:

$$\begin{aligned} R^2 &= \left( \frac{m_e r_e + m_p r_p}{M} \right)^2 \\ &= \frac{1}{M^2} (m_e^2 r_e^2 + m_p^2 r_p^2 + 2m_e m_p r_e r_p \cos \theta_{ep}) \\ &= \frac{1}{M^2} (m_e^2 r_e^2 + m_p^2 r_p^2 + m_e m_p [-r^2 + r_e^2 + r_p^2]) \end{aligned} \quad 2.114$$

By substituting the above equation into the wave function (2-101), we have:

$$\begin{aligned} \Psi(r, r_e, r_p) &= N \exp \left( -\alpha r - \beta r^2 \right. \\ &\quad \left. - \frac{\gamma}{M^2} (m_e^2 r_e^2 + m_p^2 r_p^2 \right. \\ &\quad \left. + m_e m_p [-r^2 + r_e^2 + r_p^2]) \right) \end{aligned} \quad 2.115$$

This wave function is simultaneously dependent on both single-particle and interparticle coordinates, while the interparticle angle is not present.

Now, to define the volume elements corresponding to wave function (2-115), we first define the coordinates of the first particle (here, the electron) in the usual polar coordinates  $(r_e, \theta_e, \phi_e)$ . To define the coordinates of the second particle (here, the positive particle), we rotate the coordinate system so that the z-axis lies along  $r_e$ . Then we define the coordinates of the second particle in spherical polar coordinates as  $(r_p, \theta_p, \phi_p)$  [97]. Since the z-axis is along  $r_e$ ,  $\theta_p$  is equivalent to  $\theta_{ep}$ , and we denote  $\phi_p$  by  $\chi$ . The volume element for such coordinates is  $r_p^2 \sin \theta_{ep} dr_p d\theta_{ep} d\chi$ . Essentially, we are using a relative polar coordinate system for the second particle.

Since  $r_e$  and  $r_p$  are allowed to take all values consistent with  $r$ , the integration range for the second particle's coordinates is as follows:

$$\int_0^{2\pi} \int_0^\pi \int_{|r_e-r|}^{r_e+r} r_p^2 \sin \theta_{ep} dr_p d\theta_{ep} d\chi \quad 2.116$$

Now, to eliminate the remaining angle  $\theta_{ep}$ , we use the following relation:

$$r = \sqrt{r_e^2 + r_p^2 - 2r_e r_p \cos \theta_{ep}} \Rightarrow r^2 = r_e^2 + r_p^2 - 2r_e r_p \cos \theta_{ep} \quad 2.117$$

which, by differentiating

$$2r dr = 2r_e r_p \sin \theta_{ep} d\theta_{ep} \quad 2.118$$

we arrive at the following relation:

$$\frac{dr}{d\theta_{ep}} = \frac{r_e r_p \sin \theta_{ep}}{r} \quad 2.119$$

Therefore, the volume element for the second particle transforms as follows:



$$r_p^2 \sin \theta_{ep} dr_p d\theta_{ep} d\chi = \frac{r_p^2 \sin \theta_{ep} r dr_p dr d\chi}{r_e r_p \sin \theta_{ep}} = \frac{r_p r dr_p dr d\chi}{r_e} \quad 2.120$$

By multiplying the volume element of the electron by the volume element of the positive particle, the total volume element is obtained as follows:

$$\begin{aligned} r_e^2 \sin \theta_e dr_e d\theta_e d\phi_e \frac{r_p r dr_p dr d\chi}{r_e} \\ = r_e r_p r \sin \theta_e dr_e dr_p dr d\theta_e d\phi_e d\chi \end{aligned} \quad 2.121$$

Therefore, we have:

$$d\mathbf{r}_p d\mathbf{r}_e = r_e r_p r \sin \theta_e dr_e dr_p dr d\theta_e d\phi_e d\chi \quad 2.122$$

which will have the following integration ranges:

$$\int_0^{2\pi} \int_0^{2\pi} \int_0^\pi \int_0^\infty \int_0^\infty \int_{|r_e-r|}^{r_e+r} r_e r_p r \sin \theta_e dr_p dr_e dr d\theta_e d\phi_e d\chi \quad 2.123$$

Using equation (2-123) for the wave function (2-115), which does not explicitly depend on angles, simplifies the volume elements (2-122) as follows:

$$d\mathbf{r}_p d\mathbf{r}_e = 8\pi^2 r_e r_p r dr_e dr_p dr \quad 2.124$$

Therefore, with the availability of three wave functions with different dependencies, each can be used according to the specific conditions of the problem. However, wave function (2-115) is more interesting both conceptually and computationally due to its simultaneous dependency on single-particle and interparticle coordinates, as well as the absence of angular parts.

## 2.5 Energy Components

Using the wave functions introduced in the previous section, the expectation values of energy components can be calculated in both single-particle and center-of-mass coordinate systems.

### 2.5.1 Single-Particle Coordinate System

The kinetic energy of the electron and the positive particle can be calculated using both wave functions (2-109) and (2-115) (although, computationally, wave function (2-115) is more efficient). The expected value of the kinetic energy of the electron and the positive particle, using wave function (2-109), is defined as follows:

$$\begin{aligned}\langle \hat{T}_e \rangle &= \int \int \Psi^*(\mathbf{r}_e, \mathbf{r}_p) \hat{T}_e \Psi(\mathbf{r}_e, \mathbf{r}_p) d\mathbf{r}_e d\mathbf{r}_p \\ &= -\frac{1}{2m_e} \int \int \Psi^*(\mathbf{r}_e, \mathbf{r}_p) \nabla_e^2 \Psi(\mathbf{r}_e, \mathbf{r}_p) d\mathbf{r}_e d\mathbf{r}_p\end{aligned}\tag{2.125}$$

$$\begin{aligned}\langle \hat{T}_p \rangle &= \int \int \Psi^*(\mathbf{r}_e, \mathbf{r}_p) \hat{T}_p \Psi(\mathbf{r}_e, \mathbf{r}_p) d\mathbf{r}_e d\mathbf{r}_p \\ &= -\frac{1}{2m_p} \int \int \Psi^*(\mathbf{r}_e, \mathbf{r}_p) \nabla_p^2 \Psi(\mathbf{r}_e, \mathbf{r}_p) d\mathbf{r}_e d\mathbf{r}_p\end{aligned}\tag{2.126}$$

where

$$\begin{aligned}\nabla_e^2 &= \frac{\partial^2}{\partial r_e^2} + \frac{2}{r_e} \frac{\partial}{\partial r_e} + \frac{1}{r_e^2} \frac{\partial^2}{\partial \theta_{ep}^2} + \frac{1}{r_e^2} \cot(\theta_{ep}) \frac{\partial}{\partial \theta_{ep}} \\ &\quad + \frac{1}{r_e^2 \sin^2 \theta_{ep}} \frac{\partial^2}{\partial \phi^2}\end{aligned}\tag{2.127}$$

$$\begin{aligned}\nabla_p^2 = & \frac{\partial^2}{\partial r_p^2} + \frac{2}{r_p} \frac{\partial}{\partial r_p} + \frac{1}{r_p^2} \frac{\partial^2}{\partial \theta_{ep}^2} + \frac{1}{r_p^2} \cot(\theta_{ep}) \frac{\partial}{\partial \theta_{ep}} \\ & + \frac{1}{r_p^2 \sin^2 \theta_{ep}} \frac{\partial^2}{\partial \phi^2}\end{aligned}\tag{2.128}$$

Due to the wave function (2-109) not depending on the angular part  $\phi$ , the last term in equations (2-127) and (2-128) is eliminated. By applying these Laplacians to wave function (2-109), we obtain the following expressions:

$$\begin{aligned}& \nabla_e^2 \Psi(\mathbf{r}_e, \mathbf{r}_p) \\ &= \frac{1}{\sqrt{-2r_e r_p \cos(\theta_{ep}) + r_e^2 + r_p^2}} (-2r_e r_p \cos(\theta_{ep}) (2c_e(\alpha \\ &+ c_{ep} \sqrt{-2r_e r_p \cos(\theta_{ep}) + r_e^2 + r_p^2}) + \alpha c_{ep}) + 2\alpha(2c_e r_e^2 \\ &+ c_{ep} r_p^2 - 1) + (4c_e^2 r_e^2 - 6c_e \\ &+ c_{ep}^2 r_p^2) \sqrt{-2r_e r_p \cos(\theta_{ep}) + r_e^2 + r_p^2} \\ &+ \alpha^2 \sqrt{-2r_e r_p \cos(\theta_{ep}) + r_e^2 + r_p^2}) \exp(c_{ep} r_e r_p \cos(\theta_{ep}) - c_e r_e^2 \\ &- c_p r_p^2 - \alpha \sqrt{-2r_e r_p \cos(\theta_{ep}) + r_e^2 + r_p^2})\end{aligned}\tag{2.129}$$

$$\begin{aligned}
& \nabla_p^2 \Psi(\mathbf{r}_e, \mathbf{r}_p) \\
&= \frac{1}{\sqrt{-2r_e r_p \cos(\theta_{ep}) + r_e^2 + r_p^2}} (-2r_e r_p \cos(\theta_{ep}) (2c_p(\alpha \\
&+ c_{ep} \sqrt{-2r_e r_p \cos(\theta_{ep}) + r_e^2 + r_p^2}) + \alpha c_{ep}) + 2\alpha(c_{ep} r_e^2 \\
&+ 2c_p r_p^2 - 1) + (c_{ep}^2 r_e^2 + 4c_p^2 r_p^2 \\
&- 6c_p) \sqrt{-2r_e r_p \cos(\theta_{ep}) + r_e^2 + r_p^2} \\
&+ \alpha^2 \sqrt{-2r_e r_p \cos(\theta_{ep}) + r_e^2 + r_p^2}) \exp(c_{ep} r_e r_p \cos(\theta_{ep}) - c_e r_e^2 \\
&- c_p r_p^2 - \alpha \sqrt{-2r_e r_p \cos(\theta_{ep}) + r_e^2 + r_p^2})
\end{aligned} \tag{2.130}$$

Then, by substituting equation (2-110) into equations (2-125) and (2-126), the expectation values of the kinetic energies of the electron and the positive particle are obtained from the following expression:

$$\begin{aligned}
\langle \hat{T}_e \rangle &= \\
& - \frac{1}{2m_e} \int_0^{2\pi} \int_0^\pi \int_0^\infty \int_0^{2\pi} \int_0^\pi \int_0^\infty \Psi^*(\mathbf{r}_e, \mathbf{r}_p) \nabla_e^2 \Psi(\mathbf{r}_e, \mathbf{r}_p) r_e^2 r_p^2 \sin\theta_e \sin\theta_p dr_e d\theta_e d\phi_e dr_p d\theta_p d\phi_p \\
&= - \frac{8\pi^2}{2m_e} \int_0^\infty \int_0^\pi \int_0^\infty \Psi^*(\mathbf{r}_e, \mathbf{r}_p) \nabla_e^2 \Psi(\mathbf{r}_e, \mathbf{r}_p) r_e^2 r_p^2 \sin\theta_e dr_e d\theta_e dr_p
\end{aligned} \tag{2.131}$$

$$\begin{aligned}
\langle \hat{T}_p \rangle &= - \frac{1}{2m_p} \int_0^{2\pi} \int_0^\pi \int_0^\infty \int_0^{2\pi} \int_0^\pi \int_0^\infty \Psi^*(\mathbf{r}_e, \mathbf{r}_p) \nabla_p^2 \Psi(\mathbf{r}_e, \mathbf{r}_p) r_e^2 r_p^2 \sin\theta_e \sin\theta_p dr_e d\theta_e d\phi_e dr_p d\theta_p d\phi_p \\
&= - \frac{8\pi^2}{2m_p} \int_0^\infty \int_0^\pi \int_0^\infty \Psi^*(\mathbf{r}_e, \mathbf{r}_p) \nabla_p^2 \Psi(\mathbf{r}_e, \mathbf{r}_p) r_e^2 r_p^2 \sin\theta_p dr_e d\theta_p dr_p
\end{aligned} \tag{2.13}$$

Another way to obtain the kinetic energy of the electron and the positive particle is by using wave function (2-115). For this purpose, by substituting equation (2-113) into equations (2-129) and (2-130), we transform them as follows:

$$\begin{aligned}
\nabla_e^2 \Psi(r, r_e, r_p) &= \frac{1}{r} (- (r_e^2 + r_p^2 - r^2) (2c_e(\alpha + rc_{ep}) + \alpha c_{ep}) \\
&\quad + r(4c_e^2 r_e^2 - 6c_e + c_{ep}^2 r_p^2) + 2\alpha(2c_e r_e^2 + c_{ep} r_p^2 \\
&\quad - 1) + \alpha^2 r) \exp\left(\frac{1}{2} c_{ep}(r_e^2 + r_p^2 - r^2) - c_e r_e^2 \right. \\
&\quad \left. - c_p r_p^2 - \alpha r\right)
\end{aligned} \tag{2.133}$$

$$\begin{aligned}
\nabla_p^2 \Psi(r, r_e, r_p) &= \frac{1}{r} (- (r_e^2 + r_p^2 - r^2) (\alpha c_{ep} + 2c_p(\alpha + rc_{ep})) \\
&\quad + r(c_{ep}^2 r_e^2 + 4c_p^2 r_p^2 - 6c_p) + 2\alpha(c_{ep} r_e^2 \\
&\quad + 2c_p r_p^2 - 1) + \alpha^2 r) \exp\left(\frac{1}{2} c_{ep}(r_e^2 + r_p^2 - r^2) \right. \\
&\quad \left. - c_e r_e^2 - c_p r_p^2 - \alpha r\right)
\end{aligned} \tag{2.134}$$

Therefore, the kinetic energies of the electron and the positive particle using wave function (2-115) will be as follows:

$$\begin{aligned}
\langle \hat{T}_e \rangle &= \int_0^{2\pi} \int_0^{2\pi} \int_0^\pi \int_0^\infty \int_0^\infty \int_{|r_e-r|}^{r_e+r} \Psi^*(\mathbf{r}_e, \mathbf{r}_p) \nabla_e^2 \Psi(r, r_e, r_p) r_e r_p r \sin\theta_e dr_p dr d\theta_e d\phi_e d\chi \\
&= -\frac{8\pi^2}{2m_e} \int_0^\infty \int_0^\infty \int_{|r_e-r|}^{r_e+r} \Psi^*(\mathbf{r}_e, \mathbf{r}_p) \nabla_e^2 \Psi(r, r_e, r_p) r_e r_p r dr_p dr d\theta_e d\phi_e d\chi
\end{aligned} \tag{2.135}$$

$$\begin{aligned}
\langle \hat{T}_p \rangle &= \int_0^{2\pi} \int_0^{2\pi} \int_0^\pi \int_0^\infty \int_0^\infty \int_{|r_p-r|}^{r_p+r} \Psi^*(\mathbf{r}_e, \mathbf{r}_p) \nabla_p^2 \Psi(r, r_e, r_p) r_e r_p r \sin\theta_p dr_e dr_p dr d\theta_p d\phi_p d\chi \\
&= -\frac{8\pi^2}{2m_p} \int_0^\infty \int_0^\infty \int_{|r_p-r|}^{r_p+r} \Psi^*(\mathbf{r}_e, \mathbf{r}_p) \nabla_p^2 \Psi(r, r_e, r_p) r_e r_p r dr_e dr_p dr d\theta_p d\phi_p d\chi
\end{aligned} \tag{2.136}$$

The expectation value for the potential energy of the oscillator for the electron and the positive particle, using the two wave functions (2-109) and (2-115), is defined as follows:

$$\begin{aligned}
\langle \bar{H} O_e \rangle &= \int \int \Psi^*(\mathbf{r}_e, \mathbf{r}_p) \frac{1}{2} m_e \omega^2 r_e^2 \Psi(\mathbf{r}_e, \mathbf{r}_p) d\mathbf{r}_e d\mathbf{r}_p \\
&= \frac{m_e \omega^2}{2} \int_0^{2\pi} \int_0^\pi \int_0^\infty \int_0^{2\pi} \int_0^\pi \int_0^\infty |\Psi(r_e, r_p)|^2 r_e^4 r_p^2 \sin\theta_e \sin\theta_p dr_e d\theta_e d\phi_e dr_p d\theta_p d\phi_p \\
&= \frac{m_e \omega^2}{2} \int_0^{2\pi} \int_0^{2\pi} \int_0^\pi \int_0^\infty \int_0^\infty \int_{|r_p-r|}^{r_e+r} |\Psi(r, r_e, r_p)|^2 r_e^3 r_p r \sin\theta_e dr_p dr_e dr d\theta_e d\phi_e d\chi \\
&= \frac{8\pi^2 m_e \omega^2}{2} \int_0^\infty \int_0^\pi \int_0^\infty |\Psi(r_e, r_p)|^2 r_e^4 r_p^2 \sin\theta_e dr_e d\theta_e dr_p \\
&= \frac{8\pi^2 m_e \omega^2}{2} \int_0^\infty \int_0^\infty \int_{|r_p-r|}^{r_e+r} |\Psi(r, r_e, r_p)|^2 r_e^3 r_p r dr_p dr_e dr
\end{aligned} \tag{2.137}$$

$$\begin{aligned}
\langle \bar{H} O_p \rangle &= \int \int \Psi^*(\mathbf{r}_e, \mathbf{r}_p) \frac{1}{2} m_p \omega^2 r_p^2 \Psi(\mathbf{r}_e, \mathbf{r}_p) d\mathbf{r}_e d\mathbf{r}_p \\
&= \frac{m_p \omega^2}{2} \int_0^{2\pi} \int_0^\pi \int_0^\infty \int_0^{2\pi} \int_0^\pi \int_0^\infty |\Psi(r_e, r_p)|^2 r_p^4 r_e^2 \sin\theta_e \sin\theta_p dr_e d\theta_e d\phi_e dr_p d\theta_p d\phi_p \\
&= \frac{m_p \omega^2}{2} \int_0^{2\pi} \int_0^{2\pi} \int_0^\pi \int_0^\infty \int_0^\infty \int_{|r_p-r|}^{r_p+r} |\Psi(r, r_e, r_p)|^2 r_p^3 r_e r \sin\theta_e dr_p dr_e dr d\theta_e d\phi_e d\chi \\
&= \frac{8\pi^2 m_p \omega^2}{2} \int_0^\infty \int_0^\pi \int_0^\infty |\Psi(r_e, r_p)|^2 r_p^4 r_e^2 \sin\theta_e dr_e d\theta_e dr_p \\
&= \frac{8\pi^2 m_p \omega^2}{2} \int_0^\infty \int_0^\infty \int_{|r_p-r|}^{r_p+r} |\Psi(r, r_e, r_p)|^2 r_p^3 r_e r dr_e dr_p dr
\end{aligned} \tag{2.138}$$

The expectation value of the interaction energy is also defined and calculated using the two wave functions (2-109) and (2-115) as follows:

$$\begin{aligned}
INT &= \int \int \Psi^*(\mathbf{r}_e, \mathbf{r}_p) \left(-\frac{1}{r}\right) \Psi(\mathbf{r}_e, \mathbf{r}_p) d\mathbf{r}_e d\mathbf{r}_p \\
&= \int_0^{2\pi} \int_0^\pi \int_0^\infty \int_0^{2\pi} \int_0^\pi \int_0^\infty |\Psi(r_e, r_p)|^2 \frac{1}{(r_e^2 + r_p^2 - 2r_e r_p \cos[\theta_{ep}])^{1/2}} r_e^2 r_p^2 \sin\theta_e \sin\theta_p dr_e d\theta_e d\phi_e dr_p d\theta_p d\phi_p \\
&= -8\pi^2 \int_0^{2\pi} \int_0^{2\pi} \int_0^\pi \int_0^\infty \int_0^\infty \int_{|r_p-r|}^{r_p+r} |\Psi(r, r_e, r_p)|^2 \frac{1}{r} r_e r_p r \sin\theta_e dr_p dr_e dr d\theta_e d\phi_e d\chi
\end{aligned} \tag{2.139}$$

## 2.5.2 Energy Components in Pseudo particle Coordinates

The energy components for two particles with reduced mass and the mass of the center of mass are calculated using wave function (2-101). As mentioned in the previous section, wave function (2-115) can also be used for calculations in this section due to its dependence on the interparticle distance.

For example, the kinetic energies of the pseudo particles are defined as follows:

$$\begin{aligned}
\langle \hat{T}_r \rangle &= \int \int \Psi^*(\mathbf{R}, \mathbf{r}) \hat{T}_r \Psi(\mathbf{R}, \mathbf{r}) d\mathbf{r} d\mathbf{R} \\
&= -\frac{1}{2\mu} \int_0^{2\pi} \int_0^\pi \int_0^\infty \int_0^{2\pi} \int_0^\pi \int_0^\infty \Psi^*(\mathbf{R}, \mathbf{r}) \nabla_r^2 \Psi(\mathbf{R}, \mathbf{r}) R^2 \sin\theta_R dR d\theta_R d\phi_R r^2 \sin\theta_r dr d\theta_r d\phi_r \\
&= -\frac{1}{2\mu} \int_0^{2\pi} \int_0^{2\pi} \int_0^\pi \int_0^\pi \int_0^\infty \int_{|r_p-r|}^{r_p+r} \Psi^*(r, r_e, r_p) \nabla_r^2 \Psi(r, r_e, r_p) r_e r_p r \sin\theta_e dr_e dr_p dr d\theta_p d\phi_p d\chi \\
&= -\frac{16\pi^2}{2\mu} \int_0^\infty \int_0^\pi \int_0^\infty \Psi^*(\mathbf{R}, \mathbf{r}) \nabla_r^2 \Psi(\mathbf{R}, \mathbf{r}) R^2 r^2 dR dr \\
&= -\frac{8\pi^2}{2\mu} \int_0^\infty \int_0^\infty \int_{|r_p-r|}^{r_p+r} \Psi^*(r, r_e, r_p) \nabla_r^2 \Psi(r, r_e, r_p) r_e r_p r dr_e dr_p dr
\end{aligned} \tag{2.140}$$

$$\begin{aligned}
\langle \hat{T}_R \rangle &= \int \int \Psi^*(\mathbf{R}, \mathbf{r}) \hat{T}_R \Psi(\mathbf{R}, \mathbf{r}) d\mathbf{r} d\mathbf{R} \\
&= -\frac{1}{2M} \int_0^{2\pi} \int_0^\pi \int_0^\infty \int_0^{2\pi} \int_0^\pi \int_0^\infty \Psi^*(\mathbf{R}, \mathbf{r}) \nabla_R^2 \Psi(\mathbf{R}, \mathbf{r}) R^2 \sin\theta_R dR d\theta_R d\phi_R r^2 \sin\theta_r dr d\theta_r d\phi_r \\
&= -\frac{1}{2M} \int_0^{2\pi} \int_0^{2\pi} \int_0^\pi \int_0^\pi \int_0^\infty \int_{|r_p-r|}^{r_p+r} \Psi^*(r, r_e, r_p) \nabla_R^2 \Psi(r, r_e, r_p) r_e r_p r \sin\theta_e dr_e dr_p dr d\theta_p d\phi_p d\chi \\
&= -\frac{16\pi^2}{2M} \int_0^\infty \int_0^\pi \int_0^\infty \Psi^*(\mathbf{R}, \mathbf{r}) \nabla_R^2 \Psi(\mathbf{R}, \mathbf{r}) R^2 r^2 dR dr \\
&= -\frac{8\pi^2}{2M} \int_0^\infty \int_0^\infty \int_{|r_p-r|}^{r_p+r} \Psi^*(r, r_e, r_p) \nabla_R^2 \Psi(r, r_e, r_p) r_e r_p r dr_e dr_p dr
\end{aligned} \tag{2.141}$$

In these cases, the Laplacian operators of equations (2-127) and (2-128), considering the angular independence of the wave functions under investigation, transform as follows for the reduced mass and the center of mass:

$$\nabla_r^2 = \frac{\partial^2}{\partial r^2} + \frac{2}{r} \frac{\partial}{\partial r} \tag{2.142}$$

$$\nabla_R^2 = \frac{\partial^2}{\partial R^2} + \frac{2}{R} \frac{\partial}{\partial R} \tag{2.143}$$

However, due to the product form of wave function (2-101) being divided into two parts: the center of mass and the reduced mass, and given the

independence of the operators of each part from the other, it is simpler to calculate the energy components using only wave functions (2-19) or (2-21), depending on the type of operator. In this case, the form of the integrals that appear in these calculations and their solutions are as follows:

$$\int_0^\infty x e^{-2ax-2bx^2} dx = \frac{2\sqrt{b} - a e^{\frac{a^2}{2b}} \sqrt{2\pi} \text{Erfc}[\frac{a}{\sqrt{2}\sqrt{b}}]}{8b^{3/2}} = A \quad 2.144$$

$$\int_0^\infty x^2 e^{-2ax-2bx^2} dx = \frac{-2a\sqrt{b} + (a^2 + b) e^{\frac{a^2}{2b}} \sqrt{2\pi} \text{Erfc}[\frac{a}{\sqrt{2}\sqrt{b}}]}{16b^{5/2}} \quad 2.145$$

= B

$$\int_0^\infty x^3 e^{-2ax-2bx^2} dx$$

$$= \frac{2\sqrt{b}(a^2 + 2b) - a(a^2 + 3b) e^{\frac{a^2}{2b}} \sqrt{2\pi} \text{Erfc}[\frac{a}{\sqrt{2}\sqrt{b}}]}{32b^{7/2}} = C \quad 2.146$$

$$\int_0^\infty x^4 e^{-2ax-2bx^2} dx$$

$$= \frac{-2a\sqrt{b}(a^2 + 5b) + (a^4 + 6a^2b + 3b^2) e^{\frac{a^2}{2b}} \sqrt{2\pi} \text{Erfc}[\frac{a}{\sqrt{2}\sqrt{b}}]}{64b^{9/2}} = D \quad 2.147$$

For the center of mass, the contribution to the kinetic energy is as follows:

$$T_R = \left\langle \eta_{klm}(\mathbf{R}) \left| -\frac{1}{2M} \nabla_R^2 \right| \eta_{klm}(\mathbf{R}) \right\rangle \quad 2.148$$

$$= -\frac{2\pi}{M} \int_0^\infty R^2 e^{-\frac{1}{2}M\omega R^2} \nabla_R^2 e^{-\frac{1}{2}M\omega R^2} dR = \frac{3\omega}{4}$$

and the potential energy of the harmonic oscillator is as follows:



$$\begin{aligned}
HO_R &= \left\langle \eta_{klm}(\mathbf{R}) \left| \frac{M}{2} \omega^2 R^2 \right| \eta_{klm}(\mathbf{R}) \right\rangle = 2M\pi \int_0^\infty R^4 e^{-M\omega R^2} dR \\
&= \frac{3\omega}{4}
\end{aligned} \tag{2.149}$$

and the total energy of the center of mass will be  $\frac{3\omega}{2}$ . Additionally, for the reduced mass, the kinetic energy is as follows:

$$\begin{aligned}
T_r &= \left\langle \chi_{k'l'm'}(\mathbf{r}) \left| -\frac{1}{2\mu} \nabla_r^2 \right| \chi_{k'l'm'}(\mathbf{r}) \right\rangle \\
&= -\frac{1}{2\mu} (\alpha^2 - 2\beta + 4\alpha\beta \frac{C}{B} + 4\beta^2 \frac{D}{B} - 2\alpha \frac{A}{B} \\
&\quad - 4\beta)
\end{aligned} \tag{2.150}$$

The potential energy of the harmonic oscillator:

$$HO_r = \left\langle \chi_{k'l'm'}(\mathbf{r}) \left| \frac{\mu}{2} \omega^2 r^2 \right| \chi_{k'l'm'}(\mathbf{r}) \right\rangle = \frac{1}{2} \mu \omega^2 \frac{D}{B} \tag{2.151}$$

and the interaction energy is as follows:

$$\text{INT} = \left\langle \chi_{k'l'm'}(\mathbf{r}) \left| -\frac{1}{r} \right| \chi_{k'l'm'}(\mathbf{r}) \right\rangle = -\frac{A}{B} \tag{2.152}$$

It is important to note that the results of the angular part integration ( $4\pi$ ) are not included in the above integrals, as they will cancel each other out when each of the integrals (2-144) to (2-147) is divided by the overlap integral (equation 2-145).

## 2.6 Single-Particle Densities

The normalization constant can be calculated using the normalization condition through any of the three wave functions mentioned in the previous sections, and it will yield the same numerical result. However, due to

simplicity, we will use wave function (2-101) here. The normalization condition is defined as follows:

$$\begin{aligned}
& N^2 \int \Psi(\mathbf{r}, \mathbf{R})^2 d\tau \\
& = N^2 \int \exp(-2\alpha r - 2\beta r^2 - 2\gamma R^2) d\tau \\
& = N^2 \int_0^\infty \int_0^\infty \int_0^\pi \int_0^\pi \int_0^{2\pi} \int_0^{2\pi} \exp(-2\alpha r - 2\beta r^2 \\
& \quad - 2\gamma R^2) r^2 R^2 dr dR \sin \theta_e d\theta_e \sin \theta_p d\theta_p d\phi_e d\phi_p = 1
\end{aligned} \tag{2.153}$$

As a result, the normalization constant will be:

$$N = \frac{1}{\sqrt{\int |\Psi(\mathbf{r}, \mathbf{R})|^2 d\tau}} \tag{2.154}$$

Given that wave function (2-101) lacks angular dependence, integrating over the angular part leads to the following result:

$$\int_0^{2\pi} \int_0^{2\pi} d\phi_e d\phi_p = 4\pi^2 \tag{2.155}$$

$$\int_0^\pi \int_0^\pi \sin \theta_e d\theta_e \sin \theta_p d\theta_p = 4 \tag{2.156}$$

Then, by integrating over the variable  $r$ , we have:

$$\begin{aligned}
& \int_0^\infty \exp(-2\alpha r - 2\beta r^2 - 2\gamma R^2) r^2 dr \\
& \quad e^{-2R^2\gamma} (-2\alpha\sqrt{\beta} + e^{\frac{\alpha^2}{2\beta}} \sqrt{2\pi} (\alpha^2 + \beta) \operatorname{erfc}[\frac{\alpha}{\sqrt{2\beta}}]) \\
& = \frac{e^{-2R^2\gamma} (-2\alpha\sqrt{\beta} + e^{\frac{\alpha^2}{2\beta}} \sqrt{2\pi} (\alpha^2 + \beta) \operatorname{erfc}[\frac{\alpha}{\sqrt{2\beta}}])}{16\beta^{5/2}} = \xi
\end{aligned} \tag{2.157}$$

where the complementary error function is defined as follows:

$$\operatorname{erfc}(x) = 1 - \operatorname{erf}(x) \tag{2.158}$$

Subsequently, by integrating  $\xi$  over  $R$ , we obtain the following expression:

$$\begin{aligned} \int_0^\infty \xi R^2 dR &= \frac{-\sqrt{2\pi}\alpha\sqrt{\beta} + e^{\frac{\alpha^2}{2\beta}}\pi(\alpha^2 + \beta)\operatorname{erfc}\left[\frac{\alpha}{\sqrt{2\beta}}\right]}{128\beta^{5/2}\gamma^{3/2}} \\ &= \frac{\sqrt{\pi}}{64\beta^{3/2}\gamma^{3/2}} \left( \frac{e^{\frac{\alpha^2}{2\beta}}\sqrt{\pi}(\alpha^2 + \beta)\operatorname{erfc}\left[\frac{\alpha}{\sqrt{2\beta}}\right]}{2\beta} - \frac{\alpha}{\sqrt{2\beta}} \right) \end{aligned} \quad 2.159$$

Therefore, the final expression for the normalization constant using the above equations will be:

$$N = 2\pi^{-5/4}\beta^{3/4}\gamma^{3/4} \left( \frac{e^{\frac{\alpha^2}{2\beta}}\sqrt{\pi}(\alpha^2 + \beta)\operatorname{erfc}\left[\frac{\alpha}{\sqrt{2\beta}}\right]}{2\beta} - \frac{\alpha}{\sqrt{2\beta}} \right)^{-1/2} \quad 2.160$$

It is important to note that in the following sections, the steps for calculating single-particle quantities are only explained for the electron, and only the final results are presented for the positive particle. The calculation steps for the positive particle are exactly similar to those for the electron, with the substitution of the positive particle's coordinates.

To calculate the density, we use the intermediate wave function. Since the electron density is obtained by integrating over the positive particle's coordinates (and vice versa), we first need to obtain the appropriate differentials for the density in the volume elements of the intermediate wave function. We know that the fundamental definition of electron density is as follows:

$$\rho_e(r_e) = \int_0^{2\pi} \int_0^\pi \int_0^\infty |\Psi(\mathbf{r}_e, \mathbf{r}_p)|^2 r_p^2 \sin\theta_p dr_p d\theta_p d\phi_p \quad 2.161$$

Additionally, using the normalization condition, we have:

$$\underbrace{\int_0^{2\pi} \int_0^\pi \int_0^\infty \int_0^{2\pi} \int_0^\pi \int_0^\infty |\Psi(\mathbf{r}_e, \mathbf{r}_p)|^2 r_p^2 \sin\theta_p dr_p d\theta_p d\phi_p r_e^2 \sin\theta_e dr_e d\theta_e d\phi_e}_{\rho_e(\mathbf{r}_e)} = 1 \quad 2.162$$

where the inner part of the integral is the electron density. Now, we rewrite the above equation (or the normalization condition) based on the intermediate wave function and its volume elements:

$$\int_0^{2\pi} \int_0^{2\pi} \int_0^\pi \int_0^\infty \int_0^\infty \int_{|r_e-r|}^{r_e+r} |\Psi(r, r_e, r_p)|^2 r_p r_e r \sin\theta_e dr_p dr d\theta_e d\phi_e d\chi = 1 \quad 2.163$$

By rearranging the above equation so that the electron differentials are in the outer part (like in equation 2-162), we have:

$$\int_0^{2\pi} \int_0^\pi \int_0^\infty \int_0^{2\pi} \int_0^\infty \int_{|r_e-r|}^{r_e+r} |\Psi(r, r_e, r_p)|^2 r_p r dr_p dr d\chi r_e \sin\theta_e dr_e d\theta_e d\phi_e = 1 \quad 2.164$$

Then, by multiplying and dividing the above equation by  $r_e$ , we arrive at an equation in the form of (2-162):

$$\underbrace{\int_0^{2\pi} \int_0^\pi \int_\epsilon^\infty \int_0^{2\pi} \int_0^\infty \int_{|r_e-r|}^{r_e+r} |\Psi(r, r_e, r_p)|^2 \frac{r_p r}{r_e} dr_p dr d\chi r_e^2 \sin\theta_e dr_e d\theta_e d\phi_e}_{\rho_e(\mathbf{r}_e)} = 1 \quad 2.165$$

Due to the presence of  $r_e$  in the denominator, it cannot be zero, and as a result, the lower limit of its integral starts from a very small non-zero value ( $\epsilon$ ). The electron density in the intermediate coordinates is as follows:

$$\rho_e(r_e) = \int_0^{2\pi} \int_0^\infty \int_{|r_e-r|}^{r_e+r} |\Psi(r, r_e, r_p)|^2 \frac{r_p r}{r_e} dr_p dr d\chi \quad 2.166$$

After integrating the angular part, we have:

$$\rho_e(r_e) = \frac{2\pi}{r_e} \int_0^\infty \int_{|r_e-r|}^{r_e+r} |\Psi(r, r_e, r_p)|^2 r_p r dr_p dr \quad 2.167$$

And finally, after integrating over the radial parts, we have:

$$\begin{aligned} \rho_e(r_e) &= \frac{1}{8\sqrt{2}\gamma r_e m_p (\gamma m_p^2 + \beta M^2)} \pi^{3/2} M^2 N^2 e^{-2\gamma r_e^2} \left( (\alpha M \right. \\ &\quad \left. - 2\gamma r_e m_p) \operatorname{erf} \left( \frac{\alpha M - 2\gamma r_e m_p}{\sqrt{2} M \sqrt{\beta + \frac{\gamma m_p^2}{M^2}}} \right) \exp \left( \frac{(\alpha M - 2\gamma r_e m_p)^2}{2(\gamma m_p^2 + \beta M^2)} \right) \right. \\ &\quad \left. - (2\gamma r_e m_p + \alpha M) \operatorname{erf} \left( \frac{2\gamma r_e m_p + \alpha M}{\sqrt{2} M \sqrt{\beta + \frac{\gamma m_p^2}{M^2}}} \right) \exp \left( \frac{(2\gamma r_e m_p + \alpha M)^2}{2(\gamma m_p^2 + \beta M^2)} \right) \right. \\ &\quad \left. + (\alpha M (e^{\frac{4\alpha\gamma M r_e m_p}{\gamma m_p^2 + \beta M^2}} - 1) + 2\gamma r_e m_p (e^{\frac{4\alpha\gamma M r_e m_p}{\gamma m_p^2 + \beta M^2}} \right. \\ &\quad \left. + 1)) \exp \left( \frac{(\alpha M - 2\gamma r_e m_p)^2}{2(\gamma m_p^2 + \beta M^2)} \right) \right) \quad , r_e \neq 0 \end{aligned} \quad 2.168$$

$$\begin{aligned}
\rho_p(r_p) &= \frac{1}{8\sqrt{2}\gamma m_e r_p (\gamma m_e^2 + \beta M^2) \sqrt{\beta + \frac{\gamma m_e^2}{M^2}}} \pi^{3/2} M^2 N^2 e^{-2\gamma r_p^2} ((\alpha M \\
&- 2\gamma m_e r_p) \operatorname{erf}\left(\frac{\alpha M - 2\gamma m_e r_p}{\sqrt{2}M \sqrt{\beta + \frac{\gamma m_e^2}{M^2}}}\right) \exp\left(\frac{(\alpha M - 2\gamma m_e r_p)^2}{2(\gamma m_e^2 + \beta M^2)}\right) \\
&- (2\gamma m_e r_p + \alpha M) \operatorname{erf}\left(\frac{2\gamma m_e r_p + \alpha M}{\sqrt{2}M \sqrt{\beta + \frac{\gamma m_e^2}{M^2}}}\right) \exp\left(\frac{(2\gamma m_e r_p + \alpha M)^2}{2(\gamma m_e^2 + \beta M^2)}\right) \\
&+ (\alpha M (e^{\frac{4\alpha\gamma M m_e r_p}{\gamma m_e^2 + \beta M^2}} - 1) + 2\gamma m_e r_p (e^{\frac{4\alpha\gamma M m_e r_p}{\gamma m_e^2 + \beta M^2}} \\
&+ 1)) \exp\left(\frac{(\alpha M - 2\gamma m_e r_p)^2}{2(\gamma m_e^2 + \beta M^2)}\right)) \quad , r_p \neq 0
\end{aligned} \tag{2.169}$$

Equations (2-168) and (2-169) represent the final analytical forms of the electron and positive particle densities for the intermediate wave function. Their shapes are illustrated in section 5-1-2.

## 3 Electron-Positively Charged Particle Correlation

### 3.1 Fundamental Definition of Correlation in Physics

The most general and, in a sense, fundamental mathematical definition of correlation between two particles in quantum mechanics can be presented using an inherently statistical quantity called the "pair density" or "two-particle density". The two-particle density expresses the probability of finding two particles (distinguishable or indistinguishable), one in the volume element  $d\mathbf{r}_1$  and the other in the

volume element  $d\mathbf{r}_2$ . The two-particle density for two indistinguishable particles (such as two electrons) in a system consisting of  $N$  particles, after integrating over spins, is defined as follows [98]:

$$\Gamma(\mathbf{r}_1, \mathbf{r}_2) = N(N-1) \int \dots \int |\Psi(\mathbf{r}_1, \dots, \mathbf{r}_N)|^2 d\mathbf{r}_3, \dots, d\mathbf{r}_N \quad 3.1$$

and for two distinguishable particles (such as an electron and a PCP) in a system consisting of  $N$  and  $N'$  numbers of these two particles, after integrating over spins, it is defined as follows:

$$\begin{aligned} & \Gamma(\mathbf{r}_1^e, \mathbf{r}_1^p) \\ &= NN' \int \dots \int \Psi^*(\mathbf{r}_1^e, \dots, \mathbf{r}_N^e, \mathbf{r}_1^p, \dots, \mathbf{r}_{N'}^p) \Psi(\mathbf{r}_1^e, \dots, \mathbf{r}_N^e, \mathbf{r}_1^p, \dots, \mathbf{r}_{N'}^p) d\mathbf{r}_2^e, \dots, d\mathbf{r}_N^e, d\mathbf{r}_2^p, \dots, d\mathbf{r}_{N'}^p \end{aligned} \quad 3.2$$

If the two particles are independent of each other, the two-particle density simply equals the product of the densities of each particle. Thus, whenever the two-particle density deviates from the product of the single-particle densities, we are dealing with correlated particles. Therefore, the two-particle density can be decomposed as follows:

$$\Gamma(\mathbf{r}_1^e, \mathbf{r}_1^p) = \rho_e(\mathbf{r}_1^e) \rho_p(\mathbf{r}_1^p) + \Gamma_c(\mathbf{r}_1^e, \mathbf{r}_1^p) \quad 3.3$$

Where  $\Gamma_c(\mathbf{r}_1^e, \mathbf{r}_1^p)$  represents the correlation part of the two-particle density, which is zero for uncorrelated systems. In this chapter, we will explore various aspects of e-PCP correlation, which is one of the main objectives of developing the EHM in this dissertation.



## 3.2 E-PCP Correlation

### 3.2.1 Nature

The e-PCP correlation differs fundamentally from electron-electron correlation in at least two aspects: the nature of the interaction and the mass of the particles. The e-PCP interaction, unlike the purely electronic case, is attractive, which lowers the energy level. As we saw in section 2-2-2, this attraction is one of the obstacles to achieving an analytical solution for the ground state of the EHM using the conventional power series method. Furthermore, as we will see, the attractive nature of the e-PCP correlation results in the creation of a correlation hill (as opposed to a correlation hole like in electronic correlation).

### 3.2.2 History

The PCPs examined in this study encompass a mass range from 1 (positron) to 1836 (proton) (details of the calculations will be provided in the next chapter). The e-PCP correlation has been extensively studied for particles at both ends of this mass spectrum, i.e., positrons and protons, due to the significance of positron annihilation spectroscopy in studying the electronic structure of solids and the presence of protons in atomic nuclei (hence the term electron-nucleus correlation is also used). However, other PCPs within this spectrum also have numerous applications, as mentioned in section 1-5. Below is a brief history of the research conducted on e-PCP correlation.

The electron-positron correlation gained attention early on, starting in the 1950s, due to the importance of positron annihilation. In this

context, Ferrell published a review article titled "Theory of Positron Annihilation in Solids" in 1956 [99]. In 1960, Kahana introduced a correlation function for electron-positron pairs in metals, reconciling the Sommerfeld model of a metal with experimental data, as the Sommerfeld model alone could not correctly reproduce the experimental positron annihilation rates in metals [100]. In 1966, Hamann calculated the self-energy of the positron (due to electron-positron correlation) in an electron gas [101]. Following this, in 1969, Bergersen and Pajanne calculated the effective mass of the positron, emphasizing nonlinear terms in the electron-positron interaction [102]. In 1986, Boronski and Nieminen introduced a local electron-positron correlation function [103]. In 1981, Chakraborty developed a formalism for self-consistent calculation of positron annihilation characteristics in real metals, taking into account electron-positron correlation effects [104]. Subsequently, various calculations were carried out to incorporate electron-positron correlation effects in metals and solids [105], [106]. Electron-positron correlation remains an active research area, with recent publications on the topic [107], [108].

Electron-proton correlation has been studied in scattered research efforts, such as estimating electron-proton correlation in a hydrogen atom as an entangled system using density matrix theory and von Neumann entropy [109], or investigating the effect of electron-proton correlation (especially proton movement) on hydrogen bonds in charge transfer processes within halogen-bridged complexes [110]. However, with the introduction of multi-component ab initio frameworks beyond the Born-Oppenheimer approximation, allowing for the treatment of the proton as a quantum particle, electron-proton correlation has received increased attention. One of the earliest papers in this area was

the calculation of electron-proton correlation in the hydrogen tunnelling process, published by Hammes-Schiffer and Pak in 2004 [54]. Since then, this correlation has been studied within perturbation theory frameworks [75], [111]–[113], and especially within multi-component density functional theory to develop a suitable functional for this correlation [70]–[72], [114].

Correlation of other particles, such as electron-muon correlation, has been primarily of interest in high-energy physics [115]. Recently, this correlation has entered the domain of multi-component density functional theory, and an initial functional for its calculation has been developed [73].

### 3.3 Mathematical Framework

#### 3.3.1 Pair Correlation Factor

The pair correlation factor is a measure for determining the degree of particle correlation, which is related to the two-particle density through the following relationship:

$$\Gamma(r_e, r_p) = \rho_e(r_e) \rho_p(r_p) [1 + \mathcal{F}(r_e, r_p)] \quad 3.4$$

In other words, the correlation factor indicates the deviation of the two-particle density from the product of the single-particle densities. This factor is related to the pair distribution function  $\mathcal{G}(r_e, r_p)$  through the following relationship:

$$\mathcal{G}(r_e, r_p) = 1 + \mathcal{F}(r_e, r_p) \quad 3.5$$

Based on equations (3-3), (3-4), and (3-5), we can write:

$$\mathcal{F}(r_e, r_p) = \frac{\Gamma(r_e, r_p)}{\rho_e(r_e) \rho_p(r_p)} - 1 = \frac{\Gamma_c(r_e, r_p)}{\rho_e(r_e) \rho_p(r_p)} \quad 3.6$$

$$\mathcal{G}(r_e, r_p) = \frac{\Gamma(r_e, r_p)}{\rho_e(r_e) \rho_p(r_p)} = \frac{\Gamma_c(r_e, r_p)}{\rho_e(r_e) \rho_p(r_p)} + 1 \quad 3.7$$

### 3.3.2 Correlation Hill

The correlation hill can be considered analogous to the correlation hole in electronic systems. In electronic systems, electron correlation or instantaneous interactions between two electrons lead to a depletion of density around one electron, creating a "correlation hole" around it [98]. In the EHM, due to the attractive interaction between two particles (in contrast to the repulsive interaction in electronic systems), instead of creating a hole around each particle, a hill is formed. In other words, the e-PCP correlation in a two-component system results in the accumulation of electron density around the positive particle or the accumulation of the positive particle density around the electron, creating a "correlation hill."

In electronic structure theory, the correlation hole is divided into two parts: the Fermi hole (or exchange hole) and the Coulomb hole (or correlation hole). The Fermi hole arises from the Pauli exclusion principle and exists for electrons with the same spin, while the Coulomb hole results from Coulomb repulsion between electrons. However, in the EHM, due to the distinguishability of the particles, only the Coulomb correlation hill is formed. Before presenting the mathematical framework of the correlation hill, a brief history of various definitions of the correlation hole is provided.

The quantities "correlation hole" [97], [116] and "exchange hole" [117] were first introduced by Coulson and Neilson in 1961. They defined these quantities inspired by the traditional definition of correlation energy in electronic structure theory as the difference between the exact and Hartree-Fock two-particle distribution functions (or inter-particle radial density). However, alternative definitions for these hole quantities were introduced in the 1960s, particularly in 1967 by McWeeny [118], [119]. In these definitions, instead of working with the correlation factor, which is a unitless quantity representing the difference between the two-particle density and the product of single-electron densities (equation 3-4), a new quantity called the "hole function" with the unit of single-electron density was introduced [120]. After the publication of the groundbreaking papers by Hohenberg, Kohn, and Sham [121], [122], and the birth of Density Functional Theory (DFT) in 1964, and given the better alignment of the recent hole definitions with this theory, notable papers examining various aspects of this hole definition within the DFT framework were published in subsequent years [122]–[134]. Valuable review articles on the nature and history of DFT and the development of the hole concept by prominent developers of this theory are available in references [135] and [136]. Coulson and Neilson's definitions were also used to some extent, especially within wavefunction-based frameworks [137], [138].

Since the primary goal of investigating e-PCP correlation in this study is to better understand it for developing an efficient functional within the DFT framework, we will use the appropriate correlation (hill) hole definition in DFT. However, two-particle distribution functions, mean, and variance of the two-particle distance will also be

analytically provided to gain a deeper understanding of e-PCP correlation.

In electronic systems, due to the identical nature of the two particles, there is only one type of hole. In contrast, in the two-component e-PCP system, due to the different nature of the particles (both in terms of charge and mass), two types of hills (one belonging to the electron and the other to the PCP) are formed.

Since the correlation hole and hill indicate the deviation of density around one particle interacting with a reference particle, we need a quantity that describes such a situation to define them. This quantity is called the conditional density, which indicates the probability of finding particle 2 at coordinates 2 around particle 1 (reference particle) if particle 1 is at coordinates 1. It is defined for the electron and PCP, respectively, as follows:

$$\rho^{cond}(r_e|r_p) = \frac{\Gamma(r_e, r_p)}{\rho_p(r_p)} \quad 3.8$$

$$\rho^{cond}(r_p|r_e) = \frac{\Gamma(r_e, r_p)}{\rho_e(r_e)} \quad 3.9$$

Therefore,  $\rho^{cond}(r_e|r_p)$  represents the probability of finding the electron at  $r_e$  given that the PCP is at  $r_p$  (and similarly for  $\rho^{cond}(r_p|r_e)$ ). Since  $\Gamma(r_e, r_p)$  can be decomposed as in equation (3-3), substituting (3-3) into (3-8) and (3-9) yields:

$$\rho^{cond}(r_e|r_p) = \rho_e(r_e) + \frac{\Gamma_c(r_e, r_p)}{\rho_p(r_p)} = \rho_e(r_e) + \rho_c^{hill}(r_e|r_p) \quad 3.10$$

$$\rho^{cond}(r_p|r_e) = \rho_p(r_p) + \frac{\Gamma_c(r_e, r_p)}{\rho_e(r_p)} = \rho_p(r_p) + \rho_c^{hill}(r_p|r_e) \quad 3.11$$

where  $\rho_c^{hill}(r_e|r_p)$  and  $\rho_c^{hill}(r_p|r_e)$  are the densities of the correlation hill for the electron and the PCP, respectively. Equations (3-10) and (3-11) demonstrate how the hill density deviates the conditional density from the single-particle density. Therefore, the correlation hills for the electron and PCP are defined as follows, respectively:

$$\begin{aligned} \rho_c^{hill}(r_e|r_p) &= \rho^{cond}(r_e|r_p) - \rho_e(r_e) = \frac{\Gamma(r_e, r_p)}{\rho_p(r_p)} - \rho_e(r_e) \\ &= \frac{\Gamma_c(r_e, r_p)}{\rho_p(r_p)} \end{aligned} \quad 3.12$$

$$\begin{aligned} \rho_c^{hill}(r_p|r_e) &= \rho^{cond}(r_p|r_e) - \rho_p(r_p) = \frac{\Gamma(r_e, r_p)}{\rho_e(r_e)} - \rho_p(r_p) \\ &= \frac{\Gamma_c(r_e, r_p)}{\rho_e(r_e)} \end{aligned} \quad 3.13$$

### 3.3.3 Correlation Hill Sum Rule

Since the two-particle density for a two-component system consisting of  $N$  electrons and  $N'$  PCPs is defined as in equation (3-2), integrating over it equals  $NN'$ . On the other hand, considering the decomposition of  $\Gamma(\mathbf{r}_e, \mathbf{r}_p)$  according to equation (3-3) and the correlation hill expressions (equations 3-12 and 3-13) for the electron and the PCP, we need to examine the integration over conditional densities and single-particle densities to derive the correlation hill sum rule.

Given that the integration over single-particle densities is:

$$\int \rho_e(r_e) d\mathbf{r}_e = N \quad 3.14$$

$$\int \rho_p(r_p) d\mathbf{r}_p = N' \quad 3.15$$

Integration over the conditional densities of the electron and the PCP (equations 3-8 and 3-9) results in the following:

$$\int \rho^{cond}(r_e|r_p) d\mathbf{r}_e = \int \frac{\Gamma(\mathbf{r}_e, \mathbf{r}_p)}{\rho_p(r_p)} d\mathbf{r}_e = \frac{N\rho_p(r_p)}{\rho_p(r_p)} = N \quad 3.16$$

$$\int \rho^{cond}(r_p|r_e) d\mathbf{r}_p = \int \frac{\Gamma(\mathbf{r}_e, \mathbf{r}_p)}{\rho_e(r_e)} d\mathbf{r}_p = \frac{\rho_e(r_e)N'}{\rho_e(r_e)} = N' \quad 3.17$$

Therefore, according to the above results and the correlation hill expressions (equations 3-12 and 3-13), the sum rule for them will be as follows:

$$\int \rho_c^{hill}(r_e|r_p) d\mathbf{r}_e = N - N = 0 \quad 3.18$$

$$\int \rho_c^{hill}(r_p|r_e) d\mathbf{r}_p = N' - N' = 0 \quad 3.19$$

### 3.3.4 Correlation Energy

The correlation energy of a system, which measures the degree of instantaneous interaction between two particles, can be defined in two ways: independent of an external reference and dependent on an external reference. The latter is further divided into two categories based on the type of external reference (Hartree-Fock or Kohn-Sham).



Independent correlation is defined uniformly across all approaches using only the two-particle density of the system  $\Gamma(r_e, r_p)$ . Based on equation (3-3), we can decompose the total interaction energy of two particles as follows:

$$\begin{aligned} W &= - \int \frac{\Gamma(r_e, r_p)}{r} d\mathbf{r}_e d\mathbf{r}_p \\ &= - \int \frac{\rho_e(r_e)\rho_p(r_p)}{r} d\mathbf{r}_e d\mathbf{r}_p - \int \frac{\Gamma_c(r_e, r_p)}{r} d\mathbf{r}_e d\mathbf{r}_p \end{aligned} \quad 3.20$$

For a two-component system consisting of electrons and PCPs, we can write it as follows:

$$\begin{aligned} W &= \int \rho_e(r_e) V_{coul}(r_e) d\mathbf{r}_e - \int \frac{\rho_e(r_e)\rho_c^{hill}(r_p|r_e)}{r} d\mathbf{r}_e d\mathbf{r}_p \\ &= \int \rho_p(r_p) V_{coul}(r_p) d\mathbf{r}_p \\ &\quad - \int \frac{\rho_p(r_p)\rho_c^{hill}(r_e|r_p)}{r} d\mathbf{r}_p d\mathbf{r}_e = W_{Coul} + W_c \end{aligned} \quad 3.21$$

where

$$V_{coul}(r_e) = v_e^{Jep}(r_e) = - \int \frac{\rho_p(r_p)}{|\mathbf{r}_e - \mathbf{r}_p|} d\mathbf{r}_p \quad 3.22$$

$$V_{coul}(r_p) = v_p^{Jep}(r_p) = - \int \frac{\rho_e(r_e)}{|\mathbf{r}_e - \mathbf{r}_p|} d\mathbf{r}_e \quad 3.23$$

These equations show that  $W_{Coul}$  is ultimately equal to  $J_{ep}$  (equation 1-62). Therefore, the independent correlation energy can be defined as follows:

$$W_c = W - W_{Coul} \quad 3.24$$

The traditional or external-reference-dependent correlation energy in the Hartree-Fock method is defined as the difference between the exact non-relativistic energy and the Hartree-Fock energy of the system:

$$E_c^{HF} = E_{exact} - E_{HF} \quad 3.25$$

This definition, which is the most common definition of correlation in electronic structure theory, is typically used to calculate the correlation energy using post-Hartree-Fock methods. If multi-component Hartree-Fock methods are employed, the above definition can be extended to multi-component systems. However, in this case, the calculated correlation energy is equal to the sum of all types of correlations present in the system. Separating these correlation contributions from one another in a unique manner is not possible and may vary depending on the reference definition [139]. Given that in the EHM we deal with e-PCP correlation, these complexities are not present here. To obtain the external-reference-dependent correlation energy in density functional theory, we start from the total energy functional of a two-component system consisting of an electron and a PCP (inspired by equation 1-48), defined as follows [140]:

$$\begin{aligned} E[\rho_e, \rho_p] = & \int \rho_e(\mathbf{r}_e) v_e^{ext}(\mathbf{r}_e) d\mathbf{r}_e \\ & + \int \rho_p(\mathbf{r}_p) v_p^{ext}(\mathbf{r}_p) d\mathbf{r}_p + F'[\rho_e, \rho_p] \end{aligned} \quad 3.26$$

where

$$F'[\rho_e, \rho_p] = (T_e[\rho_e] + T_p[\rho_p]) + J_{ep}[\rho_e, \rho_p] + W_c[\rho_e, \rho_p] \quad 3.27$$

On the other hand, by rewriting equation (1-59) and removing the exchange terms and interactions of similar particles, we get:

$$F[\rho_e, \rho_p] = (T_e^s[\rho_e] + T_p^s[\rho_p]) + J_{ep}[\rho_e, \rho_p] + E_{epc}[\rho_e, \rho_p] \quad 3.28$$

By equating the two equations (3-26) and the rewritten form of equation (1-58), we arrive at the following result:

$$\begin{aligned} E_{epc}[\rho_e, \rho_p] &= E_c^{KS} \\ &= (T_e[\rho_e] - T_e^s[\rho_e]) + (T_p[\rho_p] - T_p^s[\rho_p]) \\ &\quad + W_c[\rho_e, \rho_p] = T_e^c + T_p^c + W_c \end{aligned} \quad 3.29$$

where  $T_c$  represents the difference between the exact kinetic energy and the kinetic energy of the Kohn-Sham orbitals for the electron and the PCP.

On the other hand, the expectation value of the energy for the two-component system consisting of the electron and the PCP using the Kohn-Sham orbitals and the total system Hamiltonian (2-69) is defined as follows:

$$\begin{aligned} E_{KS} &= \langle \Psi_{ks} | \hat{H} | \Psi_{ks} \rangle \\ &= \int \rho_e(\mathbf{r}_e) v_e^{ext}(\mathbf{r}_e) d\mathbf{r}_e \\ &\quad + \int \rho_p(\mathbf{r}_p) v_p^{ext}(\mathbf{r}_p) d\mathbf{r}_p + F''[\rho_e, \rho_p] \end{aligned} \quad 3.30$$

where

$$F''[\rho_e, \rho_p] = (T_e^s[\rho_e] + T_p^s[\rho_p]) + J_{ep}[\rho_e, \rho_p] \quad 3.31$$

By comparing equations (3-30) and (3-26) or the rewritten form of equation (1-58), we arrive at the following final result:

$$E_c^{KS} = E_{exact} - E_{KS} \quad 3.32$$

Therefore, the external-reference-dependent correlation energy in density functional theory is also defined as the difference between the exact non-relativistic energy and the Kohn-Sham system energy. The values of the three defined correlation energies differ from one another. Since the Hartree-Fock determinant is the determinant with the lowest possible energy,  $E_{KS}$  must necessarily be greater than  $E_{HF}$ , and consequently, the DFT correlation energy should be more negative (larger in absolute value) than the HF correlation energy.

### 3.3.5 Two-Particle Distribution Functions

To gain a deeper understanding of the effects of e-PCP correlation, two-particle distribution functions can be used, as they contain the correlation information between the two particles. To define the two-particle distribution function, we express the expectation value of the distance between particles using the intermediate wavefunction (2-115) as follows:

$$\begin{aligned} \langle r \rangle &= \int_0^{2\pi} \int_0^\pi \int_0^\infty \int_0^{2\pi} \int_0^\infty \int_{|r_e-r|}^{r_e+r} r |\Psi(r, r_e, r_p)|^2 r_p r r_e dr_p dr d\chi \sin\theta_e dr_e d\theta_e d\phi_e \end{aligned} \quad 3.33$$

The above expression can be written as follows by introducing the distribution function  $f(r)$ :

$$\langle r \rangle = \int_0^\infty r f(r) dr \quad 3.34$$

This distribution function depends only on  $r$  and is averaged over all positions of the two particles. After integrating over the angular parts of (3-33), we have:

$$\langle r \rangle = \int_0^\infty r \underbrace{8\pi^2 \int_0^\infty \int_{|r_e-r|}^{r_e+r} |\Psi(r, r_e, r_p)|^2 r_p r r_e dr_p dr_e}_{f(r)} dr \quad 3.35$$

Using the normalization condition for  $f(r)$  and equation (2-164), we have:

$$\begin{aligned} \int_0^\infty f(r) dr &= 8\pi^2 \int_0^\infty \int_0^\infty \int_{|r_e-r|}^{r_e+r} |\Psi(r, r_e, r_p)|^2 r_p r r_e dr_p dr dr_e \\ &= 1 \end{aligned} \quad 3.36$$

Comparison of the above equation with equation (3-35) shows that the expression for  $f(r)$  is as follows:

$$f(r) = \int_0^\infty \underbrace{\int_{|r_e-r|}^{r_e+r} 8\pi^2 |\Psi(r, r_e, r_p)|^2 r_p r r_e dr_p}_{g(r, r_e)} dr_e \quad 3.37$$

In the above equation, by performing the inner integration over  $r_p$ , we obtain a local two-particle distribution function  $g(r, r_e)$ , which is as follows:

$$g(r, r_e) = \frac{2\pi^2 N^2 M r r_e e^{-2r(\alpha+\beta r)}}{\gamma m_p} \quad 3.38$$

$$\left( e^{-\frac{2\gamma((r_e-r)m_p+m_e r_e)^2}{M^2}} - e^{-\frac{2\gamma((r_e+r)m_p+m_e r_e)^2}{M^2}} \right)$$

This local distribution function provides a more precise picture of the correlation effect, as it is defined for different positions of the electron at  $r_e$  while considering the distance between the particles as  $r$ . Since this distribution function depends on both the distance between the particles and the location of the first particle, it will be different for the electron and the PCP.  $g(r, r_p)$  is also obtained as follows (by following the steps above):

$$g(r, r_p) = \frac{2\pi^2 N^2 M r r_p e^{-2r(\alpha+\beta r)}}{\gamma m_e} \quad 3.39$$

$$\left( e^{-\frac{2\gamma(m_e(r_p-r)+m_p r_p)^2}{M^2}} - e^{-\frac{2\gamma(m_e(r_p+r)+m_p r_p)^2}{M^2}} \right)$$

Before continuing with the calculations to obtain the average two-particle distribution function, it is interesting to note that the single-particle densities of the electron and the PCP (2-168 and 2-169) can be calculated as follows by performing the following operations on equations (3-38) and (3-39), respectively:

$$\begin{aligned} \rho_e(r_e) &= \frac{1}{4\pi r_e^2} \int_0^\infty g(r, r_e) dr \\ &= \frac{8\pi^2}{4\pi r_e^2} \int_0^\infty \int_{|r_e-r|}^{r_e+r} |\Psi(r, r_e, r_p)|^2 r_p r r_e dr_p dr \\ &= \frac{2\pi}{r_e} \int_0^\infty \int_{|r_e-r|}^{r_e+r} |\Psi(r, r_e, r_p)|^2 r_p r dr_p dr \end{aligned} \quad 3.40$$

$$\begin{aligned}
\rho_p(r_p) &= \frac{1}{4\pi r_p^2} \int_0^\infty g(r, r_p) dr \\
&= \frac{8\pi^2}{4\pi r_p^2} \int_0^\infty \int_{|r_p-r|}^{r_p+r} |\Psi(r, r_e, r_p)|^2 r_p r r_e dr_e dr \\
&= \frac{2\pi}{r_p} \int_0^\infty \int_{|r_p-r|}^{r_p+r} |\Psi(r, r_e, r_p)|^2 r_e r dr_e dr
\end{aligned} \tag{3.41}$$

Returning to equations (3-37), (3-38), and (3-39) and integrating over  $r_e$  and  $r_p$  respectively, we have:

$$f(r) = \int_0^\infty g(r, r_e) dr_e = \int_0^\infty g(r, r_p) dr_p \tag{3.42}$$

and we arrive at the final expression for the average two-particle distribution function:

$$f(r) = \frac{N^2 \sqrt{2} e^{-2r(\alpha+r\beta)} \pi^{5/2} r^2}{\gamma^{3/2}} \tag{3.43}$$

Using the definition of  $\langle r \rangle$  for the wave functions (2-17) and (2-18), we can write:

$$\begin{aligned}
\langle r \rangle &= \int \int \Psi(\mathbf{R}, \mathbf{r})^* r \Psi(\mathbf{R}, \mathbf{r}) d\mathbf{R} d\mathbf{r} \\
&= \int \int r |\eta_{klm}(\mathbf{R})|^2 |\chi_{k'l'm'}(\mathbf{r})|^2 d\mathbf{R} d\mathbf{r} \\
&= \int r |\chi_{k'l'm'}(\mathbf{r})|^2 d\mathbf{r} \\
&= \int_0^{2\pi} \int_0^\pi \int_0^\infty r r^2 |\chi_{k'l'm'}(\mathbf{r})|^2 \sin\theta_r dr d\theta_r d\phi_r \\
&= \int_0^\infty r \underbrace{4\pi r^2 |\chi_{k'l'm'}(\mathbf{r})|^2}_{f(r)} dr = \int_0^\infty r f(r) dr
\end{aligned} \tag{3.44}$$

where the fact that the wave function of the center-of-mass part has a spherical harmonic  $Y_{lm}(\theta, \phi)$  and is normalized as follows is utilized:

$$\begin{aligned}
& \int_0^\infty |\eta_{klm}(\mathbf{R})|^2 d\mathbf{R} \\
&= \int_0^{2\pi} \int_0^\pi \int_0^\infty R^2 |\eta_{klm}(\mathbf{R})|^2 \sin\theta_R dR d\theta_R d\phi_R \\
&= N_{lm}^2 \int_0^{2\pi} \int_0^\pi \int_0^\infty R^2 \tau_{lm}^2(R) Y_{lm}^2(\theta, \phi) \sin\theta_R dR d\theta_R d\phi_R = 1
\end{aligned} \tag{3.45}$$

Considering the form obtained for  $f(r)$  in equation (3-44), it can be used to calculate the two-particle interaction energy (and other components of the energy of the internal coordinates, i.e., equations 2-148 to 2-152) as follows:

$$\begin{aligned}
INT &= \int \int \Psi(\mathbf{R}, \mathbf{r})^* \left(-\frac{1}{r}\right) \Psi(\mathbf{R}, \mathbf{r}) d\mathbf{R} d\mathbf{r} \\
&= \int \int \left(-\frac{1}{r}\right) |\eta_{klm}(\mathbf{R})|^2 |\chi_{k'l'm'}(\mathbf{r})|^2 d\mathbf{R} d\mathbf{r} \\
&= \int \left(-\frac{1}{r}\right) |\chi_{k'l'm'}(\mathbf{r})|^2 d\mathbf{r} = - \int_0^\infty \frac{f(r)}{r} dr
\end{aligned} \tag{3.46}$$

which, after integration, yields:

$$INT = - \int_0^\infty \frac{f(r)}{r} dr = \frac{N^2 \pi^{5/2} (-2\sqrt{\beta} + e^{\frac{\alpha^2}{2\beta}} \sqrt{2\pi} \alpha \operatorname{Erfc}[\frac{\alpha}{\sqrt{2\beta}}])}{4\sqrt{2}(\beta\gamma)^{3/2}} \tag{3.47}$$

which is equal to the result of equation (2-152) after simplification (the results in Table 5-3 confirm this). Also, by differentiating equation (4-42) with respect to  $r$  and setting it to zero, the value of  $r$  at which  $f(r)$  is maximized is obtained as follows:



$$\frac{df(r)}{dr} = 0 \quad \Rightarrow \quad r_{max} = \frac{-\alpha + \sqrt{\alpha^2 + 8\beta}}{4\beta} \quad 3.48$$

### Differences in Two-Particle Distribution Functions

By subtracting the Hartree-Fock two-particle distribution functions from the exact two-particle distribution functions (obtained above), we arrive at the Coulson-Nielsen definition for the correlation hole. The difference in the local two-particle distribution function is defined as follows:

$$\Delta g(r, r_e) = g(r, r_e) - g_{HF}(r, r_e) \quad 3.49$$

and the difference in the average two-particle distribution function is as follows:

$$\Delta f(r) = f(r) - f_{HF}(r) \quad 3.50$$

The effects of correlation on the single-particle density can also be calculated as follows:

$$\Delta \rho(r) = \rho(r_e) - \rho_{HF}(r_e) \quad 3.51$$

### 3.3.6 Mean Inter-Particle Distance and Its Variance

Now, having the final expression for the two-particle distribution function  $f(r)$ , the mean inter-particle distance  $r$  can be calculated using equation (3-34). The desired integral can be solved analytically, and thus, the analytical form of the mean distance is obtained as follows:

$$\langle r \rangle = \frac{N^2 \pi^{5/2} (2\sqrt{\beta}(\alpha^2 + 2\beta) - e^{\frac{\alpha^2}{2\beta}} \sqrt{2\pi} \alpha (\alpha^2 + 3\beta) \text{Erfc}[\frac{\alpha}{\sqrt{2}\sqrt{\beta}}])}{16\sqrt{2}\beta^{7/2}\gamma^{3/2}} \quad 3.52$$

The variance of the inter-particle distance is also defined as follows:

$$S^2(r) = \int_0^\infty r^2 f(r) dr - \left( \int_0^\infty r f(r) dr \right)^2 \quad 3.53$$

The explicit form for it will be as follows:

$$\begin{aligned} S^2(r) = & \frac{1}{512\beta^7\gamma^3} N^2 \pi^{5/2} (-N^2 \pi^{5/2} (-2\sqrt{\beta}(\alpha^2 + 2\beta) \\ & + e^{\frac{\alpha^2}{2\beta}} \sqrt{2\pi} \alpha (\alpha^2 + 3\beta) \text{Erfc}[\frac{\alpha}{\sqrt{2}\sqrt{\beta}}])^2 \\ & + 8\sqrt{2}\beta^{5/2}\gamma^{3/2} (-2\alpha\sqrt{\beta}(\alpha^2 + 5\beta) + e^{\frac{\alpha^2}{2\beta}} \sqrt{2\pi}(\alpha^4 \\ & + 6\alpha^2\beta + 3\beta^2) \text{Erfc}[\frac{\alpha}{\sqrt{2}\sqrt{\beta}}])) \end{aligned} \quad 3.54$$

By using these two quantities, the width of the particle distribution can be compared under different conditions, and the degree of deviation from the mean inter-particle distance can be determined.

### 3.3.7 The Kato Condition

In the EHM, the Kato condition can be defined similarly to a two-electron system, as the derivative of the wave function with respect to the inter-particle distance at zero distance. This condition indicates the behavior of wave functions when the two particles coincide. To derive this condition in the EHM, after separating the center of mass and writing the wave function as a Taylor expansion [6] as follows and

applying the Hamiltonian (2-16) with the Laplacian operator in the form (2-142), we arrive at equation (3-56):

$$\Psi|_{r \rightarrow 0} = c_0 + c_1 r + c_2 r^2 + \dots \quad 3.55$$

$$H_r(\mathbf{r})\Psi = \left(\frac{c_1}{\mu} + c_0\right)\frac{1}{r} + \dots \quad 3.56$$

Therefore, for  $r \rightarrow 0$ , we have:

$$\frac{c_1}{\mu} = -c_0 \quad 3.57$$

and considering that:

$$c_1 = \left(\frac{\partial \Psi}{\partial r}\right)_{|r=0} \text{ , } c_0 = \Psi(r=0) \quad 3.58$$

we arrive at the following result:

$$\left(\frac{\partial \Psi}{\partial r}\right)_{|r=0} = -\mu \Psi(r=0) \quad 3.59$$

By applying the Kato condition to the wave function (2-101), we have:

$$\begin{aligned} \left(\frac{\partial \Psi}{\partial r}\right)_{|r=0} &= \frac{\partial[\exp(-\alpha r - \beta r^2 - \gamma R^2)]}{\partial r} = (-\alpha - 2\beta r)\Psi(r_e, r_p)|_{r=0} \\ &= -\alpha \Psi(r_e, r_p) \end{aligned} \quad 3.60$$

By comparing (3-59) and (3-60), we have:

$$\mu = \alpha \quad 3.61$$

Thus, if  $\alpha$  is equal to the reduced mass, the wave function (2-101) will satisfy the Kato condition. Numerical results for optimized  $\alpha$  and

the fitting results (sections 4-2 and 5-3) indicate that equation (3-61) is largely valid.

## 4 Numerical Data for Model Solution

### 4.1 Computational Details

All computations in this study are based on varying two parameters: the mass of the positive particle and the frequency of the oscillator field (in atomic units) over a wide range. These include ten different masses for the PCP, namely 1 (positron), 1.5, 2, 3, 10, 50, 207 (muon), 400, 900, and 1836 (proton), and nine frequencies that are arranged in the table below along with their equivalents in  $cm^{-1}$ .

Table 4-1: Range of frequencies used in the calculations of this study

Field Frequency in $\text{cm}^{-1}$	Field Frequency in Atomic Units
21.9	$10^{-4}$
219.4	$10^{-3}$
2194.7	$10^{-2}$
21947.5	$10^{-1}$
219474.6	1
$2.2 \times 10^6$	$10^1$
$2.2 \times 10^7$	$10^2$
$2.2 \times 10^8$	$10^3$
$2.2 \times 10^9$	$10^4$

This wide range of parameters allows for a more detailed examination of the system's behavior under various conditions. Thus, all calculations were performed for 90 systems. Additionally, to better scale the graphs, the relevant quantities are displayed based on the natural length of the system, which corresponds to the expected value of the inter-particle distance (equation 3-52). In numerical integrations using Mathematica, to obtain the most accurate result, depending on the problem's conditions, the "Working Precision" was set to 100

digits, the "Precision Goal" to 8 digits, and the "Max Recursion" to 20 times. The "Local Adaptive" and "Cartesian Rule" integration strategies were employed. Throughout the thesis, the accuracy of the results is reported to 6 decimal places. In all calculations, the absolute error refers to the difference between the exact value and the calculated value, and the percent error is given by the following relation:

$$\delta = \left| \frac{v_{computed} - v_{exact}}{v_{exact}} \right| * 100 \quad 4.1$$

In this study, three methods were used: variational, two-component Hartree-Fock (TC-HF), and finite element (all three methods were programmed in Mathematica). The first two methods have a variational nature, while the latter is a standard method for solving differential equations. It's worth mentioning that the variational and finite element methods were applied after separating the center of mass and for the  $\mu$  particle (although in the variational method, by adding the center of mass part to the variational wave function, the total wave function is obtained). On the other hand, the Hartree-Fock method was computed based on single-particle wave functions and the primary particle coordinates of the problem.

In this study, four methods were used: variational, two-component Hartree-Fock (TC-HF), two-component density functional theory (TC-DFT), and finite element (all four methods were programmed in Mathematica). The first three methods have a variational nature, while the latter is a standard method for solving differential equations. It's worth mentioning that the variational and finite element methods were applied after separating the center of mass and for the  $\mu$  pseudo-particles (although in the variational method, by adding the center of

mass part to the variational wave function, the total wave function is obtained). On the other hand, the Hartree-Fock method was computed based on single-particle wave functions and the primary particle coordinates of the problem.

The variational method has been fully explained in sections 2-3-2 to 2-3-5, and the TC-DFT method will be thoroughly examined in section 5-2. In the TC-HF computations for both the electron and the positive particle, the Gaussian 7s basis set (with functions placed at the bottom of potential wells) was used, denoted as [7s:7s], and all exponents were optimized for all masses and frequencies. It is worth noting that in energy calculations, the 7s basis set for both particles essentially represents the limit of the Hartree-Fock method, and extending the basis set to [7s7p7d: 7s7p7d] does not significantly improve the Hartree-Fock energy. On the other hand, the [7s:1s] basis set (7s for the electron and 1s for the PCP) was also used to more accurately investigate the changes in the exponents of PCPs and for subsequent applications.

To solve differential equations using the Finite Element Method (FEM), a discrete representation of a region, i.e., a mesh, is required. With the differential equation and boundary conditions specified, this method can be used to solve the equations. In our case, the region of interest ranges from  $r_{min} = 10^{-16}$  to  $r_{max} = 50$  in atomic units, meshed with intervals of 0.001. However, this meshing at a frequency of  $10^4$  reduced accuracy (see Figure B-1 in the appendix B), so intervals of  $10^{-4}$  were used at this frequency. The differential equation is the radial part of the Schrödinger equation (2-18), which goes to zero for  $r$  values less than  $r_{min}$ .



## 4.2 Optimized Variational Parameters

Without performing calculations, it can be easily seen that the variational parameters  $\alpha$  and  $\beta$  have a linear dependence on  $\mu$  by examining the asymptotic behavior of the variational wave function (see equations 2-73 and 2-74). However, as mentioned in section 2-3-1, we avoided separating  $\mu$  from the variational parameters for two reasons: 1) to maintain the simplicity of the wave function in subsequent calculations, and 2) to prevent  $\beta$  from approaching zero at very low frequencies, which would result in poor fitting behavior (since  $\beta$  tends to zero at very low frequencies, separating  $\mu$  would lead to zeros with infinite fitting error percentages). The optimized variational parameters with and without  $\mu$  are reported in Table 4-2.

Table 4-2: Optimized variational parameter values "with" and "without" consideration of the reduced mass, relative Hamiltonian energy, and their errors

$\omega$ /Quantities	$\mu$ included							$\mu$ excluded				
	$\alpha^1$	$\beta^2$	Variational Energy <sup>3</sup>	FEM Energy <sup>4</sup>	RMSD <sup>5</sup>	$\Delta E^6$	$(\beta/\alpha)^7$	$\alpha^8$	$\beta^9$	Variational Energy <sup>10</sup>	RMSD <sup>11</sup>	$\Delta E^{12}$
m = 1												
0.0001	0.500000	0.000000	-0.250000	-0.250000	0.000000	0.000000	0.000000	1.000000	0.000000	-0.250000	0.000000	0.000000
0.001	0.499997	0.000001	-0.249997	-0.249997	0.000000	0.000000	0.000003	0.999994	0.000003	-0.249997	0.000000	0.000000
0.01	0.499704	0.000149	-0.249701	-0.249701	0.000008	0.000000	0.000298	0.999407	0.000298	-0.249701	0.000008	0.000000
0.1	0.484707	0.010559	-0.223933	-0.223957	0.000314	-0.000024	0.021783	0.969414	0.021117	-0.223933	0.000314	-0.000024
1.0	0.438060	0.205107	0.612000	0.611853	0.000520	-0.000148	0.468217	0.876121	0.410215	0.612000	0.000520	-0.000148
10	0.414991	2.366272	12.395490	12.395303	0.000331	-0.000187	5.701982	0.829982	4.732543	12.395490	0.000331	-0.000187
100	0.407310	24.586618	141.942322	141.942127	0.000190	-0.000195	60.363374	0.814620	49.173238	141.942322	0.000190	-0.000195
1000	0.404950	248.701700	1474.690624	1474.690429	0.000108	-0.000195	614.154093	0.809723	497.405074	1474.690624	0.000108	-0.000195
10000	0.404560	2495.892300	14920.133739	14920.133541	0.000096	-0.000198	6169.399595	0.808173	4991.813767	14920.133739	0.000061	-0.000198
m = 1.5												
0.0001	0.600000	0.000000	-0.300000	-0.300000	0.000000	0.000000	0.000000	1.000000	0.000000	-0.300000	0.000000	0.000000
0.001	0.599997	0.000001	-0.299998	-0.299998	0.000000	0.000000	0.000002	0.999996	0.000003	-0.299998	0.000000	0.000000
0.01	0.599752	0.000149	-0.299750	-0.299750	0.000006	0.000000	0.000249	0.999587	0.000249	-0.299750	0.000006	0.000000
0.1	0.585320	0.011363	-0.277533	-0.277553	0.000290	-0.000020	0.019413	0.975533	0.018938	-0.277533	0.000290	-0.000020
1.0	0.529268	0.240597	0.516267	0.516098	0.000581	-0.000169	0.454585	0.882113	0.400996	0.516267	0.000581	-0.000169
10	0.499264	2.823673	12.137957	12.137735	0.000378	-0.000223	5.655669	0.832107	4.706122	12.137957	0.000378	-0.000223
100	0.489182	29.456033	141.164882	141.164648	0.000218	-0.000234	60.214909	0.815302	49.093389	141.164882	0.000218	-0.000234

$\mu$ included							$\mu$ excluded					
$\omega$ /Quantities	$\alpha^1$	$\beta^2$	Variational Energy <sup>3</sup>	FEM Energy <sup>4</sup>	RMSD <sup>5</sup>	$\Delta E^6$	$(\beta/\alpha)^7$	$\alpha^8$	$\beta^9$	Variational Energy <sup>10</sup>	RMSD <sup>11</sup>	$\Delta E^{12}$
1000	0.485964	298.293868	1472.266767	1472.266533	0.000123	-0.000234	613.818670	0.809940	497.156451	1472.266767	0.000123	-0.000234
10000	0.484945	2994.618890	14912.502746	14912.502509	0.000110	-0.000238	6175.176212	0.808241	4991.031476	14912.502746	0.000070	-0.000238
m=2												
0.0001	0.666667	0.000000	-0.333333	-0.333333	0.000000	0.000000	0.000000	1.000000	0.000000	-0.333333	0.000000	0.000000
0.001	0.666664	0.000002	-0.333331	-0.333331	0.000000	0.000000	0.000002	0.999997	0.000002	-0.333331	0.000000	0.000000
0.01	0.666443	0.000149	-0.333109	-0.333109	0.000005	0.000000	0.000224	0.999665	0.000224	-0.333109	0.000005	0.000000
0.1	0.652472	0.011795	-0.312780	-0.312797	0.000272	-0.000017	0.018077	0.978707	0.017692	-0.312780	0.000272	-0.000017
1.0	0.590509	0.263492	0.455715	0.455533	0.000619	-0.000182	0.446212	0.885764	0.395239	0.455715	0.000619	-0.000182
10	0.555616	3.126429	11.977247	11.977001	0.000408	-0.000246	5.626964	0.833423	4.689644	11.977247	0.000408	-0.000246
100	0.543817	32.695823	140.681475	140.681215	0.000236	-0.000260	60.122804	0.815726	49.043735	140.681475	0.000236	-0.000260
1000	0.540050	331.334674	1470.761234	1470.760975	0.000134	-0.000259	613.526230	0.810074	497.002015	1470.761234	0.000134	-0.000259
10000	0.538856	3327.030484	14907.764463	14907.764199	0.000119	-0.000264	6174.249590	0.808284	4990.545724	14907.764463	0.000075	-0.000264
m=3												
0.0001	0.750000	0.000000	-0.375000	-0.375000	0.000000	0.000000	0.000000	1.000000	0.000000	-0.375000	0.000000	0.000000
0.001	0.749998	0.000001	-0.374998	-0.374998	0.000000	0.000000	0.000002	0.999997	0.000002	-0.374998	0.000000	0.000000
0.01	0.749801	0.000150	-0.374800	-0.374800	0.000004	0.000000	0.000199	0.999735	0.000199	-0.374800	0.000004	0.000000
0.1	0.736443	0.012243	-0.356440	-0.356455	0.000252	-0.000015	0.016625	0.981924	0.016325	-0.356440	0.000252	-0.000015
1.0	0.667504	0.291304	0.383003	0.382805	0.000662	-0.000198	0.436408	0.890005	0.388406	0.383003	0.000662	-0.000198
10	0.626232	3.502570	11.786450	11.786175	0.000445	-0.000275	5.593084	0.834976	4.670093	11.786450	0.000445	-0.000275
100	0.612170	36.738719	140.109312	140.109020	0.000258	-0.000292	60.013926	0.816227	48.984959	140.109312	0.000258	-0.000292
1000	0.607675	372.614531	1468.980867	1468.980576	0.000146	-0.000291	613.180577	0.810234	496.819371	1468.980867	0.000146	-0.000291

$\mu$ included							$\mu$ excluded					
$\omega$ /Quantities	$\alpha^1$	$\beta^2$	Variational Energy <sup>3</sup>	FEM Energy <sup>4</sup>	RMSD <sup>5</sup>	$\Delta E^6$	$(\beta/\alpha)^7$	$\alpha^8$	$\beta^9$	Variational Energy <sup>10</sup>	RMSD <sup>11</sup>	$\Delta E^{12}$
10000	0.606251	3742.478585	14902.162752	14902.162455	0.000130	-0.000297	6173.155369	0.808335	4989.971417	14902.162750	0.000082	-0.000300
m = 10												
0.0001	0.909091	0.000000	-0.454545	-0.454545	0.000000	0.000000	0.000000	1.000000	0.000000	-0.454545	0.000000	0.000000
0.001	0.909089	0.000002	-0.454544	-0.454544	0.000000	0.000000	0.000002	0.999998	0.000002	-0.454544	0.000000	0.000000
0.01	0.908926	0.000150	-0.454381	-0.454381	0.000003	0.000000	0.000165	0.999819	0.000165	-0.454381	0.000003	0.000000
0.1	0.896744	0.012890	-0.438912	-0.438923	0.000216	-0.000011	0.014375	0.986419	0.014179	-0.438912	0.000216	-0.000011
1.0	0.815719	0.342079	0.251539	0.251315	0.000736	-0.000224	0.419359	0.897291	0.376287	0.251539	0.000736	-0.000224
10	0.761549	4.213996	11.447417	11.447087	0.000511	-0.000330	5.533453	0.837710	4.635388	11.447417	0.000511	-0.000330
100	0.742795	44.437386	139.097263	139.096910	0.000297	-0.000353	59.824535	0.817110	48.880985	139.097263	0.000297	-0.000353
1000	0.736831	451.360667	1465.835951	1465.835599	0.000168	-0.000351	612.570377	0.810515	496.496718	1465.835951	0.000168	-0.000351
10000	0.734930	4535.415827	14892.271732	14892.271372	0.000150	-0.000360	6171.223622	0.808423	4988.957410	14892.271732	0.000095	-0.000360
m = 50												
0.0001	0.980392	0.000000	-0.490196	-0.490196	0.000000	0.000000	0.000000	1.000000	0.000000	-0.490196	0.000000	0.000000
0.001	0.980391	0.000001	-0.490195	-0.490195	0.000000	0.000000	0.000002	0.999998	0.000002	-0.490195	0.000000	0.000000
0.01	0.980240	0.000150	-0.490043	-0.490043	0.000003	0.000000	0.000153	0.999844	0.000153	-0.490043	0.000003	0.000000
0.1	0.968561	0.013113	-0.475603	-0.475612	0.000201	-0.000009	0.013539	0.987933	0.013376	-0.475603	0.000201	-0.000009
1.0	0.882615	0.363909	0.195169	0.194935	0.000765	-0.000234	0.412308	0.900267	0.371188	0.195169	0.000765	-0.000234
10	0.822405	4.530152	11.304325	11.303970	0.000540	-0.000355	5.508419	0.838853	4.620756	11.304325	0.000540	-0.000355
100	0.801451	47.879691	138.671901	138.671520	0.000314	-0.000380	59.741281	0.817480	48.837283	138.671901	0.000314	-0.000380
1000	0.794737	486.628702	1464.515756	1464.515378	0.000178	-0.000378	612.313953	0.810632	496.361283	1464.515756	0.000178	-0.000378
10000	0.792600	4890.717855	14888.121166	14888.120778	0.000159	-0.000388	6170.471104	0.808460	4988.531880	14888.121166	0.000100	-0.000388

$\mu$ included							$\mu$ excluded					
$\omega$ /Quantities	$\alpha^1$	$\beta^2$	Variational Energy <sup>3</sup>	FEM Energy <sup>4</sup>	RMSD <sup>5</sup>	$\Delta E^6$	$(\beta/\alpha)^7$	$\alpha^8$	$\beta^9$	Variational Energy <sup>10</sup>	RMSD <sup>11</sup>	$\Delta E^{12}$
m = 207												
0.0001	0.995192	0.000000	-0.497596	-0.497596	0.000000	0.000000	0.000000	1.000000	0.000000	-0.497596	0.000000	0.000000
0.001	0.995191	0.000001	-0.497595	-0.497595	0.000000	0.000000	0.000002	0.999998	0.000002	-0.497595	0.000000	0.000000
0.01	0.995042	0.000150	-0.497446	-0.497446	0.000003	0.000000	0.000150	0.999850	0.000150	-0.498603	0.000003	0.000000
0.1	0.983465	0.013155	-0.483202	-0.483212	0.000199	-0.000009	0.013377	0.988260	0.013195	-0.484390	0.000198	-0.000009
1.0	0.896535	0.368372	0.183638	0.183403	0.000771	-0.000236	0.410884	0.900959	0.369991	0.181841	0.000772	-0.000236
10	0.835051	4.595580	11.275221	11.274861	0.000546	-0.000360	5.503352	0.839085	4.617781	11.275221	0.000546	-0.000360
100	0.813624	48.593656	138.585513	138.585127	0.000318	-0.000386	59.724929	0.817555	48.828408	138.585513	0.000318	-0.000386
1000	0.806758	493.947566	1464.247752	1464.247368	0.000180	-0.000384	612.262366	0.810655	496.333788	1464.247752	0.000180	-0.000384
10000	0.804581	4964.462597	14887.278700	14887.278307	0.000161	-0.000394	6170.248554	0.808469	4988.432061	14887.147551	0.000102	-0.000395
m = 400												
0.0001	0.997506	0.000000	-0.498753	-0.498753	0.000000	0.000000	0.000000	1.000000	0.000000	-0.498753	0.000000	0.000000
0.001	0.997505	0.000001	-0.498752	-0.498752	0.000000	0.000000	0.000001	0.999998	0.000002	-0.498752	0.000000	0.000000
0.01	0.997356	0.000150	-0.498603	-0.498603	0.000003	0.000000	0.000150	0.999850	0.000150	-0.498603	0.000003	0.000000
0.1	0.985796	0.013162	-0.484390	-0.484399	0.000198	-0.000009	0.013351	0.988260	0.013195	-0.484390	0.000198	-0.000009
1.0	0.898713	0.369068	0.181841	0.181605	0.000772	-0.000236	0.410663	0.900959	0.369991	0.181841	0.000772	-0.000236
10	0.837029	4.605803	11.270688	11.270328	0.000546	-0.000360	5.502564	0.839121	4.617317	11.270688	0.000546	-0.000360
100	0.815527	48.705265	138.572063	138.571677	0.000318	-0.000387	59.722424	0.817567	48.827026	138.572063	0.000318	-0.000387
1000	0.808637	495.091782	1464.206030	1464.205645	0.000181	-0.000385	612.254559	0.810659	496.329506	1464.206030	0.000181	-0.000385
10000	0.806453	4975.992079	14887.147551	14887.147157	0.000161	-0.000395	6170.223253	0.808469	4988.432061	14887.147551	0.000102	-0.000395
m = 900												

$\mu$ included							$\mu$ excluded					
$\omega$ /Quantities	$\alpha^1$	$\beta^2$	Variational Energy <sup>3</sup>	FEM Energy <sup>4</sup>	RMSD <sup>5</sup>	$\Delta E^6$	$(\beta/\alpha)^7$	$\alpha^8$	$\beta^9$	Variational Energy <sup>10</sup>	RMSD <sup>11</sup>	$\Delta E^{12}$
0.0001	0.998890	0.000000	-0.499445	-0.499445	0.000000	0.000000	0.000000	1.000000	0.000000	-0.499445	0.000000	0.000000
0.001	0.998889	0.000001	-0.499444	-0.499444	0.000000	0.000000	0.000001	0.999998	0.000002	-0.499444	0.000000	0.000000
0.01	0.998740	0.000150	-0.499295	-0.499295	0.000003	0.000000	0.000150	0.999850	0.000150	-0.499295	0.000003	0.000000
0.1	0.987190	0.013166	-0.485100	-0.485109	0.000198	-0.000009	0.013336	0.988286	0.013180	-0.485100	0.000198	-0.000009
1.0	0.900015	0.369483	0.180766	0.180530	0.000772	-0.000236	0.410530	0.901014	0.369894	0.180766	0.000772	-0.000236
10	0.838211	4.611916	11.267980	11.267619	0.000547	-0.000361	5.502092	0.839143	4.617041	11.267980	0.000547	-0.000361
100	0.816666	48.772012	138.564027	138.563640	0.000319	-0.000387	59.720902	0.817574	48.826200	138.564027	0.000319	-0.000387
1000	0.809761	495.776091	1464.181100	1464.180715	0.000181	-0.000385	612.249716	0.810661	496.326955	1464.181100	0.000181	-0.000385
10000	0.807572	4982.887482	14887.069188	14887.068792	0.000161	-0.000395	6170.207675	0.808469	4988.424026	14887.069188	0.000102	-0.000395
m = 1836												
0.0001	0.999456	0.000000	-0.499728	-0.499728	0.000000	0.000000	0.000000	1.000000	0.000000	-0.499728	0.000000	0.000000
0.001	0.999454	0.000002	-0.499726	-0.499726	0.000000	0.000000	0.000002	0.999998	0.000002	-0.499726	0.000000	0.000000
0.01	0.999306	0.000150	-0.499578	-0.499578	0.000003	0.000000	0.000150	0.999850	0.000150	-0.499578	0.000003	0.000000
0.1	0.987759	0.013167	-0.485391	-0.485400	0.000198	-0.000009	0.013331	0.988296	0.013175	-0.485391	0.000198	-0.000009
1.0	0.900546	0.369653	0.180327	0.180091	0.000772	-0.000236	0.410477	0.901037	0.369855	0.180327	0.000772	-0.000236
10	0.838695	4.614414	11.266873	11.266512	0.000547	-0.000361	5.501900	0.839152	4.616927	11.266873	0.000547	-0.000361
100	0.817131	48.799286	138.560744	138.560357	0.000319	-0.000388	59.720281	0.817577	48.825863	138.560744	0.000319	-0.000388
1000	0.810221	496.055714	1464.170918	1464.170533	0.000181	-0.000385	612.247098	0.810662	496.325903	1464.170918	0.000181	-0.000385
10000	0.808030	4985.705219	14887.037181	14887.036785	0.000161	-0.000395	6170.201461	0.808470	4988.420744	14887.037181	0.000102	-0.000395

1. Variational parameter  $\alpha$  considering reduced mass
2. Variational parameter  $\beta$  considering reduced mass

3. Internal variational energy of the system using parameters 1 and 2
4. FEM relative Hamiltonian energy
5. Root Mean Square error for the variational wave function with parameters 1 and 2 relative to the wave function obtained from fem (the error equation is  $\sqrt{\frac{1}{n}(\sum_n(\psi_{var} - \psi_{FEM}))^2}$ , where n indicates the number of points at which the wave functions were calculated)
6. Energy difference between 3 and 4
7. Ratio of parameter 2 to 1 ( $\beta/\alpha$ )
8. Variational parameter  $\alpha$  without considering reduced mass
9. Variational parameter  $\beta$  without considering reduced mass
10. Internal variational energy of the system using parameters 8 and 9
11. Root Mean Square error for the variational wave function with parameters 8 and 9 relative to the wave function obtained from FEM
12. Energy difference between 4 and 10

### 4.3 Energy and Its Components

Table 4-3 contains the total system energy data as well as the correlation energies. In this table, the total system energy is first presented using the variational method, FEM, and MC-HF (two basis sets [7s:7s] and [7s:1s]), followed by the correlation energies. The total system energy equals the sum of the relative Hamiltonian and the center of mass energies (equation 2-25). The absolute error and percentage error of the variational energy compared to the FEM energy, as well as the MC-HF/[7s:1s] energy compared to the MC-HF/[7s:7s], are also reported. The percentage error of the variational energy compared to the FEM-derived energy reaches about 0.03% in the worst-case scenario, indicating that the variational energy closely approaches the desired limit. The energy values of the wave function (2-75) and their errors for several masses are provided in Table B-1 in the appendix B, showing that this wave function has less accuracy compared to wave function (2-72).



Table 4-3: Total energy, correlation energy, and errors obtained from various methods

$\omega$ /Quantities	Total Energy				Correlation Energy		Error of variational energy		Error of $[7s:1s]$ Basis Set	
	Variational <sup>1</sup>	FEM <sup>2</sup>	MC-HF/ $[7s:7s]^3$	MC-HF/ $[7s:1s]^4$	VAR-HF <sup>5</sup>	FEM-HF <sup>6</sup>	Delta E <sup>7</sup>	% error <sup>8</sup>	Delta E <sup>9</sup>	% error <sup>10</sup>
m = 1										
0.0001	-0.249850	-0.249850	-0.108513	-0.107219	-0.141337	-0.141337	0.000000	0.000000	-0.001294	1.192040
0.001	-0.248497	-0.248497	-0.108491	-0.107198	-0.140006	-0.140006	0.000000	0.000000	-0.001293	1.192142
0.01	-0.234701	-0.234701	-0.106407	-0.105127	-0.128294	-0.128294	0.000000	0.000006	-0.001280	1.202684
0.1	-0.073933	-0.073957	0.012203	0.013286	-0.086137	-0.086160	-0.000024	0.031779	-0.001083	8.875661
1.0	2.112000	2.111853	2.171918	2.172834	-0.059918	-0.060066	-0.000148	0.006987	-0.000915	0.042140
10	27.395490	27.395303	27.448072	27.448929	-0.052581	-0.052768	-0.000187	0.000682	-0.000858	0.003125
100	291.942322	291.942127	291.992777	291.993616	-0.050455	-0.050650	-0.000195	0.000067	-0.000839	0.000287
1000	2974.690624	2974.690429	2974.740427	2974.741261	-0.049803	-0.049998	-0.000195	0.000007	-0.000834	0.000028
10000	29920.133739	29920.133541	29920.183344	29920.184180	-0.049605	-0.049804	-0.000198	0.000001	-0.000836	0.000003
m = 1.5										
0.0001	-0.299850	-0.299850	-0.131661	-0.130508	-0.168189	-0.168189	0.000000	0.000000	-0.001154	0.876152
0.001	-0.298498	-0.298498	-0.131644	-0.130490	-0.166854	-0.166854	0.000000	0.000000	-0.001153	0.876104
0.01	-0.284750	-0.284750	-0.129900	-0.128764	-0.154850	-0.154850	0.000000	0.000003	-0.001137	0.875116
0.1	-0.127533	-0.127553	-0.021539	-0.020706	-0.105994	-0.106014	-0.000020	0.015364	-0.000833	3.866629
1.0	2.016267	2.016098	2.087757	2.088293	-0.071490	-0.071659	-0.000169	0.008391	-0.000537	0.025698
10	27.137957	27.137735	27.199613	27.200050	-0.061655	-0.061878	-0.000223	0.000820	-0.000437	0.001607
100	291.164882	291.164648	291.223701	291.224105	-0.058820	-0.059054	-0.000234	0.000080	-0.000403	0.000139
1000	2972.266767	2972.266533	2972.324714	2972.325111	-0.057948	-0.058182	-0.000234	0.000008	-0.000396	0.000013

$\omega$ /Quantities	Total Energy				Correlation Energy		Error of variational energy		Error of $[7s:1s]$ Basis Set	
	Variational <sup>1</sup>	FEM <sup>2</sup>	MC-HF/ $[7s:7s]^3$	MC-HF/ $[7s:1s]^4$	VAR-HF <sup>5</sup>	FEM-HF <sup>6</sup>	Delta E <sup>7</sup>	% error <sup>8</sup>	Delta E <sup>9</sup>	% error <sup>10</sup>
10000	29912.502746	29912.502509	29912.560519	29912.560821	-0.057773	-0.058010	-0.000238	0.000001	-0.000302	0.000001
m = 2										
0.0001	-0.333183	-0.333183	-0.149328	-0.148287	-0.183855	-0.183855	0.000000	0.000000	-0.001041	0.696899
0.001	-0.331831	-0.331831	-0.149312	-0.148272	-0.182519	-0.182519	0.000000	0.000000	-0.001040	0.696854
0.01	-0.318109	-0.318109	-0.147746	-0.146721	-0.170363	-0.170363	0.000000	0.000002	-0.001024	0.693148
0.1	-0.162780	-0.162797	-0.045426	-0.044742	-0.117354	-0.117372	-0.000017	0.010597	-0.000684	1.505567
1.0	1.955715	1.955533	2.032554	2.032903	-0.076839	-0.077021	-0.000182	0.009328	-0.000349	0.017167
10	26.977247	26.977001	27.042353	27.042601	-0.065106	-0.065352	-0.000246	0.000912	-0.000248	0.000918
100	290.681475	290.681215	290.743202	290.743417	-0.061727	-0.061987	-0.000260	0.000089	-0.000215	0.000074
1000	2970.761234	2970.760975	2970.821923	2970.822132	-0.060689	-0.060948	-0.000259	0.000009	-0.000210	0.000007
10000	29907.764463	29907.764199	29907.824832	29907.825035	-0.060368	-0.060632	-0.000264	0.000001	-0.000204	0.000001
m = 3										
0.0001	-0.374850	-0.374850	-0.175573	-0.174698	-0.199277	-0.199277	0.000000	0.000000	-0.000875	0.498326
0.001	-0.373498	-0.373498	-0.175559	-0.174685	-0.197939	-0.197939	0.000000	0.000000	-0.000875	0.498281
0.01	-0.359800	-0.359800	-0.174173	-0.173313	-0.185627	-0.185627	0.000000	0.000001	-0.000860	0.493645
0.1	-0.206440	-0.206455	-0.078661	-0.078151	-0.127779	-0.127794	-0.000015	0.007104	-0.000510	0.648306
1.0	1.883003	1.882805	1.962394	1.962573	-0.079392	-0.079589	-0.000198	0.010503	-0.000179	0.009118
10	26.786450	26.786175	26.851598	26.851698	-0.065147	-0.065423	-0.000275	0.001028	-0.000100	0.000372
100	290.109312	290.109020	290.170376	290.170453	-0.061064	-0.061356	-0.000292	0.000101	-0.000077	0.000026
1000	2968.980867	2968.980576	2969.040682	2969.040755	-0.059814	-0.060105	-0.000291	0.000010	-0.000074	0.000002
10000	29902.162752	29902.162455	29902.222187	29902.222260	-0.059435	-0.059732	-0.000297	0.000001	-0.000073	0.000000

Total Energy					Correlation Energy		Error of variational energy		Error of [7s:1s] Basis Set	
$\omega$ /Quantities	Variational <sub>1</sub>	FEM <sup>2</sup>	MC-HF/[7s:7s] <sup>3</sup>	MC-HF/[7s:1s] <sup>4</sup>	VAR-HF <sup>5</sup>	FEM-HF <sup>6</sup>	Delta E <sup>7</sup>	% error <sup>8</sup>	Delta E <sup>9</sup>	% error <sup>10</sup>
m = 10										
0.0001	-0.454395	-0.454395	-0.257049	-0.256606	-0.197347	-0.197347	0.000000	0.000000	-0.000443	0.172147
0.001	-0.453044	-0.453044	-0.257037	-0.256595	-0.196007	-0.196007	0.000000	0.000000	-0.000442	0.172111
0.01	-0.439381	-0.439381	-0.255878	-0.255445	-0.183502	-0.183502	0.000000	0.000001	-0.000433	0.169154
0.1	-0.288912	-0.288923	-0.170118	-0.169934	-0.118794	-0.118805	-0.000011	0.003727	-0.000184	0.108200
1.0	1.751539	1.751315	1.810873	1.810890	-0.059334	-0.059557	-0.000224	0.012763	-0.000018	0.000971
10	26.447417	26.447087	26.490355	26.490359	-0.042938	-0.043268	-0.000330	0.001249	-0.000004	0.000014
100	289.097263	289.096910	289.135811	289.135812	-0.038548	-0.038901	-0.000353	0.000122	-0.000001	0.000000
1000	2965.835951	2965.835599	2965.873207	2965.873195	-0.037256	-0.037607	-0.000351	0.000012	0.000012	0.000000
10000	29892.271732	29892.271372	29892.308661	29892.308574	-0.036929	-0.037289	-0.000360	0.000001	0.000088	0.000000
m = 50										
0.0001	-0.490046	-0.490046	-0.353887	-0.353752	-0.136159	-0.136159	0.000000	0.000000	-0.000135	0.038033
0.001	-0.488695	-0.488695	-0.353874	-0.353739	-0.134821	-0.134821	0.000000	0.000000	-0.000135	0.038020
0.01	-0.475043	-0.475043	-0.352583	-0.352453	-0.122460	-0.122460	0.000000	0.000000	-0.000129	0.036671
0.1	-0.325603	-0.325612	-0.261510	-0.261482	-0.064093	-0.064103	-0.000009	0.002887	-0.000028	0.010724
1.0	1.695169	1.694935	1.717273	1.717273	-0.022104	-0.022337	-0.000234	0.013787	0.000000	0.000023
10	26.304325	26.303970	26.317887	26.317887	-0.013563	-0.013917	-0.000355	0.001348	0.000000	0.000000
100	288.671901	288.671520	288.683473	288.683473	-0.011572	-0.011953	-0.000380	0.000132	0.000000	0.000000
1000	2964.515756	2964.515378	2964.526763	2964.526763	-0.011007	-0.011385	-0.000378	0.000013	0.000000	0.000000
10000	29888.121166	29888.120778	29888.132005	29888.132001	-0.010839	-0.011227	-0.000388	0.000001	0.000004	0.000000
m = 207										

$\omega$ / Quantities	Total Energy				Correlation Energy		Error of variational energy		Error of $[7s:1s]$ Basis Set	
	Variational <sub>1</sub>	FEM <sup>2</sup>	MC-HF/ $[7s:7s]^3$	MC-HF/ $[7s:1s]^4$	VAR-HF <sup>5</sup>	FEM-HF <sup>6</sup>	Delta E <sup>7</sup>	% error <sup>8</sup>	Delta E <sup>9</sup>	% error <sup>10</sup>
0.0001	-0.497446	-0.497446	-0.414686143	-0.414646	-0.082760	-0.082760	0.000000	0.000000	-0.000040	0.009689
0.001	-0.496095	-0.496095	-0.414668065	-0.414628	-0.081427	-0.081427	0.000000	0.000000	-0.000040	0.009680
0.01	-0.482446	-0.482446	-0.412886483	-0.412850	-0.069560	-0.069560	0.000000	0.000000	-0.000037	0.008883
0.1	-0.333202	-0.333212	-0.306618117	-0.306615	-0.026584	-0.026594	-0.000010	0.003001	-0.000003	0.000873
1.0	1.683638441	1.683402758	1.690371599	1.690372	-0.006733	-0.006969	-0.000236	0.014000	0.000000	0.000004
10	26.27522077	26.27486117	26.27886233	26.278862	-0.003642	-0.004001	-0.000360	0.001369	0.000000	0.000000
100	288.5855131	288.5851272	288.5884904	288.588490	-0.002977	-0.003363	-0.000386	0.000134	0.000000	0.000000
1000	2964.247752	2964.247368	2964.250545	2964.250545	-0.002793	-0.003177	-0.000384	0.000013	0.000000	0.000000
10000	29887.2787	29887.27831	29887.28145	29887.281444	-0.002747	-0.003137	-0.000390	0.000001	0.000003	0.000000
m = 400										
0.0001	-0.498603	-0.498603	-0.434898	-0.434876	-0.063705	-0.063705	0.000000	0.000000	-0.000022	0.005113
0.001	-0.497252	-0.497252	-0.434876	-0.434854	-0.062375	-0.062375	0.000000	0.000000	-0.000022	0.005106
0.01	-0.483603	-0.483603	-0.432709	-0.432689	-0.050894	-0.050894	0.000000	0.000000	-0.000019	0.004457
0.1	-0.334390	-0.334399	-0.318137	-0.318136	-0.016254	-0.016263	-0.000009	0.002722	-0.000001	0.000185
1.0	1.681841	1.681605	1.685464	1.685464	-0.003624	-0.003860	-0.000236	0.014034	0.000000	0.000008
10	26.270688	26.270328	26.272493	26.272492	-0.001804	-0.002165	-0.000360	0.001372	0.000000	0.000000
100	288.572063	288.571677	288.573488	288.573487	-0.001424	-0.001811	-0.000387	0.000134	0.000000	0.000000
1000	2964.206030	2964.205645	2964.207347	2964.207347	-0.001317	-0.001702	-0.000385	0.000013	0.000000	0.000000
10000	29887.147551	29887.147157	29887.148995	29887.148842	-0.001443	-0.001838	-0.000395	0.000001	0.000153	0.000001
m = 900										
0.0001	-0.499295	-0.499295	-0.453975	-0.453965	-0.045320	-0.045320	0.000000	0.000000	-0.000011	0.002314

$\omega$ / Quantities	Total Energy				Correlation Energy		Error of variational energy		Error of $[7s:1s]$ Basis Set	
	Variational <sup>1</sup>	FEM <sup>2</sup>	MC-HF/ $[7s:7s]^3$	MC-HF/ $[7s:1s]^4$	VAR-HF <sup>5</sup>	FEM-HF <sup>6</sup>	Delta E <sup>7</sup>	% error <sup>8</sup>	Delta E <sup>9</sup>	% error <sup>10</sup>
0.001	-0.497944	-0.497944	-0.453946	-0.453935	-0.043998	-0.043998	0.000000	0.000000	-0.000010	0.002307
0.01	-0.484295	-0.484295	-0.451115	-0.451106	-0.033180	-0.033180	0.000000	0.000000	-0.000008	0.001805
0.1	-0.335100	-0.335109	-0.326729	-0.326729	-0.008372	-0.008381	-0.000009	0.002709	0.000000	0.000093
1.0	1.680766	1.680530	1.682345	1.682345	-0.001579	-0.001815	-0.000236	0.014054	0.000000	0.000014
10	26.267980	26.267619	26.268617	26.268617	-0.000638	-0.000999	-0.000361	0.001374	0.000000	0.000000
100	288.564027	288.563640	288.564475	288.564474	-0.000448	-0.000835	-0.000387	0.000134	0.000000	0.000000
1000	2964.181100	2964.180715	2964.181492	2964.181491	-0.000391	-0.000777	-0.000385	0.000013	0.000001	0.000000
10000	29887.069188	29887.068792	29887.069700	29887.069698	-0.000512	-0.000907	-0.000395	0.000001	0.000001	0.000000
m = 1836										
0.0001	-0.499578	-0.499578	-0.466417	-0.466412	-0.033161	-0.033161	0.000000	0.000000	-0.000005	0.001139
0.001	-0.498226	-0.498226	-0.466378	-0.466373	-0.031848	-0.031848	0.000000	0.000000	-0.000005	0.001134
0.01	-0.484578	-0.484578	-0.462753	-0.462749	-0.021825	-0.021825	0.000000	0.000000	-0.000003	0.000743
0.1	-0.335391	-0.335400	-0.330905	-0.330906	-0.004486	-0.004495	-0.000009	0.002704	0.000001	0.000382
1.0	1.680327	1.680091	1.681012	1.681011	-0.000684	-0.000921	-0.000236	0.014062	0.000000	0.000013
10	26.266873	26.266512	26.267013	26.267013	-0.000140	-0.000501	-0.000361	0.001375	0.000000	0.000000
100	288.560744	288.560357	288.560779	288.560778	-0.000035	-0.000422	-0.000388	0.000134	0.000000	0.000000
1000	2964.170918	2964.170533	2964.170918	2964.170916	0.000000	-0.000385	-0.000385	0.000013	0.000002	0.000000
10000	29887.037181	29887.036785	29887.037312	29887.037312	-0.000132	-0.000527	-0.000395	0.000001	0.000000	0.000000

1. Total variational energy, including the sum of relative and center of mass energies      2. FEM relative Hamiltonian energy plus center of mass Hamiltonian energy

3. Total MC-HF energy with basis Set [7s:7s]
4. Total MC-HF energy with basis Set [7s:1s]
5. Correlation energy obtained from the difference between the total energy calculated using the variational method compared to MC-HF/[7s:7s]
6. Correlation energy obtained from the difference between the total energy calculated using FEM compared to MC-HF/[7s:7s]
7. Difference between total variational and FEM Energy
8. Percentage error of variational energy compared to FEM energy
9. Difference between total MC-HF energy with [7s:1s] and [7s:7s] basis sets
10. Percentage error of MC-HF energy with [7s:1s] compared to [7s:7s]

The components of the total energy (kinetic energy, harmonic oscillator potential energy, and Coulomb interaction potential energy) for the variational and HF methods are reported in Table 4-4. These components can be presented in two ways: single-particle (section 2-5-1) and pseudo-particle (section 2-5-2), according to the following equations, respectively.

$$E = \langle T_e \rangle + \langle T_p \rangle + \langle HO_e \rangle + \langle HO_p \rangle + \langle INT_{ep} \rangle \quad 4.2$$

$$E = \langle T_R \rangle + \langle T_r \rangle + \langle HO_R \rangle + \langle HO_r \rangle + \langle INT_r \rangle \quad 4.3$$

Items 1 to 8 in the table indicate the single-particle components of the variational energy, items 9 to 15 represent the pseudo-particle components of the variational energy, and items 17 to 24 contain the single-particle components of the HF energy. The sum of the energy components must be equal in both single-particle and pseudo-particle systems. Additionally, the electron-positive particle interaction energy is the same in both systems:

$$\langle T_e \rangle + \langle T_p \rangle = \langle T_R \rangle + \langle T_r \rangle \quad 4.4$$

$$\langle HO_e \rangle + \langle HO_p \rangle = \langle HO_R \rangle + \langle HO_r \rangle \quad 4.5$$

$$\langle INT_{ep} \rangle = \langle INT_r \rangle \quad 4.6$$

The data indicate that the above equations hold true, with the maximum error being on the order of one-thousandth of a percent. Additionally, the virial ratio for the variational and MC-HF methods is presented in items 16 and 24, respectively. The virial ratio, which is a measure of the optimality of the wave function, is defined as follows:

$$vir = \frac{2\langle T \rangle}{\langle r \cdot \nabla V \rangle} \quad 4.7$$

The virial ratio is expected to be close to 1 for an accurate wave function. For the variational wave function, this ratio is equal to 1 for all masses and frequencies. According to the virial theorem,  $2\langle T \rangle = N\langle V \rangle$ , where  $N$  is the degree of homogeneity of the potential energy function. For a harmonic oscillator,  $N=2$ , and thus the kinetic energy and the potential energy of the oscillator will be exactly equal (see equations 2-148 and 2-149), each accounting for half of the total energy. The virial ratio for the HF method is reported as  $\frac{-\langle V \rangle}{\langle T \rangle}$ . Therefore, at high frequencies, where the oscillator potential dominates, this ratio approaches  $-1$ . At low frequencies, where the Coulomb interaction potential dominates with a degree of homogeneity  $N = -1$ , the virial ratio approaches 2.

The data in Table 4-4 help us observe the energy components and their relative significance. Generally, some observable trends in the data are as follows:

For the variational method:

- The magnitude of the kinetic energies increases with the oscillator frequency.
- However, at a specific frequency, the electron's kinetic energy increases with the positive particle's mass, while the positive particle's kinetic energy decreases with increasing mass.
- The harmonic oscillator potential energies (both for the electron and the positive particle) increase with frequency. At a specific frequency, they increase at a very slow rate with the positive particle's mass.



- The electron-positive particle interaction energy also increases with frequency and mass, due to the indirect effect of the decreasing average particle distance.

For the Hartree-Fock method, the trends in kinetic energy are similar to the variational method, except:

- At a specific frequency, the positive particle's kinetic energy initially increases with mass up to mass 10, then decreases with increasing mass. This can explain the change in correlation energy behavior with increasing mass.
- The harmonic oscillator potential energies of both the electron and positive particle, at a fixed mass, increase with frequency. At a fixed frequency, they decrease with increasing mass, contrary to the variational trends.
- The HF interaction energy increases with mass and frequency.

Table 4-4: Total energy, its components, and virial ratio obtained from the variational and MC-HF/[7s:7s] methods

Quantities / $\omega$	0.0001	0.001	0.01	0.1	1	10	100	1000	10000
m = 1									
Variation energy <sup>1</sup>	-0.249850	-0.248497	-0.234701	-0.073933	2.112000	27.395490	291.942322	2974.690624	29920.133739
VAR TE <sup>2</sup>	0.125038	0.125378	0.129048	0.184559	0.899854	7.857506	76.037204	753.192946	7510.009565
VAR TP <sup>3</sup>	0.125038	0.125378	0.129048	0.184559	0.899854	7.857506	76.037204	753.192946	7510.009565
Total VART <sup>4</sup>	0.250075	0.250756	0.258097	0.369119	1.799707	15.715011	152.074408	1506.385891	15020.019129
VAR HO E <sup>5</sup>	0.000038	0.000376	0.003899	0.049198	0.651951	7.185084	74.002788	746.846265	7490.029408
VAR HO P <sup>6</sup>	0.000038	0.000376	0.003899	0.049198	0.651951	7.185084	74.002788	746.846265	7490.029408
Total VAR HO <sup>7</sup>	0.000075	0.000753	0.007799	0.098395	1.303902	14.370167	148.005576	1493.692530	14980.058815
VAR INT <sup>8</sup>	-0.500000	-0.500006	-0.500596	-0.541447	-0.991609	-2.689688	-8.137662	-25.387791	-79.944206
REL T <sup>9</sup>	0.250000	0.250006	0.250597	0.294119	1.049707	8.215011	77.074408	756.385886	7520.019128
REL INT <sup>10</sup>	-0.500000	-0.500006	-0.500596	-0.541447	-0.991609	-2.689688	-8.137662	-25.387791	-79.944206
REL HO <sup>11</sup>	0.000000	0.000003	0.000299	0.023395	0.553902	6.870167	73.005576	743.692530	7480.058817
COM T <sup>12</sup>	0.000075	0.000750	0.007500	0.075000	0.750000	7.500000	75.000000	750.000000	7500.000000
COM HO <sup>13</sup>	0.000075	0.000750	0.007500	0.075000	0.750000	7.500000	75.000000	750.000000	7500.000000
Total RC T <sup>14</sup>	0.250075	0.250756	0.258097	0.369119	1.799707	15.715011	152.074408	1506.385886	15020.019128
Total RC HO <sup>15</sup>	0.000075	0.000753	0.007799	0.098395	1.303902	14.370167	148.005576	1493.692530	14980.058817
VAR Virial ratio <sup>16</sup>	1.000000	1.000000	1.000000	1.000000	1.000000	1.000000	1.000000	0.999999	0.999998
MC-HF/[7s:7s] E <sup>17</sup>	-0.108513	-0.108491	-0.106407	0.012203	2.171918	27.448072	291.992777	2974.740427	29920.183344
MC-HF TE <sup>18</sup>	0.054257	0.054278	0.056302	0.127546	0.865636	7.830022	76.011617	753.168064	7509.987785
MC-HF TP <sup>19</sup>	0.054257	0.054278	0.056302	0.127546	0.865636	7.830022	76.011614	753.168062	7509.987545

Quantities $/\omega$	0.0001	0.001	0.01	0.1	1	10	100	1000	10000
Total MC-HF T <sup>20</sup>	0.108514	0.108556	0.112604	0.255092	1.731273	15.660044	152.023231	1506.336126	15019.975330
MC-HF HO E <sup>21</sup>	0.000000	0.000011	0.001033	0.044549	0.650532	7.184686	74.002667	746.846090	7490.026332
MC-HF HO P <sup>22</sup>	0.000000	0.000011	0.001033	0.044549	0.650532	7.184686	74.002670	746.846092	7490.026573
Total MC-HF HO <sup>23</sup>	0.000000	0.000021	0.002066	0.089098	1.301064	14.369372	148.005337	1493.692181	14980.052905
MC-HF INT <sup>24</sup>	-0.217027	-0.217069	-0.221077	-0.331987	-0.860418	-2.581344	-8.035792	-25.287881	-79.844891
MC-HF Virial Ratio <sup>25</sup>	1.999989	1.999400	1.944965	0.952162	-0.254521	-0.752746	-0.920712	-0.974818	-0.992026
m=1.5									
Variation energy <sup>1</sup>	-0.299850	-0.298498	-0.284750	-0.127533	2.016267	27.137957	291.164882	2972.266767	29912.502746
VAR TE <sup>2</sup>	0.180030	0.180303	0.183299	0.233614	0.955011	7.975708	76.368579	754.202362	7513.166676
VAR TP <sup>3</sup>	0.120045	0.120452	0.124699	0.180742	0.886674	7.817139	75.912386	752.801576	7508.777784
Total VART <sup>4</sup>	0.300075	0.300755	0.307998	0.414356	1.841685	15.792847	152.280966	1507.003938	15021.944459
VAR HO E <sup>5</sup>	0.000030	0.000301	0.003150	0.042365	0.621590	7.086161	73.689169	745.854141	7486.889440
VAR HO P <sup>6</sup>	0.000045	0.000451	0.004600	0.053243	0.664394	7.224107	74.126113	747.236094	7491.259627
Total VAR HO <sup>7</sup>	0.000075	0.000752	0.007749	0.095608	1.285984	14.310268	147.815282	1493.090235	14978.149067
VAR INT <sup>8</sup>	-0.600000	-0.600005	-0.600498	-0.637497	-1.111402	-2.965158	-8.931366	-27.827407	-87.590782
REL T <sup>9</sup>	0.300000	0.300005	0.300498	0.339356	1.091685	8.292847	77.280966	757.003939	7521.944461
REL INT <sup>10</sup>	-0.600000	-0.600005	-0.600498	-0.637497	-1.111402	-2.965158	-8.931366	-27.827407	-87.590782
REL HO <sup>11</sup>	0.000000	0.000002	0.000249	0.020608	0.535984	6.810268	72.815282	743.090235	7478.149067
COM T <sup>12</sup>	0.000075	0.000750	0.007500	0.075000	0.750000	7.500000	75.000000	750.000000	7500.000000
COM HO <sup>13</sup>	0.000075	0.000750	0.007500	0.075000	0.750000	7.500000	75.000000	750.000000	7500.000000
Total RC T <sup>14</sup>	0.300075	0.300755	0.307998	0.414356	1.841685	15.792847	152.280966	1507.003939	15021.944461

Quantities $/\omega$	0.0001	0.001	0.01	0.1	1	10	100	1000	10000
Total RC HO <sup>15</sup>	0.000075	0.000752	0.007749	0.095608	1.285984	14.310268	147.815282	1493.090235	14978.149067
VAR Virial ratio <sup>16</sup>	1.000000	1.000000	1.000000	1.000000	1.000000	1.000000	1.000000	1.000000	1.000000
MC-HF/[7s:7s] E <sup>17</sup>	-0.131661	-0.131644	-0.129900	-0.021539	2.087757	27.199613	291.223701	2972.324714	29912.560519
MC-HF TE <sup>18</sup>	0.071904	0.071923	0.073710	0.145309	0.902448	7.934121	76.330067	754.164780	7513.129370
MC-HF TP <sup>19</sup>	0.059756	0.059773	0.061403	0.127650	0.856317	7.793882	75.891153	752.780910	7508.754787
Total MC-HF T <sup>20</sup>	0.131660	0.131696	0.135112	0.272959	1.758765	15.728003	152.221220	1506.945690	15021.884157
MC-HF HO E <sup>21</sup>	0.000000	0.000008	0.000797	0.039402	0.624862	7.091596	73.695222	745.860380	7486.895746
MC-HF HO P <sup>22</sup>	0.000000	0.000010	0.000941	0.044406	0.657312	7.217609	74.119712	747.229757	7491.255910
Total MC-HF HO <sup>23</sup>	0.000000	0.000018	0.001737	0.083807	1.282174	14.309205	147.814934	1493.090137	14978.151656
MC-HF INT <sup>24</sup>	-0.263321	-0.263358	-0.266750	-0.378305	-0.953182	-2.837595	-8.812453	-27.711113	-87.475293
MC-HF Virial Ratio <sup>25</sup>	2.000008	1.999600	1.961425	1.078908	-0.187058	-0.729375	-0.913161	-0.972417	-0.991266
m = 2									
Variation energy <sup>1</sup>	-0.333183	-0.331831	-0.318109	-0.162780	1.955715	26.977247	290.681475	2970.761234	29907.764463
VAR TE <sup>2</sup>	0.222247	0.222475	0.225021	0.271652	0.996139	8.061391	76.606651	754.925466	7515.424558
VAR TP <sup>3</sup>	0.111161	0.111613	0.116261	0.173326	0.873070	7.780696	75.803326	752.462738	7507.712279
Total VART <sup>4</sup>	0.333408	0.334088	0.341282	0.444978	1.869209	15.842087	152.409976	1507.388204	15023.136838
VAR HO E <sup>5</sup>	0.000025	0.000251	0.002650	0.037711	0.599983	7.015407	73.464767	745.144321	7484.644733
VAR HO P <sup>6</sup>	0.000050	0.000501	0.005075	0.056355	0.674992	7.257704	74.232383	747.572161	7492.322367
Total VAR HO <sup>7</sup>	0.000075	0.000752	0.007724	0.094066	1.274975	14.273111	147.697150	1492.716482	14976.967100
VAR INT <sup>8</sup>	-0.666667	-0.666672	-0.667115	-0.701824	-1.188468	-3.137952	-9.425652	-29.343461	-92.339475
REL T <sup>9</sup>	0.333333	0.333338	0.333782	0.369978	1.119209	8.342087	77.409976	757.388213	7523.136838

Quantities / $\omega$	0.0001	0.001	0.01	0.1	1	10	100	1000	10000
REL INT <sup>10</sup>	-0.666667	-0.666671	-0.667115	-0.701824	-1.188468	-3.137951	-9.425652	-29.343461	-92.339475
REL HO <sup>11</sup>	0.000000	0.000002	0.000224	0.019066	0.524975	6.773111	72.697150	742.716482	7476.967100
COM T <sup>12</sup>	0.000075	0.000750	0.007500	0.075000	0.750000	7.500000	75.000000	750.000000	7500.000000
COM HO <sup>13</sup>	0.000075	0.000750	0.007500	0.075000	0.750000	7.500000	75.000000	750.000000	7500.000000
Total RC T <sup>14</sup>	0.333408	0.334088	0.341282	0.444978	1.869209	15.842087	152.409976	1507.388213	15023.136838
Total RC HO <sup>15</sup>	0.000075	0.000752	0.007724	0.094066	1.274975	14.273111	147.697150	1492.716482	14976.967100
VAR Virial ratio <sup>16</sup>	1.000000	1.000000	1.000000	1.000000	1.000000	1.000000	1.000000	1.000000	1.000000
MC-HF/[7s:7s] E <sup>17</sup>	-0.149328	-0.149312	-0.147746	-0.045426	2.032554	27.042353	290.743202	2970.821923	29907.824832
MC-HF TE <sup>18</sup>	0.086372	0.086389	0.088052	0.159882	0.930716	8.010659	76.560034	754.880100	7515.379561
MC-HF TP <sup>19</sup>	0.062955	0.062970	0.064390	0.127220	0.848021	7.762520	75.787062	752.447064	7507.696782
Total MC-HF T <sup>20</sup>	0.149327	0.149359	0.152442	0.287101	1.778737	15.773179	152.347096	1507.327164	15023.076343
MC-HF HO E <sup>21</sup>	0.000000	0.000007	0.000672	0.036065	0.606838	7.025252	73.475454	745.155265	7484.655762
MC-HF HO P <sup>22</sup>	0.000000	0.000009	0.000893	0.044493	0.663592	7.246592	74.221331	747.561103	7492.311315
Total MC-HF HO <sup>23</sup>	0.000000	0.000016	0.001565	0.080558	1.270430	14.271844	147.696786	1492.716368	14976.967077
MC-HF INT <sup>24</sup>	-0.298655	-0.298687	-0.301753	-0.413086	-1.016614	-3.002670	-9.300680	-29.221608	-92.218589
MC-HF Virial Ratio <sup>25</sup>	2.000006	1.999687	1.969194	1.158223	-0.142695	-0.714452	-0.908426	-0.970920	-0.990792
m=3									
Variation energy <sup>1</sup>	-0.374850	-0.373498	-0.359800	-0.206440	1.883003	26.786450	290.109312	2968.980867	29902.162752
VAR TE <sup>2</sup>	0.281269	0.281440	0.283424	0.325262	1.052436	8.175910	76.922433	755.882362	7518.410271
VAR TP <sup>3</sup>	0.093806	0.094313	0.099475	0.158421	0.850812	7.725303	75.640811	751.960794	7506.136756
Total VART <sup>4</sup>	0.375075	0.375754	0.382899	0.483683	1.903248	15.901213	152.563244	1507.843156	15024.547027

Quantities / $\omega$	0.0001	0.001	0.01	0.1	1	10	100	1000	10000
VAR HO E <sup>5</sup>	0.000019	0.000189	0.002025	0.031811	0.571563	6.921916	73.168139	744.206011	7481.677445
VAR HO P <sup>6</sup>	0.000056	0.000563	0.005675	0.060604	0.690521	7.307305	74.389380	748.068670	7493.892482
Total VAR HO <sup>7</sup>	0.000075	0.000752	0.007700	0.092414	1.262084	14.229221	147.557519	1492.274681	14975.569926
VAR INT <sup>8</sup>	-0.750000	-0.750004	-0.750399	-0.782537	-1.282329	-3.343984	-10.011451	-31.136990	-97.954202
REL T <sup>9</sup>	0.375000	0.375004	0.375399	0.408683	1.153248	8.401213	77.563244	757.843176	7524.547027
REL INT <sup>10</sup>	-0.750000	-0.750004	-0.750399	-0.782537	-1.282329	-3.343984	-10.011451	-31.136990	-97.954202
REL HO <sup>11</sup>	0.000000	0.000002	0.000200	0.017414	0.512084	6.729221	72.557519	742.274681	7475.569926
COM T <sup>12</sup>	0.000075	0.000750	0.007500	0.075000	0.750000	7.500000	75.000000	750.000000	7499.999998
COM HO <sup>13</sup>	0.000075	0.000750	0.007500	0.075000	0.750000	7.500000	75.000000	750.000000	7500.000002
Total RC T <sup>14</sup>	0.375075	0.375754	0.382899	0.483683	1.903248	15.901213	152.563244	1507.843176	15024.547026
Total RC HO <sup>15</sup>	0.000075	0.000752	0.007700	0.092414	1.262084	14.229221	147.557519	1492.274681	14975.569928
VAR Virial ratio <sup>16</sup>	1.000000	1.000000	1.000000	1.000000	1.000000	1.000000	1.000000	1.000000	1.000000
MC-HF/[7s:7s] E <sup>17</sup>	-0.175573	-0.175559	-0.174173	-0.078661	1.962394	26.851598	290.170376	2969.040682	29902.222187
MC-HF TE <sup>18</sup>	0.109323	0.109339	0.110873	0.183072	0.972233	8.116130	76.868367	755.830037	7518.358479
MC-HF TP <sup>19</sup>	0.066251	0.066263	0.067464	0.125904	0.835049	7.715334	75.632449	751.952935	7506.129002
Total MC-HF T <sup>20</sup>	0.175574	0.175602	0.178338	0.308975	1.807282	15.831464	152.500816	1507.782972	15024.487481
MC-HF HO E <sup>21</sup>	0.000000	0.000005	0.000540	0.031885	0.582797	6.936918	73.184129	744.222289	7481.693785
MC-HF HO P <sup>22</sup>	0.000000	0.000009	0.000848	0.044886	0.673762	7.290771	74.372922	748.052211	7493.876075
Total MC-HF HO <sup>23</sup>	0.000000	0.000014	0.001389	0.076771	1.256559	14.227689	147.557051	1492.274500	14975.569861
MC-HF INT <sup>24</sup>	-0.351147	-0.351175	-0.353899	-0.464408	-1.101447	-3.207555	-9.887490	-31.016790	-97.835154
MC-HF Virial Ratio <sup>25</sup>	1.999997	1.999758	1.976646	1.254586	-0.085826	-0.696091	-0.902746	-0.969143	-0.990232

Quantities $/\omega$	0.0001	0.001	0.01	0.1	1	10	100	1000	10000
m=10									
Variation energy <sup>1</sup>	-0.454395	-0.453044	-0.439381	-0.288912	1.751539	26.447417	289.097263	2965.835951	29892.271732
VAR TE <sup>2</sup>	0.413230	0.413294	0.414204	0.446475	1.174993	8.416433	77.578073	757.862074	7524.580388
VAR TP <sup>3</sup>	0.041390	0.042004	0.048170	0.112147	0.792499	7.591643	75.257807	750.786207	7502.458035
Total VART <sup>4</sup>	0.454620	0.455299	0.462375	0.558622	1.967492	16.008077	152.835880	1508.648281	15027.038423
VAR HO E <sup>5</sup>	0.000007	0.000070	0.000832	0.020367	0.513343	6.728936	72.555477	742.267944	7475.548526
VAR HO P <sup>6</sup>	0.000068	0.000682	0.006833	0.069537	0.726334	7.422894	74.755548	749.226795	7497.554878
Total VAR HO <sup>7</sup>	0.000075	0.000752	0.007665	0.089903	1.239677	14.151830	147.311025	1491.494739	14973.103404
VAR INT <sup>8</sup>	-0.909091	-0.909094	-0.909420	-0.937438	-1.455630	-3.712490	-11.049642	-34.307070	-107.870080
REL T <sup>9</sup>	0.454545	0.454549	0.454875	0.483622	1.217492	8.508077	77.835880	758.648277	7527.038427
REL INT <sup>10</sup>	-0.909091	-0.909094	-0.909420	-0.937438	-1.455630	-3.712490	-11.049642	-34.307069	-107.870081
REL HO <sup>11</sup>	0.000000	0.000002	0.000165	0.014903	0.489677	6.651830	72.311025	741.494743	7473.103386
COM T <sup>12</sup>	0.000075	0.000750	0.007500	0.075000	0.750000	7.500000	75.000000	750.000000	7500.000000
COM HO <sup>13</sup>	0.000075	0.000750	0.007500	0.075000	0.750000	7.500000	75.000000	750.000000	7500.000000
Total RC T <sup>14</sup>	0.454620	0.455299	0.462375	0.558622	1.967492	16.008077	152.835880	1508.648277	15027.038427
Total RC HO <sup>15</sup>	0.000075	0.000752	0.007665	0.089903	1.239677	14.151830	147.311025	1491.494743	14973.103386
VAR Virial ratio <sup>16</sup>	1.000000	1.000000	1.000000	1.000000	1.000000	1.000000	1.000000	1.000000	1.000000
MC-HF/[7s:7s] E <sup>17</sup>	-0.257049	-0.257037	-0.255878	-0.170118	1.810873	26.490355	289.135811	2965.873207	29892.308661
MC-HF TE <sup>18</sup>	0.190221	0.190237	0.191653	0.265936	1.090860	8.363320	77.532992	757.819352	7524.538502
MC-HF TP <sup>19</sup>	0.066828	0.066837	0.067719	0.117340	0.797477	7.596780	75.262833	750.790852	7502.460544
Total MC-HF T <sup>20</sup>	0.257048	0.257074	0.259372	0.383277	1.888337	15.960100	152.795825	1508.610204	15026.999046

Quantities $/\omega$	0.0001	0.001	0.01	0.1	1	10	100	1000	10000
MC-HF HO E <sup>21</sup>	0.000000	0.000003	0.000326	0.023032	0.527705	6.745695	72.572511	742.284996	7475.565480
MC-HF HO P <sup>22</sup>	0.000000	0.000008	0.000837	0.048020	0.705366	7.404457	74.738088	749.209996	7497.540355
Total MC-HF HO <sup>23</sup>	0.000000	0.000012	0.001164	0.071053	1.233070	14.150152	147.310599	1491.494992	14973.105835
MC-HF INT <sup>24</sup>	-0.514097	-0.514123	-0.516413	-0.624448	-1.310535	-3.619897	-10.970613	-34.231990	-107.796219
MC-HF Virial Ratio <sup>25</sup>	2.000001	1.999854	1.986531	1.443852	0.041023	-0.659786	-0.892302	-0.965964	-0.989240
m = 50									
Variation energy <sup>1</sup>	-0.490046	-0.488695	-0.475043	-0.325603	1.695169	26.304325	288.671901	2964.515756	29888.121166
VAR TE <sup>2</sup>	0.480586	0.480602	0.481031	0.508885	1.236361	8.533208	77.893163	758.810580	7527.533827
VAR TP <sup>3</sup>	0.009685	0.010347	0.016971	0.083678	0.759727	7.520664	75.057863	750.176211	7500.550737
Total VART <sup>4</sup>	0.490271	0.490949	0.498002	0.592562	1.996089	16.053873	152.951026	1508.986791	15028.084564
VAR HO E <sup>5</sup>	0.000001	0.000016	0.000297	0.015183	0.485705	6.636666	72.262395	741.340705	7472.616132
VAR HO P <sup>6</sup>	0.000074	0.000735	0.007356	0.073804	0.744714	7.482733	74.945248	749.826814	7499.452322
Total VAR HO <sup>7</sup>	0.000075	0.000752	0.007653	0.088986	1.230419	14.119399	147.207643	1491.167520	14972.068454
VAR INT <sup>8</sup>	-0.980392	-0.980395	-0.980698	-1.007152	-1.531339	-3.868947	-11.486768	-35.638555	-112.031793
REL T <sup>9</sup>	0.490196	0.490199	0.490502	0.517562	1.246089	8.553873	77.951026	758.986791	7528.084504
REL INT <sup>10</sup>	-0.980392	-0.980395	-0.980698	-1.007152	-1.531339	-3.868947	-11.486768	-35.638555	-112.031793
REL HO <sup>11</sup>	0.000000	0.000002	0.000153	0.013986	0.480419	6.619399	72.207642	741.167520	7472.068455
COM T <sup>12</sup>	0.000075	0.000750	0.007500	0.075000	0.750000	7.500000	75.000000	750.000000	7500.000000
COM HO <sup>13</sup>	0.000075	0.000750	0.007500	0.075000	0.750000	7.500000	75.000000	750.000000	7500.000000
Total RC T <sup>14</sup>	0.490271	0.490949	0.498002	0.592562	1.996089	16.053873	152.951026	1508.986791	15028.084504
Total RC HO <sup>15</sup>	0.000075	0.000752	0.007653	0.088986	1.230419	14.119399	147.207642	1491.167520	14972.068455



Quantities $/\omega$	0.0001	0.001	0.01	0.1	1	10	100	1000	10000
VAR Virial ratio <sup>16</sup>	1.000000	1.000000	1.000000	1.000000	1.000000	1.000000	1.000000	1.000000	1.000000
MC-HF $/[7s:7s]$ E <sup>17</sup>	-0.353887	-0.353874	-0.352583	-0.261510	1.717273	26.317887	288.683473	2964.526763	29888.132005
MC-HF TE <sup>18</sup>	0.302339	0.302356	0.304056	0.382721	1.196668	8.513224	77.877443	758.796032	7527.519574
MC-HF TP <sup>19</sup>	0.051554	0.051563	0.052416	0.099684	0.766004	7.524732	75.061373	750.179559	7500.554606
Total MC-HF T <sup>20</sup>	0.353893	0.353919	0.356473	0.482406	1.962672	16.037956	152.938816	1508.975591	15028.074181
MC-HF HO E <sup>21</sup>	0.000000	0.000002	0.000219	0.017187	0.492317	6.643259	72.268755	741.346974	7472.622430
MC-HF HO P <sup>22</sup>	0.000000	0.000011	0.001076	0.056445	0.734331	7.475350	74.938677	749.820484	7499.445439
Total MC-HF HO <sup>23</sup>	0.000000	0.000013	0.001295	0.073632	1.226648	14.118608	147.207432	1491.167458	14972.067869
MC-HF INT <sup>24</sup>	-0.707780	-0.707806	-0.710350	-0.817548	-1.472047	-3.838676	-11.462775	-35.616286	-112.010044
MC-HF Virial Ratio <sup>25</sup>	1.999983	1.999873	1.989088	1.542095	0.125033	-0.640975	-0.887575	-0.964596	-0.988820
m = 207									
Variation energy <sup>1</sup>	-0.497446	-0.496095	-0.482446	-0.333202	1.683638	26.275221	288.585513	2964.247752	29887.278700
VAR TE <sup>2</sup>	0.495204	0.495210	0.495540	0.522468	1.249601	8.558126	77.960160	759.012015	7528.160741
VAR TP <sup>3</sup>	0.002467	0.003139	0.009858	0.077162	0.752414	7.505112	75.014300	750.043536	7500.135624
Total VART <sup>4</sup>	0.497671	0.498349	0.505397	0.599630	2.002014	16.063238	152.974461	1509.055552	15028.296365
VAR HO E <sup>5</sup>	0.000000	0.000005	0.000186	0.014103	0.479856	6.617085	72.200178	741.143887	7471.993785
VAR HO P <sup>6</sup>	0.000075	0.000746	0.007465	0.074706	0.748695	7.495735	74.986474	749.957217	7499.864699
Total VAR HO <sup>7</sup>	0.000075	0.000752	0.007651	0.088809	1.228551	14.112820	147.186652	1491.101104	14971.858484
VAR INT <sup>8</sup>	-0.995192	-0.995195	-0.995493	-1.021642	-1.546927	-3.900836	-11.575591	-35.908903	-112.876573
REL T <sup>9</sup>	0.497596	0.497599	0.497897	0.524630	1.252015	8.563238	77.974457	759.055552	7528.296783
REL INT <sup>10</sup>	-0.995192	-0.995195	-0.995493	-1.021642	-1.546927	-3.900837	-11.575600	-35.908903	-112.876573

Quantities $/\omega$	0.0001	0.001	0.01	0.1	1	10	100	1000	10000
REL HO <sup>11</sup>	0.000000	0.000002	0.000151	0.013809	0.478551	6.612820	72.186657	741.101104	7471.858489
COM T <sup>12</sup>	0.000075	0.000750	0.007500	0.075000	0.750000	7.500000	75.000000	750.000000	7500.000008
COM HO <sup>13</sup>	0.000075	0.000750	0.007500	0.075000	0.750000	7.500000	75.000000	750.000000	7499.999992
Total RC T <sup>14</sup>	0.497671	0.498349	0.505397	0.599630	2.002015	16.063238	152.974457	1509.055552	15028.296791
Total RC HO <sup>15</sup>	0.000075	0.000752	0.007651	0.088809	1.228551	14.112820	147.186657	1491.101104	14971.858481
VAR Virial ratio <sup>16</sup>	1.000000	1.000000	1.000000	1.000000	1.000000	1.000000	1.000000	1.000000	1.000000
MC-HF/[7s:7s] E <sup>17</sup>	-0.414686	-0.414668	-0.412886	-0.306618	1.690372	26.278862	288.588490	2964.250545	29887.281447
MC-HF TE <sup>18</sup>	0.380422	0.380447	0.382855	0.460480	1.236019	8.552262	77.955792	759.008048	7528.156876
MC-HF TP <sup>19</sup>	0.034267	0.034278	0.035356	0.086426	0.754936	7.506531	75.015478	750.044648	7500.136990
Total MC-HF T <sup>20</sup>	0.414689	0.414725	0.418211	0.546906	1.990955	16.058793	152.971270	1509.052696	15028.293866
MC-HF HO E <sup>21</sup>	0.000000	0.000002	0.000182	0.015011	0.482015	6.619078	72.202063	741.145729	7471.995624
MC-HF HO P <sup>22</sup>	0.000000	0.000016	0.001593	0.065086	0.745097	7.493475	74.984525	749.955355	7499.863016
Total MC-HF HO <sup>23</sup>	0.000000	0.000018	0.001774	0.080097	1.227112	14.112553	147.186588	1491.101084	14971.858640
MC-HF INT <sup>24</sup>	-0.829375	-0.829411	-0.832872	-0.933620	-1.527695	-3.892484	-11.569367	-35.903235	-112.871059
MC-HF Virial Ratio <sup>25</sup>	1.999993	1.999863	1.987268	1.560641	0.150975	-0.636416	-0.886554	-0.964312	-0.988734
m = 400									
Variation energy <sup>1</sup>	-0.498603	-0.497252	-0.483603	-0.334390	1.681841	26.270688	288.572063	2964.206030	29887.147551
VAR TE <sup>2</sup>	0.497510	0.497514	0.497828	0.524612	1.251687	8.562043	77.970678	759.043651	7528.259187
VAR TP <sup>3</sup>	0.001319	0.001992	0.008726	0.076124	0.751254	7.502655	75.007427	750.022610	7500.070071
Total VART <sup>4</sup>	0.498828	0.499506	0.506553	0.600736	2.002941	16.064698	152.978105	1509.066261	15028.329257
VAR HO E <sup>5</sup>	0.000000	0.000003	0.000169	0.013935	0.478938	6.614010	72.190415	741.112979	7471.896060

Quantities $/\omega$	0.0001	0.001	0.01	0.1	1	10	100	1000	10000
VAR HO P <sup>6</sup>	0.000075	0.000748	0.007482	0.074847	0.749322	7.497785	74.992976	749.977782	7499.929081
Total VAR HO <sup>7</sup>	0.000075	0.000752	0.007650	0.088782	1.228261	14.111795	147.183391	1491.090762	14971.825141
VAR INT <sup>8</sup>	-0.997506	-0.997509	-0.997806	-1.023908	-1.549360	-3.905805	-11.589431	-35.950992	-113.008083
REL T <sup>9</sup>	0.498753	0.498756	0.499053	0.525736	1.252941	8.564698	77.978106	759.066260	7528.329835
REL INT <sup>10</sup>	-0.997506	-0.997509	-0.997806	-1.023908	-1.549361	-3.905805	-11.589432	-35.950992	-113.008083
REL HO <sup>11</sup>	0.000000	0.000002	0.000150	0.013782	0.478261	6.611795	72.183390	741.090762	7471.825800
COM T <sup>12</sup>	0.000075	0.000750	0.007500	0.075000	0.750000	7.500000	75.000000	750.000000	7500.000000
COM HO <sup>13</sup>	0.000075	0.000750	0.007500	0.075000	0.750000	7.500000	75.000000	750.000000	7500.000000
Total RC T <sup>14</sup>	0.498828	0.499506	0.506553	0.600736	2.002941	16.064698	152.978106	1509.066260	15028.329835
Total RC HO <sup>15</sup>	0.000075	0.000752	0.007650	0.088782	1.228261	14.111795	147.183390	1491.090762	14971.825800
VAR Virial ratio <sup>16</sup>	1.000000	1.000000	1.000000	1.000000	1.000000	1.000000	1.000000	1.000000	1.000000
MC-HF/[ $7s:7s$ ] E <sup>17</sup>	-0.434898	-0.434876	-0.432709	-0.318137	1.685464	26.272493	288.573488	2964.207347	29887.148995
MC-HF TE <sup>18</sup>	0.407640	0.407671	0.410598	0.484326	1.244006	8.558972	77.968471	759.041682	7528.264288
MC-HF TP <sup>19</sup>	0.027261	0.027274	0.028544	0.082313	0.752732	7.503458	75.008085	750.023229	7500.072894
Total MC-HF T <sup>20</sup>	0.434901	0.434945	0.439142	0.566639	1.996738	16.062429	152.976556	1509.064911	15028.337182
MC-HF HO E <sup>21</sup>	0.000000	0.000002	0.000172	0.014501	0.480129	6.615097	72.191440	741.113975	7471.890187
MC-HF HO P <sup>22</sup>	0.000000	0.000021	0.001972	0.068337	0.747277	7.496544	74.991916	749.976771	7499.927138
Total MC-HF HO <sup>23</sup>	0.000000	0.000022	0.002144	0.082838	1.227406	14.111641	147.183356	1491.090747	14971.817325
MC-HF INT <sup>24</sup>	-0.869799	-0.869844	-0.873995	-0.967613	-1.538680	-3.901577	-11.586424	-35.948311	-113.005512
MC-HF Virial Ratio <sup>25</sup>	1.999995	1.999842	1.985350	1.561445	0.155891	-0.635649	-0.886390	-0.964268	-0.988720
m = 900									

Quantities $/\omega$	0.0001	0.001	0.01	0.1	1	10	100	1000	10000
Variation energy <sup>1</sup>	-0.499295	-0.497944	-0.484295	-0.335100	1.680766	26.267980	288.564027	2964.181100	29887.069188
VAR TE <sup>2</sup>	0.498891	0.498895	0.499199	0.525896	1.252936	8.564387	77.976976	759.062587	7528.318124
VAR TP <sup>3</sup>	0.000629	0.001303	0.008046	0.075501	0.750559	7.501184	75.003308	750.010071	7500.031464
Total VART <sup>4</sup>	0.499520	0.500198	0.507245	0.601397	2.003495	16.065571	152.980284	1509.072658	15028.349588
VAR HO E <sup>5</sup>	0.000000	0.000002	0.000158	0.013834	0.478389	6.612170	72.184564	741.094479	7471.837554
VAR HO P <sup>6</sup>	0.000075	0.000749	0.007492	0.074932	0.749698	7.499014	74.996872	749.990101	7499.968708
Total VAR HO <sup>7</sup>	0.000075	0.000752	0.007650	0.088766	1.228087	14.111184	147.181435	1491.084580	14971.806262
VAR INT <sup>8</sup>	-0.998890	-0.998893	-0.999190	-1.025263	-1.550816	-3.908762	-11.597701	-35.976141	-113.086663
REL T <sup>9</sup>	0.499445	0.499448	0.499745	0.526397	1.253495	8.565570	77.980287	759.072657	7528.349589
REL INT <sup>10</sup>	-0.998890	-0.998893	-0.999190	-1.025263	-1.550816	-3.908774	-11.597698	-35.976141	-113.086663
REL HO <sup>11</sup>	0.000000	0.000002	0.000150	0.013766	0.478087	6.611184	72.181438	741.084584	7471.806262
COM T <sup>12</sup>	0.000075	0.000750	0.007500	0.075000	0.750000	7.500000	75.000000	750.000000	7500.000000
COM HO <sup>13</sup>	0.000075	0.000750	0.007500	0.075000	0.750000	7.500000	75.000000	750.000000	7500.000000
Total RC T <sup>14</sup>	0.499520	0.500198	0.507245	0.601397	2.003495	16.065570	152.980287	1509.072657	15028.349589
Total RC HO <sup>15</sup>	0.000075	0.000752	0.007650	0.088766	1.228087	14.111184	147.181438	1491.084584	14971.806262
VAR Virial ratio <sup>16</sup>	1.000000	1.000000	1.000000	1.000000	1.000000	1.000000	1.000000	1.000000	1.000000
MC-HF/[7s:7s] E <sup>17</sup>	-0.453975	-0.453946	-0.451115	-0.326729	1.682345	26.268617	288.564475	2964.181492	29887.069700
MC-HF TE <sup>18</sup>	0.433917	0.433958	0.437715	0.503895	1.249292	8.563130	77.976156	759.061875	7528.324535
MC-HF TP <sup>19</sup>	0.020059	0.020076	0.021677	0.078944	0.751287	7.501566	75.003618	750.010409	7500.032322
Total MC-HF T <sup>20</sup>	0.453976	0.454034	0.459392	0.582838	2.000579	16.064696	152.979773	1509.072284	15028.356856
MC-HF HO E <sup>21</sup>	0.000000	0.000002	0.000164	0.014127	0.478928	6.612669	72.185040	741.094950	7471.831068

Quantities $/\omega$	0.0001	0.001	0.01	0.1	1	10	100	1000	10000
MC-HF HO P <sup>22</sup>	0.000000	0.000028	0.002596	0.071253	0.748715	7.498434	74.996383	749.989591	7499.967679
Total MC-HF HO <sup>23</sup>	0.000000	0.000030	0.002760	0.085380	1.227642	14.111103	147.181422	1491.084542	14971.798747
MC-HF INT <sup>24</sup>	-0.907952	-0.908011	-0.913266	-0.994947	-1.545876	-3.907182	-11.596721	-35.975334	-113.085904
MC-HF Virial Ratio <sup>25</sup>	1.999999	1.999806	1.981981	1.560582	0.159071	-0.635177	-0.886292	-0.964241	-0.988712
m = 1836									
Variation energy <sup>1</sup>	-0.499578	-0.498226	-0.484578	-0.335391	1.680327	26.266873	288.560744	2964.170918	29887.037181
VAR TE <sup>2</sup>	0.499456	0.499459	0.499759	0.526422	1.253447	8.565660	77.979554	759.070327	7528.342222
VAR TP <sup>3</sup>	0.000347	0.001022	0.007768	0.075246	0.750274	7.500580	75.001623	750.004944	7500.016692
Total VART <sup>4</sup>	0.499803	0.500481	0.507528	0.601667	2.003721	16.066240	152.981177	1509.075271	15028.358915
VAR HO E <sup>5</sup>	0.000000	0.000002	0.000154	0.013792	0.478164	6.610983	72.182175	741.086918	7471.813632
VAR HO P <sup>6</sup>	0.000075	0.000750	0.007496	0.074967	0.749852	7.499516	74.998465	749.995145	7499.984648
Total VAR HO <sup>7</sup>	0.000075	0.000752	0.007650	0.088759	1.228016	14.110499	147.180640	1491.082063	14971.798280
VAR INT <sup>8</sup>	-0.999456	-0.999459	-0.999755	-1.025817	-1.551410	-3.909978	-11.601062	-35.986413	-113.118759
REL T <sup>9</sup>	0.499728	0.499731	0.500028	0.526667	1.253721	8.565927	77.981177	759.075268	7528.357659
REL INT <sup>10</sup>	-0.999456	-0.999459	-0.999755	-1.025817	-1.551410	-3.909987	-11.601074	-35.986413	-113.118759
REL HO <sup>11</sup>	0.000000	0.000002	0.000150	0.013759	0.478016	6.610933	72.180641	741.082063	7471.798280
COM T <sup>12</sup>	0.000075	0.000750	0.007500	0.075000	0.750000	7.500000	75.000000	750.000000	7500.000000
COM HO <sup>13</sup>	0.000075	0.000750	0.007500	0.075000	0.750000	7.500000	75.000000	750.000000	7500.000000
Total RC T <sup>14</sup>	0.499803	0.500481	0.507528	0.601667	2.003721	16.065927	152.981177	1509.075268	15028.357659
Total RC HO <sup>15</sup>	0.000075	0.000752	0.007650	0.088759	1.228016	14.110933	147.180641	1491.082063	14971.798280
VAR Virial ratio <sup>16</sup>	1.000000	1.000000	1.000000	1.000000	1.000000	1.000000	1.000000	1.000000	1.000000

Quantities $/\omega$	0.0001	0.001	0.01	0.1	1	10	100	1000	10000
MC-HF/[7s:7s] E <sup>17</sup>	-0.466417	-0.466378	-0.462753	-0.330905	1.681012	26.267013	288.560779	2964.170918	29887.037312
MC-HF TE <sup>18</sup>	0.451373	0.451428	0.456066	0.514174	1.251621	8.564874	77.979324	759.070160	7528.348933
MC-HF TP <sup>19</sup>	0.015040	0.015061	0.017054	0.077175	0.750653	7.500779	75.001780	750.005100	7500.015695
Total MC-HF T <sup>20</sup>	0.466413	0.466489	0.473120	0.591350	2.002274	16.065653	152.981104	1509.075260	15028.364628
MC-HF HO E <sup>21</sup>	0.000000	0.000002	0.000159	0.013946	0.478411	6.611663	72.182412	741.087157	7471.807132
MC-HF HO P <sup>22</sup>	0.000000	0.000037	0.003299	0.072886	0.749348	7.499221	74.998220	749.994900	7499.984305
Total MC-HF HO <sup>23</sup>	0.000000	0.000039	0.003458	0.086832	1.227758	14.110884	147.180632	1491.082057	14971.791437
MC-HF INT <sup>24</sup>	-0.932830	-0.932906	-0.939331	-1.009087	-1.549020	-3.909524	-11.600958	-35.986399	-113.118753
MC-HF Virial Ratio <sup>25</sup>	2.000010	1.999763	1.978087	1.559575	0.160449	-0.634979	-0.886251	-0.964230	-0.988709

- |  |   |
|--|---|
| 1. Total variational energy  | 8. E-PCP interaction energy component in variational method                   |
| 2. Electron's kinetic energy component in variational method                       | 9. Kinetic energy component of relative coordinates                           |
| 3. PCP's kinetic energy component in variational method                            | 10. Interaction energy component of relative coordinates                      |
| 4. Total kinetic energy component in variational method                            | 11. Harmonic oscillator potential energy component of relative coordinates    |
| 5. Electron's harmonic oscillator potential energy component in variational method | 12. Kinetic energy component of the center of mass                            |
| 6. PCP's harmonic oscillator potential energy component in variational method      | 13. Harmonic oscillator potential energy component of the center of mass      |
| 7. Total harmonic oscillator potential energy component in variational method      | 14. Total kinetic energy component of relative and center of mass coordinates |

15. Total harmonic oscillator potential energy component of relative and center of mass coordinates
16. Variational virial ratio
17. Total MC-HF energy for basis set [7s:7s]
18. Electron's kinetic energy component in MC-HF
19. PCP's kinetic energy component in MC-HF
20. Total kinetic energy component in MC-HF
21. Electron's harmonic oscillator potential energy component in MC-HF
22. PCP's harmonic oscillator potential energy component in MC-HF
23. Total harmonic oscillator potential energy component in MC-HF
24. E-PCP interaction energy component in MC-HF
25. MC-HF virial ratio

## 4.4 Exponents and Coefficients of MC-HF Calculations

Table 4-5 is dedicated to the exponents and coefficients for the Hartree-Fock calculations using the [7s:7s] basis set, which were provided to us in an optimized form. In this table, the exponents and their corresponding coefficients are presented in order (based on the magnitude of the coefficients) for the electron and PCP orbitals (expansions 1-37 and 1-38). Similar data for the [7s:1s] basis set are reported in Table B-2 of the appendix B.

Finding a consistent and precise pattern among the coefficients and exponents is challenging, but at least a few trends can be roughly observed:

- As the frequency strength increases for a given mass, the magnitude of the exponents (for both the electron and the PCP) increases.
- The magnitude of the dominant exponent (having the largest coefficient) for the electron orbitals at each frequency does not depend on the mass of the PCP, meaning that the dominant orbital exponent at each frequency remains relatively constant regardless of the mass of the PCP.
- The dominant exponent at each frequency (having a larger linear coefficient) usually has a smaller magnitude.
- At higher frequencies, the dominance of a single exponent becomes more significant, and in some cases, the dominant



exponent can be selected as the only effective exponent in the calculations, neglecting the other exponents.

- For the PCP, the exponents are very sensitive to both increasing frequency and mass, reaching the order of millions for a mass and frequency of  $10^4$ .
- Additionally, for the PCP, with increasing mass, the dominant exponent shifts to a larger magnitude exponent.

Table 4-5: Optimized coefficients and exponents of the [7s:7s] basis set in the MC-HF framework. The top and bottom rows for each frequency, respectively, show the absolute values of the sorted coefficients (from largest to smallest) and their corresponding exponents.

Sorted Linear coefficients and corresponding exponents for Electron Orbitals								Sorted Linear coefficients and corresponding exponents for PC Orbitals						
$\omega$ /Basis	1s	2s	3s	4s	5s	6s	7s	1s	2s	3s	4s	5s	6s	7s
m = 1														
0.0001	0.3371	0.2945	0.2297	0.1191	0.0664	0.0036	0.0032	0.4536	0.2173	0.1781	0.1505	0.0374	0.0132	0.0030
	0.0562	0.0324	0.0241	0.0142	0.1101	0.0070	0.0095	0.0288	0.0649	0.0460	0.0146	0.1060	0.1600	0.1950
0.0010	0.3745	0.2937	0.2094	0.1317	0.0286	0.0086	0.0008	0.4419	0.2821	0.1792	0.1556	0.0716	0.0664	0.0064
	0.0403	0.0250	0.0703	0.0155	0.1282	0.0085	0.1646	0.0290	0.0700	0.0435	0.0148	0.0975	0.1274	0.1671
0.0100	0.3539	0.2825	0.2454	0.1227	0.0375	0.0041	0.0005	0.5185	0.3519	0.1494	0.0534	0.0189	0.0090	0.0003
	0.0501	0.0214	0.0329	0.0934	0.0118	0.2077	0.2700	0.0304	0.0622	0.0150	0.1529	0.1899	0.0116	0.5134
0.1000	0.5381	0.1703	0.1617	0.1417	0.0355	0.0289	0.0061	0.6487	0.3024	0.0544	0.0190	0.0002	0.0001	0.0001
	0.0743	0.0526	0.1208	0.1554	0.4216	0.5147	0.6643	0.0701	0.1361	0.0438	0.2970	8.4040	5.9399	11.9810
1	0.7138	0.1151	0.1028	0.0707	0.0060	0.0006	0.0002	0.5855	0.3641	0.0690	0.0139	0.0107	0.0074	0.0067
	0.5417	0.4651	0.7639	1.0044	1.9316	3.8172	5.4195	0.5000	0.6412	1.1070	1.4234	0.3872	1.7406	1.2656
10	0.8355	0.1070	0.0582	0.0024	0.0009	0.0006	0.0003	0.9270	0.1190	0.0609	0.0139	0.0023	0.0012	0.0001
	5.1246	4.7648	7.9818	19.7336	36.1043	59.8889	73.1219	5.0719	7.7344	8.4000	10.8375	3.8500	13.8906	3.0469
100	0.7978	0.2381	0.0396	0.0068	0.0025	0.0004	0.0002	0.6675	0.6598	0.5120	0.4888	0.0183	0.0133	0.0026
	51.7598	44.6831	39.3719	127.5706	165.3781	346.0825	402.5625	120.7188	122.0313	48.7500	52.4966	81.1172	167.2031	204.9219
1000	0.8148	0.1889	0.0047	0.0014	0.0007	0.0006	0.0000	0.5705	0.4971	0.0444	0.0334	0.0075	0.0030	0.0000
	508.4658	469.8193	372.3223	1205.0781	2717.5828	3008.7031	5038.5383	475.0000	536.3672	626.1328	369.5313	321.4844	971.2891	3865.0000
10000	0.7729	0.2436	0.0193	0.0029	0.0001	0.0000	0.0000	0.7670	0.4619	0.1751	0.0710	0.0234	0.0088	0.0026
	5094.9219	4643.1782	3577.8125	2833.8281	26213.7188	45381.3281	312053.9375	5301.9775	4346.2891	4051.4160	7264.3127	10207.7637	14162.3535	17021.8262
m = 1.5														
0.0001	0.3037	0.2373	0.2257	0.1998	0.0463	0.0404	0.0001	0.3196	0.2675	0.2301	0.1784	0.0289	0.0091	0.0081
	0.0562	0.0383	0.0251	0.0945	0.0142	0.1725	0.7570	0.0649	0.0460	0.1060	0.0288	0.1950	0.0146	0.1600
0.0010	0.3487	0.3218	0.2011	0.1079	0.0670	0.0070	0.0004	0.4285	0.3038	0.1920	0.0632	0.0453	0.0090	0.0000
	0.0403	0.0703	0.0260	0.1282	0.0155	0.2585	0.4146	0.0544	0.0975	0.0290	0.0435	0.1827	0.0148	0.6274

Sorted Linear coefficients and corresponding exponents for Electron Orbitals								Sorted Linear coefficients and corresponding exponents for PC Orbitals						
$\omega$ /Basis	1s	2s	3s	4s	5s	6s	7s	1s	2s	3s	4s	5s	6s	7s
0.0100	0.3892	0.2469	0.2063	0.1615	0.0302	0.0111	0.0069	0.5605	0.2532	0.1900	0.0325	0.0099	0.0072	0.0016
	0.0501	0.0934	0.0329	0.0214	0.1763	0.0118	0.2077	0.0617	0.0309	0.1215	0.1451	0.2634	0.2025	0.0086
0.1000	0.4673	0.2383	0.1430	0.1104	0.0705	0.0025	0.0006	0.5584	0.3315	0.1337	0.0024	0.0005	0.0004	0.0002
	0.0743	0.1208	0.1554	0.0526	0.2647	0.4216	0.6643	0.1361	0.0857	0.2638	0.0438	8.4040	5.9399	11.9810
1	0.6616	0.1677	0.0963	0.0731	0.0138	0.0005	0.0001	0.6217	0.5758	0.4259	0.3849	0.2414	0.0091	0.0000
	0.5417	0.7639	0.4651	1.1294	1.9316	2.8172	5.4195	0.9234	0.6412	1.7656	1.7719	0.5625	0.3872	3.1070
10	0.8334	0.0882	0.0757	0.0302	0.0240	0.0006	0.0000	0.7058	0.2167	0.0519	0.0243	0.0063	0.0042	0.0010
	5.1246	4.7648	7.9818	19.7336	21.1043	37.8889	73.1219	7.7344	7.8688	6.0719	13.3906	10.8375	3.8500	3.0469
100	0.8082	0.2139	0.0298	0.0096	0.0008	0.0004	0.0002	3.5325	3.4418	0.9834	0.1835	0.0709	0.0186	0.0138
	51.7598	44.6831	38.8719	114.0706	165.3781	346.0825	402.5625	120.3438	122.0313	81.1094	61.9966	167.2031	48.7500	203.4219
1000	0.7900	0.2136	0.0054	0.0024	0.0006	0.0005	0.0000	0.9881	0.0187	0.0049	0.0034	0.0028	0.0011	0.0000
	509.9658	469.8193	372.3223	1205.0781	2717.5828	3008.7031	5038.5383	747.8828	971.2891	533.3672	543.0000	369.5313	321.4844	3865.0000
10000	0.6629	0.3601	0.0261	0.0031	0.0001	0.0000	0.0000	2.0540	2.0268	0.9853	0.0888	0.0866	0.0147	0.0045
	5145.9219	4679.6782	3643.3125	2833.8281	26213.7188	45381.3281	312053.9375	4641.3672	4695.4775	7264.3127	4123.9160	9641.7637	14162.3535	17017.8262
m=2														
0.0001	0.4567	0.2583	0.1690	0.1162	0.0916	0.0598	0.0257	0.4004	0.3115	0.1559	0.1013	0.0367	0.0292	0.0031
	0.0562	0.1139	0.0265	0.0324	0.2664	0.2799	0.0144	0.1060	0.0649	0.0460	0.1950	0.0288	0.1600	0.3896
0.0010	0.3621	0.3233	0.1631	0.1408	0.0308	0.0196	0.0181	0.4335	0.2912	0.1649	0.1010	0.0413	0.0074	0.0011
	0.0703	0.0403	0.1282	0.0250	0.0155	0.2585	0.1646	0.0975	0.0513	0.1749	0.0700	0.0290	0.3774	0.5148
0.0100	0.3435	0.3029	0.1841	0.1050	0.0866	0.0322	0.0025	0.4057	0.3611	0.1511	0.1466	0.1171	0.0824	0.0072
	0.0817	0.0462	0.0329	0.1450	0.0195	0.2077	0.3868	0.0622	0.1053	0.2634	0.1587	0.2650	0.0357	0.0304
0.1000	0.4162	0.2664	0.1512	0.1158	0.0800	0.0114	0.0023	0.6135	0.4672	0.1521	0.1158	0.0441	0.0147	0.0043
	0.0743	0.1208	0.1554	0.2647	0.0526	0.5466	0.6643	0.1332	0.2521	0.3618	0.5076	0.7478	0.9185	0.0575
1	0.6362	0.1856	0.0865	0.0817	0.0250	0.0005	0.0001	0.6531	0.3176	0.1996	0.1378	0.1060	0.0133	0.0033
	0.5417	0.7639	1.1294	0.4651	1.9316	3.9195	2.8172	1.1070	1.2656	1.4859	1.8031	0.7975	0.5000	0.3872
10	0.8765	0.0812	0.0354	0.0151	0.0032	0.0004	0.0000	0.5732	0.4354	0.1280	0.1047	0.0163	0.0003	0.0000
	5.1246	8.0443	4.5148	16.7336	21.1043	37.8889	73.1219	10.8375	9.4000	6.7344	6.5719	17.3906	4.1000	3.2969

Sorted Linear coefficients and corresponding exponents for Electron Orbitals								Sorted Linear coefficients and corresponding exponents for PC Orbitals						
$\omega$ /Basis	1s	2s	3s	4s	5s	6s	7s	1s	2s	3s	4s	5s	6s	7s
100	0.8089	0.1913	0.0116	0.0109	0.0005	0.0005	0.0003	7.1415	6.5958	0.4206	0.0569	0.0185	0.0088	0.0046
	51.7598	45.1831	110.0706	36.3719	165.3781	346.0825	402.5625	119.2031	120.5313	90.6172	167.2031	59.4966	204.9219	48.7500
1000	0.7839	0.2189	0.0054	0.0032	0.0004	0.0004	0.0000	0.8366	0.1674	0.0678	0.0633	0.0013	0.0007	0.0001
	510.4658	469.8193	372.3223	1204.0781	3008.7031	2717.5828	5038.5383	1017.7891	923.6328	537.5000	533.3672	369.5313	321.4844	3812.0000
10000	1.0088	0.0322	0.0225	0.0010	0.0002	0.0000	0.0000	0.9958	0.0325	0.0286	0.0110	0.0092	0.0027	0.0011
	4958.1782	4195.8125	6361.4219	2842.3281	26211.2188	45381.3281	312053.9375	10028.2637	4495.2891	4839.9775	6784.8127	4123.4160	14162.3535	17021.8262
m=3														
0.0001	0.3542	0.3477	0.1533	0.1085	0.0594	0.0362	0.0049	0.3118	0.2752	0.2415	0.1720	0.0255	0.0252	0.0178
	0.0886	0.0480	0.1549	0.0288	0.2507	0.0193	0.4758	0.1216	0.1600	0.0771	0.2575	0.0460	0.5649	0.5913
0.0010	0.6654	0.4322	0.3739	0.1984	0.1003	0.0403	0.0014	0.5210	0.2488	0.2387	0.0567	0.0496	0.0289	0.0030
	0.0481	0.0813	0.0546	0.1567	0.0228	0.2975	0.5155	0.1274	0.2225	0.0700	0.0460	0.0421	0.3560	0.5290
0.0100	0.4159	0.3793	0.1331	0.1252	0.0095	0.0009	0.0002	0.2926	0.2901	0.2366	0.1192	0.0586	0.0352	0.0002
	0.0501	0.1012	0.2077	0.0251	0.4433	0.0079	1.0200	0.1007	0.1366	0.2025	0.0622	0.3415	0.2154	1.3149
0.1000	0.3480	0.2837	0.1687	0.1625	0.0504	0.0294	0.0051	0.8058	0.7904	0.4673	0.4488	0.0850	0.0002	0.0000
	0.0743	0.1208	0.2647	0.1554	0.0526	0.4841	0.6643	0.1673	0.1688	0.1951	0.2970	0.5123	1.6899	0.7790
1	0.5811	0.1598	0.1569	0.0699	0.0504	0.0062	0.0034	0.6636	0.2675	0.1116	0.0965	0.0601	0.0030	0.0003
	0.5417	0.7014	1.0044	0.4651	1.9316	4.8172	5.4195	1.6227	1.4859	2.4438	1.1250	0.9850	0.5747	0.3281
10	0.8792	0.0890	0.0170	0.0166	0.0052	0.0005	0.0000	3.4301	3.2772	0.5906	0.5441	0.0269	0.0101	0.0022
	5.1246	7.9818	14.2336	4.2648	21.1043	37.8889	73.1219	9.9844	9.9625	13.2125	16.7969	6.7594	4.8500	3.7344
100	0.7674	0.2195	0.0155	0.0041	0.0036	0.0008	0.0003	2.1322	1.5441	0.3868	0.0429	0.0128	0.0067	0.0019
	51.7598	46.4331	97.5706	34.8719	165.3781	346.0825	402.5625	131.7188	126.3281	167.2031	90.6172	204.9219	59.4966	48.7500
1000	0.7687	0.2337	0.0059	0.0040	0.0002	0.0001	0.0000	0.9969	0.1664	0.1654	0.0045	0.0007	0.0002	0.0002
	511.4658	469.8193	372.3223	1204.0781	2717.5828	3008.7031	5038.5383	1505.2891	536.3672	534.5000	922.1328	369.5313	321.4844	3814.0000
10000	0.7601	0.2886	0.0538	0.0051	0.0004	0.0000	0.0000	0.9897	0.0109	0.0054	0.0048	0.0008	0.0005	0.0002
	5137.4219	4475.6782	3685.8125	2834.8281	22866.2188	45381.3281	312053.9375	14988.8535	17021.3262	4495.4775	4603.2891	4115.9160	10950.7637	7264.3127
m=10														
0.0001	0.3863	0.3329	0.1780	0.1492	0.0269	0.0261	0.0154	0.5276	0.3857	0.0897	0.0364	0.0175	0.0008	0.0003

Sorted Linear coefficients and corresponding exponents for Electron Orbitals								Sorted Linear coefficients and corresponding exponents for PC Orbitals						
$\omega$ /Basis	1s	2s	3s	4s	5s	6s	7s	1s	2s	3s	4s	5s	6s	7s
0.0010	0.0866	0.1755	0.0435	0.3708	0.8058	0.0226	0.0249	0.5350	0.3200	1.0460	0.1947	1.3774	4.4040	6.3560
	2.4389	2.2629	0.5776	0.1568	0.1159	0.0417	0.0158	0.5274	0.3857	0.0892	0.0363	0.0166	0.0008	0.0003
	0.0996	0.1062	0.1589	0.0382	0.3645	0.4790	0.9237	0.5350	0.3200	1.0421	0.1947	1.3774	4.4040	6.3560
0.0100	0.3683	0.3377	0.1864	0.1256	0.1153	0.0702	0.0207	0.6204	0.3478	0.0830	0.0305	0.0028	0.0022	0.0004
	0.0661	0.1321	0.2271	0.0349	0.4141	0.0449	0.8678	0.5321	0.2911	1.2614	1.6400	5.4399	7.4040	11.8560
0.1000	0.4044	0.2797	0.2706	0.1068	0.0179	0.0152	0.0099	0.7369	0.4444	0.3919	0.2202	0.0011	0.0010	0.0003
	0.1443	0.0782	0.2893	0.6141	1.3278	0.0734	0.0459	0.7960	1.1400	1.0350	0.5700	5.9399	8.9040	11.9810
1	0.6302	0.2494	0.0825	0.0548	0.0179	0.0027	0.0004	0.9061	0.0854	0.0103	0.0007	0.0001	0.0001	0.0000
	0.5686	1.0044	2.1531	0.4407	4.7633	7.3379	13.3386	5.3750	4.4375	10.1372	20.0797	199.0375	136.9000	292.4000
10	0.7632	0.1223	0.0931	0.0296	0.0054	0.0001	0.0000	0.9260	0.0751	0.0016	0.0010	0.0004	0.0002	0.0001
	5.1246	8.1039	4.9602	18.2688	47.6278	251.2469	567.7014	51.0000	45.9000	37.4000	118.6719	172.6000	425.7750	467.5000
100	0.8843	0.2005	0.1032	0.0192	0.0034	0.0003	0.0000	0.8462	0.1938	0.0489	0.0235	0.0085	0.0072	0.0011
	51.7598	40.2886	37.9070	120.9788	316.2973	816.6250	1702.4875	486.2500	611.9043	949.0000	1359.0000	321.2500	1977.7500	2902.4063
1000	0.8946	0.1524	0.0521	0.0056	0.0012	0.0003	0.0001	0.8590	0.1797	0.0475	0.0227	0.0082	0.0067	0.0011
	508.9235	433.1982	401.6191	1252.7391	3526.2813	4413.5383	7435.5469	4862.5000	6130.8685	9487.5586	13510.0000	3212.5000	19850.0000	29185.7031
10000	0.8337	0.1846	0.0232	0.0041	0.0011	0.0001	0.0000	0.8362	0.2254	0.0556	0.0072	0.0033	0.0021	0.0000
	5094.8980	4498.8301	3480.1563	2833.8281	16863.1328	47646.9531	161858.6250	48624.0234	59724.7276	72750.0000	32446.8750	192150.0000	230775.0000	653117.5781
m=50														
0.0001	0.4294	0.3346	0.1617	0.1424	0.0361	0.0026	0.0000	0.5941	0.2894	0.1107	0.0164	0.0030	0.0015	0.0013
	0.1235	0.2868	0.0529	0.6763	1.6223	3.5866	6.8660	1.5700	2.3900	1.0350	3.2960	5.4399	11.4040	11.8560
0.0010	0.4282	0.3353	0.1610	0.1431	0.0362	0.0028	0.0001	0.5942	0.2895	0.1105	0.0165	0.0030	0.0015	0.0013
	0.1232	0.2857	0.0528	0.6738	1.6093	3.4538	6.8521	1.5700	2.3900	1.0350	3.2921	5.4399	11.4040	11.8560
0.0100	0.4273	0.3311	0.1625	0.1433	0.0390	0.0035	0.0000	0.5939	0.3065	0.0913	0.0187	0.0034	0.0010	0.0001
	0.1242	0.2861	0.0534	0.6624	1.5547	3.4577	6.9575	1.5700	2.3900	1.0350	3.2960	5.9399	8.3560	11.4040
0.1000	0.3581	0.3216	0.1824	0.1549	0.0706	0.0150	0.0001	0.8580	0.1690	0.0346	0.0306	0.0273	0.0128	0.0044
	0.1443	0.2873	0.6141	0.0779	1.4274	3.6047	18.7647	3.1400	5.0460	7.4399	1.0700	1.0350	11.4040	13.9810
1	0.5835	0.2815	0.1081	0.0406	0.0330	0.0073	0.0005	0.8123	0.1876	0.0002	0.0001	0.0001	0.0001	0.0000

Sorted Linear coefficients and corresponding exponents for Electron Orbitals								Sorted Linear coefficients and corresponding exponents for PC Orbitals						
$\omega$ /Basis	1s	2s	3s	4s	5s	6s	7s	1s	2s	3s	4s	5s	6s	7s
10	0.5686	1.0044	2.2577	0.4407	5.8135	16.2643	44.4820	25.8750	24.0797	56.7500	103.5122	178.4000	281.0375	388.9000
	0.9429	0.1333	0.1046	0.0355	0.0094	0.0020	0.0002	0.5286	0.4784	0.3280	0.3135	0.0218	0.0003	0.0001
	5.1246	8.1039	5.2531	18.2688	48.0672	138.0633	374.3421	245.2125	258.4000	549.9219	553.9000	433.5375	923.7500	90.0625
100	0.8966	0.2664	0.1840	0.0214	0.0045	0.0009	0.0001	0.6175	0.4049	0.0224	0.0001	0.0000	0.0000	0.0000
	51.7598	38.8238	37.4188	123.6644	341.1997	1027.5625	3014.9875	2484.0000	2540.2500	2699.0000	5086.0000	6035.0000	517.5000	258.7500
1000	0.9139	0.1214	0.0408	0.0060	0.0012	0.0002	0.0000	0.5731	0.4822	0.0366	0.0224	0.0039	0.0003	0.0000
	508.9235	420.9912	384.5293	1338.1883	3915.4914	12474.6094	38985.2656	26100.0000	23588.1250	18865.0000	30699.3750	13631.2500	7675.0000	4462.5000
10000	0.8300	0.1857	0.0199	0.0032	0.0014	0.0002	0.0000	0.9462	0.0647	0.0104	0.0007	0.0002	0.0001	0.0000
	5094.9219	4525.6855	3499.6875	2833.8281	16994.9688	54521.9531	187210.1875	251523.2834	219125.0000	182446.8750	546400.0000	805217.1875	51749.0234	25875.0000
m = 207														
0.0001	0.3848	0.3492	0.1762	0.1261	0.0640	0.0180	0.0034	0.5200	0.4006	0.0628	0.0193	0.0071	0.0018	0.0007
	0.1281	0.2908	0.6666	0.0562	1.5226	3.3366	6.8660	4.1400	5.7960	3.0700	8.4399	11.4040	13.8560	2.0350
0.0010	0.3843	0.3485	0.1765	0.1265	0.0645	0.0182	0.0034	0.5248	0.3870	0.0607	0.0279	0.0083	0.0010	0.0009
	0.1282	0.2903	0.6640	0.0563	1.5155	3.3288	6.8521	4.1400	5.7921	3.0700	7.4399	11.4040	15.8560	2.0350
0.0100	0.3834	0.3481	0.1770	0.1260	0.0653	0.0187	0.0035	0.5592	0.2775	0.1570	0.0081	0.0073	0.0006	0.0005
	0.1286	0.2908	0.6634	0.0566	1.5118	3.3327	6.9575	4.1400	5.7960	6.4399	11.4040	2.0700	15.8560	1.0350
0.1000	0.3321	0.3313	0.2075	0.1152	0.0957	0.0318	0.0060	0.8612	0.1680	0.0333	0.0072	0.0020	0.0001	0.0000
	0.2893	0.1443	0.6141	0.0782	1.4216	3.6984	10.7647	11.4040	14.4810	8.9399	5.7960	4.1400	2.0700	1.0350
1	0.5710	0.2880	0.1148	0.0383	0.0364	0.0106	0.0019	0.9587	0.0481	0.0071	0.0016	0.0009	0.0003	0.0001
	0.5686	1.0044	2.2547	5.8379	0.4407	17.3386	61.6695	103.5122	124.0797	178.4000	281.0375	56.7500	388.9000	25.8750
10	0.9288	0.1353	0.0942	0.0370	0.0104	0.0026	0.0004	0.8825	0.1176	0.0135	0.0103	0.0035	0.0005	0.0000
	5.1246	8.1039	5.2531	18.2688	48.7997	151.2469	567.7014	1038.2750	1017.5000	258.4000	268.6719	237.4000	472.6000	113.5000
100	0.8965	0.2637	0.1820	0.0221	0.0048	0.0011	0.0002	0.9977	0.0023	0.0000	0.0000	0.0000	0.0000	0.0000
	51.7598	38.8238	37.4188	123.6644	349.9888	1152.5625	4702.4875	10352.7500	10086.0000	1449.0000	2484.0000	1035.0000	517.5000	258.7500
1000	0.9151	0.1156	0.0363	0.0062	0.0012	0.0002	0.0000	0.9967	0.0033	0.0000	0.0000	0.0000	0.0000	0.0000
	508.9235	420.9912	382.0879	1350.3953	4101.0383	14310.5469	58047.7656	103510.0000	102350.0000	44840.0000	14490.0000	10350.0000	5175.0000	2587.5000
10000	0.8377	0.1827	0.0243	0.0029	0.0014	0.0002	0.0000	0.6910	0.3138	0.0049	0.0003	0.0002	0.0000	0.0000

Sorted Linear coefficients and corresponding exponents for Electron Orbitals								Sorted Linear coefficients and corresponding exponents for PC Orbitals						
$\omega$ /Basis	1s	2s	3s	4s	5s	6s	7s	1s	2s	3s	4s	5s	6s	7s
	5094.9219	4486.6230	3577.8125	2833.8281	17619.9688	63662.5781	305803.9375	1022600.0000	1058900.0000	798400.0000	209750.0000	182446.8750	51749.0234	25875.0000
m = 400														
0.0001	0.3721	0.3551	0.1860	0.1131	0.0719	0.0238	0.0048	0.5434	0.4778	0.0484	0.0204	0.0170	0.0017	0.0013
	0.1281	0.2908	0.6666	0.0564	1.5226	3.4928	8.4910	8.4399	5.7960	4.1400	13.8560	3.0700	2.0350	11.4040
0.0010	0.3710	0.3542	0.1868	0.1136	0.0727	0.0239	0.0047	0.5088	0.2994	0.1862	0.0069	0.0050	0.0011	0.0002
	0.1282	0.2898	0.6630	0.0565	1.5155	3.5007	8.5083	7.4399	5.7921	9.9040	4.1400	15.8560	3.0700	2.0350
0.0100	0.3701	0.3534	0.1874	0.1129	0.0741	0.0246	0.0048	0.6626	0.2561	0.0514	0.0411	0.0050	0.0002	0.0000
	0.1286	0.2903	0.6614	0.0568	1.5118	3.5358	8.7700	7.9399	5.7960	11.8560	11.4040	4.1400	2.0700	1.0350
0.1000	0.3367	0.3118	0.2268	0.1111	0.1011	0.0313	0.0057	0.9015	0.1093	0.0172	0.0112	0.0045	0.0005	0.0001
	0.2844	0.1443	0.6219	0.0791	1.5515	4.4718	15.1865	22.4810	16.9040	8.9399	5.7960	4.1400	2.0700	1.0350
1	0.5448	0.2982	0.1158	0.0561	0.0366	0.0094	0.0016	1.0019	0.0065	0.0039	0.0012	0.0005	0.0001	0.0000
	0.5686	1.0090	2.3615	0.4712	6.5276	21.3058	87.8414	200.2750	149.0797	281.0375	103.5122	388.9000	56.7500	25.8750
10	0.8432	0.1272	0.0357	0.0110	0.0028	0.0006	0.0001	0.7957	0.2643	0.0771	0.0191	0.0024	0.0007	0.0004
	5.1222	8.2937	18.1009	46.7550	143.4344	492.9944	1731.8156	2038.2750	1770.1188	1385.8375	1017.5000	582.2500	268.6719	222.6000
100	0.9007	0.2241	0.1461	0.0220	0.0046	0.0010	0.0002	0.8291	0.1712	0.0003	0.0000	0.0000	0.0000	0.0000
	51.7598	38.5796	36.9305	126.1058	370.4966	1306.8594	6100.9250	20056.7031	19727.7500	13734.0000	2699.0000	1035.0000	517.5000	258.7500
1000	0.8153	0.1776	0.0073	0.0014	0.0003	0.0001	0.0000	1.0000	0.0000	0.0000	0.0000	0.0000	0.0000	0.0000
	508.9235	474.8547	1217.5903	3603.8133	11732.8742	40850.8379	147930.5781	200006.2500	192340.0000	451010.0000	71990.0000	10350.0000	5175.0000	2587.5000
10000	0.9829	0.0461	0.0347	0.0166	0.0106	0.0003	0.0000	0.7028	0.2977	0.0003	0.0002	0.0000	0.0000	0.0000
	5094.9100	3577.8125	8197.3889	10432.4688	2833.8281	62962.1406	377295.3906	2022600.0000	1948400.0000	4374024.5117	582446.8750	209750.0000	51749.0234	25875.0000
m = 900														
0.0001	0.3598	0.3593	0.1960	0.1028	0.0809	0.0276	0.0055	0.6499	0.2487	0.1298	0.0410	0.0279	0.0109	0.0013
	0.1281	0.2903	0.6666	0.0567	1.5578	3.8991	11.0378	11.4040	15.8560	8.4399	5.7960	4.1400	3.0700	2.0350
0.0010	0.3593	0.3586	0.1962	0.1031	0.0815	0.0277	0.0055	0.7149	0.2250	0.1028	0.0532	0.0231	0.0079	0.0009
	0.1282	0.2898	0.6640	0.0567	1.5507	3.8913	11.0396	11.4040	16.1060	7.4399	5.7921	4.1400	3.0700	2.0350
0.0100	0.3568	0.3556	0.1972	0.1057	0.0834	0.0281	0.0055	0.6081	0.3982	0.0276	0.0187	0.0082	0.0010	0.0001
	0.1295	0.2908	0.6624	0.0578	1.5547	3.9772	11.5356	11.4040	15.8560	5.7960	6.4399	4.1400	2.0700	1.0350

Sorted Linear coefficients and corresponding exponents for Electron Orbitals								Sorted Linear coefficients and corresponding exponents for PC Orbitals						
$\omega$ /Basis	1s	2s	3s	4s	5s	6s	7s	1s	2s	3s	4s	5s	6s	7s
0.1000	0.3752	0.3149	0.2298	0.0914	0.0867	0.0260	0.0046	0.9939	0.0071	0.0029	0.0024	0.0015	0.0002	0.0000
	0.2920	0.1384	0.6990	1.8942	0.0762	5.9777	23.4522	47.5123	26.4040	5.7960	8.9399	4.1400	2.0700	1.0350
1	0.6105	0.3018	0.0981	0.0362	0.0131	0.0031	0.0005	0.9819	0.0209	0.0029	0.0004	0.0003	0.0000	0.0000
	0.5592	1.0576	2.4469	5.6059	15.3061	52.0276	207.7633	451.4000	406.0375	328.4000	124.0797	103.5122	56.7500	25.8750
10	0.8434	0.1270	0.0359	0.0110	0.0028	0.0006	0.0001	0.5413	0.4587	0.0042	0.0030	0.0013	0.0000	0.0000
	5.1231	8.3118	18.2230	47.8231	150.2703	544.2639	2278.6906	4472.6000	4534.3688	258.4000	268.6719	237.4000	1017.5000	113.5000
100	0.9067	0.2922	0.2193	0.0216	0.0044	0.0009	0.0001	0.9796	0.0204	0.0000	0.0000	0.0000	0.0000	0.0000
	51.7750	37.6030	36.4422	129.7679	396.8638	1480.6875	7671.2375	45007.8750	44727.7500	17484.0000	1035.0000	1449.0000	517.5000	258.7500
1000	0.8302	0.1631	0.0071	0.0013	0.0003	0.0001	0.0000	0.8370	0.1631	0.0000	0.0000	0.0000	0.0000	0.0000
	508.9235	472.4133	1260.0098	3845.5125	11810.9992	32100.8379	127930.5781	451010.0000	444850.0000	137340.0000	10350.0000	14490.0000	5175.0000	2587.5000
10000	0.9829	0.0462	0.0347	0.0166	0.0107	0.0003	0.0000	0.8964	0.1037	0.0001	0.0000	0.0000	0.0000	0.0000
	5094.9165	3577.8125	8197.3889	10432.4688	2833.8281	62649.6406	390850.0781	4508887.7930	4422600.0000	1898400.0000	232446.8750	209750.0000	51749.0234	25875.0000
m=1836														
0.0001	0.3580	0.3527	0.2039	0.0992	0.0880	0.0281	0.0052	0.6772	0.5561	0.3422	0.1999	0.1272	0.0458	0.0051
	0.2908	0.1291	0.6666	0.0573	1.6242	4.4850	14.3035	20.8560	12.4040	8.9399	5.7960	4.1400	3.0700	2.0350
0.0010	0.3547	0.3482	0.2065	0.1010	0.0902	0.0291	0.0054	0.6817	0.3666	0.1040	0.0789	0.0222	0.0034	0.0001
	0.2874	0.1291	0.6533	0.0577	1.5858	4.3835	14.1646	20.7310	13.6540	7.4399	5.7921	4.1400	3.0700	2.0350
0.0100	0.3609	0.3489	0.2079	0.0966	0.0886	0.0279	0.0051	0.8065	0.2572	0.2518	0.2442	0.0569	0.0048	0.0006
	0.2893	0.1286	0.6693	0.0573	1.6563	4.6647	15.3638	22.5435	13.6540	6.9399	5.7960	4.1400	2.0700	1.0350
0.1000	0.3997	0.3414	0.2225	0.0812	0.0605	0.0218	0.0039	0.9998	0.0039	0.0026	0.0026	0.0012	0.0001	0.0000
	0.3064	0.1345	0.7818	2.2399	0.0699	7.4875	32.4522	94.4810	8.9399	5.7960	11.4040	4.1400	2.0700	1.0350
1	0.6142	0.3032	0.0995	0.0329	0.0109	0.0026	0.0004	0.7167	0.2834	0.0002	0.0001	0.0001	0.0000	0.0000
	0.5603	1.0721	2.5865	6.4162	18.1076	64.2591	291.9430	913.9000	931.0375	328.4000	174.0797	103.5122	56.7500	25.8750
10	0.8425	0.1279	0.0361	0.0109	0.0028	0.0006	0.0001	0.7870	0.2193	0.0064	0.0003	0.0002	0.0000	0.0000
	5.1222	8.2946	18.2993	48.6776	157.1063	605.7874	2864.6281	9288.2750	8722.6000	6508.4000	1017.5000	862.4000	268.6719	113.5000
100	0.9103	0.0837	0.0212	0.0139	0.0042	0.0008	0.0001	0.5801	0.4301	0.0102	0.0000	0.0000	0.0000	0.0000
	51.7750	39.3719	133.1859	31.6216	421.2778	1634.0078	9241.5500	92852.7500	90086.0000	79046.5000	1035.0000	1449.0000	517.5000	258.7500



Sorted Linear coefficients and corresponding exponents for Electron Orbitals								Sorted Linear coefficients and corresponding exponents for PC Orbitals						
$\omega$ /Basis	1s	2s	3s	4s	5s	6s	7s	1s	2s	3s	4s	5s	6s	7s
1000	0.8212	0.1718	0.0073	0.0014	0.0003	0.0001	0.0000	0.9372	0.0628	0.0000	0.0000	0.0000	0.0000	0.0000
	508.9235	473.9392	1232.8491	3640.8332	10500.7859	28702.4004	130508.7031	918470.9375	911100.0000	14490.0000	10350.0000	44840.0000	5175.0000	2587.5000
10000	0.9832	0.0460	0.0347	0.0164	0.0106	0.0003	0.0000	0.9563	0.0437	0.0000	0.0000	0.0000	0.0000	0.0000
	5094.9213	3577.8125	8168.2637	10432.4306	2833.8281	63245.3438	414600.0781	9183802.3438	9097600.0000	209750.0000	182446.8750	1198400.0000	51749.0234	25875.0000

## 4.5 Asymptotic Behavior of the Variational Wave Function and System Nature

According to the discussion in section 2-3-2, we can compare the radial distribution function of the variational system ( $RDF_{var}$ )

$$RDF_{var} = r^2 e^{-2\alpha r - 2\beta r^2} \quad 4.8$$

The radial distribution function of the hydrogen-like atom ( $RDF_{HL}$ )

$$RDF_{HL}(r) = 4\mu^3 r^2 \exp(-2\mu r) \quad 4.9$$

and the radial distribution function of the harmonic oscillator ( $RDF_{HO}$ )

$$RDF_{HO}(r) = 4 \frac{(\mu\omega)^{3/2}}{\pi^{1/2}} r^2 \exp(-\mu\omega r^2) \quad 4.10$$

at any specific mass and frequency, and as a result, examine the overall behavior of the variational wave function and its similarity to the two mentioned systems, especially its asymptotic behavior. This comparison at frequencies  $10^{-4}$  and  $10^4$  can confirm the accuracy of the asymptotic behavior of the variational wave function (2-72). Figures 4-1 to 4-10 illustrate these points.

As expected, the behavior of the variational wave function at frequencies of  $10^{-4}$  corresponds closely to that of a hydrogen-like atom; and at frequencies of  $10^4$ , it matches the behavior of a harmonic oscillator. This behavior can be evaluated using equation (4-8) by examining  $\frac{\beta}{\alpha}$  ratio. This ratio is reported as item 7 in Table 4-2. It is expected that, at low frequencies, this ratio approaches zero, and at high frequencies, it tends towards infinity. The numerical data of this ratio confirms this behavior.

As mass increases, the rate of system behavior changes (or changes in nature) decreases. This means that the lower the mass of the PCP, the faster the system's behavior (at lower frequencies) transitions to oscillator-like behavior. This correctly shows that the lower the mass of the PCP, the more sensitive the system is to the presence of an oscillatory field. Given that the binding energy of hydrogen (mass 1836) is greater compared to positronium (mass 1) and its radius is smaller, it demonstrates more stability in maintaining atomic structure against external fields.

Based on the above explanations, it can be said that at low frequencies, the system has a nature similar to hydrogen-like atoms, and the two particles are bound to each other, making the concept of an atom and, consequently, the correlation energy meaningful. However, at high frequencies, the system's behavior diverges from that of a hydrogen-like atom and aligns with that of a harmonic oscillator. Therefore, in these regions, the two particles (even with a very small distance) are not bound to each other and are only held together by an oscillatory potential. As a result, the concept of atomic structure is meaningless, and one can only speak of two particles trapped in a powerful oscillatory potential.

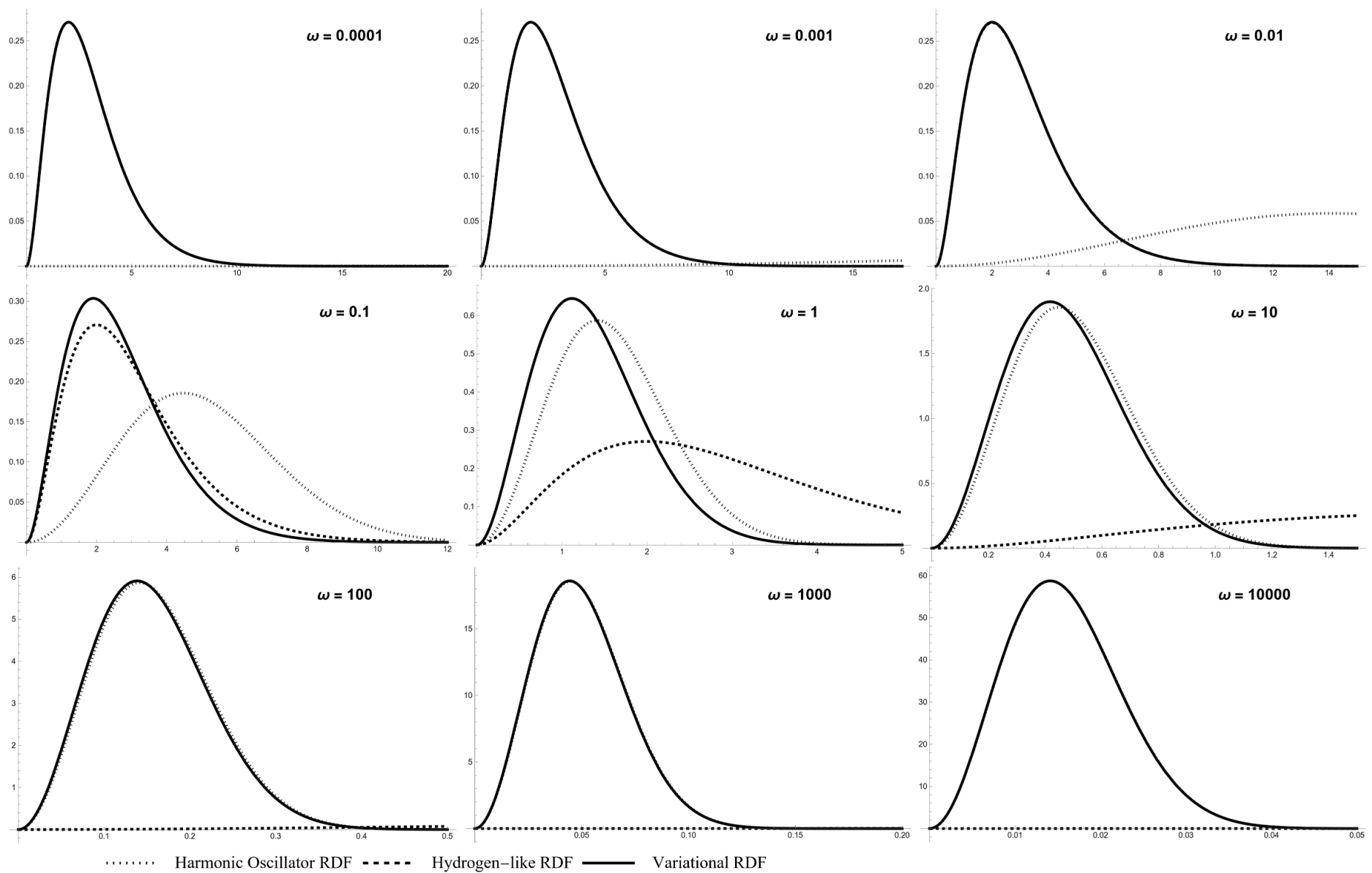


Figure 4-1: Comparison of the radial distribution functions with respect to inter-particle distance for variational, hydrogen-like, and harmonic oscillator systems at mass 1.

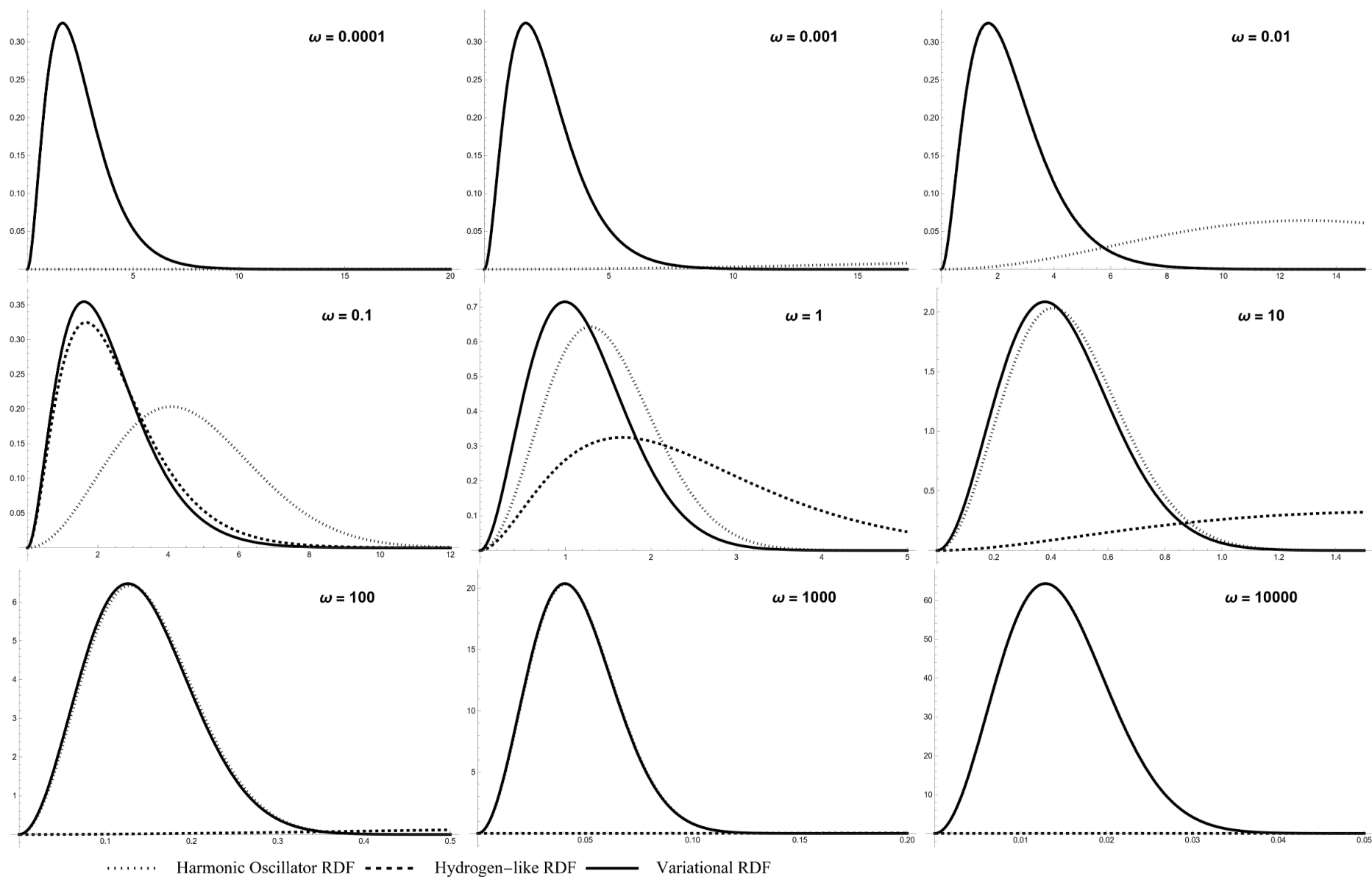


Figure 4-2: Comparison of the radial distribution functions with respect to inter-particle distance for variational, hydrogen-like, and harmonic oscillator systems at mass 1.5.

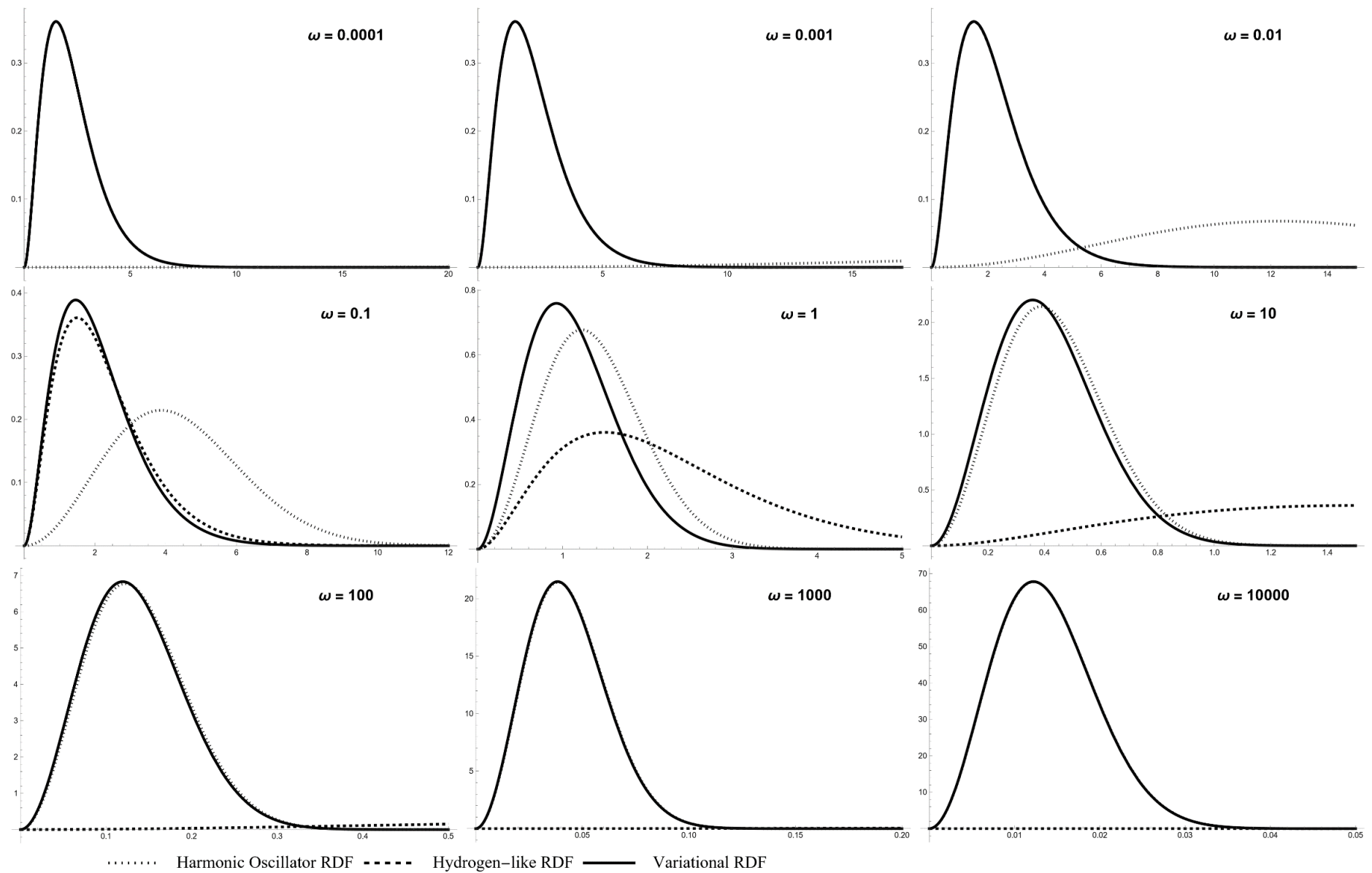


Figure 4-3: Comparison of the radial distribution functions with respect to inter-particle distance for variational, hydrogen-like, and harmonic oscillator systems at mass 2.

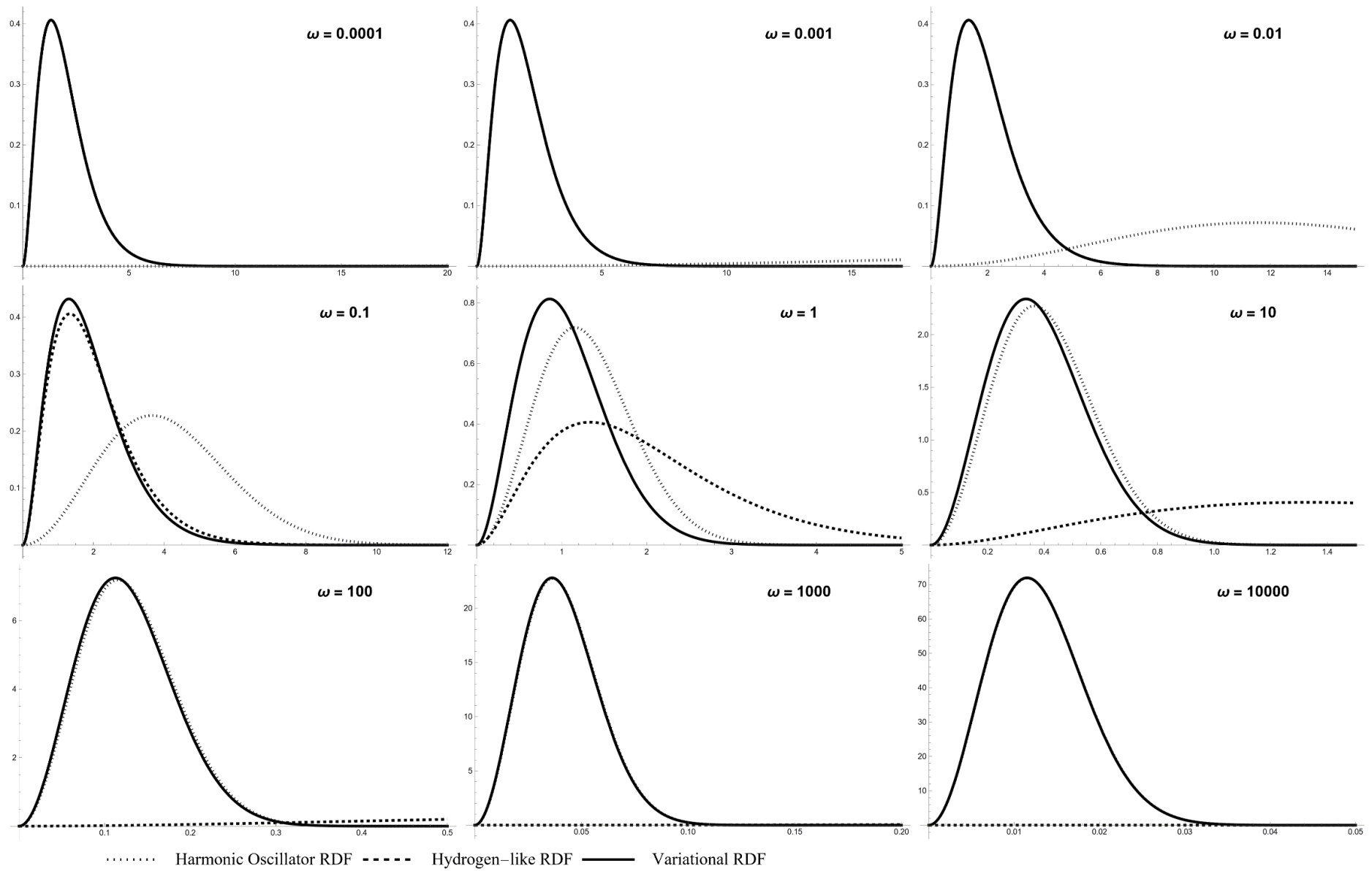


Figure 4-4: Comparison of the radial distribution functions with respect to inter-particle distance for variational, hydrogen-like, and harmonic oscillator systems at mass 3.

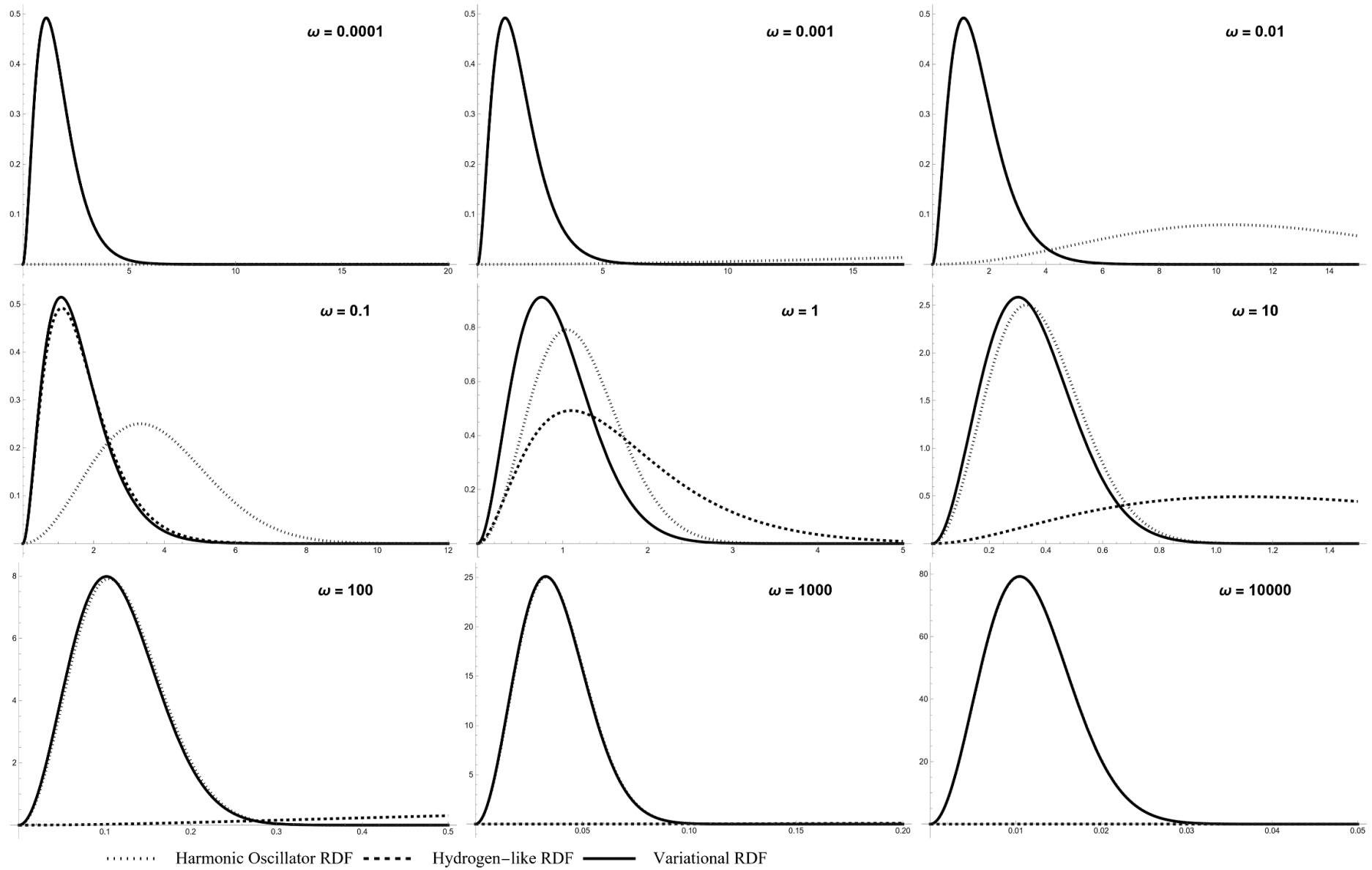


Figure 4-5: Comparison of the radial distribution functions with respect to inter-particle distance for variational, hydrogen-like, and harmonic oscillator systems at mass 10.



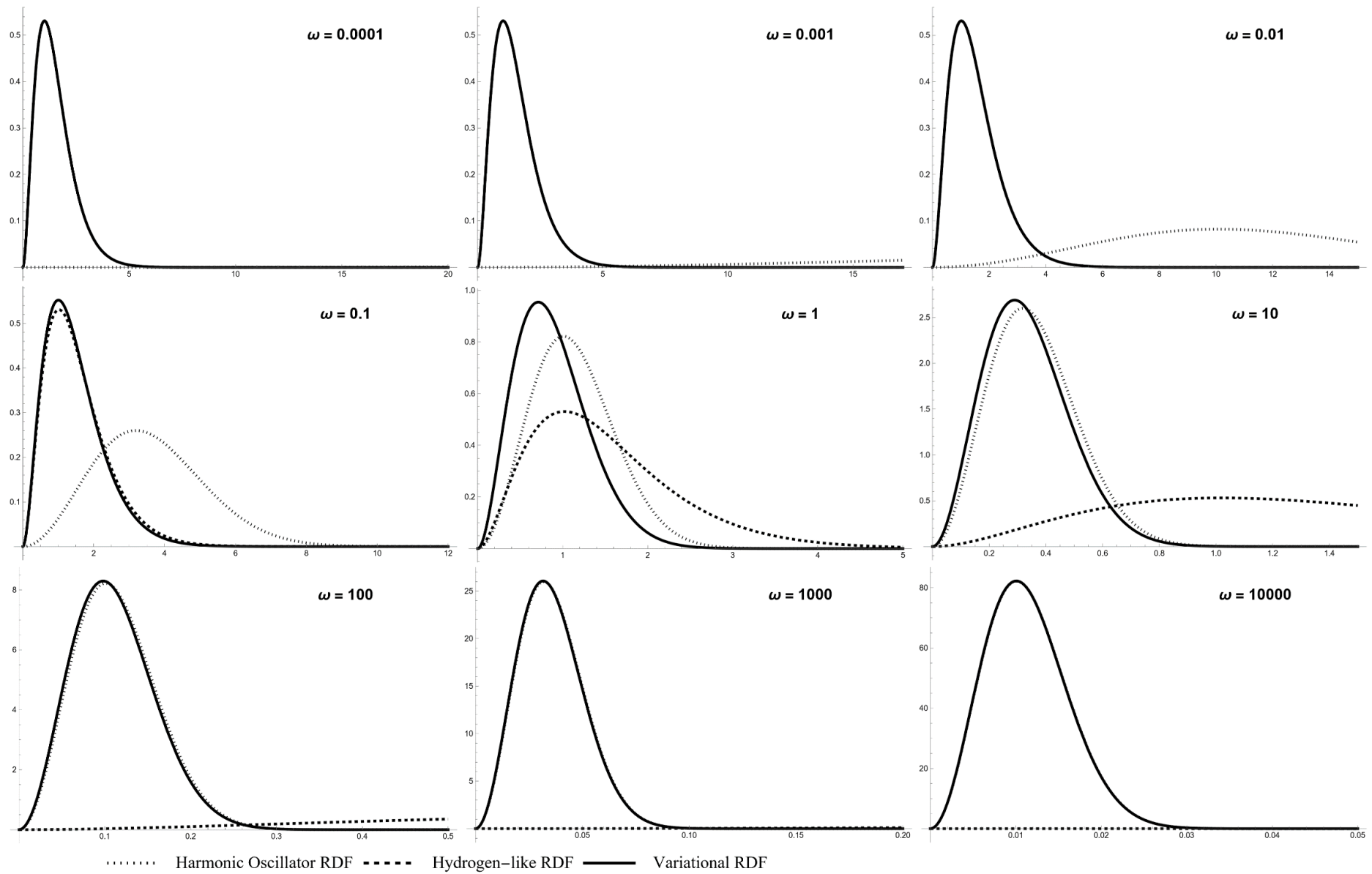


Figure 4-6: Comparison of the radial distribution functions with respect to inter-particle distance for variational, hydrogen-like, and harmonic oscillator systems at mass 50.

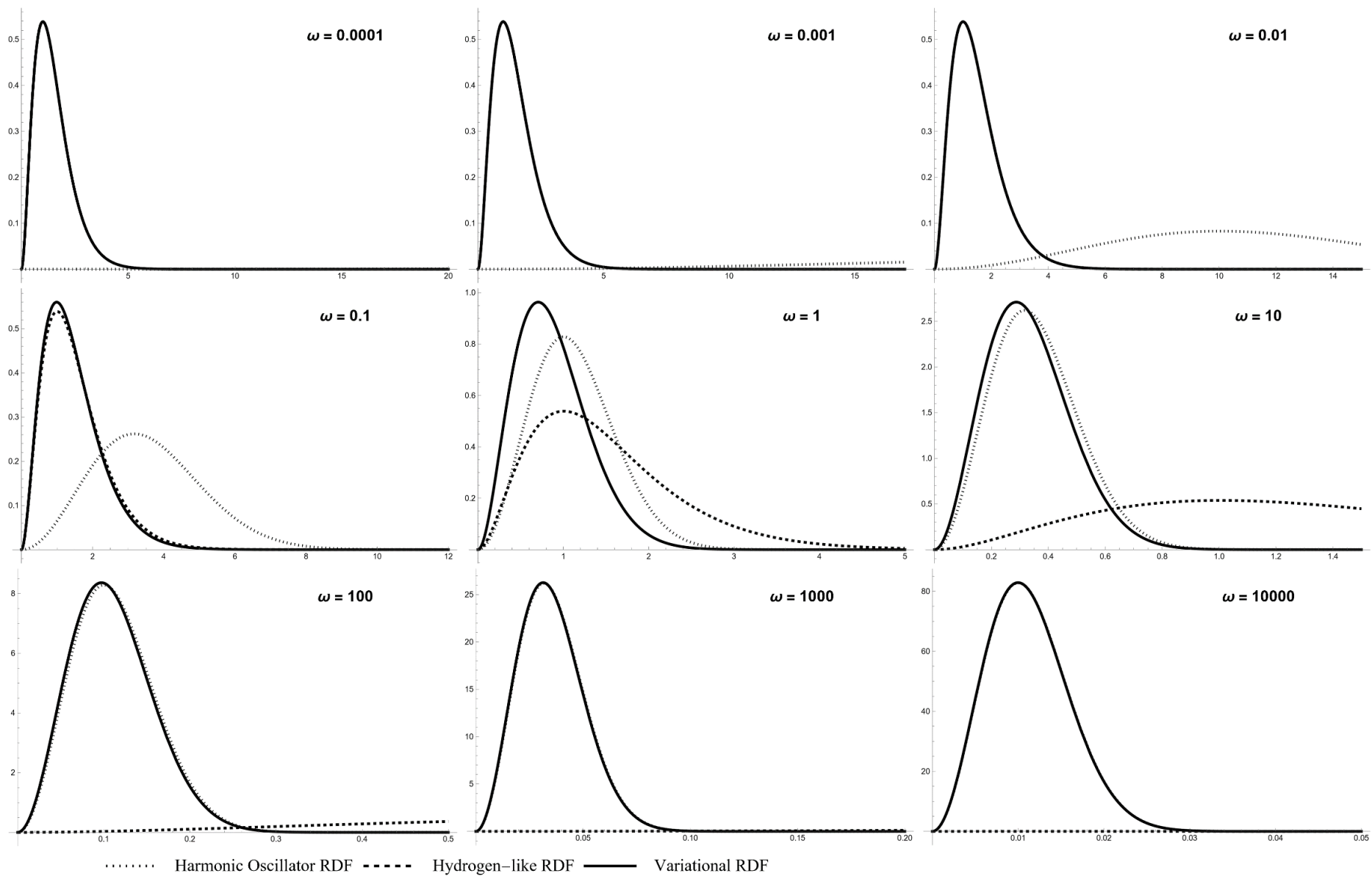


Figure 4-7: Comparison of the radial distribution functions with respect to inter-particle distance for variational, hydrogen-like, and harmonic oscillator systems at mass 207.

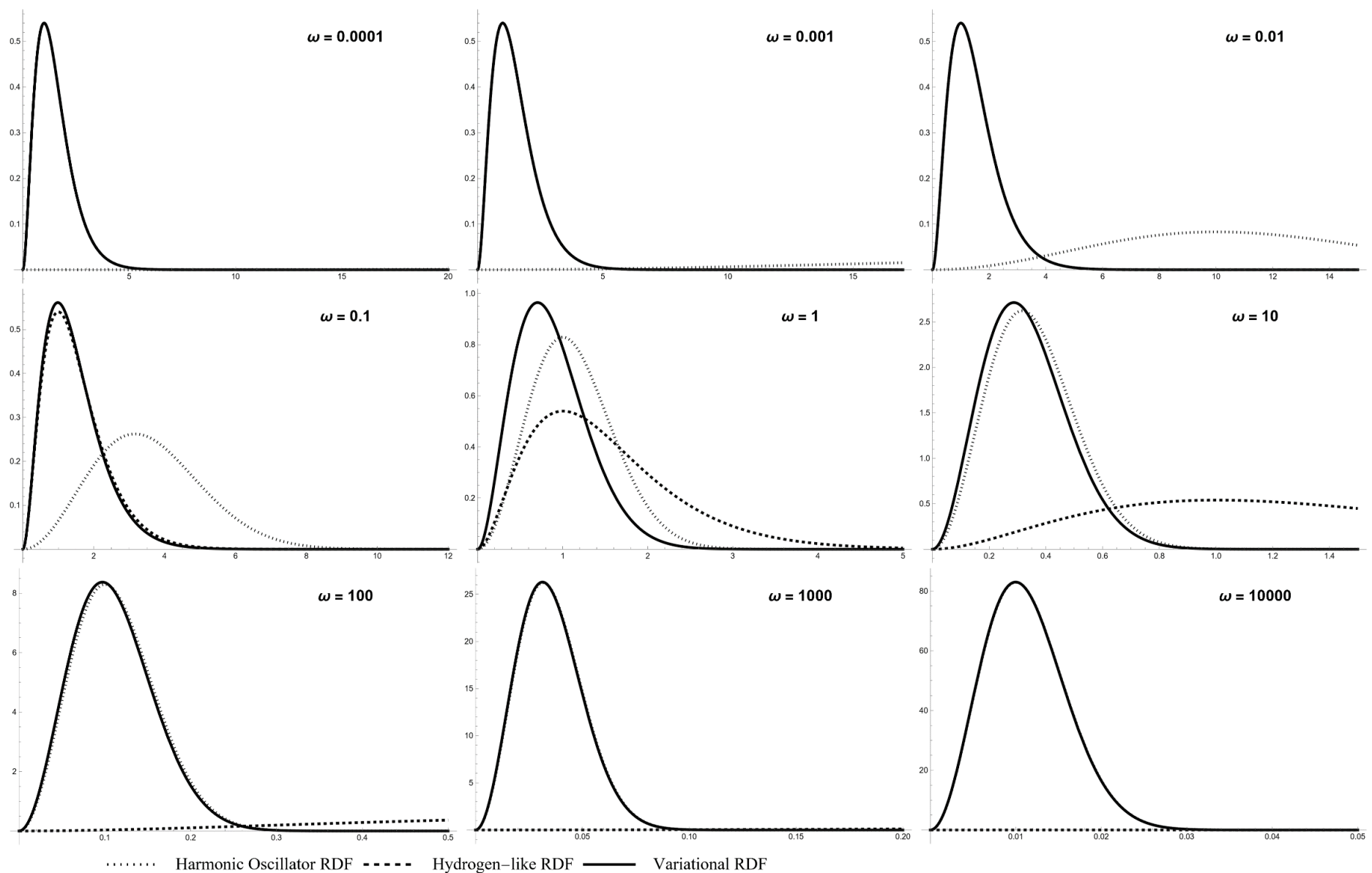


Figure 4-8: Comparison of the radial distribution functions with respect to inter-particle distance for variational, hydrogen-like, and harmonic oscillator systems at mass 400.

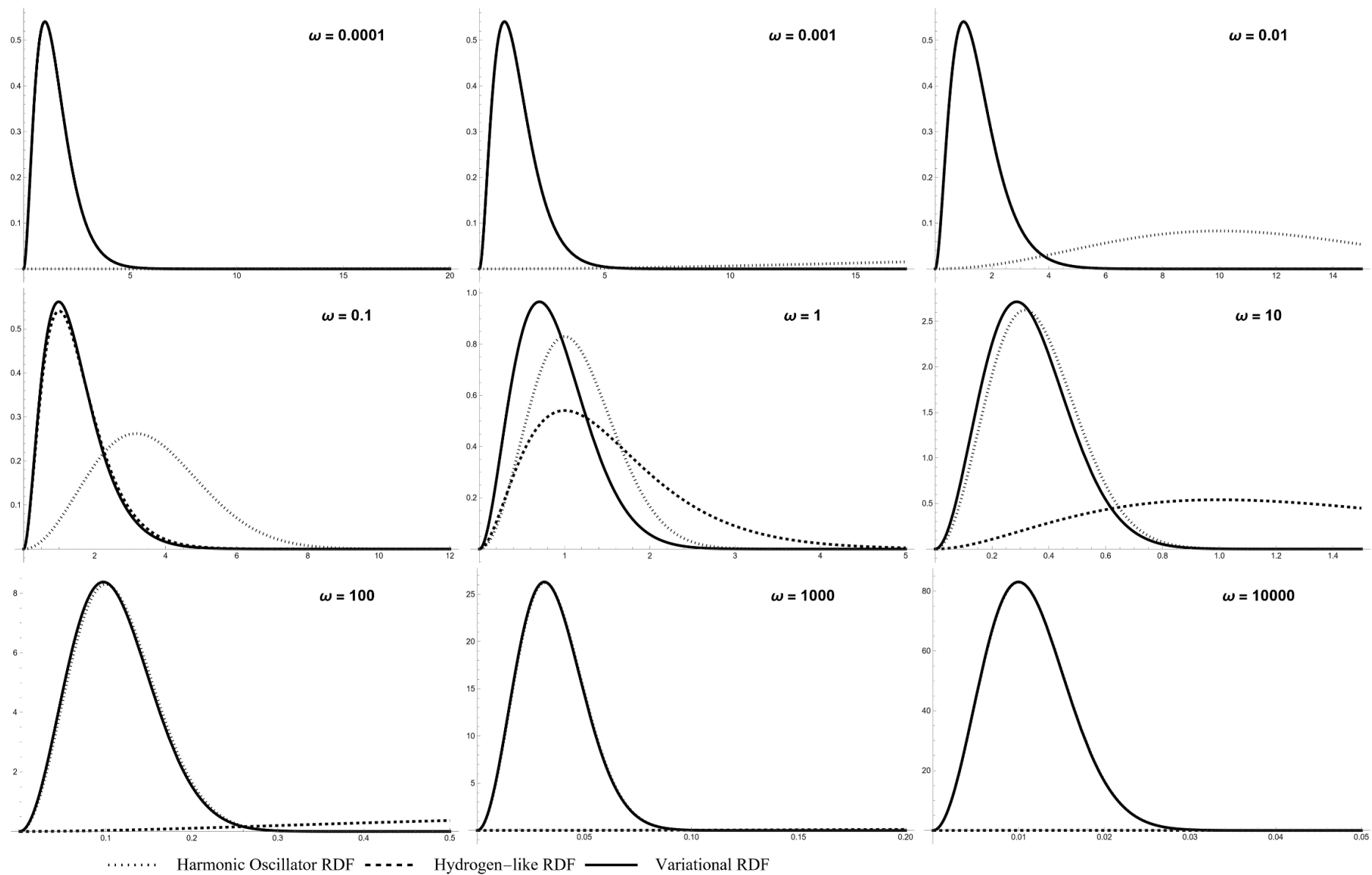


Figure 4-9: Comparison of the radial distribution functions with respect to inter-particle distance for variational, hydrogen-like, and harmonic oscillator systems at mass 900.

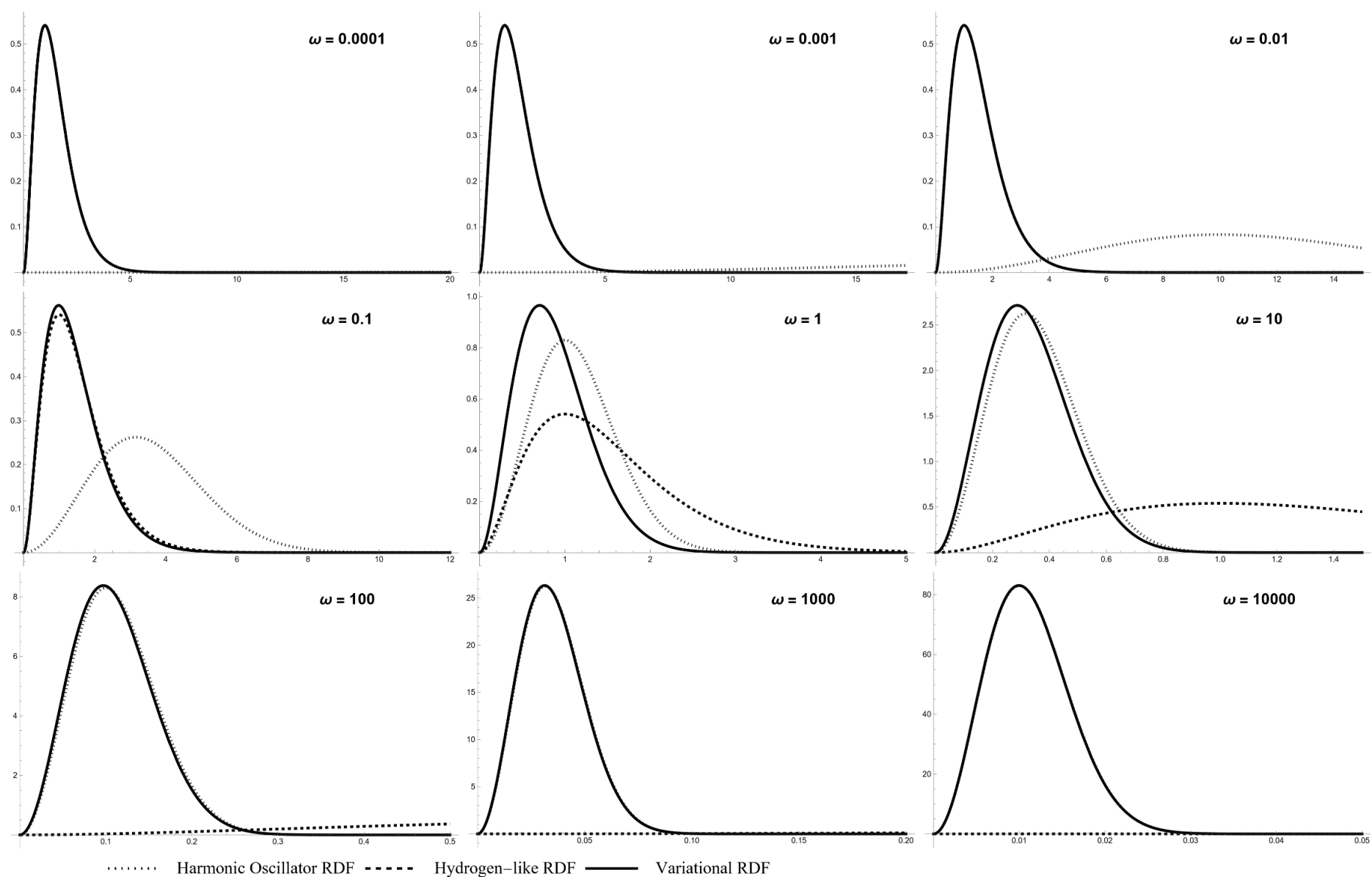


Figure 4-10: Comparison of the radial distribution functions with respect to inter-particle distance for variational, hydrogen-like, and harmonic oscillator systems at mass 1836

## 5 Electron-Positively Charged Particle Correlation in the Exotic Harmonium Model

### 5.1 Correlation in Wavefunction-Based Approaches

#### 5.1.1 Correlation Energy

In this study, the correlation energies (3-24) and (3-25) for the entire range of mass and HO frequencies are calculated and reported in Table 5-1. However, DFT calculations using analytical single-particle densities were not feasible due to complexity. Therefore, the density forms were simplified through fitting only for selected masses

and HO frequencies. Subsequently, the DFT calculations, including the correlation energy (3-32), were also performed only for these selected parameters.

The Hartree-Fock correlation energy, defined by equation (3-25) as the difference in energy between correlated methods and the MC-HF method, is reported for both the variational and FEM methods in items 5 and 6 of Table 4-3, respectively. These numerical data, along with Figures 5-1 and 5-2, show that the magnitude of correlation energy decreases with increasing HO frequency for a given mass. Conversely, as mass increases from 1 to 3, the magnitude of correlation energy initially increases and then decreases for masses above 10. Therefore, the magnitude of correlation energy inversely correlates with oscillator frequency and PCP mass, except for a small range between masses 1 and 3 where this relationship is direct.

Table 5-1 shows the correlation energy components relative to the MC-HF reference, obtained from the differences in variational and MC-HF energy components (Table 4-4). The difference in electron kinetic energy decreases with increasing frequency for a given mass and initially increases (up to mass 10) and then decreases with increasing mass for a given frequency. The difference in the kinetic energy of the PCP at a specific frequency decreases with increasing mass and changes sign, decreasing in magnitude for masses above 10.

The difference in the harmonic oscillator potential energy for the electron at a given mass changes sign and becomes negative with increasing frequency, with its magnitude increasing. However, its magnitude decreases with increasing mass for a given frequency. The difference in the harmonic oscillator potential energy for the PCP is

always positive and increases with frequency for a given mass. At a specific frequency, it initially increases and then decreases for intermediate masses (e.g., 50 and 207). Additionally, the difference in e-PCP interaction energy is always negative, and its magnitude decreases with increasing frequency for a given mass. At a specific frequency, it initially increases and then decreases for intermediate masses.

The correlation energy has two major components: kinetic energy, which depends on mass changes, and potential energy, which depends on frequency changes.



Table 5-1: Correlation energy values relative to MC-HF reference and its components

$\omega$ /Quantities	Correlation E <sup>1</sup>	$\Delta$ TE <sup>2</sup>	$\Delta$ TP <sup>3</sup>	$\Delta$ HO E <sup>4</sup>	$\Delta$ HO P <sup>5</sup>	$\Delta$ INT <sup>6</sup>
m = 1						
0.0001	-0.141337	0.070781	0.070781	0.000037	0.000037	-0.282973
0.001	-0.140006	0.071100	0.071100	0.000366	0.000366	-0.282937
0.01	-0.128294	0.072746	0.072746	0.002867	0.002867	-0.279520
0.1	-0.086137	0.057013	0.057013	0.004648	0.004648	-0.209460
1	-0.059918	0.034217	0.034217	0.001419	0.001419	-0.131191
10	-0.052581	0.027484	0.027484	0.000398	0.000398	-0.108344
100	-0.050455	0.025587	0.025590	0.000121	0.000118	-0.101870
1000	-0.049803	0.024882	0.024883	0.000175	0.000173	-0.099911
10000	-0.049605	0.021779	0.022020	0.003076	0.002835	-0.099315
m = 1.5						
0.0001	-0.168189	0.108126	0.060289	0.000030	0.000045	-0.336679
0.001	-0.166854	0.108380	0.060679	0.000293	0.000441	-0.336647
0.01	-0.154850	0.109589	0.063297	0.002353	0.003659	-0.333748
0.1	-0.105994	0.088305	0.053092	0.002963	0.008837	-0.259192
1	-0.071490	0.052563	0.030357	-0.003271	0.007081	-0.158220
10	-0.061655	0.041587	0.023257	-0.005435	0.006498	-0.127562
100	-0.058820	0.038512	0.021233	-0.006052	0.006401	-0.118913
1000	-0.057948	0.037582	0.020665	-0.006239	0.006337	-0.116294
10000	-0.057773	0.037306	0.022997	-0.006305	0.003717	-0.115488
m = 2						
0.0001	-0.183855	0.135875	0.048206	0.000025	0.000050	-0.368011
0.001	-0.182519	0.136086	0.048643	0.000245	0.000492	-0.367985
0.01	-0.170363	0.136970	0.051871	0.001978	0.004182	-0.365363
0.1	-0.117354	0.111770	0.046106	0.001646	0.011862	-0.288738
1	-0.076839	0.065423	0.025049	-0.006855	0.011399	-0.171855
10	-0.065106	0.050733	0.018175	-0.009845	0.011112	-0.135281
100	-0.061727	0.046616	0.016264	-0.010688	0.011052	-0.124972
1000	-0.060689	0.045367	0.015674	-0.010944	0.011058	-0.121852
10000	-0.060368	0.044998	0.015497	-0.011029	0.011051	-0.120886
m = 3						
0.0001	-0.199277	0.171946	0.027555	0.000019	0.000056	-0.398853
0.001	-0.197939	0.172102	0.028050	0.000184	0.000554	-0.398829
0.01	-0.185627	0.172551	0.032010	0.001484	0.004827	-0.396500
0.1	-0.127779	0.142191	0.032517	-0.000074	0.015718	-0.318130
1	-0.079392	0.080203	0.015763	-0.011235	0.016759	-0.180882

$\omega$ /Quantities	Correlation E <sup>1</sup>	$\Delta$ TE <sup>2</sup>	$\Delta$ TP <sup>3</sup>	$\Delta$ HO E <sup>4</sup>	$\Delta$ HO P <sup>5</sup>	$\Delta$ INT <sup>6</sup>
10	-0.065147	0.059780	0.009969	-0.015002	0.016534	-0.136429
100	-0.061064	0.054066	0.008362	-0.015990	0.016457	-0.123961
1000	-0.059814	0.052325	0.007859	-0.016278	0.016460	-0.120200
10000	-0.059435	0.051791	0.007754	-0.016340	0.016406	-0.119048
m=10						
0.0001	-0.197347	0.223009	-0.025437	0.000007	0.000068	-0.394994
0.001	-0.196007	0.223057	-0.024833	0.000066	0.000673	-0.394971
0.01	-0.183502	0.222552	-0.019549	0.000505	0.005996	-0.393007
0.1	-0.118794	0.180539	-0.005193	-0.002666	0.021516	-0.312990
1	-0.059334	0.084132	-0.004977	-0.014362	0.020969	-0.145095
10	-0.042938	0.053113	-0.005136	-0.016759	0.018437	-0.092593
100	-0.038548	0.045080	-0.005026	-0.017034	0.017459	-0.079028
1000	-0.037256	0.042722	-0.004645	-0.017052	0.016799	-0.075081
10000	-0.036929	0.041886	-0.002508	-0.016954	0.014523	-0.073860
m=50						
0.0001	-0.136159	0.178247	-0.041869	0.000001	0.000073	-0.272612
0.001	-0.134821	0.178246	-0.041216	0.000014	0.000724	-0.272589
0.01	-0.122460	0.176975	-0.035446	0.000078	0.006280	-0.270348
0.1	-0.064093	0.126163	-0.016007	-0.002004	0.017359	-0.189603
1	-0.022104	0.039693	-0.006276	-0.006612	0.010383	-0.059291
10	-0.013563	0.019984	-0.004068	-0.006593	0.007384	-0.030271
100	-0.011572	0.015720	-0.003510	-0.006360	0.006571	-0.023993
1000	-0.011007	0.014548	-0.003348	-0.006269	0.006330	-0.022269
10000	-0.010839	0.014253	-0.003870	-0.006298	0.006883	-0.021748
m=207						
0.0001	-0.082760	0.114782	-0.031800	0.000000	0.000074	-0.165817
0.001	-0.081427	0.114763	-0.031139	0.000003	0.000730	-0.165784
0.01	-0.069560	0.112685	-0.025499	0.000004	0.005872	-0.162622
0.1	-0.026584	0.061989	-0.009265	-0.000908	0.009619	-0.088022
1	-0.006733	0.013582	-0.002522	-0.002159	0.003598	-0.019232
10	-0.003642	0.005864	-0.001419	-0.001994	0.002260	-0.008353
100	-0.002977	0.004369	-0.001178	-0.001885	0.001949	-0.006223
1000	-0.002793	0.003967	-0.001112	-0.001843	0.001862	-0.005668
10000	-0.002747	0.003865	-0.001366	-0.001839	0.001684	-0.005513
m=400						
0.0001	-0.063705	0.089870	-0.025943	0.000000	0.000075	-0.127707
0.001	-0.062375	0.089844	-0.025282	0.000002	0.000727	-0.127666

$\omega$ /Quantities	Correlation E <sup>1</sup>	$\Delta$ TE <sup>2</sup>	$\Delta$ TP <sup>3</sup>	$\Delta$ HO E <sup>4</sup>	$\Delta$ HO P <sup>5</sup>	$\Delta$ INT <sup>6</sup>
0.01	-0.050894	0.087230	-0.019818	-0.000004	0.005510	-0.123812
0.1	-0.016254	0.040286	-0.006189	-0.000566	0.006510	-0.056295
1	-0.003624	0.007681	-0.001478	-0.001190	0.002045	-0.010680
10	-0.001804	0.003071	-0.000803	-0.001086	0.001241	-0.004228
100	-0.001424	0.002208	-0.000658	-0.001025	0.001060	-0.003007
1000	-0.001317	0.001969	-0.000620	-0.000996	0.001011	-0.002681
10000	-0.001443	-0.005101	-0.002824	0.005873	0.001943	-0.002571
m = 900						
0.0001	-0.045320	0.064974	-0.019430	0.000000	0.000075	-0.090938
0.001	-0.043998	0.064936	-0.018772	0.000001	0.000721	-0.090882
0.01	-0.033180	0.061483	-0.013630	-0.000006	0.004896	-0.085924
0.1	-0.008372	0.022002	-0.003443	-0.000293	0.003679	-0.030317
1	-0.001579	0.003644	-0.000729	-0.000539	0.000983	-0.004939
10	-0.000638	0.001257	-0.000382	-0.000498	0.000579	-0.001580
100	-0.000448	0.000821	-0.000310	-0.000476	0.000489	-0.000980
1000	-0.000391	0.000712	-0.000338	-0.000471	0.000509	-0.000807
10000	-0.000512	-0.006410	-0.000858	0.006486	0.001029	-0.000759
m = 1836						
0.0001	-0.033161	0.048083	-0.014693	0.000000	0.000075	-0.066626
0.001	-0.031848	0.048031	-0.014040	0.000000	0.000712	-0.066552
0.01	-0.021825	0.043694	-0.009286	-0.000006	0.004197	-0.060424
0.1	-0.004486	0.012247	-0.001929	-0.000154	0.002081	-0.016730
1	-0.000684	0.001826	-0.000378	-0.000246	0.000504	-0.002389
10	-0.000140	0.000786	-0.000199	-0.000680	0.000295	-0.000454
100	-0.000035	0.000230	-0.000157	-0.000238	0.000245	-0.000104
1000	0.000000	0.000167	-0.000156	-0.000239	0.000245	-0.000013
10000	-0.000132	-0.006711	-0.000997	0.006500	0.000343	-0.000006

1. Correlation energy relative to MC-HF/[7s:7s] reference (equation 3-25)
2. Electron's kinetic energy contribution to correlation energy
3. PCP's kinetic energy contribution to correlation energy
4. Electron's harmonic oscillator potential energy contribution to correlation energy
5. PCP's harmonic oscillator potential energy contribution to correlation energy
6. E-PCP interaction energy contribution to correlation energy

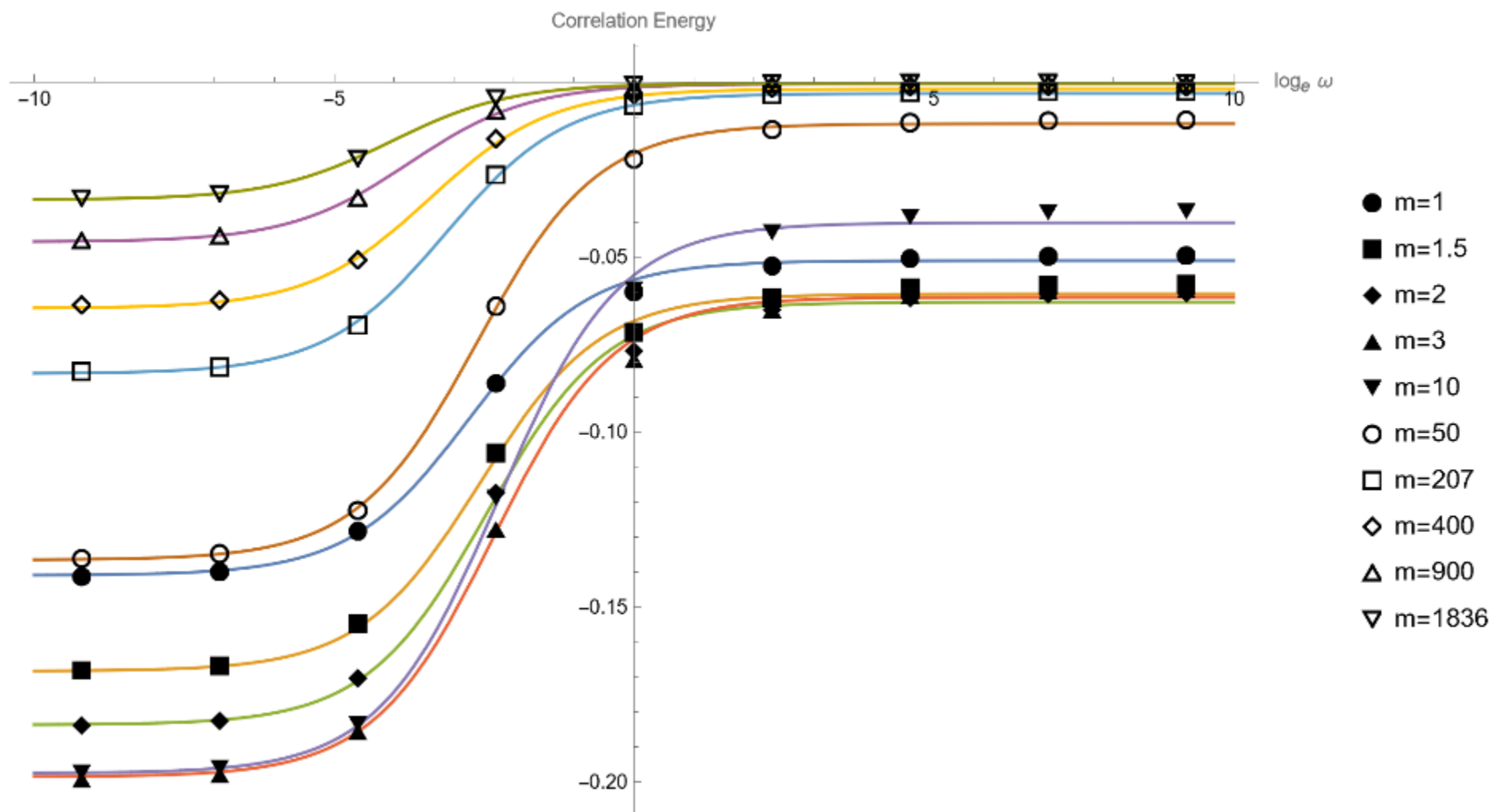


Figure 5-1: Correlation energies plotted (shapes) against the natural logarithm of HO frequency for different masses, along with lines obtained from fitting functions.

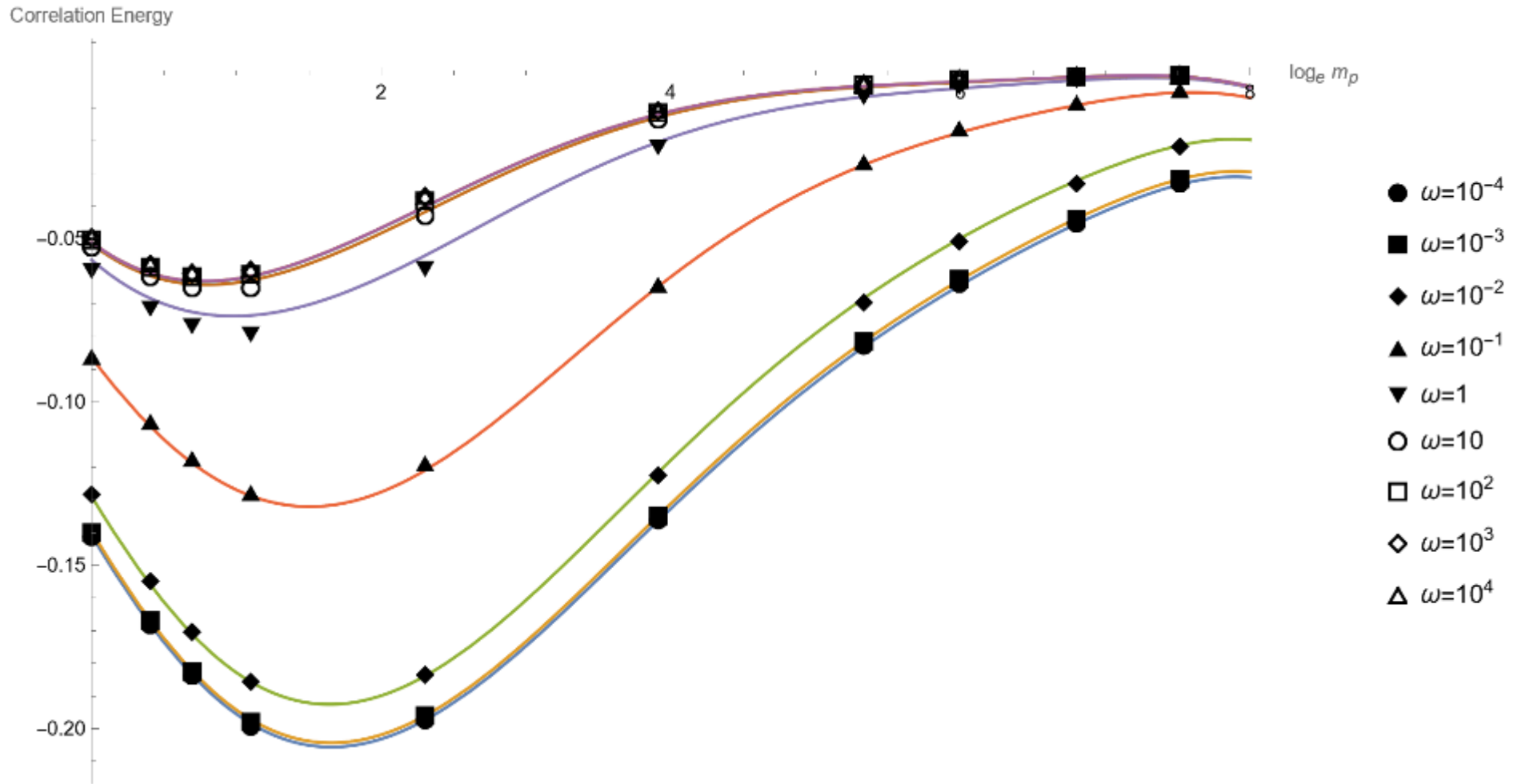


Figure 5-2: Correlation energies plotted (shapes) against the natural logarithm of the PCP's mass for different HO frequencies, along with lines obtained from fitting functions.

The reference-independent correlation energies ( $w_c$ ), as well as the values of  $w$  and  $w_{col}$  in equation (3-24), are presented in Table 2-5. Since the total two-particle interaction energy ( $w$ ) equals the interaction energy from wavefunction-based calculations (equations 2-139 and 2-152), these two values are reported for comparison in items 1 and 2, and their difference in item 6 of Table 5-2, where the zeros confirm the data's accuracy. The values of  $w_c$  and  $w_{col}$  are presented in items 4 and 3, respectively. To check the data's accuracy based on equation (3-21), the sum of  $w_c$  and  $w_{col}$  is given in item 5, which equals item 2 across all systems (while this equality seems obvious according to equation 3-21, it is noteworthy that the definition of  $w_c$  in the codes was derived using the integrand of equation 3-20, and the integration was ultimately performed to obtain the numerical values. Consequently, this test indicates any potential errors in the integration process).

The data in Table 5-2 show that the trends of reference-independent correlation energy match the Hartree-Fock correlation energy trends. However, their values, especially at low masses and HO frequencies, differ significantly. At high HO frequencies, these energy values converge, reflecting the system's effective transformation into two harmonic oscillators. In such a scenario, the particles are not correlated, and the effective system's wavefunction reduces to the product of the electron and positive particle wavefunctions, resembling the two-component Hartree-Fock total wavefunction.

Table 5-2: values of e-PCP interaction energy, Hartree potential, reference-independent correlation energy, and MC-HF correlation energy

$\omega$ /Quantities	INT <sup>1</sup>	$\mathbf{w}^2$	$\mathbf{w}_{col}^3$	$\mathbf{w}_c^4$	TEST1 <sup>5</sup>	TEST2 <sup>6</sup>	MC-HF corr <sup>7</sup>
m = 1							
0.0001	-0.5000	-0.5000	-0.0113	-0.4887	-0.5000	0.0000	-0.141337
0.001	-0.5000	-0.5000	-0.0356	-0.4644	-0.5000	0.0000	-0.140006
0.01	-0.5006	-0.5006	-0.1107	-0.3899	-0.5006	0.0000	-0.128294
0.1	-0.5414	-0.5414	-0.3127	-0.2288	-0.5414	0.0000	-0.086137
1	-0.9916	-0.9916	-0.8589	-0.1327	-0.9916	0.0000	-0.059918
10	-2.6897	-2.6897	-2.5813	-0.1084	-2.6897	0.0000	-0.052581
100	-8.1377	-8.1377	-8.0359	-0.1017	-8.1377	0.0000	-0.050455
1000	-25.3878	-25.3878	-25.2881	-0.0997	-25.3878	0.0000	-0.049803
10000	-79.9442	-79.9442	-79.8451	-0.0991	-79.9442	0.0000	-0.049605
m = 1.5							
0.0001	-0.6000	-0.6000	-0.0126	-0.5874	-0.6000	0.0000	-0.168189
0.001	-0.6000	-0.6000	-0.0398	-0.5602	-0.6000	0.0000	-0.166854
0.01	-0.6005	-0.6005	-0.1240	-0.4765	-0.6005	0.0000	-0.154850
0.1	-0.6375	-0.6375	-0.3516	-0.2859	-0.6375	0.0000	-0.105994
1	-1.1114	-1.1114	-0.9518	-0.1596	-1.1114	0.0000	-0.071490
10	-2.9652	-2.9652	-2.8378	-0.1274	-2.9652	0.0000	-0.061655
100	-8.9314	-8.9314	-8.8128	-0.1186	-8.9314	0.0000	-0.058820
1000	-27.8274	-27.8274	-27.7114	-0.1160	-27.8274	0.0000	-0.057948
10000	-87.5908	-87.5908	-87.4756	-0.1152	-87.5908	0.0000	-0.057773
m = 2							
0.0001	-0.6667	-0.6667	-0.0138	-0.6528	-0.6667	0.0000	-0.183855
0.001	-0.6667	-0.6667	-0.0436	-0.6231	-0.6667	0.0000	-0.182519
0.01	-0.6671	-0.6671	-0.1357	-0.5314	-0.6671	0.0000	-0.170363
0.1	-0.7018	-0.7018	-0.3828	-0.3191	-0.7018	0.0000	-0.117354
1	-1.1885	-1.1885	-1.0165	-0.1720	-1.1885	0.0000	-0.076839
10	-3.1380	-3.1380	-3.0035	-0.1344	-3.1380	0.0000	-0.065106
100	-9.4257	-9.4257	-9.3013	-0.1243	-9.4257	0.0000	-0.061727
1000	-29.3435	-29.3435	-29.2221	-0.1213	-29.3435	0.0000	-0.060689
10000	-92.3395	-92.3395	-92.2192	-0.1204	-92.3395	0.0000	-0.060368
m = 3							
0.0001	-0.7500	-0.7500	-0.0160	-0.7340	-0.7500	0.0000	-0.199277
0.001	-0.7500	-0.7500	-0.0504	-0.6997	-0.7500	0.0000	-0.197939
0.01	-0.7504	-0.7504	-0.1562	-0.5942	-0.7504	0.0000	-0.185627
0.1	-0.7825	-0.7825	-0.4323	-0.3502	-0.7825	0.0000	-0.127779
1	-1.2823	-1.2823	-1.1049	-0.1775	-1.2823	0.0000	-0.079392

$\omega$ / Quantities	INT <sup>1</sup>	$\mathbf{W}^2$	$\mathbf{W}_{col}^3$	$\mathbf{W}_{\mathbf{c}}^4$	TEST1 <sup>5</sup>	TEST2 <sup>6</sup>	MC-HF corr <sup>7</sup>
10	-3.3440	-3.3440	-3.2099	-0.1341	-3.3440	0.0000	-0.065147
100	-10.0115	-10.0114	-9.8887	-0.1227	-10.0114	0.0000	-0.061064
1000	-31.1370	-31.1369	-31.0176	-0.1193	-31.1369	0.0000	-0.059814
10000	-97.9542	-97.9542	-97.8359	-0.1183	-97.9542	0.0000	-0.059435
m = 10							
0.0001	-0.9091	-0.9091	-0.0264	-0.8826	-0.9091	0.0000	-0.197347
0.001	-0.9091	-0.9091	-0.0832	-0.8259	-0.9091	0.0000	-0.196007
0.01	-0.9094	-0.9094	-0.2515	-0.6579	-0.9094	0.0000	-0.183502
0.1	-0.9374	-0.9374	-0.6124	-0.3250	-0.9374	0.0000	-0.118794
1	-1.4556	-1.4556	-1.3269	-0.1287	-1.4556	0.0000	-0.059334
10	-3.7125	-3.7125	-3.6258	-0.0867	-3.7125	0.0000	-0.042938
100	-11.0496	-11.0496	-10.9732	-0.0765	-11.0496	0.0000	-0.038548
1000	-34.3071	-34.3071	-34.2335	-0.0735	-34.3071	0.0000	-0.037256
10000	-107.8701	-107.8701	-107.7974	-0.0726	-107.8701	0.0000	-0.036929
m = 50							
0.0001	-0.9804	-0.9804	-0.0568	-0.9236	-0.9804	0.0000	-0.136159
0.001	-0.9804	-0.9804	-0.1758	-0.8046	-0.9804	0.0000	-0.134821
0.01	-0.9807	-0.9807	-0.4723	-0.5084	-0.9807	0.0000	-0.122460
0.1	-1.0072	-1.0072	-0.8454	-0.1617	-1.0072	0.0000	-0.064093
1	-1.5313	-1.5313	-1.4860	-0.0454	-1.5313	0.0000	-0.022104
10	-3.8689	-3.8689	-3.8420	-0.0270	-3.8689	0.0000	-0.013563
100	-11.4868	-11.4868	-11.4638	-0.0229	-11.4868	0.0000	-0.011572
1000	-35.6386	-35.6386	-35.6167	-0.0218	-35.6386	0.0000	-0.011007
10000	-112.0318	-112.0318	-112.0103	-0.0215	-112.0318	0.0000	-0.010839
m = 207							
0.0001	-0.9952	-0.9952	-0.1139	-0.8813	-0.9952	0.0000	-0.082760
0.001	-0.9952	-0.9952	-0.3327	-0.6624	-0.9952	0.0000	-0.081427
0.01	-0.9954	-0.9954	-0.7068	-0.2886	-0.9954	0.0000	-0.069560
0.1	-1.0216	-1.0216	-0.9613	-0.0603	-1.0216	0.0000	-0.026584
1	-1.5469	-1.5469	-1.5232	-0.0237	-1.5469	0.0000	-0.006733
10	-3.9008	-3.9008	-3.8932	-0.0076	-3.9008	0.0000	-0.003642
100	-11.5756	-11.5756	-11.5692	-0.0064	-11.5756	0.0000	-0.002977
1000	-35.9089	-35.9089	-35.9029	-0.0060	-35.9089	0.0000	-0.002793
10000	-112.8766	-112.8766	-112.8707	-0.0059	-112.8766	0.0000	-0.002747
m = 400							
0.0001	-0.9975	-0.9975	-0.1567	-0.8408	-0.9975	0.0000	-0.063705
0.001	-0.9975	-0.9975	-0.4326	-0.5649	-0.9975	0.0000	-0.062375
0.01	-0.9978	-0.9978	-0.7984	-0.1994	-0.9978	0.0000	-0.050894



$\omega$ / Quantities	INT <sup>1</sup>	$\mathbf{W}$ <sup>2</sup>	$\mathbf{W}_{col}$ <sup>3</sup>	$\mathbf{W}_c$ <sup>4</sup>	TEST1 <sup>5</sup>	TEST2 <sup>6</sup>	MC-HF corr <sup>7</sup>
0.1	-1.0239	-1.0239	-0.9886	-0.0354	-1.0239	0.0000	-0.016254
1	-1.5494	-1.5494	-1.4583	-0.0910	-1.5494	0.0000	-0.003624
10	-3.9058	-3.9058	-3.9017	-0.0041	-3.9058	0.0000	-0.001804
100	-11.5894	-11.5894	-11.5860	-0.0034	-11.5894	0.0000	-0.001424
1000	-35.9510	-35.9510	-35.9478	-0.0032	-35.9510	0.0000	-0.001317
10000	-113.0081	-113.0081	-113.0049	-0.0032	-113.0081	0.0000	-0.001443
m = 900							
0.0001	-0.9989	-0.9989	-0.2297	-0.7692	-0.9989	0.0000	-0.045320
0.001	-0.9989	-0.9989	-0.5693	-0.4295	-0.9989	0.0000	-0.043998
0.01	-0.9992	-0.9992	-0.8826	-0.1166	-0.9992	0.0000	-0.033180
0.1	-1.0253	-1.0252	-1.0077	-0.0175	-1.0252	0.0000	-0.008372
1	-1.5508	-1.5508	-1.1976	-0.3532	-1.5508	0.0000	-0.001579
10	-3.9088	-3.9088	-3.9069	-0.0019	-3.9088	0.0000	-0.000638
100	-11.5977	-11.5977	-11.5961	-0.0016	-11.5977	0.0000	-0.000448
1000	-35.9761	-35.9761	-35.9747	-0.0015	-35.9761	0.0000	-0.000391
10000	-113.0867	-113.0867	-113.0852	-0.0014	-113.0867	0.0000	-0.000512
m = 1836							
0.0001	-0.9995	-0.9995	-0.3156	-0.6838	-0.9995	0.0000	-0.033161
0.001	-0.9994	-0.9993	-0.6875	-0.3119	-0.9994	-0.0001	-0.031848
0.01	-0.9998	-0.9998	-0.9315	-0.0683	-0.9997	0.0000	-0.021825
0.1	-1.0258	-1.0258	-1.0166	-0.0092	-1.0258	0.0000	-0.004486
1	-1.5514	-1.5514	-1.5497	-0.0018	-1.5514	0.0000	-0.000684
10	-3.9100	-3.9100	-3.9090	-0.0009	-3.9100	0.0000	-0.000140
100	-11.6011	-11.6011	-11.6003	-0.0008	-11.6011	0.0000	-0.000035
1000	-35.9864	-35.9864	-35.9857	-0.0007	-35.9864	0.0000	0.000000
10000	-113.1188	-113.1188	-113.1180	-0.0007	-113.1188	0.0000	-0.000132

1. E-PCP interaction energy calculated based on wave function (equations 2-139 and 2-152)
2. E-PCP interaction energy calculated using two-particle density (equation 3-20)
3. Hartree potential energy or coulomb contribution to interaction energy (equation 3-21)
4. Reference-independent correlation energy (equation 3-24)
5. First test: sum of items 3 and 4 to ensure reproduction of item 2 according to equation (3-21)
6. Second test: difference between items 1 and 2
7. Correlation energy relative to MC-HF reference

### 5.1.2 Single-Particle Densities

The electron and PCP densities were calculated using the variational method (with equations 2-168 and 2-169) and the MC-HF method, as shown in Figures 5-3 to 5-14. These figures are grouped into three mass categories: Category 1 includes masses 1 to 3, Category 2 includes masses 10 and 50, and Category 3 includes masses 207 to 1836. This categorization is done to account for the different localization extents of various masses, ensuring image clarity and better comparison.

It is important to note that the densities given by equations (2-168) and (2-169) are not defined for  $r = 0$ . However, comparing the densities obtained from the numerical calculation of equation (2-161), which includes  $r = 0$ , shows that the densities (2-168) and (2-169) produce very accurate results at all points except  $r = 0$ . Figures (C-1) and (C-2) in the appendix C show the percentage error of the densities with form (2-168) compared to form (2-161).

There is a notable difference between the variational density and the HF density (illustrated in Figures C-3 to C-7 in the appendix C) at a frequency of  $10^{-4}$  (especially at mass 1). This difference is not unexpected since, as shown in Table 4-3, the MC-HF method exhibits significant energy errors in this range, hence the produced density is expected to have substantial errors. A clear pattern observed in all densities is the increased localization with increasing frequency. This means that at a given mass, as the frequency increases, the potential well narrows, forcing the particles to be confined in a smaller space, which leads to increased localization of the densities with increasing frequency. Additionally, at a given frequency, increased mass of the PCP also results in more localized densities. At a frequency of  $10^4$ , as the mass of the PCP increases, the electron density remains constant,

but the PCP density becomes more localized. This trend is consistent with the fact that heavier particles are more localized.

In general, the MC-HF densities, particularly for the PCP, clearly show over-localization. This is especially evident in the system with mass 1 and frequency  $10^{-4}$ . In this system, the masses of the positive and negative particles are equal, and the harmonic oscillator potential approaches zero. The variational densities demonstrate that the single-particle density in this system is significantly delocalized, nearing zero at  $r_e = 200$ . Meanwhile, the MC-HF single-particle density approaches zero at approximately  $r_e = 10$ . This over-localization is precisely the effect observed in real molecule calculations multiple times, indicating that the EHM can reproduce it accurately.

At low frequencies, the Coulomb interaction between the electron and the PCP in equation (2-16) dominates the harmonic oscillator potential, and the two particles are completely bound to each other. However, they oscillate as a single particle with mass  $M$ , according to equation (2-15). This means that at low frequencies, the lighter particle is attached to the heavier one (closer to the center of mass), and these two particles oscillate together as a total mass  $M$ . Naturally, the heavier the PCP, the smaller the oscillation amplitude of this mass  $M$ . Therefore, at mass 1, the oscillation amplitude is very large because both particles have equal and light masses, allowing either to induce oscillations in the other.

At high frequencies, the situation in equation (2-16) is reversed, and the harmonic oscillator potential now dominates the Coulomb potential. Thus, the two particles are not bound to each other. In this case, the two particles form two separate oscillators.

Finally, the normalization condition for the densities is defined as follows:

$$4\pi \int_0^\infty \rho_e(r_e) r_e^2 dr_e = 1 \quad 5.1$$

$$4\pi \int_0^\infty \rho_p(r_p) r_p^2 dr_p = 1 \quad 5.2$$

This condition was verified for the electron and PCP densities calculated at the variational, FEM, and HF levels, and all of them satisfy the above equation.

The limit of single-particle densities as  $m_p \rightarrow \infty$  was examined due to the system's approach to the clamped nuclei approximation. For the EHM with  $m_p \rightarrow \infty$ , the electron density in the limit  $\omega \rightarrow 0$  approaches the electron density of a hydrogen atom with a clamped nucleus. In the limit  $\omega \rightarrow 0$ , the strength of the harmonic oscillator potential and thus the perturbation caused by it becomes very small, allowing it to be approximated by a free hydrogen atom. Since  $m_p \rightarrow \infty$ , the electron experiences conditions identical to those of a hydrogen atom with a clamped nucleus (considering the PCP is clamped, we can assume  $r_p = 0$  and therefore  $r = |r_e - r_p| = r_e$ ), resulting in the electron density (in the limit of equation 2-168) being equal to the electron density of a hydrogen atom with a clamped nucleus:

$$\lim_{m_p \rightarrow \infty, \omega \rightarrow 0} \rho_e(r_e) \rightarrow \frac{e^{-2r_e}}{\pi} = \rho_H(r) \quad 5.3$$

In this case, the density of the PCP approaches a Dirac delta function. Additionally, for sufficiently large frequencies, since the mass of the PCP is assumed to be infinite, its kinetic energy term in the Hamiltonian approaches zero. Given that in this limit,  $r_p = 0$ , the oscillatory term of the PCP is eliminated, and the e-PCP interaction term can be neglected. Consequently, only the electron's kinetic and oscillatory energy terms remain. Therefore, in the limit  $m_p \rightarrow \infty$  and

sufficiently large frequencies, the electron density approaches a Gaussian function (the ground state of the oscillator):

$$\lim_{\substack{m_p \rightarrow \infty \\ \text{large } \omega}} \rho_e(r_e) \rightarrow \left(\frac{\omega}{\pi}\right)^{3/2} e^{-\omega r_e^2} = \rho_{HO}(r) \quad 5.4$$

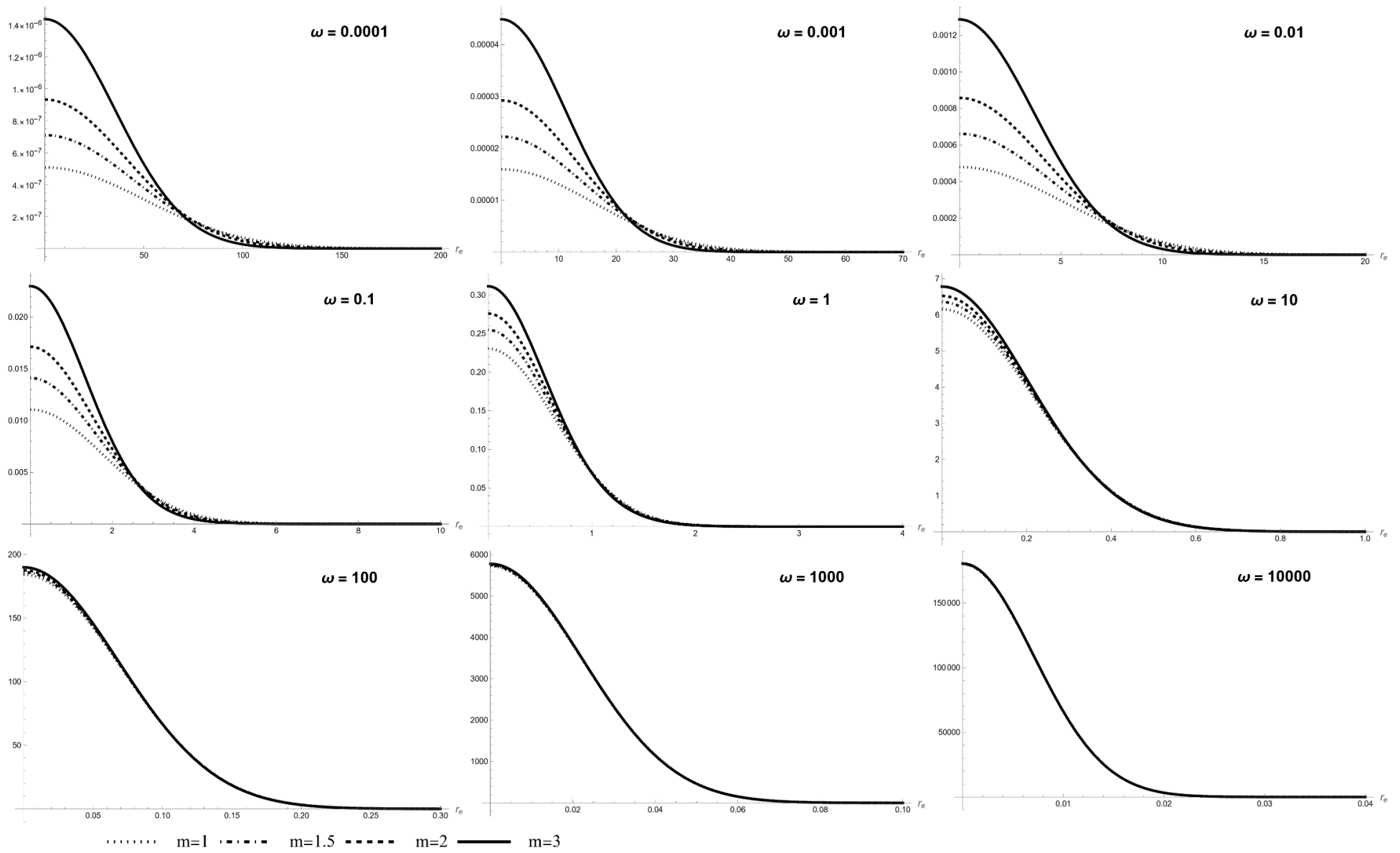


Figure 5-3: Variational electron density as a function of  $r_e$  for different frequencies across the four lower masses.

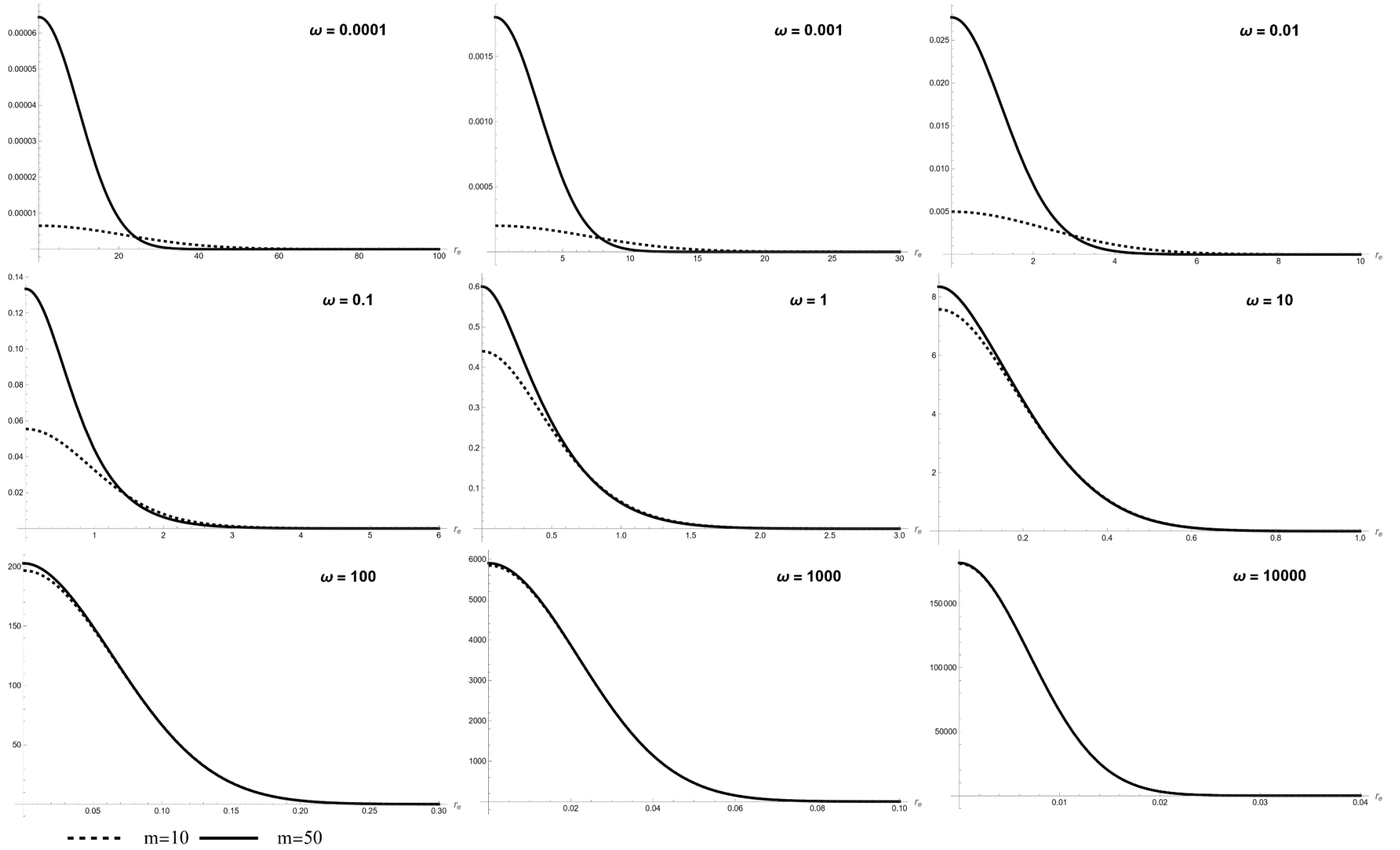


Figure 5-4: Variational electron density as a function of  $r_e$  for different frequencies across the two middle masses.

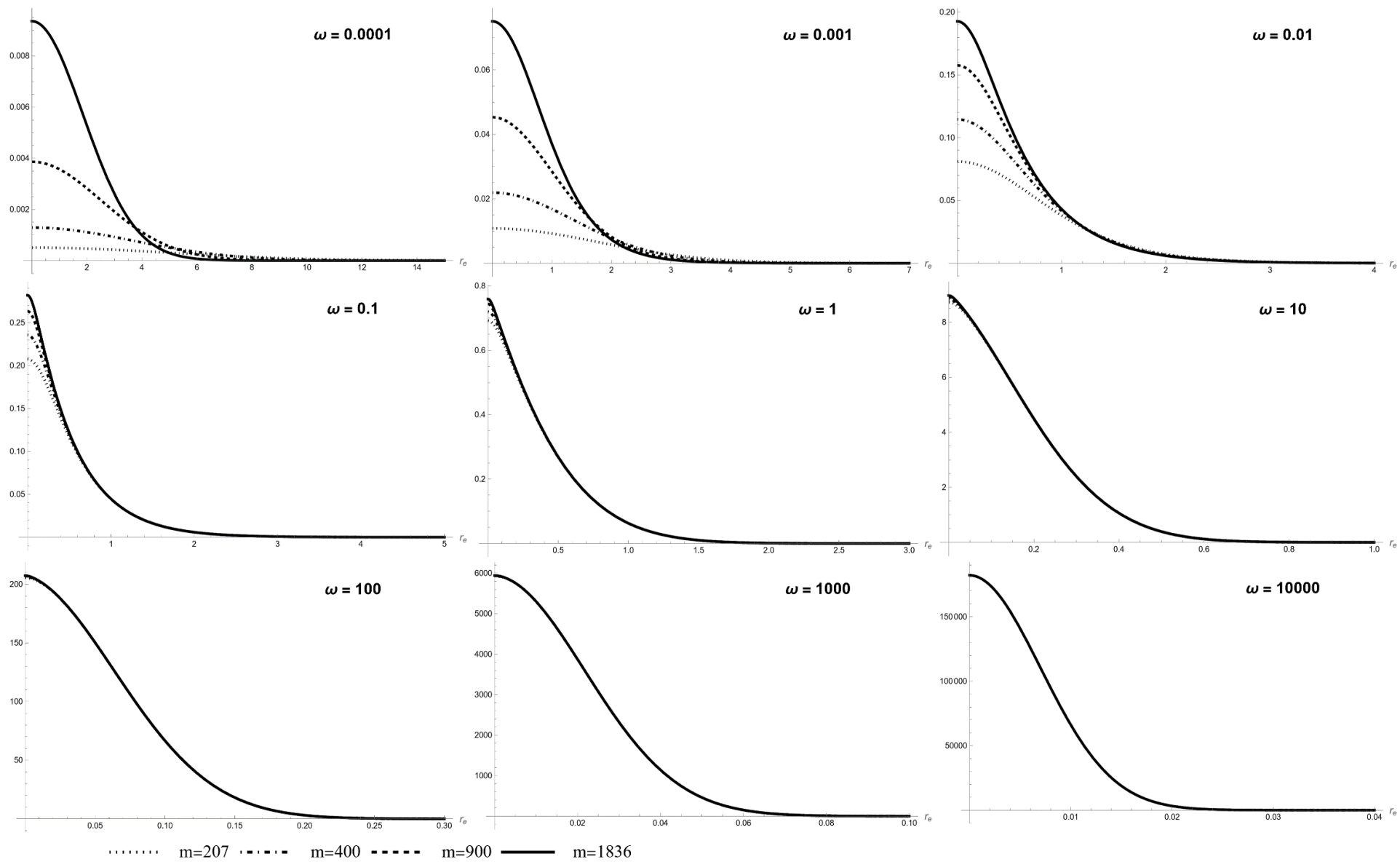


Figure 5-5: Variational electron density as a function of  $r_e$  for different frequencies across the four higher masses.



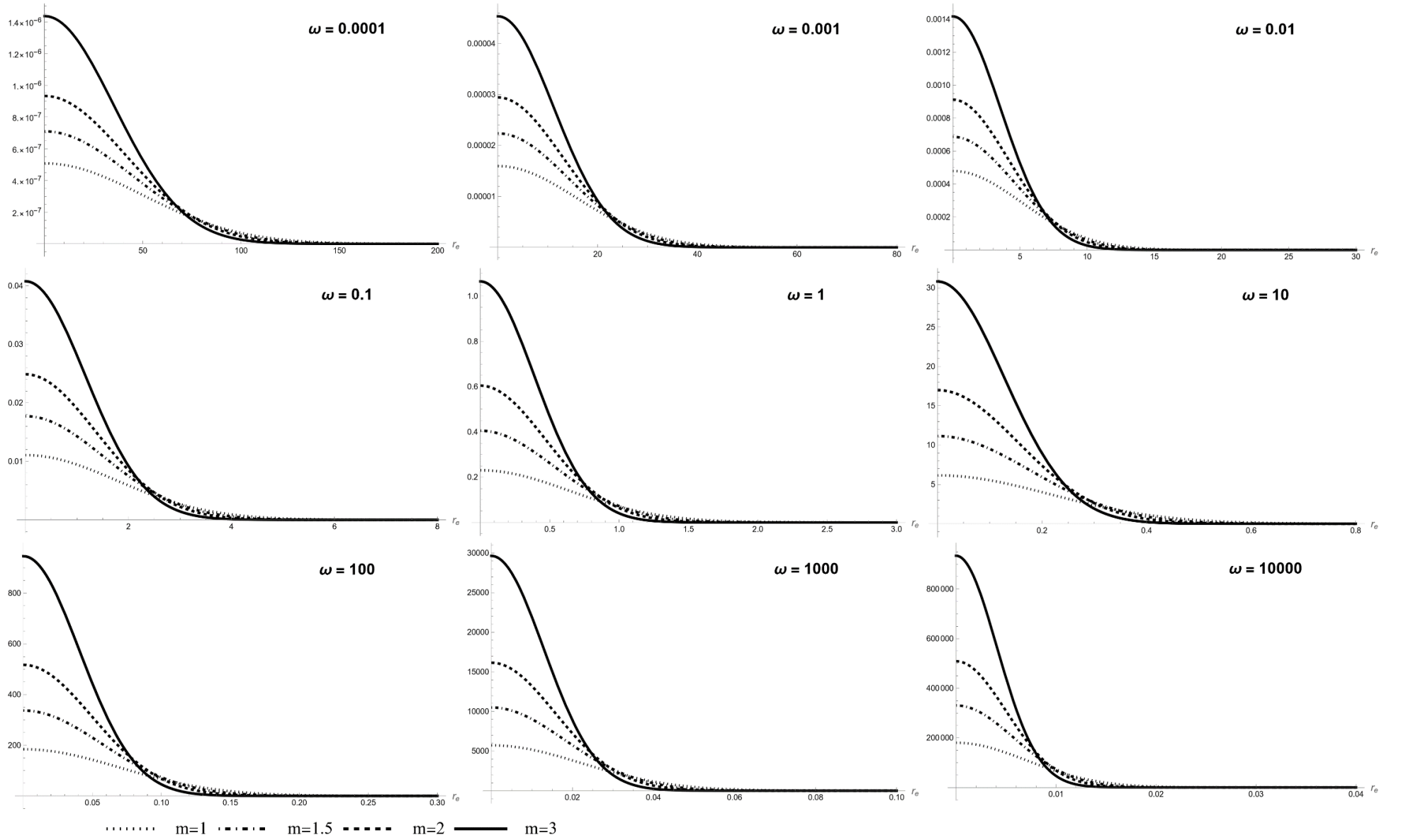


Figure 5-6: Variational PCP density as a function of  $r_p$  for different frequencies across the four lower masses.

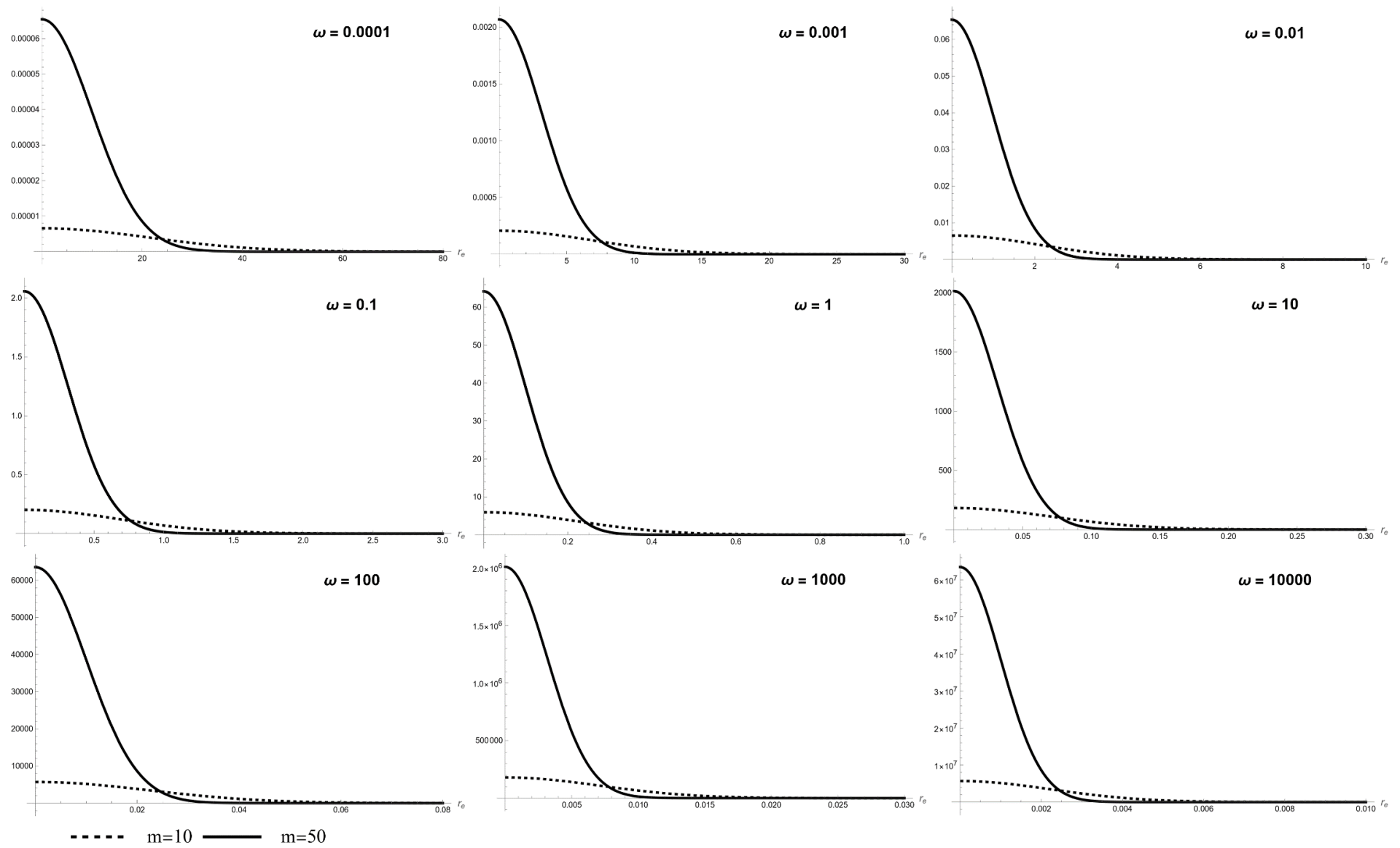


Figure 5-7: Variational PCP density as a function of  $r_p$  for different frequencies across the two middle masses.

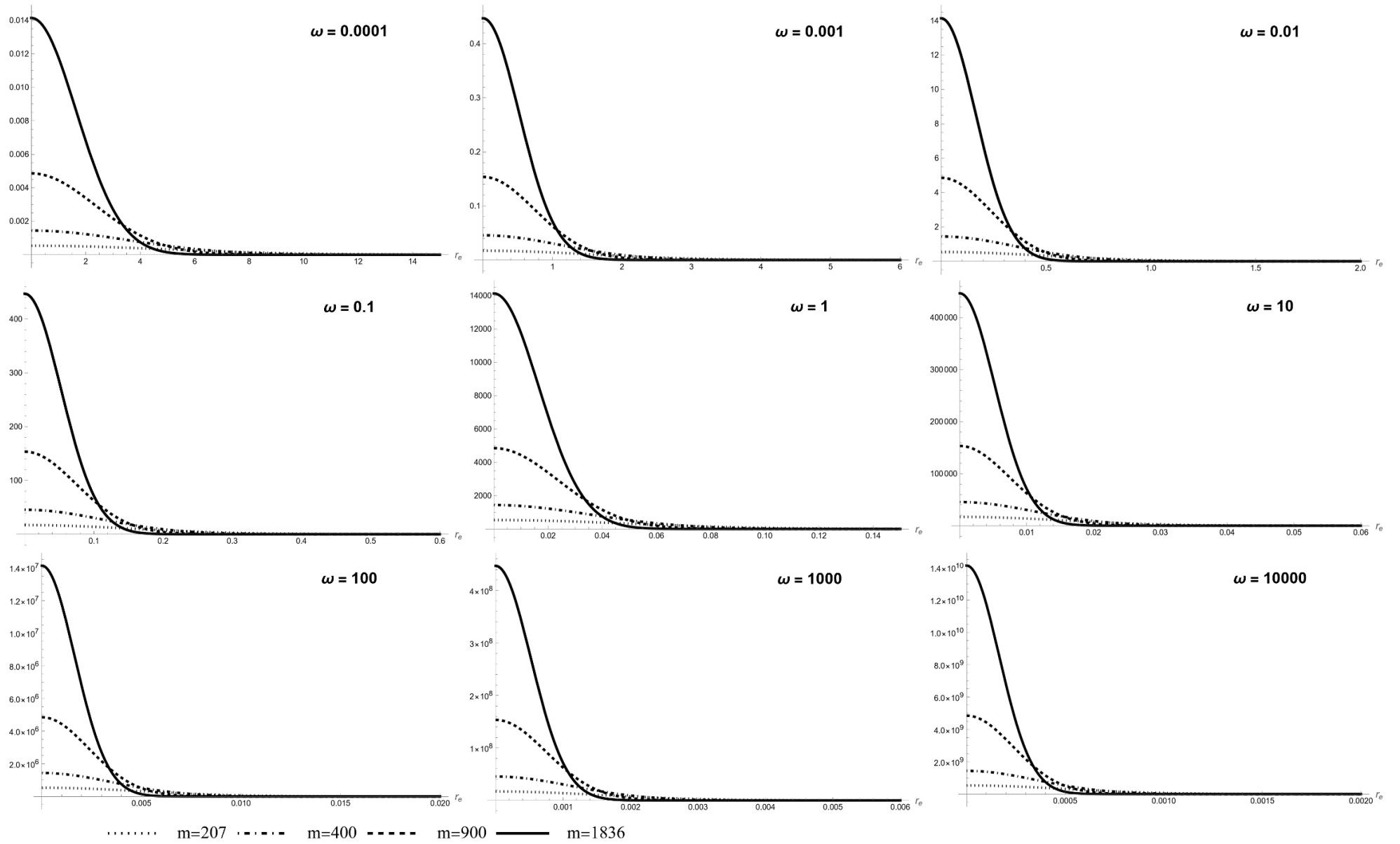


Figure 5-8: Variational PCP density as a function of  $r_p$  for different frequencies across the four higher masses.

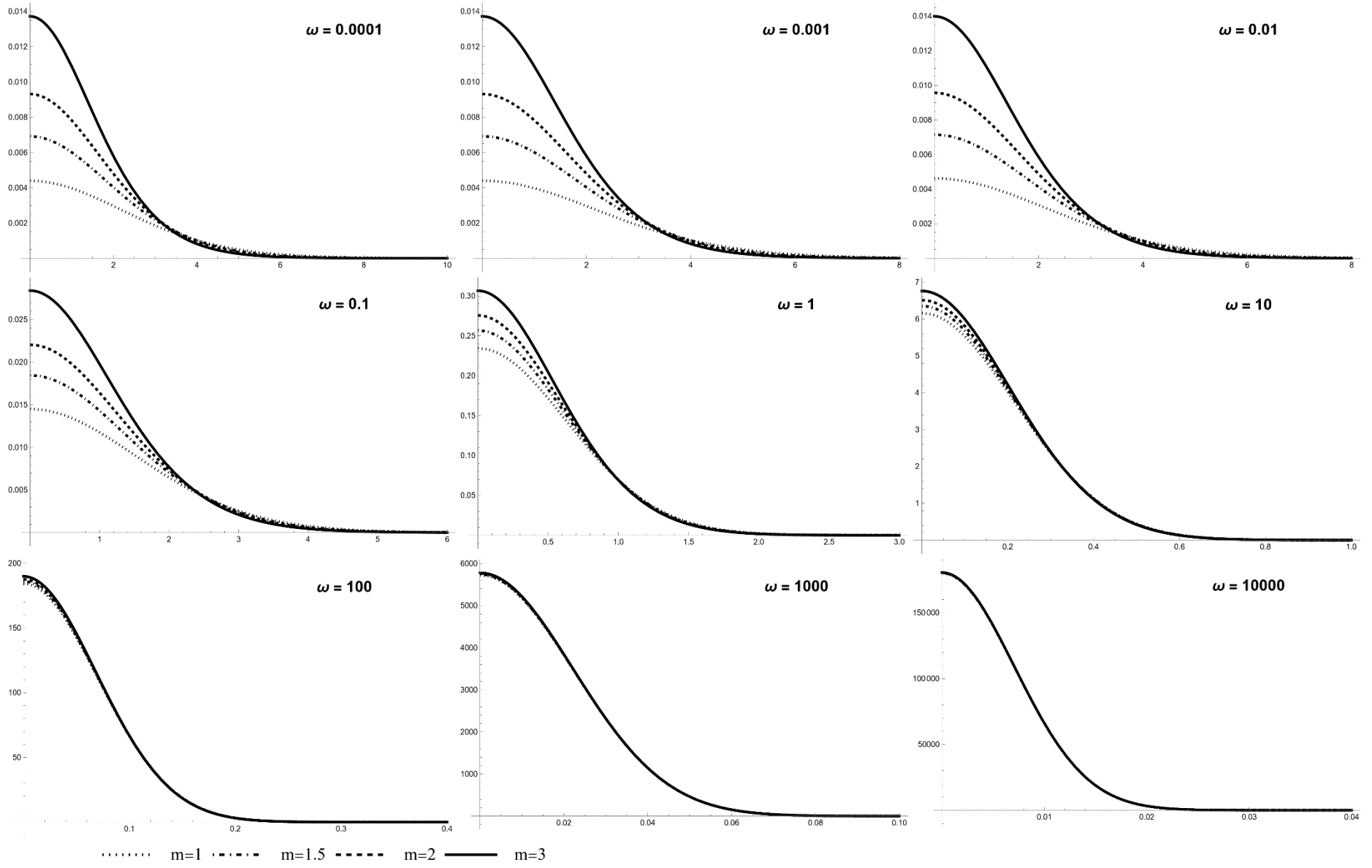


Figure 5-9: TC-HF electron density as a function of  $r_s$  for different frequencies across the four lower masses.

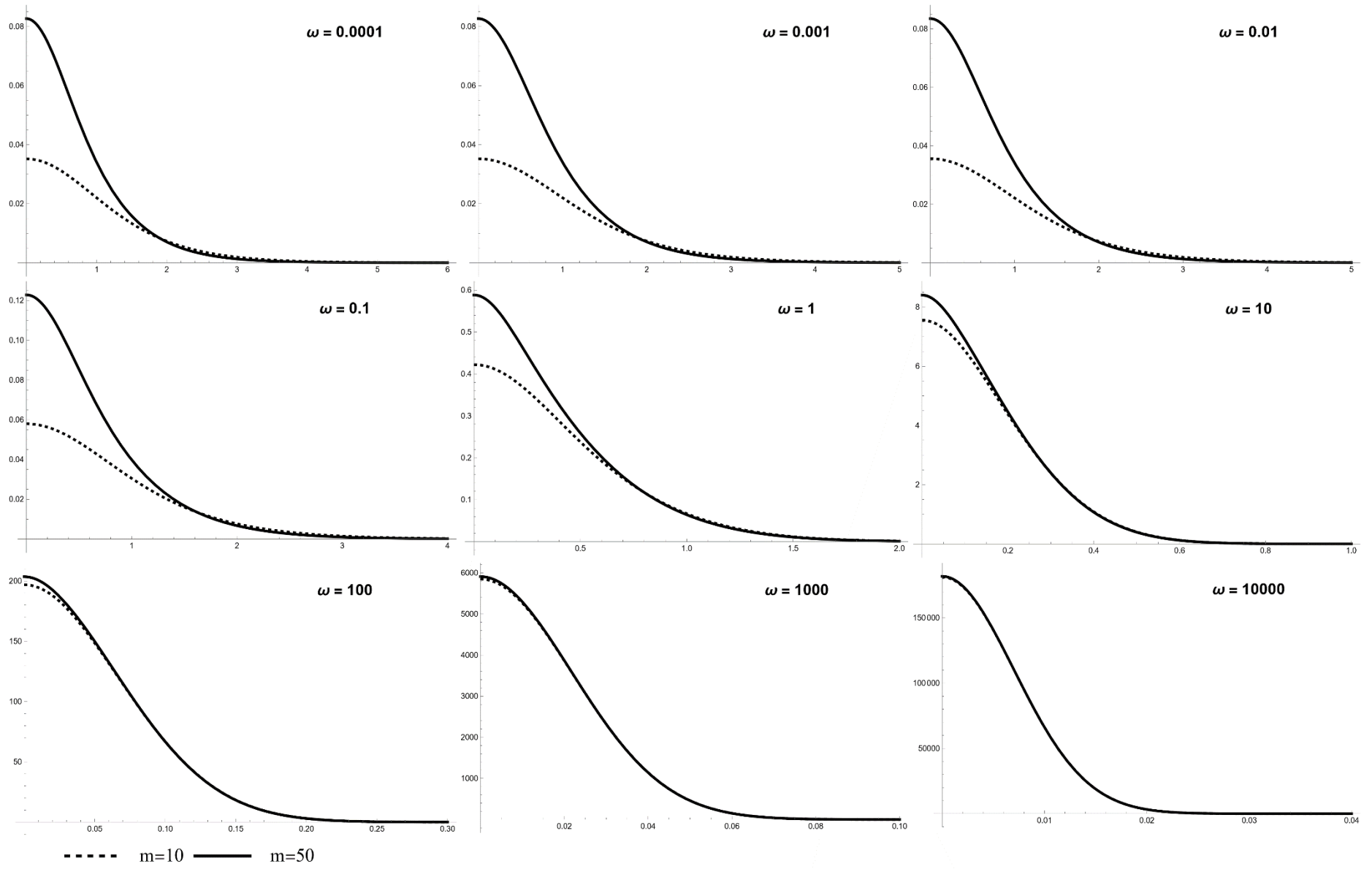


Figure 5-10: TC-HF electron density as a function of  $r_s$  for different frequencies across the two middle masses.

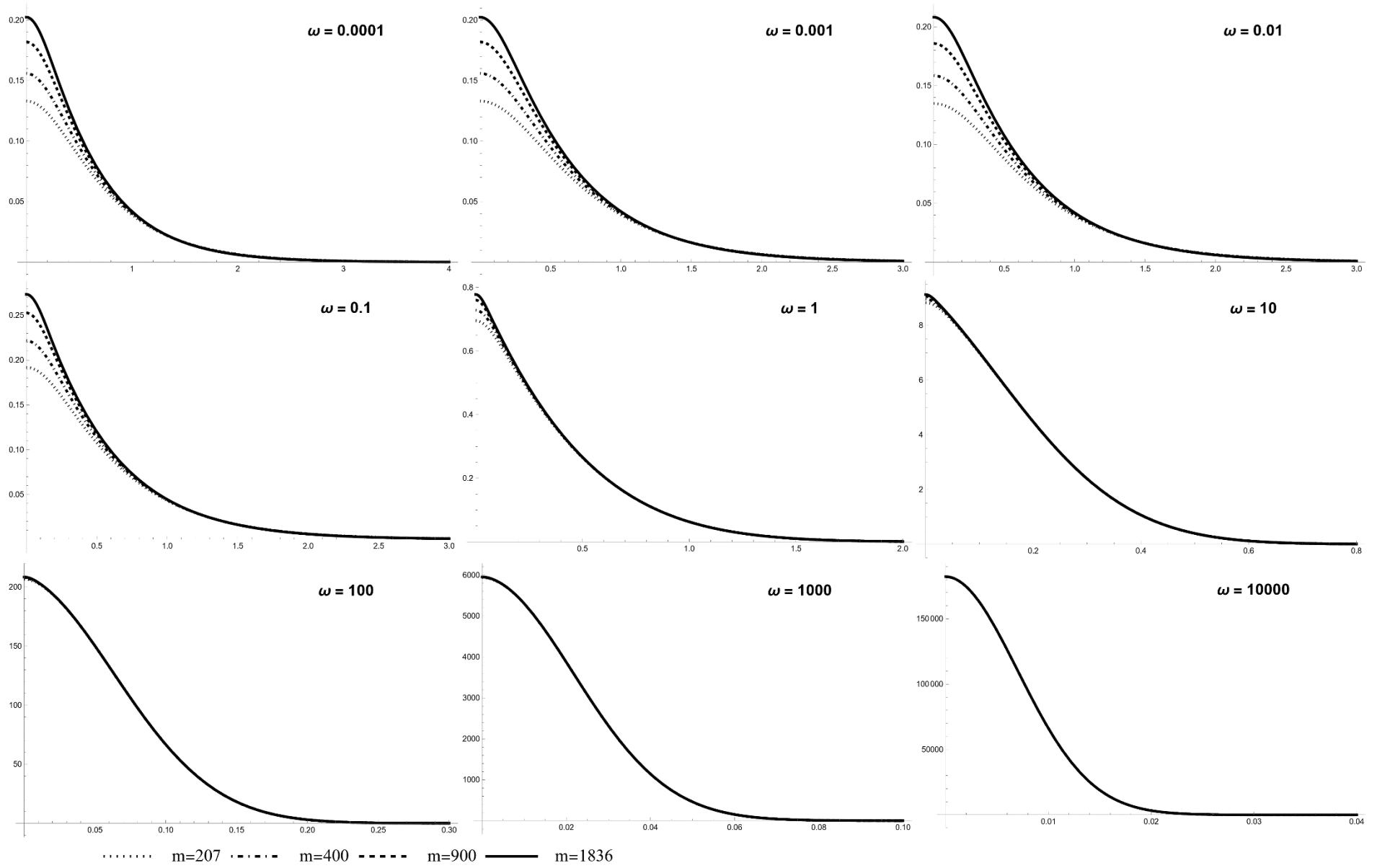


Figure 5-11: TC-HF electron density as a function of  $r_e$  for different frequencies across the four higher masses.

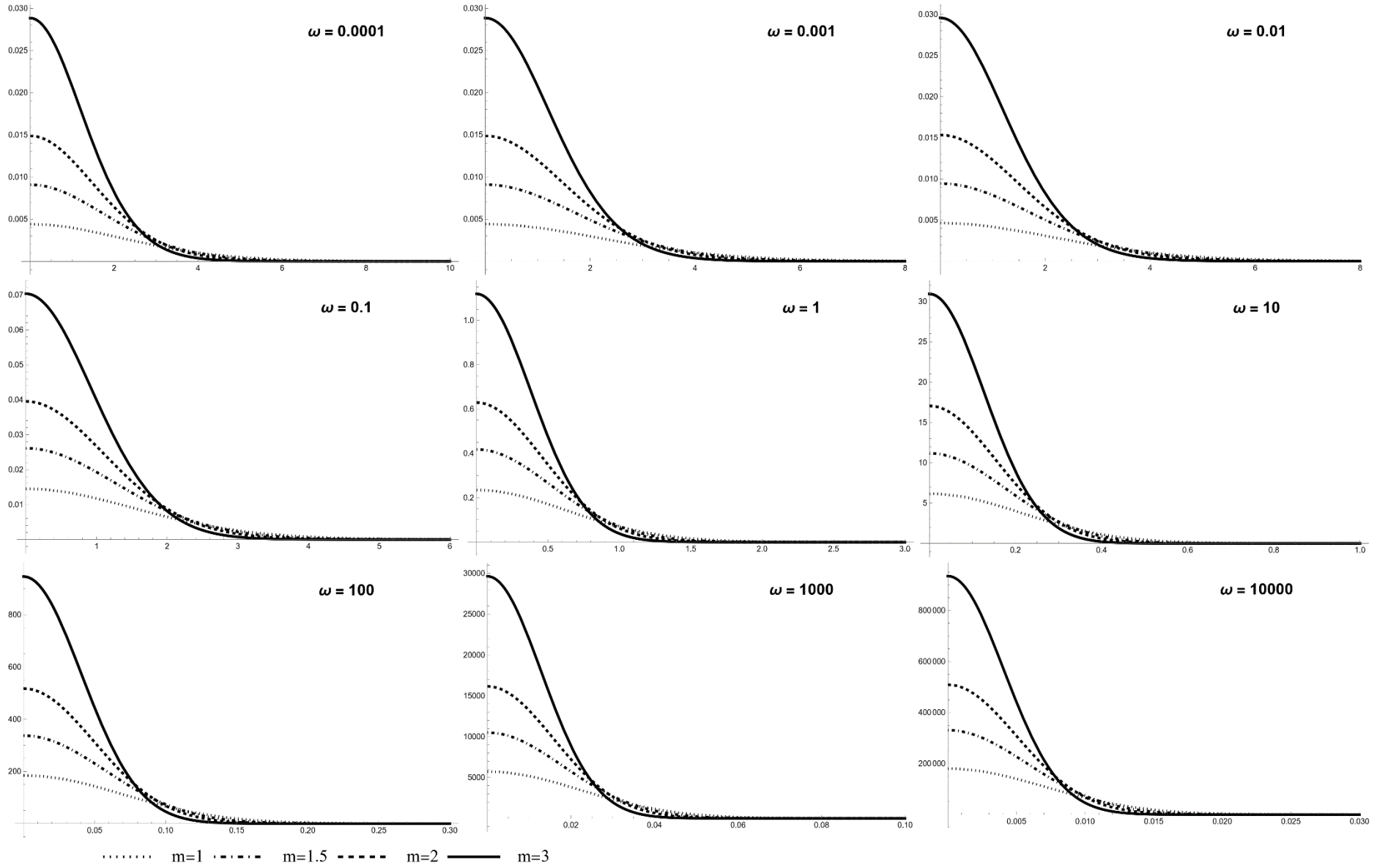


Figure 5-12: TC-HF PCP density as a function of  $r_p$  for different frequencies across the four lower masses.

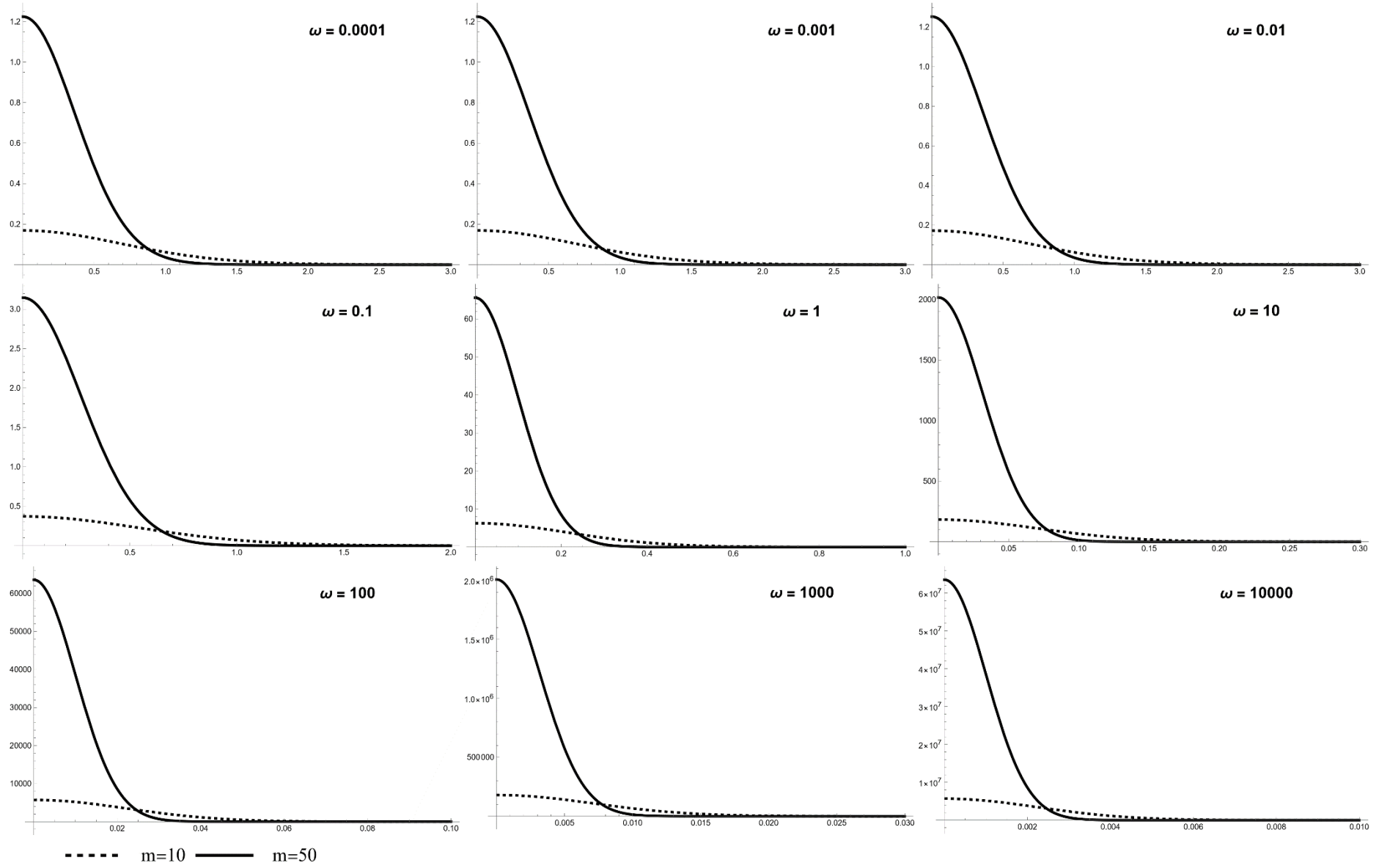


Figure 5-13: TC-HF PCP density as a function of  $r_p$  for different frequencies across the two middle masses.



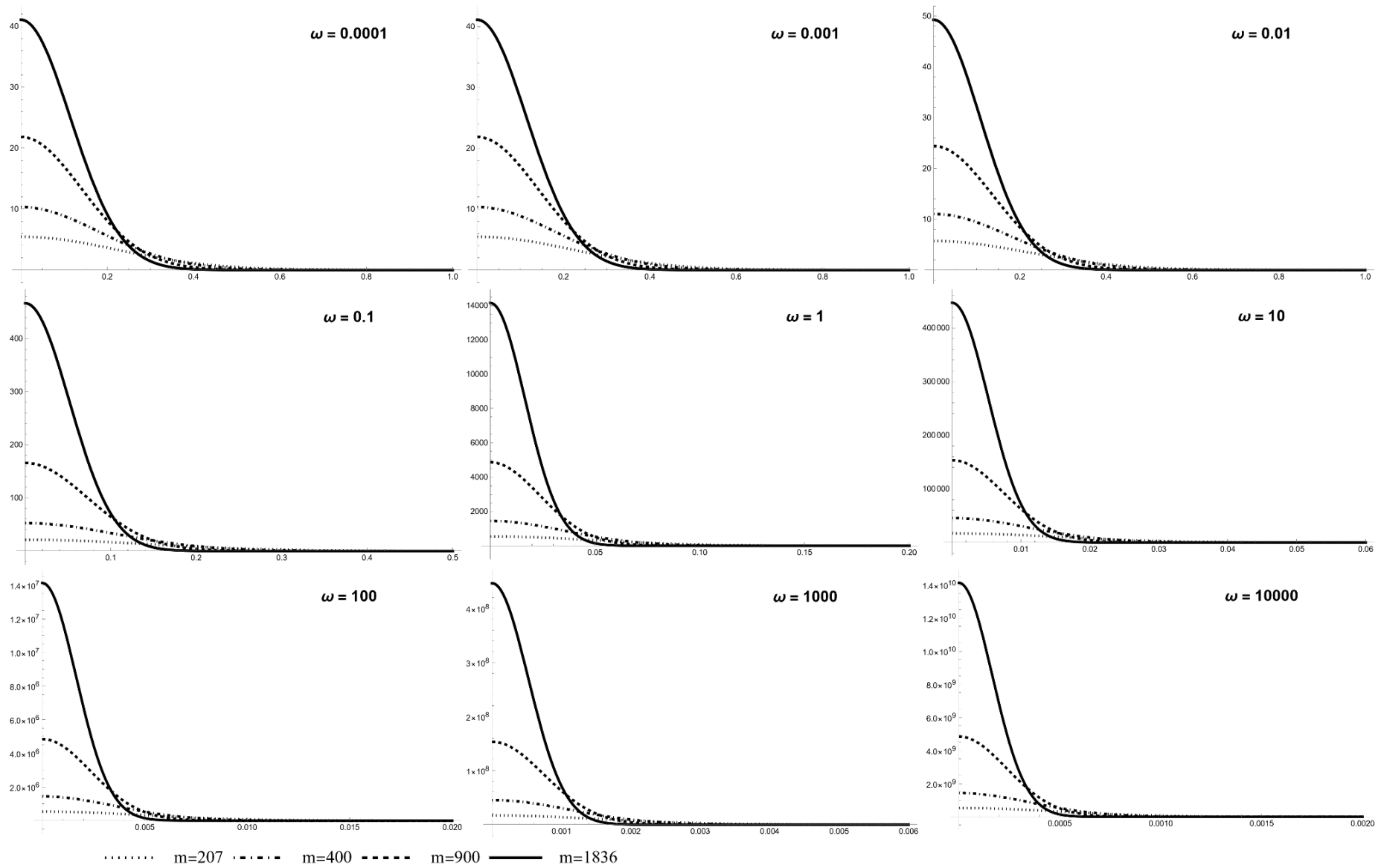


Figure 5-14: TC-HF PCP density as a function of  $r_p$  for different frequencies across the four higher masses.

### 5.1.3 Correlation Hill

The correlation hills, obtained using the variational equations (3-12 and 3-13), are presented for different masses for the electron and the PCP in Figures 5-15 to 5-34. In all these figures, to simplify the computational process, the reference particle is placed at the center of the potential well (i.e.,  $r_e = 0$  and  $r_p = 0$  for the reference electron and PCP, respectively). In this configuration, due to the isotropy of the harmonic oscillator potential, the angular dependence is eliminated, resulting in  $r_p = r$  and  $r_e = r$  for the reference electron and PCP, respectively.

Since, according to the aforementioned equations, the correlation hill density is derived from the difference between the conditional density and the single-particle density, both quantities are included in the correlation hill figures for better comparison. Additionally, an inset is plotted within each main graph to better compare the positive and negative parts of the graph.

The term "correlation hill" is aptly named in contrast to the "correlation hole" observed in electron-electron correlation within electronic systems. Due to the repulsive nature of the interaction, electron-electron correlation creates a hole around each electron (reference particle) and reduces the probability of another electron being nearby. Conversely, e-PCP correlation, due to the attractive nature of the interaction, creates a hill around each reference particle, increasing the probability of another particle being present. Accordingly, the correlation hill plots show high density near the reference particle. As one moves away from the reference particle, this density reaches zero and then turns negative, which is the exact opposite behavior of the electron correlation hole.

However, similar to the correlation hole, the sum rule of the correlation hill (equations 3-18 and 3-19) indicates that the sum of the positive and negative parts should be zero. Integration over the correlation hills of the electron and PCP was performed for all systems, resulting in a net value of zero, confirming the sum rule for all correlation hills.

The correlation hill figures show that as  $\omega$  increases for a fixed mass, the zero-crossing boundary of the correlation hill moves to smaller distances closer to the reference particle. This distance is essentially the "effective radius" of the correlation, beyond which correlation effects do not operate, thus serving as a good measure of the correlation range in real space. This effective radius is highly sensitive to the mass of the PCP and decreases with increasing mass.

For a more detailed examination, the numerical values of the correlation radius for different masses and frequencies were calculated and presented in Table (C-1) of the appendix C. This radius indicates the distance at which the correlation hill intersects the horizontal axis and changes sign. Analysis of these values reveals that, in general, the effective radius of the PCP is smaller than that of the electron. Additionally, for both particles, increasing frequency or mass (while keeping the other parameter constant) results in a decrease in the effective radius.

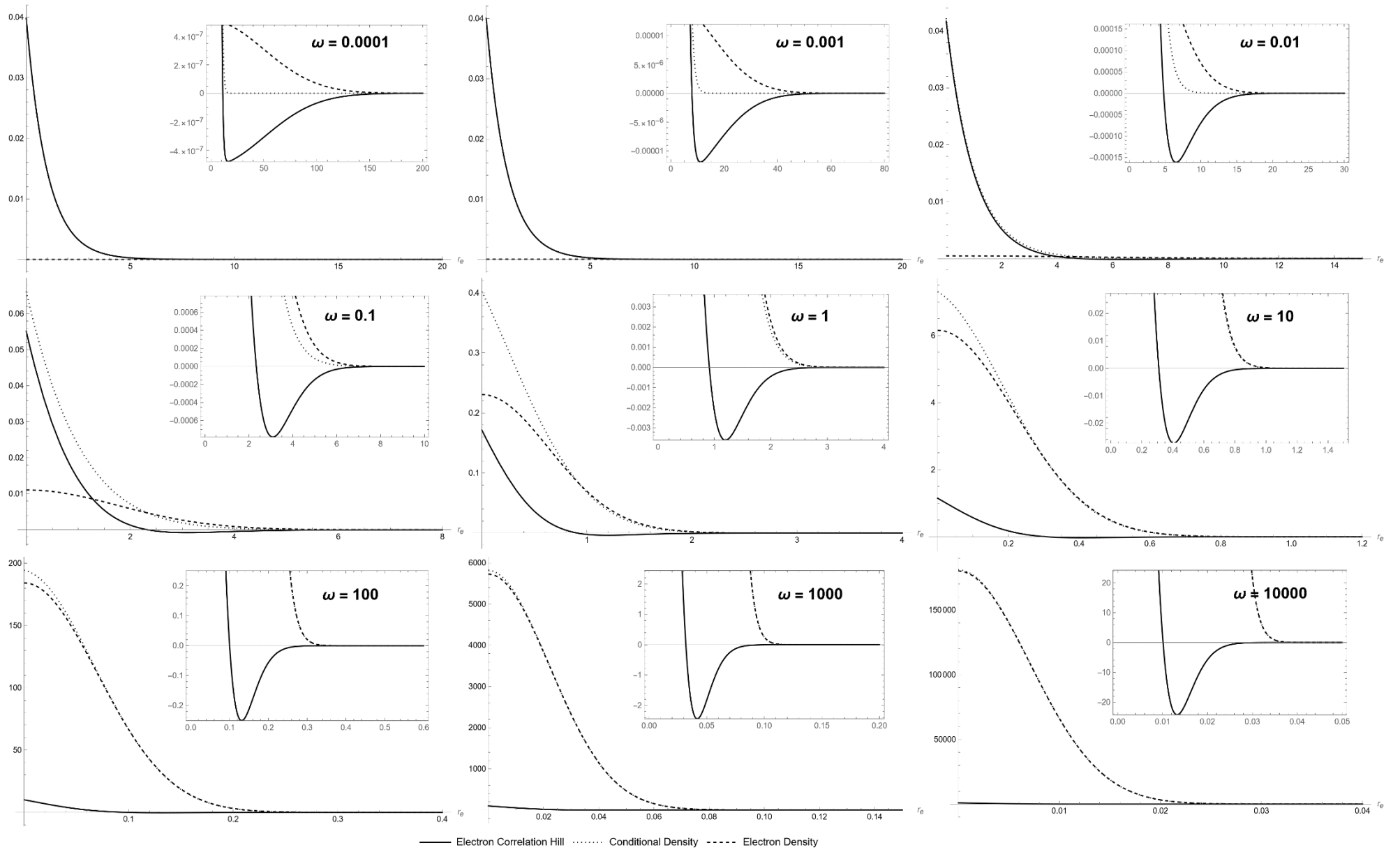


Figure 5-15: Comparison of the correlation hill, conditional density, and single-particle density of electron for mass 1.

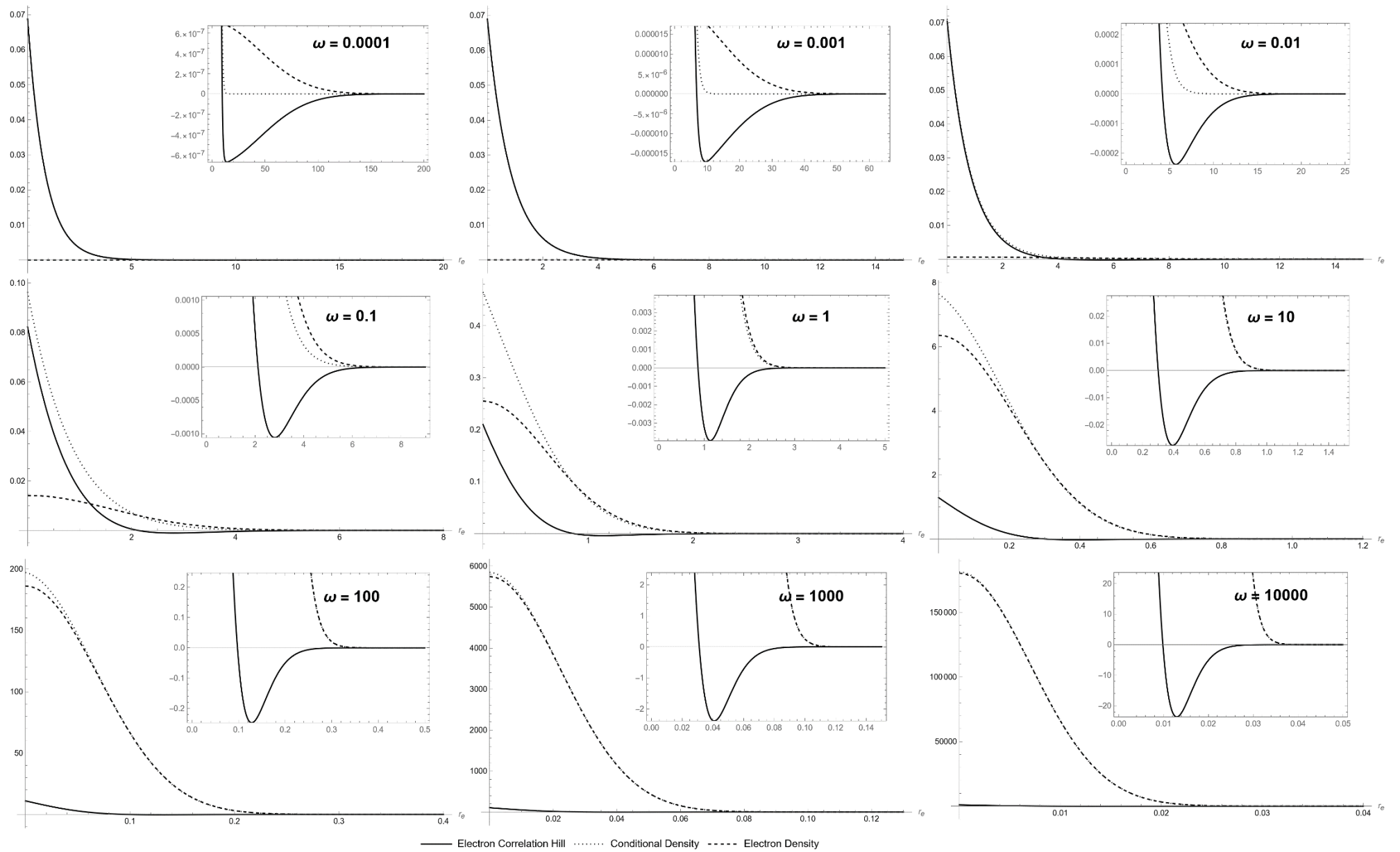


Figure 5-16: Comparison of the correlation hill, conditional density, and single-particle density of electron for mass 1.5

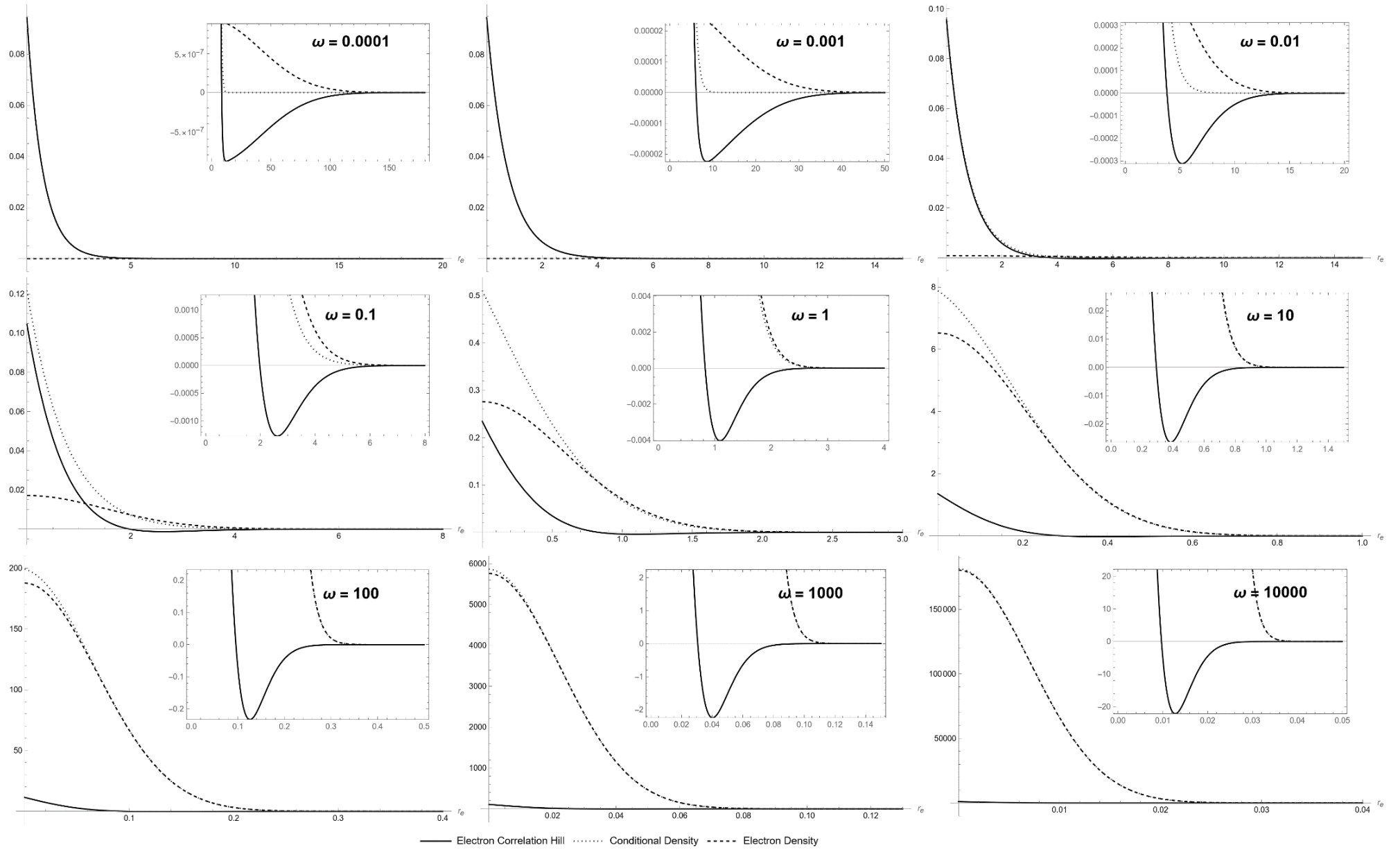


Figure 5-17: Comparison of the correlation hill, conditional density, and single-particle density of electron for mass 2

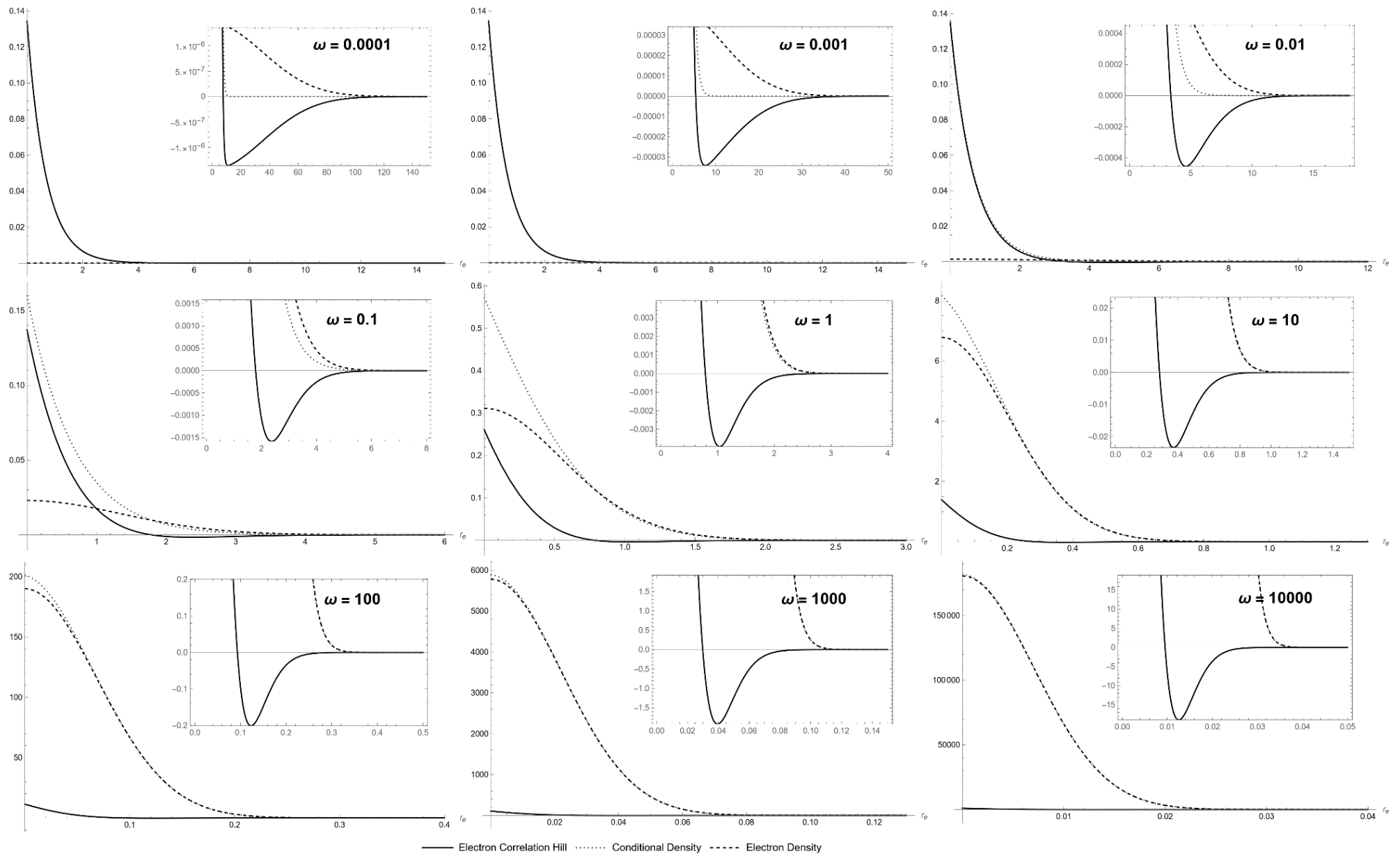


Figure 5-18: Comparison of the correlation hill, conditional density, and single-particle density of electron for mass 3

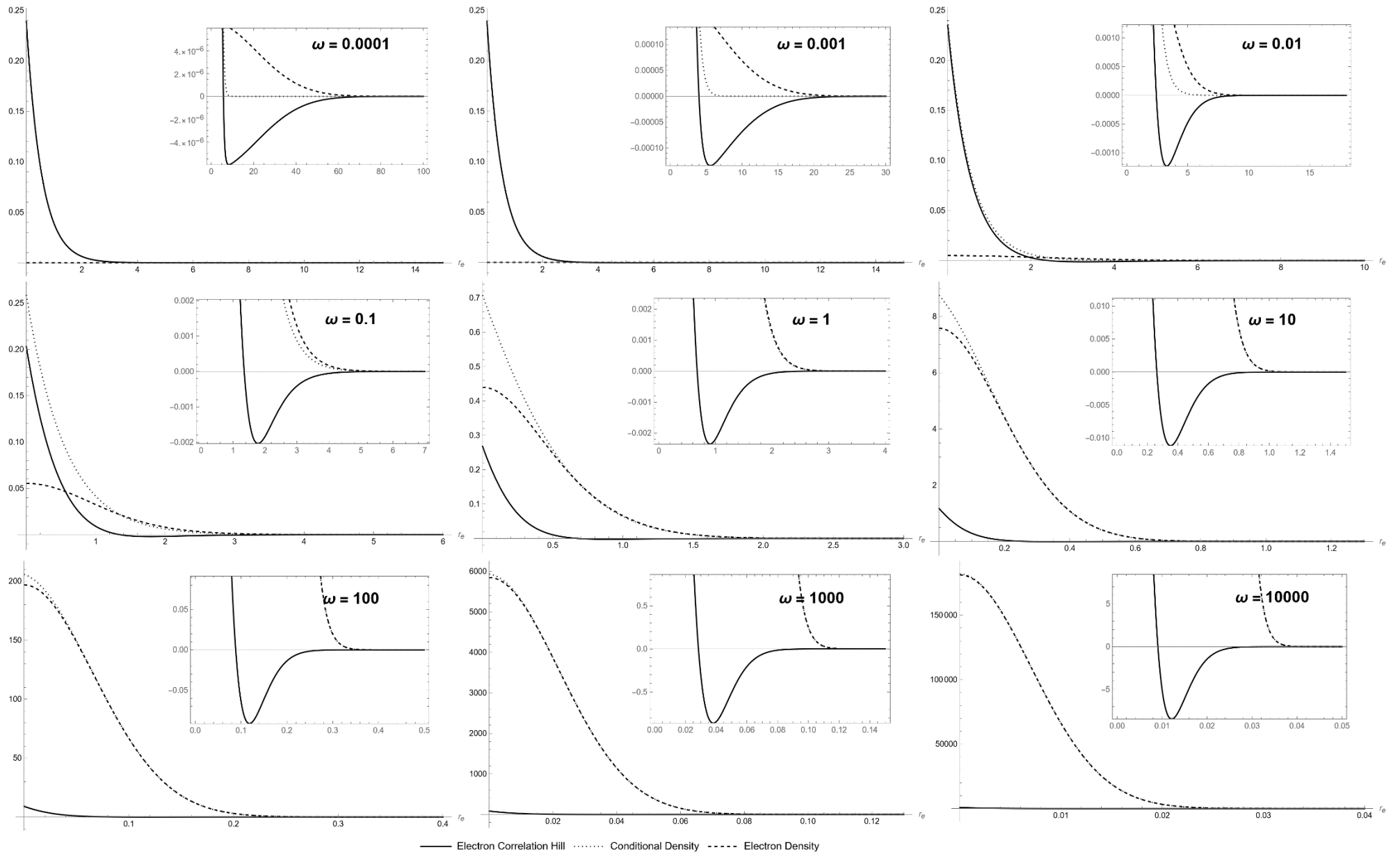


Figure 5-19: Comparison of the correlation hill, conditional density, and single-particle density of electron for mass 10



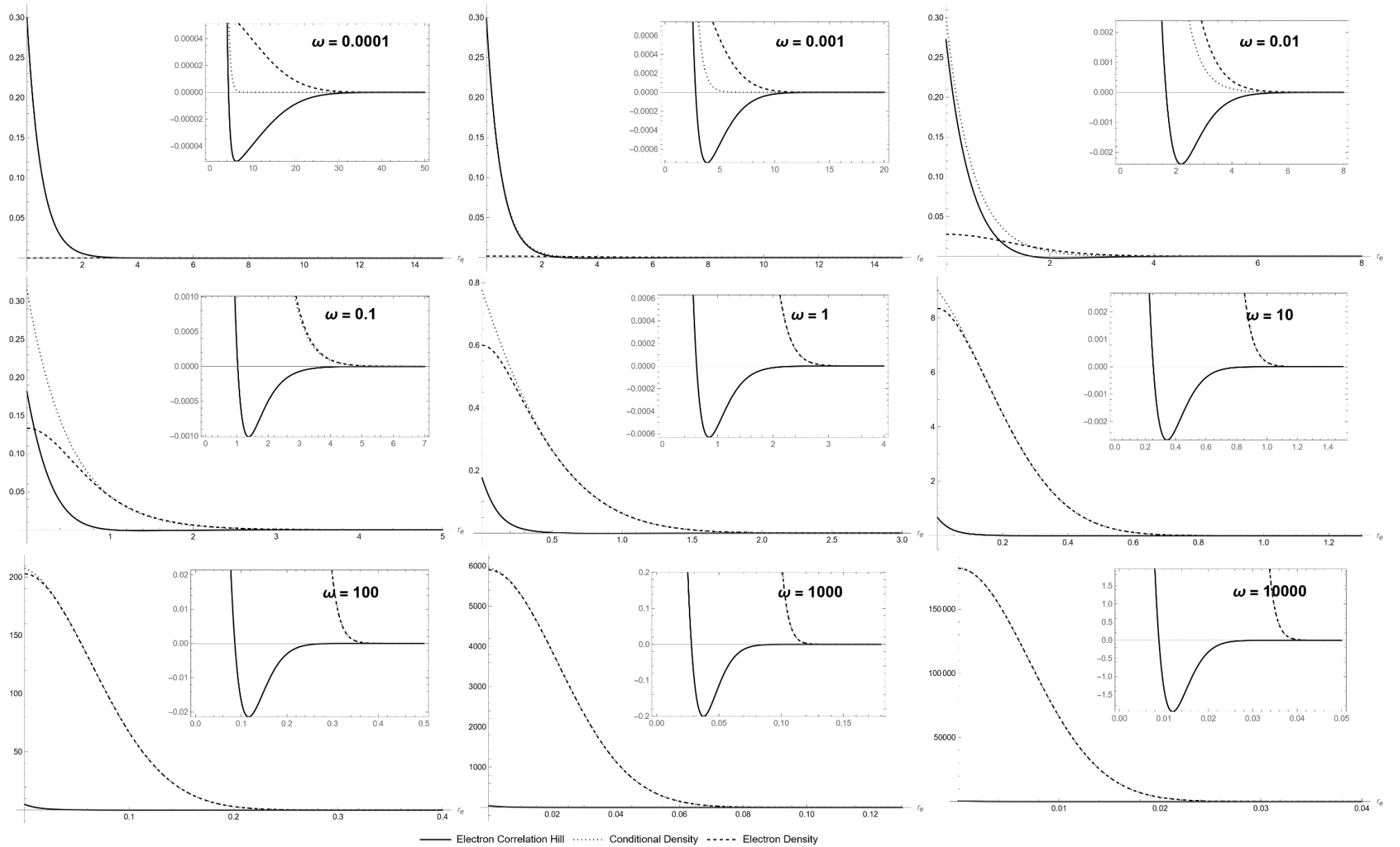


Figure 5-20: Comparison of the correlation hill, conditional density, and single-particle density of electron for mass 50

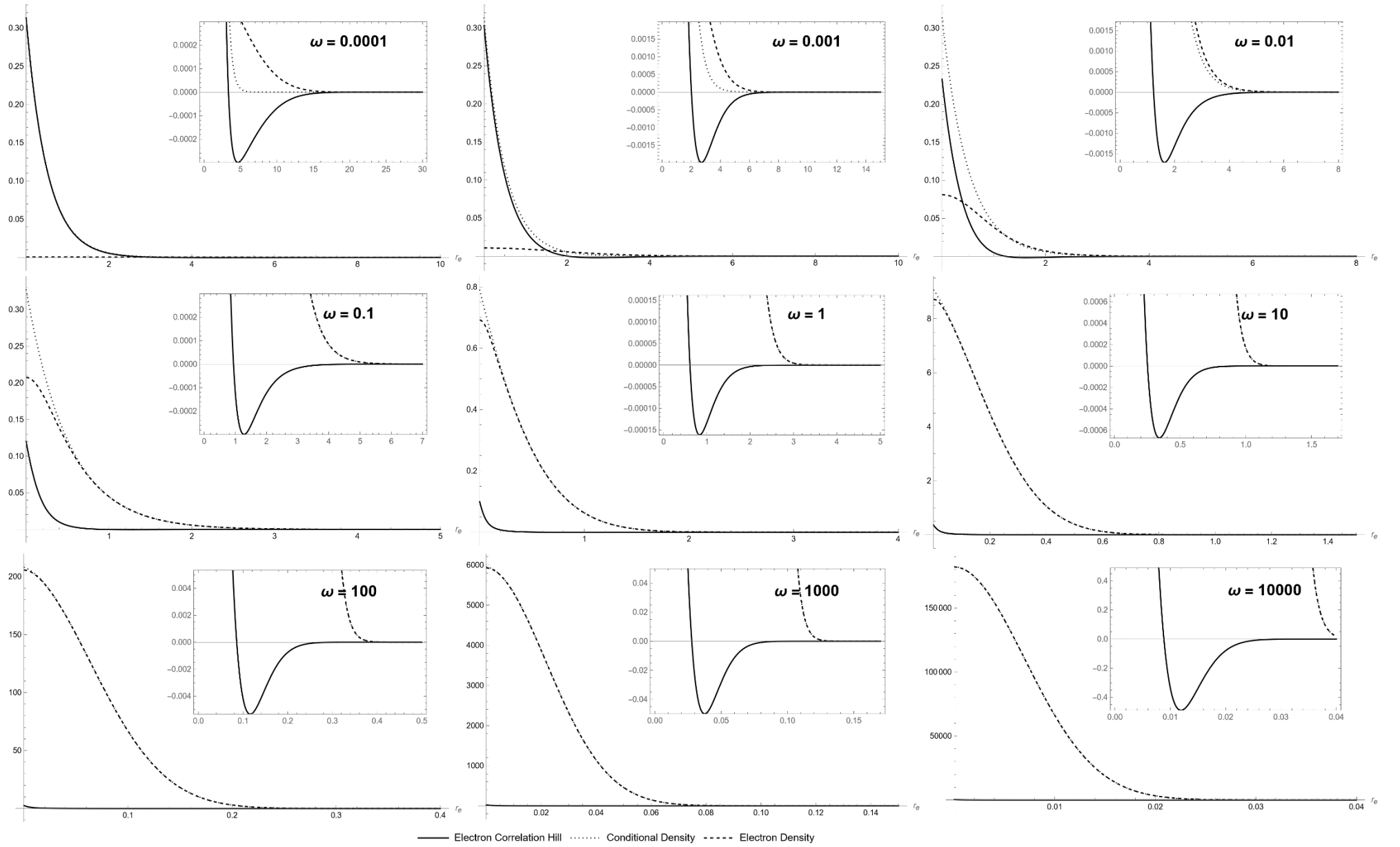


Figure 5-21: Comparison of the correlation hill, conditional density, and single-particle density of electron for mass 207

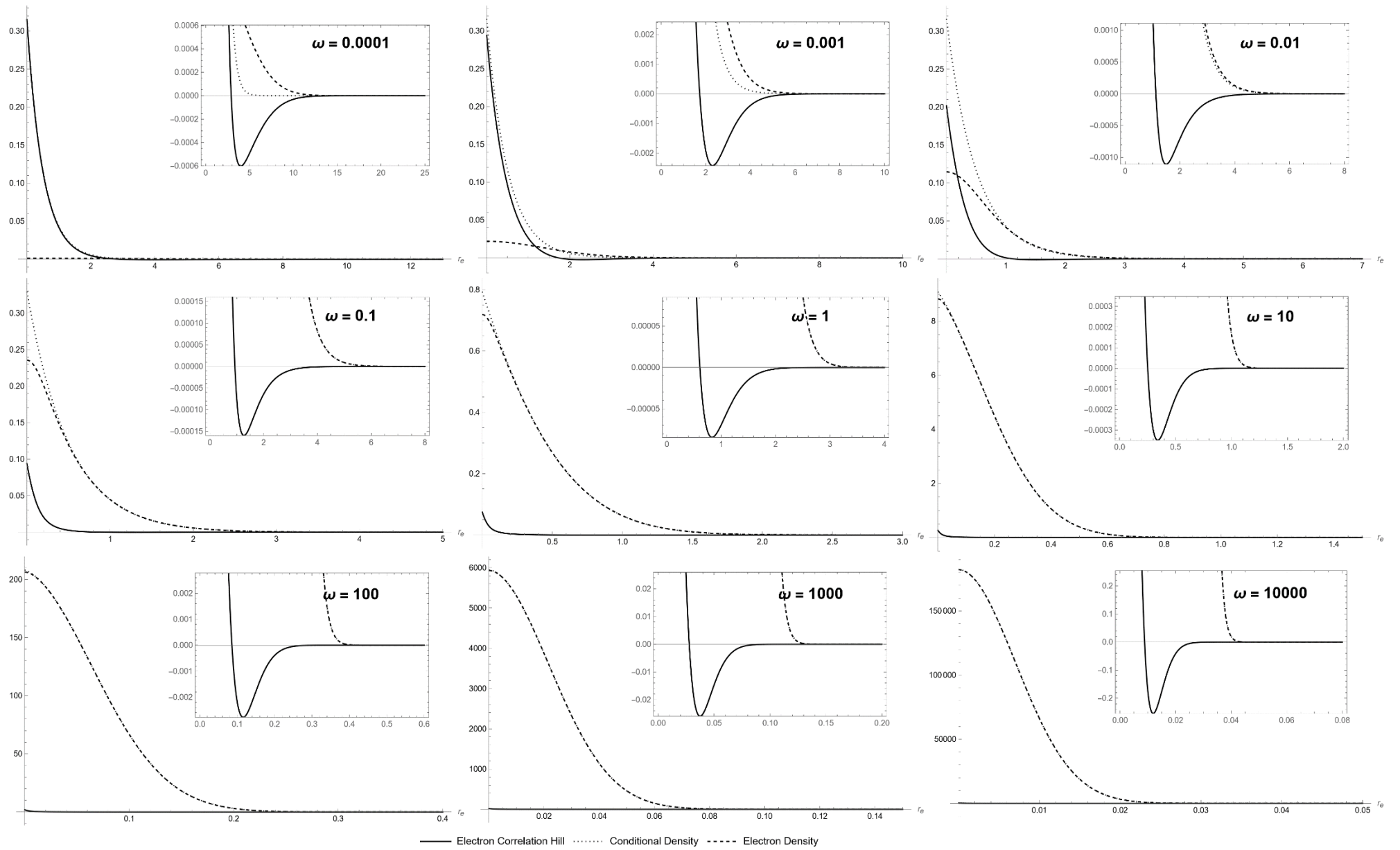


Figure 5-22: Comparison of the correlation hill, conditional density, and single-particle density of electron for mass 400

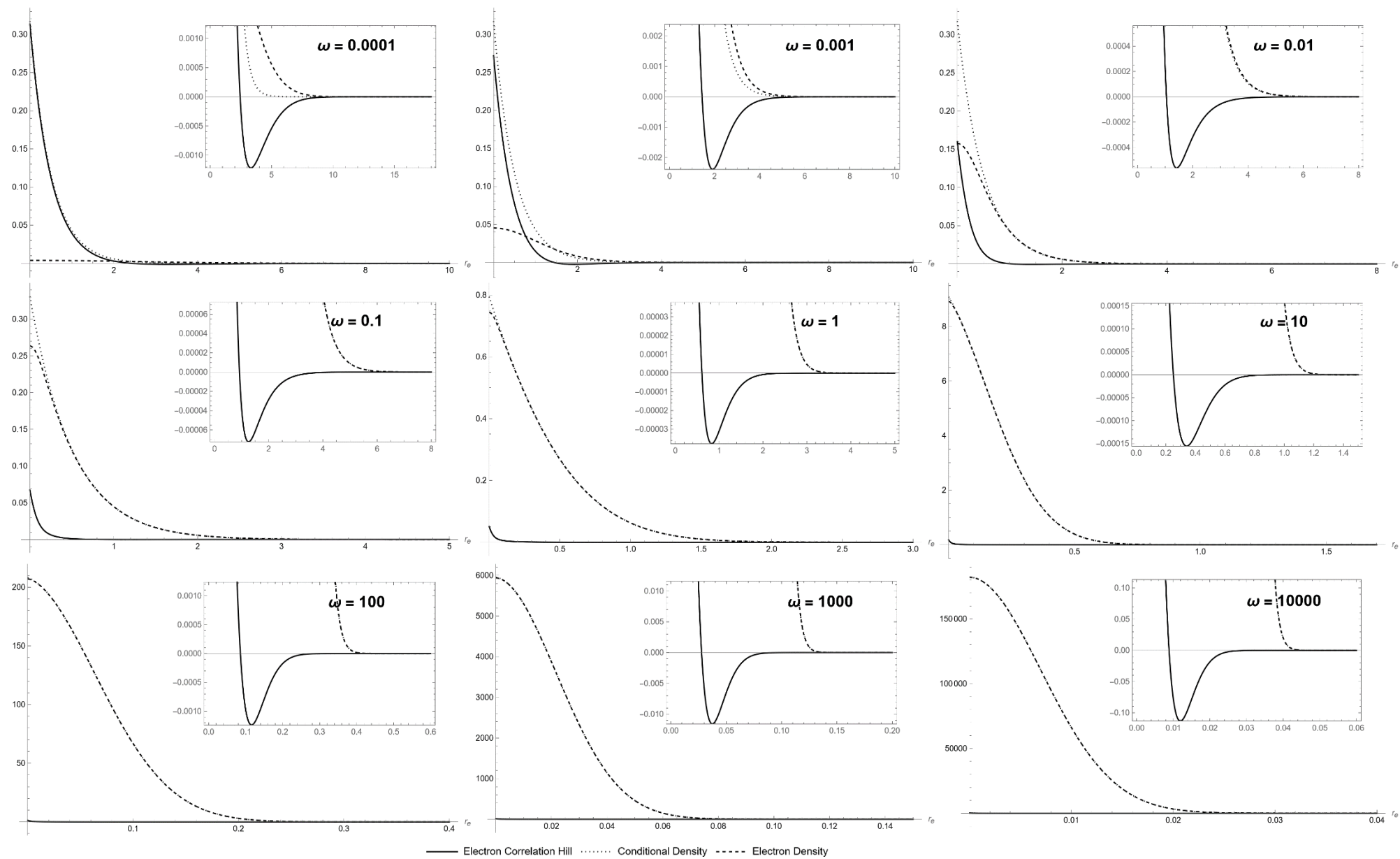


Figure 5-23: Comparison of the correlation hill, conditional density, and single-particle density of electron for mass 900

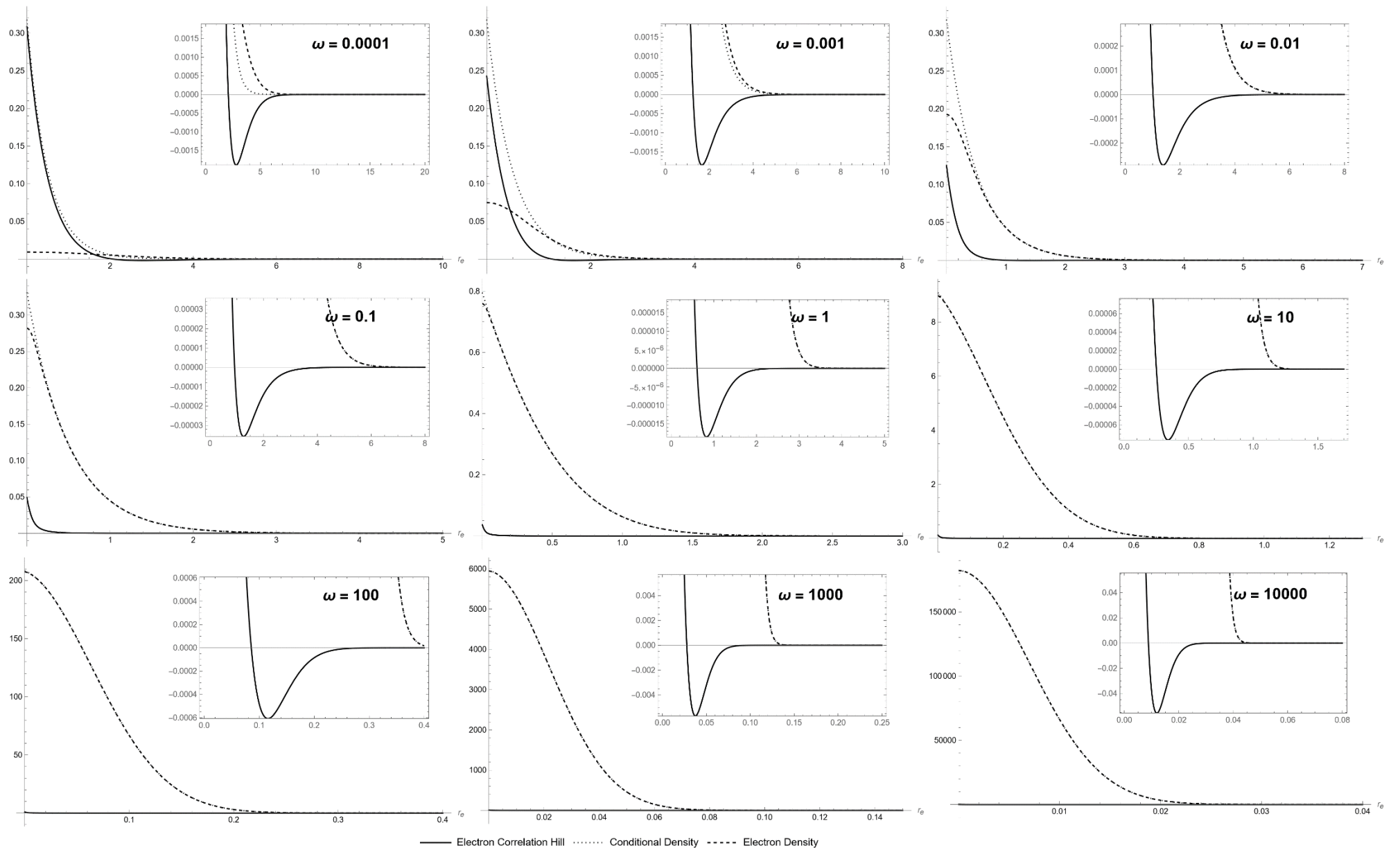


Figure 5-24: Comparison of the correlation hill, conditional density, and single-particle density of electron for mass 1836

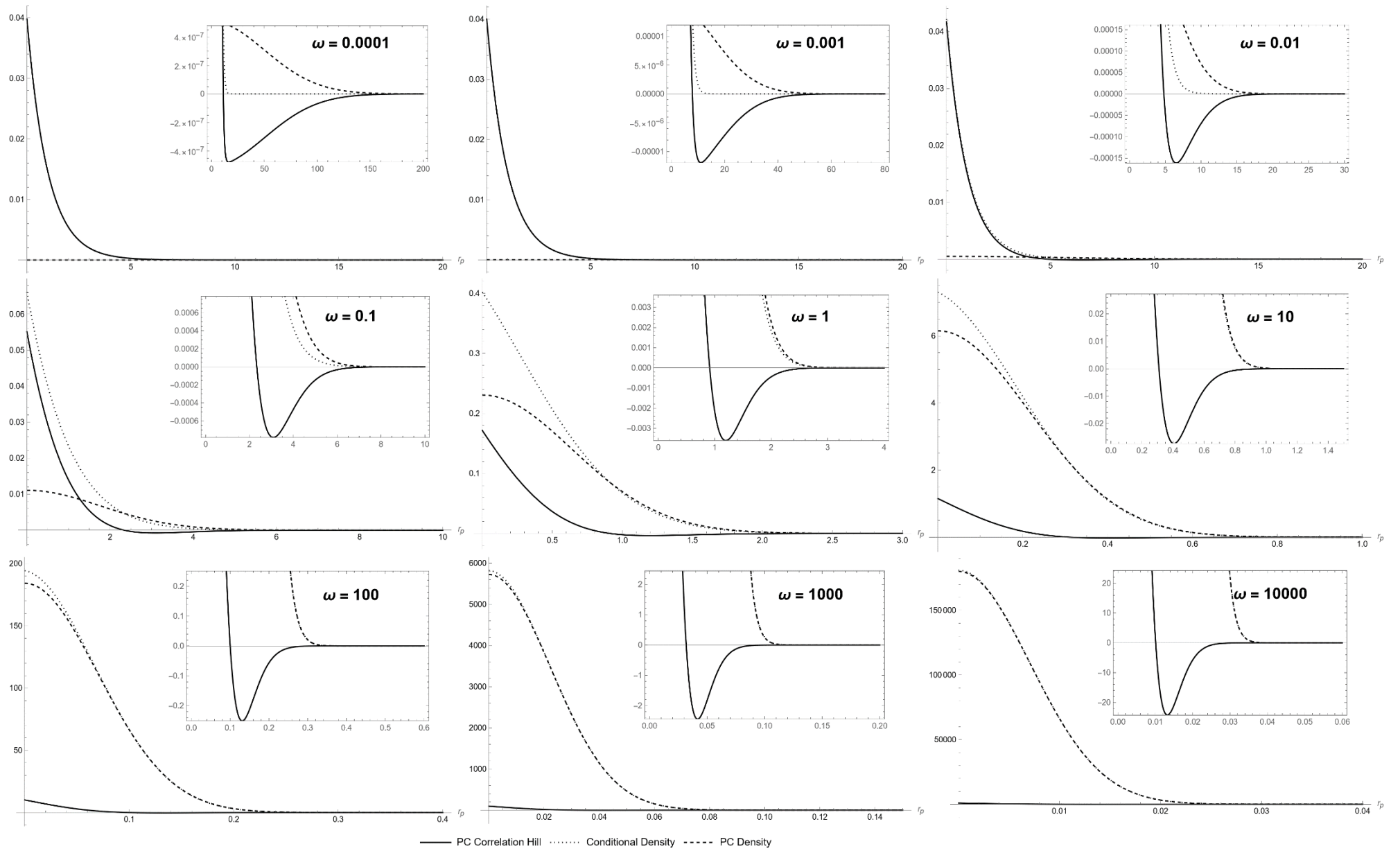


Figure 5-25: Comparison of the correlation hill, conditional density, and single-particle density of PCP for mass 1

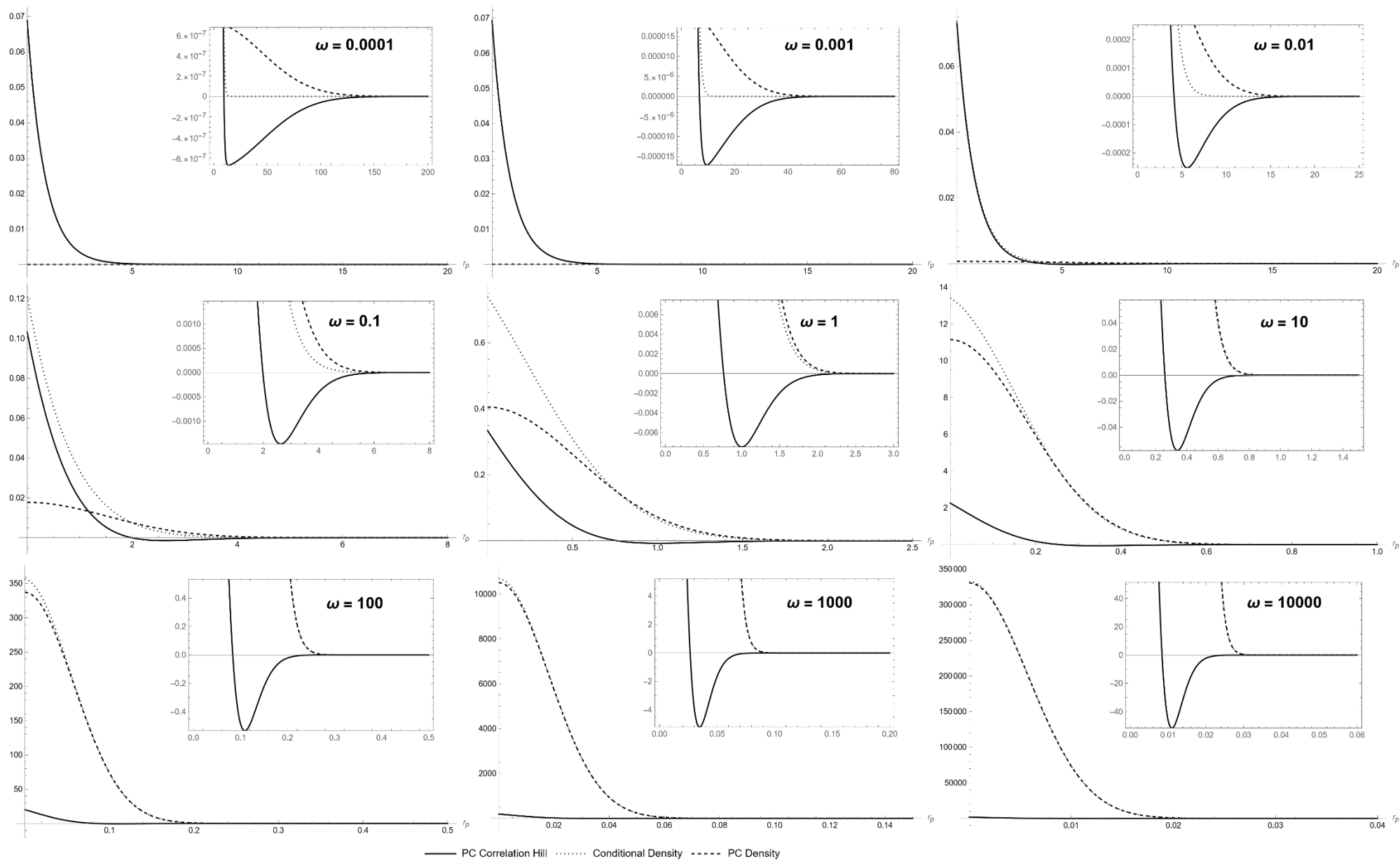


Figure 5-26: Comparison of the correlation hill, conditional density, and single-particle density of PCP for mass 1.5

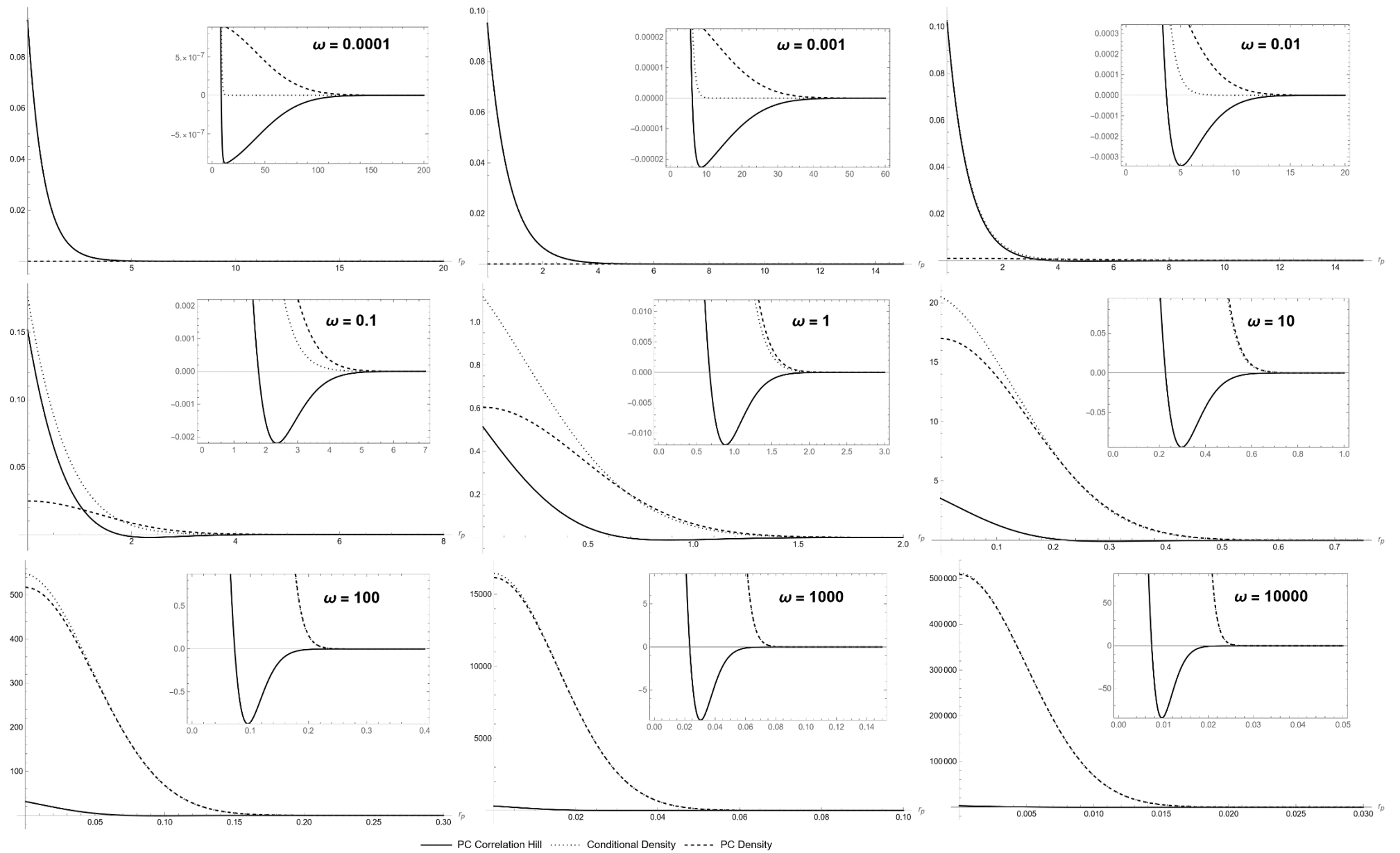


Figure 5-27: Comparison of the correlation hill, conditional density, and single-particle density of PCP for mass 2



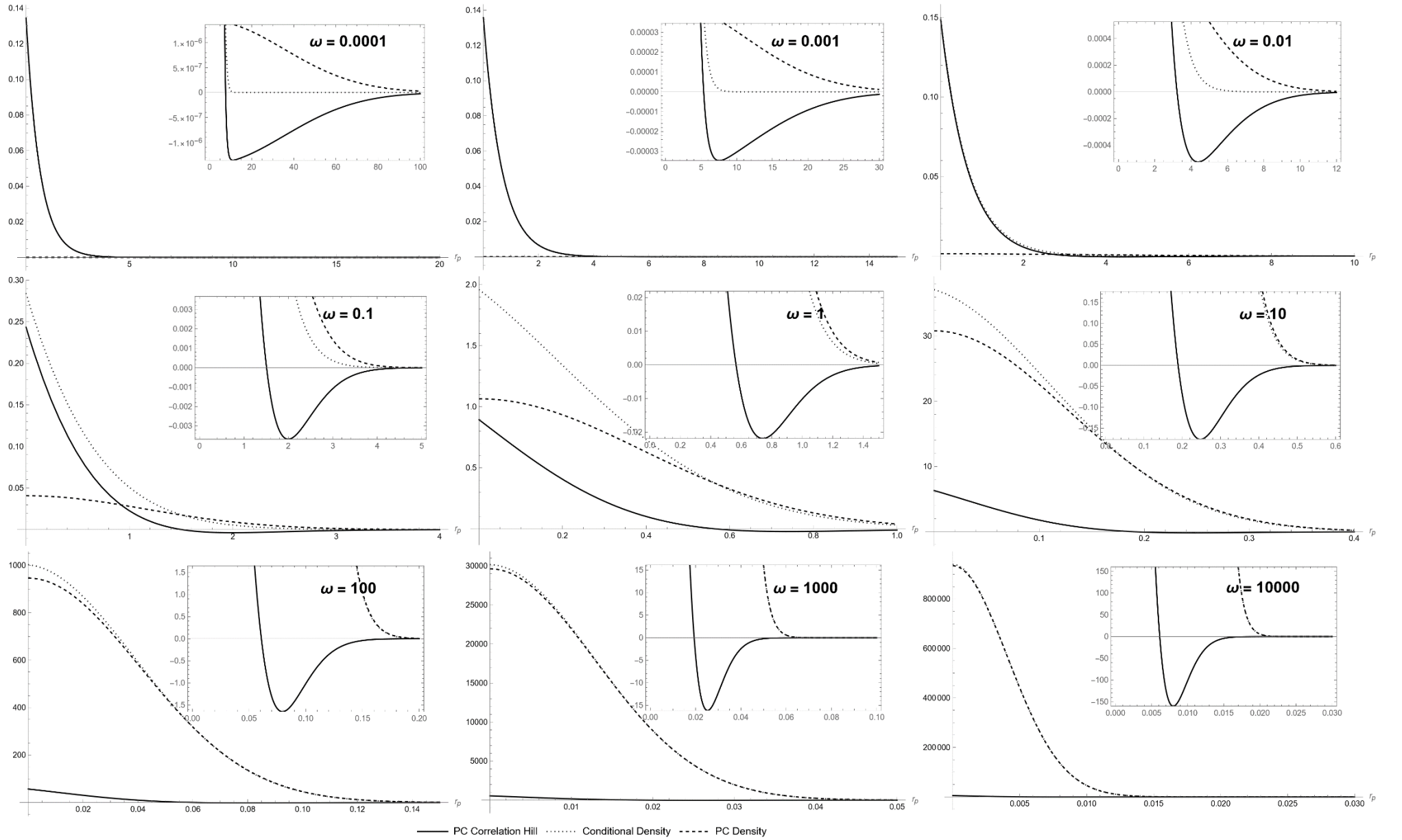


Figure 5-28: Comparison of the correlation hill, conditional density, and single-particle density of PCP for mass 3

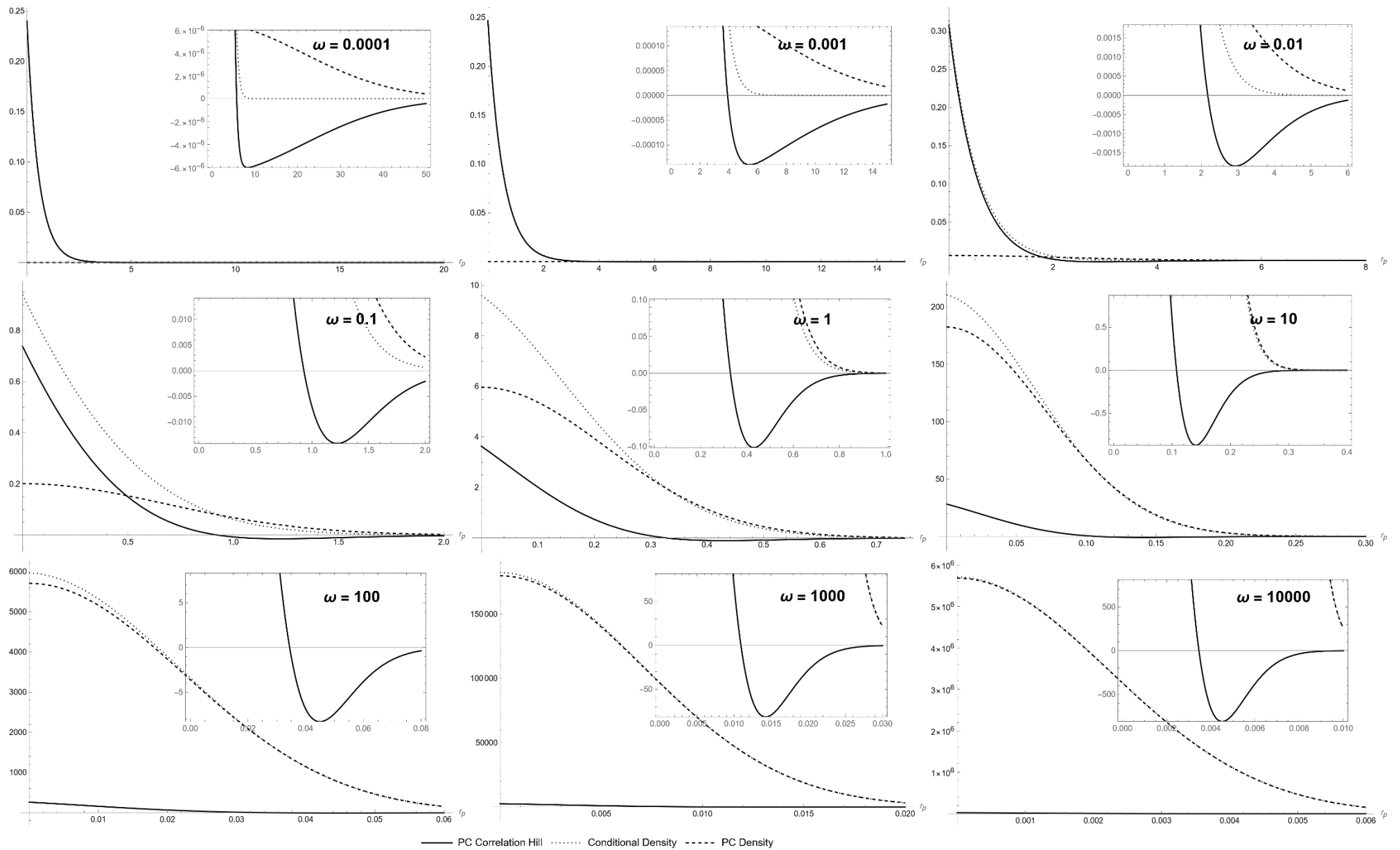


Figure 5-29: Comparison of the correlation hill, conditional density, and single-particle density of PCP for mass 10

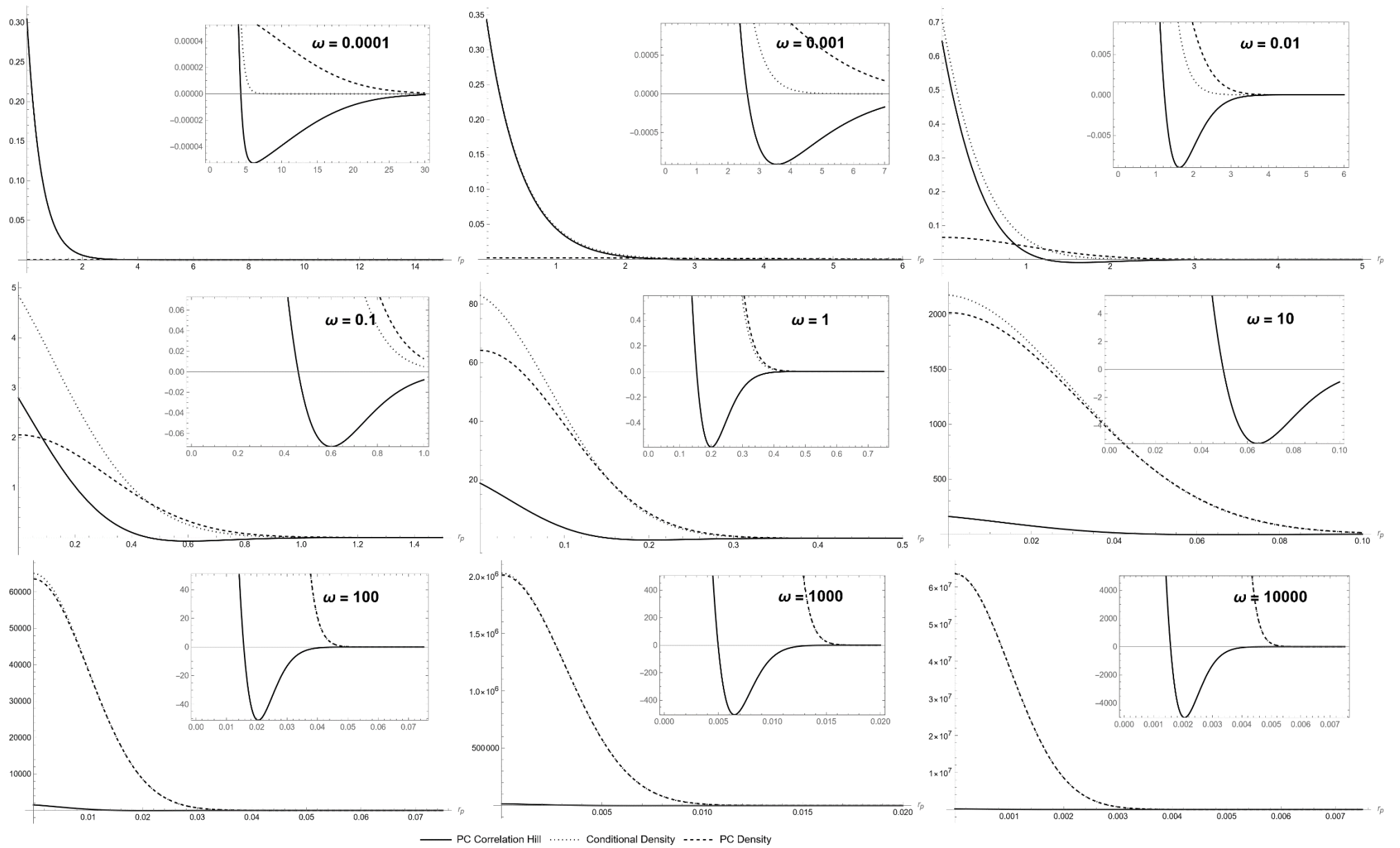


Figure 5-30: Comparison of the correlation hill, conditional density, and single-particle density of PCP for mass 50

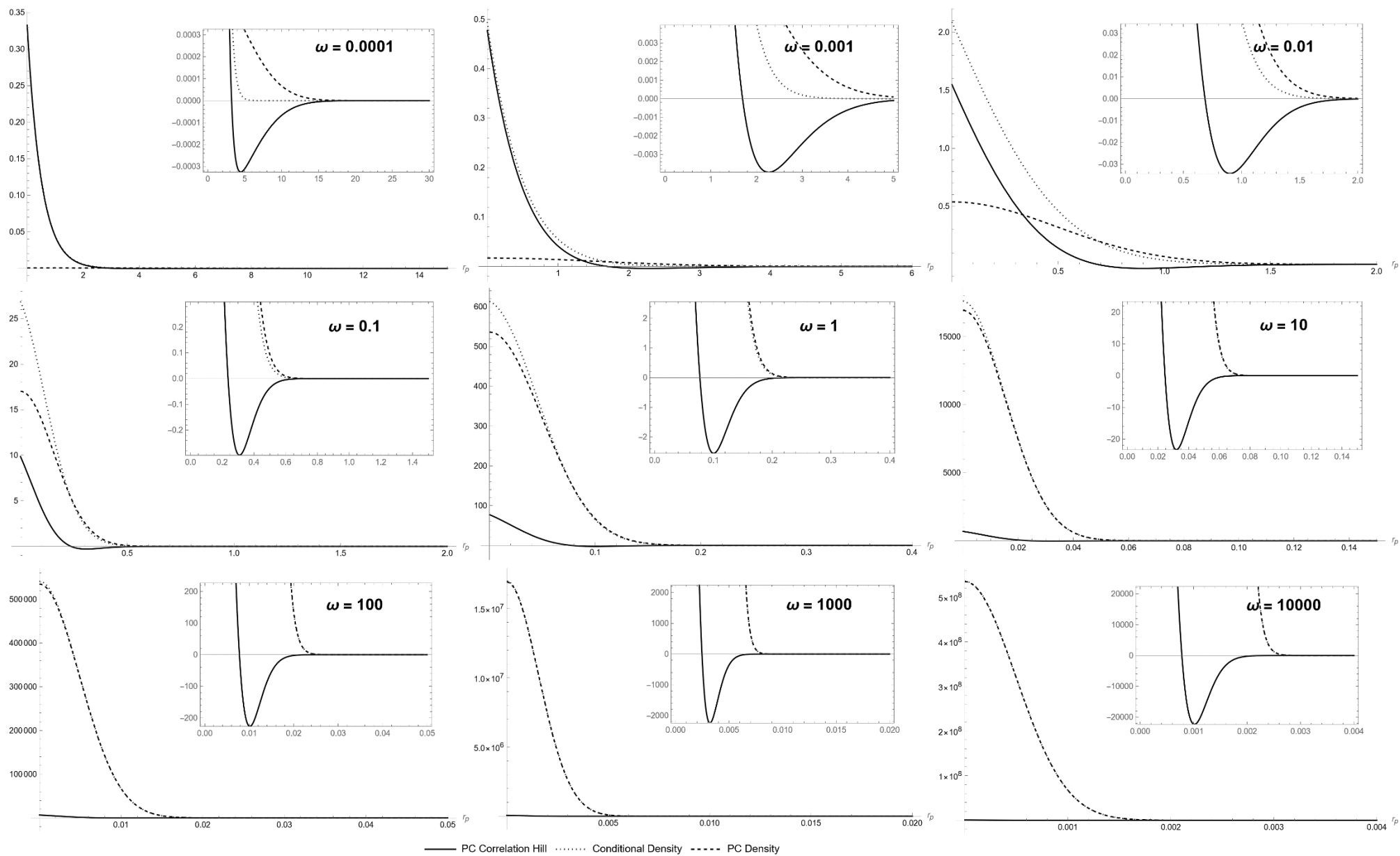


Figure 5-31: Comparison of the correlation hill, conditional density, and single-particle density of PCP for mass 207

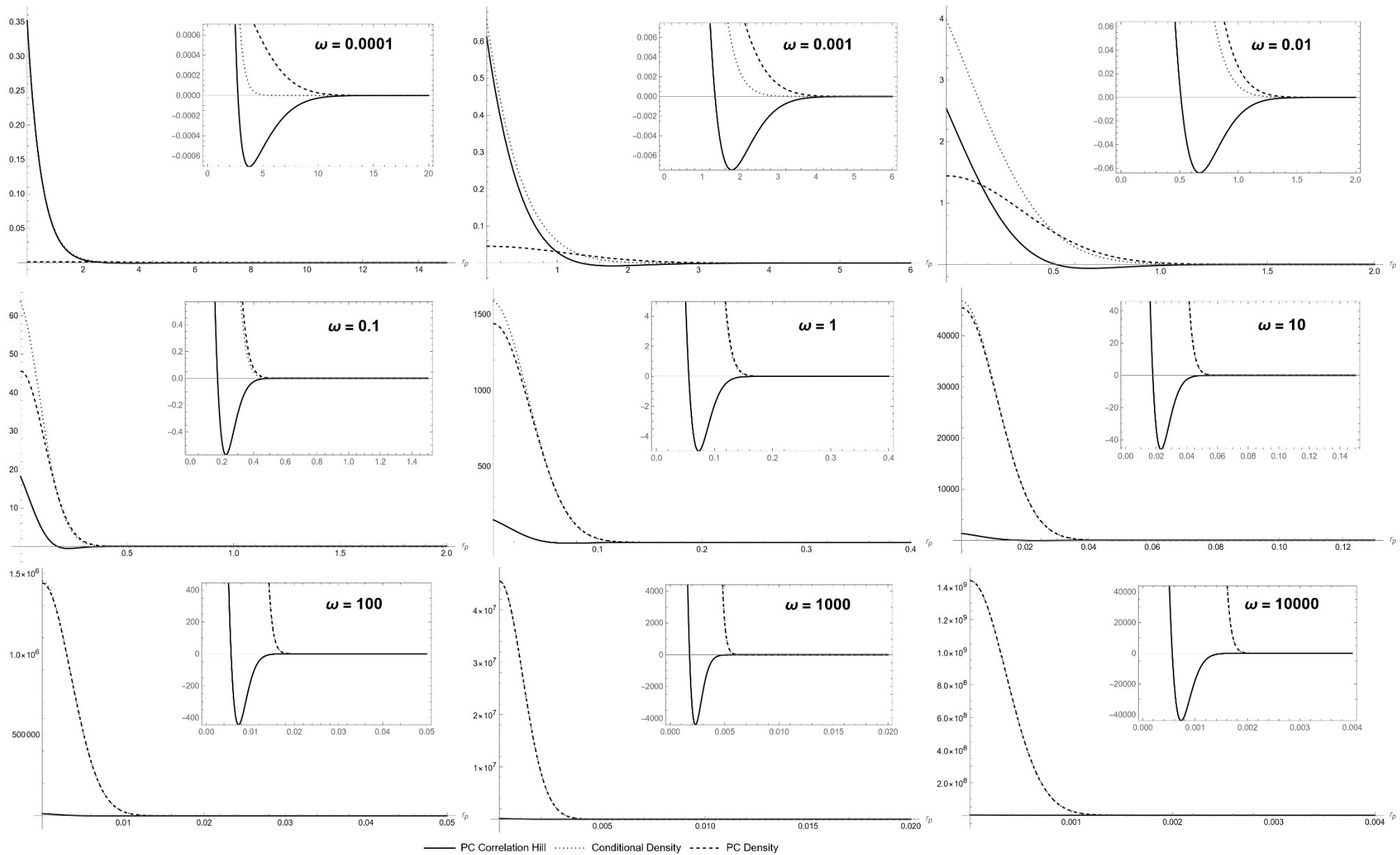


Figure 5-32: Comparison of the correlation hill, conditional density, and single-particle density of PCP for mass 400

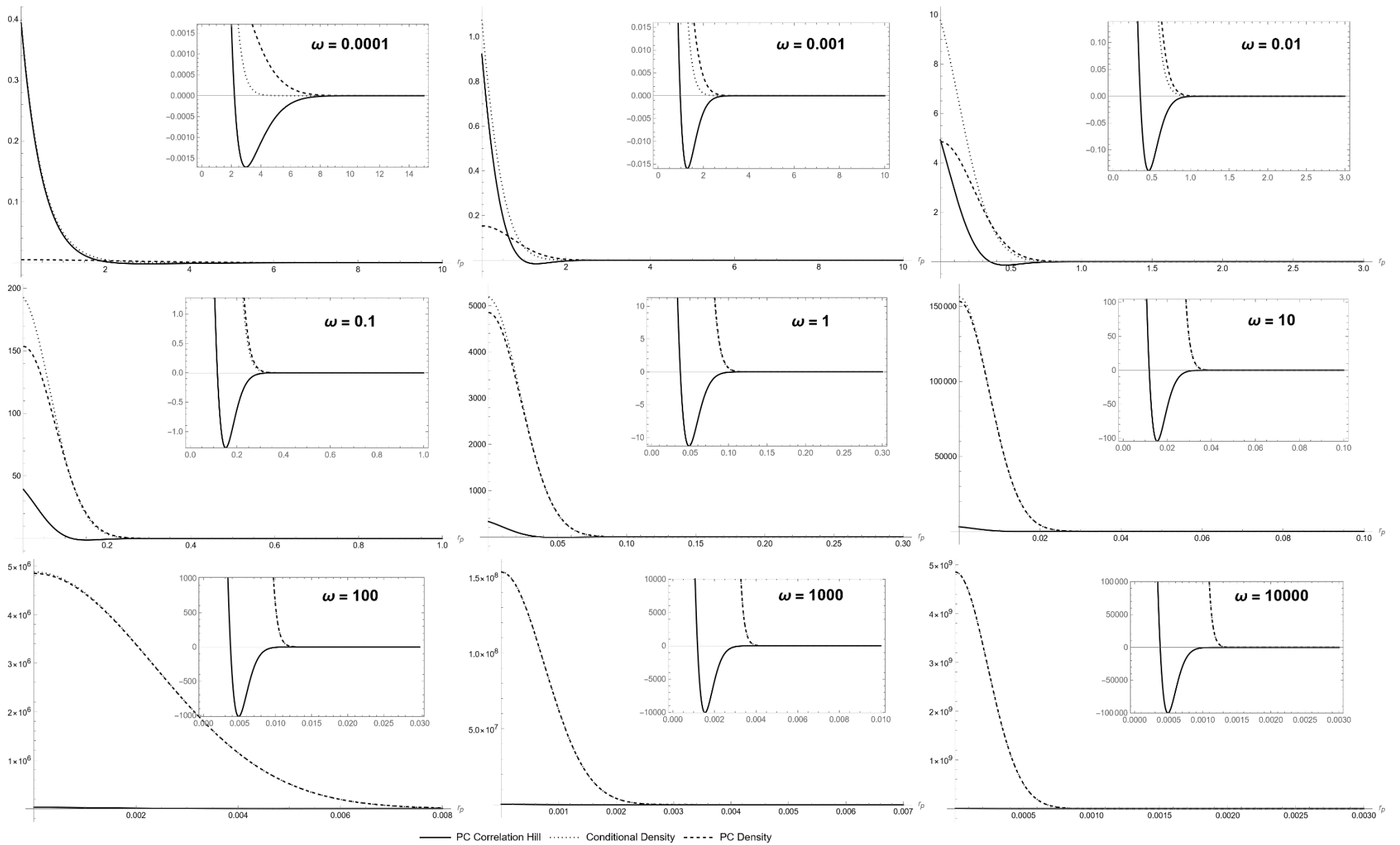


Figure 5-33: Comparison of the correlation hill, conditional density, and single-particle density of PCP for mass 900

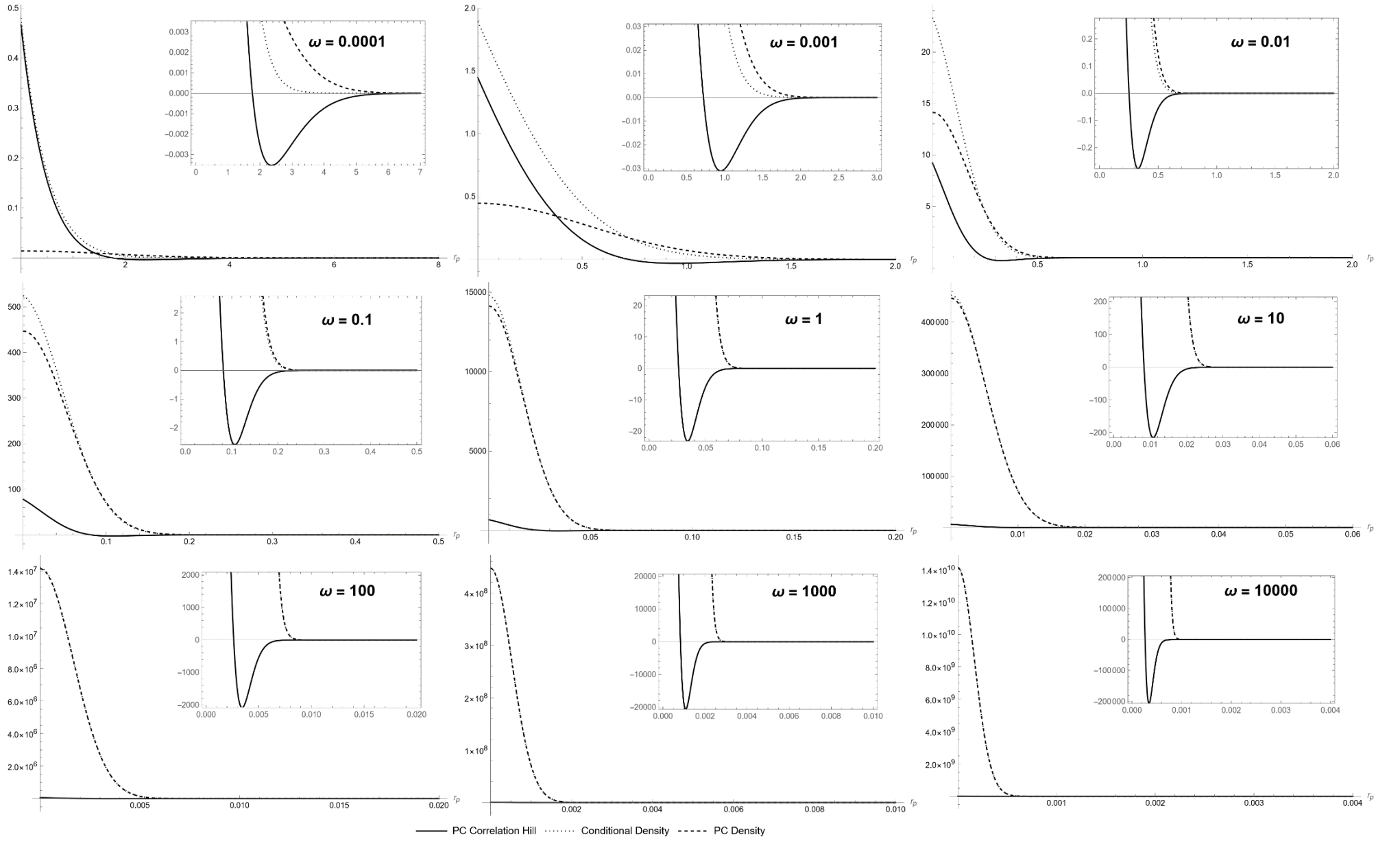


Figure 5-34: Comparison of the correlation hill, conditional density, and single-particle density of PCP for mass 1836

#### 5.1.4 Two-Particle Distribution Functions

Figures 5-35, 5-36, and 5-37 respectively represent the average two-particle distribution functions (3-42) obtained using the variational, FEM, and MC-HF methods. Figure 5-38 shows the difference between the average two-particle distribution functions (equation 3-50) obtained by the variational and MC-HF methods.

The average two-particle distribution function has a Gaussian-like shape that becomes more localized with increasing frequency and mass, indicating that the two particles are closer to each other at a frequency of  $10^4$  and high mass. Since the MC-HF method lacks correlation effects, the difference between the variational and MC-HF distribution functions can be interpreted as an indicator of e-PCP correlation effects. In most cases, the difference in the average two-particle distribution functions of variational and TC-HF methods shows an oscillatory pattern, being positive at short inter-particle distances and negative at long inter-particle distances. However, at high masses and frequencies, it is initially negative, then positive, then negative again, and finally positive at very short distances.

For electron correlation, the correlation effect always tends to keep electrons further apart, but conversely, for e-PCP correlation, the correlation effect, due to its attractive nature, tends to bring the two particles closer together. This is consistent with the positive correlation function differences at short inter-particle distances shown in Figure 5-38.

Integration of the average two-particle distribution function with respect to the inter-particle distance must equal 1 (equation 3-36), a condition that was verified for the average variational, numerical, and MC-HF two-particle distribution functions, all of which satisfy this requirement.



The limit of the average two-particle distribution function as  $m_p \rightarrow \infty$  and  $\omega \rightarrow 0$  was also examined, and the result is equal to the radial distribution function of a hydrogen atom with a clamped nucleus:

$$\lim_{m_p \rightarrow \infty, \omega \rightarrow 0} f(\mathbf{r}) = 4r^2 e^{-2r} = \text{RDF}_H(\mathbf{r}) \quad 5.5$$

The difference between the two-particle distribution function of the two-component system and the radial distribution function of a hydrogen atom with a clamped nucleus is due to the finite mass of the PCP and the harmonic oscillator potential, both of which disappear in the mentioned limit. This can be clearly observed in Figure 5-35 for a frequency of 0.0001 and a mass of 1836.

From Figure 5-38, it can be concluded that correlation causes the electron and PCP to be closer on average. In other words, in a fully correlated state, the electron and the PCP spend more time together, which is consistent with the concept of the correlation hill discussed in the previous section.

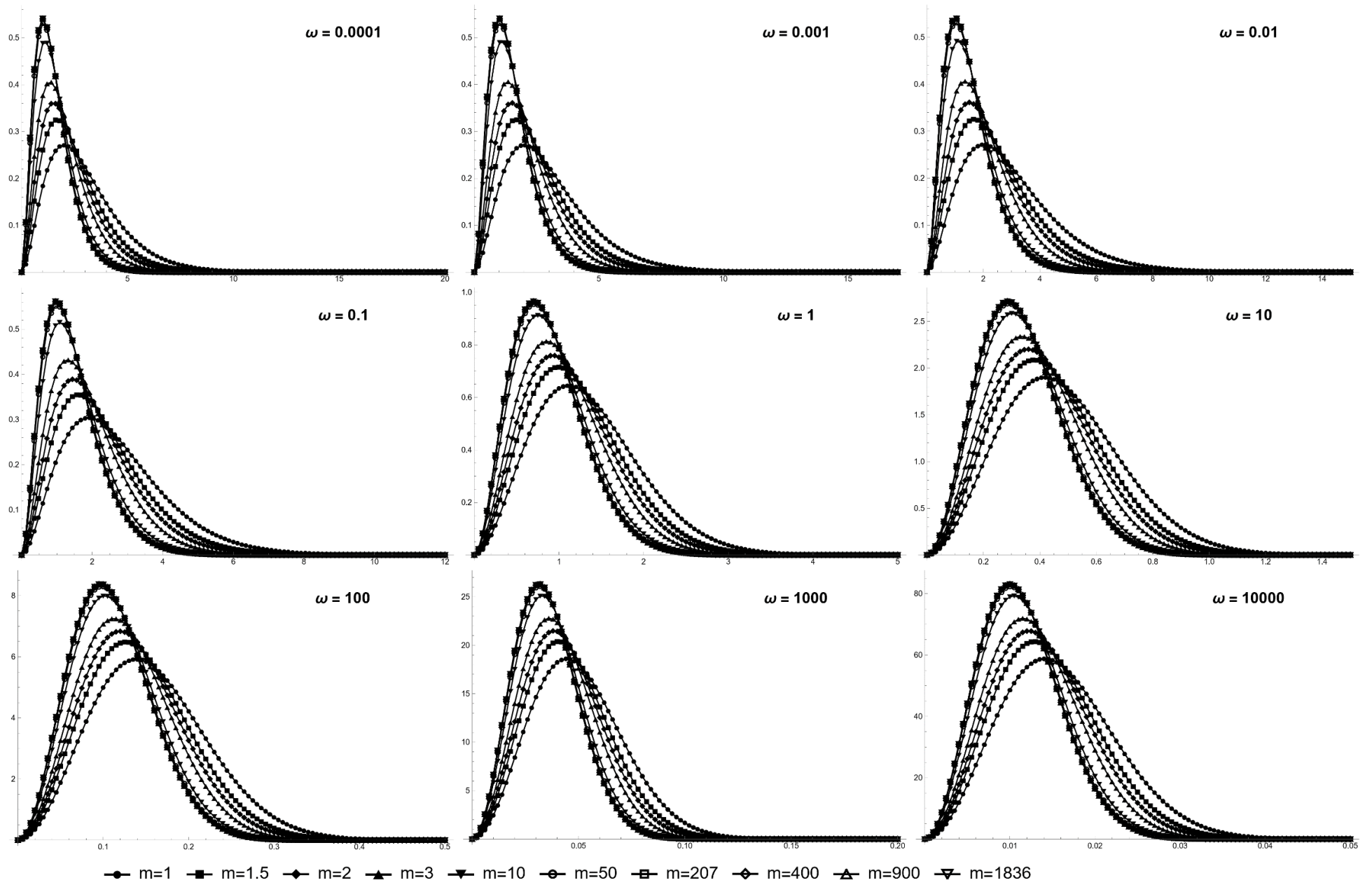


Figure 5-35: Variational average two-particle distribution function as a function of  $r$  for different frequencies and masses.

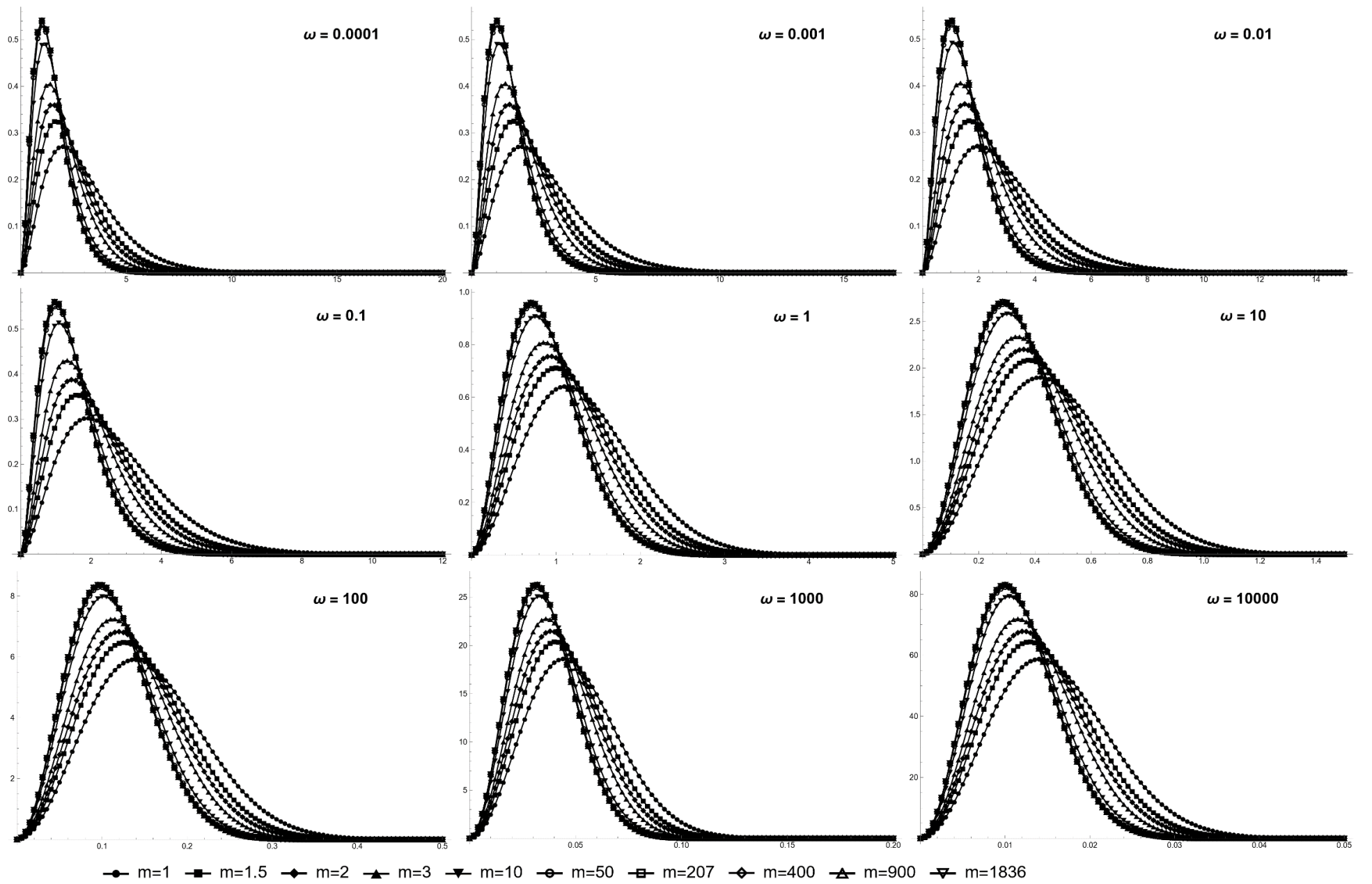


Figure 5-36: FEM average two-particle distribution function as a function of  $r$  for different frequencies and masses.

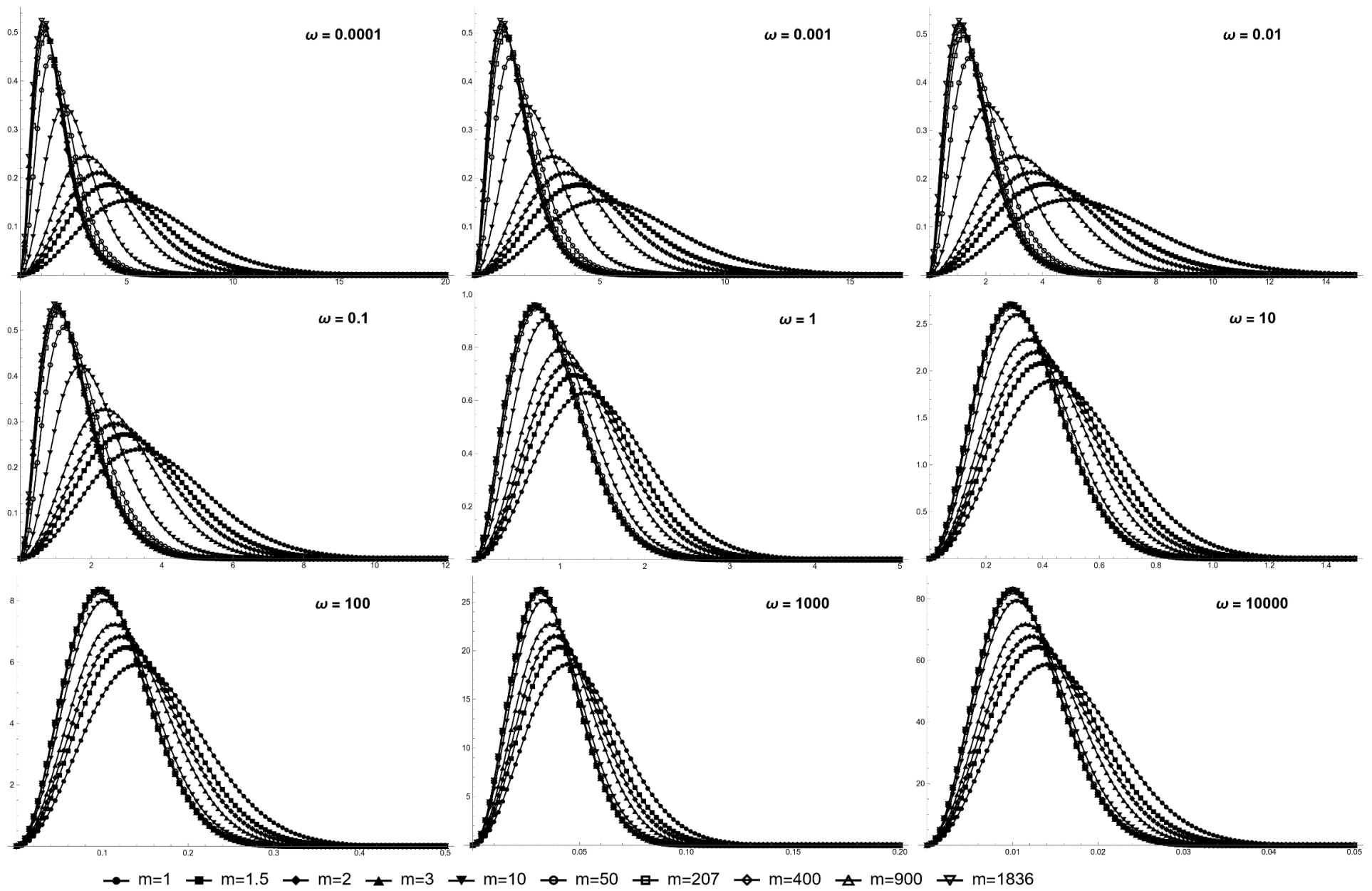


Figure 5-37: TC-HF average two-particle distribution function as a function of  $r$  for different frequencies and masses.

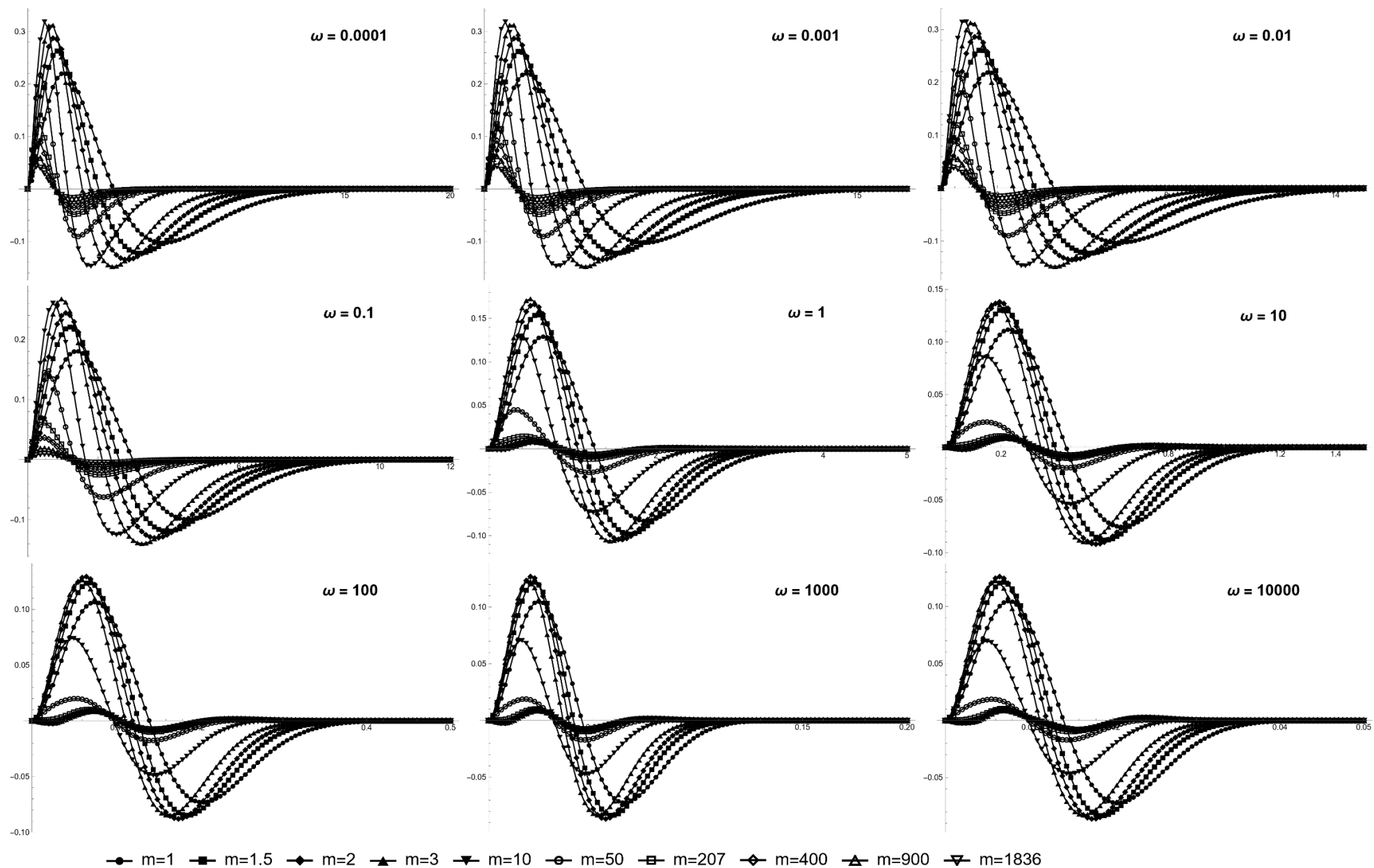


Figure 5-38: Difference between the variational and TC-HF average two-particle distribution functions

### 5.1.5 Mean Inter-particle Distance and its Variance

The results for mean inter-particle distances (equation 3-44) and their variances for the three methods—variational, FEM, and MC-HF—are reported in Table 5-3, which confirm the results mentioned in previous sections. The inter-particle distance decreases with increasing frequency and mass. The variance, which indicates the spread from the mean value, follows the same trend, which is logical given that the particles are closer to each other at higher frequencies and masses. The data show that with increasing  $\omega$ , the average distance difference between the fully correlated variational method and the MC-HF method disappears. This result aligns with the idea that correlation effects decrease with increasing  $\omega$ , confirming the results of previous sections. Additionally, this difference decreases with increasing mass, meaning that correlation effects are more significant for lighter PCPs. This pattern, observed for correlation energy, is exactly seen here for variance as well.

Furthermore, the results for reproducing the e-PCP interaction energy through the two-particle distribution function (equation 3-46) using variational and FEM methods are presented in items 8 and 9 of Table 5-3, which match exactly with the interaction energies presented in items 1 and 2 of Table 5-2. It is worth noting that due to computational issues, these values were not calculated for the HF method.

Table 5-3: The quantities obtained based on the average two-particle distribution function.

$\omega$ /Quantities	Average of r				Variance of r			$\int \mathbf{f}/\mathbf{r} \, d\mathbf{r} = \text{INT}$	
	$f_{\max}^1$	Variational <sup>2</sup>	FEM <sup>3</sup>	MC-HF <sup>4</sup>	Variational <sup>5</sup>	FEM <sup>6</sup>	MC-HF <sup>7</sup>	Variational <sup>8</sup>	FEM <sup>9</sup>
m = 1									
0.0001	2.000000	2.999999	2.999999	5.981602	2.999998	2.999998	7.190049	-0.500000	-0.500000
0.001	1.999988	2.999946	2.999946	5.980384	2.999820	2.999808	7.186729	-0.500006	-0.500006
0.01	1.998803	2.994651	2.994653	5.867637	2.982239	2.981093	6.884944	-0.500596	-0.500596
0.1	1.904998	2.686954	2.688387	3.871700	2.138349	2.121882	2.829622	-0.541447	-0.541407
1	1.116163	1.349412	1.350134	1.484141	0.394696	0.392679	0.399454	-0.991609	-0.991837
10	0.417919	0.480650	0.480729	0.493695	0.043782	0.043706	0.043653	-2.689688	-2.690048
100	0.138524	0.157206	0.157214	0.158491	0.004488	0.004486	0.004482	-8.137662	-8.138049
1000	0.044433	0.050227	0.050227	0.050354	0.000452	0.000452	0.000452	-25.387791	-25.388180
10000	0.014113	0.015934	0.015934	0.015947	0.000045	0.000045	0.000045	-79.944206	-79.944309
m = 1.5									
0.0001	1.666667	2.500000	2.500000	4.934280	2.083333	2.083332	4.920492	-0.600000	-0.600000
0.001	1.666660	2.499969	2.499969	4.933588	2.083247	2.083241	4.918910	-0.600005	-0.600005
0.01	1.665973	2.496896	2.496897	4.868394	2.074733	2.074173	4.773718	-0.600498	-0.600498
0.1	1.608070	2.296002	2.296978	3.404134	1.597607	1.586164	2.212973	-0.637497	-0.637453
1	0.992970	1.209767	1.210470	1.340977	0.323077	0.321298	0.327920	-1.111402	-1.111648
10	0.378914	0.436646	0.436726	0.449270	0.036349	0.036280	0.036223	-2.965158	-2.965584
100	0.126200	0.143301	0.143309	0.144540	0.003736	0.003734	0.003730	-8.931366	-8.931830
1000	0.040536	0.045830	0.045831	0.045953	0.000377	0.000377	0.000376	-27.827407	-27.827882
10000	0.012881	0.014544	0.014544	0.014556	0.000038	0.000038	0.000038	-87.590782	-87.591125
m = 2									

$\omega$ /Quantities	Average of r				Variance of r			$\int \mathbf{f}/\mathbf{r} \, d\mathbf{r} = \text{INT}$	
	$f_{\max}^1$	Variational <sup>2</sup>	FEM <sup>3</sup>	MC-HF <sup>4</sup>	Variational <sup>5</sup>	FEM <sup>6</sup>	MC-HF <sup>7</sup>	Variational <sup>8</sup>	FEM <sup>9</sup>
0.0001	1.500000	2.250000	2.250000	4.357798	1.687499	1.687499	3.878840	-0.666667	-0.666667
0.001	1.499995	2.249977	2.249977	4.357315	1.687443	1.687439	3.877865	-0.666671	-0.666671
0.01	1.499494	2.247734	2.247735	4.311394	1.681848	1.681478	3.786690	-0.667115	-0.667115
0.1	1.455992	2.092163	2.092922	3.125413	1.342596	1.333497	1.894119	-0.701824	-0.701779
1	0.926837	1.134680	1.135371	1.259215	0.287424	0.285774	0.291646	-1.188468	-1.188724
10	0.357940	0.412985	0.413064	0.424824	0.032637	0.032571	0.032496	-3.137951	-3.138421
100	0.119574	0.135825	0.135833	0.136980	0.003361	0.003358	0.003354	-9.425652	-9.426166
1000	0.038441	0.043466	0.043467	0.043580	0.000339	0.000339	0.000339	-29.343461	-29.343988
10000	0.012219	0.013796	0.013796	0.013808	0.000034	0.000034	0.000034	-92.339475	-92.339464
m=3									
0.0001	1.333333	2.000000	2.000000	3.720384	1.333333	1.333333	2.893677	-0.750000	-0.750000
0.001	1.333330	1.999984	1.999984	3.720075	1.333298	1.333295	2.893121	-0.750004	-0.750004
0.01	1.332978	1.998407	1.998407	3.690477	1.329799	1.329567	2.842222	-0.750399	-0.750399
0.1	1.301551	1.882410	1.882969	2.794381	1.100335	1.093412	1.560897	-0.782537	-0.782494
1	0.857032	1.055298	1.055973	1.166177	0.251903	0.250390	0.254800	-1.282329	-1.282593
10	0.335763	0.387965	0.388044	0.398227	0.028929	0.028867	0.028759	-3.343984	-3.344507
100	0.112569	0.127921	0.127929	0.128910	0.002985	0.002983	0.002977	-10.011451	-10.012028
1000	0.036226	0.040966	0.040967	0.041064	0.000301	0.000301	0.000301	-31.136990	-31.137584
10000	0.011518	0.013006	0.013006	0.013016	0.000030	0.000030	0.000030	-97.954202	-97.954818
m=10									
0.0001	1.100000	1.650000	1.650000	2.590797	0.907500	0.907500	1.561928	-0.909091	-0.909091
0.001	1.099998	1.649991	1.649991	2.590647	0.907483	0.907482	1.561559	-0.909094	-0.909094
0.01	1.099801	1.649104	1.649104	2.579139	0.905859	0.905751	1.547241	-0.909420	-0.909420



$\omega$ /Quantities	Average of r				Variance of r			$\int \mathbf{f}/\mathbf{r} \, d\mathbf{r} = \text{INT}$	
	$f_{\max}^1$	Variational <sup>2</sup>	FEM <sup>3</sup>	MC-HF <sup>4</sup>	Variational <sup>5</sup>	FEM <sup>6</sup>	MC-HF <sup>7</sup>	Variational <sup>8</sup>	FEM <sup>9</sup>
0.1	1.081518	1.578456	1.578774	2.129586	0.787219	0.782964	1.031733	-0.937438	-0.937401
1	0.751829	0.935327	0.935972	0.997221	0.202453	0.201149	0.202034	-1.455630	-1.455900
10	0.302230	0.350136	0.350215	0.355189	0.023745	0.023690	0.023564	-3.712490	-3.713113
100	0.101978	0.115970	0.115978	0.116434	0.002459	0.002457	0.002452	-11.049642	-11.050341
1000	0.032877	0.037188	0.037189	0.037233	0.000248	0.000248	0.000248	-34.307069	-34.307788
10000	0.010459	0.011811	0.011811	0.011815	0.000025	0.000025	0.000025	-107.870081	-107.870362
m = 50									
0.0001	1.020000	1.530000	1.530000	1.949965	0.780300	0.780300	1.031171	-0.980392	-0.980392
0.001	1.019998	1.529993	1.529993	1.949900	0.780288	0.780287	1.031121	-0.980395	-0.980395
0.01	1.019841	1.529285	1.529286	1.943441	0.779086	0.779006	1.024910	-0.980698	-0.980698
0.1	1.005104	1.471429	1.471680	1.698090	0.688120	0.684652	0.779651	-1.007152	-1.007117
1	0.713362	0.891326	0.891957	0.910909	0.185594	0.184366	0.184251	-1.531339	-1.531607
10	0.289923	0.336252	0.336330	0.337618	0.021971	0.021917	0.021869	-3.868947	-3.869613
100	0.098091	0.111585	0.111593	0.111704	0.002279	0.002277	0.002276	-11.486768	-11.487519
1000	0.031649	0.035801	0.035802	0.035813	0.000230	0.000230	0.000230	-35.638555	-35.639330
10000	0.010071	0.011372	0.011373	0.011374	0.000023	0.000023	0.000023	-112.031793	-112.031719
m = 207									
0.0001	1.004831	1.507246	1.507246	1.713677	0.757264	0.757264	0.874958	-0.995192	-0.995192
0.001	1.004829	1.507240	1.507240	1.713614	0.757252	0.757252	0.874906	-0.995195	-0.995195
0.01	1.004679	1.506563	1.506563	1.707620	0.756121	0.756045	0.870034	-0.995493	-0.995493
0.1	0.990562	1.450974	1.451212	1.537190	0.669862	0.666534	0.702137	-1.021642	-1.021608
1	0.705910	0.882792	0.883421	0.888875	0.182403	0.181191	0.181130	-1.546927	-1.547195
10	0.287535	0.333558	0.333637	0.333973	0.021634	0.021582	0.021568	-3.900837	-3.901511

$\omega$ /Quantities	Average of r				Variance of r			$\int \mathbf{f}/\mathbf{r} \, d\mathbf{r} = \text{INT}$	
	$f_{\max}^1$	Variational <sup>2</sup>	FEM <sup>3</sup>	MC-HF <sup>4</sup>	Variational <sup>5</sup>	FEM <sup>6</sup>	MC-HF <sup>7</sup>	Variational <sup>8</sup>	FEM <sup>9</sup>
100	0.097337	0.110734	0.110742	0.110771	0.002245	0.002243	0.002243	-11.575600	-11.576362
1000	0.031410	0.035532	0.035533	0.011263	0.000227	0.000227	0.001363	-35.908903	-35.909690
10000	0.009995	0.011287	0.011288	0.011288	0.000023	0.000023	0.000023	-112.876573	-112.876468
m = 400									
0.0001	1.002500	1.503750	1.503750	1.652347	0.753755	0.753755	0.837699	-0.997506	-0.997506
0.001	1.002498	1.503743	1.503743	1.652281	0.753743	0.753743	0.837669	-0.997509	-0.997509
0.01	1.002349	1.503072	1.503072	1.645959	0.752622	0.752547	0.832830	-0.997806	-0.997806
0.1	0.988325	1.447826	1.448062	1.499710	0.667072	0.663765	0.685196	-1.023908	-1.023874
1	0.704761	0.881475	0.882104	0.885056	0.181913	0.180703	0.180670	-1.549361	-1.549628
10	0.287167	0.333142	0.333221	0.333398	0.021583	0.021530	0.021523	-3.905805	-3.906481
100	0.097221	0.110603	0.110611	0.110626	0.002240	0.002238	0.002238	-11.589432	-11.590196
1000	0.031373	0.035491	0.035492	0.035493	0.000226	0.000226	0.000226	-35.950992	-35.951780
10000	0.009984	0.011274	0.011274	0.011275	0.000023	0.000023	0.000023	-113.008083	-113.007974
m = 900									
0.0001	1.001111	1.501667	1.501667	1.600851	0.751667	0.751667	0.807377	-0.998890	-0.998890
0.001	1.001110	1.501660	1.501660	1.600772	0.751656	0.751656	0.807323	-0.998893	-0.998893
0.01	1.000961	1.500991	1.500991	1.593711	0.750542	0.750467	0.802209	-0.999190	-0.999190
0.1	0.986993	1.445950	1.446185	1.472460	0.665412	0.662117	0.673072	-1.025263	-1.025229
1	0.704075	0.880690	0.881318	0.460130	0.181621	0.180413	0.292910	-1.550816	-1.551083
10	0.286947	0.332894	0.332973	0.333053	0.021552	0.021499	0.021496	-3.908774	-3.909451
100	0.097151	0.110525	0.110533	0.110539	0.002237	0.002235	0.002235	-11.597698	-11.598462
1000	0.031351	0.035466	0.035467	0.035467	0.000226	0.000226	0.000226	-35.976141	-35.976930
10000	0.009977	0.011266	0.011267	0.011267	0.000023	0.000023	0.000023	-113.086663	-113.086551

$\omega$ /Quantities	Average of $r$				Variance of $r$			$\int \mathbf{f}/\mathbf{r} \, d\mathbf{r} = \text{INT}$	
	$f_{\max}^1$	Variational <sup>2</sup>	FEM <sup>3</sup>	MC-HF <sup>4</sup>	Variational <sup>5</sup>	FEM <sup>6</sup>	MC-HF <sup>7</sup>	Variational <sup>8</sup>	FEM <sup>9</sup>
$m = 1836$									
0.0001	1.000545	1.500817	1.500817	1.570352	0.750817	0.750817	0.789786	-0.999456	-0.999456
0.001	1.000543	1.500810	1.500810	1.570256	0.750806	0.750805	0.789707	-0.999459	-0.999459
0.01	1.000394	1.500142	1.500143	1.562364	0.749694	0.749619	0.784314	-0.999755	-0.999755
0.1	0.986450	1.445184	1.445419	1.459412	0.664734	0.661445	0.667317	-1.025817	-1.025783
1	0.703795	0.880370	0.880997	0.454000	0.181502	0.180294	0.290106	-1.551410	-1.551677
10	0.286857	0.332793	0.332872	0.332911	0.021539	0.021487	0.021485	-3.909987	-3.910664
100	0.097123	0.110493	0.110501	0.110504	0.002235	0.002234	0.002234	-11.601074	-11.601838
1000	0.031343	0.035456	0.035457	0.035457	0.000226	0.000226	0.000226	-35.986413	-35.987203
10000	0.009974	0.011263	0.011263	0.011263	0.000023	0.000023	0.000023	-113.118759	-113.118645

1. The value of  $r$  at which the variational mean two-particle distribution function is maximum.
2. The mean distance  $r$  calculated using the variational method.
3. The mean distance  $r$  calculated using the FEM method.
4. The mean distance  $r$  calculated using the MC-HF method.
5. The variance of the distance  $r$  calculated using the variational method.
6. The variance of the distance  $r$  calculated using the FEM method.
7. The variance of the distance  $r$  calculated using the MC-HF method.
8. The e-PCP interaction energy obtained through the variational two-particle distribution function.
9. The e-PCP interaction energy obtained through the FEM two-particle distribution function.

## 5.2 E-PCP Correlation in Density Functional Theory

Since the exact wavefunction is not available for most physical systems, the conventional approach in density functional theory is to solve the Kohn-Sham equations using an approximate but suitable exchange-correlation functional to obtain the Kohn-Sham orbitals and ultimately the total energy and densities. However, fortunately, the EHM (like the harmonium model) falls into the rare category of systems for which we have the exact solution of the Schrödinger equation and the corresponding single-particle densities. Therefore, we can take a reverse approach compared to the usual method: First, using equations (1-54) and (1-55), we obtain the Kohn-Sham single-orbital for the electron and the Kohn-Sham single-orbital for the PCP. Then, by substituting them into the Kohn-Sham equations (equations 1-65 and 1-66), we calculate the e-PCP correlation potential (equations 1-67 and 1-68).

The correlation potential provides deeper insight into the nature of correlation within the DFT framework. Therefore, in this section, we first obtain the exact correlation potentials of the electron and the PCP for the EHM using the inversion of Kohn-Sham equations. Then, we compute the potentials using existing e-PCP correlation functionals and compare them with their exact counterparts. This way, in addition to analyzing the exact correlation potentials and interpreting their behavior, we can gain a better understanding of the reasons behind the success or failure of existing e-PCP correlation functionals.

### 5.2.1 Simplification of Densities

To facilitate calculations, and since the analytical form of the electron and PCP densities (equations 2-168 and 2-169, respectively) for performing calculations within the framework of two-component density functional theory for muons and protons are complex, their simplification was considered. The strategy used for simplification involves identifying the dominant terms and approximating the density with them. Accordingly, after determining the dominant term in the PCP density and calculating the normalization constant, the simplified density ( $\rho_p^{sim}$ ) was obtained as follows:

$$\rho_p^{sim}(r_p) = \frac{2\sqrt{2}\gamma^{3/2}}{\pi^{3/2}} e^{-2r_p^2\gamma} \quad 5.6$$

However, for the analytical electron density, the constituent terms contribute almost equally to the final density, rendering simplification through identifying the dominant term ineffective. Another strategy for simplifying the electron density is to fit it with well-behaved known functions. Therefore, the electron densities and their square roots were fitted with several Gaussian functions, which were then used for working with the two-component DFT equations presented in section 1-7-1. Additionally, in all the following calculations, the system parameters were limited to the following two cases:

Table 5-4: Masses and frequencies used in DFT calculations.

HO Frequency	PCP mass
0.02	207
0.01	1836

Fitting the electron densities and Kohn-Sham orbitals (which are related through equation 1-54) were performed using 4, 5, and 6 Gaussian functions over different ranges of  $r_e$ . Ultimately, based on the relative errors and overlap integral values for each specific fit, the following fits were selected for Table 5-4:

Table 5-5: Characteristics of the fittings performed for the simplification of single-particle densities.

Number of points	$r_e$ range	Number of Gaussians	Fitted quantity	Frequency	PCP mass
200	0-5	6	density	0.02	207
200	0-5	6	KS Orbital	0.02	207
200	0-5	6	density	0.01	1836
200	0-5	6	KS Orbital	0.01	1836

The relative error percentages for  $r_e$  for the four selected fits are shown in Figure 5-39. Additionally, the relative error percentages and overlap integral values for all fits performed are presented in Table (C-1) of the appendix C. Although the relative errors were calculated for each of the 200 points used in the fits, due to space constraints, the relative error is reported only for the first 10 points with the highest errors. The linear coefficients and Gaussian exponents obtained from the fits are also available in Table (C-3) of the appendix C. It is worth mentioning that

some coefficients became zero during the fitting process, effectively resulting in four Gaussian terms instead of six.

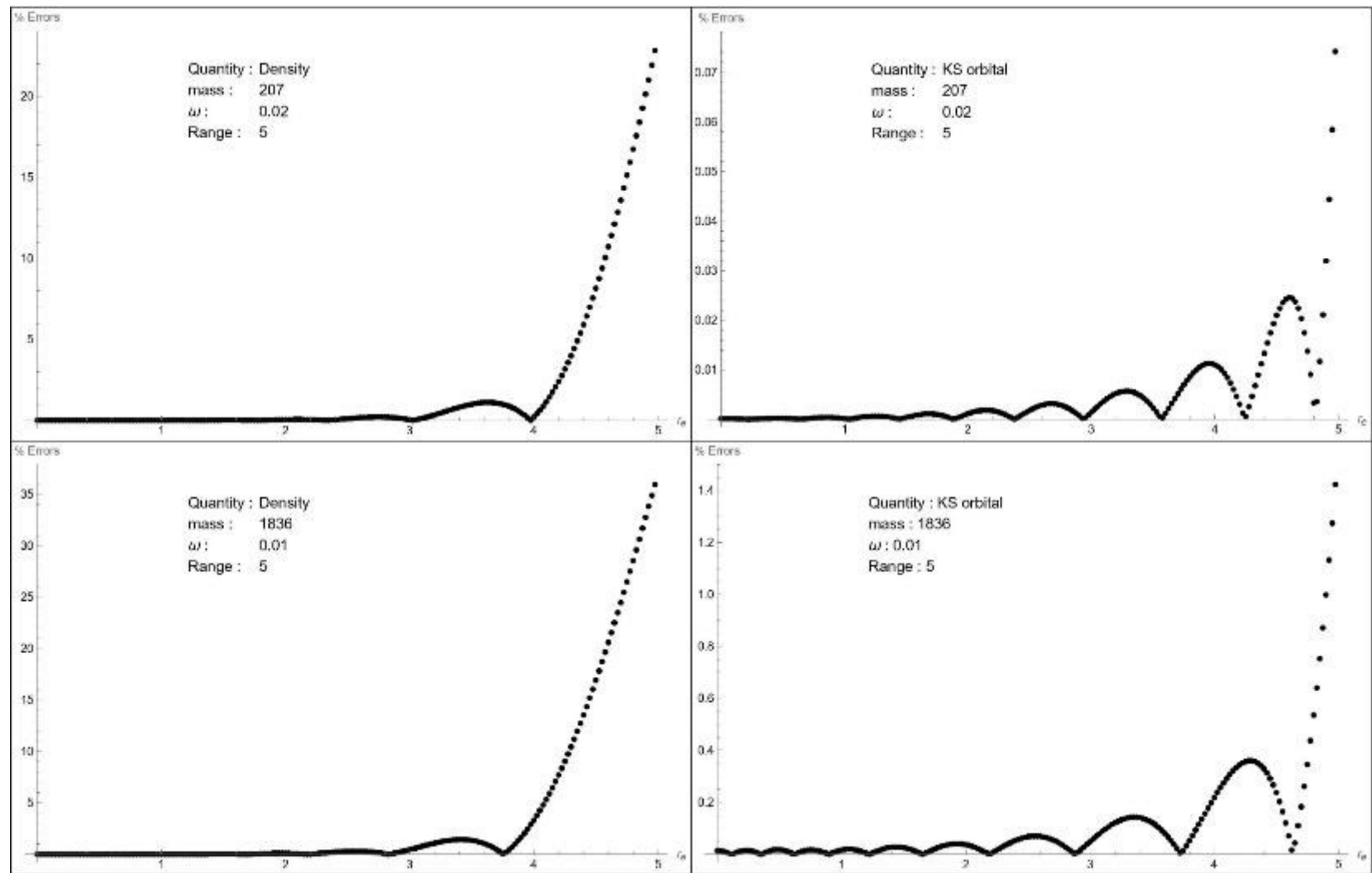


Figure 5-39: Relative error percentage versus electronic distance for the fits with four functions from Table 5-4.



The  $T_e^s[\rho_e]$  and  $T_p^s[\rho_p]$  (equations 1-56 and 1-57) can be calculated using different volume elements (section 2-4) as follows:

$$\begin{aligned}
\langle \hat{T}_e^s \rangle &= \int \int \psi^{ks}(\mathbf{r}_e, \mathbf{r}_p)^* \hat{T}_e^s \psi^{ks}(\mathbf{r}_e, \mathbf{r}_p) d\mathbf{r}_e d\mathbf{r}_p \\
&= -\frac{1}{2m_e} \int \int \psi^{ks}(\mathbf{r}_e, \mathbf{r}_p)^* \nabla_e^2 \psi^{ks}(\mathbf{r}_e, \mathbf{r}_p) d\mathbf{r}_e d\mathbf{r}_p \\
&= -\frac{16\pi^2}{2m_e} \int \int \phi_e^{ks}(\mathbf{r}_e)^* \nabla_e^2 \phi_e^{ks}(\mathbf{r}_e) |\phi_p^{ks}(\mathbf{r}_p)|^2 r_e^2 r_p^2 d\mathbf{r}_e d\mathbf{r}_p \\
&= -\frac{8\pi^2}{2m_e} \int_0^\infty \int_0^\infty \int_{|r_e-r|}^{r_e+r} \phi_e^{ks}(\mathbf{r}_e)^* \nabla_e^2 \phi_e^{ks}(\mathbf{r}_e) |\phi_p^{ks}(\mathbf{r}_p)|^2 r_e r_p r d\mathbf{r}_p d\mathbf{r}_e dr \\
&= -\frac{4\pi}{2m_e} \int_0^\infty \phi_e^{ks}(\mathbf{r}_e)^* \nabla_e^2 \phi_e^{ks}(\mathbf{r}_e) r_e^2 d\mathbf{r}_e
\end{aligned} \tag{5.7}$$

$$\begin{aligned}
\langle \hat{T}_p^s \rangle &= \int \int \psi^{ks}(\mathbf{r}_e, \mathbf{r}_p)^* \hat{T}_p^s \psi^{ks}(\mathbf{r}_e, \mathbf{r}_p) d\mathbf{r}_e d\mathbf{r}_p \\
&= -\frac{1}{2m_p} \int \int \psi^{ks}(\mathbf{r}_e, \mathbf{r}_p)^* \nabla_p^2 \psi^{ks}(\mathbf{r}_e, \mathbf{r}_p) d\mathbf{r}_e d\mathbf{r}_p \\
&= -\frac{16\pi^2}{2m_p} \int \int \phi_p^{ks}(\mathbf{r}_p)^* \nabla_p^2 \phi_p^{ks}(\mathbf{r}_p) |\phi_e^{ks}(\mathbf{r}_e)|^2 r_e^2 r_p^2 d\mathbf{r}_e d\mathbf{r}_p \\
&= -\frac{8\pi^2}{2m_p} \int_0^\infty \int_0^\infty \int_{|r_p-r|}^{r_p+r} \phi_p^{ks}(\mathbf{r}_p)^* \nabla_p^2 \phi_p^{ks}(\mathbf{r}_p) |\phi_e^{ks}(\mathbf{r}_e)|^2 r_e r_p r d\mathbf{r}_e d\mathbf{r}_p dr \\
&= -\frac{4\pi}{2m_p} \int_0^\infty \phi_p^{ks}(\mathbf{r}_p)^* \nabla_p^2 \phi_p^{ks}(\mathbf{r}_p) r_p^2 d\mathbf{r}_p
\end{aligned} \tag{5.8}$$

The external potentials in the EHM for the electron and PCP are defined as follows:

$$v_e^{ext}(\mathbf{r}_e) = \frac{1}{2} m_e \omega^2 r_e^2 \tag{5.9}$$

$$v_p^{ext}(\mathbf{r}_p) = \frac{1}{2} m_p \omega^2 r_p^2 \tag{5.10}$$

Thus, the energy components of the EHM within the DFT were calculated using the fitted densities and are presented in Table 5-6. Furthermore, to verify previous results, and since the reference system densities are the same as the actual system, the Hartree energy term  $J_{ep}[\rho_e, \rho_p]$  (equation 1-62) was also calculated using the simplified

densities. The data in Table 5-6 show that the Hartree energy calculated using the fitted orbitals matches the exact data more closely, and their normalization constant is nearer to one, indicating their greater accuracy compared to the data obtained from direct density fitting. The contribution of the kinetic correlation energy terms  $T_e^c$  and  $T_p^c$  (equation 3-29) for electrons is much larger than for muons and protons, and in both cases, they constitute the main component of the total kinetic correlation energy. Additionally, the absolute value of the KS correlation energy for the system comprising a muon and an electron is more than twice that of the system comprising a proton and an electron. Thus, as the mass of the PCP decreases, the absolute value of the KS correlation energy, like the wavefunction-based correlation energy discussed in previous sections, increases. On the other hand, the absolute value of the KS correlation energy is smaller by a factor of two compared to the reference-independent correlation energy.

Table 5-6: Quantities Calculated within the DFT

Quantities/m	1836	1836	207	207
$\omega$	0.01	0.01	0.02	0.02
Power <sup>1</sup>	1	0.5	1	0.5
Norm P <sup>2</sup>	1	1	1	1
Norm E <sup>3</sup>	0.9970	0.9995	0.9979	0.9998
Exact HAR <sup>4</sup>	-0.9315	-0.9315	-0.8035	-0.8035
KS HAR <sup>5</sup>	-0.9309	-0.9314	-0.8031	-0.8035
$\Delta$ HAR <sup>6</sup>	-0.0006	-0.0001	-0.0004	0.0000
TSE1 <sup>7</sup>	0.4659	0.4649	0.3952	0.3944
TSE2 <sup>8</sup>	0.4659	0.4649	0.3952	0.3944
TSE3 <sup>9</sup>	0.4659	0.4649	0.3952	0.3944
TSP1 <sup>10</sup>	0.0075	0.0075	0.0150	0.0151
TSP2 <sup>11</sup>	0.0075	0.0075	0.0150	0.0151
TSP3 <sup>12</sup>	0.0075	0.0075	0.0151	0.0151
EXT E <sup>13</sup>	0.0001	0.0002	0.0007	0.0007
EXT P <sup>14</sup>	0.0075	0.0075	0.0149	0.0149
TE <sup>15</sup>	0.4998	0.4998	0.4965	0.4965
TP <sup>16</sup>	0.0078	0.0078	0.0173	0.0173
TC E <sup>17</sup>	0.0339	0.0349	0.1013	0.1021
TC P <sup>18</sup>	0.0003	0.0003	0.0023	0.0023
IND Corr <sup>19</sup>	-0.0683	-0.0683	-0.1929	-0.1929
KS Corr <sup>20</sup>	-0.0341	-0.0331	-0.0893	-0.0885
Exact Etot <sup>21</sup>	-0.4846	-0.4846	-0.4670	-0.4670
KS Etot <sup>22</sup>	-0.4846	-0.4846	-0.4670	-0.4670
$\Delta E$ <sup>23</sup>	0.0000	0.0000	0.0000	0.0000

1. Density term power in the fit (1 means density, and 0.5 means KS orbital).
2. Normalization condition for electron density and KS orbital (equation 1-52).
3. Normalization condition for PCP density and KS orbital (equation 1-53).
4. Exact Hartree energy calculated using analytical densities (equation 1-62).
5. Hartree energy calculated using fitted densities (equation 1-62).
6. Difference between items 4 and 5.
7. Electron kinetic energy in the reference system using the third line of equation 5-7.
8. Electron kinetic energy in the reference system using the fourth line of equation 5-7.
9. Electron kinetic energy in the reference system using the fifth line of equation 5-7.
10. PCP kinetic energy in the reference system using the third line of equation 5-8.
11. PCP kinetic energy in the reference system using the fourth line of equation 5-8.

12. PCP kinetic energy in the reference system using the fifth line of equation 5-8.
13. Electron external potential energy (equation 5-9, comparable with item 5 of Table 4-4).
14. PCP external potential energy (equation 5-10, comparable with item 6 of Table 4-4).
15. Exact electron kinetic energy (equation 2-135 and item 2 of Table 4-4).
16. Exact PCP kinetic energy (equation 2-136 and item 3 of Table 4-4).
17. Electron kinetic correlation energy (first parenthesis in equation 3-29).
18. PCP kinetic correlation energy (second parenthesis in equation 3-29).
19. Reference-independent correlation energy (equation 3-24 and item 4 of Table 5-2).
20. Correlation energy within the DFT (equation 3-29).
21. Exact total energy (item 1 in Table 4-4).
22. Total energy of the model within the DFT (equation 3-26).
23. Difference between items 21 and 22.

### 5.2.2 Calculating Correlation Potentials via Inversion of Kohn-Sham Equations

The effective potentials in the Kohn-Sham equations (1-67) and (1-68) for the EHM reduce to the following forms:

$$V_{\text{eff}}^e(\mathbf{r}_e) = v_e^{\text{ext}}(\mathbf{r}_e) + v_e^{J_{ep}}(\mathbf{r}_e) + v_e^{\text{epc}}(\mathbf{r}_e) \quad 5.11$$

$$V_{\text{eff}}^p(\mathbf{r}_p) = v_p^{\text{ext}}(\mathbf{r}_p) + v_p^{J_{ep}}(\mathbf{r}_p) + v_p^{\text{epc}}(\mathbf{r}_p) \quad 5.12$$

where  $v_e^{J_{ep}}$  and  $v_e^{\text{ext}}$  can be calculated using equations (3-22) and (5-9) respectively, and  $v_p^{J_{ep}}$  and  $v_p^{\text{ext}}$  can be calculated using equations (3-23) and (5-10). By inverting the Kohn-Sham equations for the electron and the PCP (equations 1-65 and 1-66), the Kohn-Sham correlation potentials can be calculated as follows:

$$v_e^{\text{epc}}(\mathbf{r}_e) = \epsilon_e^{ks} - v_e^{\text{ext}}(\mathbf{r}_e) - v_e^{J_{ep}}(\mathbf{r}_e) - v_e^{KE}(\mathbf{r}_e) \quad 5.13$$

$$v_p^{\text{epc}}(\mathbf{r}_p) = \epsilon_p^{ks} - v_p^{\text{ext}}(\mathbf{r}_p) - v_p^{J_{ep}}(\mathbf{r}_p) - v_p^{KE}(\mathbf{r}_p) \quad 5.14$$

where the following terms are introduced as kinetic energy potentials:

$$v_e^{KE}(\mathbf{r}_e) = -\frac{1}{2m_e} \frac{\nabla_e^2 \phi_e^{ks}(\mathbf{r}_e)}{\phi_e^{ks}(\mathbf{r}_e)} \quad 5.15$$

$$v_p^{KE}(\mathbf{r}_p) = -\frac{1}{2m_p} \frac{\nabla_p^2 \phi_p^{ks}(\mathbf{r}_p)}{\phi_p^{ks}(\mathbf{r}_p)} \quad 5.16$$

Thus, the only unknown quantities in equations (5-13) and (5-14) are the orbital energies  $\epsilon_e^{ks}$  and  $\epsilon_p^{ks}$ , which we can obtain by analyzing and fitting the asymptotic behavior of the correlation potential components and the condition of this potential approaching zero at infinity. It's important to note that these energies can be analytically

calculated if the exact wavefunction of the system is available, by examining the asymptotic behavior of the correlation potential [83], [141]. However, since the wavefunction presented here is obtained through the variational theorem and is not the exact wavefunction of the system, this method cannot be used. Nevertheless, a similar approach can be employed to estimate the approximate values of the orbital energies.

The correlation potential's dependency is determined by the three components presented in equations (5-11) and (5-12): kinetic energy potential, external potential, and Hartree potential. The first condition regarding the dependency of the correlation potential is that it approaches zero at infinite distance. By using this condition and analyzing the asymptotic behavior of each component of the correlation potential, we can estimate the orbital energy. The simplest component is the external potential, which here is equal to the potential of a harmonic oscillator and for the electron and PCP is given by equations (5-9) and (5-10) respectively, in the form of  $\lambda r^2$  where  $\lambda = \frac{1}{2}m\omega^2$ , thus having a  $r^2$  dependency. The next component, the Hartree potential, has a  $-\frac{1}{r}$  dependency at long inter-particle distances and hence should approach zero at infinite distance, as shown in Figure (5-40). Given that the density of the PCP is more localized compared to the electron density, and also considering the presence of the second particle's density in the Hartree potential of the first particle, the electron's Hartree potential reaches the  $-\frac{1}{r}$  dependency faster, whereas this occurs at further distances for the PCPs.

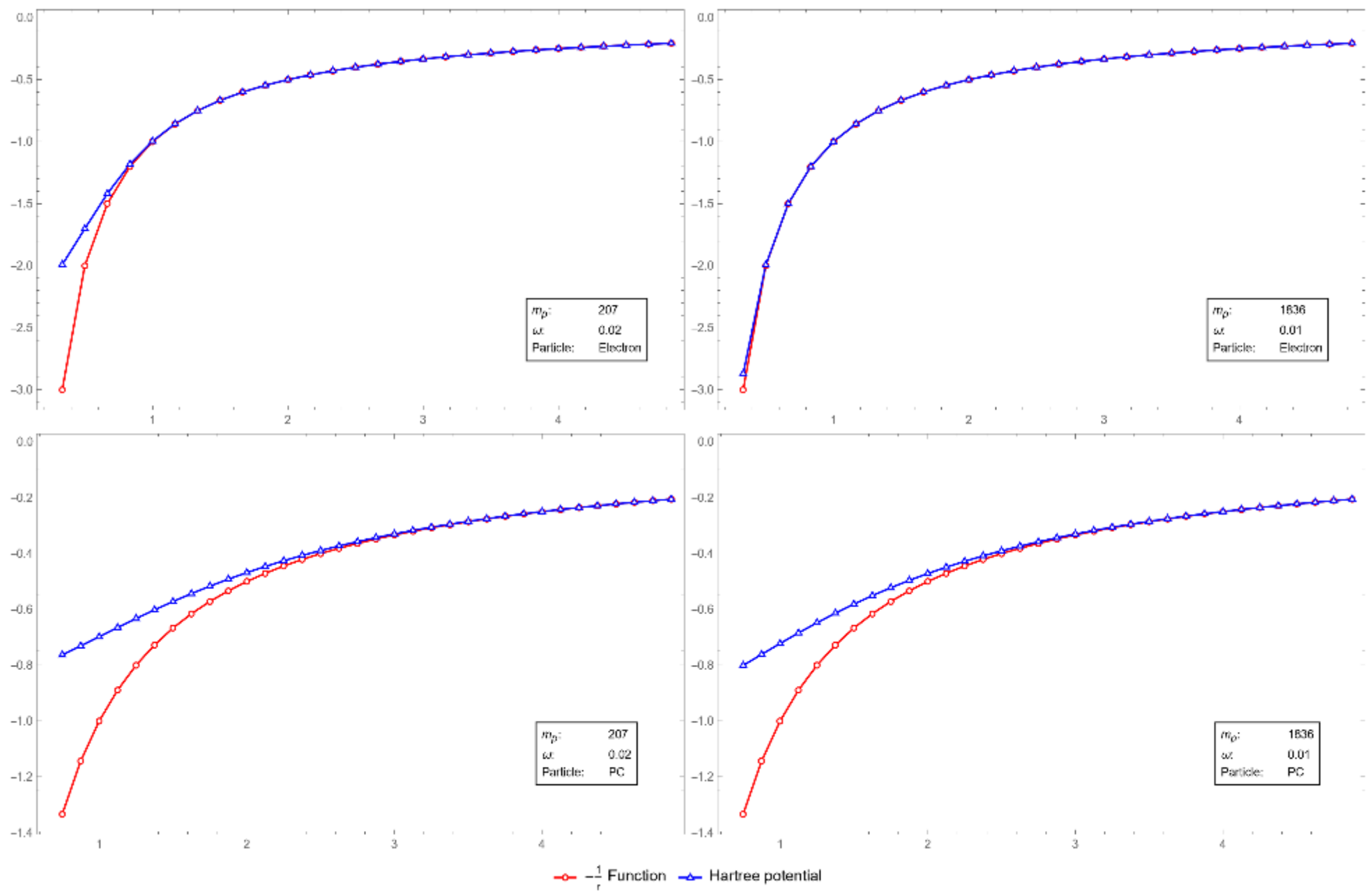


Figure 5-40: Consistency of the asymptotic behavior of the Hartree potential with the  $-\frac{1}{r}$  potential.

The third component of the correlation potential is the kinetic energy potential, whose dependency on distance is not explicitly known. However, the condition that the correlation potential approaches zero at infinite distance can help determine its dependency and estimate the orbital energy. Given that both the correlation and Hartree potentials approach zero at infinite distance, we have:

$$\epsilon_e^{ks} = \lim_{r_e \rightarrow \infty} (v_e^{ext}(\mathbf{r}_e) + v_e^{asym-KE}[\rho_e]) \quad 5.17$$

$$\epsilon_p^{ks} = \lim_{r_p \rightarrow \infty} (v_p^{ext}(\mathbf{r}_p) + v_p^{asym-KE}[\rho_p]) \quad 5.18$$

Given that we know the values  $\epsilon_e^{ks}$  and  $\epsilon_p^{ks}$  are numerical constants, the dependency of the kinetic energy potential plus a numerical constant (equivalent to the orbital energy) must be such that the sum of the harmonic oscillator potential and the orbital energy equals zero at infinite distance; that is:

$$v_e^{ext} - \epsilon_e^{ks} + (v_e^{asyKE} + \epsilon_e^{ks}) = 0 \quad 5.19$$

$$v_p^{ext} - \epsilon_p^{ks} + (v_p^{asyKE} + \epsilon_p^{ks}) = 0 \quad 5.20$$

Thus, the kinetic energy dependency at long distances must be in the form of  $-\lambda' r^2$ , where for the exact wavefunction,  $\lambda' = \lambda$ , and these two terms completely cancel each other out. However, for the variational wavefunction, we know that there is a slight difference between the coefficients:

$$v_e^{ext} + v_e^{asyKE} = (\lambda_e - \lambda'_e) r^2 + \epsilon_e^{ks} \quad 5.21$$

$$v_p^{ext} + v_p^{asyKE} = (\lambda_p - \lambda'_p) r^2 + \epsilon_p^{ks} \quad 5.22$$

As a result, by fitting the kinetic energy potential data to a function of the form  $-a r^2 - b$ , we can estimate the orbital energy, which is a



numerical constant and ensures the correlation potential approaches zero at infinite distance.

In Figure 5-41, the data for the best fit of the kinetic energy potential with the function  $-ar^2 - b$  in different systems and the quantities related to the fit quality are presented. As shown in the graphs, the fit quality for the PCP data is significantly better than that for the electron data, due to the oscillatory behavior of the PCP. Given that the density of the PCP can be very accurately approximated by a Gaussian function (unlike the electron), its behavior here is also similar to that of a harmonic oscillator. Therefore, the fit of the kinetic energy potential over all distances for the PCP has very high quality, whereas for the electron, the fit reaches acceptable quality only at long distances.

Considering the above explanations, the coefficients of the function ( $a$  or  $\lambda'$ ) should have values close to  $\frac{1}{2}m\omega^2$ , which is evident in the values presented in the tables of Figure 5-41. Furthermore, the numerical constants ( $b$ ) or orbital energies for the PCP, which behaves similarly to a harmonic oscillator, should practically be equal to its zero-point energy ( $\frac{3}{2}\omega$ ). The expected values of  $a$  and  $b$  are shown in the “Expectation” column of the tables in Figure 5-41.

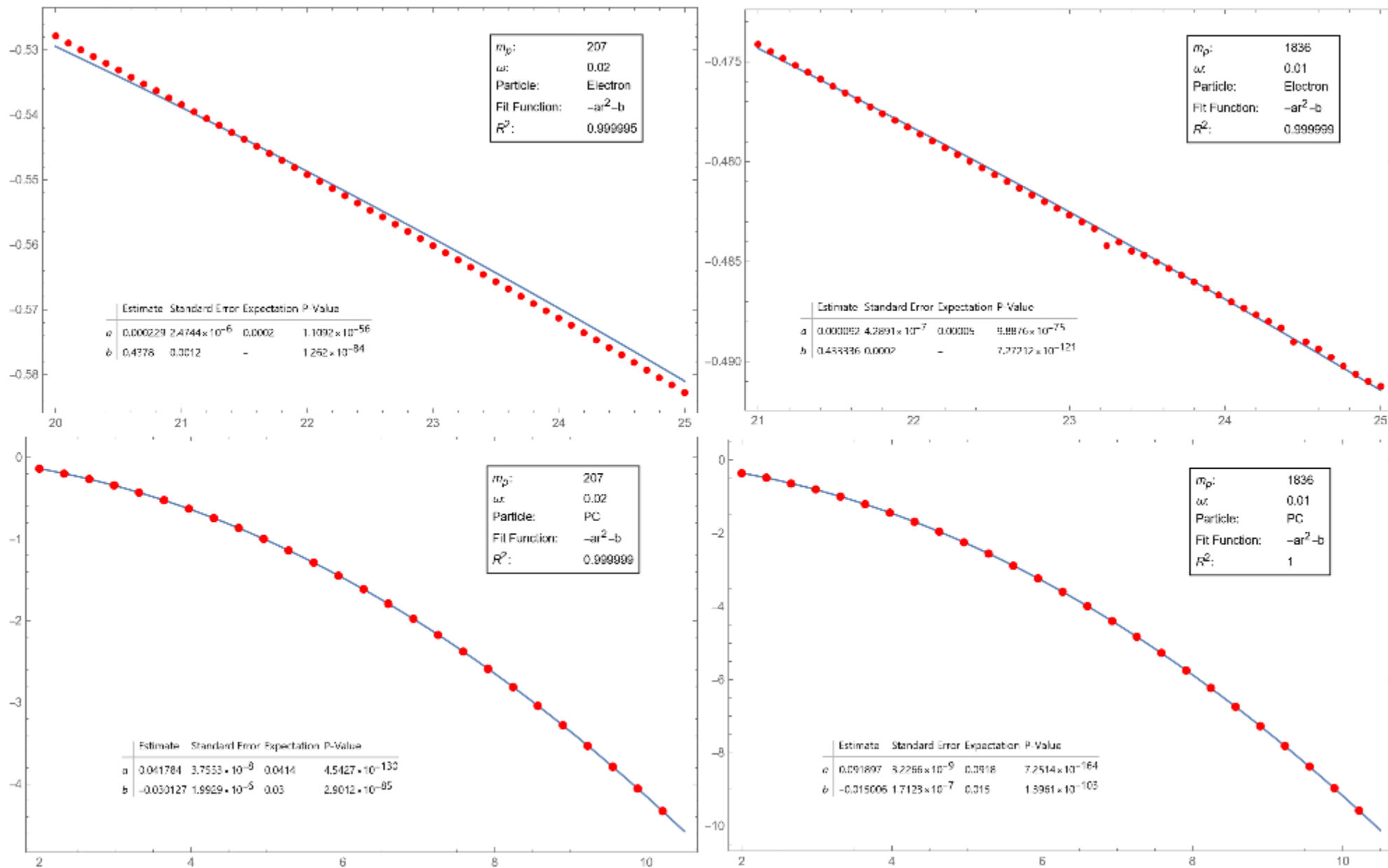


Figure 5-41: Fitting of the kinetic energy potential (dots and lines represent actual data and fitted functions, respectively).

By obtaining the orbital energies, the correlation potentials can be calculated using both FEM densities and variational (fitted) densities, as presented and compared in Figure 5-42. In all cases, there is a very high degree of consistency between them. The qualitative difference in the behavior of the correlation potentials for electrons and PCPs is quite evident in this figure.

It is noteworthy that, to ensure the correlation potential approaches zero at infinite distance, a value of  $-0.06$  was added to the electron orbital energies obtained from the fit, which was  $-0.43$  for both systems, resulting in a final electron orbital energy of  $-0.49$  for both systems. This value is very close to the ground state energy of an electron in a free hydrogen atom.

To conduct a more precise analysis of the Kohn-Sham effective potential (the sum of Hartree, external, and correlation potentials), its components are displayed in Figure 5-43. In the Kohn-Sham effective potentials for electrons, the Hartree potential is the dominant term and controls the overall shape of the potential. This control increases with the mass of the PCP. The correlation potential, and especially the external potential, play a minor role in determining the shape of the total potential. Hence, the presence or absence of an e-PCP correlation functional has little impact on the shape of the Kohn-Sham effective potential for electrons.

In contrast, the role of the correlation potential in the Kohn-Sham potentials for the PCP is highly significant. In fact, the correlation potential neutralizes the effect of the Hartree potential, causing the final shape of the Kohn-Sham potential to align completely with the external potential (harmonic oscillator), as previous data confirm that the PCP behaves exactly like a harmonic oscillator. Therefore, the

presence of an e-PCP correlation functional in the Kohn-Sham equations for the PCP is crucial.

The accuracy of the obtained orbital energies can also be verified using the equations related to the sum of orbital energy values. By extending the standard equations of DFT to their two-component versions, we get:

$$\sum_i^N \epsilon_e^{ks} = T_e^s[\rho_e] + \int \rho_e(\mathbf{r}_e) V_{\text{eff}}^e(\mathbf{r}_e) d\mathbf{r}_e \quad 5.23$$

$$\sum_{i'}^{N'} \epsilon_p^{ks} = T_p^s[\rho_p] + \int \rho_p(\mathbf{r}_p) V_{\text{eff}}^p(\mathbf{r}_p) d\mathbf{r}_p \quad 5.24$$

Considering that the functions  $V_{\text{eff}}^e(\mathbf{r}_e)$  and  $V_{\text{eff}}^p(\mathbf{r}_p)$  are themselves the sum of several potentials, integrating them leads to numerical difficulties. Therefore, we first fitted them using six Gaussian functions, and then used the result of this fitting in the above equations. The fitting details and results are shown in Table 5-7, which confirm the accuracy of the orbital energies obtained from the previous method. It is also worth noting that during the fitting process, some coefficients of the functions became zero, resulting in only four Gaussian functions in the final result.

Table 5-7: Details of fitting effective potentials and predicted and obtained orbital energy values

Particle/Quantity	$m_p$	$\omega$	Fitted $V_{\text{eff}}$	$R^2$ of fitting <sup>1</sup>	$V_{\text{eff}}$ $\rho$ Integral <sup>2</sup>	$T_s$ <sup>3</sup>	Obtained $\epsilon$ <sub>4</sub>	Expected $\epsilon$ <sup>5</sup>
Electron	207	0.02	$-1.1828198631201177e^{-1.6958106783662794x^2}$ $-0.6030099153338793e^{-0.5137363920720693x^2}$ $-0.345016638782312e^{-0.13227251840688656x^2}$ $-0.2580958806954125e^{-0.014719066831130966x^2}$	0.9999996	-0.8842	0.3944	-0.4898	-0.49
PC	207	0.02	$-0.3730298834254647e^{-0.059013127132755056x^2}$ $+0.37286336846293927e^{0.05342619762675789x^2}$	0.9999998	0.0149	0.0151	0.0300	0.03
Electron	1836	0.01	$-2.3691654995926226e^{-9.064309621783845x^2}$ $-1.4389052306037728e^{-2.175416017302567x^2}$ $-0.6836181104321617e^{-0.3893475435267434x^2}$ $-0.4079586697626854e^{-0.03108796523905667x^2}$	0.9999951	-0.9595	0.4649	-0.4946	0.-49
PC	1836	0.01	$-0.905641219740176e^{-0.05317938771639458x^2}$ $+0.9055837583856249e^{0.048591942739784226x^2}$	0.9999999	0.0074	0.0075	0.0149	0.015

1. Coefficient of determination for fitting effective potential functions.
2. Result of the two integrals in equations (5-23) and (5-24).
3. Kohn-Sham kinetic energy values (items 7 to 13 in Table 5-6).
4. Final obtained values for orbital energies using equations (5-23) and (5-24).
5. Expected values for orbital energies (obtained from fitting the kinetic energy potentials).

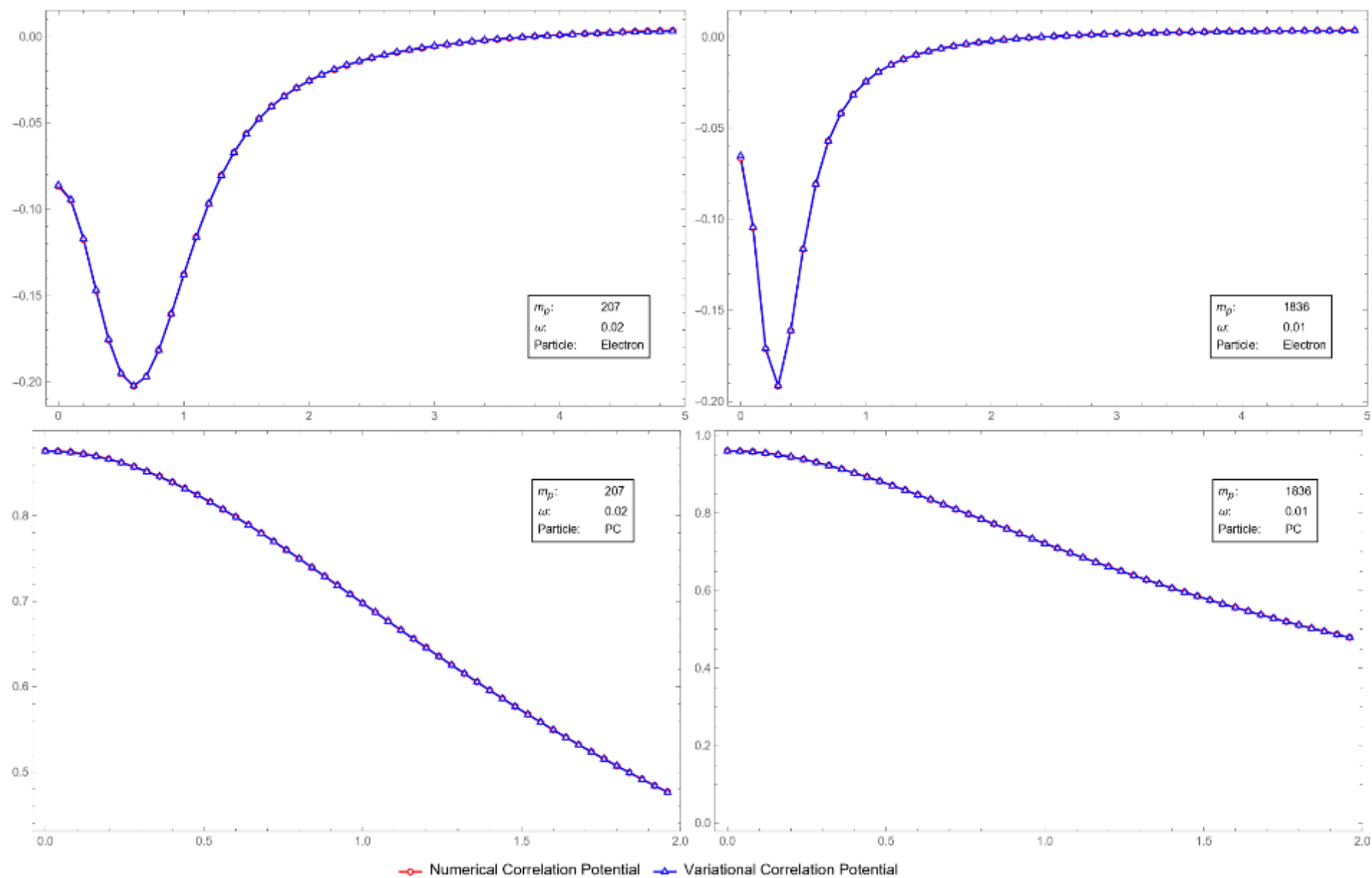


Figure 5-42: Comparison of FEM and variational correlation potentials

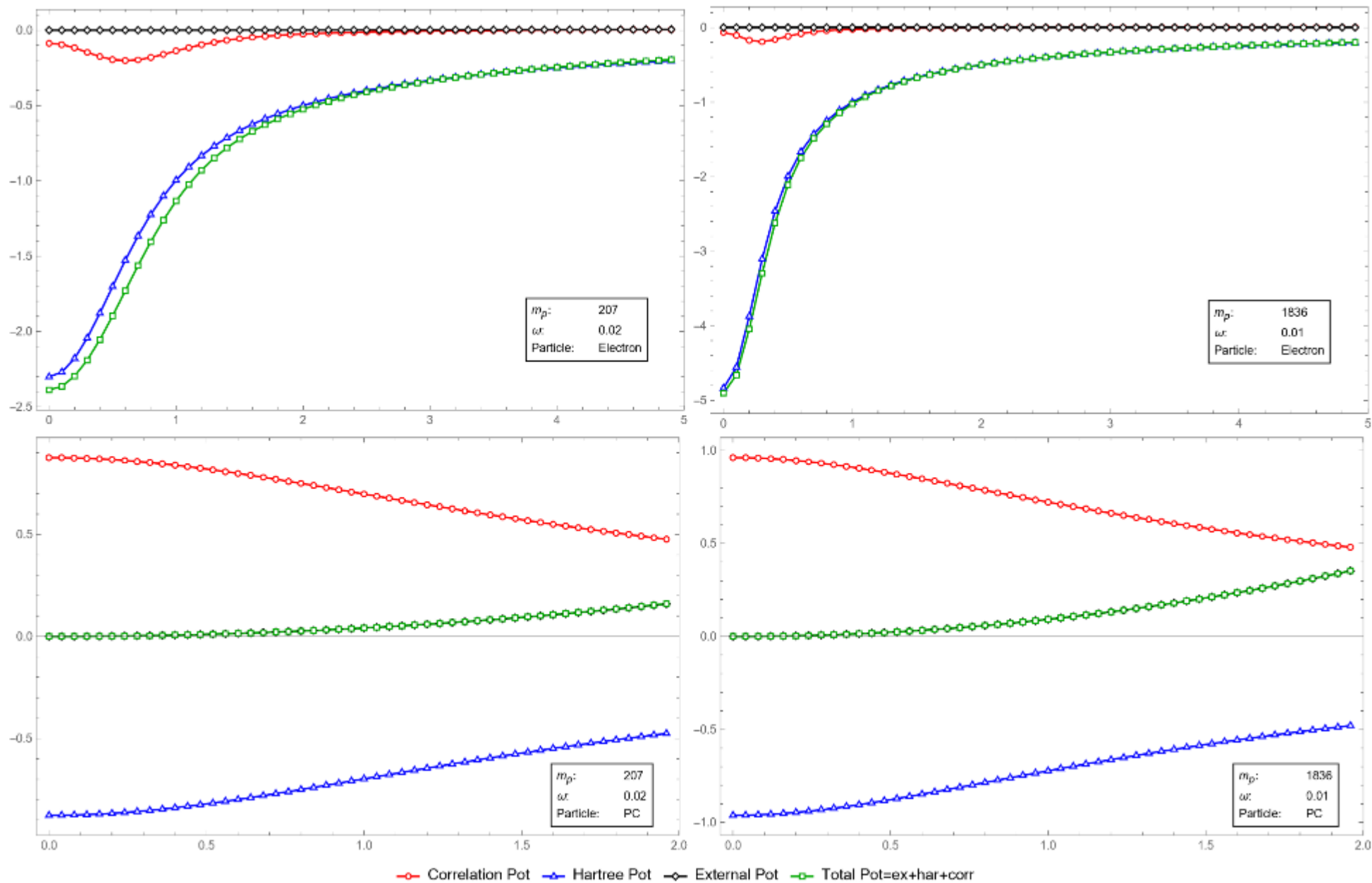


Figure 5-43: Comparison of different components of the Kohn-Sham effective potential

### 5.2.3 Evaluating the Efficiency of Existing Electron-PCP Functionals

In this section, the accuracy of five proposed local functionals for calculating the e-PCP correlation energy is examined. The parameters of four of them (*epc17-1*, *epc17-2*, *epc18-1*, *epc18-2*) have been optimized for electron-proton correlation, and one of them (*emc1*) has been designed for electron-muon correlation. The explicit forms of the electron-proton correlation functionals are as follows:

$$E_{epc17}[\rho_e, \rho_p] = - \int \frac{\rho_e \rho_p}{a - b(\rho_e)^{1/2}(\rho_p)^{1/2} + c\rho_e \rho_p} d\mathbf{r} \quad 5.25$$

$$E_{epc18}[\rho_e, \rho_p] = - \int \frac{\rho_e \rho_p}{\left(a - b + (\rho_e^{1/3} + \rho_p^{1/3})^3 + c(\rho_e^{1/3} + \rho_p^{1/3})^6\right)} d\mathbf{r} \quad 5.26$$

where their forms are the same for both open-shell and closed-shell cases. For the two functional forms *epc17* and *epc18*, two different sets of parameters are introduced, each set making the functional describe a specific observable more accurately. The parameters for these four functionals are provided in the table below:

Table 5-8: Parameters for electron-proton correlation functionals

Functional/parameter	a	b	c
Epc17-1	2.35	2.4	3.2
Epc17-2	2.35	2.4	6.6
Epc18-1	1.8	0.1	0.03
Epc18-2	3.9	0.5	0.06

The form of electron-muon correlation functional in the closed-shell case is as follows:



$$E_{e\mu c1-cs}[\rho_e, \rho_p] = -\int \frac{2\rho_e \rho_p - \rho_e(\rho_p)^{3/2}}{1 + 4\rho_e \rho_p + 2\rho_e(\rho_p)^{3/2}} d\mathbf{r} \quad 5.27$$

while the open-shell case is as follows:

$$\begin{aligned} E_{e\mu c1-os}[\rho_e^\alpha, \rho_e^\beta, \rho_\mu] \\ = -\int \frac{2\rho_e^\alpha \rho_\mu - \rho_e^\alpha(\rho_\mu)^{3/2}}{1 + 8\rho_e^\alpha \rho_\mu + 4\rho_e^\alpha(\rho_\mu)^{3/2}} \\ + \frac{2\rho_e^\beta \rho_\mu - \rho_e^\beta(\rho_\mu)^{3/2}}{1 + 8\rho_e^\beta \rho_\mu + 4\rho_e^\beta(\rho_\mu)^{3/2}} d\mathbf{r} \end{aligned} \quad 5.28$$

where  $\rho_e^\alpha$  and  $\rho_e^\beta$  are the spin-up and spin-down electron densities, respectively. The following convention holds for all the above functionals:

$$\int d\mathbf{r} = \int d\mathbf{r}_e \int d\mathbf{r}_p \delta(\mathbf{r}_e - \mathbf{r}_p) \quad 5.29$$

The e-PCP correlation energy was calculated using the five functionals introduced above, employing the exact one-particle densities. The results are presented in Table 5-9.

Table 5-9: Comparison of independent and dependent correlation energies with values obtained from 5 functionals

Table 5-9: Comparison of independent and dependent correlation energies with values obtained from 5 functionals

Corr Energy/mp	207	1836
omega	0.02	0.01
epc17-1	-0.0406	-0.0564
epc17-2	-0.0367	-0.0345
epc18-1	-0.0461	-0.0427
epc18-2	-0.0257	-0.0292
$e\mu$ c1(OS)	-0.0699	-0.0191
KS	-0.0885	-0.0331
HF	-0.0592	-0.0218
IND	-0.1929	-0.0683

In the case of the muon system, the *emc-1* functional clearly has greater accuracy in reproducing the exact Kohn-Sham correlation energy compared to the other functionals. Meanwhile, for the proton system, the *epc17-2* and *epc18-2* functionals show a better match with the Kohn-Sham correlation energy. This aligns well with the idea that the parameters of these functionals have been optimized to accurately reproduce the total system energy. It appears that the designed functionals are generally successful in reproducing the correlation energy.

Additionally, the Kohn-Sham correlation energy values for a mass of 1836 at frequencies of 0.1 and 0.001 were found to be  $-0.0049$  and  $-0.1380$ , respectively, indicating that the Kohn-Sham correlation

energy is sensitive to the field frequency ( $\omega$ ), and the matching of correlation energies at a frequency of 0.01 is not coincidental. Therefore, the existing functionals are efficient in reproducing the correlation energy.

#### 5.2.4 Calculating the Correlation Potentials of the Functionals

In this section, we extract the correlation potentials from the functionals presented in equations (5-25) to (5-28) and compare them with the analytical potentials (equations 5-13 and 5-14) to evaluate their accuracy. By differentiating the above-mentioned functionals with respect to the electron and PCP densities, we obtain the electron and PCP correlation potentials, respectively:

$$v_e^{epc}(\mathbf{r}_e) = \frac{\delta E_{epc}[\rho_e, \rho_p]}{\delta \rho_e} \quad 5.30$$

$$v_p^{epc}(\mathbf{r}_p) = \frac{\delta E_{epc}[\rho_e, \rho_p]}{\delta \rho_p} \quad 5.31$$

Generally, the derivative of a functional of the form below can be calculated as shown in equation (5-33) [77].

$$F[\rho] = \int f(x, \rho, \rho^{(1)}, \rho^{(2)}, \dots, \rho^{(n)}) dx \quad 5.32$$

$$\begin{aligned} \frac{\delta F}{\delta \rho(x)} = & \frac{\partial f}{\partial \rho} - \frac{d}{dx} \left( \frac{\partial f}{\partial \rho^{(1)}} \right) + \frac{d^2}{dx^2} \left( \frac{\partial f}{\partial \rho^{(2)}} \right) \\ & - \dots + (-1)^n \frac{d^n}{dx^n} \left( \frac{\partial f}{\partial \rho^{(n)}} \right) \end{aligned} \quad 5.33$$

In the calculation of the electron and PCP correlation potentials from the above-mentioned local functionals, only the first term in the

above expression has a non-zero value. The forms of the correlation potentials obtained from the functionals are as follows:

$$v_e^{epc171}(\mathbf{r}_e) = \frac{b_{171}\sqrt{\rho_e(r_e)}\rho_p(r_e)^{3/2} - 2a_{171}\rho_p(r_e)}{2(a_{171} - b_{171}\sqrt{\rho_e(r_e)}\sqrt{\rho_p(r_e)} + c_{171}\rho_e(r_e)\rho_p(r_e))^2} \quad 5.34$$

$$v_e^{epc172}(\mathbf{r}_e) = \frac{b_{172}\sqrt{\rho_e(r_e)}\rho_p(r_e)^{3/2} - 2a_{172}\rho_p(r_e)}{2(a_{172} - b_{172}\sqrt{\rho_e(r_e)}\sqrt{\rho_p(r_e)} + c_{172}\rho_e(r_e)\rho_p(r_e))^2} \quad 5.35$$

$$v_e^{epc181}(\mathbf{r}_e) = (a_{181} + (\sqrt[3]{\rho_e(r_e)} + \sqrt[3]{\rho_p(r_e)})^3(c_{181}(\sqrt[3]{\rho_e(r_e)} + \sqrt[3]{\rho_p(r_e)})^3 - b_{181}))^{-2} \left( \rho_p(r_e)(-a_{181} + b_{181}\sqrt[3]{\rho_p(r_e)}(\sqrt[3]{\rho_e(r_e)} + \sqrt[3]{\rho_p(r_e)})^2 + c_{181}(\sqrt[3]{\rho_e(r_e)} - \sqrt[3]{\rho_p(r_e)})(\sqrt[3]{\rho_e(r_e)} + \sqrt[3]{\rho_p(r_e)})^5) \right) \quad 5.36$$

$$v_e^{epc182}(\mathbf{r}_e) = (a_{182} + (\sqrt[3]{\rho_e(r_e)} + \sqrt[3]{\rho_p(r_e)})^3(c_{182}(\sqrt[3]{\rho_e(r_e)} + \sqrt[3]{\rho_p(r_e)})^3 - b_{182}))^{-2} \left( \rho_p(r_e)(-a_{182} + b_{182}\sqrt[3]{\rho_p(r_e)}(\sqrt[3]{\rho_e(r_e)} + \sqrt[3]{\rho_p(r_e)})^2 + c_{182}(\sqrt[3]{\rho_e(r_e)} - \sqrt[3]{\rho_p(r_e)})(\sqrt[3]{\rho_e(r_e)} + \sqrt[3]{\rho_p(r_e)})^5) \right) \quad 5.37$$

$$v_e^{e\mu c10}(\mathbf{r}_e) = \frac{(\sqrt{\rho_p(r_e)} - 2)\rho_p(r_e)}{(4\rho_e(r_e)(\sqrt{\rho_p(r_e)} + 2)\rho_p(r_e) + 1)^2} \quad 5.38$$

$$v_e^{e\mu c1c}(\mathbf{r}_e) = \frac{(\sqrt{\rho_p(r_e)} - 2)\rho_p(r_e)}{(2\rho_e(r_e)(\sqrt{\rho_p(r_e)} + 2)\rho_p(r_e) + 1)^2} \quad 5.39$$

$$\begin{aligned} v_p^{epc171}(\mathbf{r}_p) \\ = \frac{b_{17}\rho_e(r_p)^{3/2}\sqrt{\rho_p(r_p)} - 2a_{17}\rho_e(r_p)}{2(a_{17} - b_{17}\sqrt{\rho_e(r_p)}\sqrt{\rho_p(r_p)} + c_{171}\rho_e(r_p)\rho_p(r_p))^2} \end{aligned} \quad 5.40$$

$$\begin{aligned} v_p^{epc172}(\mathbf{r}_p) \\ = \frac{b_{17}\rho_e(r_p)^{3/2}\sqrt{\rho_p(r_p)} - 2a_{17}\rho_e(r_p)}{2(a_{17} - b_{17}\sqrt{\rho_e(r_p)}\sqrt{\rho_p(r_p)} + c_{172}\rho_e(r_p)\rho_p(r_p))^2} \end{aligned} \quad 5.41$$

$$\begin{aligned} v_p^{epc181}(\mathbf{r}_p) = & (a_{181} \\ & + (\sqrt[3]{\rho_e(r_p)} + \sqrt[3]{\rho_p(r_p)})^3(c_{181}(\sqrt[3]{\rho_e(r_p)} \\ & + \sqrt[3]{\rho_p(r_p)})^3 - b_{181}))^{-2} \left( \rho_e(r_p)(a_{181} \right. \\ & + (\sqrt[3]{\rho_e(r_p)} + \sqrt[3]{\rho_p(r_p)})^2(-\sqrt[3]{\rho_e(r_p)}(b_{181} \\ & + 2c_{181}\rho_p(r_p)) + c_{181}\rho_e(r_p)^{4/3} \\ & \left. + 2c_{181}\rho_e(r_p)\sqrt[3]{\rho_p(r_p)} - c_{181}\rho_p(r_p)^{4/3})) \right) \end{aligned} \quad 5.42$$

$$\begin{aligned}
v_p^{epc182}(\mathbf{r}_p) = & (a_{182} \\
& + (\sqrt[3]{\rho_e(r_p)} + \sqrt[3]{\rho_p(r_p)})^3 (c_{182}(\sqrt[3]{\rho_e(r_p)} \\
& + \sqrt[3]{\rho_p(r_p)})^3 - b_{182}))^{-2} \left( \rho_e(r_p)(a_{182} \right. \\
& + (\sqrt[3]{\rho_e(r_p)} + \sqrt[3]{\rho_p(r_p)})^2 (-\sqrt[3]{\rho_e(r_p)}(b_{182} \\
& + 2c_{182}\rho_p(r_p)) + c_{182}\rho_e(r_p)^{4/3} \\
& \left. + 2c_{182}\rho_e(r_p)\sqrt[3]{\rho_p(r_p)} - c_{182}\rho_p(r_p)^{4/3})) \right)
\end{aligned} \tag{5.43}$$

$$v_p^{e\mu c10}(\mathbf{r}_p) = -\frac{\rho_e(r_p)(-16\rho_e(r_p)\rho_p(r_p)^{3/2} - 3\sqrt{\rho_p(r_p)} + 4)}{2(4\rho_e(r_p)(\sqrt{\rho_p(r_p)} + 2)\rho_p(r_p) + 1)^2} \tag{5.44}$$

$$v_p^{e\mu c1C}(\mathbf{r}_p) = -\frac{\rho_e(r_p)(-8\rho_e(r_p)\rho_p(r_p)^{3/2} - 3\sqrt{\rho_p(r_p)} + 4)}{2(2\rho_e(r_p)(\sqrt{\rho_p(r_p)} + 2)\rho_p(r_p) + 1)^2} \tag{5.45}$$

Figures 5-44 and 5-45 show the comparison of the exact potentials with the potentials obtained from the aforementioned functionals (equations 5-34 to 5-45) for electrons and PCPs. Although these functionals reproduce the approximate shape of the exact electron correlation potential with limited accuracy, they completely fail in reproducing the exact PCP correlation potential. Consequently, it seems that the success of the functionals in reproducing the correlation energy, as mentioned in the previous section, is unrelated to their ability to accurately reproduce the exact correlation potential.

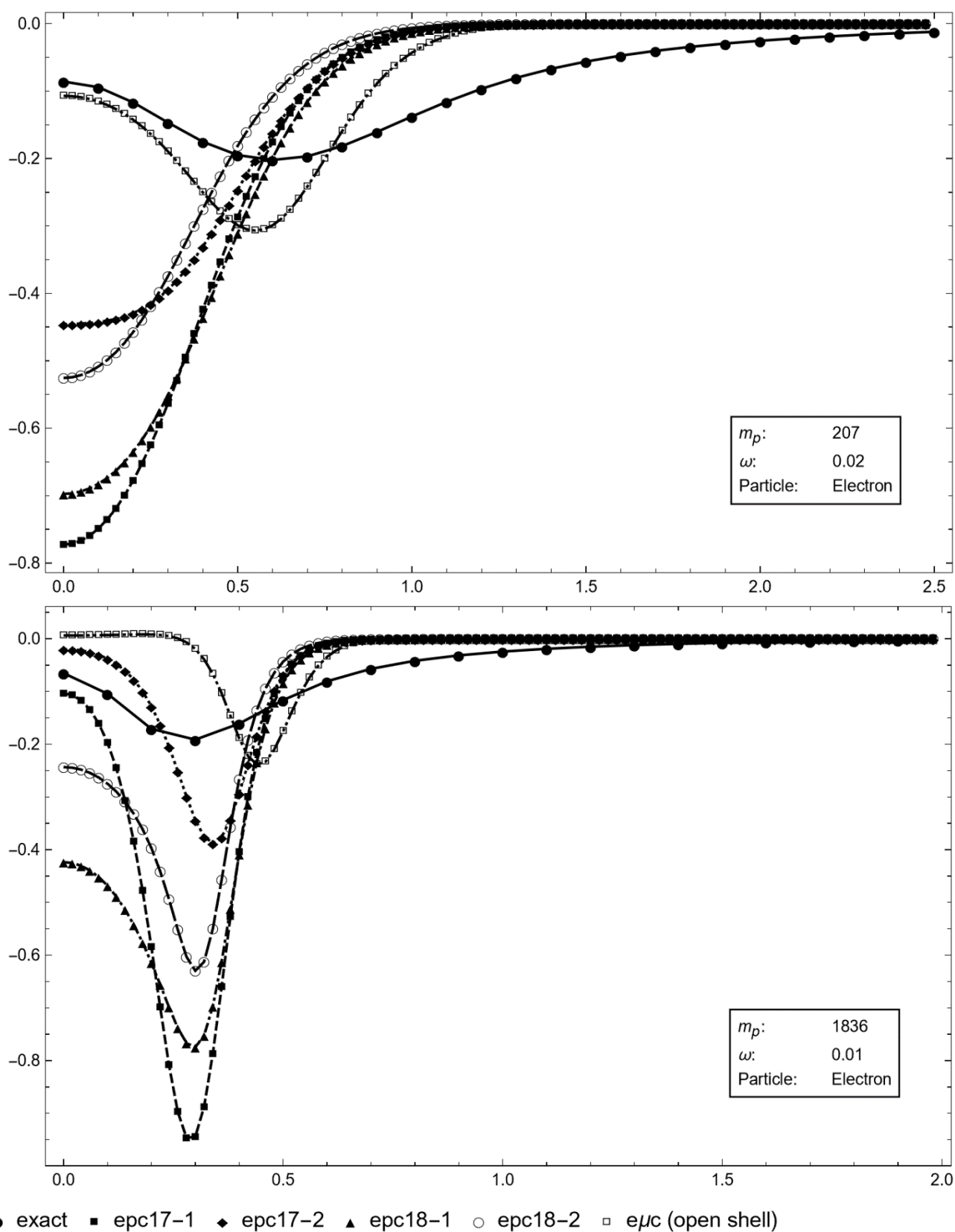


Figure 5-44: Comparison of exact correlation potentials and functional-derived potentials for electrons

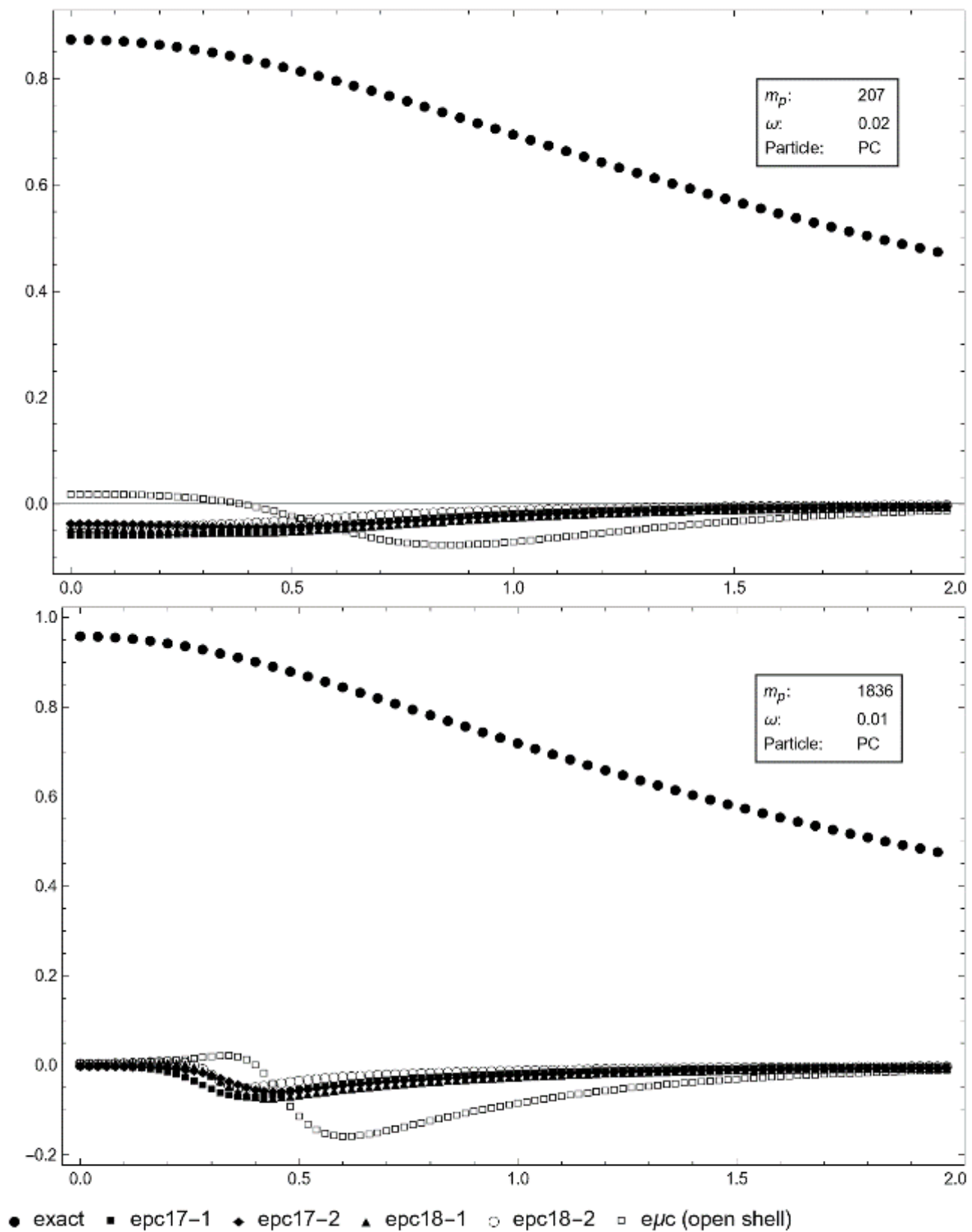


Figure 5-45: Comparison of exact correlation potentials and functional-derived potentials for PCP



## 5.3 Data Fitting

To propose an explicit functional dependence on the two main variational parameters of the problem (field frequency and the mass of the PCP), data fitting was performed in three sections: parameters of the variational wave function, nuclear exponents of Hartree-Fock wave functions, and correlation energies. In essence, data fitting allows us to propose an explicit form for the functions, thus providing a deeper insight into how the system's components behave under different conditions.

### 5.3.1 Fitting Variational Parameters

The fitting of variational parameters was performed both in two stages (i.e., first finding the dependence of the data on the frequency and then on the mass) and in a single stage (i.e., fitting the data simultaneously with respect to frequency and mass). Accordingly, the parameter  $\alpha$  was fitted with a logistic function (LOG) in the form:

$$L(\kappa) = \mu \left( \frac{l_1}{1 + \exp(\kappa)} + l_2 \right) \quad 5.46$$

and a specific form of the error function (ERR) as follows:

$$E(\kappa) = \mu(a_1 - a_2 \operatorname{erf}(\kappa\sqrt{a_3\mu})) \quad 5.47$$

where

$$\kappa = \operatorname{Log}_e[\omega] \quad 5.48$$

Additionally, the optimized parameter  $\beta$  shows good agreement with the analytical form of this parameter based on the harmonic oscillator model (SIM1):

$$\beta = \frac{1}{2} \mu \omega \quad 5.49$$

although the data can also be fitted with the following exponential function (EXP), which can be represented in linear form as well:

$$Z(\omega) = \mu b_3 \exp(\kappa) = \mu b_3 \omega \quad 5.50$$

However, to improve accuracy, the difference between the optimized parameter  $\beta$  values and those obtained from (5-49) was also fitted to the exponential function (5-50) and added to the values obtained from (5-49). This resulted in a relatively simple yet precise form (SIM2) for this parameter, as shown below, which led to a significant increase in accuracy.

$$\mathcal{S}(\kappa) = |1/2 \mu \omega - b_1 \mu \exp[b_2 \kappa]| = |1/2 \mu \omega - b_1 \mu \omega^{b_2}| \quad 5.51$$

With the values of the constants as shown in the table below, the expressions obtained for the fundamental parameters  $\alpha$  and  $\beta$  will be as shown in Table 5-11.

Table 5-10: Constants for fitting variational parameters

	$l_1$	$l_2$	$a_1$	$a_2$	$a_3$	$b_1$	$b_2$	$b_3$
Variational (exact)	0.2	0.8	0.9	0.096	0.1333	0.1	0.5	0.48

Table 5-11: Explicit forms obtained from fitting for variational parameters

Parameter	Explicit form
$\alpha_{LOG}$	$\frac{\mu}{5} (4 + \frac{1}{1 + \exp[\kappa]})$
$\alpha_{ERR}$	$\mu (a_1 - a_2 \text{Erf}[\kappa \sqrt{a_3 \mu}])$
$\beta_{EXP}$	$b_3 \mu \text{Exp}[\kappa]$
$\beta_{SIM1}$	$1/2 \mu \omega$
$\beta_{SIM2}$	$ 1/2 \mu \omega - b_1 \mu \text{Exp}[b_2 \kappa] $

Comparing the optimized parameter  $\alpha_{OPT}$  with the two fitting parameters  $\alpha_{LOG}$  and  $\alpha_{ERR}$  over the range of frequencies and reporting the error percentage for each case at different masses shows that, on average, the highest error percentage for both methods occurs at intermediate frequencies (particularly at  $\omega = 1$ ). While the error percentage decreases for  $\alpha_{ERR}$  at higher frequencies, it remains significant for  $\alpha_{LOG}$ . Overall, the error percentage for  $\alpha_{ERR}$  is lower (with an overall mean error of 0.82% and a variance of 0.2), making it a more suitable choice for reproducing the alpha parameter.

Comparing the optimized parameter  $\beta_{OPT}$  with the three fitting parameters  $\beta_{EXP}$ ,  $\beta_{SIM1}$ , and  $\beta_{SIM2}$  over the range of frequencies and reporting the error percentage for all three cases shows that the error percentage is very high at low frequencies (with an average of 99%). Since the beta values in these regions are very small, even a slight difference from the optimized value results in large error percentages. However, as reported in Table (C-4) of the appendix C, due to the small contribution of beta to the energy in these regions, large errors in beta do not lead to large errors in the energy (with an overall mean error of about 0.06%). The error percentage for all three forms of beta

decreases with increasing frequency, and overall,  $\beta_{SIM2}$  has the lowest error percentage (with an overall mean error of 35.78%).

Comparison of the energy values obtained from the combination of the two parameters  $\alpha_{LOG}$  and  $\alpha_{ERR}$ , and the three parameters  $\beta_{EXP}$ ,  $\beta_{SIM1}$ , and  $\beta_{SIM2}$  over the range of frequencies, along with the error percentage report for each case relative to the energy obtained from the optimized parameters, is also presented in Table (C-4) of the appendix C. The error percentages for the six different parameter combinations show that, once again, the highest error occurs at intermediate frequencies (particularly at  $\omega = 1$ ) and decreases at higher frequencies. This indicates that at intermediate frequencies (especially at  $\omega = 1$ ), the alpha parameter plays a more significant role compared to the beta parameter, and thus the error pattern follows that of the alpha parameter. However, at higher frequencies, the beta parameter quickly surpasses the alpha parameter, and consequently, the energy error pattern aligns with the error pattern of the beta parameter. The data show that among the six different parameter combinations, the combination of  $\alpha_{ERR}\beta_{SIM2}$  provides the best results (with the least errors). Using this combination, the total wave function is transformed into the form below:

$$\chi_{fit} = \exp\left(-\mu(a_1 - a_2 \text{Erf}[\kappa\sqrt{a_3\mu}])r - \mu\left|-b_1\omega^{b_2} + \frac{\omega}{2}\right|r^2\right) \quad 5.52$$

In this case, the variational wave function (2-72) can be simply obtained by specifying the reduced mass and the oscillator field frequency through the explicit form (5-52). Additionally, all quantities obtained in the previous sections can be derived by substituting these two parameters. For example, the average two-particle distribution function based on the fitting results will be as follows:

$$f(r) = \sqrt{2} \gamma^{-3/2} N^2 \pi^{5/2} r^2 e^{-2\mu r(r|\frac{\omega}{2} - \omega^{b_2} b_1| + (a_1 - \text{Erf}[\kappa\sqrt{\mu a_3}] a_2))} \quad 5.53$$

Overall, the form of the wave function obtained from the fitting shows that the hydrogen-like part, in addition to a linear dependence on  $\mu$ , also has a nonlinear dependence on it as well as on the field frequency. On the other hand, for the oscillator part, only a linear behavior with respect to  $\mu$  is observable, but its dependence on the field frequency is both linear and nonlinear. In general, comparing (5-52) with the two equations (2-73) and (2-74) shows that the deviation of each part from its reference state (the alpha values with respect to the exponent of the hydrogen-like wave function and the beta values with respect to the exponent of the harmonic oscillator wave function) appears as a nonlinear term. Naturally, the form of this nonlinear term can vary depending on the type of function chosen for fitting and its accuracy (for example, both the error function and the logistic function can be used for alpha, with accuracy being the deciding factor for preferring one over the other).

## 5.4 Comparison of Non-Adiabatic and Correlation Energy Contributions

One of the interesting topics in multi-component quantum chemistry is the comparison of non-adiabatic energy and e-PCP correlation energy. Since accurate non-adiabatic energy of the system is required for this comparison and such capability is usually not available due to the complexity of calculations for real molecular systems, the EHM is used here to compare these two energies.

### 5.4.1 Analysis of the EHM in the Adiabatic Framework

Comparing the non-adiabatic energy and the e-PCP correlation energy helps us understand under which conditions non-adiabatic two-component methods are efficient and when they lose their effectiveness. To perform such a comparison, three energies are required: the exact non-adiabatic energy of the system, the exact adiabatic energy of the system, and the two-component Hartree-Fock limit energy of the system. The difference between the first two energies is the non-adiabatic energy; and the difference between the first and the third energies is the e-PCP correlation energy of the system:

$$E_{non-ad} = E_{exact} - E_{ad} \quad 5.54$$

$$E_{corr} = E_{exact} - E_{TC-HF} \quad 5.55$$

Of the three aforementioned energies, the first and third have already been calculated and are presented in Table (4-3); therefore, only the adiabatic energy of the EHM needs to be calculated. To calculate the system's energy within the adiabatic approximation

framework, it is necessary, as with all adiabatic formulations, to consider the heavier particle as a clamped point charge (with infinite mass) and then place the origin of the coordinate system on this particle. After making these changes to the EHM, the Hamiltonians within the adiabatic framework are obtained as follows:

$$H(\mathbf{r}_e) = -\frac{1}{2}\nabla_{\mathbf{r}_e}^2 + \frac{1}{2}\omega^2 r_e^2 - \frac{1}{r_e} \quad 5.56$$

$$H(\mathbf{r}_p) = -\frac{1}{2m_p}\nabla_{\mathbf{r}_p}^2 + \frac{1}{2}m_p\omega^2 r_p^2 \quad 5.57$$

The energy of equation (5-67) is simply equivalent to the energy of a three-dimensional harmonic oscillator and can be calculated from equation (2-17). The energy in equation (5-56), representing the electronic energy, is similar to the relative motion part in the original EHM, except here the reduced mass equals the electron mass (1 in atomic units), and the distance between the two particles is reduced to the electron's distance from the coordinate system's center (the clamped particle). The energy of this equation can be computed variationally or using the FEM, similar to equation (2-18).

Therefore, the total ground state energy of the adiabatic system is obtained by summing the ground state energies of these two equations:

$$E_{ad} = E_{ad}^p + E_{ad}^e = E_{3D-HO} + E_{ad}^e = \frac{3}{2}\omega + E_{ad}^e \quad 5.58$$

As a result, to calculate  $E_{ad}$ , it is only necessary to compute the energy  $E_{ad}^e$ , which will be addressed in the next section.

#### 5.4.2 Calculation of Electronic Energy

The energy of the electronic part is calculated numerically and variationally (using the wave function 2-72), and the results are

presented in Table (5-12). The electronic energy is parametrically dependent only on the frequency, and here we encounter 9 systems with different field frequencies.



Table 5-12: Electronic energies

$\omega$	$\alpha^{ad}$ <sup>1</sup>	$\beta^{ad}$ <sup>2</sup>	N <sup>3</sup>	FEM $E_{ad}^e$ <sup>4</sup>	Var $E_{ad}^e$ <sup>5</sup>	$\Delta E_{ad}^e$ <sup>6</sup>
0.0001	1.000000	0.000000	0.564190	-0.500000	-0.500000	0.000000
0.001	0.999999	0.000002	0.564191	-0.499999	-0.499999	0.000000
0.01	0.999850	0.000150	0.564316	-0.499850	-0.499850	0.000000
0.1	0.988307	0.013169	0.575925	-0.485679	-0.485670	0.000009
1.0	0.901059	0.369817	0.892146	0.179668	0.179905	0.000236
10	0.839160	4.616819	3.015105	11.265447	11.265809	0.000361
100	0.817579	48.825540	14.430261	138.557198	138.557585	0.000388
1000	0.810663	496.324903	77.139839	1464.160725	1464.161119	0.000394
10000	0.808470	4988.417578	426.915815991	14887.005984	14887.006379	0.000396

1. Optimized variational parameter  $\alpha^{ad}$
2. Optimized variational parameter  $\beta^{ad}$
3. Variational normalization coefficient
4. FEM energy
5. Variational energy
6. Difference between 4 and 5

•

To utilize the maximum accuracy of the FEM, a meshing of 0.0001 distance in atomic units was used for all frequencies. Additionally, the accuracy of the calculations was tested by comparing the results with the perturbative trends of the problem. Similar to the discussion in section 2-3-2, there are two perturbative regimes in this problem: one at low frequencies, where the interaction of the electron with the clamped positive particle dominates the Hamiltonian (equivalent to the energy of a hydrogen atom with a clamped nucleus), and the oscillator potential of the electron can be considered a perturbation. The other regime is at high frequencies, where the electron's oscillator potential becomes very large and dominant (similar to the energy of a three-dimensional harmonic oscillator), and the Coulomb interaction between the electron and the clamped positive particle can be considered a perturbation. The first-order perturbation at low

frequencies is  $\frac{3\pi\omega^2}{2}$  and at high frequencies is  $-\frac{2\sqrt{\omega}}{\sqrt{\pi}}$ . Therefore, the total adiabatic electronic energy at low and high frequencies will be as follows:

$$E_{ad}^{e-low\omega} \approx \frac{3\pi\omega^2 - 1}{2} \quad 5.59$$

$$E_{ad}^{e-high\omega} \approx \frac{3}{2}\omega - \frac{2\sqrt{\omega}}{\sqrt{\pi}} \quad 5.60$$

The data in Table 5-13 show that the adiabatic electronic energies are close to equation (5-59) at low frequencies and close to equation (5-60) at high frequencies. Additionally, the calculation of the components of adiabatic electronic energy indicates that the kinetic and oscillator potential energy components approach their corresponding values for a three-dimensional harmonic oscillator at high frequencies. The only factor causing deviation from these values is the expectation value of the interaction energy, which increases in absolute value with increasing frequency.

Table 5-13: Asymptotic behavior and components of electronic energy

$\omega$	0.0001	0.001	0.01	0.1	1	10	100	1000	10000
Num $\mathbf{E}_{ad}^e$ <sup>1</sup>	-0.500000	-0.499999	-0.499850	-0.485679	0.179668	11.265447	138.557198	1464.160725	14887.005984
$\mathbf{E}_{ad}^e$ low $\omega$ <sub>2</sub>	-0.500000	-0.499995	-0.499529	-0.452876	4.212389	-	-	-	-
$\Delta E$ low $\omega$ <sub>3</sub>	0.000000	0.000003	0.000321	0.032803	4.032721	-	-	-	-
% low $\omega$ <sup>4</sup>	0.000011	0.000648	0.064288	6.754031	2244.534471	-	-	-	-
$\mathbf{E}_{ad}^e$ high $\omega$ <sub>5</sub>	-	-	-	-	0.371621	11.431752	138.716208	1464.317518	14887.162083
$\Delta E$ high $\omega$ <sub>6</sub>	-	-	-	-	0.191952	0.166304	0.159011	0.156793	0.156100
% high $\omega$ <sup>7</sup>	-	-	-	-	106.836989	1.476233	0.114762	0.010709	0.001049
HO coms <sup>8</sup>	0.000075	0.000750	0.007500	0.075000	0.750000	7.500000	75.000000	750.000000	7500.000000
$\mathbf{INT}_{ad}^e$ <sup>9</sup>	-1.000000	-1.000003	-1.000300	-1.026316	-1.552250	-3.911832	-11.605088	-35.997084	-113.150437
$\mathbf{HO}_{ad}^e$ <sup>10</sup>	0.000000	0.000001	0.000150	0.013740	0.477897	6.610682	72.179871	741.079633	7471.790600
$\mathbf{T}_{ad}^e$ <sup>11</sup>	0.500001	0.500004	0.500301	0.526898	1.254023	8.566641	77.984665	759.139868	7529.547941

1. Numerical exact energy of the system
2. Perturbative energy of the system at low frequencies (equation 5-59)
3. Difference between 1 and 2
4. Error percentage of 2
5. Perturbative energy of the system at high frequencies (equation 5-60)
6. Difference between 1 and 5
7. Error percentage of 5

8. Components of kinetic/potential oscillator energy for a three-dimensional harmonic oscillator (equal to  $\frac{3}{4}\omega$  from equations 2-148 and 2-149)
9. Expectation value of electron-clamped positive particle interaction energy
10. Expectation value of oscillator potential energy
11. Expectation value of kinetic energy

### 5.4.3 Comparison of Non-Adiabatic and Correlation Energy Contributions

After calculating the electronic energies, the total adiabatic energy can be obtained using equation (5-58). This gives us the three energies needed to compare the non-adiabatic part of the total energy and the e-PCP correlation energy (i.e., equations 5-54 and 5-55).

The numerical results of this comparison, presented in Table 5-14, show that the non-adiabatic energy contribution increases with increasing frequency for any given mass, while the correlation energy decreases at a slower rate under the same conditions. On the other hand, the non-adiabatic energy contribution decreases with increasing mass for any given frequency, showing a uniform pattern, unlike the correlation energy. It is worth mentioning that since the adiabatic energy depends only on the frequency and is therefore the same for different masses, its values for each mass are presented repeatedly in Table 5-14 for easier comparison.

Figures 5-46 and 5-47, which illustrate the differences between the non-adiabatic energy and the magnitude of the correlation energy (item 6 in Table 5-18), clearly show the aforementioned trends. To better visualize the points, the graphs are plotted on a natural logarithmic scale of frequencies. For the two masses of 1 and 1.5, the non-adiabatic energies are greater than the correlation energies across the entire frequency range. However, for larger masses, particularly at low frequencies, the non-adiabatic energy is smaller than the correlation energy, but gradually surpasses it as the frequency increases. As the mass increases, the frequency at which the sign of the difference between the non-adiabatic energy and the magnitude of the correlation energy changes shifts to higher frequencies.

Overall, the results indicate that with increasing mass, the non-adiabatic effects become smaller (as expected), eventually becoming smaller than the correlation energies.

Unfortunately, non-adiabatic energies are rarely reported due to the lack of exact solutions for obtaining the energies of systems. However, reference [12] provides these data for six hydride systems using the Monte Carlo method. Fitting the data from reference [12] and extrapolating the non-adiabatic energy for the single-electron system yields a value of 0.0003 Hartree, which matches the values obtained for the proton (mass 1836) at low frequencies in Table 5-18. The current data seem to confirm that for the physical masses of 1, 207, and 1836, only the mass of 1 (positron) has the property that the electron-positron correlation energy is smaller than the non-adiabatic energy. Consequently, it is reliable to use two-component quantum chemistry methods for calculations involving it. In the case of muons and protons, the adiabatic approximation and its perturbative corrections appear to be a better approach.

Table 5-14: Comparison of non-adiabatic and correlation energy contributions for the EHM

omega	$E_{exact}^1$	$E_{TC-HF}^2$	$E_{ad}^3$	$E_{non-ad}^4$	$E_{Corr}^5$	$\Delta E^6$
m = 1						
0.0001	-0.249850	-0.108513	-0.499850	0.250000	-0.141337	0.108663
0.001	-0.248497	-0.108491	-0.498499	0.250002	-0.140006	0.109996
0.01	-0.234701	-0.106407	-0.484850	0.250149	-0.128294	0.121856
0.1	-0.073957	0.012203	-0.335679	0.261722	-0.086160	0.175562
1.0	2.111853	2.171918	1.679668	0.432184	-0.060066	0.372118
10	27.395303	27.448072	26.265447	1.129856	-0.052768	1.077088
100	291.942127	291.992777	288.557198	3.384929	-0.050650	3.334279
1000	2974.690429	2974.740427	2964.160725	10.529704	-0.049998	10.479706
10000	29920.133541	29920.183344	29887.005984	33.127557	-0.049804	33.077754
m = 1.5						
0.0001	-0.299850	-0.131661	-0.499850	0.200000	-0.168189	0.031811
0.001	-0.298498	-0.131644	-0.498499	0.200001	-0.166854	0.033147
0.01	-0.284750	-0.129900	-0.484850	0.200100	-0.154850	0.045250
0.1	-0.127553	-0.021539	-0.335679	0.208126	-0.106014	0.102112
1.0	2.016098	2.087757	1.679668	0.336429	-0.071659	0.264771
10	27.137735	27.199613	26.265447	0.872287	-0.061878	0.810410
100	291.164648	291.223701	288.557198	2.607450	-0.059054	2.548396
1000	2972.266533	2972.324714	2964.160725	8.105808	-0.058182	8.047626
10000	29912.502509	29912.560519	29887.005984	25.496525	-0.058010	25.438515
m = 2						
0.0001	-0.333183	-0.149328	-0.499850	0.166667	-0.183855	-0.017188
0.001	-0.331831	-0.149312	-0.498499	0.166667	-0.182519	-0.015851
0.01	-0.318109	-0.147746	-0.484850	0.166742	-0.170363	-0.003622
0.1	-0.162797	-0.045426	-0.335679	0.172882	-0.117372	0.055510
1.0	1.955533	2.032554	1.679668	0.275864	-0.077021	0.198843
10	26.977001	27.042353	26.265447	0.711553	-0.065352	0.646201
100	290.681215	290.743202	288.557198	2.124018	-0.061987	2.062031
1000	2970.760975	2970.821923	2964.160725	6.600250	-0.060948	6.539302
10000	29907.764199	29907.824832	29887.005984	20.758216	-0.060632	20.697583
m = 3						
0.0001	-0.374850	-0.175573	-0.499850	0.125000	-0.199277	-0.074277
0.001	-0.373498	-0.175559	-0.498499	0.125001	-0.197939	-0.072938

omega	$E_{exact}^1$	$E_{TC-HF}^2$	$E_{ad}^3$	$E_{non-ad}^4$	$E_{Corr}^5$	$\Delta E^6$
0.01	-0.359800	-0.174173	-0.484850	0.125050	-0.185627	-0.060578
0.1	-0.206455	-0.078661	-0.335679	0.129224	-0.127794	0.001430
1.0	1.882805	1.962394	1.679668	0.203136	-0.079589	0.123547
10	26.786175	26.851598	26.265447	0.520728	-0.065423	0.455305
100	290.109020	290.170376	288.557198	1.551823	-0.061356	1.490466
1000	2968.980576	2969.040682	2964.160725	4.819851	-0.060105	4.759746
10000	29902.162455	29902.222187	29887.005984	15.156471	-0.059732	15.096739
m = 10						
0.0001	-0.454395	-0.257049	-0.499850	0.045455	-0.197347	-0.151892
0.001	-0.453044	-0.257037	-0.498499	0.045455	-0.196007	-0.150552
0.01	-0.439381	-0.255878	-0.484850	0.045470	-0.183502	-0.138033
0.1	-0.288923	-0.170118	-0.335679	0.046756	-0.118805	-0.072049
1.0	1.751315	1.810873	1.679668	0.071647	-0.059557	0.012090
10	26.447087	26.490355	26.265447	0.181639	-0.043268	0.138371
100	289.096910	289.135811	288.557198	0.539712	-0.038901	0.500811
1000	2965.835599	2965.873207	2964.160725	1.674875	-0.037607	1.637267
10000	29892.271372	29892.308661	29887.005984	5.265389	-0.037289	5.228100
m = 50						
0.0001	-0.490046	-0.353887	-0.499850	0.009804	-0.136159	-0.126355
0.001	-0.488695	-0.353874	-0.498499	0.009804	-0.134821	-0.125017
0.01	-0.475043	-0.352583	-0.484850	0.009807	-0.122460	-0.112653
0.1	-0.325612	-0.261510	-0.335679	0.010067	-0.064103	-0.054036
1.0	1.694935	1.717273	1.679668	0.015267	-0.022337	-0.007070
10	26.303970	26.317887	26.265447	0.038523	-0.013917	0.024606
100	288.671520	288.683473	288.557198	0.114323	-0.011953	0.102370
1000	2964.515378	2964.526763	2964.160725	0.354653	-0.011385	0.343268
10000	29888.120778	29888.132005	29887.005984	1.114795	-0.011227	1.103568
m = 207						
0.0001	-0.497446	-0.414686	-0.499850	0.002404	-0.082760	-0.080356
0.001	-0.496095	-0.414668	-0.498499	0.002404	-0.081427	-0.079023
0.01	-0.482446	-0.412886	-0.484850	0.002404	-0.069560	-0.067155
0.02	-0.466994	-0.407763	-0.469401	0.002407	-0.059231	-0.056824
0.1	-0.333212	-0.306618	-0.335679	0.002467	-0.026594	-0.024127
1.0	1.683403	1.690372	1.679668	0.003734	-0.006969	-0.003235
10	26.274861	26.278862	26.265447	0.009414	-0.004001	0.005413

omega	$E_{exact}^1$	$E_{TC-HF}^2$	$E_{ad}^3$	$E_{non-ad}^4$	$E_{Corr}^5$	$\Delta E^6$
100	288.585127	288.588490	288.557198	0.027930	-0.003363	0.024566
1000	2964.247368	2964.250545	2964.160725	0.086643	-0.003177	0.083467
10000	29887.278310	29887.281447	29887.005984	0.272326	-0.003137	0.269189
m = 400						
0.0001	-0.498603	-0.434898	-0.499850	0.001247	-0.063705	-0.062458
0.001	-0.497252	-0.434876	-0.498499	0.001247	-0.062375	-0.061128
0.01	-0.483603	-0.432709	-0.484850	0.001247	-0.050894	-0.049647
0.1	-0.334399	-0.318137	-0.335679	0.001280	-0.016263	-0.014983
1.0	1.681605	1.685464	1.679668	0.001936	-0.003860	-0.001923
10	26.270328	26.272493	26.265447	0.004880	-0.002165	0.002716
100	288.571677	288.573488	288.557198	0.014479	-0.001811	0.012668
1000	2964.205645	2964.207347	2964.160725	0.044921	-0.001702	0.043219
10000	29887.147157	29887.148995	29887.005984	0.141173	-0.001838	0.139335
m = 900						
0.0001	-0.499295	-0.453975	-0.499850	0.000555	-0.045320	-0.044765
0.001	-0.497944	-0.453946	-0.498499	0.000555	-0.043998	-0.043443
0.01	-0.484295	-0.451115	-0.484850	0.000555	-0.033180	-0.032625
0.1	-0.335109	-0.326729	-0.335679	0.000570	-0.008381	-0.007811
1.0	1.680530	1.682345	1.679668	0.000862	-0.001815	-0.000954
10	26.267619	26.268617	26.265447	0.002171	-0.000999	0.001173
100	288.563640	288.564475	288.557198	0.006442	-0.000835	0.005607
1000	2964.180715	2964.181492	2964.160725	0.019991	-0.000777	0.019214
10000	29887.068792	29887.069700	29887.005984	0.062809	-0.000907	0.061902
m = 1836						
0.0001	-0.499578	-0.466417	-0.499850	0.000272	-0.033161	-0.032889
0.001	-0.498226	-0.466378	-0.498499	0.000272	-0.031848	-0.031576
0.01	-0.484578	-0.462753	-0.484850	0.000272	-0.021825	-0.021553
0.1	-0.335400	-0.330905	-0.335679	0.000279	-0.004495	-0.004216
1.0	1.680091	1.681012	1.679668	0.000423	-0.000921	-0.000498
10	26.266512	26.267013	26.265447	0.001065	-0.000501	0.000564
100	288.560357	288.560779	288.557198	0.003159	-0.000422	0.002737
1000	2964.170533	2964.170918	2964.160725	0.009808	-0.000385	0.009423
10000	29887.036785	29887.037312	29887.005984	0.030802	-0.000527	0.030275

1. Numerical exact energy
2. Two-component Hartree-Fock energy with [7s:7s] basis sets



3. Adiabatic energy
4. Non-adiabatic energy (difference between 1 and 3)
5. Correlation energy (difference between 1 and 2)
6. Difference between 4 and the magnitude of 5 ( $\Delta E = E_{non-ad} - |E_{corr}|$ )

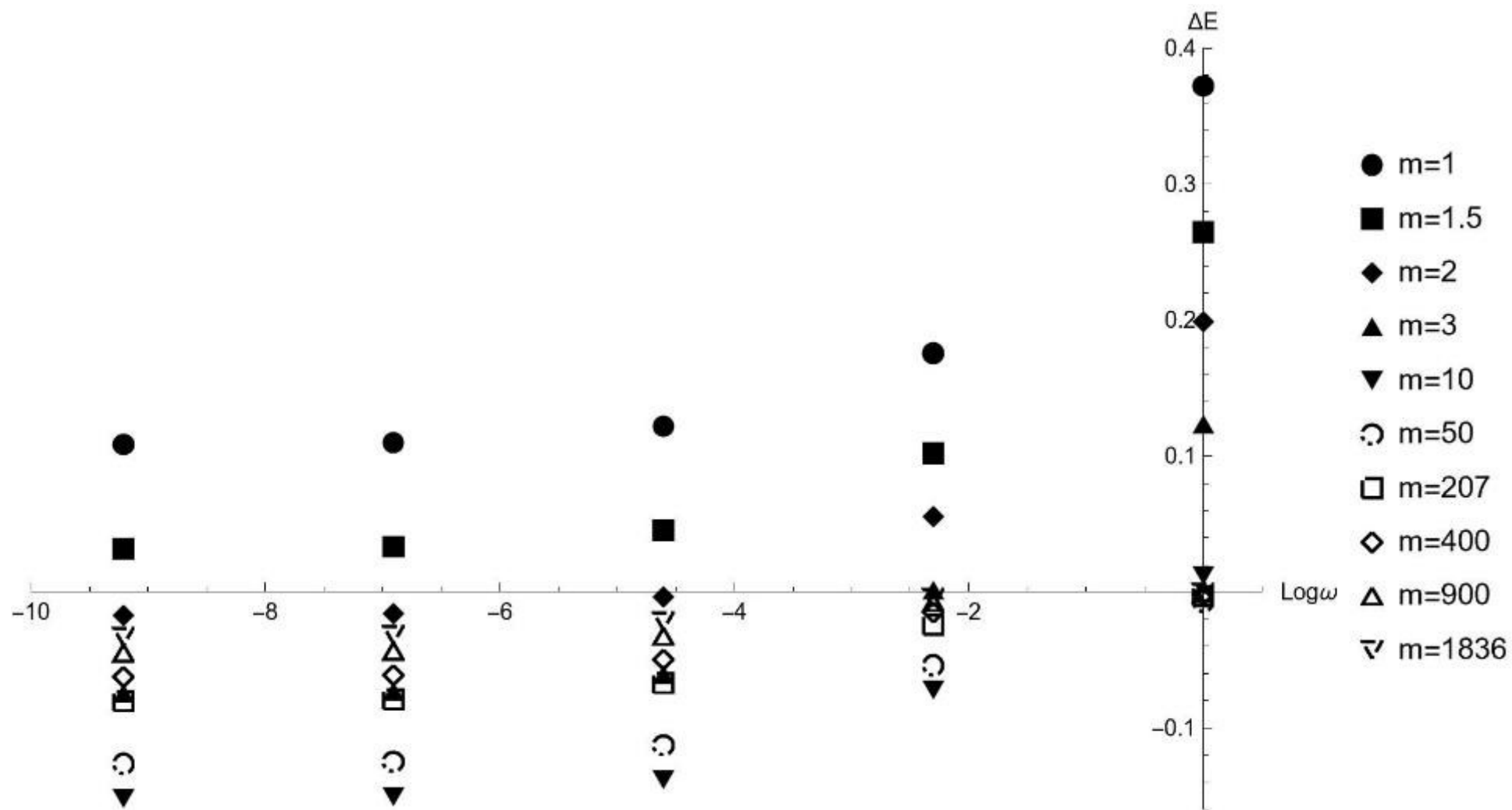


Figure 5-46: Comparison of the magnitude differences between non-adiabatic and correlation energies in the logarithmic frequency range (0.0001 to 1)

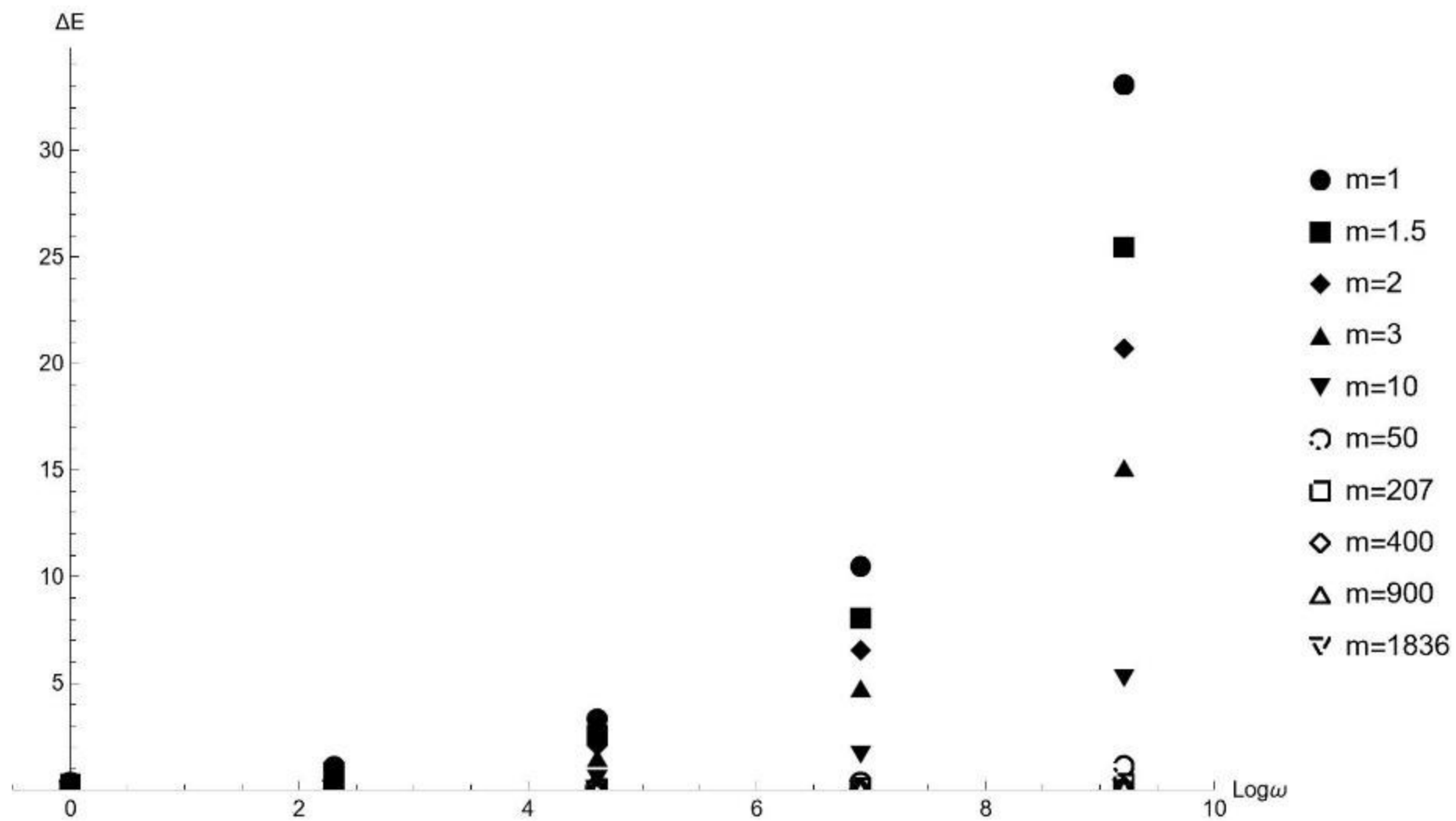


Figure 5-47: Comparison of the magnitude differences between non-adiabatic and correlation energies in the logarithmic frequency range (1 to 10000)

## 6 Conclusion

The term "model," in its most common usage, refers to a simplified version of the so-called target system, which is the part or aspect of the world that we are interested in [142]. The history of science, especially quantum physics, is replete with models that have significantly contributed to understanding real physical phenomena [143]. Models serve three important purposes: developing new theories, exploring and testing existing ones [144], and these purposes are made possible because models provide a deep understanding of the real system [145], even though they are only representations of the external world and, in this sense, are fictional systems. From the famous Solar System model to the ideal gas model, our work in this study was also inspired by a very important model in the field of electron-electron correlation: the Harmonium model.

The problem of calculating e-PCP correlation is one of the challenges of quantum chemistry beyond the adiabatic approximation. One could say that the ultimate goal of ab initio two-component methods is to better estimate this type of correlation. To this end, we developed a simple model for better understanding, inspired by its electronic counterpart, the Harmonium model, which aimed to better understand electronic correlation. However, e-PCP correlation has fundamental differences from electron-electron correlation (as discussed in Chapter 3), and since it involves particles with positive charge and variable mass, we named it the "Exotic Harmonium."

In the first step, we attempted to apply the method used to obtain analytical equations in the Harmonium model to the Exotic Harmonium, but encountered challenges that are detailed in Chapter 2. These challenges led us to the most straightforward method for finding the ground state in quantum mechanics, the variational method. Fortunately, by predicting the asymptotic behavior of the system, we were able to obtain a very simple yet accurate variational wave function. Since having the wave function essentially allows access to all the properties of the system, we obtained the main quantities such as energy and its components, as well as single-particle densities. As discussed in Chapter 2, by performing a series of transformations, we wrote the wave function in three coordinate systems, each of which could be used for a specific purpose and provided a different perspective on the system.

In Chapter 3, we developed the most important concepts and quantities for studying electronic correlation, particularly in the Harmonium model for the EHM, while also reviewing their history. The key idea introduced in Chapter 3 was the "correlation hill," which

is akin to the correlation hole in the Harmonium model but has an inverse shape here, hence the name "correlation hill." This quantity clearly revealed the different nature of e-PCP correlation compared to electron-electron correlation, and precisely for this reason, e-PCP correlation cannot be considered a generalization of electron-electron correlation.

In Chapter 4, the numerical data obtained from solving the model, including the expectation values achievable with the variational wave function, were presented. Additionally, all numerical data related to the quantities and concepts introduced for extracting correlation information from the EHM were reported in Chapter 5, making this chapter the first to present applications of the EHM. Three types of correlation classifications were introduced: reference-independent, MC-HF, and MC-DFT. Although MC-DFT correlation was reported for only a few systems due to the need for simplification and density fitting, other two-particle quantities related to particle interactions were also examined.

Another application of the EHM is to benchmark existing functionals for e-PCP correlation, just as successful electron functionals like LYP have been benchmarked using the Harmonium model [83], [141], [146]. Here, we also benchmarked five existing functionals for e-PCP correlation using the EHM. Another important step reported in Chapter 5 was the fitting of the variational wave function parameters, which enabled us to derive a simple yet accurate form for the wave function in terms of the two main variables of the problem: the frequency of the oscillator field and the mass of the PCP. This form of the wave function explicitly shows its dependency on these variables, providing valuable insight into the system's behavior

with respect to these two variables. Given that the range of variations in the frequency of the oscillator field and the mass of the PCP was considered very wide (from very high and very low frequencies compared to typical molecular systems to the smallest possible mass, positron, and the most significant large mass, proton), the e-PCP correlation can be examined for a wide range of real systems using the EHM.

There are many opportunities for future research in this field. The primary mission of this study was the development of the EHM. However, much like the Harmonium model, which has long been used to extract information about electron-electron correlation, the EHM will certainly have a broader scope beyond the applications presented in this dissertation.

Unlike the Harmonium model, this model deals not just with one type of particle, but with a general PCP, which can be any particle within the studied mass spectrum, such as positrons, muons, kaons, pions, protons, etc. Consequently, the EHM can be applied to each of these exotic particles (briefly discussed in Chapter 1).

Therefore, although the importance of e-PCP correlation in quantum chemistry and atomic physics calculations is not as significant as that of electron-electron correlation, the ability to investigate a wide range of PCPs makes the EHM a vital tool.

The model itself can also be considered more complex in future research. For example, to better simulate molecular environments, the harmonic oscillator can be replaced with an anharmonic oscillator, as atomic vibrations along and perpendicular to the bond axis have different frequencies. Given the capabilities of the Harmonium model

in providing deep insights into electronic correlation, many studies in the field of DFT have been conducted on Harmonium, and almost all of them are applicable to Exotic Harmonium as well [147], [148], [157]–[163], [149]–[156].

The above examples show that research work in this area has just begun, and as the history of science has shown, the development of any model is equivalent to opening a window to a new world, each corner of which requires further exploration.



## 7 Appendix A

### Mathematical Framework of Ab Initio Multi-Component Methods

In this section, the mathematical details of the multi-component Hartree-Fock method are provided. Since the Hartree-Fock method is a mean-field theory, comparing it with exact methods will reveal the correlation effects. Given that the details of deriving the multi-component Hartree-Fock equations are not reported in the references, an effort has been made to present all the derivation steps in this section.

#### A.1 Derivation of the Energy Expression

The general approach to obtaining MC-HF equations, similar to electronic structure theory, is to derive an expression for the system's energy and then vary it with respect to both the electronic and PCP orbitals simultaneously. To achieve this goal, we need to evaluate the expectation value of the energy, which has the following general form:

$$\begin{aligned}
E_0 &= \langle \Psi_0 | \hat{H}_{NEO} | \Psi_0 \rangle \\
&= \langle \Psi_0 | \hat{T}_{NEO}^e | \Psi_0 \rangle + \langle \Psi_0 | \hat{V}_{ext}^e | \Psi_0 \rangle \\
&+ \langle \Psi_0 | \hat{T}_{NEO}^p | \Psi_0 \rangle + \langle \Psi_0 | \hat{V}_{ext}^p | \Psi_0 \rangle \\
&+ \langle \Psi_0 | \hat{V}_{NEO}^{ee} | \Psi_0 \rangle + \langle \Psi_0 | \hat{V}_{NEO}^{ep} | \Psi_0 \rangle \\
&+ \langle \Psi_0 | \hat{V}_{NEO}^{pp} | \Psi_0 \rangle
\end{aligned} \tag{A.1}$$

#### Kinetic Energy Operators

For the first term in Equation A-1, we have:

$$\begin{aligned}
&\langle \Phi_0^e | \hat{T}_{NEO}^e + \hat{V}_{ext}^e | \Phi_0^e \rangle = \langle \Phi_0^e | \sum_i^N h_i | \Phi_0^e \rangle \\
&= \sum_i^N \int dx_1^e dx_2^e \dots dx_N^e \left[ (N!)^{-\frac{1}{2}} \left( \chi_1^e(x_1^e) \dots \chi_k^e(x_N^e) \right. \right. \\
&\quad \left. \left. - \chi_k^e(x_N^e) \dots \chi_1^e(x_1^e) \right) \right]^* \\
&\times h_i \left[ (N!)^{-\frac{1}{2}} \left( \chi_1^e(x_1^e) \dots \chi_k^e(x_N^e) - \chi_k^e(x_N^e) \dots \chi_1^e(x_1^e) \right) \right] \\
&= \frac{1}{N!} \sum_i^N \int dx_1^e dx_2^e \dots dx_N^e \{ \chi_1^{e*}(x_1^e) \dots \chi_k^{e*}(x_N^e) h_i \chi_1^e(x_1^e) \dots \chi_k^e(x_N^e) \\
&\quad + \chi_k^{e*}(x_N^e) \dots \chi_1^{e*}(x_1^e) h_i \chi_k^e(x_N^e) \dots \chi_1^e(x_1^e) \\
&\quad - \chi_1^{e*}(x_1^e) \dots \chi_k^{e*}(x_N^e) h_i \chi_k^e(x_N^e) \dots \chi_1^e(x_1^e) \\
&\quad - \chi_k^{e*}(x_N^e) \dots \chi_1^{e*}(x_1^e) h_i \chi_1^e(x_1^e) \dots \chi_k^e(x_N^e) \}
\end{aligned} \tag{A.2}$$

By integrating over all variables except  $x_i^e$ , the above terms will be equal to one (the first two terms) or zero (the last two terms) due to the orthonormality of the electronic spin-orbitals, as follows:

$$\int dx^e \chi_i^{e*} \chi_j^e = \langle \chi_i^e | \chi_j^e \rangle = \delta_{ij} = \begin{cases} 1 & \text{if } i = j \\ 0 & \text{if } i \neq j \end{cases} \quad \text{A.3}$$

As a result, we will have:

$$\begin{aligned} & \langle \Phi_0^e | \sum_i^N h_i | \Phi_0^e \rangle \\ &= \sum_i^N \int dx_i^e \{ \chi_1^{e*}(x_1^e) \dots \chi_k^{e*}(x_N^e) h_i \chi_1^e(x_1^e) \dots \chi_k^e(x_N^e) \} \end{aligned} \quad \text{A.4}$$

On the other hand, by convention, the dummy integration variables for the one-electron operators are chosen such that they correspond to the coordinates of the first electron. Therefore, we have:

$$\langle \Phi_0^e | \sum_i^N h_i | \Phi_0^e \rangle = \sum_i^N \int dx_1^e \chi_i^{e*}(x_1^e) h_i \chi_i^e(x_1^e) \quad \text{A.5}$$

Following similar steps for  $h_{i'}$  (Equation 1-20), we arrive at the following result:

$$\langle \Phi_0^p | \sum_i^{N'} h_{i'} | \Phi_0^p \rangle = \sum_i^{N'} \int dx_1^p \chi_{i'}^{p*}(x_1^p) h_{i'} \chi_{i'}^p(x_1^p) \quad \text{A.6}$$

## Two-Particle Operators

Now, let's evaluate the matrix elements of the two-particle operators in Equation (A-1). Starting with  $\hat{V}_{NEO}^{ee}$ , we have:

$$\begin{aligned}
& \langle \Phi_0^e | \sum_i^N \sum_{j>i}^N \left( \frac{1}{r_{ij}} \right) | \Phi_0^e \rangle \\
&= \sum_i^N \sum_{j>i}^N \left\{ \int dx_1^e dx_2^e \dots dx_N^e \left[ (N!)^{-\frac{1}{2}} \left( \chi_1^e(x_1^e) \dots \chi_k^e(x_N^e) \right. \right. \right. \\
&\quad \left. \left. \left. - \chi_k^e(x_N^e) \dots \chi_1^e(x_1^e) \right) \right]^* \right. \\
&\quad \left. \times \frac{1}{r_{ij}} \left[ (N!)^{-\frac{1}{2}} \left( \chi_1^e(x_1^e) \dots \chi_k^e(x_N^e) - \chi_k^e(x_N^e) \dots \chi_1^e(x_1^e) \right) \right] \right\}
\end{aligned} \tag{A.7}$$

To evaluate the matrix elements of the operator  $\frac{1}{r_{ij}}$ , we use the general rules of electronic structure theory for evaluating two-electron integrals known as the Slater-Condon rules, resulting in the following expression [164]:

$$\begin{aligned}
& \langle \Phi_0^e | \sum_i^N \sum_{j>i}^N \frac{1}{r_{ij}} | \Phi_0^e \rangle \\
&= \sum_i^N \sum_{j>i}^N \left[ \int dx_1^e dx_2^e \chi_i^{e*}(x_1^e) \chi_j^{e*}(x_2^e) \frac{1}{r_{ij}} \chi_i^e(x_1^e) \chi_j^e(x_2^e) \right. \\
&\quad \left. - \int dx_1^e dx_2^e \chi_i^{e*}(x_1^e) \chi_j^{e*}(x_2^e) \frac{1}{r_{ij}} \chi_j^e(x_1^e) \chi_i^e(x_2^e) \right]
\end{aligned} \tag{A.8}$$

In the following, by convention, we write these expressions using standard notation. Here, we use the following notation:

$$[ij|kl] = \int dx_1 dx_2 \chi_i^*(x_1) \chi_j(x_1) r_{12}^{-1} \chi_k^*(x_2) \chi_l(x_2) \tag{A.9}$$

Finally, we can write the two-electron integrals as follows:

$$\langle \Phi_0^e | \sum_i^N \sum_{j>i}^N \frac{1}{r_{ij}} | \Phi_0^e \rangle = \frac{1}{2} \sum_i^N \sum_j^N ([\chi_i^e \chi_i^e | \chi_j^e \chi_j^e] - [\chi_i^e \chi_j^e | \chi_i^e \chi_j^e]) \tag{A.10}$$

The coefficient  $\frac{1}{2}$  appears because we have avoided imposing the condition  $j > i$  for the sums. The matrix elements of the two-particle operator for the PCP also yield the following results through a similar process:

$$\begin{aligned} \left\langle \Phi_0^p \left| \sum_{i'}^{N'} \sum_{j' > i'}^{N'} \frac{1}{r_{i'j'}} \right| \Phi_0^p \right\rangle \\ = \frac{1}{2} \sum_{i'}^{N'} \sum_{j'}^{N'} \left( \left[ \chi_{i'}^p \chi_{i'}^p \left| \chi_{j'}^p \chi_{j'}^p \right] - \left[ \chi_{i'}^p \chi_{j'}^p \left| \chi_{i'}^p \chi_{j'}^p \right] \right) \end{aligned} \quad \text{A.11}$$

The two-particle operator for electron-PCP interaction has a form similar to other two-particle operators, but it simultaneously involves both the electronic and PCP coordinates. In other words, we should note that the exchange integrals in this case are zero because electrons and PCPs do not exhibit exchange effects with each other. Therefore, the fourth term in Equation (A-1) is calculated as follows:

$$\begin{aligned} \left\langle \Psi_0 \left| \sum_i^N \sum_{i'}^{N'} \frac{Z_{i'}}{r_{ii'}} \right| \Psi_0 \right\rangle &= \left\langle \Phi_0^e(r^e) \Phi_0^p(r^p) \left| \sum_i^N \sum_{i'}^{N'} \frac{Z_{i'}}{r_{ii'}} \right| \Phi_0^e(r^e) \Phi_0^p(r^p) \right\rangle \\ &= \frac{1}{N!} \frac{1}{N'!} \int dx_1^e dx_1^p \left[ \left( \chi_1^e(x_1^e) \chi_1^p(x_1^p) \right) \right]^* \sum_i^N \sum_{i'}^{N'} \frac{Z_{i'}}{r_{ii'}} \left[ \left( \chi_1^e(x_1^e) \chi_1^p(x_1^p) \right) \right] \quad \text{A.1} \\ &= \sum_i^N \sum_{i'}^{N'} \int dx_1^e dx_1^p \left[ \left( \chi_1^e(x_1^e) \chi_1^p(x_1^p) \right) \right]^* \frac{Z_{i'}}{r_{ii'}} \left[ \left( \chi_1^e(x_1^e) \chi_1^p(x_1^p) \right) \right] \quad 2 \end{aligned}$$

According to the rules of electronic structure theory [164], we have:

$$\left\langle \Psi_0 \left| \sum_i^N \sum_{i'}^{N'} \frac{Z_{i'}}{r_{ii'}} \right| \Psi_0 \right\rangle = \sum_i^N \sum_{i'}^{N'} Z_{i'} [\chi_i^e \chi_i^e | \chi_{i'}^p \chi_{i'}^p] \quad \text{A.13}$$

In the end, the energy expression is obtained as follows:

$$\begin{aligned} E_0 = & \sum_i^N [\chi_i^e | h^e | \chi_i^e] + \frac{1}{2} \sum_i^N \sum_j^N ([\chi_i^e \chi_i^e | \chi_j^e \chi_j^e] - [\chi_i^e \chi_j^e | \chi_j^e \chi_i^e]) \\ & + \sum_{i'}^{N'} [\chi_{i'}^p | h^p | \chi_{i'}^p] \\ & + \frac{1}{2} \sum_{i'}^{N'} \sum_{i'}^{N'} ([\chi_{i'}^p \chi_{i'}^p | \chi_{j'}^p \chi_{j'}^p] - [\chi_{i'}^p \chi_{j'}^p | \chi_{j'}^p \chi_{i'}^p]) \\ & - \sum_i^N \sum_{i'}^{N'} Z_{i'} [\chi_i^e \chi_i^e | \chi_{i'}^p \chi_{i'}^p] \end{aligned} \quad \text{A.14}$$

### Transformation of Spin-Orbitals to Spatial Orbitals

So far, we have used spin-orbitals, but to simplify subsequent calculations, it is necessary to integrate out the spin functions from the electronic and PCP spin-orbitals. Therefore, we will use spatial orbitals instead of spin-orbitals. In the restricted Hartree-Fock approach, the  $\alpha$  and  $\beta$  spins have the same spatial orbitals, and each spatial orbital is occupied by two electrons with different spins. In other words, the electronic wave function consists of  $N/2$  spin-orbitals with  $\alpha$  spin and  $N/2$  spin-orbitals with  $\beta$  spin, i.e.:

$$\sum_i^N \chi_i^e = \sum_i^{N/2} \psi_i^e + \sum_i^{N/2} \bar{\psi}_i^e \quad \text{A.15}$$

where the  $\beta$  spin is indicated with a bar symbol. Using the orthonormality of the spin functions, the one-electron integrals are evaluated as follows:

$$\begin{aligned} \sum_i^N [\chi_i^e | h^e | \chi_i^e] &= \sum_i^{N/2} [\psi_i^e | h^e | \psi_i^e] + \sum_i^{N/2} [\bar{\psi}_i^e | h^e | \bar{\psi}_i^e] \\ &= 2 \sum_i^{N/2} (\psi_i^e | h^e | \psi_i^e) \end{aligned} \quad \text{A.16}$$

Similarly, for the double sums, we have:

$$\begin{aligned}
\sum_i^N \sum_j^N \chi_i^e \chi_j^e &= \sum_i^N \chi_i^e \sum_j^N \chi_j^e \\
&= \sum_i^{N/2} (\psi_i^e + \bar{\psi}_i^e) \sum_j^{N/2} (\psi_j^e + \bar{\psi}_j^e) \\
&= \sum_i^{N/2} \sum_j^{N/2} \psi_i^e \psi_j^e + \sum_i^{N/2} \sum_j^{N/2} \psi_i^e \bar{\psi}_j^e + \sum_i^{N/2} \sum_j^{N/2} \bar{\psi}_i^e \psi_j^e \\
&\quad + \sum_i^{N/2} \sum_j^{N/2} \bar{\psi}_i^e \bar{\psi}_j^e
\end{aligned} \tag{A.17}$$

Therefore, the integrals of the operator  $\frac{1}{r_{ij}}$  can be expressed as follows:

$$\begin{aligned}
&\frac{1}{2} \sum_i^N \sum_j^N ([\chi_i^e \chi_i^e | \chi_j^e \chi_j^e] - [\chi_i^e \chi_j^e | \chi_j^e \chi_i^e]) \\
&= \frac{1}{2} \left\{ \sum_i^{N/2} \sum_j^{N/2} [(\psi_i^e \psi_i^e | \psi_j^e \psi_j^e) - (\psi_i^e \psi_j^e | \psi_j^e \psi_i^e)] \right. \\
&\quad + \sum_i^{N/2} \sum_j^{N/2} [(\psi_i^e \psi_i^e | \bar{\psi}_j^e \bar{\psi}_j^e) - (\psi_i^e \bar{\psi}_j^e | \bar{\psi}_j^e \psi_i^e)] \\
&\quad + \sum_i^{N/2} \sum_j^{N/2} [(\bar{\psi}_i^e \bar{\psi}_i^e | \psi_j^e \psi_j^e) - (\bar{\psi}_i^e \psi_j^e | \psi_j^e \bar{\psi}_i^e)] \\
&\quad \left. + \sum_i^{N/2} \sum_j^{N/2} [(\bar{\psi}_i^e \bar{\psi}_i^e | \bar{\psi}_j^e \bar{\psi}_j^e) - (\bar{\psi}_i^e \bar{\psi}_j^e | \bar{\psi}_j^e \bar{\psi}_i^e)] \right\}
\end{aligned} \tag{A.18}$$



It is clear that when the bar symbol appears on one side of the two-electron integrals, the term becomes zero due to the orthogonality of the spins.

Here, we consider the PCPs in the high-spin open-shell configuration, where all the orbitals of the PCPs have the same spin state (either all have alpha spin or beta spin). All that needs to be done here is to convert the spin-orbital notation (brackets) to spatial orbital notation (parentheses). By convention, for the integrals belonging to the operator  $\frac{1}{r_{ij}}$ , we have:

$$\begin{aligned}
& \sum_{i'}^{N'} [\chi_{i'}^p | h^p | \chi_{i'}^p] + \frac{1}{2} \sum_{i'}^{N'} \sum_i^{N'} Z_{i'} Z_j \left( [\chi_{i'}^p \chi_{i'}^p | \chi_j^p \chi_j^p] \right. \\
& \quad \left. - [\chi_{i'}^p \chi_j^p | \chi_{i'}^p \chi_j^p] \right) \\
& = \sum_{i'}^{N'} h_{ii'}^p \\
& \quad + \frac{1}{2} \sum_{i'}^{N'} \sum_i^{N'} Z_{i'} Z_j \left[ (\psi_{i'}^p \psi_{i'}^p | \psi_j^p \psi_j^p) \right. \\
& \quad \left. - (\psi_{i'}^p \psi_j^p | \psi_{i'}^p \psi_j^p) \right]
\end{aligned} \tag{A.19}$$

In the final step, we need to obtain the spatial orbital notation for the electron-PCP interaction. Based on the above explanations, we can write:

$$\begin{aligned}
& \sum_i^N \sum_{i'}^{N'} [\chi_i^e \chi_i^e | \chi_{i'}^p \chi_{i'}^p] \\
&= \sum_i^{N/2} \sum_{i'}^{N'} [\psi_i^e \psi_i^e | \psi_{i'}^p \psi_{i'}^p] \\
&+ \sum_i^{N/2} \sum_{i'}^{N'} [\bar{\psi}_i^e \bar{\psi}_i^e | \psi_{i'}^p \psi_{i'}^p] \\
&= 2 \sum_i^{N/2} \sum_{i'}^{N'} (\psi_i^e \psi_i^e | \psi_{i'}^p \psi_{i'}^p)
\end{aligned} \tag{A.20}$$

Finally, the energy expression in terms of spatial orbitals is obtained as follows:

$$\begin{aligned}
E = & 2 \sum_i^{N/2} h_{ii}^e + \sum_i^{N/2} \sum_j^{N/2} [2(\psi_i^e \psi_i^e | \psi_j^e \psi_j^e) - (\psi_i^e \psi_j^e | \psi_j^e \psi_i^e)] \\
& + \sum_{i'}^{N'} h_{i'i'}^p \\
& + \frac{1}{2} \sum_{i'}^{N'} \sum_{i'}^{N'} Z_{i'} Z_{j'} [(\psi_{i'}^p \psi_{i'}^p | \psi_{j'}^p \psi_{j'}^p) \\
& - (\psi_{i'}^p \psi_{j'}^p | \psi_{i'}^p \psi_{j'}^p)] \\
& - 2 \sum_i^{\frac{N}{2}} \sum_{i'}^{N'} Z_{i'} (\psi_i^e \psi_i^e | \psi_{i'}^p \psi_{i'}^p)
\end{aligned} \tag{A.21}$$

where the integrals are defined as follows:

$$h_{ij}^e = \int dr_1 \psi_i^{e*}(1) h^e(1) \psi_j^e(1) \quad \text{A.22}$$

$$h_{ij'}^p = \int dr_1 \psi_i^{p*}(1) h^p(1) \psi_{j'}^p(1) \quad \text{A.23}$$

$$(\psi_i^e \psi_j^e | \psi_k^e \psi_l^e) = \int dr_1 \int dr_2 \psi_i^{e*}(1) \psi_j^e(1) r_{12}^{-1} \psi_k^{e*}(2) \psi_l^e(2) \quad \text{A.24}$$

### Minimizing the Energy Expression

At this stage, the energy expression (Equation A-21) is minimized simultaneously with respect to both the electronic and PCP orbitals under a suitable constraint using the Lagrange multiplier method. The appropriate constraints for applying the variational principle to the energy expression are the orthonormality of the electronic and PCP orbitals, as follows:

$$\int dr_1 \psi_i^*(1) \psi_j(1) = [\psi_i | \psi_j] = \delta_{ij} \quad \text{A.25}$$

$$\int dr_1 \psi_i'^*(1) \psi_{j'}(1) = [\psi_i' | \psi_{j'}] = \delta_{ij'} \quad \text{A.26}$$

$$[\psi_i | \psi_{j'}] - \delta_{ij'} = 0 \quad \text{A.27}$$

$$[\psi_i | \psi_j] - \delta_{ij} = 0 \quad \text{A.28}$$

The functional form of the Lagrangian is given by:

$$\begin{aligned}
\mathcal{L}[\{\psi_i^e\}, \{\psi_{i'}^p\}] &= E_0[\{\psi_i^e\}, \{\psi_{i'}^p\}] \\
&\quad - \sum_i^{N/2} \sum_j^{N/2} \varepsilon_{ij} ([\psi_i | \psi_j] - \delta_{ij}) \\
&\quad - \sum_{i'}^{N'} \sum_{j'}^{N'} \varepsilon_{i'j'} ([\psi_{i'} | \psi_{j'}] - \delta_{i'j'})
\end{aligned} \tag{A.29}$$

where  $E_0$  is the expectation value of the total wave function energy, which was finally obtained as the expression in Equation (A-21). By minimizing  $\mathcal{L}[\{\psi_i^e\}, \{\psi_{i'}^p\}]$ , with respect to the constraints and with an infinitesimal variation of the electronic and PCP orbitals as follows:

$$\psi_i^e \rightarrow \psi_i^e + \delta\psi_i^e \tag{A.30}$$

$$\psi_{i'}^p \rightarrow \psi_{i'}^p + \delta\psi_{i'}^p \tag{A.31}$$

The first variation in  $\mathcal{L}$  must be equal to zero:

$$\begin{aligned}
\delta\mathcal{L} &= \delta E_0 - 2 \sum_i^{N/2} \sum_j^{N/2} \varepsilon_{ij} \delta([\psi_i | \psi_j] - \delta_{ij}) \\
&\quad - \sum_{i'}^{N'} \sum_{j'}^{N'} \varepsilon_{i'j'} \delta([\psi_{i'} | \psi_{j'}] - \delta_{i'j'}) = 0
\end{aligned} \tag{A.32}$$

Since the variation of a constant is zero,  $\delta_{ij}$  and  $\delta_{i'j'}$  will be zero. Now, we will evaluate each term to reach the final result. By varying the overlap integrals, we obtain:

$$\delta[\psi_i | \psi_j] = [\delta\psi_i | \psi_j] + [\psi_i | \delta\psi_j] \tag{A.33}$$

$$\delta[\psi_{i'}|\psi_{j'}] = [\delta\psi_{i'}|\psi_{j'}] + [\psi_{i'}|\delta\psi_{j'}] \quad \text{A.34}$$

In the next step, by varying the energy expression, we have:

$$\begin{aligned} \delta E_0 = \delta \left\{ 2 \sum_i^{\frac{N}{2}} h_{ii}^e \right. \\ + \sum_i^{\frac{N}{2}} \sum_j^{\frac{N}{2}} [2(\psi_i^e \psi_i^e | \psi_j^e \psi_j^e) - (\psi_i^e \psi_j^e | \psi_j^e \psi_i^e)] \\ + \sum_{i'}^{N'} h_{i'i'}^p \\ + \frac{1}{2} \sum_{i'}^{N'} \sum_{j'}^{N'} Z_{i'} Z_{j'} [(\psi_{i'}^p \psi_{i'}^p | \psi_{j'}^p \psi_{j'}^p) \\ - (\psi_{i'}^p \psi_{j'}^p | \psi_{j'}^p \psi_{i'}^p)] \\ \left. - 2 \sum_i^{\frac{N}{2}} \sum_{i'}^{N'} Z_{i'} (\psi_i^e \psi_i^e | \psi_{i'}^p \psi_{i'}^p) \right\} \quad \text{A.35} \end{aligned}$$

To evaluate such a term, we need to find the complex conjugate parts and then put them all into a separate expression. Starting with  $h_i^e$ , we have:

$$\begin{aligned}
2 \sum_i^{\frac{N}{2}} \delta h_{ii}^e &= 2 \sum_i^{N/2} \delta(\psi_i^e | h_i^e | \psi_i^e) \\
&= 2 \sum_i^{N/2} [(\delta\psi_i^e | h_i^e | \psi_i^e) + (\psi_i^e | h_i^e | \delta\psi_i^e)] \\
&= 2 \sum_i^{N/2} (\delta\psi_i^e | h_i^e | \psi_i^e)
\end{aligned} \tag{A.36}$$

where the second term inside the brackets is the complex conjugate of the first one. For the subsequent terms, we obtain:

$$\begin{aligned}
\sum_i^{\frac{N}{2}} \sum_j^{\frac{N}{2}} \delta \left[ 2 \left( \psi_i^e \psi_i^e \left| \psi_j^e \psi_j^e \right. \right) - \left( \psi_i^e \psi_j^e \left| \psi_j^e \psi_i^e \right. \right) \right] \\
= 2 \sum_i^{\frac{N}{2}} \sum_j^{\frac{N}{2}} \left[ \left( \delta\psi_i^e \psi_i^e \left| \psi_j^e \psi_j^e \right. \right) + \left( \psi_i^e \delta\psi_i^e \left| \psi_j^e \psi_j^e \right. \right) \right. \\
+ \left( \psi_i^e \psi_i^e \left| \delta\psi_j^e \psi_j^e \right. \right) + \left( \psi_i^e \psi_i^e \left| \psi_j^e \delta\psi_j^e \right. \right) \Big] \\
- \sum_i^{\frac{N}{2}} \sum_j^{\frac{N}{2}} \left[ \left( \delta\psi_i^e \psi_j^e \left| \psi_j^e \psi_i^e \right. \right) + \left( \psi_i^e \delta\psi_j^e \left| \psi_j^e \psi_i^e \right. \right) \right. \\
+ \left( \psi_i^e \psi_j^e \left| \delta\psi_j^e \psi_i^e \right. \right) + \left( \psi_i^e \psi_j^e \left| \psi_j^e \delta\psi_i^e \right. \right) \Big]
\end{aligned} \tag{A.37}$$

In the first bracket (Coulomb terms), the first two terms are complex conjugates (CC) of each other, and the same is true for the next two terms, meaning:

$$\left( \delta\psi_i^e \psi_i^e \left| \psi_j^e \psi_j^e \right. \right) = \left( \psi_i^e \delta\psi_i^e \left| \psi_j^e \psi_j^e \right. \right)^* \tag{A.38}$$

$$\left(\psi_i^e \psi_i^e \middle| \delta \psi_j^e \psi_j^e\right) = \left(\psi_i^e \psi_i^e \middle| \psi_j^e \delta \psi_j^e\right)^* \quad \text{A.39}$$

Therefore:

$$\begin{aligned} & \left(\delta \psi_i^e \psi_i^e \middle| \psi_j^e \psi_j^e\right) + \left(\psi_i^e \delta \psi_i^e \middle| \psi_j^e \psi_j^e\right) + \left(\psi_i^e \psi_i^e \middle| \delta \psi_j^e \psi_j^e\right) \\ & \quad + \left(\psi_i^e \psi_i^e \middle| \psi_j^e \delta \psi_j^e\right) \\ & = \left(\delta \psi_i^e \psi_i^e \middle| \psi_j^e \psi_j^e\right) + \left(\psi_i^e \psi_i^e \middle| \delta \psi_j^e \psi_j^e\right) + \text{CC} \end{aligned} \quad \text{A.40}$$

These two terms are also equal through the change of indices in the double sum, which results in the exchange of the integral variables. In fact, since the sum over  $i$  and  $j$  of these quantities is equal, it is possible to exchange the variables in the sum (exchange  $i$  and  $j$ ) and the integral (exchange both sides of the parenthesis), therefore:

$$\left(\delta \psi_i^e \psi_i^e \middle| \psi_j^e \psi_j^e\right) = \left(\delta \psi_j^e \psi_j^e \middle| \psi_i^e \psi_i^e\right) = \left(\psi_i^e \psi_i^e \middle| \delta \psi_j^e \psi_j^e\right) \quad \text{A.41}$$

We also have:

$$\begin{aligned} & \left(\delta \psi_i^e \psi_i^e \middle| \psi_j^e \psi_j^e\right) + \left(\psi_i^e \delta \psi_i^e \middle| \psi_j^e \psi_j^e\right) + \left(\psi_i^e \psi_i^e \middle| \delta \psi_j^e \psi_j^e\right) \\ & \quad + \left(\psi_i^e \psi_i^e \middle| \psi_j^e \delta \psi_j^e\right) = 2 \left(\delta \psi_i^e \psi_i^e \middle| \psi_j^e \psi_j^e\right) + \text{CC} \end{aligned} \quad \text{A.42}$$

We can apply these manipulations to the exchange terms as well. In this way, each of the four Coulomb term expressions is identical:

$$\left(\delta \psi_i^e \psi_j^e \middle| \psi_j^e \psi_i^e\right) = \left(\delta \psi_j^e \psi_i^e \middle| \psi_i^e \psi_j^e\right) = \left(\psi_i^e \delta \psi_j^e \middle| \psi_j^e \psi_i^e\right)^* \quad \text{A.43}$$

$$(\psi_i^e \psi_j^e | \delta \psi_j^e \psi_i^e) = (\psi_j^e \psi_i^e | \delta \psi_i^e \psi_j^e) = (\psi_i^e \psi_j^e | \psi_j^e \delta \psi_i^e)^* \quad \text{A.44}$$

Therefore, we have:

$$\begin{aligned} \sum_i^{\frac{N}{2}} \sum_j^{\frac{N}{2}} & \left[ (\delta \psi_i^e \psi_j^e | \psi_j^e \psi_i^e) + (\psi_i^e \delta \psi_j^e | \psi_j^e \psi_i^e) + (\psi_i^e \psi_j^e | \delta \psi_j^e \psi_i^e) \right. \\ & \left. + (\psi_i^e \psi_j^e | \psi_j^e \delta \psi_i^e) \right] \\ & = (\delta \psi_i^e \psi_j^e | \psi_j^e \psi_i^e) + (\psi_i^e \psi_j^e | \delta \psi_j^e \psi_i^e) + \text{CC} \end{aligned} \quad \text{A.45}$$

And since:

$$(\delta \psi_i^e \psi_j^e | \psi_j^e \psi_i^e) = (\delta \psi_j^e \psi_i^e | \psi_i^e \psi_j^e) = (\psi_i^e \psi_j^e | \delta \psi_j^e \psi_i^e) \quad \text{A.46}$$

So, we have:

$$\begin{aligned} \sum_i^{\frac{N}{2}} \sum_j^{\frac{N}{2}} & \left[ (\delta \psi_i^e \psi_j^e | \psi_j^e \psi_i^e) + (\psi_i^e \delta \psi_j^e | \psi_j^e \psi_i^e) + (\psi_i^e \psi_j^e | \delta \psi_j^e \psi_i^e) \right. \\ & \left. + (\psi_i^e \psi_j^e | \psi_j^e \delta \psi_i^e) \right] \\ & = \sum_i^{\frac{N}{2}} \sum_j^{\frac{N}{2}} 2 (\delta \psi_i^e \psi_j^e | \psi_j^e \psi_i^e) + \text{CC} \end{aligned} \quad \text{A.47}$$

Ultimately, we obtain:



$$\begin{aligned}
& \sum_i^{\frac{N}{2}} \sum_j^{\frac{N}{2}} \delta \left[ 2 \left( \psi_i^e \psi_i^e \middle| \psi_j^e \psi_j^e \right) - \left( \psi_i^e \psi_j^e \middle| \psi_j^e \psi_i^e \right) \right] \\
& = 2 \sum_i^{\frac{N}{2}} \sum_j^{\frac{N}{2}} \left\{ 2 \left( \delta \psi_i^e \psi_i^e \middle| \psi_j^e \psi_j^e \right) \right. \\
& \quad \left. - \left( \delta \psi_i^e \psi_j^e \middle| \psi_j^e \psi_i^e \right) + \text{cc} \right\}
\end{aligned} \tag{A.48}$$

For the PCP terms, we also have:

$$\begin{aligned}
& \frac{1}{2} \sum_{i'}^{N'} \sum_j^{N'} Z_{i'} Z_j \delta \left[ \left( \psi_{i'}^p \psi_{i'}^p \middle| \psi_j^p \psi_j^p \right) - \left( \psi_{i'}^p \psi_j^p \middle| \psi_j^p \psi_{i'}^p \right) \right] \\
& = \sum_{i'}^{N'} \sum_j^{N'} \left[ \left( \delta \psi_{i'}^p \psi_{i'}^p \middle| \psi_j^p \psi_j^p \right) \right. \\
& \quad \left. - \left( \delta \psi_{i'}^p \psi_j^p \middle| \psi_j^p \psi_{i'}^p \right) \right]
\end{aligned} \tag{A.49}$$

And the electron-PCP operator gives:

$$\begin{aligned}
& 2 \sum_i^{\frac{N}{2}} \sum_{i'}^{N'} Z_{i'} (\psi_i^e \psi_i^e \middle| \psi_{i'}^p \psi_{i'}^p) \\
& = 2 \sum_i^{\frac{N}{2}} \sum_{i'}^{N'} (\delta \psi_i^e \psi_i^e \middle| \psi_{i'}^p \psi_{i'}^p) \\
& \quad + (\psi_i^e \delta \psi_i^e \middle| \psi_{i'}^p \psi_{i'}^p) + (\psi_i^e \psi_i^e \middle| \delta \psi_{i'}^p \psi_{i'}^p) \\
& \quad + (\psi_i^e \psi_i^e \middle| \psi_{i'}^p \delta \psi_{i'}^p)
\end{aligned} \tag{A.50}$$

On the other hand, we have:

$$(\delta\psi_i^e\psi_i^e|\psi_{i'}^p\psi_{i'}^p) = (\psi_i^e\delta\psi_i^e|\psi_{i'}^p\psi_{i'}^p)^* \quad \text{A.51}$$

$$(\psi_i^e\psi_i^e|\delta\psi_{i'}^p\psi_{i'}^p) = (\psi_i^e\psi_i^e|\psi_{i'}^p\delta\psi_{i'}^p)^* \quad \text{A.52}$$

Since the sum over  $i$  and  $i'$  for these quantities is not equal, we are not allowed to exchange variables. Therefore, ultimately, we obtain:

$$\begin{aligned} 2 \sum_i^{\frac{N}{2}} \sum_{i'}^{N'} Z_{i'} (\psi_i^e\psi_i^e|\psi_{i'}^p\psi_{i'}^p) \\ = 2 \sum_i^{\frac{N}{2}} \sum_{i'}^{N'} Z_{i'} (\delta\psi_i^e\psi_i^e|\psi_{i'}^p\psi_{i'}^p) \\ + (\psi_i^e\psi_i^e|\delta\psi_{i'}^p\psi_{i'}^p) + \text{CC} \end{aligned} \quad \text{A.53}$$

The same process applies to the integrals for PCPs. In the variation of the overlap integrals, we can exchange the dummy variables because, in these terms, we are dealing with only one electron:

$$\begin{aligned} \sum_i^{N/2} \sum_j^{N/2} \varepsilon_{ij} ([\delta\psi_i|\psi_j] + [\psi_i|\delta\psi_j]) &= 2 \sum_i^{N/2} \sum_j^{N/2} \varepsilon_{ij} [\delta\psi_i|\psi_j] \\ &+ \sum_i^{N/2} \sum_j^{N/2} \varepsilon_{ij} [\psi_i|\delta\psi_j] \\ &= 2 \left( \sum_i^{N/2} \sum_j^{N/2} \varepsilon_{ij} [\delta\psi_i|\psi_j] + \sum_i^{N/2} \sum_j^{N/2} \varepsilon_{ji} [\psi_j|\delta\psi_i] \right) \end{aligned} \quad \text{A.54}$$

$$\begin{aligned}
&= 2 \left( \sum_i^{N/2} \sum_j^{N/2} \varepsilon_{ij} [\delta\psi_i | \psi_j] + \sum_i^{N/2} \sum_j^{N/2} \varepsilon_{ij}^* [\delta\psi_i | \psi_j]^* \right) \\
&= 2 \sum_i^{N/2} \sum_j^{N/2} \varepsilon_{ij} [\delta\psi_i | \psi_j] + \text{CC}
\end{aligned}$$

By applying the same process to the overlap integrals of the PCP, we obtain:

$$\sum_{i'}^{N'} \sum_{j'}^{N'} \varepsilon_{i'j'} \delta[\psi_{i'} | \psi_{j'}] = \sum_{i'}^{N'} \sum_{j'}^{N'} \varepsilon_{i'j'} [\delta\psi_{i'} | \psi_{j'}] + \text{CC} \quad \text{A.55}$$

We can now obtain the final form of the Hartree-Fock equation. Using the results above, the final Lagrangian expression is equal to:

$$\begin{aligned}
\delta\mathcal{L} = & 2 \sum_i^{N/2} (\delta\psi_i^e | h^e | \psi_i^e) + \sum_{i'}^{N'} (\delta\psi_{i'}^p | h^p | \psi_{i'}^p) \\
& + 2 \sum_i^{\frac{N}{2}} \sum_j^{\frac{N}{2}} \{ 2(\delta\psi_i^e \psi_j^e | \psi_j^e \psi_i^e) \\
& - (\delta\psi_i^e \psi_j^e | \psi_j^e \psi_i^e) \} \\
& + \sum_{i'}^{N'} \sum_{i'}^{N'} Z_{i'} Z_{j'} [(\delta\psi_{i'}^p \psi_{i'}^p | \psi_{j'}^p \psi_{j'}^p) \\
& - (\delta\psi_{i'}^p \psi_{j'}^p | \psi_{j'}^p \psi_{i'}^p)] \\
& - 2 \sum_i^{\frac{N}{2}} \sum_{i'}^{N'} Z_{i'} (\delta\psi_i^e \psi_i^e | \psi_{i'}^p \psi_{i'}^p) \\
& - 2 \sum_i^{\frac{N}{2}} \sum_j^{\frac{N}{2}} \varepsilon_{ij} [\delta\psi_i | \psi_j] \\
& - \sum_{i'}^{N'} \sum_{j'}^{N'} \varepsilon_{i'j'} [\delta\psi_{i'} | \psi_{j'}] + \text{CC} = 0
\end{aligned} \tag{A.56}$$

where the integrals are defined as follows:

$$(\delta\psi_i^e \psi_i^e | \psi_j^e \psi_j^e) = \int dr_1^e dr_2^e \delta\psi_i^{e*}(1) \psi_i^e(1) r_{12}^{-1} \psi_j^{e*}(2) \psi_j^e(2) \tag{A.57}$$

$$(\delta\psi_i^e \psi_i^e | \psi_{i'}^p \psi_{i'}^p) = \int dr_1^e dr_2^p \delta\psi_i^{e*}(1) \psi_i^e(1) r_{12}^{-1} \psi_{i'}^{p*}(2) \psi_{i'}^p(2) \tag{A.58}$$

Due to space limitations, we will define some operators using the operators we introduced earlier. The Coulomb operators are as follows:

$$J_j^{ee}(1)\psi_i^e(1) = \left[ \int dr_2^e \psi_j^{e*}(2) \hat{V}_{NEO}^{ee} \psi_j^e(2) \right] \psi_i^e(1) \quad \text{A.59}$$

$$J_j^{pp}(1)\psi_i^p(1) = \left[ \int dr_2^p \psi_j^{p*}(2) \hat{V}_{NEO}^{pp} \psi_j^p(2) \right] \psi_i^p(1) \quad \text{A.60}$$

$$J_i^{pe}(1)\psi_i^e(1) = \left[ \int dr_2^p \psi_i^{p*}(2) \hat{V}_{NEO}^{pe} \psi_i^p(2) \right] \psi_i^e(1) \quad \text{A.61}$$

$$J_i^{ep}(1)\psi_i^p(1) = \left[ \int dr_2^e \psi_i^{e*}(2) \hat{V}_{NEO}^{ep} \psi_i^e(2) \right] \psi_i^p(1) \quad \text{A.62}$$

And the exchange operators are defined as follows:

$$K_j^e(1)\psi_i^e(1) = \left[ \int dr_2^e \psi_j^{e*}(2) \hat{V}_{NEO}^{ee} \psi_i^e(2) \right] \psi_j^e(1) \quad \text{A.63}$$

$$K_j^p(1)\psi_i^p(1) = \left[ \int dr_2^p \psi_j^{p*}(2) \hat{V}_{NEO}^{pp} \psi_i^p(2) \right] \psi_j^p(1) \quad \text{A.64}$$

Likewise, similar operators for PCPs are defined. Ultimately, we have:

$$\begin{aligned}
\delta\mathcal{L} = & 2 \sum_i^{N/2} \int dr_1^e \delta\psi_i^{e*}(1) \left[ h^e(1)\psi_i^e(1) \right. \\
& + \sum_j^{N/2} \left( 2J_j^{ee}(1) - K_j^{ee}(1) \right) \psi_i^e(1) \\
& \left. - \sum_{i'}^{N'} J_{i'}^{ep} \psi_i^e(1) - \sum_j^{N/2} \varepsilon_{ij} \psi_j^e(1) \right] \\
& + \sum_{i'}^{N'} \int dr_1^p \delta\psi_{i'}^{p*}(1) \left[ h^p(1)\psi_{i'}^p(1) \right. \\
& + \sum_{j'}^{N'} \left( J_{j'}^{pp}(1) - K_{j'}^{pp}(1) \right) \psi_{i'}^p(1) \\
& \left. - 2 \sum_i^{N/2} J_i^{pe}(1)\psi_{i'}^p(1) - \sum_{j'}^{N'} \varepsilon_{i'j'} \psi_{j'}^p(1) \right] + \text{CC} \\
& = 0
\end{aligned} \tag{A.65}$$

In the above expression, the quantities inside the brackets must be zero because  $\delta\psi_i^{e*}(1)$  and  $\delta\psi_{i'}^{p*}(1)$  are arbitrary, meaning:

$$\begin{aligned}
& \left[ h^e(1) + \sum_j^{N/2} \left( 2J_j^{ee}(1) - K_j^{ee}(1) \right) + \sum_{i'}^{N'} J_{i'}^{ep} \right] \psi_i^e(1) \\
& = \sum_j^{N/2} \varepsilon_{ij} \psi_j^e(1)
\end{aligned} \tag{A.66}$$

$$\begin{aligned}
& \left[ h^p(1) + \sum_{j'}^{N'} \left( J_{j'}^{pp}(1) - K_{j'}^{pp}(1) \right) + 2 \sum_i^{\frac{N}{2}} J_i^{pe}(1) \right] \psi_i^p(1) \\
& = \sum_{j'}^{N'} \varepsilon_{ij'} \psi_{j'}^e(1)
\end{aligned} \tag{A.67}$$

After performing a unitary transformation to diagonalize the matrices  $\varepsilon_{ij}$  and  $\varepsilon_{ij'}$ , we reach the final form of the Hartree-Fock equations:

$$f^e(1) \psi_i^e(1) = \varepsilon_i \psi_i^e(1) \tag{A.68}$$

$$f^p(1) \psi_i^p(1) = \varepsilon_i \psi_i^p(1) \tag{A.69}$$

In which  $f^e$  and  $f^p$  are called the electronic and PCP Fock operators, respectively, and are equal to the expressions inside the brackets in equations (A-66) and (A-67).

#### Roothaan Equations

We can expand the orbitals of PCPs and electrons using a series of basis functions ( $\phi_v^e$ ), which are commonly Gaussian functions. This approach transforms an integro-differential equation into a matrix equation that is easier to solve:

$$\psi_i^e(1) = \sum_v^B c_{vi}^e \phi_v^e(1) \tag{A.70}$$

$$\psi_i^p(1) = \sum_{v'}^{B'} c_{v'i}^p \phi_{v'}^p(1) \quad \text{A.71}$$

where  $B$  and  $B'$  are the number of basis functions for the electron and the PCP, respectively. By substituting the above expansions into the Hartree-Fock equations (A-68) and (A-69), we obtain the following results:

$$\sum_v^B f^e(1) c_{vi}^e \phi_v^e(1) = \varepsilon_i \sum_v^B c_{vi}^e \phi_v^e(1) \quad \text{A.72}$$

$$\sum_{v'}^{B'} f^p(1) c_{v'i}^p \phi_{v'}^p(1) = \varepsilon_{i'} \sum_{v'}^{B'} c_{v'i}^p \phi_{v'}^p(1) \quad \text{A.73}$$

By multiplying  $\phi_\mu^{e*}$  and  $\phi_\mu^{p*}$  on the left side of the above equations, respectively, and then integrating, we have:

$$\sum_v^B c_{vi}^e \int dr_1^e \phi_\mu^{e*}(1) f^e(1) \phi_v^e(1) = \varepsilon_i \sum_v^B c_{vi}^e \int \phi_\mu^{e*}(1) \phi_v^e(1) \quad \text{A.74}$$

$$\begin{aligned} \sum_{v'}^{B'} c_{v'i}^p \int dr_1^p \phi_\mu^{p*}(1) f^p(1) \phi_{v'}^p(1) \\ = \varepsilon_{i'} \sum_{v'}^{B'} c_{v'i}^p \int \phi_\mu^{p*}(1) \phi_{v'}^p(1) \end{aligned} \quad \text{A.75}$$

The above expressions can be summarized by introducing the overlap matrices and the Fock matrices as follows:



$$S_{\mu\nu}^e = \int dr_1^e \phi_\mu^{e*}(1) \phi_\nu^e(1) \quad \text{A.76}$$

$$S_{\mu'v'}^p = \int dr_1^p \phi_{\mu'}^{p*}(1) \phi_{v'}^p(1) \quad \text{A.77}$$

$$F_{\mu\nu}^e = \int dr_1^e \phi_\mu^{e*}(1) f^e(1) \phi_\nu^e(1) \quad \text{A.78}$$

$$F_{\mu'v'}^p = \int dr_1^p \phi_{\mu'}^{p*}(1) f^p(1) \phi_{v'}^p(1) \quad \text{A.79}$$

By substituting the above expressions into equations (A-68) and (A-69), we arrive at the following equations:

$$\sum_v^B F_{\mu\nu}^e c_{vi}^e = \varepsilon_i \sum_v^B c_{vi}^e S_{\mu\nu}^e \quad \text{A.80}$$

$$\sum_{v'}^{B'} F_{\mu'v'}^p c_{v'i'}^p = \varepsilon_{i'} \sum_{v'}^{B'} c_{v'i'}^p S_{\mu'v'}^p \quad \text{A.81}$$

These are the Roothaan equations. In equation (A-80) which pertains to electrons,  $c$  and  $\varepsilon$  are square matrices of size  $B \times B$  (similarly for equation A-81 for PCPs). The Fock operator can be defined using the basis function expansion. In fact, the Fock matrix is a matrix representation of the Fock operator and has the following form:

$$\begin{aligned}
F_{\mu\nu}^e &= \int dr_1^e \phi_\mu^{e*}(1) f^e(1) \phi_\nu^e(1) \\
&= \int dr_1^e \phi_\mu^{e*}(1) h^e(1) \phi_\nu^e(1) \\
&\quad + \sum_j^{N/2} \int dr_1^e \phi_\mu^{e*}(1) [2J_j^{ee}(1) - K_j^{ee}(1)] \phi_\nu^e(1) \\
&\quad + \sum_i^{N'} \int dr_1^e \phi_\mu^{e*}(1) J_i^{ep} \phi_\nu^e(1)
\end{aligned} \tag{A.82}$$

A similar equation is obtained for PCPs by following the above process:

$$\begin{aligned}
F_{\mu'\nu'}^p &= \int dr_1^p \phi_{\mu'}^{p*}(1) f^p(1) \phi_{\nu'}^p(1) \\
&= \int dr_1^p \phi_{\mu'}^{p*}(1) h^p(1) \phi_{\nu'}^p(1) \\
&\quad + \sum_j^{N'} \int dr_1^p \phi_{\mu'}^{p*}(1) [J_j^{pp}(1) - K_j^{pp}(1)] \phi_{\nu'}^p(1) \\
&\quad + \sum_i^{N/2} \int dr_1^p \phi_{\mu'}^{p*}(1) J_i^{pe} \phi_{\nu'}^p(1)
\end{aligned} \tag{A.83}$$

By defining the core Hamiltonians as follows:

$$H_{\mu\nu}^{coreE} = \int dr_1^e \phi_\mu^{e*}(1) h^e(1) \phi_\nu^e(1) \tag{A.84}$$

$$H_{\mu'\nu'}^{coreP} = \int dr_1^p \phi_{\mu'}^{p*}(1) h^p(1) \phi_{\nu'}^p(1) \tag{A.85}$$

We can write equation (A-82) as follows:

$$\begin{aligned}
F_{\mu\nu}^e &= H_{\mu\nu}^{coreE} + \sum_j^{N/2} \left[ 2 \left( \phi_\mu^e \phi_\nu^e | \psi_j^e \psi_j^e \right) - \left( \phi_\mu^e \psi_j^e | \psi_j^e \phi_\nu^e \right) \right] \\
&\quad - 2 \sum_i^{N'} Z_{i'} \left( \phi_\mu^e \phi_\nu^e | \psi_{i'}^p \psi_{i'}^p \right)
\end{aligned} \tag{A.86}$$

By substituting the basis functions  $\sigma$  and  $\lambda$  into the above expression, we have:

$$\begin{aligned}
F_{\mu\nu}^e &= H_{\mu\nu}^{core} + \sum_j^{N/2} \sum_{\sigma\lambda}^B c_{\lambda j}^e c_{\sigma j}^{e*} \left[ 2 \left( \phi_\mu^e \phi_\nu^e | \phi_\sigma^e \phi_\lambda^e \right) \right. \\
&\quad \left. - \left( \phi_\mu^e \phi_\lambda^e | \phi_\sigma^e \phi_\nu^e \right) \right] \\
&\quad - 2 \sum_i^{N'} \sum_{\sigma'\lambda'}^{B'} Z_{i'} c_{\lambda i'}^p c_{\sigma i'}^{p*} \left( \phi_\mu^e \phi_\nu^e | \psi_{\sigma'}^p \psi_{\lambda'}^p \right) \\
&= H_{\mu\nu}^{coreE} + G_{\mu\nu}^e - \sum_{\lambda'\sigma'}^{B'} P_{\lambda'\sigma'}^p \left( \phi_\mu^e \phi_\nu^e | \psi_{\sigma'}^p \psi_{\lambda'}^p \right)
\end{aligned} \tag{A.87}$$

By following the same procedure for the equations of PCPs, we obtain:

$$\begin{aligned}
F_{\mu'v'}^p &= H_{\mu'v'}^{coreP} + \sum_{j'}^{N'} \sum_{\sigma'\lambda'}^{B'} Z_{j'} c_{\lambda j'}^p c_{\sigma j'}^{p*} [(\phi_{\mu'}^p \phi_{v'}^p | \phi_{\sigma'}^p \phi_{\lambda'}^p) \\
&\quad - (\phi_{\mu'}^p \phi_{\lambda'}^p | \phi_{\sigma'}^p \phi_{v'}^p)] \\
&\quad - \sum_{i'}^{N'} \sum_{\sigma\lambda}^B Z_{i'} c_{\lambda i'}^e c_{\sigma i'}^{e*} (\phi_{\mu'}^p \phi_{v'}^p | \psi_{\sigma}^e \psi_{\lambda}^e) \\
&= H_{\mu'v'}^{coreP} + G_{\mu'v'}^p - \sum_{\lambda\sigma}^B P_{\lambda\sigma}^e (\phi_{\mu'}^p \phi_{v'}^p | \psi_{\sigma}^e \psi_{\lambda}^e)
\end{aligned} \tag{A.88}$$

where

$$G_{\mu v}^p = \sum_{\sigma\lambda}^B P_{\lambda\sigma}^p \left[ (\phi_{\mu}^p \phi_v^p | \phi_{\sigma}^p \phi_{\lambda}^p) - \frac{1}{2} (\phi_{\mu}^p \phi_{\lambda}^p | \phi_{\sigma}^p \phi_v^p) \right] \tag{A.89}$$

$$G_{\mu'v'}^p = Z_{i'} \sum_{\sigma'\lambda'}^{B'} P_{\sigma'\lambda'}^p [(\phi_{\mu'}^p \phi_{v'}^p | \phi_{\sigma'}^p \phi_{\lambda'}^p) - (\phi_{\mu'}^p \psi_{\sigma'}^p | \phi_{v'}^p \psi_{\lambda'}^p)] \tag{A.90}$$

In these expressions, the new quantities  $P_{v\mu}^e$  and  $P_{v'\mu'}^p$ , called the density matrices, are defined as follows:

$$P_{v\mu}^e = 2 \sum_i^{N/2} c_{vi}^e c_{\mu i}^{e*} \tag{A.91}$$

$$P_{v'\mu'}^p = \sum_{i'}^{N'} Z_{i'} c_{v'i'}^p c_{\mu'i'}^{p*} \tag{A.92}$$

The factor of 2 appearing in the electronic density matrix arises from the transition of spin-orbitals to closed-shell spatial orbitals.

Equations (A-87) and (A-88) represent the final forms of the electronic and PCP Fock operators, respectively, expanded using the basis functions. Therefore, the derivation of the multi-component Hartree-Fock equations concludes here. These equations show that the electronic (PCP) Fock matrix also includes the PCP (electronic) density matrix; hence, they are sometimes referred to as coupled Hartree-Fock equations.

The mathematical framework presented here forms the theoretical foundation of the multi-component Hartree-Fock method. However, for coding this framework, specific mathematical techniques are employed to further simplify the calculations, especially the two-particle integrals, which can be found in references [165], [166], [175], [176], [167]–[174].

## 8 Appendix B

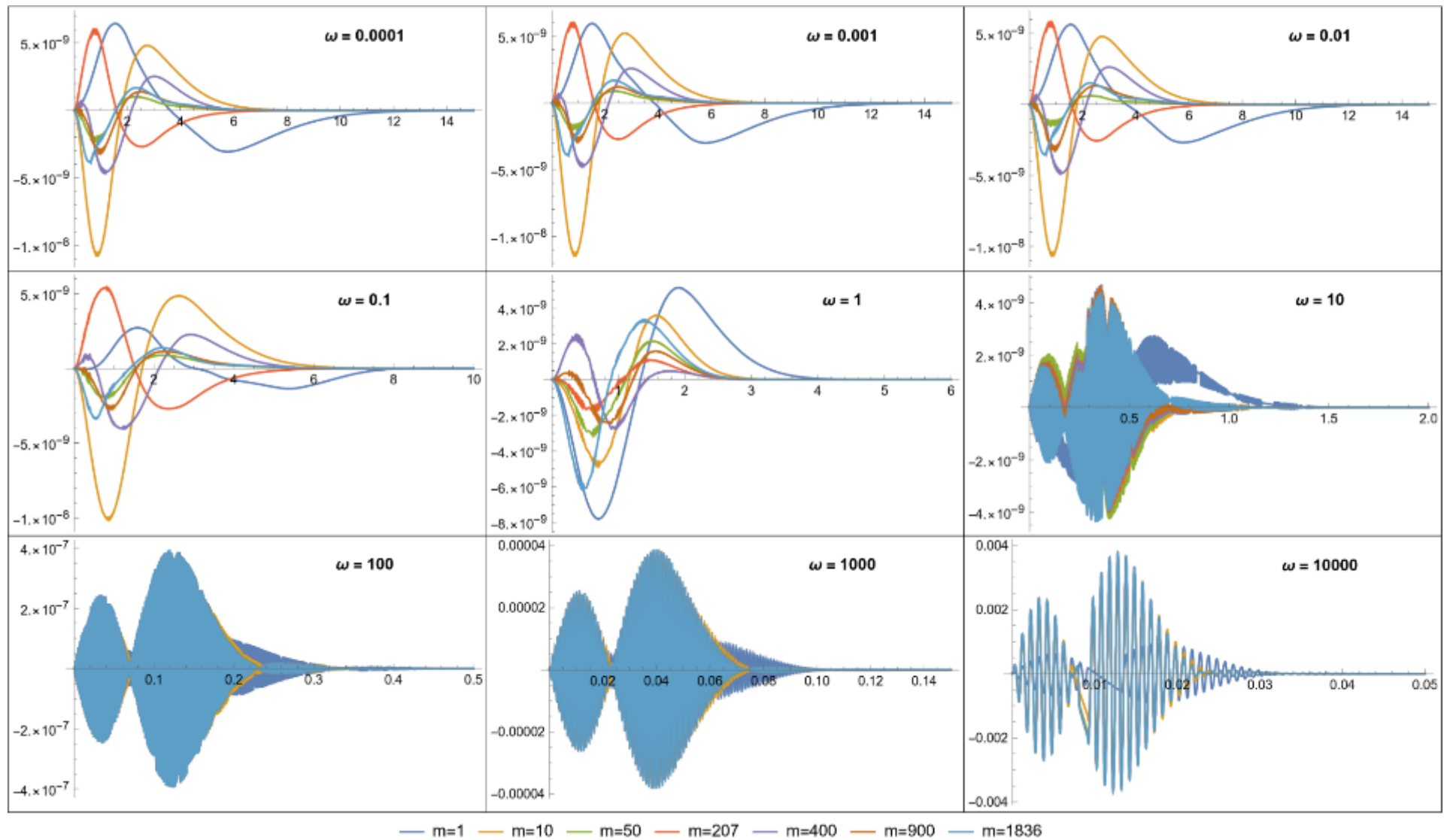


Figure B-1: Energy difference using the finite element method for two mesh sizes, 0.001 and 0.0001. This difference becomes significant only at a frequency of 10,000, therefore, a mesh size of 0.0001 was used at this frequency.

Table B-1: Variational parameters, variational energy of relative motion, and their errors for wavefunction (2-75)

$\omega$ /Quantities	$\alpha''^1$	$\beta''^2$	Variational Energy <sup>3</sup>	FEM Energy <sup>4</sup>	$\Delta E^5$	%error <sup>6</sup>
m = 1						
0.0001	0.999996	1.000002	-0.250000	-0.250000	0.000000	0.000000
0.001	0.999989	1.000012	-0.249997	-0.249997	0.000000	0.000000
0.01	1.000314	1.000458	-0.249700	-0.249701	0.000000	-0.000070
0.1	0.919436	1.091479	-0.223717	-0.223957	-0.000240	-0.106998
1.0	1.103504	1.559082	0.614439	0.611853	-0.002587	0.422747
10	5.476005	1.851585	12.398910	12.395303	-0.003607	0.029097
100	48.724976	1.952538	141.945987	141.942127	-0.003861	0.002720
1000	487.383633	1.984942	1474.694360	1474.690429	-0.003931	0.000267
10000	4932.850820	1.995251	14920.137495	14920.135808	-0.001687	0.000011
m = 10						
0.0001	0.999987	1.000010	-0.454545	-0.454545	0.000000	0.000000
0.001	0.999988	1.000012	-0.454544	-0.454544	0.000000	0.000000
0.01	0.999794	1.000429	-0.454381	-0.454381	0.000000	-0.000003
0.1	0.985483	1.035773	-0.438836	-0.438923	-0.000088	-0.019938
1.0	1.183071	1.434114	0.254978	0.251315	-0.003663	1.457446
10	5.325488	1.801301	11.453381	11.447087	-0.006295	0.054991
100	47.379844	1.936102	139.103860	139.096910	-0.006950	0.004997
1000	480.153146	1.979707	1465.842722	1465.835599	-0.007123	0.000486
10000	4900.246695	1.993594	14892.278556	14892.271372	-0.007183	0.000048
m = 50						



0.0001	0.999985	1.000012	-0.490196	-0.490196	0.000000	0.000000
0.001	0.999986	1.000014	-0.490195	-0.490195	0.000000	0.000000
0.01	0.999847	1.000372	-0.490043	-0.490043	0.000000	-0.000002
0.1	0.989384	1.031384	-0.475538	-0.475612	-0.000075	-0.015672
1.0	1.190500	1.417222	0.198722	0.194935	-0.003787	1.942556
10	5.297276	1.793893	11.310715	11.303970	-0.006745	0.059668
100	47.164546	1.933659	138.679004	138.671520	-0.007484	0.005397
1000	487.383633	1.984942	1474.694360	1474.690429	-0.003931	0.000267
10000	4895.212995	1.993348	14888.128524	14888.120778	-0.007746	0.000052
m = 207						
0.0001	0.999985	1.000013	-0.497596	-0.497596	0.000000	0.000000
0.001	0.999986	1.000014	-0.497595	-0.497595	0.000000	0.000000
0.01	0.999857	1.000361	-0.497446	-0.497446	0.000000	-0.000002
0.1	0.990073	1.030571	-0.483139	-0.483212	-0.000072	-0.014930
1.0	1.191882	1.413851	0.187213	0.183403	-0.003810	2.077655
10	5.291400	1.792392	11.281699	11.274861	-0.006838	0.060645
100	47.120482	1.933164	138.592722	138.585127	-0.007595	0.005480
1000	478.795133	1.978769	1464.255161	1464.247368	-0.007792	0.000532
10000	4894.205763	1.993299	14887.286169	14887.278307	-0.007863	0.000053
m = 400						
0.0001	0.999985	1.000013	-0.498753	-0.498753	0.000000	0.000000
0.001	0.999986	1.000014	-0.498752	-0.498752	0.000000	0.000000
0.01	0.999856	1.000361	-0.498603	-0.498603	0.000000	-0.000002

0.1	0.990178	1.030446	-0.484327	-0.484399	-0.000072	-0.014818
1.0	1.192093	1.413328	0.185419	0.181605	-0.003814	2.100237
10	5.290481	1.792159	11.277180	11.270328	-0.006852	0.060797
100	47.113599	1.933086	138.579288	138.571677	-0.007612	0.005493
1000	478.759328	1.978744	1464.213456	1464.205645	-0.007810	0.000533
10000	4894.031446	1.993290	14887.155037	14887.147157	-0.007881	0.000053
m = 900						
0.0001	0.999985	1.000013	-0.499445	-0.499445	0.000000	0.000000
0.001	0.999986	1.000014	-0.499444	-0.499444	0.000000	0.000000
0.01	0.999857	1.000360	-0.499295	-0.499295	0.000000	-0.000002
0.1	0.990240	1.030372	-0.485038	-0.485109	-0.000072	-0.014752
1.0	1.192219	1.413015	0.184346	0.180530	-0.003816	2.113946
10	5.289932	1.792020	11.274480	11.267619	-0.006861	0.060889
100	47.109533	1.933041	138.571262	138.563640	-0.007622	0.005501
1000	478.738007	1.978729	1464.188536	1464.180715	-0.007821	0.000534
10000	4893.940977	1.993286	14887.076684	14887.068793	-0.007892	0.000053
m = 1836						
0.0001	0.999985	1.000013	-0.499728	-0.499728	0.000000	0.000000
0.001	0.999986	1.000014	-0.499726	-0.499726	0.000000	0.000000
0.01	0.999858	1.000359	-0.499578	-0.499578	0.000000	-0.000002
0.1	0.990265	1.030342	-0.485328	-0.485400	-0.000071	-0.014725
1.0	1.192270	1.412888	0.183908	0.180091	-0.003817	2.119593
10	5.289708	1.791963	11.273377	11.266512	-0.006864	0.060926

100	47.107820	1.933022	138.567983	138.560357	-0.007626	0.005504
1000	478.740821	1.978733	1464.178358	1464.170533	-0.007825	0.000534
10000	4893.907688	1.993284	14887.044681	14887.036785	-0.007896	0.000053

1. Variational parameter  $\alpha''$
2. Variational parameter  $\beta''$
3. Variational energy of the Hamiltonian for the relative motion of the system using parameters 1 and 2
4. FEM energy of the Hamiltonian for the relative motion of the system using parameters 1 and 2
5. Energy difference between 3 and 4
6. Percentage error of the variational energy relative to the FEM energy of the Hamiltonian for relative motion

Table B-2: Coefficients and exponents of MC-HF basis set [7s:1s]: the top and bottom rows for each frequency respectively represent the absolute values of the sorted coefficients (from largest to smallest) and their corresponding exponents.

Sorted electron and PC coefficients and corresponding exponents								
m = 1								
$\omega$ / basis set	1s	2s	3s	4s	5s	6s	7s	1s
0.0001	0.319802	0.318093	0.223462	0.125915	0.051273	0.004274	0.001406	1
	0.056193	0.032409	0.024091	0.014230	0.100768	0.110112	0.005600	0.036377
0.001	0.480059	0.309318	0.150645	0.070601	0.023273	0.011134	-0.000783	1
	0.037353	0.019479	0.065922	0.079692	0.009443	0.134079	0.148314	0.036377
0.01	0.751009	0.264841	0.233746	0.006087	0.000389	-0.000569	-0.213076	1
	0.036651	0.071272	0.017227	0.177794	0.914376	0.753855	0.041752	0.037689
0.1	0.426653	0.264646	0.260619	0.111251	0.005225	-0.001106	-0.044230	1
	0.074259	0.052490	0.109068	0.174970	0.351791	0.443185	0.045903	0.085144
1	0.700127	0.131542	0.121834	0.051798	0.002541	0.000003	-0.000031	1
	0.541680	0.763898	0.465139	1.102035	1.931633	16.317160	5.419529	0.577278
10	0.830460	0.110435	0.059221	0.005317	0.001988	-0.000579	-0.004335	1
	5.124563	4.764844	7.859766	19.733625	36.104344	44.263938	26.246875	5.220210
100	0.797798	0.238146	0.006739	0.000421	-0.000235	-0.002480	-0.039593	1
	51.759766	44.683125	127.570625	346.082500	402.562500	165.378125	39.371875	50.674434
1000	0.814668	0.189003	0.001467	0.000294	-0.000020	-0.000423	-0.004737	1
	508.465772	469.819336	1205.078125	3008.703125	5038.538281	2522.270313	372.322266	502.112311
10000	0.797600	0.211149	0.000917	0.000025	-0.000094	-0.001887	-0.007633	1
	5094.914424	4643.193124	15178.937500	64174.160156	37568.828125	10588.718750	3577.812500	5006.657809

m = 1.5								
$\omega$ /basis set	1s	2s	3s	4s	5s	6s	7s	1s
0.0001	0.521302	0.339283	0.202026	0.019858	0.012632	-0.007539	-0.036752	1
	0.053282	0.025131	0.120039	0.010869	0.368693	0.428893	0.160714	0.060120
0.001	0.324401	0.265691	0.232998	0.145646	0.048941	0.029086	0.003973	1
	0.059814	0.025981	0.040329	0.102216	0.014165	0.142455	0.226510	0.060120
0.01	0.356345	0.285918	0.236219	0.144662	0.026523	0.000002	-0.000098	1
	0.035385	0.054391	0.093414	0.018956	0.177684	6.886778	0.598310	0.061722
0.1	0.472133	0.234186	0.146582	0.112009	0.065784	0.000671	0.000041	1
	0.074259	0.120849	0.155439	0.052560	0.264653	0.508041	1.202818	0.127792
1	0.638380	0.173114	0.116400	0.070425	0.013669	0.000007	-0.000070	1
	0.541680	0.763898	0.473410	1.129379	1.871389	11.357029	3.806633	0.856476
10	0.890747	0.068393	0.035699	0.009586	0.000073	-0.000006	-0.000490	1
	5.124563	7.981836	4.452344	14.733625	37.888938	73.121875	21.104344	7.794067
100	0.808387	0.213605	0.009387	0.001201	-0.000271	-0.001348	-0.029671	1
	51.759766	44.683125	114.070625	271.082500	352.562500	215.378125	38.871875	75.891419
1000	0.790644	0.212843	0.002496	0.000164	-0.000015	-0.000255	-0.005466	1
	509.904736	469.819336	1189.453125	3008.703125	5038.538281	2342.582813	372.322266	752.781105
10000	0.662884	0.360082	0.003146	0.000148	0.000001	-0.000040	-0.026090	1
	5145.921875	4679.678223	2833.828125	26213.718750	311428.937500	45381.328125	3643.312500	7508.756638
m = 2								
$\omega$ /basis set	1s	2s	3s	4s	5s	6s	7s	1s
0.0001	0.474146	0.276934	0.248649	0.027532	0.027172	0.001241	-0.000085	1

	0.056193	0.028325	0.113935	0.014342	0.224923	0.032409	0.795639	0.084515
0.001	0.360990	0.328335	0.172251	0.142398	0.031848	0.020079	-0.000352	1
	0.070260	0.040329	0.128173	0.025004	0.015502	0.234052	0.359868	0.084515
0.01	0.481508	0.375742	0.165785	0.040314	0.004777	-0.000917	-0.012412	1
	0.069488	0.032943	0.153319	0.015706	0.445993	0.745799	0.227522	0.086327
0.1	0.459492	0.373823	0.080416	0.058739	0.055216	0.011088	-0.001075	1
	0.112715	0.064190	0.261459	0.204772	0.196330	0.462646	0.357736	0.169869
1	0.636545	0.185479	0.086305	0.081854	0.024910	0.000411	-0.000128	1
	0.541680	0.763898	1.129379	0.465139	1.931633	3.919529	2.817160	1.130886
10	0.876809	0.080993	0.035215	0.015527	0.000684	-0.000224	-0.003713	1
	5.124563	8.044336	4.514844	16.733625	37.888938	48.121875	21.104344	10.350143
100	0.802263	0.203540	0.012380	0.001445	0.000366	-0.001273	-0.017001	1
	51.759766	45.183125	108.508125	290.378125	402.562500	346.082500	37.934375	101.049347
1000	0.783587	0.219261	0.003230	0.000156	-0.000018	-0.000163	-0.005505	1
	510.465772	469.819336	1200.171875	3008.703125	5038.538281	2217.582813	372.322266	1003.262711
10000	1.004939	0.007057	0.000755	0.000617	0.000000	-0.000383	-0.012811	1
	4988.695801	7032.808594	3169.476563	21445.593750	312053.937500	23662.578125	4234.875000	10010.263443
m = 3								
$\omega$ /basis set	1s	2s	3s	4s	5s	6s	7s	1s
0.0001	0.352795	0.351487	0.158219	0.107902	0.051423	0.037391	0.003306	1
	0.048034	0.088627	0.154855	0.028849	0.250654	0.019272	0.426940	0.133343
0.001	0.417539	0.367490	0.109416	0.106654	0.045026	0.012869	0.003496	1
	0.047378	0.096113	0.205571	0.022998	0.130126	0.249948	0.466673	0.133343

0.01	0.426570	0.369535	0.132757	0.127499	0.004831	0.001125	-0.000455	1
	0.051072	0.102752	0.025131	0.207685	0.443309	0.531743	0.789122	0.135727
0.1	0.470043	0.220474	0.174890	0.157130	0.031048	0.022885	-0.029553	1
	0.120849	0.253972	0.063578	0.070871	0.615463	1.094420	1.034345	0.252075
1	0.562292	0.190519	0.144298	0.076475	0.044051	0.003650	-0.000488	1
	0.541680	0.701398	1.053207	0.465139	1.980461	4.035910	5.419529	1.670284
10	0.879206	0.088949	0.016960	0.016570	0.005163	0.000514	-0.000022	1
	5.124563	7.981836	14.233625	4.264844	21.104344	37.888938	73.121875	15.430786
100	0.766365	0.220560	0.015879	0.003209	0.000687	-0.000018	-0.004279	1
	51.759766	46.433125	97.570625	165.378125	271.082500	402.562500	34.871875	151.265259
1000	0.763792	0.241446	0.004179	0.000389	0.000150	-0.000276	-0.008912	1
	511.465772	469.819336	1188.453125	3258.703125	5717.582813	5038.538281	387.947266	1503.905487
10000	0.760091	0.288561	0.005070	0.000417	0.000001	-0.000048	-0.053849	1
	5137.421875	4475.678223	2834.828125	22866.218750	312053.937500	45381.328125	3685.812500	15012.256622
m = 10								
$\omega$ /basis set	1s	2s	3s	4s	5s	6s	7s	1s
0.0001	0.388898	0.329896	0.176012	0.147766	0.028571	0.012238	-0.000179	1
	0.086591	0.175541	0.043527	0.364731	0.757365	0.021117	0.610533	0.447388
0.001	2.555506	0.293038	-0.060568	-0.150463	-0.411872	-0.848858	-2.459807	1
	0.108504	0.474365	0.686081	0.037615	0.424077	0.146650	0.099557	0.447578
0.01	0.415687	0.406983	0.167362	0.156054	0.021592	0.005461	-0.090118	1
	0.086591	0.190434	0.041656	0.383605	0.822250	0.017405	0.242013	0.453301
0.1	0.404281	0.271201	0.267376	0.105556	0.017807	0.007462	0.000014	1

	0.144286	0.289291	0.078166	0.614083	1.291197	0.042851	6.323408	0.782700
1	0.630393	0.249179	0.082967	0.054674	0.024589	0.001483	-0.005450	1
	0.568586	1.004379	2.153098	0.440725	4.763279	10.213555	4.212883	5.316467
10	0.829252	0.118976	0.029841	0.029229	0.011795	0.001256	-0.006822	1
	5.124563	8.103906	17.672735	4.721738	48.104618	79.585498	55.578330	50.645339
100	0.882683	0.218492	0.019251	0.003494	0.000455	-0.000157	-0.119803	1
	51.759766	40.288594	119.786735	307.714275	877.660156	1092.135938	38.145450	501.753938
1000	0.887617	0.146405	0.005756	0.001340	0.000252	-0.000491	-0.039470	1
	508.923535	438.920288	1218.406787	3327.916992	6214.843750	4413.538281	401.619141	5005.275726
10000	0.833737	0.184573	0.004061	0.001111	0.000141	0.000001	-0.023176	1
	5094.898033	4498.830078	2833.828125	16863.132813	47646.953125	161858.625000	3480.156250	50016.428232
m = 50								
$\omega$ / basis set	1s	2s	3s	4s	5s	6s	7s	1s
0.0001	0.429978	0.336113	0.160200	0.141464	0.054536	0.003005	-0.018707	1
	0.123092	0.286850	0.052706	0.676339	1.524596	3.391279	1.397221	1.722260
0.001	0.428235	0.335157	0.161103	0.142172	0.041051	0.005194	-0.006336	1
	0.123168	0.285690	0.052836	0.670724	1.609252	3.063154	2.164555	1.722260
0.01	0.426080	0.334006	0.161343	0.141930	0.037014	0.003866	0.002352	1
	0.123603	0.285354	0.053321	0.662423	1.488774	2.335997	3.457685	1.750488
0.1	0.358258	0.321585	0.181824	0.154887	0.067386	0.015595	0.003122	1
	0.144286	0.287338	0.614083	0.077922	1.390807	2.956547	5.167158	3.323288
1	0.584607	0.281076	0.107669	0.040117	0.032969	0.007394	0.000585	1
	0.568586	1.005905	2.257712	0.440725	5.776848	15.849297	40.966404	25.532837



10	0.942087	0.133246	0.035496	0.009349	0.002003	0.000164	-0.103743	1
	5.124563	8.103906	18.268781	48.067234	137.109607	374.342063	5.253125	250.824745
100	0.896380	0.267331	0.021409	0.004474	0.000936	0.000114	-0.184690	1
	51.759766	38.823750	123.425956	338.338665	995.137573	2831.882031	37.418750	2502.048564
1000	0.911749	0.135577	0.006065	0.001194	0.000227	0.000019	-0.052943	1
	508.923535	420.991211	1321.022144	3801.050488	11772.705078	34590.734375	390.251343	25005.971909
10000	0.829951	0.185719	0.003163	0.001352	0.000239	0.000035	-0.019860	1
	5094.921875	4525.685547	2833.828125	16994.968750	54521.953125	187210.187500	3499.687500	250018.472672
m = 207								
$\omega$ /basis set	1s	2s	3s	4s	5s	6s	7s	1s
0.0001	0.384872	0.349120	0.176316	0.126117	0.063879	0.018202	0.003192	1
	0.128112	0.290756	0.666574	0.056193	1.522643	3.336591	6.865971	4.733582
0.001	0.384333	0.348393	0.176602	0.126459	0.064362	0.018336	0.003213	1
	0.128173	0.290329	0.664010	0.056254	1.515502	3.328779	6.852055	4.735107
0.01	0.383444	0.347966	0.177153	0.125943	0.065187	0.018876	0.003340	1
	0.128570	0.290756	0.663400	0.056590	1.511778	3.332685	6.957524	4.883118
0.1	0.332073	0.331309	0.207517	0.115229	0.095650	0.031774	0.005999	1
	0.289291	0.144286	0.614083	0.078166	1.421568	3.698408	10.764653	11.928101
1	0.577244	0.286546	0.115459	0.038367	0.031301	0.010332	0.001800	1
	0.568586	1.004379	2.254660	5.898918	0.428518	17.826836	64.110936	104.179688
10	0.928031	0.135150	0.037035	0.010388	0.002578	0.000436	-0.093366	1
	5.124563	8.103906	18.268781	49.038075	153.392642	577.238181	5.253125	1035.908413
100	0.896466	0.264013	0.022122	0.004789	0.001058	0.000168	-0.182197	1

	51.759766	38.823750	123.664375	351.896099	1177.358032	4839.816602	37.418750	10352.169991
1000	0.914321	0.116832	0.006144	0.001224	0.000254	0.000038	-0.036783	1
	508.983140	420.991211	1350.395313	4070.520703	14005.371094	56582.921875	382.087891	103506.202698
10000	0.831705	0.190324	0.002972	0.001365	0.000238	0.000034	-0.025996	1
	5098.259735	4486.623047	2833.828125	17886.997559	65585.185547	314348.859375	3593.071289	1035019.111633
m = 400								
$\omega$ /basis set	1s	2s	3s	4s	5s	6s	7s	1s
0.0001	0.372058	0.355170	0.185951	0.113121	0.072028	0.023719	0.004821	1
	0.128112	0.290756	0.666574	0.056437	1.522643	3.492841	8.368901	7.275696
0.001	0.371008	0.354149	0.186814	0.113562	0.072696	0.023936	0.004713	1
	0.128173	0.289840	0.663034	0.056498	1.515502	3.500654	8.447270	7.279511
0.01	0.370070	0.353460	0.187261	0.112953	0.074224	0.024426	0.004799	1
	0.128570	0.290268	0.661447	0.056834	1.511778	3.535810	8.647954	7.615204
0.1	0.340196	0.309990	0.228335	0.110706	0.099598	0.030297	0.005471	1
	0.283931	0.143810	0.627618	0.079142	1.583876	4.586286	15.514592	21.950836
1	0.550809	0.298031	0.116308	0.050487	0.036292	0.009042	0.001493	1
	0.568586	1.008957	2.372916	0.463613	6.649650	22.038262	91.259373	200.734253
10	0.842814	0.127762	0.035518	0.010841	0.002920	0.000629	0.000083	1
	5.121582	8.293687	18.177229	46.449803	137.483447	462.476828	1631.717969	2000.933838
100	0.902013	0.252253	0.021919	0.004594	0.000974	0.000149	-0.175394	1
	51.759766	38.341191	126.821037	376.695446	1348.821045	6345.065625	36.930469	20002.161980
1000	0.812100	0.180735	0.007367	0.001467	0.000319	0.000062	0.000008	1
	508.923535	475.331574	1207.815170	3531.334033	11519.251172	40606.697266	147930.578125	200006.122589

10000	1.001042	0.003257	0.001313	0.000648	0.000143	0.000025	-0.005777	1
	5005.264568	9891.114471	3840.908203	27583.347656	93388.166016	433203.593750	4630.668945	2000018.310547
m = 900								
$\omega$ /basis set	1s	2s	3s	4s	5s	6s	7s	1s
0.0001	0.359796	0.359360	0.195998	0.102762	0.081234	0.027364	0.005330	1
	0.128112	0.290268	0.666574	0.056681	1.561614	3.944868	11.159916	12.044067
0.001	0.359450	0.358300	0.196746	0.103016	0.081827	0.027189	0.005315	1
	0.128173	0.289840	0.664010	0.056742	1.562102	3.959944	11.161625	12.051697
0.01	0.356834	0.355530	0.197377	0.105719	0.083521	0.027914	0.005407	1
	0.129546	0.290756	0.662423	0.057810	1.558562	4.007734	11.611943	13.013001
0.1	0.378321	0.321745	0.227120	0.088628	0.083929	0.024734	0.004307	1
	0.296030	0.138427	0.716211	1.960982	0.075497	6.237104	24.382939	47.368164
1	0.605674	0.305034	0.102249	0.034542	0.012201	0.003185	0.000505	1
	0.558167	1.047342	2.464087	5.880607	15.580742	51.417287	215.575779	450.780029
10	0.842907	0.127864	0.035649	0.010799	0.002856	0.000611	0.000087	1
	5.122201	8.311807	18.342214	47.823094	146.932452	531.866171	2278.690625	4500.905228
100	0.909988	0.288465	0.021206	0.004241	0.000862	0.000127	-0.218327	1
	51.789926	37.126210	132.390495	412.837795	1565.564514	8312.106641	35.965350	45002.138138
1000	0.820272	0.172740	0.007264	0.001413	0.000309	0.000066	0.000012	1
	508.923535	474.082260	1229.969025	3650.962940	11772.852246	40889.900391	168457.921875	450006.122589
10000	0.982866	0.046181	0.016577	0.000303	0.000035	-0.010655	-0.034658	1
	5094.916511	3577.812500	10432.468750	62649.640625	390850.078125	2833.828125	8197.388886	4500018.310547
m = 1836								

$\omega$ /basis set	1s	2s	3s	4s	5s	6s	7s	1s
0.0001	0.357678	0.351737	0.206584	0.099427	0.087382	0.027318	0.005037	1
	0.289802	0.129089	0.667527	0.057292	1.649001	4.568952	14.486577	18.414612
0.001	0.354395	0.347732	0.207895	0.101077	0.090344	0.028465	0.005238	1
	0.286922	0.129150	0.653268	0.057719	1.601073	4.459760	14.256108	18.437500
0.01	0.361614	0.348298	0.208746	0.096891	0.087817	0.027372	0.005093	1
	0.289291	0.128570	0.672120	0.057441	1.675383	4.710493	15.363774	20.878906
0.1	0.397827	0.354195	0.216193	0.077677	0.061671	0.020193	0.003338	1
	0.316156	0.136905	0.813279	2.361521	0.069388	8.094007	35.748051	94.456787
1	0.610738	0.305425	0.102108	0.032507	0.010123	0.002524	0.000404	1
	0.559455	1.064460	2.591307	6.667961	18.931572	65.540822	303.661717	918.828125
10	0.841922	0.128848	0.036014	0.010652	0.002769	0.000578	0.000082	1
	5.121247	8.294641	18.478113	49.214028	155.437320	599.111655	2956.180859	9180.938721
100	0.911097	0.086886	0.021078	0.004115	0.000802	0.000114	-0.017506	1
	51.789926	39.014247	134.497162	432.245067	1719.838501	9867.160352	32.098439	91802.234650
1000	0.816580	0.176323	0.007324	0.001452	0.000323	0.000070	0.000011	1
	508.923535	474.654465	1217.590332	3572.168652	11576.530566	42252.205078	205948.156250	918006.134033
10000	0.983239	0.045958	0.016368	0.000305	0.000035	-0.010581	-0.034672	1
	5094.920813	3577.812500	10432.430603	63245.343750	414600.078125	2833.828125	8168.263672	9180018.615723

## 9 Appendix C

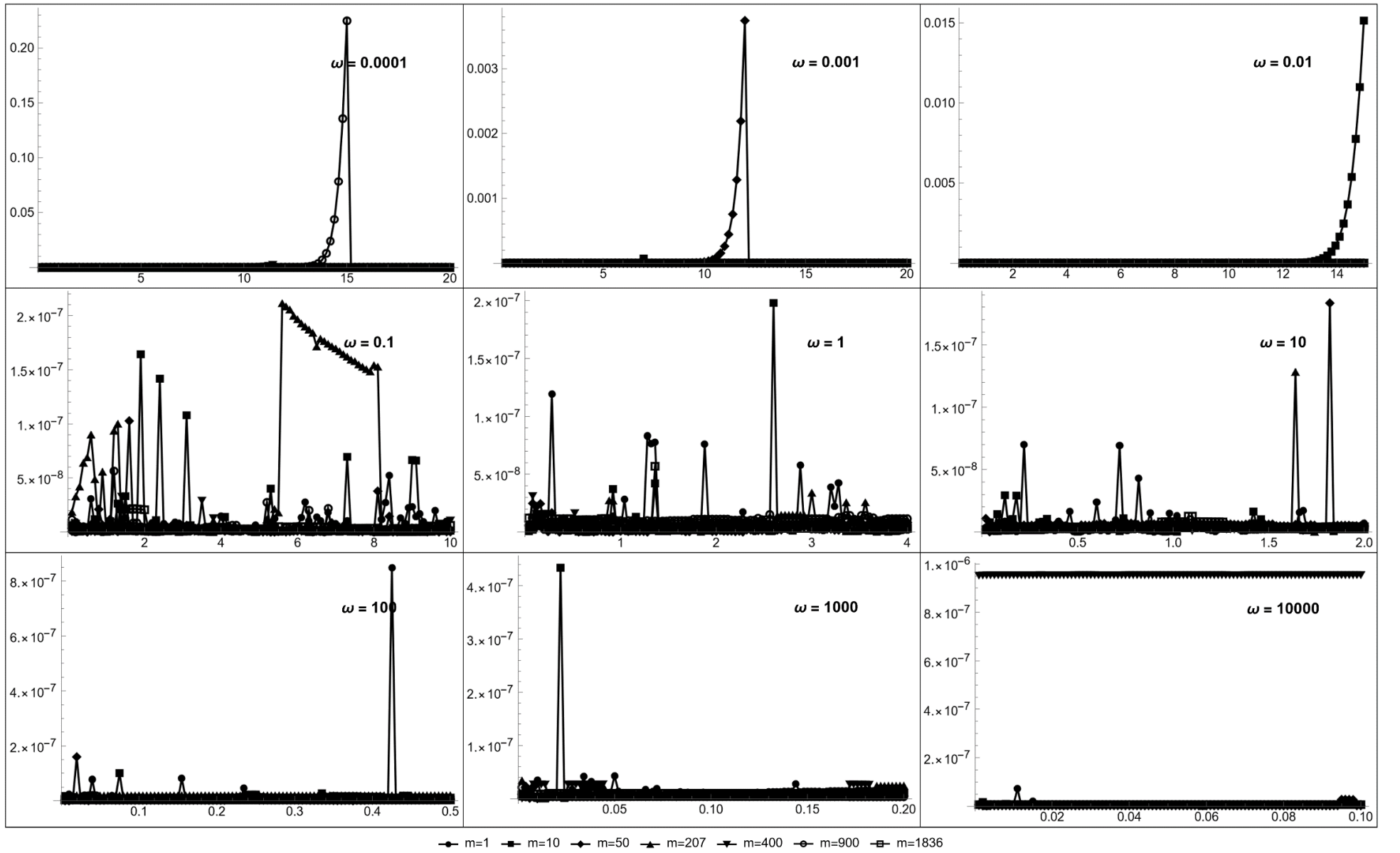


Figure C-1: Percentage error of analytical electron density from equation (2-168) relative to FEM density from equation (2-161) versus  $r_e$  for different frequencies

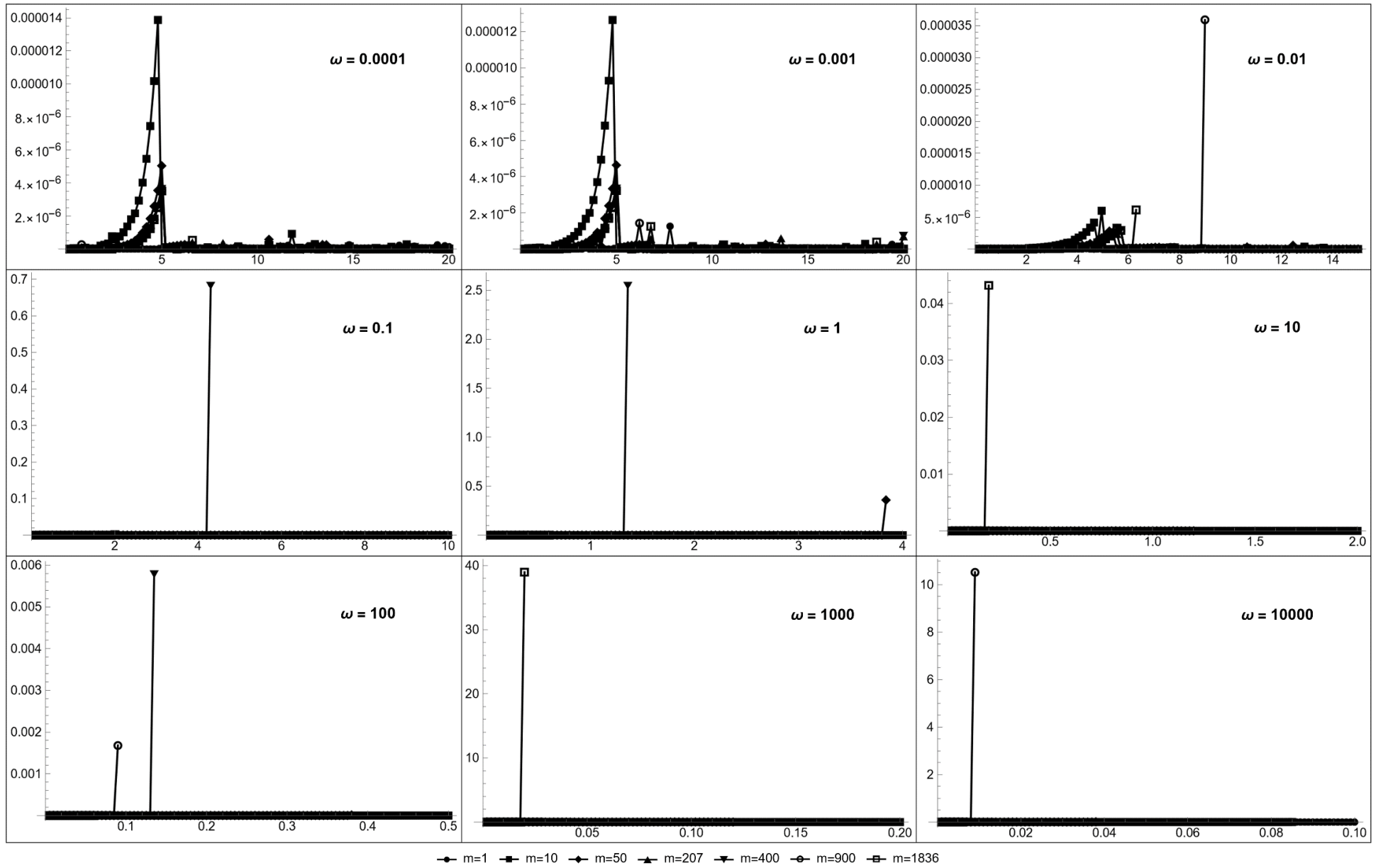


Figure C-2: Percentage error of PCP densities from equation (2-169) and FEM density from equivalent equation (2-161) versus  $r_p$  for different frequencies

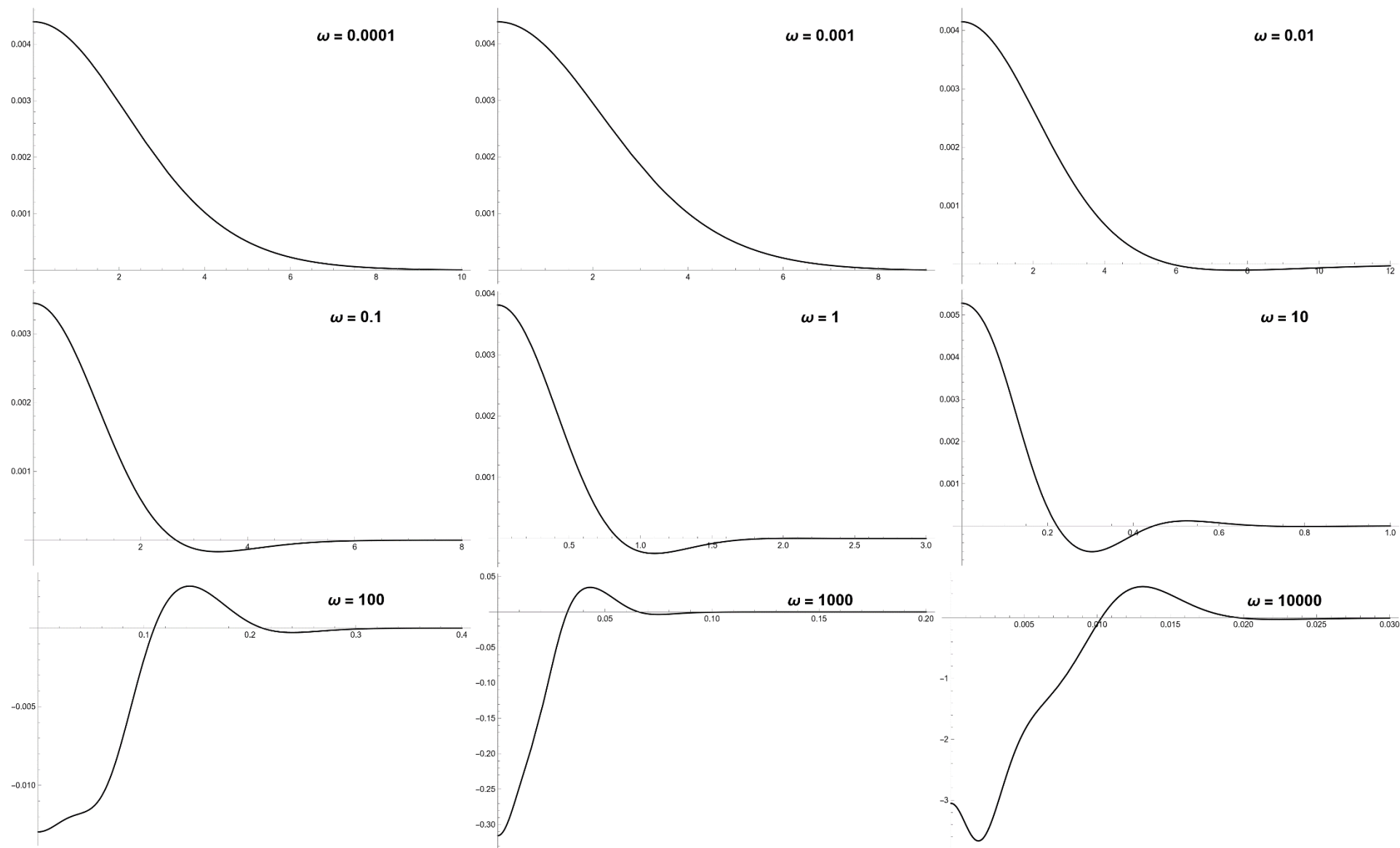


Figure C-3: Difference in electron (PCP) densities between variational and TC-HF for mass 1 at different frequencies



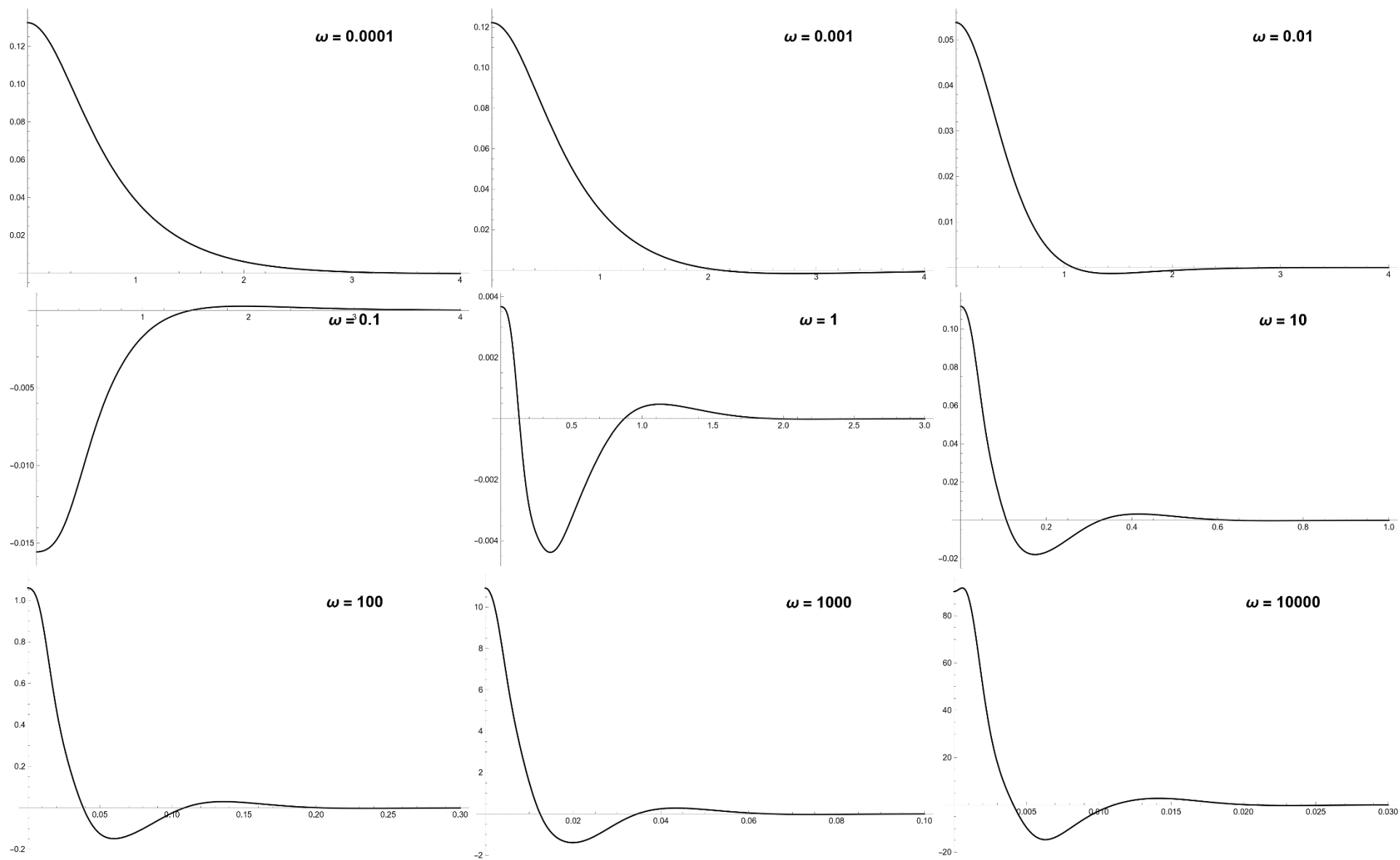


Figure C-4: Difference in electron densities between variational and TC-HF for mass 207 at different frequencies

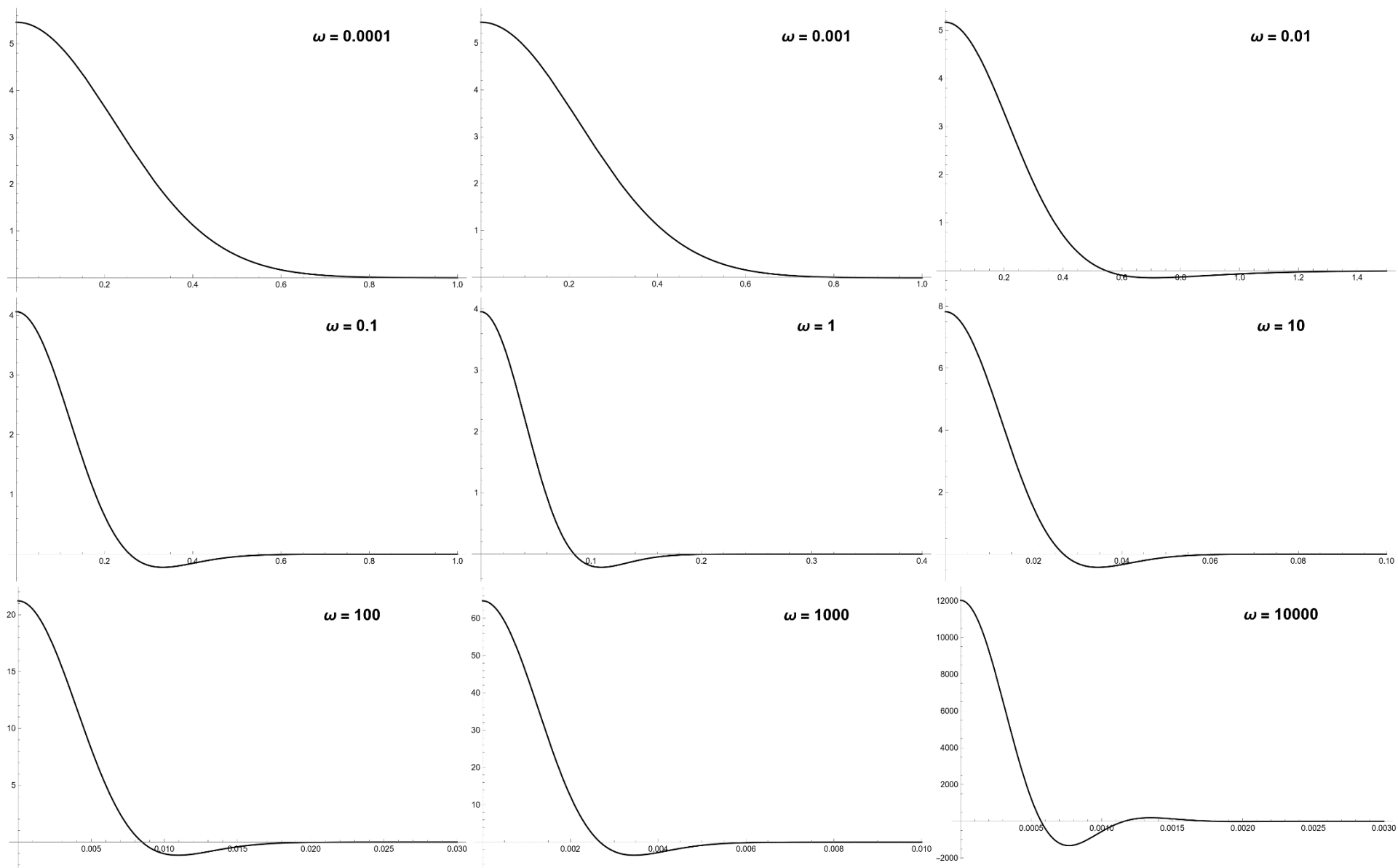


Figure C-5: Difference in PCP densities between variational and TC-HF for mass 207 at different frequencies

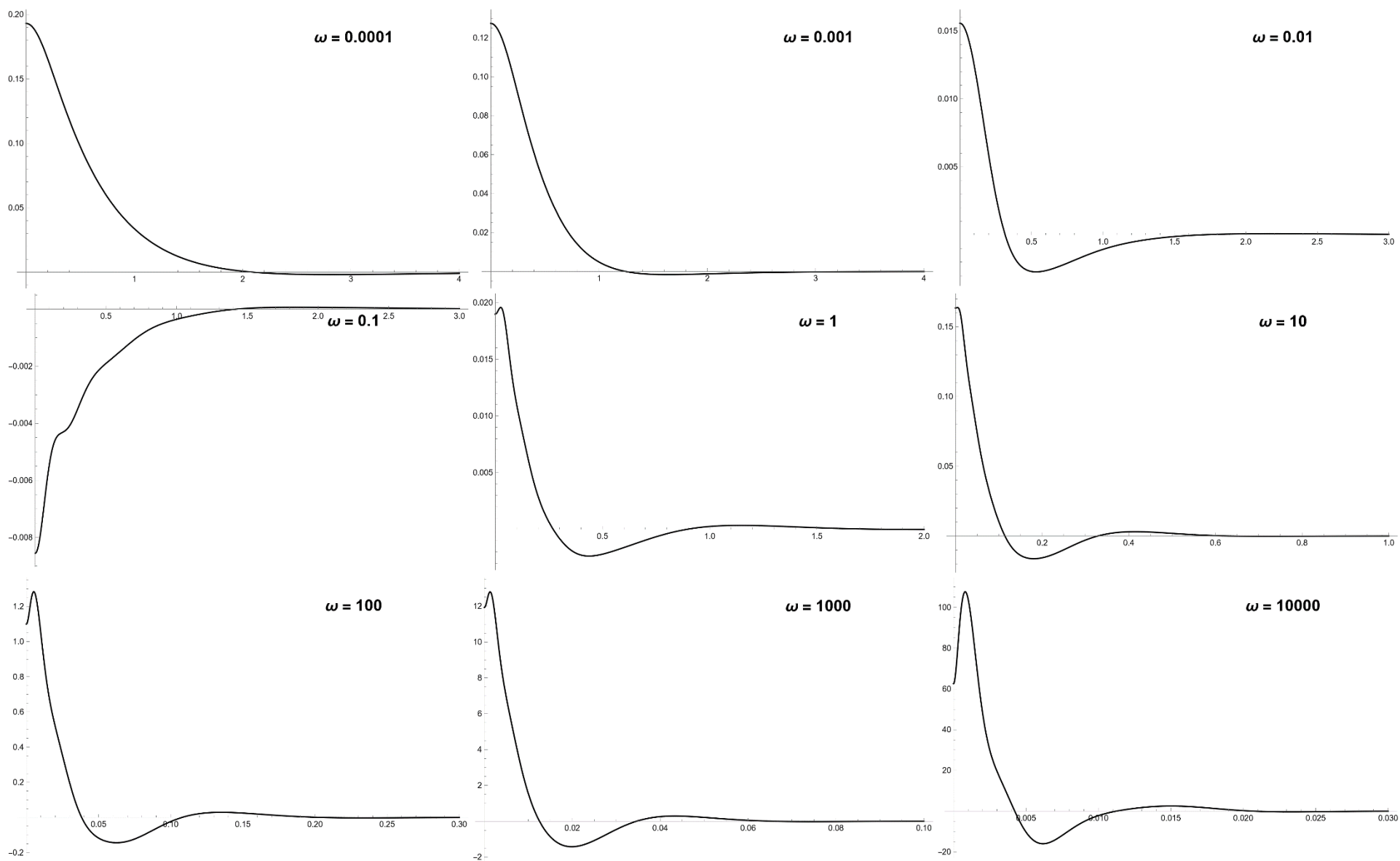


Figure C-6: Difference in electron densities between variational and TC-HF for mass 1836 at different frequencies

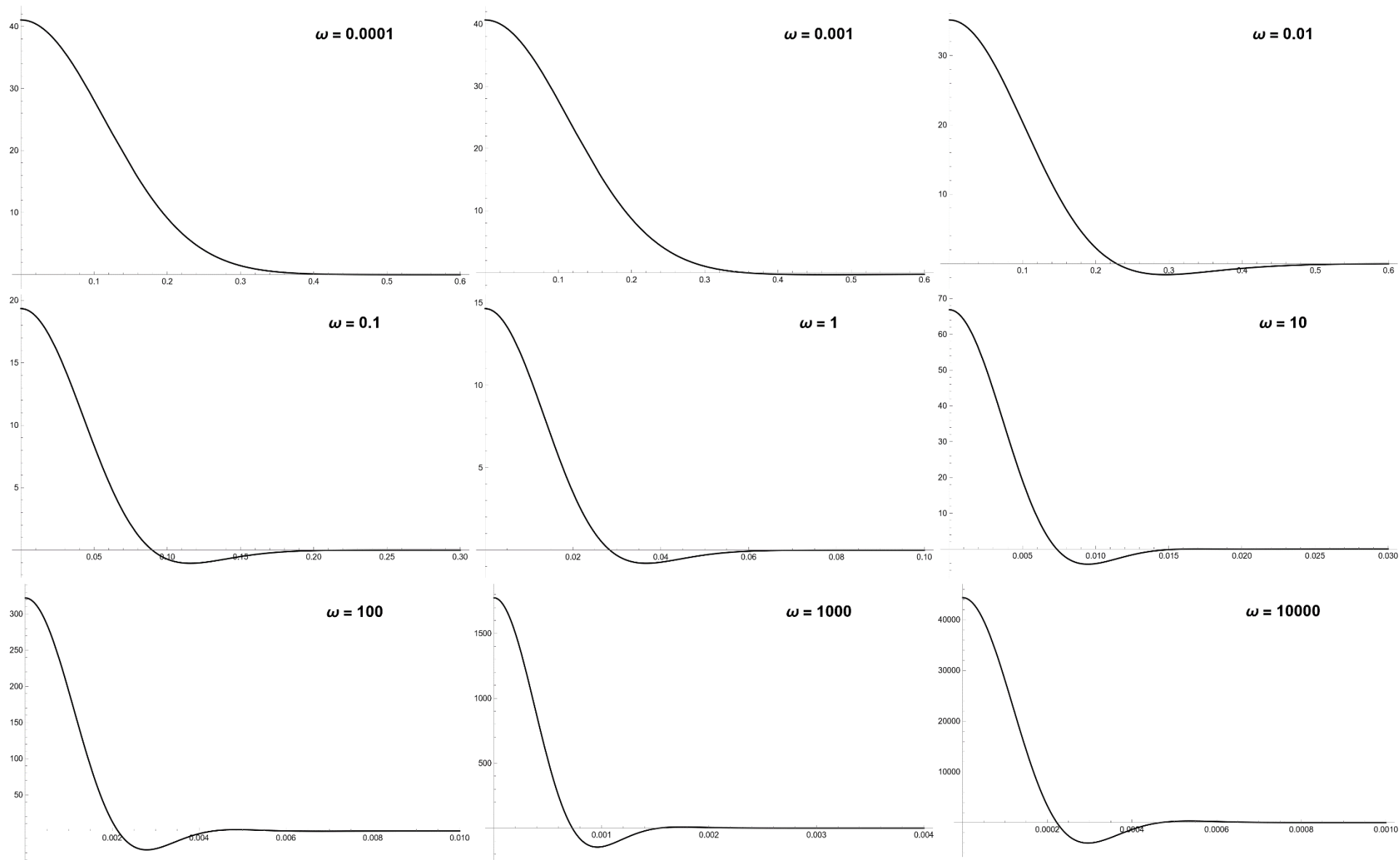


Figure C-7: Difference in PCP densities between variational and TC-HF for mass 1836 at different frequencies

Table C-1: Effective correlation hill radii for electron and PCP as a function of their position vectors ( $r_e$  and  $r_p$  respectively)

$\omega/\text{mp}$	1	1.5	2	3	10	50	207	400	900	1836
Electron										
0.0001	11.28902	9.584436	8.658497	7.645748	5.799772	4.356237	3.341128	2.916228	2.439233	2.070306
0.001	7.920257	6.778073	6.13538	5.408981	3.989535	2.794661	2.014594	1.729134	1.44638	1.261239
0.01	4.802232	4.185704	3.813969	3.369773	2.427789	1.641467	1.229876	1.120673	1.047728	1.018109
0.1	2.334938	2.120617	1.976072	1.787824	1.350063	1.029548	0.941931	0.928476	0.920483	0.917229
1	0.910885	0.864609	0.831099	0.785004	0.67705	0.620979	0.609572	0.6078	0.606742	0.60631
10	0.309557	0.299782	0.29269	0.283029	0.262315	0.253149	0.251324	0.251041	0.250872	0.250803
100	0.100111	0.097575	0.095749	0.093293	0.088289	0.086208	0.085799	0.085736	0.085699	0.085683
1000	0.031881	0.031136	0.030602	0.029887	0.028459	0.027879	0.027766	0.027749	0.027738	0.027734
10000	0.010104	0.009874	0.00971	0.00949	0.009054	0.008878	0.008844	0.008838	0.008835	0.008834
PCP										
0.0001	11.28902	9.580604	8.652869	7.637951	5.783146	4.309265	3.229977	2.757817	2.207241	1.763979
0.001	7.920257	6.758847	6.107092	5.370028	3.912109	2.615676	1.695086	1.339603	0.975366	0.722557
0.01	4.802232	4.11391	3.708008	3.225829	2.178893	1.231347	0.685288	0.511316	0.351989	0.251319
0.1	2.334938	1.984361	1.770639	1.508874	0.928101	0.459662	0.236703	0.172503	0.116294	0.081972
1	0.910885	0.764794	0.67521	0.565573	0.328969	0.153875	0.077052	0.055708	0.037297	0.02618
10	0.309557	0.258642	0.227375	0.189177	0.107825	0.049499	0.024574	0.017725	0.011843	0.008303
100	0.100111	0.083508	0.073309	0.060859	0.034466	0.015732	0.007791	0.005615	0.00375	0.002628
1000	0.031881	0.02658	0.023323	0.019349	0.010935	0.004983	0.002465	0.001777	0.001186	0.000831
10000	0.010104	0.008422	0.007389	0.006129	0.003462	0.001576	0.00078	0.000562	0.000375	0.000263

Table C-2: Fit details for simplifying single-particle densities and Kohn-Sham orbitals

mass	$\omega$	NO <sup>1</sup>	Power <sup>2</sup>	Range <sup>3</sup>	Overlap <sup>4</sup>	Percentage errors of 10 first points sorted by absolute values <sup>5</sup>									
1836	0.01	fit4	1	4	0.969661	76.8	76.0	75.2	74.4	73.6	72.8	71.9	71.0	70.2	69.3
1836	0.01	fit4	1	5	0.973641	97.1	96.9	96.7	96.5	96.3	96.1	95.8	95.5	95.3	95.0
1836	0.01	fit5	1	4	0.969661	76.8	76.0	75.2	74.4	73.6	72.8	71.9	71.0	70.2	69.3
1836	0.01	fit5	1	5	0.996404	36.3	35.2	34.1	33.1	32.0	30.9	29.9	28.8	27.8	26.8
1836	0.01	fit6	1	4	0.985610	6.8	6.4	5.9	5.5	5.1	4.7	4.3	3.9	3.6	3.3
1836	0.01	fit6	1	5	0.996413	36.0	34.9	33.8	32.7	31.7	30.6	29.6	28.5	27.5	26.5
1836	0.01	fit4	0.5	5	0.989540	78.3	77.7	77.0	76.3	75.6	74.9	74.2	73.5	72.8	72.0
1836	0.01	fit4	0.5	6	0.998900	55.5	54.6	53.7	52.7	51.8	50.8	49.9	48.9	47.9	46.9
1836	0.01	fit4	0.5	7	0.999187	79.7	79.0	78.3	77.6	76.8	76.1	75.3	74.5	73.7	72.9
1836	0.01	fit5	0.5	5	0.996800	29.0	28.2	27.3	26.5	25.7	24.9	24.1	23.3	22.5	21.7
1836	0.01	fit5	0.5	6	0.999432	18.4	17.7	16.9	16.2	15.5	14.8	14.2	13.5	12.8	12.2
1836	0.01	fit5	0.5	7	0.999859	38.7	37.7	36.7	35.7	34.8	33.8	32.8	31.8	30.9	29.9
1836	0.01	fit6	0.5	5	0.997111	6.9	6.5	6.1	5.7	5.3	5.0	4.6	4.3	3.9	3.6
1836	0.01	fit6	0.5	6	0.999432	18.4	17.7	16.9	16.2	15.5	14.8	14.2	13.5	12.8	12.2
1836	0.01	fit6	0.5	7	0.999901	12.1	11.5	10.9	10.3	9.7	9.1	8.6	8.1	7.5	7.0
207	0.02	fit4	1	4	0.982082	27.7	26.8	25.9	25.0	24.1	23.2	22.4	21.5	20.6	19.8
207	0.02	fit4	1	5	0.992173	70.2	69.3	68.4	67.4	66.4	65.4	64.4	63.4	62.3	61.3
207	0.02	fit5	1	4	0.982082	27.7	26.8	25.9	25.0	24.1	23.2	22.4	21.5	20.6	19.8
207	0.02	fit5	1	5	0.992173	70.2	69.3	68.4	67.4	66.4	65.4	64.4	63.4	62.3	61.3
207	0.02	fit6	1	4	0.983708	0.4	0.3	0.3	0.2	0.2	0.1	0.1	0.1	0.1	0.1
207	0.02	fit6	1	5	0.996388	22.8	21.9	21.0	20.1	19.3	18.4	17.6	16.7	15.9	15.1

207	0.02	fit4	0.5	5	0.996720	0.8	0.7	0.6	0.6	0.5	0.4	0.3	0.3	0.2	0.2
207	0.02	fit4	0.5	6	0.999384	3.4	3.1	2.8	2.6	2.3	2.1	1.9	1.7	1.5	1.3
207	0.02	fit4	0.5	7	0.999808	45.8	44.8	43.8	42.8	41.8	40.8	39.8	38.8	37.8	36.8
207	0.02	fit5	0.5	5	0.996698	8.4	8.0	7.5	7.1	6.6	6.2	5.8	5.4	5.0	4.7
207	0.02	fit5	0.5	6	0.999335	22.7	21.9	21.1	20.4	19.6	18.8	18.1	17.3	16.6	15.9
207	0.02	fit5	0.5	7	0.999808	45.8	44.8	43.8	42.8	41.8	40.8	39.8	38.8	37.8	36.8
207	0.02	fit6	0.5	5	0.996721	0.1	0.1	0.0	0.0	0.0	0.0	0.0	0.0	0.0	0.0
207	0.02	fit6	0.5	6	0.999385	0.3	0.3	0.2	0.2	0.1	0.1	0.1	0.1	0.1	0.1
207	0.02	fit6	0.5	7	0.999808	45.8	44.8	43.8	42.8	41.8	40.8	39.8	38.8	37.8	36.8

1. Number of Gaussian terms used in the fitting process
2. Power, where 1 means single-particle density and 0.5 means Kohn-Sham orbitals
3. Range of  $r$  used in the fitting process
4. Integral overlap values between the exact quantity and the fitted quantity
5. Percentage error of the fitted points relative to the original density points for the first 10 points with the highest error

Table C-3: Gaussian functions resulting from fitting electronic densities and Kohn-Sham orbitals in TC-DFT calculations

quantity/mp	207	1836
One-electron density	$0.022451e^{-2.67952\text{re}^2} + 0.05146e^{-1.26742\text{re}^2}$ $+ 0.0363588e^{-0.563362\text{re}^2} + 0.006425e^{-0.247975\text{re}^2}$	$0.0202244 e^{-10.2106\text{re}^2} + 0.262169e^{-3.94531\text{re}^2}$ $- 0.207595e^{-3.91606\text{re}^2} + 0.0675395e^{-1.58444\text{re}^2}$ $+ 0.0425351e^{-0.644867\text{re}^2}$ $+ 0.00775279e^{-0.2684\text{re}^2}$
KS electronic orbital	$0.116145e^{-1.8118\text{re}^2} - 0.17711e^{-1.54565\text{re}^2} + 0.157897e^{-1.25662\text{re}^2}$ $+ 0.112317e^{-0.503436\text{re}^2} + 0.10058e^{-0.215329\text{re}^2}$ $+ 0.0317891e^{-0.0863076\text{re}^2}$	$0.06247 e^{-5.62925\text{re}^2} + 0.142094e^{-1.40685\text{re}^2}$ $+ 0.165614e^{-0.393182\text{re}^2} + 0.0684561e^{-0.118032\text{re}^2}$



Table C-4: Details of fitting variational parameters

Quantities/ $\omega$		0.0001	0.001	0.01	0.1	1	10	100	1000	10000
m = 1										
a parameter	OPT $\alpha^1$	0.500000	0.499997	0.499704	0.484707	0.438060	0.414991	0.407310	0.404861	0.404086
	LOG $\alpha^2$	0.499990	0.499900	0.499010	0.490909	0.450000	0.409091	0.400990	0.400100	0.400010
	ERR $\alpha^3$	0.497963	0.497440	0.493553	0.478778	0.450000	0.421222	0.406447	0.402560	0.402037
	%LOG <sup>4</sup>	0.002000	0.019383	0.139038	1.263419	2.653261	1.442263	1.576125	1.190062	1.019060
	%ERR <sup>5</sup>	0.409065	0.513939	1.246274	1.238431	2.653261	1.479361	0.212303	0.571789	0.509742
b parameter	OPT $\beta^6$	0.000000	0.000001	0.000149	0.010559	0.205107	2.366272	24.586618	248.702541	2495.906884
	SIM $\beta^7$	0.000025	0.000250	0.002500	0.025000	0.250000	2.500000	25.000000	250.000000	2500.000000
	SIM2 $\beta^8$	0.000475	0.001331	0.002500	0.009189	0.200000	2.341886	24.500000	248.418861	2495.000000
	EXP $\beta^9$	0.000024	0.000240	0.002400	0.024000	0.240000	2.400000	24.000000	240.000000	2400.000000
	%SIM <sup>10</sup>	99.952980	99.400089	94.038998	57.765854	17.957021	5.349138	1.653527	0.518984	0.163725
	%SIM2 <sup>11</sup>	99.997525	99.887331	94.038998	14.908943	2.553724	1.041273	0.353544	0.114194	0.036348
	%EXP <sup>12</sup>	99.951021	99.375093	93.790623	56.006098	14.538564	1.405352	2.444243	3.626059	3.996120
Energy	VAR Energy <sup>13</sup>	-0.250000	-0.249997	-0.249701	-0.223933	0.612000	12.395490	141.942322	1474.690624	14920.133739
	LS Energy <sup>14</sup>	-0.250000	-0.249994	-0.249474	-0.217075	0.630344	12.412923	141.960439	1474.709359	14920.152718
	ES Energy <sup>15</sup>	-0.249996	-0.249995	-0.249582	-0.218556	0.630344	12.415904	141.961799	1474.709979	14920.153233
	LE Energy <sup>16</sup>	-0.250000	-0.249995	-0.249493	-0.217839	0.623950	12.396391	141.986041	1475.633840	14931.610696
	EE Energy <sup>17</sup>	-0.249996	-0.249995	-0.249595	-0.219238	0.623950	12.397175	141.983937	1475.629363	14931.597794
	LS2 Energy <sup>18</sup>	-0.249989	-0.249917	-0.249474	-0.223914	0.612047	12.396473	141.943590	1474.691879	14920.134976
	ES2 Energy <sup>19</sup>	-0.249997	-0.249949	-0.249582	-0.223730	0.612047	12.395899	141.943252	1474.691721	14920.134846

Quantities/ $\omega$		0.0001	0.001	0.01	0.1	1	10	100	1000	10000
	%LS <sup>20</sup>	0.000011	0.001064	0.090900	3.159465	2.910089	0.140437	0.012762	0.001270	0.000127
	%LE <sup>21</sup>	0.000010	0.000977	0.083307	2.797517	1.915165	0.007267	0.030791	0.063919	0.076863
	%LS2 <sup>22</sup>	0.004237	0.031838	0.090900	0.008562	0.007715	0.007924	0.000893	0.000085	0.000008
	%ES <sup>23</sup>	0.001427	0.000749	0.047595	2.460411	2.910089	0.164414	0.013720	0.001312	0.000131
	%EE <sup>24</sup>	0.001435	0.000778	0.042332	2.141776	1.915165	0.013592	0.029309	0.063616	0.076777
	%ES2 <sup>25</sup>	0.001325	0.019291	0.047595	0.091086	0.007715	0.003301	0.000655	0.000074	0.000007
m=1.5										
a parameter	OPT a	0.600000	0.599997	0.599752	0.585320	0.529268	0.499264	0.489182	0.485964	0.484945
	LOG a	0.599988	0.599880	0.598812	0.589091	0.540000	0.490909	0.481188	0.480120	0.480012
	ERR a	0.597587	0.597270	0.593829	0.577035	0.540000	0.502965	0.486171	0.482730	0.482413
	%LOG	0.002000	0.019567	0.157023	0.640109	1.987402	1.701975	1.661221	1.217252	1.027617
	%ERR	0.403828	0.456625	0.997417	1.435817	1.987402	0.735804	0.619313	0.670015	0.524751
b parameter	OPT b	0.000000	0.000001	0.000149	0.011363	0.240597	2.823673	29.456033	298.293868	2994.618890
	SIM b	0.000030	0.000300	0.003000	0.030000	0.300000	3.000000	30.000000	300.000000	3000.000000
	SIM2 b	0.000570	0.001597	0.003000	0.011026	0.240000	2.810263	29.400000	298.102633	2994.000000
	EXP b	0.000029	0.000288	0.002880	0.028800	0.288000	2.880000	28.800000	288.000000	2880.000000
	%SIM	99.960817	99.500074	95.022645	62.124846	19.800854	5.877564	1.813225	0.568711	0.179370
	%SIM2	99.997938	99.906109	95.022645	3.049174	0.248932	0.477170	0.190587	0.064151	0.020671
	%EXP	99.959184	99.479244	94.815255	60.546715	16.459223	1.955796	2.277891	3.574260	3.979823
Energy	VAR Energy	-0.300000	-0.299998	-0.299750	-0.277533	0.516267	12.137957	141.164882	1472.266767	14912.502746
	LS Energy	-0.300000	-0.299995	-0.299560	-0.270893	0.536833	12.158441	141.186484	1472.289203	14912.525507
	ES Energy	-0.299996	-0.299996	-0.299644	-0.272214	0.536833	12.161337	141.187713	1472.289860	14912.526117

Quantities/ $\omega$		0.0001	0.001	0.01	0.1	1	10	100	1000	10000
	LE Energy	-0.300000	-0.299996	-0.299576	-0.271605	0.530186	12.139720	141.203219	1473.183252	14923.884672
	EE Energy	-0.299996	-0.299996	-0.299656	-0.272854	0.530186	12.140650	141.201573	1473.178978	14923.870779
	LS2 Energy	-0.299991	-0.299931	-0.299560	-0.277528	0.516339	12.138319	141.165405	1472.267268	14912.503233
	ES2 Energy	-0.299998	-0.299958	-0.299644	-0.277451	0.516339	12.138034	141.165225	1472.267172	14912.503146
	%LS	0.000007	0.000726	0.063548	2.451169	3.830983	0.168474	0.015300	0.001524	0.000153
	%LE	0.000007	0.000666	0.058202	2.182577	2.625281	0.014523	0.027150	0.062211	0.076267
	%LS2	0.002948	0.022194	0.063548	0.001689	0.013945	0.002976	0.000371	0.000034	0.000003
	%ES	0.001424	0.000628	0.035430	1.954141	3.830983	0.192247	0.016171	0.001569	0.000157
	%EE	0.001432	0.000654	0.031585	1.714720	2.625281	0.022179	0.025985	0.061921	0.076173
	%ES2	0.000795	0.013020	0.035430	0.029552	0.013945	0.000631	0.000244	0.000028	0.000003
m = 2										
a parameter	OPT a	0.666667	0.666664	0.666443	0.652472	0.590509	0.555616	0.543817	0.540050	0.538856
	LOG a	0.666653	0.666533	0.665347	0.654545	0.600000	0.545455	0.534653	0.533467	0.533347
	ERR a	0.663993	0.663771	0.660661	0.642776	0.600000	0.557224	0.539339	0.536229	0.536007
	%LOG	0.001991	0.019631	0.164833	0.316852	1.581817	1.862860	1.713983	1.234041	1.032945
	%ERR	0.402594	0.435954	0.875224	1.508335	1.581817	0.288593	0.830334	0.712439	0.531571
b parameter	OPT b	0.000000	0.000002	0.000149	0.011795	0.263492	3.126429	32.695823	331.334674	3327.030484
	SIM b	0.000033	0.000333	0.003333	0.033333	0.333333	3.333333	33.333333	333.333333	3333.333333
	SIM2 b	0.000633	0.001775	0.003333	0.012251	0.266667	3.122515	32.666667	331.225148	3326.666667
	EXP b	0.000032	0.000320	0.003200	0.032000	0.320000	3.200000	32.000000	320.000000	3200.000000
	%SIM	99.931437	99.544514	95.516568	64.616431	20.952291	6.207122	1.912531	0.599598	0.189085
	%SIM 2	99.996391	99.914456	95.516568	3.729827	1.190363	0.125362	0.089254	0.033067	0.010936

Quantities/ $\omega$		0.0001	0.001	0.01	0.1	1	10	100	1000	10000
%EXP		99.928580	99.525536	95.329758	63.142115	17.658636	2.299086	2.174447	3.542086	3.969703
Energy	VAR Energy	-0.333333	-0.333331	-0.333109	-0.312780	0.455715	11.977247	140.681475	1470.761234	14907.764463
	LS Energy	-0.333333	-0.333329	-0.332937	-0.306322	0.477606	11.999709	140.705382	1470.786132	14907.789743
	ES Energy	-0.333329	-0.333329	-0.333009	-0.307529	0.477606	12.002497	140.706531	1470.786827	14907.790419
	LE Energy	-0.333333	-0.333329	-0.332952	-0.307002	0.470830	11.979676	140.716665	1471.661343	14919.087618
	EE Energy	-0.333329	-0.333329	-0.333020	-0.308144	0.470830	11.980658	140.715256	1471.657090	14919.073056
	LS2 Energy	-0.333325	-0.333271	-0.332937	-0.312767	0.455934	11.977383	140.681703	1470.761441	14907.764658
	ES2 Energy	-0.333331	-0.333297	-0.333009	-0.312734	0.455934	11.977250	140.681599	1470.761380	14907.764601
	%LS	0.000006	0.000581	0.051475	2.108383	4.583484	0.187193	0.016991	0.001693	0.000170
	%LE	0.000005	0.000532	0.047121	1.882285	3.210322	0.020279	0.025008	0.061163	0.075897
	%LS2	0.002389	0.018001	0.051475	0.004119	0.048049	0.001140	0.000162	0.000014	0.000001
	%ES	0.001434	0.000607	0.029805	1.707677	4.583484	0.210376	0.017807	0.001740	0.000174
	%EE	0.001440	0.000633	0.026604	1.504499	3.210322	0.028472	0.024007	0.060874	0.075800
	%ES2	0.000610	0.010216	0.029805	0.014645	0.048049	0.000030	0.000088	0.000010	0.000001
m = 3										
a parameter	OPT a	0.750000	0.749998	0.749801	0.736443	0.667504	0.626232	0.612170	0.607675	0.606251
	LOG a	0.749985	0.749850	0.748515	0.736364	0.675000	0.613636	0.601485	0.600150	0.600015
	ERR a	0.746997	0.746856	0.744160	0.725175	0.675000	0.624825	0.605840	0.603144	0.603003
	%LOG	0.002000	0.019717	0.171842	0.010793	1.110486	2.052664	1.776395	1.253885	1.039226
	%ERR	0.401975	0.420761	0.758074	1.553884	1.110486	0.225182	1.044784	0.751156	0.538599
b parameter	OPT b	0.000000	0.000001	0.000150	0.012243	0.291304	3.502570	36.738719	372.614531	3742.478585
	SIM b	0.000038	0.000375	0.003750	0.037500	0.375000	3.750000	37.500000	375.000000	3750.000000

Quantities/ $\omega$		0.0001	0.001	0.01	0.1	1	10	100	1000	10000
Energy	SIM 2 b	0.000713	0.001997	0.003750	0.013783	0.300000	3.512829	36.750000	372.628292	3742.500000
	EXP b	0.000036	0.000360	0.003600	0.036000	0.360000	3.600000	36.000000	360.000000	3600.000000
	%SIM	99.968654	99.600163	96.011650	67.350968	22.318911	6.598141	2.030082	0.636125	0.200571
	%SIM 2	99.998350	99.924907	96.011650	11.169846	2.898639	0.292057	0.030696	0.003693	0.000572
	%EXP	99.967347	99.583503	95.845469	65.990592	19.082199	2.706397	2.051998	3.504036	3.957738
	VAR Energy	-0.375000	-0.374998	-0.374800	-0.356440	0.383003	11.786450	140.109312	1468.980867	14902.162752
	LS Energy	-0.375000	-0.374996	-0.374648	-0.350229	0.406395	11.811329	140.136081	1469.008837	14902.191178
	ES Energy	-0.374995	-0.374996	-0.374709	-0.351292	0.406395	11.813936	140.137143	1469.009589	14902.191937
	LE Energy	-0.375000	-0.374996	-0.374661	-0.350871	0.399493	11.789789	140.140971	1469.861834	14913.416659
	EE Energy	-0.374995	-0.374996	-0.374718	-0.351878	0.399493	11.790793	140.139799	1469.857536	14913.401287
	LS2 Energy	-0.374993	-0.374945	-0.374648	-0.356411	0.383501	11.786472	140.109354	1468.980895	14902.162773
	ES2 Energy	-0.374998	-0.374969	-0.374709	-0.356414	0.383501	11.786487	140.109321	1468.980875	14902.162756
	%LS	0.000005	0.000452	0.040535	1.773442	5.756019	0.210632	0.019102	0.001904	0.000191
	%LE	0.000004	0.000414	0.037081	1.587124	4.127785	0.028322	0.022591	0.059935	0.075462
	%LS2	0.001889	0.014233	0.040535	0.008151	0.129934	0.000188	0.000030	0.000002	0.000000
a parameter	%ES	0.001448	0.000614	0.024455	1.465585	5.756019	0.232655	0.019860	0.001955	0.000196
	%EE	0.001454	0.000639	0.021856	1.296455	4.127785	0.036835	0.021755	0.059643	0.075359
	%ES2	0.000482	0.007681	0.024455	0.007435	0.129934	0.000315	0.000006	0.000001	0.000000
	m = 10									
a parameter	OPT a	0.909091	0.909089	0.908926	0.896745	0.815720	0.761554	0.742827	0.736831	0.734930
	LOG a	0.909073	0.908909	0.907291	0.892562	0.818182	0.743802	0.729073	0.727454	0.727291
	ERR a	0.905454	0.905396	0.903416	0.883033	0.818182	0.753331	0.732948	0.730968	0.730910

	Quantities/ $\omega$	0.0001	0.001	0.01	0.1	1	10	100	1000	10000
b parameter	%LOG	0.001999	0.019796	0.180272	0.468653	0.300949	2.386751	1.886491	1.288926	1.050314
	%ERR	0.401661	0.407912	0.609998	1.552838	0.300949	1.091638	1.347800	0.802095	0.550021
	OPT b	0.000000	0.000002	0.000150	0.012890	0.342079	4.213989	44.437261	451.360667	4535.415827
	SIM b	0.000045	0.000455	0.004545	0.045455	0.454545	4.545455	45.454545	454.545455	4545.454545
	SIM2 b	0.000864	0.002420	0.004545	0.016707	0.363636	4.257975	44.545455	451.670657	4536.363636
	EXP b	0.000044	0.000436	0.004364	0.043636	0.436364	4.363636	43.636364	436.363636	4363.636364
	%SIM	99.974139	99.666836	96.705464	71.641569	24.742679	7.292248	2.238026	0.700653	0.220852
	%SIM2	99.998639	99.937429	96.705464	22.843536	5.928349	1.033028	0.242884	0.068632	0.020894
	%EXP	99.973062	99.652954	96.568191	70.459967	21.606958	3.429426	1.835389	3.436820	3.936613
	VAR Energy	-0.454545	-0.454544	-0.454381	-0.438912	0.251539	11.447417	139.097263	1465.835951	14892.271732
	LS Energy	-0.454545	-0.454542	-0.454257	-0.433193	0.277382	11.476745	139.129440	1465.869766	14892.306161
	ES Energy	-0.454539	-0.454541	-0.454301	-0.433986	0.277382	11.478902	139.130376	1465.870646	14892.307079
	LE Energy	-0.454545	-0.454543	-0.454268	-0.433772	0.270320	11.452664	139.123182	1466.683692	14903.403985
	EE Energy	-0.454539	-0.454541	-0.454310	-0.434524	0.270320	11.453602	139.122323	1466.679201	14903.387167
	LS2 Energy	-0.454540	-0.454500	-0.454257	-0.438853	0.252744	11.447614	139.097398	1465.836106	14892.271901
Energy	ES2 Energy	-0.454544	-0.454523	-0.454301	-0.438885	0.252744	11.447801	139.097454	1465.836166	14892.271967
	%LS	0.000003	0.000298	0.027217	1.320309	9.316719	0.255541	0.023127	0.002307	0.000231
	%LE	0.000003	0.000272	0.024865	1.185062	6.947797	0.045813	0.018630	0.057800	0.074696
	%LS2	0.001286	0.009682	0.027217	0.013473	0.476625	0.001722	0.000097	0.000011	0.000001
	%ES	0.001472	0.000674	0.017403	1.135127	9.316719	0.274290	0.023800	0.002367	0.000237
	%EE	0.001477	0.000699	0.015575	1.009911	6.947797	0.054004	0.018013	0.057494	0.074583
	%ES2	0.000401	0.004667	0.017403	0.006157	0.476625	0.003355	0.000138	0.000015	0.000002

Quantities/ $\omega$		0.0001	0.001	0.01	0.1	1	10	100	1000	10000
m = 50										
a parameter	OPT a	0.980392	0.980391	0.980240	0.968561	0.882615	0.822405	0.801451	0.794737	0.792600
	LOG a	0.980373	0.980196	0.978451	0.962567	0.882353	0.802139	0.786255	0.784510	0.784333
	ERR a	0.976470	0.976432	0.974726	0.953971	0.882353	0.810735	0.789980	0.788274	0.788236
	%LOG	0.001995	0.019833	0.182826	0.622755	0.029713	2.526509	1.932654	1.303698	1.054025
	%ERR	0.401625	0.405446	0.565690	1.529464	0.029713	1.439423	1.452002	0.819909	0.553752
b parameter	OPT b	0.000000	0.000001	0.000150	0.013113	0.363909	4.530152	47.879691	486.628702	4890.717855
	SIM b	0.000049	0.000490	0.004902	0.049020	0.490196	4.901961	49.019608	490.196078	4901.960784
	SIM2 b	0.000931	0.002610	0.004902	0.018017	0.392157	4.591934	48.039216	487.095806	4892.156863
	EXP b	0.000047	0.000471	0.004706	0.047059	0.470588	4.705882	47.058824	470.588235	4705.882353
	%SIM	99.946254	99.696529	96.945106	73.248938	25.762490	7.584890	2.325431	0.727745	0.229356
	%SIM2	99.997171	99.943005	96.945106	27.216803	7.203112	1.345427	0.332073	0.095896	0.029415
	%EXP	99.944015	99.683884	96.817819	72.134311	22.669260	3.734260	1.744342	3.408599	3.927754
Energy	VAR Energy	-0.490196	-0.490195	-0.490043	-0.475603	0.195169	11.304325	138.671901	1464.515756	14888.121166
	LS Energy	-0.490196	-0.490193	-0.489929	-0.470101	0.221956	11.335583	138.706479	1464.552184	14888.158282
	ES Energy	-0.490189	-0.490191	-0.489969	-0.470779	0.221956	11.337506	138.707376	1464.553126	14888.159273
	LE Energy	-0.490196	-0.490193	-0.489939	-0.470655	0.214849	11.310479	138.695595	1465.349772	14899.202603
	EE Energy	-0.490189	-0.490191	-0.489977	-0.471298	0.214849	11.311351	138.694834	1465.345176	14899.185181
	LS2 Energy	-0.490191	-0.490154	-0.489929	-0.475534	0.196730	11.304731	138.672232	1464.516133	14888.121569
	ES2 Energy	-0.490194	-0.490176	-0.489969	-0.475569	0.196730	11.304954	138.672317	1464.516230	14888.121674
	%LS	0.000003	0.000252	0.023211	1.170328	12.068611	0.275749	0.024929	0.002487	0.000249
	%LE	0.000002	0.000231	0.021191	1.051297	9.160081	0.054411	0.017084	0.056916	0.074376

Quantities/ $\omega$		0.0001	0.001	0.01	0.1	1	10	100	1000	10000
	%LS2	0.001106	0.008318	0.023211	0.014624	0.793266	0.003588	0.000239	0.000026	0.000003
	%ES	0.001481	0.000708	0.015108	1.024639	12.068611	0.292667	0.025576	0.002552	0.000256
	%EE	0.001485	0.000733	0.013524	0.913430	9.160081	0.062117	0.016536	0.056602	0.074259
	%ES2	0.000400	0.003797	0.015108	0.007166	0.793266	0.005568	0.000300	0.000032	0.000003
m = 207										
a parameter	OPT a	0.995192	0.995191	0.995042	0.983465	0.896535	0.835051	0.813624	0.806758	0.804581
	LOG a	0.995172	0.994993	0.993222	0.977098	0.895673	0.814248	0.798125	0.796353	0.796174
	ERR a	0.991211	0.991176	0.989523	0.968708	0.895673	0.822639	0.801823	0.800170	0.800135
	%LOG	0.001973	0.019832	0.183285	0.651678	0.096203	2.554842	1.942031	1.306622	1.055913
	%ERR	0.401600	0.405063	0.557750	1.523451	0.096203	1.508864	1.471793	0.823295	0.555636
b parameter	OPT b	0.000000	0.000001	0.000150	0.013155	0.368372	4.595580	48.593656	493.947566	4964.462597
	SIM b	0.000050	0.000498	0.004976	0.049760	0.497596	4.975962	49.759615	497.596154	4975.961538
	SIM2 b	0.000945	0.002649	0.004976	0.018289	0.398077	4.661254	48.764423	494.449079	4966.009615
	EXP b	0.000048	0.000478	0.004777	0.047769	0.477692	4.776923	47.769231	477.692308	4776.923077
	%SIM	99.837207	99.698596	96.990537	73.562010	25.969647	7.644388	2.343183	0.733243	0.231090
	%SIM2	99.991432	99.943393	96.990537	28.068596	7.462059	1.408942	0.350187	0.101429	0.031152
	%EXP	99.830424	99.686037	96.865143	72.460428	22.885049	3.796237	1.725851	3.402872	3.925948
Energy	VAR Energy	-0.497596	-0.497595	-0.497446	-0.483202	0.183638	11.275221	138.585513	1464.247752	14887.278700
	LS Energy	-0.497596	-0.497593	-0.497334	-0.477745	0.210611	11.306874	138.620589	1464.284722	14887.316374
	ES Energy	-0.497589	-0.497591	-0.497372	-0.478400	0.210611	11.308747	138.621479	1464.285678	14887.317380
	LE Energy	-0.497596	-0.497594	-0.497343	-0.478294	0.203496	11.281566	138.608770	1465.078999	14898.349839
	EE Energy	-0.497589	-0.497591	-0.497380	-0.478915	0.203496	11.282422	138.608027	1465.074380	14898.332295



Quantities/ $\omega$		0.0001	0.001	0.01	0.1	1	10	100	1000	10000
	LS2 Energy	-0.497591	-0.497554	-0.497334	-0.483131	0.185275	11.275678	138.585896	1464.248187	14887.279163
	ES2 Energy	-0.497594	-0.497577	-0.497372	-0.483167	0.185275	11.275907	138.585986	1464.248291	14887.279276
	%LS	0.000002	0.000244	0.022484	1.142266	12.806657	0.279951	0.025303	0.002525	0.000253
	%LE	0.000002	0.000223	0.020525	1.026232	9.758351	0.056248	0.016779	0.056737	0.074311
	%LS2	0.001073	0.008071	0.022484	0.014785	0.883052	0.004055	0.000276	0.000030	0.000003
	%ES	0.001482	0.000715	0.014680	1.003882	12.806657	0.296465	0.025945	0.002590	0.000260
	%EE	0.001487	0.000740	0.013142	0.895267	9.758351	0.063829	0.016243	0.056422	0.074194
	%ES2	0.000401	0.003643	0.014680	0.007405	0.883052	0.006084	0.000341	0.000037	0.000004
m = 400										
a parameter	OPT a	0.997506	0.997505	0.997356	0.985796	0.898713	0.837029	0.815527	0.808637	0.806453
	LOG a	0.997486	0.997307	0.995531	0.979370	0.897756	0.816141	0.799980	0.798204	0.798025
	ERR a	0.993516	0.993481	0.991836	0.971012	0.897756	0.824499	0.803675	0.802030	0.801995
	%LOG	0.001997	0.019838	0.183350	0.656112	0.106591	2.559249	1.943426	1.307042	1.056055
	%ERR	0.401623	0.405012	0.556540	1.522480	0.106591	1.519636	1.474771	0.823783	0.555778
b parameter	OPT b	0.000000	0.000001	0.000150	0.013162	0.369068	4.605803	48.705265	495.091782	4975.992079
	SIM b	0.000050	0.000499	0.004988	0.049875	0.498753	4.987531	49.875312	498.753117	4987.531172
	SIM2 b	0.000948	0.002656	0.004988	0.018331	0.399002	4.672092	48.877805	495.598726	4977.556110
	EXP b	0.000048	0.000479	0.004788	0.047880	0.478803	4.788030	47.880299	478.802993	4788.029925
	%SIM	99.976431	99.701653	96.997178	73.610356	26.001949	7.653653	2.345943	0.734098	0.231359
	%SIM2	99.998760	99.943968	96.997178	28.200132	7.502436	1.418833	0.353003	0.102289	0.031422
	%EXP	99.975449	99.689222	96.872060	72.510787	22.918696	3.805889	1.722976	3.401982	3.925668
VAR Energy		-0.498753	-0.498752	-0.498603	-0.484390	0.181841	11.270688	138.572063	1464.206030	14887.147551

Quantities/ $\omega$		0.0001	0.001	0.01	0.1	1	10	100	1000	10000
Energy	LS Energy	-0.498753	-0.498750	-0.498491	-0.478940	0.208842	11.302404	138.607217	1464.243085	14887.185312
	ES Energy	-0.498746	-0.498748	-0.498530	-0.479591	0.208842	11.304269	138.608106	1464.244042	14887.186320
	LE Energy	-0.498753	-0.498751	-0.498501	-0.479488	0.201726	11.277064	138.595252	1465.036846	14898.217088
	EE Energy	-0.498746	-0.498748	-0.498538	-0.480105	0.201726	11.277917	138.594512	1465.032224	14898.199524
	LS2 Energy	-0.498748	-0.498712	-0.498491	-0.484318	0.183489	11.271154	138.572455	1464.206474	14887.148024
	ES2 Energy	-0.498751	-0.498734	-0.498530	-0.484354	0.183489	11.271383	138.572545	1464.206580	14887.148138
	%LS	0.000002	0.000243	0.022374	1.137965	12.928849	0.280608	0.025362	0.002531	0.000254
	%LE	0.000002	0.000222	0.020424	1.022389	9.857606	0.056537	0.016731	0.056710	0.074301
	%LS2	0.001068	0.008033	0.022374	0.014808	0.898097	0.004130	0.000282	0.000030	0.000003
	%ES	0.001482	0.000716	0.014615	1.000699	12.928849	0.297059	0.026003	0.002596	0.000260
	%EE	0.001487	0.000741	0.013083	0.892480	9.857606	0.064097	0.016197	0.056394	0.074183
	%ES2	0.000402	0.003619	0.014615	0.007443	0.898097	0.006166	0.000348	0.000038	0.000004
m = 900										
a parameter	OPT a	0.998890	0.998889	0.998740	0.987189	0.900014	0.838211	0.816666	0.809761	0.807572
	LOG a	0.998870	0.998691	0.996912	0.980728	0.899001	0.817274	0.801090	0.799312	0.799132
	ERR a	0.994894	0.994860	0.993220	0.972390	0.899001	0.825612	0.804782	0.803143	0.803108
	%LOG	0.001989	0.019839	0.183392	0.658753	0.112695	2.561894	1.944300	1.307321	1.056147
	%ERR	0.401615	0.404980	0.555823	1.521896	0.112695	1.526080	1.476585	0.824102	0.555870
b parameter	OPT b	0.000000	0.000001	0.000150	0.013166	0.369484	4.611916	48.772012	495.776091	4982.887482
	SIM b	0.000050	0.000499	0.004994	0.049945	0.499445	4.994451	49.944506	499.445061	4994.450610
	SIM2 b	0.000949	0.002659	0.004994	0.018357	0.399556	4.678574	48.945616	496.286293	4984.461709
	EXP b	0.000048	0.000479	0.004795	0.047947	0.479467	4.794673	47.946726	479.467259	4794.672586

Quantities/ $\omega$		0.0001	0.001	0.01	0.1	1	10	100	1000	10000
Energy	%SIM	99.918331	99.702440	97.001346	73.639192	26.021163	7.659192	2.347595	0.734609	0.231520
	%SIM 2	99.995702	99.944116	97.001346	28.278589	7.526454	1.424746	0.354688	0.102804	0.031583
	%EXP	99.914928	99.690042	96.876402	72.540825	22.938712	3.811659	1.721255	3.401449	3.925500
	VAR Energy	-0.499445	-0.499444	-0.499295	-0.485100	0.180766	11.267980	138.564027	1464.181100	14887.069188
	LS Energy	-0.499445	-0.499442	-0.499184	-0.479654	0.207784	11.299732	138.599227	1464.218206	14887.107001
	ES Energy	-0.499438	-0.499440	-0.499222	-0.480303	0.207784	11.301592	138.600115	1464.219165	14887.108010
	LE Energy	-0.499445	-0.499442	-0.499193	-0.480202	0.200668	11.274373	138.587175	1465.011659	14898.137767
	EE Energy	-0.499438	-0.499440	-0.499230	-0.480817	0.200668	11.275225	138.586437	1465.007035	14898.120192
	LS2 Energy	-0.499440	-0.499404	-0.499184	-0.485028	0.182421	11.268450	138.564423	1464.181550	14887.069666
	ES2 Energy	-0.499443	-0.499426	-0.499222	-0.485064	0.182421	11.268680	138.564514	1464.181656	14887.069781
	%LS	0.000002	0.000242	0.022308	1.135404	13.002865	0.281001	0.025397	0.002534	0.000254
	%LE	0.000002	0.000221	0.020364	1.020101	9.917757	0.056710	0.016703	0.056693	0.074295
	%LS2	0.001065	0.008011	0.022308	0.014822	0.907236	0.004176	0.000286	0.000031	0.000003
	%ES	0.001483	0.000717	0.014576	0.998803	13.002865	0.297413	0.026038	0.002600	0.000261
	%EE	0.001487	0.000742	0.013048	0.890820	9.917757	0.064258	0.016170	0.056378	0.074177
	%ES2	0.000402	0.003605	0.014576	0.007465	0.907236	0.006215	0.000352	0.000038	0.000004
$m = 1836$										
a parameter	OPT a	0.999456	0.999454	0.999306	0.987759	0.900546	0.838695	0.817131	0.810221	0.808030
	LOG a	0.999436	0.999256	0.997477	0.981284	0.899510	0.817736	0.801544	0.799764	0.799584
	ERR a	0.995458	0.995423	0.993785	0.972954	0.899510	0.826067	0.805235	0.803597	0.803563
	%LOG	0.001999	0.019831	0.183417	0.659830	0.115213	2.562955	1.944655	1.307538	1.056183
	%ERR	0.401625	0.404958	0.555539	1.521656	0.115213	1.528692	1.477324	0.824336	0.555905

Quantities/ $\omega$		0.0001	0.001	0.01	0.1	1	10	100	1000	10000
b parameter	OPT b	0.000000	0.000002	0.000150	0.013167	0.369653	4.614414	48.799286	496.055715	4985.705219
	SIM b	0.000050	0.000500	0.004997	0.049973	0.499728	4.997278	49.972782	499.727817	4997.278171
	SIM2 b	0.000949	0.002661	0.004997	0.018367	0.399782	4.681223	48.973326	496.567261	4987.283615
	EXP b	0.000048	0.000480	0.004797	0.047974	0.479739	4.797387	47.973870	479.738704	4797.387044
	%SIM	99.976477	99.696982	97.003375	73.650960	26.029034	7.661449	2.348269	0.734821	0.231585
	%SIM2	99.998762	99.943091	97.003375	28.310605	7.536292	1.427155	0.355377	0.103017	0.031648
	%EXP	99.975497	99.684357	96.878515	72.553083	22.946910	3.814010	1.720553	3.401229	3.925432
Energy	VAR Energy	-0.499728	-0.499726	-0.499578	-0.485391	0.180327	11.266873	138.560744	1464.170918	14887.037181
	LS Energy	-0.499728	-0.499725	-0.499467	-0.479946	0.207352	11.298641	138.595963	1464.208044	14887.075015
	ES Energy	-0.499720	-0.499723	-0.499505	-0.480594	0.207352	11.300499	138.596851	1464.209003	14887.076025
	LE Energy	-0.499728	-0.499725	-0.499476	-0.480494	0.200236	11.273274	138.583876	1465.001371	14898.105369
	EE Energy	-0.499720	-0.499723	-0.499513	-0.481108	0.200236	11.274125	138.583138	1464.996747	14898.087789
	LS2 Energy	-0.499722	-0.499686	-0.499467	-0.485319	0.181985	11.267346	138.561143	1464.171370	14887.037661
	ES2 Energy	-0.499726	-0.499708	-0.499505	-0.485354	0.181985	11.267576	138.561234	1464.171476	14887.037777
	%LS	0.000002	0.000242	0.022281	1.134360	13.033316	0.281162	0.025411	0.002536	0.000254
	%LE	0.000002	0.000221	0.020339	1.019168	9.942509	0.056780	0.016692	0.056686	0.074293
	%LS2	0.001064	0.008002	0.022281	0.014827	0.911001	0.004194	0.000287	0.000031	0.000003
	%ES	0.001483	0.000717	0.014560	0.998029	13.033316	0.297558	0.026052	0.002601	0.000261
	%EE	0.001487	0.000742	0.013034	0.890143	9.942509	0.064324	0.016159	0.056371	0.074175
	%ES2	0.000402	0.003600	0.014560	0.007475	0.911001	0.006235	0.000353	0.000038	0.000004

1. Parameter  $\alpha$  alpha using logistic function
2. Parameter  $\alpha$  alpha using error function

3. Error percentage of parameter  $\alpha$  alpha using logistic function
4. Error percentage of parameter  $\alpha$  using error function
5. Optimized variational parameter  $\beta$
6. Parameter  $\beta$  using simple form 1
7. Parameter  $\beta$  using simple form 2
8. Parameter  $\beta$  using exponential function
9. Error percentage of parameter  $\beta$  using simple form 1
10. Error percentage of parameter  $\beta$  using simple form 2
11. Error percentage of parameter  $\beta$  using exponential function
12. Variational energy of relative motion Hamiltonian using optimized parameters
13. Variational energy of relative motion Hamiltonian using parameters from items 2 and 7
14. Variational energy of relative motion Hamiltonian using parameters from items 3 and 7
15. Variational energy of relative motion Hamiltonian using parameters from items 2 and 9
16. Variational energy of relative motion Hamiltonian using parameters from items 3 and 9
17. Variational energy of relative motion Hamiltonian using parameters from items 2 and 8
18. Variational energy of relative motion Hamiltonian using parameters from items 3 and 8
19. Error percentage for item 14
20. Error percentage for item 15
21. Error percentage for item 16
22. Error percentage for item 17
23. Error percentage for item 18
24. Error percentage for item 19



## 10 References

- [1] S. M. Blinder and J. E. House, “Mathematical physics in theoretical chemistry: A volume in developments in physical & theoretical chemistry,” *Math. Phys. Theor. Chem.*, pp. 1–408, Jan. 2018, doi: 10.1016/C2016-0-04521-7.
- [2] J. Leszczynski, *Handbook of computational chemistry*. Springer, 2012.
- [3] P. W. Atkins and J. De Paula, “Atkins’ Physical Chemistry, 8th Ed.; Oxford University Press,” 2006.
- [4] “Электронная библиотека БГУ: On the Quantum Theory of Molecules.” [Online]. Available: <https://elib.bsu.by/handle/123456789/154381>. [Accessed: 21-May-2022].
- [5] M. Born and V. Fock, “Beweis des Adiabatsatzes,” *Zeitschrift für*

- Phys. 1928 513*, vol. 51, no. 3, pp. 165–180, Mar. 1928, doi: 10.1007/BF01343193.
- [6] L. Piela, *Ideas of Quantum Chemistry*. Elsevier, 2020.
  - [7] D. J. (David J. Griffiths and D. F. Schroeter, *Introduction to quantum mechanics*, 3rd editio. Cambridge University Press, 2018.
  - [8] P. Atkins and R. Friedman, *Molecular Quantum Mechanics*, 5th Edition, Oxford University Press, 2011.
  - [9] Jensen Frank, *Introduction to Computational Chemistry*, 3rd Edition. Wiley, 2017.
  - [10] F. Agostini and B. F. E. Curchod, “Chemistry without the Born–Oppenheimer approximation,” *Philos. Trans. R. Soc. A Math. Phys. Eng. Sci.*, vol. 380, no. 2223, May 2022, doi: 10.1098/RSTA.2020.0375.
  - [11] M. Born and K. Huang, *Dynamical Theory of Crystal Lattices*, New Ed. Oxford: Clarendon Press, 1954.
  - [12] Y. Yang, I. Kylänpää, N. M. Tubman, J. T. Krogel, S. Hammes-Schiffer, and D. M. Ceperley, “How large are nonadiabatic effects in atomic and diatomic systems?,” *J. Chem. Phys.*, vol. 143, no. 12, p. 124308, Sep. 2015, doi: 10.1063/1.4931667.
  - [13] P. M. Kozłowski and L. Adamowicz, “Equivalent Quantum Approach to Nuclei and Electrons in Molecules,” *Chem. Rev.*, vol. 93, no. 6, pp. 2007–2022, 1993, doi: 10.1021/cr00022a003.
  - [14] S. Hammes-Schiffer, “Current theoretical challenges in proton-coupled electron transfer: Electron-proton nonadiabaticity, proton relays, and ultrafast dynamics,” *J. Phys. Chem. Lett.*, vol. 2, no. 12, pp. 1410–1416, Jun. 2011, doi: 10.1021/jz200277p.
  - [15] I. Navrotskaya and S. Hammes-Schiffer, “Electrochemical proton-coupled electron transfer: Beyond the golden rule,” *J. Chem. Phys.*, vol. 131, no. 2, p. 024112, Jul. 2009, doi: 10.1063/1.3158828.
  - [16] A. Reyes, F. Moncada, and J. Charry, “The any particle molecular



- orbital approach: A short review of the theory and applications,” *Int. J. Quantum Chem.*, vol. 119, no. 2, p. e25705, Jan. 2019, doi: 10.1002/qua.25705.
- [17] M. Cafiero, S. Bubin, and L. Adamowicz, “Non-Born-Oppenheimer calculations of atoms and molecules,” *Phys. Chem. Chem. Phys.*, vol. 5, no. 8, pp. 1491–1501, Apr. 2003, doi: 10.1039/b211193d.
  - [18] J. Hartmann, “Exotic atoms,” *Access Sci.*, 2000, doi: 10.1036/1097-8542.YB000560.
  - [19] K. Nagamine, *Introductory Muon Science*. Cambridge University Press, 2003.
  - [20] F. R. Attila Vertes, Sandor Nagy, Zoltan Klencsar, Rezso G. Lovas, Ed., *Handbook of Nuclear Chemistry*. Springer US, 2011.
  - [21] C. J. Rhodes, “Muonium - The second radioisotope of hydrogen - And its contribution to free radical chemistry,” *J. Chem. Soc. Perkin Trans. 2*, no. 8, pp. 1379–1396, 2002, doi: 10.1039/b100699l.
  - [22] I. McKenzie, “The positive muon and  $\mu$ Sr spectroscopy: Powerful tools for investigating the structure and dynamics of free radicals and spin probes in complex systems,” *Annu. Reports Prog. Chem. - Sect. C*, vol. 109, pp. 65–112, 2013, doi: 10.1039/c3pc90005c.
  - [23] B. D. Patterson, “Muonium states in semiconductors,” *Rev. Mod. Phys.*, vol. 60, no. 1, pp. 69–159, 1988, doi: 10.1103/RevModPhys.60.69.
  - [24] C. M. Surko, G. F. Gribakin, and S. J. Buckman, “Low-energy positron interactions with atoms and molecules,” *J. Phys. B At. Mol. Opt. Phys.*, vol. 38, no. 6, 2005, doi: 10.1088/0953-4075/38/6/R01.
  - [25] M. J. Puska and R. M. Nieminen, “Theory of positrons,” *Rev. Mod. Phys.*, vol. 66, no. 3, pp. 841–897, 1994.
  - [26] F. Tuomisto and I. Makkonen, “Defect identification in semiconductors with positron annihilation: Experiment and theory,” *Rev. Mod. Phys.*, vol. 85, no. 4, pp. 1583–1631, 2013, doi: 10.1103/RevModPhys.85.1583.

- [27] D. L. Bailey and D. W. Townsend, *Positron Emission Tomography: Basic Sciences*. Springer, 2006.
- [28] S. D. Bass, S. Mariazzi, P. Moskal, and E. Stepien, “Positronium Physics and Biomedical Applications,” vol. 95, no. June, pp. 1–21, 2023, doi: 10.1103/RevModPhys.95.021002.
- [29] T. Okumura *et al.*, “Proof-of-Principle Experiment for Testing Strong-Field Quantum Electrodynamics with Exotic Atoms : High Precision X-Ray Spectroscopy of Muonic Neon,” *Phys. Rev. Lett.*, vol. 130, no. 17, p. 173001, 2023, doi: 10.1103/PhysRevLett.130.173001.
- [30] J. S. Rigden, *Hydrogen: The Essential Element*. Harvard University Press, 2003.
- [31] M. Hori, H. Aghai-Khozani, A. Sótér, A. Dax, and D. Barna, “Recent results of laser spectroscopy experiments of pionic helium atoms at PSI,” *SciPost Phys. Proc.*, vol. 5, no. 5, p. 026, Sep. 2021, doi: 10.21468/SCIPOSTPHYSPROC.5.026.
- [32] M. Hori, A. Sótér, and V. I. Korobov, “Proposed method for laser spectroscopy of pionic helium atoms to determine the charged-pion mass,” *Phys. Rev. A - At. Mol. Opt. Phys.*, vol. 89, no. 4, p. 042515, Apr. 2014, doi: 10.1103/PHYSREVA.89.042515/FIGURES/11/MEDIUM.
- [33] E. D. Kena and G. B. Adera, “Solving the Dirac equation in central potential for muonic hydrogen atom with point-like nucleus,” *J. Phys. Commun.*, vol. 5, no. 10, p. 105018, Oct. 2021, doi: 10.1088/2399-6528/AC2FBC.
- [34] M. Hori, H. Aghai-Khozani, A. Sótér, A. Dax, and D. Barna, “Laser spectroscopy of pionic helium atoms,” *Nature*, vol. 581, no. 7806, pp. 37–41, May 2020, doi: 10.1038/S41586-020-2240-X.
- [35] D. Gotta, “Precision spectroscopy of light exotic atoms,” *Prog. Part. Nucl. Phys.*, vol. 52, no. 1, pp. 133–195, 2004, doi: 10.1016/j.ppnp.2003.09.003.
- [36] A. D. Bochevarov, E. F. Valeev, and C. D. Sherrill, “The electron and

- nuclear orbitals model: Current challenges and future prospects,” *Mol. Phys.*, vol. 102, no. 1, pp. 111–123, Jan. 2004, doi: 10.1080/00268970410001668525.
- [37] M. Goli and S. Shahbazian, “The two-component quantum theory of atoms in molecules (TC-QTAIM): Foundations,” *Theor. Chem. Acc.*, vol. 131, no. 5, pp. 1–19, Apr. 2012, doi: 10.1007/s00214-012-1208-9.
  - [38] I. L. Thomas and H. W. Joy, “Protonic structure of molecules. II. Methodology, center-of-mass transformation, and the structure of methane, ammonia, and water,” *Phys. Rev. A*, vol. 2, no. 4, pp. 1200–1208, Oct. 1970, doi: 10.1103/PhysRevA.2.1200.
  - [39] I. L. Thomas, “Protonic structure of molecules. I. Ammonia molecules,” *Phys. Rev.*, vol. 185, no. 1, pp. 90–94, 1969, doi: 10.1103/PhysRev.185.90.
  - [40] P. M. Kozłowski and L. Adamowicz, “An effective method for generating nonadiabatic many-body wave function using explicitly correlated Gaussian-type functions,” *J. Chem. Phys.*, vol. 95, no. 9, pp. 6661–6668, 1991, doi: 10.1063/1.461538.
  - [41] S. Bubin, M. Pavanello, W. C. Tung, K. L. Sharkey, and L. Adamowicz, “Born-oppenheimer and non-born-oppenheimer, atomic and molecular calculations with explicitly correlated gaussians,” *Chem. Rev.*, vol. 113, no. 1, pp. 36–79, 2013, doi: 10.1021/cr200419d.
  - [42] S. Bubin and L. Adamowicz, “Variational calculations of excited states with zero total angular momentum (vibrational spectrum) of H<sub>2</sub> without use the Born-Oppenheimer approximation,” *J. Chem. Phys.*, vol. 118, no. 7, pp. 3079–3082, Feb. 2003, doi: 10.1063/1.1537719.
  - [43] M. Cafiero and L. Adamowicz, “Non-Born-Oppenheimer molecular structure and one-particle densities for H<sub>2</sub>D<sup>+</sup>,” *J. Chem. Phys.*, vol. 122, no. 18, p. 184305, 2005, doi: 10.1063/1.1891707.
  - [44] H. Nakai, “Nuclear orbital plus molecular orbital theory: Simultaneous determination of nuclear and electronic wave functions without Born–Oppenheimer approximation,” *Int. J. Quantum Chem.*, vol. 107, no.

14, pp. 2849–2869, Nov. 2007, doi: 10.1002/qua.21379.

- [45] M. Tachikawa, K. Mori, K. Suzuki, and K. Iguchi, “Full variational molecular orbital method: Application to the positron-molecule complexes,” *Int. J. Quantum Chem.*, vol. 70, no. 3, pp. 491–501, 1998, doi: 10.1002/(SICI)1097-461X(1998)70:3<491::AID-QUA5>3.0.CO;2-P.
- [46] M. Tachikawa, K. Mori, H. Nakai, and K. Iguchi, “An extension of ab initio molecular orbital theory to nuclear motion,” *Chem. Phys. Lett.*, vol. 290, no. 4–6, pp. 437–442, Jul. 1998, doi: 10.1016/S0009-2614(98)00519-3.
- [47] H. Nakai, “Simultaneous determination of nuclear and electronic wave functions without Born-Oppenheimer approximation: Ab initio NO+MO/HF theory,” *Int. J. Quantum Chem.*, vol. 86, no. 6, pp. 511–517, Feb. 2002, doi: 10.1002/qua.1106.
- [48] H. Nakai and K. Sodeyama, “Many-body effects in nonadiabatic molecular theory for simultaneous determination of nuclear and electronic wave functions: Ab initio NOMO/MBPT and CC methods,” *J. Chem. Phys.*, vol. 118, no. 3, pp. 1119–1127, Jan. 2003, doi: 10.1063/1.1528951.
- [49] H. Nakai, M. Hoshino, K. Miyamoto, and S. Hyodo, “Elimination of translational and rotational motions in nuclear orbital plus molecular orbital theory,” *J. Chem. Phys.*, vol. 122, no. 16, p. 164101, Apr. 2005, doi: 10.1063/1.1871914.
- [50] B. T. Sutcliffe, “The idea of a potential energy surface,” *J. Mol. Struct. THEOCHEM*, vol. 341, no. 1–3, pp. 217–235, Oct. 1995, doi: 10.1016/0166-1280(95)04125-P.
- [51] M. Hoshino and H. Nakai, “Elimination of translational and rotational motions in nuclear orbital plus molecular orbital theory: Application of Møller-Plesset perturbation theory,” *J. Chem. Phys.*, vol. 124, no. 19, p. 194110, May 2006, doi: 10.1063/1.2193513.
- [52] H. Nishizawa, M. Hoshino, Y. Imamura, and H. Nakai, “Evaluation of electron repulsion integral of the explicitly correlated Gaussian-

- nuclear orbital plus molecular orbital theory,” *Chem. Phys. Lett.*, vol. 521, pp. 142–149, Jan. 2012, doi: 10.1016/j.cplett.2011.11.023.
- [53] S. P. Webb, T. Iordanov, and S. Hammes-Schiffer, “Multiconfigurational nuclear-electronic orbital approach: Incorporation of nuclear quantum effects in electronic structure calculations,” *J. Chem. Phys.*, vol. 117, no. 9, pp. 4106–4118, Sep. 2002, doi: 10.1063/1.1494980.
  - [54] M. V. Pak and S. Hammes-Schiffer, “Electron-Proton Correlation for Hydrogen Tunneling Systems,” *Phys. Rev. Lett.*, vol. 92, no. 10, p. 103002, Mar. 2004, doi: 10.1103/PHYSREVLETT.92.103002/FIGURES/2/MEDIUM.
  - [55] C. Swalina, M. V. Pak, A. Chakraborty, and S. Hammes-Schiffer, “Explicit dynamical electron-proton correlation in the nuclear-electronic orbital framework,” *J. Phys. Chem. A*, vol. 110, no. 33, pp. 9983–9987, Aug. 2006, doi: 10.1021/jp0634297.
  - [56] A. Chakraborty, M. V. Pak, and S. Hammes-Schiffer, “Inclusion of explicit electron-proton correlation in the nuclear-electronic orbital approach using Gaussian-type geminal functions,” *J. Chem. Phys.*, vol. 129, no. 1, p. 014101, Jul. 2008, doi: 10.1063/1.2943144.
  - [57] C. Ko, M. V. Pak, C. Swalina, and S. Hammes-Schiffer, “Alternative wavefunction ansatz for including explicit electron-proton correlation in the nuclear-electronic orbital approach,” *J. Chem. Phys.*, vol. 135, no. 5, p. 054106, Aug. 2011, doi: 10.1063/1.3611054.
  - [58] A. Sirjoosingh, M. V. Pak, C. Swalina, and S. Hammes-Schiffer, “Reduced explicitly correlated Hartree-Fock approach within the nuclear-electronic orbital framework: Theoretical formulation,” *J. Chem. Phys.*, vol. 139, no. 3, p. 034102, 2013, doi: 10.1063/1.4812257.
  - [59] K. R. Brorsen, A. Sirjoosingh, M. V. Pak, and S. Hammes-Schiffer, “Nuclear-electronic orbital reduced explicitly correlated Hartree-Fock approach: Restricted basis sets and open-shell systems,” *J. Chem. Phys.*, vol. 142, no. 21, p. 214108, Jun. 2015, doi: 10.1063/1.4921304.

- [60] F. Pavošević, T. Culpitt, and S. Hammes-Schiffer, “Multicomponent Quantum Chemistry: Integrating Electronic and Nuclear Quantum Effects via the Nuclear-Electronic Orbital Method,” *Chem. Rev.*, vol. 120, no. 9, pp. 4222–4253, 2020, doi: 10.1021/acs.chemrev.9b00798.
- [61] S. Hammes-Schiffer, “Nuclear-electronic orbital methods: Foundations and prospects,” *J. Chem. Phys.*, vol. 155, no. 3, pp. 1–11, 2021, doi: 10.1063/5.0053576.
- [62] J. F. Capitani, R. F. Nalewajski, and R. G. Parr, “NonBorn – Oppenheimer density functional theory of molecular systems Non-Born-Oppenheimer density functional theory of molecular systems,” *J. Chem. Phys.*, no. 76, p. 568, 1982, doi: 10.1063/1.442703.
- [63] Y. Shigeta, H. Takahashi, S. Yamanaka, M. Mitani, H. Nagao, and K. Yamaguchi, “Density functional theory without the Born–Oppenheimer approximation and its application,” *Int. J. Quantum Chem.*, vol. 70, no. 45, pp. 659–669, 1998, doi: 10.1002/(sici)1097-461x(1998)70:4/5<659::aid-qua12>3.3.co;2-s.
- [64] T. Kreibich and E. K. U. Gross, “Multicomponent density-functional theory for electrons and nuclei,” *Phys. Rev. Lett.*, vol. 86, no. 14, pp. 2984–2987, Apr. 2001, doi: 10.1103/PhysRevLett.86.2984.
- [65] M. V. Pak, A. Chakraborty, and S. Hammes-Schiffer, “Density functional theory treatment of electron correlation in the nuclear-electronic orbital approach,” *J. Phys. Chem. A*, vol. 111, no. 20, pp. 4522–4526, 2007, doi: 10.1021/jp0704463.
- [66] A. Chakraborty, M. V. Pak, and S. Hammes-Schiffer, “Properties of the exact universal functional in multicomponent density functional theory,” *J. Chem. Phys.*, vol. 131, no. 12, p. 124115, 2009, doi: 10.1063/1.3236844.
- [67] A. Sirjoosingh, M. V. Pak, and S. Hammes-Schiffer, “Derivation of an electron-proton correlation functional for multicomponent density functional theory within the nuclear-electronic orbital approach,” *J. Chem. Theory Comput.*, vol. 7, no. 9, pp. 2689–2693, Sep. 2011, doi: 10.1021/ct200473r.

- [68] A. Sirjoosingh, M. V. Pak, and S. Hammes-Schiffer, "Multicomponent density functional theory study of the interplay between electron-electron and electron-proton correlation," *J. Chem. Phys.*, vol. 136, no. 17, p. 174114, May 2012, doi: 10.1063/1.4709609.
- [69] Y. Yang, K. R. Brorsen, T. Culpitt, M. V. Pak, and S. Hammes-Schiffer, "Development of a practical multicomponent density functional for electron-proton correlation to produce accurate proton densities," *J. Chem. Phys.*, vol. 147, no. 11, p. 114113, Sep. 2017, doi: 10.1063/1.4996038.
- [70] K. R. Brorsen, Y. Yang, and S. Hammes-Schiffer, "Multicomponent Density Functional Theory: Impact of Nuclear Quantum Effects on Proton Affinities and Geometries," *J. Phys. Chem. Lett.*, vol. 8, no. 15, pp. 3488–3493, 2017, doi: 10.1021/acs.jpcllett.7b01442.
- [71] K. R. Brorsen, P. E. Schneider, and S. Hammes-Schiffer, "Alternative forms and transferability of electron-proton correlation functionals in nuclear-electronic orbital density functional theory," *J. Chem. Phys.*, vol. 149, no. 4, p. 044110, 2018, doi: 10.1063/1.5037945.
- [72] Z. Tao, Y. Yang, and S. Hammes-Schiffer, "Multicomponent density functional theory: Including the density gradient in the electron-proton correlation functional for hydrogen and deuterium," *J. Chem. Phys.*, vol. 151, no. 12, p. 124102, 2019, doi: 10.1063/1.5119124.
- [73] M. Goli and S. Shahbazian, "Two-component density functional theory for muonic molecules: Inclusion of the electron–positive muon correlation functional," *J. Chem. Phys.*, vol. 156, no. 4, p. 044104, Jan. 2022, doi: 10.1063/5.0077179.
- [74] F. Pavošević, T. Culpitt, and S. Hammes-Schiffer, "Multicomponent Coupled Cluster Singles and Doubles Theory within the Nuclear-Electronic Orbital Framework," *J. Chem. Theory Comput.*, vol. 15, no. 1, pp. 338–347, Jan. 2019, doi: 10.1021/acs.jctc.8b01120.
- [75] C. Swalina, M. V. Pak, and S. Hammes-Schiffer, "Alternative formulation of many-body perturbation theory for electron-proton correlation," *Chem. Phys. Lett.*, vol. 404, no. 4–6, pp. 394–399, Mar.

2005, doi: 10.1016/j.cplett.2005.01.115.

- [76] F. Pavošević, B. J. G. Rousseau, and S. Hammes-Schiffer, “Multicomponent Orbital-Optimized Perturbation Theory Methods: Approaching Coupled Cluster Accuracy at Lower Cost,” *J. Phys. Chem. Lett.*, vol. 11, no. 4, pp. 1578–1583, 2020, doi: 10.1021/acs.jpclett.0c00090.
- [77] R. G. Parr and Y. Weitao, *Density-Functional Theory of Atoms and Molecules*. Oxford University Press, 1989.
- [78] T. Gould, D. P. Kooi, P. Gori-Giorgi, and S. Pittalis, “Electronic Excited States in Extreme Limits via Ensemble Density Functionals,” *Phys. Rev. Lett.*, vol. 130, no. 10, p. 106401, 2023, doi: 10.1103/physrevlett.130.106401.
- [79] M. Taut, “Two electrons in an external oscillator potential: Particular analytic solutions of a Coulomb correlation problem,” *Phys. Rev. A*, vol. 48, no. 5, pp. 3561–3566, Nov. 1993, doi: 10.1103/PhysRevA.48.3561.
- [80] N. R. Kestner and O. Sinanoğlu, “Study of Electron Correlation in Helium-Like Systems Using an Exactly Soluble Model,” *Phys. Rev.*, vol. 128, no. 6, pp. 2687–2692, Dec. 1962, doi: 10.1103/PhysRev.128.2687.
- [81] E. A. Hylleraas, “Über den Grundzustand des Heliumatoms,” *Zeitschrift für Phys.*, vol. 48, no. 7–8, pp. 469–494, 1928, doi: 10.1007/BF01340013.
- [82] E. A. Hylleraas, “Neue Berechnung der Energie des Heliums im Grundzustande, sowie des tiefsten Terms von Ortho-Helium,” *Zeitschrift für Phys.*, vol. 54, no. 5–6, pp. 347–366, 1929, doi: 10.1007/BF01375457.
- [83] P. M. Laufer and J. B. Krieger, “Test of density-functional approximations in an exactly soluble model,” *Phys. Rev. A*, vol. 33, no. 3, pp. 1480–1491, Mar. 1986, doi: 10.1103/PhysRevA.33.1480.
- [84] S. K. Ghosh and A. Samanta, “Study of correlation effects in an exactly



- solvable model two-electron system,” *J. Chem. Phys.*, vol. 94, no. 1, pp. 517–522, Aug. 1991, doi: 10.1063/1.460368.
- [85] A. Samanta and S. K. Ghosh, “Correlation in an exactly solvable two-particle quantum system,” *Phys. Rev. A*, vol. 42, no. 3, pp. 1178–1183, 1990, doi: 10.1103/PhysRevA.42.1178.
  - [86] A. G. Ushveridze, *Quasi-exactly solvable models in quantum mechanics*. Taylor & Francis, 1994.
  - [87] J. Karwowski and L. Cyrnek, “Harmonium,” *Ann. Phys.*, vol. 13, no. 4, pp. 181–193, Apr. 2004, doi: 10.1002/andp.200310071.
  - [88] J. Karwowski, “Influence of confinement on the properties of quantum systems,” *J. Mol. Struct. THEOCHEM*, vol. 727, no. 1-3 SPEC. ISS., pp. 1–7, Aug. 2005, doi: 10.1016/j.theochem.2005.02.038.
  - [89] J. Karwowski and H. A. Witek, “Biconfluent Heun equation in quantum chemistry: Harmonium and related systems,” *Theor. Chem. Acc.*, vol. 133, no. 7, pp. 1–11, May 2014, doi: 10.1007/s00214-014-1494-5.
  - [90] J. Karwowski, “Inverse problems in quantum chemistry,” *Int. J. Quantum Chem.*, vol. 109, no. 11, pp. 2456–2463, Jan. 2009, doi: 10.1002/qua.22048.
  - [91] J. Karwowski, “Few-particle systems: Quasi-exactly solvable models,” *J. Phys. Conf. Ser.*, vol. 104, no. 1, p. 12033, 2008, doi: 10.1088/1742-6596/104/1/012033.
  - [92] J. Karwowski and H. A. Witek, “Schrödinger equations with power potentials,” *Mol. Phys.*, vol. 114, no. 7–8, pp. 932–940, Apr. 2016, doi: 10.1080/00268976.2015.1115565.
  - [93] J. Cioslowski and K. Strasburger, “Five- and six-electron harmonium atoms: Highly accurate electronic properties and their application to benchmarking of approximate 1-matrix functionals,” *J. Chem. Phys.*, vol. 148, no. 14, p. 144107, 2018, doi: 10.1063/1.5021419.
  - [94] K. D. Sen, *Electronic structure of quantum confined atoms and molecules*. Springer, 2014.

- [95] P. C. Deshmukh, J. Jose, H. R. Varma, and S. T. Manson, “Electronic structure and dynamics of confined atoms,” *Eur. Phys. J. D*, vol. 75, no. 6, pp. 1–32, 2021, doi: 10.1140/epjd/s10053-021-00151-2.
- [96] P. A. Maksym and T. Chakraborty, “Quantum dots in a magnetic field: Role of electron-electron interactions,” *Phys. Rev. Lett.*, vol. 65, no. 1, pp. 108–111, 1990, doi: 10.1103/PhysRevLett.65.108.
- [97] C. A. Coulson and A. H. Neilson, “Electron correlation in the ground state of helium,” *Proc. Phys. Soc.*, vol. 78, no. 5, pp. 831–837, 1961, doi: 10.1088/0370-1328/78/5/328.
- [98] W. Koch and M. C. Holthausen, *A Chemist’s Guide to Density Functional Theory*. Wiley, 2001.
- [99] R. A. Ferrell, “Theory of Positron Annihilation in Solids,” *Rev. Mod. Phys.*, vol. 28, p. 308, 1956.
- [100] S. Kahana, “Positron annihilation in metals,” *Phys. Rev.*, vol. 117, no. 1, pp. 123–128, 1960, doi: 10.1103/PhysRev.117.123.
- [101] D. R. Hamann, “Effective mass of positrons in metals,” *Phys. Rev.*, vol. 146, no. 1, pp. 277–281, 1966, doi: 10.1103/PhysRev.146.277.
- [102] B. Bergersen and E. Pajanne, “Positron-electron correlation-polarization potentials for the calculation of positron collisions with atoms and molecules,” *Phys. Rev.*, vol. 186, no. 2, pp. 375–380, Oct. 1969, doi: 10.1103/PhysRev.186.375.
- [103] E. Boroński and R. M. Nieminen, “Electron-positron density-functional theory,” *Phys. Rev. B*, vol. 34, no. 6, pp. 3820–3831, 1986, doi: 10.1103/PhysRevB.34.3820.
- [104] B. Chakraborty, “Effects of electron-positron correlation on positron annihilation: Self-consistent band-structure calculations in Al,” *Phys. Rev. B*, vol. 24, no. 12, pp. 7423–7426, Dec. 1981, doi: 10.1103/PhysRevB.24.7423.
- [105] B. Barbiellini, M. Hakala, M. Puska, R. Nieminen, and A. Manuel, “Correlation effects for electron-positron momentum density in solids,” *Phys. Rev. B - Condens. Matter Mater. Phys.*, vol. 56, no. 12,

- pp. 7136–7142, 1997, doi: 10.1103/PhysRevB.56.7136.
- [106] G. Kontrym-Sznajd and J. Majsnerowski, “Electronic structure and electron-positron correlation effects in Mg,” *J. Phys. Condens. Matter*, vol. 2, no. 49, pp. 9927–9939, 1990, doi: 10.1088/0953-8984/2/49/017.
  - [107] J. Franz, “Positron-electron correlation-polarization potentials for the calculation of positron collisions with atoms and molecules\*,” *Eur. Phys. J. D*, vol. 71, no. 2, 2017, doi: 10.1140/epjd/e2017-70591-2.
  - [108] J. A. Charry Martinez, M. Barborini, and A. Tkatchenko, “Correlated Wave Functions for Electron-Positron Interactions in Atoms and Molecules,” *J. Chem. Theory Comput.*, vol. 18, no. 4, pp. 2267–2280, 2022, doi: 10.1021/acs.jctc.1c01193.
  - [109] P. Tommasini, E. Timmermans, and A. F. R. de Toledo Piza, “The hydrogen atom as an entangled electron–proton system,” *Am. J. Phys.*, vol. 66, no. 10, pp. 881–886, 1998, doi: 10.1119/1.18977.
  - [110] E. Matsushita, “Model of electron-proton correlation in quasi-one-dimensional halogen-bridged mixed-valence complexes: Role of proton motion,” *Phys. Rev. B. Condens. Matter*, vol. 51, no. 24, pp. 17332–17337, 1995, doi: 10.1103/PHYSREVB.51.17332.
  - [111] T. Ishimoto, M. Tachikawa, and U. Nagashima, “Electron-electron and electron-nucleus correlation effects on exponent values of Gaussian-type functions for quantum protons and deuterons,” *J. Chem. Phys.*, vol. 125, no. 14, p. 144103, 2006, doi: 10.1063/1.2352753.
  - [112] O. J. Fajen and K. R. Brorsen, “Separation of electron-electron and electron-proton correlation in multicomponent orbital-optimized perturbation theory,” *J. Chem. Phys.*, vol. 152, no. 19, p. 194107, 2020, doi: 10.1063/5.0006743.
  - [113] Z. Chen and J. Yang, “Nucleus-electron correlation revising molecular bonding fingerprints from the exact wavefunction factorization,” *J. Chem. Phys.*, vol. 155, no. 10, p. 104111, 2021, doi: 10.1063/5.0056773.

- [114] T. Udagawa, T. Tsuneda, and M. Tachikawa, “Electron-nucleus correlation functional for multicomponent density-functional theory,” *Phys. Rev. A - At. Mol. Opt. Phys.*, vol. 89, no. 5, pp. 1–6, 2014, doi: 10.1103/PhysRevA.89.052519.
- [115] Y. Akamatsu, T. Hatsuda, and T. Hirano, “Electron-muon correlation as a new probe of strongly interacting quark-gluon plasma,” *Phys. Rev. C - Nucl. Phys.*, vol. 80, no. 3, pp. 33–36, 2009, doi: 10.1103/PhysRevC.80.031901.
- [116] R. J. Boyd and C. A. Coulson, “Coulomb hole in some excited states of helium,” *J. Phys. B At. Mol. Phys.*, vol. 6, no. 5, pp. 782–793, 1973, doi: 10.1088/0022-3700/6/5/012.
- [117] C. Boyd, “On the Fermi hole in atoms,” *J. Phys. B At. Mol. Phys.*, vol. 7, no. 14, pp. 1805–1816, 1975, doi: 10.1088/0022-3700/8/8/002.
- [118] R. McWeeny, “Some recent advances in density matrix theory,” *Rev. Mod. Phys.*, vol. 32, no. 2, pp. 335–369, 1960, doi: 10.1103/RevModPhys.32.335.
- [119] R. Mcweeny, “The nature of electron correlation in molecules,” *Int. J. Quantum Chem.*, vol. 1, no. 1 S, pp. 351–359, 1967, doi: 10.1002/qua.560010641.
- [120] A. J. Thakkar, “Extracules, Intracules, Correlation Holes, Potentials, Coefficients and All That,” in *Density Matrices and Density Functionals*, 1987, pp. 553–581, doi: 10.1007/978-94-009-3855-7\_30.
- [121] W. Kohn and L. J. Sham, “Self-consistent equations including exchange and correlation effects,” *Phys. Rev.*, vol. 140, no. 4A, pp. A1133–A1138, Nov. 1965, doi: 10.1103/PHYSREV.140.A1133/FIGURE/1/THUMB.
- [122] P. Hohenberg and W. Kohn, “Inhomogeneous electron gas,” *Phys. Rev.*, vol. 136, no. 3B, pp. B864–B871, Nov. 1964, doi: 10.1103/PHYSREV.136.B864/FIGURE/1/THUMB.
- [123] B. I. Gunnarsson, O. Lundqvist, “Exchange and correlation in atoms, molecules, and solids by the spin-density-functional formalism,” *Phys.*

- Rev. B*, vol. 13, no. 10, pp. 4274–4298, 1976.
- [124] D. C. Langreth and J. P. Perdew, “THE EXCHANGE-CORRELATION ENERGY OF A METALLIC SURFACE,” *Phys. Rev. B*, vol. 15, no. 6, pp. 2884–2901, 1977.
  - [125] J. Harris, “The role of occupation numbers in HKS theory,” *Int. J. Quantum Chem.*, vol. 16, no. 13 S, pp. 189–193, 1979, doi: 10.1002/qua.560160821.
  - [126] J. Harris, “Adiabatic-connection approach to Kohn-Sham theory,” *Phys. Rev. A*, vol. 29, no. 4, pp. 1648–1659, 1984, doi: 10.1103/PhysRevA.29.1648.
  - [127] A. D. Becke, “Correlation energy of an inhomogeneous electron gas: A coordinate-space model,” *J. Chem. Phys.*, vol. 88, no. 2, pp. 1053–1062, 1988, doi: 10.1063/1.454274.
  - [128] K. Burke, J. P. Perdew, and D. C. Langreth, “Is the local density approximation exact for short wavelength fluctuations?,” *Phys. Rev. Lett.*, vol. 73, no. 9, pp. 1283–1286, 1994, doi: 10.1103/PhysRevLett.73.1283.
  - [129] T. Leininger, H. Stoll, H. J. Werner, and A. Savin, “Combining long-range configuration interaction with short-range density functional,” *Chem. Phys. Lett.*, vol. 275, no. 3–4, pp. 151–160, 1997, doi: 10.1016/S0009-2614(97)00758-6.
  - [130] J. Cioslowski and G. Liu, “Electron intracule densities and Coulomb holes from energy-derivative two-electron reduced density matrices,” *J. Chem. Phys.*, vol. 109, no. 19, pp. 8225–8231, 1998, doi: 10.1063/1.477484.
  - [131] K. Burke, J. P. Perdew, and M. Ernzerhof, “Why semilocal functionals work: Accuracy of the on-top pair density and importance of system averaging,” *J. Chem. Phys.*, vol. 109, no. 10, pp. 3760–3771, 1998, doi: 10.1063/1.476976.
  - [132] Z. Yan, J. P. Perdew, and S. Kurth, “Density functional for short-range correlation: Accuracy of the random-phase approximation for

- isoelectronic energy changes,” *Phys. Rev. B - Condens. Matter Mater. Phys.*, vol. 61, no. 24, pp. 16430–16439, 2000, doi: 10.1103/PhysRevB.61.16430.
- [133] T. M. Henderson and R. J. Bartlett, “Short-range corrections to the correlation hole,” *Phys. Rev. A*, vol. 70, no. 2, pp. 1–12, 2004, doi: 10.1103/PhysRevA.70.022512.
- [134] T. M. Henderson and R. J. Bartlett, “Theory of the short-range correlation hole model,” *Mol. Phys.*, vol. 103, no. 15–16, pp. 2093–2103, 2005, doi: 10.1080/09500340500131442.
- [135] A. D. Becke, “Perspective: Fifty years of density-functional theory in chemical physics,” *J. Chem. Phys.*, vol. 140, no. 18, 2014, doi: 10.1063/1.4869598.
- [136] A. Pribram-Jones, D. A. Gross, and K. Burke, “DFT: A theory full of holes,” *Annu. Rev. Phys. Chem.*, vol. 66, pp. 283–304, 2015, doi: 10.1146/annurev-physchem-040214-121420.
- [137] D. P. O’Neill and P. M. W. Gill, “Wave functions and two-electron probability distributions of the Hooke’s-law atom and helium,” *Phys. Rev. A - At. Mol. Opt. Phys.*, vol. 68, no. 2, p. 7, 2003, doi: 10.1103/PhysRevA.68.022505.
- [138] J. Makarewicz, “Coulomb and Fermi holes in a two-electron model atom,” *Am. J. Phys.*, vol. 56, no. 12, pp. 1100–1104, 1988, doi: 10.1119/1.15760.
- [139] P. Cassam-Chenaï, B. Suo, and W. Liu, “A quantum chemical definition of electron–nucleus correlation,” *Theor. Chem. Acc.*, vol. 136, no. 4, 2017, doi: 10.1007/s00214-017-2081-3.
- [140] E. J. Baerends and O. V Gritsenko, “A Quantum Chemical View of Density Functional Theory,” *J. Phys. Chem. A.*, vol. 101, no. 30, pp. 5384–5403, 1997, doi: 10.1021/jp9703768.
- [141] S. Kais, D. R. Herschbach, N. C. Handy, C. W. Murray, and G. J. Laming, “Density functionals and dimensional renormalization for an exactly solvable model,” *J. Chem. Phys.*, vol. 99, no. 1, pp. 417–425,

- 1993, doi: 10.1063/1.465765.
- [142] R. Frigg, “Models in physics,” *Routledge Encyclopedia of Philosophy Online*. Routledge, 2009, doi: 10.4324/9780415249126-Q135-1.
  - [143] B. Sutherland, *Beautiful Models*. World Scientific, 2004.
  - [144] M. B. Hesse, “Models in physics,” *Br. J. Philos. Sci.*, vol. 4, no. 15, pp. 198–214, 1953, doi: 10.1093/bjps/IV.15.198.
  - [145] M. W. W. Robert S. Cohen, Ed., *Boston Studies in the Philosophy of Science*, vol. 5. springer, 1968.
  - [146] C. Filippi, C. J. Umrigar, and M. Taut, “Comparison of exact and approximate density functionals for an exactly soluble model,” *J. Chem. Phys.*, vol. 100, no. 2, pp. 1290–1296, 1994, doi: 10.1063/1.466658.
  - [147] S. Majumdar and A. K. Roy, “Density functional study of atoms spatially confined inside a hard sphere,” *Int. J. Quantum Chem.*, vol. 121, no. 11, pp. 1–21, 2021, doi: 10.1002/qua.26630.
  - [148] R. Singh, A. Kumar, M. K. Harbola, and P. Samal, “Semianalytical wavefunctions and Kohn-Sham exchange-correlation potentials for two-electron atomic systems in two-dimensions,” *J. Phys. B At. Mol. Opt. Phys.*, vol. 53, no. 3, 2020, doi: 10.1088/1361-6455/ab56be.
  - [149] T. Chachiyo and H. Chachiyo, “Understanding electron correlation energy through density functional theory,” *Comput. Theor. Chem.*, vol. 1172, no. September 2019, p. 112669, 2020, doi: 10.1016/j.comptc.2019.112669.
  - [150] D. P. Kooi and P. Gori-Giorgi, “Local and global interpolations along the adiabatic connection of DFT: a study at different correlation regimes,” *Theor. Chem. Acc.*, vol. 137, no. 12, pp. 1–12, 2018, doi: 10.1007/s00214-018-2354-5.
  - [151] R. S. Chauhan and M. K. Harbola, “Study of adiabatic connection in density functional theory with an accurate wavefunction for two-electron spherical systems,” *Int. J. Quantum Chem.*, vol. 117, no. 8, 2017, doi: 10.1002/qua.25344.

- [152] S. F. Vyboishchikov, “A Simple Local Correlation Energy Functional for Spherically Confined Atoms from ab Initio Correlation Energy Density,” *ChemPhysChem*, vol. 18, no. 23, pp. 3478–3484, 2017, doi: 10.1002/cphc.201700774.
- [153] J. Cioslowski, M. Piris, and E. Matito, “Robust validation of approximate 1-matrix functionals with few-electron harmonium atoms,” *J. Chem. Phys.*, vol. 143, no. 21, 2015, doi: 10.1063/1.4936583.
- [154] J. P. Coe, A. Sudbery, and I. D’Amico, “Entanglement and density-functional theory: Testing approximations on Hooke’s atom,” *Phys. Rev. B - Condens. Matter Mater. Phys.*, vol. 77, no. 20, pp. 1–14, 2008, doi: 10.1103/PhysRevB.77.205122.
- [155] M. Seidl, “Adiabatic connection in density-functional theory: Two electrons on the surface of a sphere,” *Phys. Rev. A - At. Mol. Opt. Phys.*, vol. 75, no. 6, pp. 1–11, 2007, doi: 10.1103/PhysRevA.75.062506.
- [156] S. Ragot, “Exact Kohn-Sham versus Hartree-Fock in momentum space: Examples of two-fermion systems,” *J. Chem. Phys.*, vol. 125, no. 1, 2006, doi: 10.1063/1.2212935.
- [157] D. Gómez, E. V. Ludeña, V. Karasiev, and P. Nieto, “Application of exact analytic total energy functional for Hooke’s atom to He, Li<sup>+</sup> and Be<sup>++</sup>: An examination of the universality of the energy functional in DFT,” *Theor. Chem. Acc.*, vol. 116, no. 4–5, pp. 608–613, 2006, doi: 10.1007/s00214-006-0106-4.
- [158] P. Capuzzi, N. H. March, and M. P. Tosi, “Differential equation for the ground-state density of artificial two-electron atoms with harmonic confinement,” *J. Phys. A. Math. Gen.*, vol. 38, no. 24, 2005, doi: 10.1088/0305-4470/38/24/L01.
- [159] E. V. Ludeña, D. Gómez, V. Karasiev, and P. Nieto, “Exact analytic total energy functional for Hooke’s atom generated by local-scaling transformations,” *Int. J. Quantum Chem.*, vol. 99, no. 4, pp. 297–307, 2004, doi: 10.1002/qua.10858.



- [160] C. Amovilli and N. H. March, “Exact density matrix for a two-electron model atom and approximate proposals for realistic two-electron systems,” *Phys. Rev. A - At. Mol. Opt. Phys.*, vol. 67, no. 2, p. 6, 2003, doi: 10.1103/PhysRevA.67.022509.
- [161] D. Frydel, W. M. Terilla, and K. Burke, “Adiabatic connection from accurate wave-function calculations,” *J. Chem. Phys.*, vol. 112, no. 12, pp. 5292–5297, 2000, doi: 10.1063/1.481099.
- [162] Z. Qian and V. Sahni, “Physics of transformation from Schrödinger theory to Kohn-Sham density-functional theory: Application to an exactly solvable model,” *Phys. Rev. A - At. Mol. Opt. Phys.*, vol. 57, no. 4, pp. 2527–2538, 1998, doi: 10.1103/PhysRevA.57.2527.
- [163] K. Lam, F. G. Cruz, and K. Burke, “Virial Exchange-Correlation Energy Density in Hooke’s Atom,” *Int. J. Quantum Chem.*, vol. 69, pp. 533–540, 1998.
- [164] N. S. O. Attila Szabo, *Modern Quantum Chemistry: Introduction to Advanced Electronic Structure Theory*. Dover Publications, 1982.
- [165] H. Taketa, S. Huzinaga, and K. O-ohata, “Gaussian-Expansion Methods for Molecular Integrals,” *J. Phys. Soc. Japan*, vol. 21, no. 11, pp. 2313–2324, 1966, doi: 10.1143/JPSJ.21.2313.
- [166] I. I. Guseinov and B. A. Mamedov, “Evaluation of the Boys function using analytical relations,” *J. Math. Chem.*, vol. 40, no. 2, pp. 179–183, 2006, doi: 10.1007/s10910-005-9023-3.
- [167] E. W. Ng and M Geller, “Table of Integrals of the Error Functions,” *U S Bur Stand. Res. Sci.*, vol. 73 B, no. 1, pp. 1–20, 1969, doi: 10.6028/jres.073b.001.
- [168] E. R. D. Larry E McMurchie, “One- and two-electron integrals over cartesian gaussian functions,” *J. Comput. Phys.*, vol. 26, pp. 218–231, 1978.
- [169] T. Helgaker, P. Jørgensen, and J. Olsen, *Molecular electronic-structure theory*. Wiley, 2014.
- [170] I. I. Guseinov, “Analytical evaluation of one- and two-center Coulomb

- and two-center hybrid integrals for Slater-type orbitals,” *J. Chem. Phys.*, vol. 67, no. 8, pp. 3837–3839, 1977, doi: 10.1063/1.435329.
- [171] Peter M.W. Gill, “Molecular Integrals,” in *Advances in Quantum Chemistry*, vol. 25, J. R. M. C. Z. Sabin, Ed. Academic Press, 1994, p. 65.
- [172] J. A. Rosal Sandberg, “New efficient integral algorithms for quantum chemistry,” KTH Royal Institute of Technology, 2014.
- [173] G. M. J. Barca and P. F. Loos, “Recurrence Relations for Four-Electron Integrals Over Gaussian Basis Functions,” *Adv. Quantum Chem.*, vol. 76, no. 3, pp. 147–165, 2018, doi: 10.1016/bs.aiq.2017.03.004.
- [174] T. Helgaker and P. R. Taylor, “Gaussian Basis Sets and Molecular Integrals,” in *Modern Electronic Structure Theory*, worldscientific, 1995, pp. 725–856.
- [175] S. Obara and A. Saika, “Efficient recursive computation of molecular integrals over Cartesian Gaussian functions,” *J. Chem. Phys.*, vol. 84, no. 7, pp. 3963–3974, 1985, doi: 10.1063/1.450106.
- [176] W. H. Press, S. a Teukolsky, W. T. Vetterling, and B. P. Flannery, *Numerical Recipes 3rd Edition: The Art of Scientific Computing*, 3rd ed., vol. 1. Cambridge University Press, 2007.